VNIVERSITAT DE VALÈNCIA

Tesis Doctoral

Aranzazu Martínez de Marañón Peris

2021

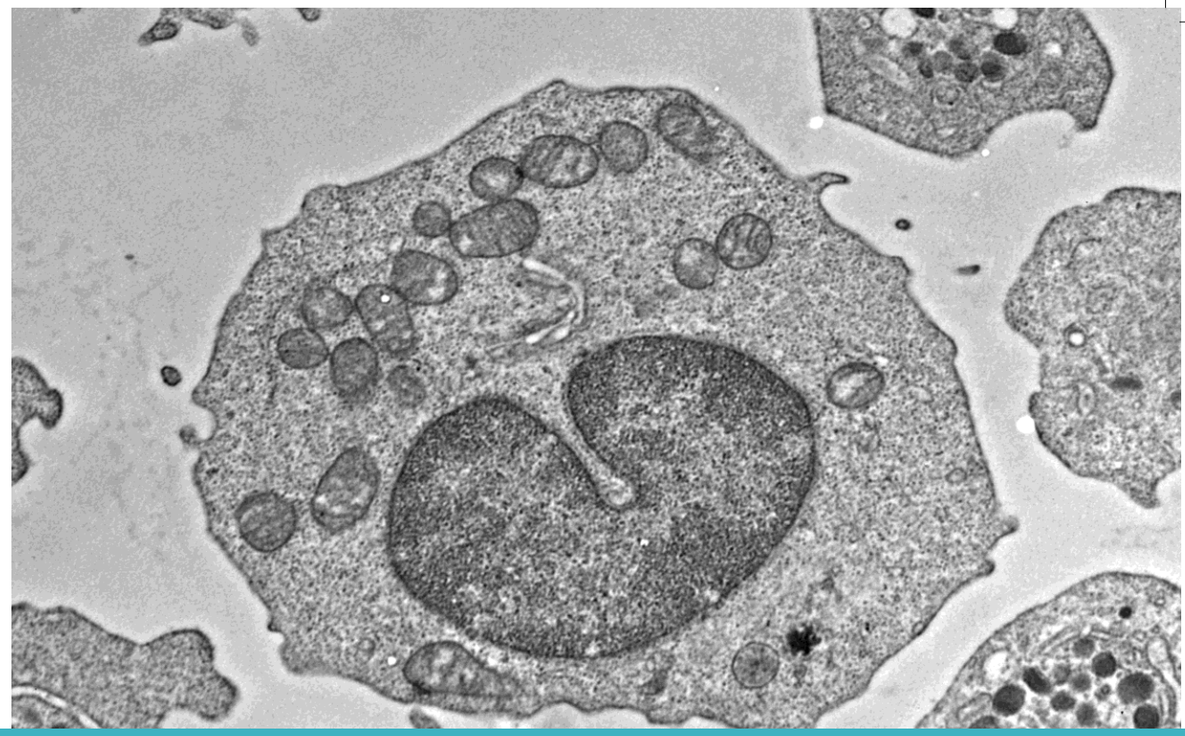

Study of mitochondrial dynamics and function and autophagy and their relationship with cardiovascular complications in type 2 diabetes

Doctorado en Biomedicina y Farmacia

Tesis Doctoral
Aranzazu Martínez de Marañón Peris

Directores:
Víctor Manuel Víctor González
Milagros Rocha Barajas
Miguel Martí Cabrera

VNIVERSITAT DE VALÈNCIA

Valencia, 2021

VNIVERSITAT DE VALÈNCIA

Universitat de València

Programa de Doctorado en Biomedicina y Farmacia

Study of mitochondrial dynamics and function and autophagy and their relationship with cardiovascular complications in type 2 diabetes

Tesis doctoral

Aranzazu Martínez de Marañón Peris

Directores:

Víctor Manuel Víctor González

Milagros Rocha Barajas

Miguel Martí Cabrera

Valencia, Octubre de 2021

Comisión Académica del Programa de Doctorado en Biomedicina y Farmacia

D. Víctor M. Víctor González, Profesor Titular del Departamento de Fisiología de la Facultad de Medicina y Odontología de la Universitat de València e Investigador en la Fundació per al Foment de la Investigació Sanitària i Biomèdica de la Comunitat Valenciana (FISABIO) – Hospital Universitario Doctor Peset de València; Dña Milagros Rocha Barajas, Investigadora Senior en la Fundació per al Foment de la Investigació Sanitària i Biomèdica de la Comunitat Valenciana (FISABIO) – Hospital Universitario Doctor Peset de València; y D. Miguel Martí Cabrera, Catedrático en Farmacología en la Universitat de Valencia:

CERTIFICAN:

Que el trabajo presentado por la Gda. **Aranzazu Martínez de Marañon Peris,** titulado "Study of mitochondrial dynamics and function, autophagy and their relationship with cardiovascular complications in type 2 diabetes", para obtener el grado de Doctor, ha sido realizado bajo nuestra dirección y asesoramiento.

Concluido el trabajo experimental y bibliográfico, autorizamos la presentación de la Tesis, para que sea juzgado por el tribunal correspondiente.

Lo que firmamos en Valencia septiembre 2021

Firmado por VICTOR MANUEL VICTOR GONZALEZ - NIF:08927488S el día 27/09/2021 con un certificado emitido por ACCVCA-120

MIGUEL |MARTI| CABRERA

Firmado digitalmente por MIGUEL|MARTI|CABRERA
Fecha: 2021.09.27 19:43:28 +02'00'

ROCHA BARAJAS, MARÍA MILAGROS (FIRMA)

Firmado digitalmente por ROCHA BARAJAS, MARÍA MILAGROS (FIRMA)
Fecha: 2021.09.27 14:38:39 +02'00'

Víctor M. Víctor González | Miguel Martí Cabrera | Milagros Rocha Barajas

Esta Tesis Doctoral se ha llevado a cabo gracias a las siguientes fuentes de financiación:

- Contrato predoctoral para la formación de Investigadores otorgada por el Instituto de Investigación Sanitaria Carlos III, con código FI17/00126.

- Proyecto de concurrencia competitiva financiado por FISABIO en la II Convocatoria de Ayudas para el desarrollo de proyectos de investigación para Grupos de Investigación Consolidados titulado "Efecto de los antioxidantes con diana en la mitocondria SS31 y MitoQ sobre la disfunción mitocondrial y el estrés de retículo endoplasmático en la diabetes tipo 2: implicaciones fisiopatológicas, clínicas y terapéuticas", con referencia UGP-15-193, y cuyo Investigador Principal ha sido Víctor Manuel Víctor González, siendo el periodo de ejecución desde el 24/05/2016 hasta el 23/12/2017.

- Proyecto de concurrencia competitiva financiado por el Instituto de Salud Carlos III en la Convocatoria AES 2016 - Proyecto de Investigación en Salud- titulado "Estudio de la dinámica y la función mitocondrial, el inflamasoma y su relación con las complicaciones cardiovasculares en la diabetes tipo 2: Implicaciones fisiopatológicas y clínicas." con referencia PI16/01083, y cuyo Investigador Principal ha sido Víctor Manuel Víctor González, siendo el periodo de ejecución desde el 01/01/2017 hasta el 31/12/2019.

- Proyecto de concurrencia competitiva financiado por el Instituto de Salud Carlos III en la Convocatoria AES 2019 - Proyectos de Investigación en Salud- "Estudio de la función mitocondrial, la autofagia y la mitofagia en la diabetes tipo 2: relación con las complicaciones cardiovasculares e implicaciones clinicas." con referencia PI19/00838, y cuyo Investigador Principal es Víctor Manuel Víctor González, siendo el periodo de ejecución desde el 01/01/2020 hasta el 31/12/2022.

- Proyecto de concurrencia competitiva financiado por la Conselleria de Innovacion, Universidades, Ciencia y Sociedad Digital de la Generalitat Valenciana – Subvenciones programa Prometeo para grupos de investigación de excelencia- "Patofisiología de las enfermedades cardiometabólicas" con referencia PROMETEO/2019/027, y cuyo Investigador Principal es Víctor Manuel Víctor González, siendo el periodo de ejecución desde el 01/03/2020 hasta el 30/04/2023.

- Proyecto de concurrencia competitiva financiado por el Instituto de Salud Carlos III en la Convocatoria AES 2013 - Proyectos de Investigación en Salud- "Efecto de la pérdida de peso sobre marcadores de estrés de retículo endoplasmático en la obesidad mórbida: Implicaciones fisiopatológicas y nuevas dianas terapéuticas" con referencia PI13/00073, y cuya Investigadora Principal es Milagros Rocha Barajas, siendo el periodo de ejecución desde el 01/01/2014 hasta el 31/12/2016.

- Proyecto de concurrencia competitiva financiado por el Instituto de Salud Carlos III en la Convocatoria AES 2013 - Proyectos de Investigación en Salud- “Papel de la autofagia y el inflamasoma en la fisiopatología de la obesidad: Efecto de la pérdida de peso y posibles implicaciones terapéuticas” con referencia PI16/00301, y cuya Investigadora Principal es Milagros Rocha Barajas, siendo el periodo de ejecución desde el 01/01/2017 hasta el 31/12/2019.

Life is not easy for any of us. But ...what of that? We must have perseverance and, above all, confidence in ourselves. We must believe that we are gifted for something, and that this thing, at whatever cost, must be attained.

Marie Curie

A mis padres y mi hermana.

A Víctor.

AGRADECIMIENTOS

En primer lugar, agradezdo a mis directores Víctor, Milagros y Miguel por darme la oportunidad de realizar esta tesis doctoral. A Víctor, por acogerme en el grupo donde he podido iniciar mis andaduras científicas, por empujarme a hacer todo un poco mejor cada vez y por recordarme siempre que la fama cuesta. A Milagros, por su paciencia, por todas las correcciones que me han hecho aprender a mejorar y a cuidar los detalles en todo lo que hago. A Miguel, por su ayuda incondicional cuando la he necesitado.

Quiero a gradecer a los miembros del Servicio de Endocrinología y Nutrición del Hospital Dr Peset por su colaboración y a todos los pacientes y voluntarios que han participado en el estudio. En especial, gracias al jefe del servicio, el Dr Morillas, por creer en nuestro proyecto; a Juan Diego, por su ayuda y por poner las cosas fáciles; y a Begoña, por su disponibilidad y colaboración. Gracias también al departamento de farmacología de la UV, en especial a la Dra Apostolova, por haberme ayudado en el planteamiento y la corrección de los artículos; a Mamen, por tu disponibilidad en todo momento y por no dejarme sola en ningún trámite; y a Brian por todas sus correcciones, incluida ésta tesis.

Gracias a todos los miembros del lab: A las personas con las que empecé: gracias a Susana por tu acogida, por ser una referencia como persona y como científica; a Noelia, por enseñarme lo que es la excelencia científica y el cuidado del detalle; a Irene, por su sonrisa y optimismo incansable que me ayudó a llevar mejor los días en el sótano; y a Francesca, porque me ha enseñado que la alegría no está reñida con el trabajo duro y el esfuerzo. Gracias a la gente que ha estado siempre: a Celia, por haber creido en mí en mis inicios y por seguir haciéncolo, por tus buenos consejos y tu guía; a Rosa, por la complicidad (Escorpio), por ser más que una compañera y saber cuidarme siempre. A Sandra, por mostrarme que nunca hay que rendirse y que siempre hay una puerta abierta cuando otra parece cerrarse. Y a los de ahora, en especial a Zaida, mi pollito que ya ha crecido, gracias por los momentos compartidos, tanto los buenos como los menos buenos. Gracias por tu apoyo y por ser ejemplo de entrega, estoy orgullosa de haberte visto crecer como persona y como científica. A Pancho, gracias por transmitirme tu paz y por ser tan amable; y a Pedro por recordarme que siempre hay un mundo fuera de la tesis. A Teresa, por tu ayuda y apoyo incondicional, por tu alegría innata y por transmitirme que, al final, todo irá bien. A Silvia y a Oscar, por las tertulias cuando hay tiempo, por su cariño y sus palabras de ánimo. A los demás, Mey, Celia, Belén, por cada una de las sonrisas que me habeis sacado.

A la gente querida con la que he compartido momentos durante este tiempo: A mis amigos de siempre, Inma, Diana, Daniela, Víctor, Javi, Marian, por los momentos en los que nos hemos juntado para contarnos la vida y que así todo parezca más fácil. A Isa, por estar cuando hace falta y cuando no, por nuestras quedadas esporádicas pero necesarias. A Mireia, por haber caminado este tiempo juntas y demostrar que la gente importante se queda en tu vida. A Lorena, por demostrarme que la vida tiene muchos caminos posibles y que solamente tú decides hacia donde quieres caminar. A Borja y a Aldana, por nuestras tertulias cinematográficas, filosóficas y de juegos. Por las risas y los buenos momentos que compatimos y que nos hacen sobrellevar lo demás. A Ana Cris por ser reflejo de que con esfuerzo y dedicación se puede llegar a cualquier sitio. A Patri, por nuestras quedadas donde hemos prendido fuego a todo y a todos, gracias por estar ahí. A la gente de la parroquia, por saber dónde encontrar una segunda casa siempre que la he necesitado. A aquellas personas que me dejo pero que han sido especiales durante éste periodo, gracias.

También agradezco a las personas que me acogieron en la estancia, al Dr Luca Scorrano, por transmitirme su excelencia científica y el amor por la ciencia bien hecha. A Lukáš, por no soltarme durante esos meses, por su simpatía y por ser para mí un ejemplo a seguir. A Lorenza, por todas tus enseñanzas y nuestro intercambio cultural y lingüístico. A los españoles padovanos, en especial, a Matías, gracias por hacer de guía turístico y que por culpa de esos paseos ahora seas un amigo en la distancia.

Finalmente, gracias a mis padres, por creer en mí incondicionalmente, por vuestros ánimos y apoyo. Gracias por los valores que me habeis transmitido y que me han ayudado a ser feliz durante todo este tiempo. Gracias a mi hermana, por poder ver cómo con perseverancia y trabajo se puede llegar a conseguir lo que sueñas. Gracias a mi amoña, por sus ánimos desde la distancia, por acordarse de mí en cuanto ve una bata blanca. Gracias a los que ya no están, a mi yaya y a mi aitona, porque sé que desde el cielo me habeis dado fuerzas y ahora estaréis más que orgullosos de mí. Gracias a Víctor, por no soltar mi mano, por acompañarme en lo bueno y lo malo, por creer en mí siempre y querer que llegue adonde yo quiera llegar. Por hacer sencillos los días que lo veo todo difícil, por entender el entusiasmo con el que vivo la ciencia. Por ser mi compañero de vida y mi centro adonde siempre quiero volver.

FOREWORD

Type 2 diabetes (T2D) is a chronic metabolic disease with an inflammatory basis and whose incidence has been increasing over recent years. Identifying the molecular and cellular basis of T2D would contribute to its early detection and prevention of associated complications. This doctoral thesis outlines some of the molecular homeostatic mechanisms associated to the physiopathology of T2D in leukocytes isolated from T2D patients. To this end, observational studies have been carried out in different T2D cohorts recruited from the Endocrinology and Nutrition Service of University Hospital Dr Peset, Valencia, Spain.

The data obtained from the recruited volunteers have rendered the results presented in this thesis and published in scientific journals indexed in the Journal Citations Report (JCR), all in the first quartile. The thesis consists of a global summary with an introduction, the main objectives, the methods employed and the results, followed by a discussion and conclusions. The four original articles included in this thesis can be found in the results and after the summary. In short, the first article details how autophagy, a cellular homeostatic process, is altered in the leukocytes of T2D patients. Moreover, the data supports that this alteration is related to leukocyte activation. In the second article it is detailed how poorly controlled T2D patients present a rise in some markers of inflammation and cardiovascular risk, and how maintaining glycated haemoglobin in range can reduce these alterations. The third article describes the functional and dynamic state of mitochondria in leukocytes from type 2 diabetic patients and their inflammatory state, all of which are ameliorated by treatment with metformin. Finally, the fourth article explores the effect of a mitochondria-targeted antioxidant compound, SS-31, on different homeostatic cellular processes and mitochondrial function in leukocytes from T2D patients.

This PhD thesis complies with the regulations approved by the doctoral School and the Academic Committee of the Phd Programme in Biomedicine and Pharmacy of the University of Valencia to be considered for the International Doctorate Mention. During the PhD, Ms. Aranzazu Martínez de Marañón has spent 4 months in a reseach institute outside Spain (Veneto Institute of Molecular Medicine, Italy). The core of this PhD thesis is written in English, and includes summary in Spanish (Resumen), since it is one of the official languages of the University of Valencia.

INDEX

Figure Index

TABLE INDEX

ABBREVIATIONS:

AARE: Aminoacid response elements.

ABCD3: ATP-binding cassette subfamily D member 3.

ACC: Acetyl-CoA carboxylase.

ADP: Adenosine diphosphate.

AGEs: Advanced glycation endproducts.

AIDS: Acquired immunodeficiency syndrome.

AKT: Protein kinase B/AKR mouse thymoma kinase.

ALG12: Asparagine-linked glycosilaton 12.

AMBRA1: Activating molecule in Beclin1-regulated autophagy protein 1.

AMPK: AMPK-activated protein kinase.

ApoE: Apolipoprotein E.

ARE: Adenylate-uridylate rich elements.

ASK: Apoptosis signal regulated kinase.

ATF: Activating transcription factor.

ATF3: Activating transcription factor 3.

ATF4: Activating transcription factor 4.

ATF5: Activating transcription factor 5.

ATF6: Activating transcription factor 6.

Atg: Autophagy-related protein.

ATII: Angiotensin II.

ATP: Adenosine triphosphate.

ATPase: ATP synthase.

Bcl-2: B cell CLL/Lymphoma 2.

BECLIN1: Coiled-coil myosin-like BCL2-interacting protein 1.

BIP: Immunoglobulin heavy chain –binding protein.

Bmal-1: Brain and muscle Arnt-like protein-1.

BNIP3: Bcl2-interacting protein 3.

BNIP3L/NIX: BCL2/adenovirus E1B interacting protein 3-like.

BP: Blood pressure.

B-ZIP: basic leucine zipper.

CAMKIII: Ca^{2+}/Calmodulin-dependent protein kinase III.

cAMP: Cyclic AMP.

CASTOR: Cytosolic arginine sensor for mTOR.

CCL: C-C chemokines motif ligand.

CCS: Copper chaperone for superoxide dismutase.

CHOP: CCAAT-enhancer-binding protein homologous protein.

CIMT: Carotid intima-media thickness.

CMA: Chaperone mediated autophagy.

CNS: Central nervous system.

CoQ: Coenzyme Q.

COX2: Cyclooxygenase 2.

CRE: CHOP response elements.

CREB: cAMP responsive element binding protein.

CRELD2: Cysteine-rich with EGF-like domains 2.

CRP: C-reactive protein.

CVD: Cardiovascular disease

CXCL: Chemokine (C-X-C motif) ligand.

CytC: Cytochrome C.

DAG: Diacylglycerol.

DALY: Disability-adjusted life years.

DBP: Diastolic blood pressure.

DPP-IV: Dipeptidyl peptidase IV.

DRP1: Dynamin-like protein 1.

E2F1: E2 transcription factor 1.

EDHF: Endothelium-derived hyperpolarizing factor.

Egfl7: Epidermal growth factor-like 7.

eIF2α: Eukaryotic initiation factor 2α.

ELK1: ETS-like 1.

ER: Endoplasmic reticulum.

ERAD: Endoplasmic reticulum associated protein degradation.

ERdj4: ER-localized DnaJ 4.

ERO1α: Endoplasmic reticulum oxidase 1.

ERSE: Endoplasmic reticulum stress elements.

ESCRT: Endosomal sorting complex required for transport.

ET-1: Endothelin-1.

ETC: Electron transport chain.

FAD: Flavin adenine dinucleotide.

FAM134B: Family with sequence similarity 134 Member B.

FASL: Fas ligand.

FFA: Free fatty acids.

FGF21: Fibroblast growth factor 21.

FIP200: Fak-family interacting protein of 200 KDa.

FIS1: Fission protein 1.

FMN: Flavin mononucleotide.

FOXO: Forkhead family box O.

FPG: Fasting plasma glucose.

FUNDC1: FUN14 domain containing 1.

FXR: Farnesoid X receptor.

GABARAPL1: Gamma-aminobutyric acid receptor-associated protein like 1.

GADD34: Growth arrest and DNA damage-inducible protein.

GAPDH: Glyceraldehyde-3-phosphate dehydrogenase.

GFAP: Glial fibrillary acidic protein.

GIP: Glucagon inhibitory protein.

GIPR: GIP receptor.

GLC: Glutamate-gated chloride channel.

GLP-1: Glucagon-like protein 1.

GLP1R: GLP1 receptor.

GLUT: Glucose transporter.

GPCR: G protein coupled receptor.

GRP78: Glucose-regulated protein 78.

GSH: Glutathione.

GSK3β: Glycogen synthase kinase 3 β.

GST: Glutathione-S-transferase.

H_2O: Hydrogen peroxide.

HbA_{1c}%: Glycated haemoglobin.

HDL: High density lipoprotein

HFD: High fat diet.

hIAPP: Human islet amyloid peptide.

HIF1α: Hypoxia-induced factor 1α.

HKDC1: Hexokinase domain component 1.

HMOX1: Heme oxygenase-1.

HOMA-IR: Homeostatic model assessment of insulin resistance.

hsCRP: High sensitivity C-reactive protein.

HSP70: Heat-shock protein 70.

HSP90: Heat-shock protein 90.

HSPA8: Heat-shock protein A8.

ICAM-1: Intercellular adhesion molecule 1.

IKKβ: Inhibitor of nuclear factor kappa B subunit beta.

IL-1RA: Interleukin 1 receptor antagonist.

IL-1β: Interleukin-1β.

IL-6: Interleukin 6.

IL-6R: Interleukin 6 receptor.

IMM: Inner mitochondrial membrane.

IP3R: Inositol-1, 4, 5-phosphate receptor.

IR: Insulin resistance.

IRAK: Interleukin associated receptor kinase.

IRE1: Inositol-requiring enzyme 1.

IRS: Insulin receptor substrate.

JNK: Janus kinase.

KEAP1: Kelch like ECH associated protein 1.

KRT16: Keratin 16.

LAMP2B: Lysosome-associated membrane protein 2B.

LC3: Microtubule-associated protein 1A/1B-light chain 3.

LDL-c: Low density lipoprotein.

LFA-1: Lymphocyte function associated antigen 1.

LKB1: Liver kinase B1.

MafA: Mast cell function-associated antigen.

MAPK: Mitogen-activated protein kinase.

MARCH5: Membrane-associated ring-CH-type finger 5.

MDG1: Microvascular-endothelial differentiation gene 1 protein.

MFN1: Mitofusin1.

MFN2: Mitofusin 2.

MLC: Myosine light chain.

MODY: Maturity onset diabetes of the young.

MPPs: Mitochondria penetrating peptides.

mTFA: Mitochondrial transcription factor A.

mTORC: Mammal target of rapamycin complex.

mtROS: Mitochondrial ROS.

NADH: Nicotinamide adenine dinucleotide.

NADPH: Nicotinamide adenine dinucleotide phosphate.

NAFLD: Non-alcoholic fatty liver disease.

NASH: Non alcoholic steatohepatitis.

NBR1: Next-to BRC1A autophagy cargo receptor 1.

NDP52: Nuclear dot protein 52.

NETs: Neutrophils extracellular traps.

NFκB: Nuclear factor κB.

NFY: Nuclear transcription factor Y.

NLP2: Niban-like protein 2.

NLRP3: NLR-family pyrin-domain containing 3.

NLS: Nuclear-locating sequence.

NO: Nitric oxide.

NOS: NO synthase.

NOX: NADPH oxidase.

NQO1: NADPH-quinone oxidorreductase-1.

NRBF2: Nuclear receptor-binding factor 2.

NRF2: Nuclear respiratory factor 2.

Nvj1: Nuclear-vacuolar junctions 1.

OCR: Oxygen consumption rate.

OCT: Organic cation transporter.

OGGT: Oral glucose tolerance test.

OMM: Outer mitochondrial membrane.

OPA1: Optic atrophy-1.

OPTN: Optineurin.

OSBP: Oxysterol-binding protein.

oxLDL: Oxidized low-density lipoprotein.

OXPHOS: Oxidative phosphorylation.

PAI-1: Plasminogen activator inhibitor 1.

PARL: Presenylins-associated rhomboid-like.

PARP: Poly-ADP ribose polymerase.

PBMCs: Peripheral blood mononuclear cells.

PDGF: Platelet-derived growth factor.

PDI: Protein disulfide isomerase.

PDK: Phosphoinositide–dependent kinase.

PDX-1: Pancreatic and duodenal homeobox 1.

PECAM: Platelet endothelial cell adhesion molecule.

PEPCK: Phosphoenolpyruvate carboxykinase.

PERK: Protein kinase RNA-like endoplasmic reticulum kinase.

PEX2: Peroxisome biogenesis factor 2.

PEX3: Peroxisome biogenesis factor 3.

PFK2: Phosphofructokinase 2.

PG: Plasma glucose.

PGC1: PPAR gamma coactivator 1.

PHB2: Prohibitin 2.

PHLPP1: Pleckstrin homology domain leucine-rich repeat protein phosphatase.

PI3K: Phosphoinositol-3-kinase.

PI3KK: Phosphoinositol-3-kinase related kinase.

PINK: PTEN-induced kinase.

PIP_3: Phosphatidil insolitol (3, 4, 5) triphosphate.

PKA: Protein kinase A.

PKC: Protein kinase C.

PLC: Phospholipase C.

PLIN2: Perilipin 2.

PMNs: Polymorphonuclear cells.

PBMCs: Peripheral blood mononuclear cells.

PP2A: Protein phosphatase 2A.

PPAR: Peroxisome proliferation activated receptor.

PPARγ: Peroxisome proliferator associated receptor γ.

PTEN: Phosphate and tensin homolog.

PTP1B: Protein tyrosine phosphatase 1B.

PUFA: Polyunsaturated acids.

RAGE: Receptor of AGEs.

Ras: Rat sarcoma.

RER: Rough endoplasmic reticulum.

Rheb: Ras homolog enriched in brain.

RIP: Regulated intermembrane processing.

ROCK: Rho kinase.

RORα: RAR-related orphan receptor α.

ROS: Reactive oxygen species.

SAMTOR: S-adenosyl-methionine sensor upstream of mTORC1.

SBP: Systolic blood pressure.

SER: Smooth endoplasmic reticulum.

SGLT: Sodium-glucose linked transporters.

SHIP2: SH2-containing inositol phosphatase 2.

SIRT1: Sirtuin-1.

SOCS: Suppressor of cytokine signalling protein.

SOD: Superoxide dismutase.

SQSTM1/p62: Sequestosome 1.

SS: Szeto-Schiller peptides.

STAT3: Signal transducer and activator of transcription 3.

STZ: Streptozotocin.

SUR1: Sulphonylurea receptor 1.

T2D: Type 2 diabetes.

TAG: Triacylglycerol.

TAK1: TGFβ-activated kinase 1.

TBC1D4: RabGAP TBC1 domain family member 4.

TBK1: TAK binding kinase 1.

TCA: Tricarboxilic acid.

TEPCR1: Tectonin β-propeller repeat containing 1.

TFEB: Transcription factor EB.

TG: Triglycerides.

tHBQ: TerButylhydroquinone.

TIRAP: TIR domain containing adaptor protein.

TLRs: Toll-like receptors.

TNFα: Tumour-necrosis factor α.

TOLLIP: Toll-interacting protein.

TRADD: TNFR1-associated death domain protein.

TRAF2: TNF-associated factor 2.

TRB3: Tribbles homolog 3.

TSC2: Tuberous sclerosis complex 2.

TXNIP: Thioredoxin interacting protein.

UDP: Uridine diphosphate.

UDP-GlnNAC: Uridyl diphosphate-N-acetylglucosamine.

ULK: Unc-51 like autophagy activating kinase.

uORF: Upstream open reading frame.

UPR: Unfolded protein response.

UPRE: Unfolded protein response elements.

UVRAG: UV radiation resistance associated gene protein.

Vac8: Vacuolar protein 8.

VCAM-1: Vascular cell adhesion molecule 1.

VEGF: Vascular endothelial growth factor.

VLA-1: Very late antigen 1.

VLDL: Very low density lipoprotein.

Vps34: Vacuolar protein sorting 34.

VSMC: Vascular smooth muscle cells.

vWF: von Willebrand factor.

WIPI: WD-repeat protein interacting with phosphoinositides.

WPB: Weibel-palade bodies.

XBP1: X-box binding protein 1.

YmeL1: YME-like protein 1.

YY1: Yin-yang 1.

ZFD: Zucker diabetic fatty.

RESUMEN

Introducción

Actualmente, hay un preocupante incremento de las enfermedades metabólicas atribuible a un estilo de vida menos saludable, en el cual las dietas industrializadas con alimentos ultraprocesados y el aumento del sedentarismo conllevan un equilibrio energético positivo. En consecuencia, se favorece el desarrollo de sobrepeso y la obesidad, que son el origen de enfermedades metabólicas crónicas como el síndrome metabólico y la diabetes tipo 2 (T2D del inglés *type 2 diabetes*).

La T2D es una enfermedad metabólica crónica de base inflamatoria, que cursa con tres síntomas principales, que son la hiperglucemia, la hiperlipidemia y la resistencia a la insulina (IR, del inglés *insulin resistance*). Inicialmente, el exceso de glucosa y lípidos circulantes provocan un estrés en el organismo que conlleva al mal funcionamiento de los órganos y tejidos encargados del metabolismo energético, tales como el páncreas, el hígado, el músculo esquelético o el tejido adiposo. El estrés celular resultante da lugar a una alta producción de moléculas proinflamatorias que desencadenan un estado inflamatorio de bajo grado. Gradualmente, la inflamación inhibe la acción de la insulina en los tejidos periféricos, llevando a un estado de IR. Simultáneamente, el exceso de nutrientes en sangre y la inflamación dan lugar a una hiperfunción del páncreas que provoca la hiperinsulinemia. Debido a esta situación – inflamación crónica, estrés oxidativo y alta demanda de insulina – llega un momento en el que se puede producir un fallo en el funcionamiento del páncreas. Todo este cuadro clínico es característico de la T2D.

La principal hormona en la fisiopatología de la T2D es la insulina, sintetizada en las células β en los islotes pancreáticos en respuesta a la internalización de glucosa. El proceso de liberación de insulina comienza con la entrada de glucosa por los canales GLUT2 (del inglés

glucose transporter 2) y la generación de ATP. El aumento de energía celular provoca la apertura de los canales de potasio, despolarizando la membrana y aumentando las concentraciones de Ca^{2+} citosólico. Este incremento provoca la exocitosis de las vesículas preformadas de insulina, que se libera al torrente circulatorio y actúa sobre los tejidos periféricos donde estimula la captación de glucosa y lípidos favoreciendo la biosíntesis de macromoléculas e inhibe las rutas catabólicas. El mecanismo de acción de la insulina comienza cuando los receptores de insulina, al unirse a su ligando, se dimerizan y fosforilan, actuando como anclaje para la proteína IRS (del inglés *insulin receptor substrate*). Ésta activa una cascada de señalización que termina en la quinasa AKT (del inglés, AKR mouse thymoma kinase), responsable de activar la glucólisis y la síntesis de lípidos y proteínas, e inhibir la gluconeogénesis.

La acción de la insulina se puede alterar por cambios en las concentraciones de lípidos y glucosa circulantes, comenzando por la síntesis y acumulación de lípidos en el músculo esquelético. En este caso, la infiltración de lípidos entre las fibras musculares perjudica la señalización de la insulina en los miocitos a través de intermediarios metabólicos como el diacilglicerol (DAG). Esta molécula inhibe la señalización de la insulina a través de la PKC (del inglés, *proteín kinase C*) provocando un cambio metabólico que implica la inhibición del almacenamiento muscular de glucógeno y un aumento de la síntesis hepática de glucógeno y lípidos que de nuevo genera DAG e inhibe la señalización de insulina. Por ello, la glucosa no se internaliza en los tejidos dependientes de insulina y permanece en circulación. Además, la síntesis de glucosa y la liberación de lípidos por parte de éstos tejidos acentúan el estado de hiperglucemia e hiperlipidemia. Este complejo proceso que involucra a diferentes tejidos y tipos celulares se denomina IR, y puede terminar agravándose hasta afectar e impedir la función pancreática.

Pese a que la T2D es una enfermedad crónica, existen tratamientos eficaces para controlar sus desencadenantes y sus síntomas a través de diferentes aproximaciones: las sulfonilureas, las biguanidas, las tiazolidinedionas, las glitazonas, los inhibidores de SGLT2 (del inglés, sodium-glucose cotransporter 2), los inhibidores de DPP-IV (del inglés, *dipeptidyl peptidase IV*) o los análogos de GLP-1 (del inglés, *glucagon-like peptide 1*). De entre todos ellos, la metformina es el fármaco de primera elección perteneciente al grupo de las biguanidas. A nivel celular, la metformina inhibe la gluconeogénesis, el complejo I de la cadena de transporte electrónico mitocondrial y activa a la AMPK (del inglés *AMP-activated kinase*). Se ha visto que la metformina es capaz de mejorar la función de la mitocondria, reducir el estrés oxidativo y, por tanto, paliar los efectos del estrés metabólico al que están expuestas las células.

A nivel celular, la diabetes tiene importantes repercusiones ya que se provocan alteraciones en la bioenergética y sobre los niveles de estrés celular. Uno de los mecanismos fisiopatológicos más importantes es la presencia de estrés oxidativo, una alteración en el equilibrio entre especies prooxidantes y antioxidantes. La principal fuente de especies reactivas de oxígeno (ROS, del inglés *reactive oxygen species*) es la mitocondria, aunque existen otras fuentes en el citosol entre las que se incluyen la ruta de la hexoquinasa, la de las pentosas fosfato, y enzimas como la NADPH (del inglés, *nicotinamide-adenine dinucleotide phosphate*) oxidasa o la NO (del inglés, *nitric oxide*) sintasa entre otras. La mitocondria es el orgánulo encargado de sintetizar energía en forma de ATP a través de la cadena de transporte electrónico. Los electrones necesarios se generan en los procesos catabólicos como la glucólisis, la β-oxidación y el ciclo de Krebs, y son transportados por los intermediarios energéticos NADH y $FADH_2$. Ambas moléculas ceden los electrones que fluyen a través de los complejos I, II, III y IV de la cadena de transporte electrónico ubicados en la membrana interna de la mitocondria hasta el complejo IV donde generan H_2O junto a una molécula de O_2. Al mismo tiempo, la ATP sintasa

que forma el complejo V emplea la energía resultante de disipar el gradiente electroquímico de H^+ para generar ATP a partir de ADP. El exceso de glucosa, característico de la T2D, genera un exceso de intermediarios energéticos que conlleva a una hiperactividad de la cadena de transporte electrónico, superando el balance adecuado entre ATP y ADP, lo que inhibe la ATP sintasa, despolariza la membrana por desacoplamiento del potencial de membrana y ralentiza el transporte de electrones. Además, los electrones libres pueden reaccionar con las moléculas de O_2 generando anión superóxido en los complejos I y III, provocando un aumento de los ROS.

La acumulación de ROS provoca una situación de estrés celular causada por diferentes motivos. Uno de ellos es el daño al ADN mitocondrial, que altera su función afectando especialmente a células con una alta demanda energética. Simultáneamente, los ROS inhiben la señalización de la insulina a nivel de la IRS e inducen la activación de rutas apoptóticas como JNK o IKK (del inglés *c-JUN N-terminal kinase* e *IκB kinase*). La inhibición en la señalización de la insulina favorece el uso y acumulación de lípidos que da como subproducto las ceramidas o el DAG, que contribuyen a la IR.

A nivel sistémico, el exceso de ROS favorece las reacciones de glicación y oxidación entre moléculas. La glicación da lugar a productos de glicación avanzada (AGE, del inglés *advanced glycation end products*), que a través de su receptor RAGE (del inglés *receptor for advanced glycation end products*) puede activar rutas proinflamatorias en los tejidos que lo expresan. También, dentro de las reacciones que implican glicosilación se encuentra el aumento en la hemoglobina glicosilada (HbA_{1C}), que se emplea para monitorizar el estado de control de la T2D. En cuanto a la oxidación, las más importantes son las de las LDL, dando lugar a partículas de LDL oxidadas (oxLDL, del inglés *oxidized low-density lipoprotein*), que activan al endotelio y a las células inmunitarias favoreciendo el desarrollo temprano de lesión aterosclerótica.

Ante el aumento de las concentraciones de ROS celular, existen mecanismos antioxidantes, como las enzimas catalasa o superóxido dismutasa, que neutralizan los ROS y equilibran la balanza entre los antioxidantes/prooxidantes. También se han diseñado moléculas capaces de neutralizar los ROS, entre las cuales se encuentran los antioxidantes con diana en la mitocondria y de carácter peptídico como el SS-31, que además cuenta con la capacidad de acumularse en la mitocondria sin alterar a su función. Su actividad antioxidante se debe a un residuo dimetiltirosina, que no posee su análogo sin capacidad antioxidante, el SS-20.

Una de las explicaciones al aumento patológico de ROS observado en la T2D es la disfunción mitocondrial. Se define por el defecto en la función de las mitocondrias que impide producir la cantidad necesaria de ATP, y se detecta mediante diferentes marcadores como la alteración del potencial de membrana, la disminución del consumo de O_2 o la alta producción de ROS mitocondriales. Cabe destacar que el acúmulo de ROS afecta funciones celulares como la señalización de la insulina, la señalización por Ca^{2+} o la acumulación de DAG, que provocan tanto disfunción mitocondrial como IR. Por tanto, ambos procesos están estrechamente relacionados y son característicos de la fisiopatología de la T2D.

Frente a la disfunción mitocondrial se establecen una serie de respuestas homeostáticas dentro de las cuales se encuentra la regulación de la dinámica mitocondrial. Ésta consiste en una serie de procesos por los cuales las mitocondrias se fusionan y fisionan para optimizar su estado metabólico en respuesta a las necesidades celulares. Cuando existe un daño celular, las mitocondrias se fisionan principalmente a través de las moléculas DRP-1 (del inglés *dynamin-related protein 1*) y FIS-1 (del inglés *fission protein-1*), entre otras, para aislar la mitocondria dañada y eliminarla o tratar de reparar el daño. En cambio, en ausencia de daño, las

mitocondrias se fusionan mediante las proteínas MFN1 y 2 (del inglés *mitofusin*) y OPA1 (del inglés *optic atrophy-1*) para optimizar la fosforilación oxidativa.

Otro de los mecanismos moleculares activados por la hiperglucemia e hiperlipidemia es el estrés de retículo endoplásmico (ER, del inglés *endoplasmic reticulum*) y la respuesta a proteínas mal plegadas (UPR, del inglés, *unfolded protein response*). Durante el estado de estrés celular y oxidativo, hay un problema de acumulación de proteínas mal plegadas y no funcionales, que se une a un estado de mayor demanda de síntesis proteica. El ER en esta situación, activa la UPR, una combinación de 3 vías de señalización que tienen por objetivo maximizar la capacidad de procesamiento y plegamiento en el ER y de degradación de proteínas alteradas. En caso de que esta respuesta no consiga resolver la situación, se activarán rutas apoptóticas. Las 3 rutas implicadas se inician con la activación de la proteína chaperona GRP78/BiP, que se disocia de las proteínas iniciadoras al detectar proteínas mal plegadas. La primera comienza con la dimerización de PERK (del inglés, *protein kinase- r like ER kinase*), que se fosforila y a su vez fosforila a eIF2α (del inglés, *eukaryotic transcription initiation factor 2 alpha*), inhibiéndola. Con ello se reduce la síntesis proteica generalizada, aunque algunos genes con secuencias específicas como el factor de transcripción ATF4 (del inglés, *activating transcription factor 4*) se siguen expresando. La segunda ruta se inicia con la proteína ATF6 (del inglés, *activating transcription factor 6*), que tras la disociación de GRP78 se trasloca al aparato de Golgi donde escinde su dominio citoplásmico que puede actuar de factor de transcripción. La tercera vía implica a la proteína transmembrana IRE1 (del inglés, *inositol-requiring enzyme 1*), que dimeriza y se autofosforila, activando su actividad endonucleasa que permite procesar el ARN mensajero del gen XBP1 (del inglés, *X-Box binding protein 1*) a su forma sXBP1 que actúa como factor de transcripción. Las 3 vías activan un programa transcripcional de respuesta a estrés, conformado por chaperonas, proteínas de degradación y autofagia, así como de respuesta antioxidante. En

particular, la primera vía tiene como diana el gen CHOP (del inglés, *C/EBP homologous protein*) que, en situación de estrés crónico, activa genes implicados en la apoptosis.

Otra vía de homeostasis celular implicada en situaciones de estrés es la autofagia. Se encarga de degradar componentes defectuosos o de suplir de nutrientes a la célula en situaciones de estrés. Existen diferentes tipos de autofagia, aunque en esta tesis nos centraremos en la macroautofagia. Se inicia cuando las vías de señalización celulares activan al complejo ULK (del inglés, *Unc-51 like autophagy activating kinase 1*), que crea un dominio de nucleación para el anclaje de proteínas implicadas en la autofagia. A su vez, son reclutadas en este dominio las proteínas iniciadoras de la formación del autofagosoma, como Beclina-1, ATG4B (del inglés, *autophagy related 4B cysteine peptidase*), ATG9 (del inglés, *autophagy related protein 9*) o AMBRA1 (del inglés, *autophagy and Beclin-1 regulator 1*). Una vez formado, ULK activa al complejo de iniciación que a través del complejo PI3K (del inglés, *phosphoinositol 3 kinase*) expande la membrana mediante la síntesis de PI3P (del inglés, *phosphoinositol-3-phosphate*). Posteriormente, diferentes proteínas se involucran en el proceso de expandir la membrana y curvarla, como LC3/ATG8 (del inglés, *autophagy related protein 8*). Esta membrana englobará las moléculas, orgánulos o componentes celulares que se necesitan degradar, que pueden ser transportados por chaperonas o por proteínas específicas, como SQSTM/p62 (del inglés, *sequestosome p62*). Estas últimas interactúan específicamente con proteínas del autofagosoma como LC3. Una vez el autofagosoma se ha cerrado, se fusiona con un lisosoma que verterá sus enzimas en el lumen del autofagolisosoma, degradando la membrana interna y el contenido del mismo. Posteriormente, los componentes digeridos se liberarán de nuevo al citoplasma para su reciclaje. Este proceso está altamente regulado por el coste celular que conlleva su activación y ejecución. Principalmente, está regulado por rutas celulares que controlan el ayuno y la disponibilidad de nutrientes, como mTOR (del inglés, *mammal target of*

rapamycin) o AMPK. Otras vías como FOXO (del inglés, *forkhead box transcription factor*) también lo regulan en respuesta a factores de crecimiento o estimulación por señalización de insulina a través de AKT.

La inflamación crónica de bajo grado es otra de las características que definen a la T2D y es responsable en gran medida de su fisiopatología. A nivel sistémico se refleja en los niveles elevados de citoquinas y moléculas proinflamatorias circulantes. Las más estudiadas han sido las citoquinas TNFα (del inglés, *tumour necrosis factor alpha*), IL-6, IL-1β o moléculas proinflamatorias como CRP (del inglés, *C-reactive protein*), que ya se pueden detectar en estadios tempranos de la T2D. El aumento de estas moléculas en fases iniciales del desarrollo de T2D refleja las primeras alteraciones como consecuencia de la hiperglucemia e hiperlipidemia, que junto con los ROS, las oxLDL o las AGE activan rutas implicadas en la inflamación, como NFκB (del inglés, *nuclear factor kappa B*) o JNK. A su vez, las citoquinas proinflamatorias que se producen activan cascadas de señalización proinflamatorias, amplificando la respuesta. Uno de los tejidos más expuestos a estas agresiones es el tejido vascular y, concretamente, las células endoteliales que recubren los vasos sanguíneos. La principal función de este tipo celular es mantener la homeostasis vascular, regulando procesos como la permeabilidad celular o la coagulación sanguínea. El endotelio se activa en respuesta a diferentes alteraciones como un aumento de células inmunitarias activadas circulantes, la presencia de oxLDL o un flujo sanguíneo turbulento, siguiendo un proceso que comprende dos fases sucesivas. En la primera, la célula libera los cuerpos de Weibel-Pallade, que almacenan moléculas proinflamatorias; y en la segunda, sintetiza moléculas de adhesión, selectinas e integrinas, que van a mediar las interacciones con las células inmunitarias para su extravasación. Este segundo paso requiere de la coestimulación por parte de los leucocitos circulantes activados.

La importancia de este proceso radica en que es el origen de una de las complicaciones más frecuentes de la T2D, la formación de placa aterosclerótica. Dicho proceso se inicia con la expresión y liberación por parte del endotelio y de los leucocitos de citoquinas y quimiocinas, que facilitan la interacción celular y su activación que suele estar mediada por la acumulación de oxLDL circulantes, en especial, de los macrófagos. En respuesta a esta activación, ambos tipos celulares sintetizan moléculas de adhesión, que provocan el rodamiento, anclaje firme y posterior extravasación del leucocito. Al extravasarse, los macrófagos pueden endocitar las moléculas de oxLDL, convirtiéndose progresivamente en células espumosas que se acumulan en la capa íntima-media de la vasculatura. La acumulación de este tipo celular produce grandes cantidades de moléculas inflamatorias que mantiene la activación de las células endoteliales e inicia la activación de las células musculares y fibroblastos. La inflamación crónica provocará la necrosis de las células espumosas, que crean un núcleo necrótico cuya característica es la producción de moléculas proinflamatorias y proapoptóticas. En este entorno inflamatorio, las células musculares modifican sus propiedades, adquiriendo la capacidad de migrar y calcificarse y, por tanto, estabilizar la lesión aterosclerótica.

Las combinación de las manifestaciones a nivel celular de la T2D pueden derivar, como en el caso de las lesiones ateroscleróticas, en diferentes complicaciones cardiovasculares. Estas complicaciones son responsables de un porcentaje muy representativo de las muertes totales dentro de esta patología, y se pueden prevenir mediante estrategias combinadas de cambios en el estilo de vida y tratamiento farmacológico. Hay diferentes tipos de complicaciones cardiovasculares dependiendo de qué proceso se ve alterado: las complicaciones microvasculares implican a vasos pequeños, capilares principalmente, cuyas células que generalmente no están reguladas por insulina y que, por tanto, están expuestas a las altas concentraciones de glucosa circulante; las complicaciones macrovasculares se relacionan con la

aparición de placa de ateroma, que puede desencadenar diferentes patologías entre las que se incluye el infarto de miocardio.

Las alteraciones macrovasculares tienen su origen en el estado proinflamatorio que, en combinación con la hiperglucemia e hiperlipidemia de la T2D, conllevan una activación crónica de las células endoteliales. La cronificación causa un estado protrombótico que favorece la aparición de placas de ateroma. Las posibles consecuencias de esta patología dependen de su fisiopatología, pudiendo ocasionarse por bloqueo del vaso (eventos isquémicos) o por desestabilización y rotura de la placa, dando lugar a un trombo (eventos trombóticos). Ambas presentaciones pueden originar enfermedad coronaria arterial (infarto, fallo cardíaco, isquemia de miocardio), enfermedad cerebrovascular (ictus) o enfermedad vascular periférica. La prevención temprana y el correcto control de la enfermedad parece ser la mejor aproximación terapéutica para este tipo de complicaciones. En este sentido, marcadores como la medición del grosor de la capa íntima-media de la carótida (CIMT, del inglés, carotid intima media thickness) son de utilidad para monitorizar y prevenir de manera precoz la aparición y el desarrollo de estas complicaciones. En combinación con otros marcadores moleculares pueden ser una buena herramienta para el cribado temprano de pacientes con susceptibilidad a desarrollar complicaciones.

Hipótesis y objetivos:

La T2D es una enfermedad crónica con base inflamatoria y que cursa con hiperglucemia, hiperlipidemia e IR. El exceso de nutrientes y la IR generan un estrés en la mitocondria que conlleva la producción y acumulación de ROS, que causan alteraciones en la señalización de la insulina y modificaciones en los componentes celulares, así como la afectación de la función mitocondrial y los mecanismos de rescate de la misma. Por tanto, es importante investigar el

estatus de las mitocondrias en la T2D para poder comprender mejor el mecanismo de la enfermedad.

Asimismo, los procesos celulares de respuesta a estrés como la UPR o la autofagia se encuentran alterados en la mayor parte de los tejidos y órganos en la T2D. La IR, la hiperglucemia y la hiperlipidemia ejercen un papel fundamental en la regulación de estos procesos, pudiendo activarlos o inhibirlos dependiendo del tipo celular. Nuestra hipótesis se basa en que hay una activación de estos procesos que permitiría el restablecimiento de la homeostasis celular.

Las complicaciones cardiovasculares son uno de los mayores problemas de salud asociados a la T2D. En la base de su desarrollo están las interacciones leucocito-endotelio, que corresponde a las etapas iniciales de la formación de la placa de ateroma y, por tanto, medir diferentes parámetros de esta interacción puede ser un buen indicador del estado del paciente. También hay otras estrategias que miden la aparición de placa aterosclerótica y que además sirven como marcador de riesgo cardiovascular como determinar el CIMT. Por ello, determinar estos dos parámetros y establecer su relación con otras variables que se encuentran alteradas en la T2D puede de ser de interés para establecer el riesgo cardiovascular de estos pacientes.

También nos preguntamos si las estrategias terapéuticas actuales son capaces de atenuar las consecuencias a nivel celular de la T2D. El control glucémico es una herramienta preventiva que se ha asociado a una menor incidencia de complicaciones a largo plazo. En este sentido, se necesitan marcadores fiables que permitan, junto a los niveles de HbA_{1C}, monitorizar y detectar de manera precoz este tipo de alteraciones, como el CIMT. En cuanto al tratamiento farmacológico, la metformina ha sido desde su descubrimiento una de los tratamientos habituales en la farmacoterapia de la T2D. Sin embargo, se necesitan más estudios para

profundizar en sus mecanismos de acción a nivel celular. Por otra parte, el desarrollo de nuevos tratamientos antioxidantes experimentales con diana en la mitocondria como el SS-31, se plantea como uno de las áreas con mayor proyección a nivel farmacológico, aunque muchos de los mecanismos de acción y su efecto exacto aún son desconocidos.

Todas estas alteraciones afectan profundamente al metabolismo y la función de las células del sistema inmunitario que están expuestas durante su ciclo de vida a las situaciones de hiperglucemia, hiperlipidemia e IR comentadas previamente. Estas agresiones alteran su función favoreciendo la producción excesiva de ROS, la respuesta inflamatoria, la activación de rutas de rescate y el aumento de las interacciones con el endotelio. No obstante, todos estos mecanismos han sido poco estudiados en este tipo celular, tan relevante en la fisiopatología de la T2D.

En base a lo expuesto, nos planteamos los siguientes objetivos:

1. Evaluar el estado de la autofagia y su relación con la función mitocondrial y la inflamación en leucocitos de pacientes T2D.

2. Estudiar la presencia de marcadores de riesgo cardiometabólico en pacientes T2D, reflejadas por el nivel de citoquinas circulantes, el grosor de la capa íntima-media de la carótida y las interacciones leucocito-endotelio; y la influencia del control glucémico estricto sobre todos éstos parámetros.

3. Evaluar la influencia del tratamiento con metformina en la dinámica mitocondrial en leucocitos de pacientes T2D.

4. Analizar el efecto del antioxidante con diana mitocondrial SS-31 en el estrés de ER, la autofagia y el estrés oxidativo.

Material y métodos:

Sujetos de estudio:

Para la realización de esta tesis reclutamos pacientes T2D y voluntarios sanos en el Servicio de Endocrinología y Nutrición del Hospital Universitario Dr Peset. Los pacientes firmaron el consentimiento informado que detallaba los procedimientos experimentales, aprobados por el Comité de Ética para la Investigación Clínica del hospital, con códigos 97/16 y 98/19, de acuerdo con los principios de la declaración de Helsinki. El diagnóstico de T2D se realizó de acuerdo a los criterios de la ADA (del inglés, American Diabetes Association). Los criterios de exclusión fueron: presencia de obesidad mórbida, tratamiento con insulina o presencia de enfermedades de origen autoinmune, hematológico, infeccioso, u otras enfermedades inflamatorias o neoplásicas.

Recogida de muestras y análisis antropométrico y bioquímico:

La recogida de muestras la realizó una enfermera especialista que extrajo 30 mL de sangre periférica de la vena braquial en tubos de recogida con el anticoagulante EDTA y un tubo de gelosa del que se aisló el suero. Previamente, se determinó la presión arterial, el peso, la altura y la circunferencia de cintura y cadera. Los parámetros bioquímicos que se analizaron en el Laboratorio Central de Análisis Clínicos fueron la glucosa en ayunas, el % de HbA_{1C}, la insulina, el colesterol total, el colesterol HDL, VLDL y los triglicéridos, las apolipoproteínas y la CRP ultrasensible. Se calcularon posteriormente el IMC, las concentraciones de LDL según la fórmula de Friedewald y el índice HOMA-IR.

Determinación del grosor de capa íntima-media de la carótida.

Un subgrupo de los pacientes se derivó al Servicio de Cardiología para medir el grosor de la capa íntima-media de las arterias carótidas. Lo realizaron especialistas en ecosonografía según las guías de la Asociación Americana de Ecocardiografía. La medida se realizó por triplicado en un segmento de 1 cm de la carótida de los pacientes a lo largo del eje longitudinal con un dispositivo Aloka 5500 (Hitachi, Aloka, Tokyo (Japón)).

Ensayos funcionales:

- *Aislamiento de leucocitos:* Los leucocitos polimorfonucleares (PMNs) y los mononucleares (PBMCs, del inglés peripheral blood mononuclear cells) se aislaron a partir de las muestras de sangre mediante un gradiente de densidades con Ficoll hystopaque 1119 y 10771. Tras una centrifugación, se generó un halo y un sedimento que correspondieron a las poblaciones de PBMCs y PMNs respectivamente. Las células se lavaron sucesivamente hasta obtener una población limpia que se repartió en alícuotas para su posterior uso. Parte de las células se trataron con diferentes estímulos como SS-31, SS-20, rotenona, thapsigargina o rapamicina.

- *Citometría estática:* Se sembraron $3x10^5$ PBMCs/pocillo en placas de 24 pocillos y por duplicado para cada muestra. Tras su adhesión al fondo de la placa, los PBMCs se marcaron con los fluoróforos TMRM, Fluo4, DCFH-DA y el marcador nuclear HOESCHT 33342. Después de incubar 20 minutos y lavar los pocillos con HBSS, se visualizó la fluorescencia con un microscopio Olympus IX81 y el software ScanR. Se calculó la media de 16 imágenes por pocillo y se relativizó frente al control interno.

- *Citometría de flujo:* Una alícuota de sangre entera se marcó con anti-CD45 y DCFH-DA para visualizar los ROS totales de los leucocitos. El protocolo comprende un paso de lisis de eritrocitos y lavados para poder visualizar posteriormente la población de interés. La muestra se analizó en el citómetro Accuri C6 con un láser de 488 nm de emisión y el filtro FL-1 (FITC). Se midió la intensidad de DCFH en la población de los leucocitos, que se aisló por morfología y por marcaje de CD45, frente a un control interno.

- *Ensayo de consumo de O_2:* Se midió el consumo de O_2 en una alícuota de $5x10^5$ PBMCs con un electrodo de O_2 de tipo Clark, y la monitorización del consumo se realizó con el software Duo.18. Se calculó el consumo máximo de O_2 con los substratos endógenos mediante GraphPad.

- *Análisis de la interacción leucocito-endotelio:* En este ensayo se analizó la interacción de $1.2x10^6$ PMNs con una monocapa confluente de células endoteliales de cordón umbilical humano sembrada en una placa petri de 35 mm de diámetro. En el experimento se pasó la disolución de PMNs sobre la monocapa a una velocidad de 0,3 mL/min en una cámara de flujo paralelo Glycotech, grabando 5 minutos de vídeo. En este vídeo se determinaron los siguientes parámetros: número de PMNs que ruedan sobre el endotelio en 1 minuto, velocidad de estos leucocitos y la adhesión de los PMNs en 5 campos aleatorios.

- *Determinación de citoquinas y moléculas de adhesión solubles:* Estos experimentos se realizaron con muestras de sueros de pacientes y sujetos control con un analizador Luminex-200 y kits Milliplex MAP específicos siguiendo las instrucciones del fabricante. Las moléculas que se detectaron fueron TNFα, IL-6, VCAM-1, ICAM-1 y P-selectina.

Análisis de expresión génica y proteica:

La expresión génica se analizó mediante RT-PCR con ARN extraído de muestras de PBMCs congeladas a -80ºC. La extracción se realizó con el GeneAll Ribospin total RNA extraction kit y cuantificado por Nanodrop 2000c. La retrotranscripción se realizó con el RevertAid first Strand c-DNA Synthesis kit, y 2µg se destinaron a analizar la expresión génica con cebadores específicos y el reactivo fluorescente KAPA SYBR FAST master mix. La expresión de cada gen se cuantificó mediante el método comparativo $2^{-\Delta\Delta Ct}$.

En análisis de expresión proteica se llevó a cabo con 25 µg de proteína extraída de los PBMCs mediante un tampón de lisis y su cuantificación mediante el método BCA. La proteína se separó en geles comerciales de porcentaje específico dependiendo de la proteína de interés y se transfirió mediante un método de transferencia húmeda a una membrana de nitrocelulosa. Posteriormente, las proteínas de interés se detectaron mediante bloqueo de las membranas con leche o BSA, incubación durante la noche con anticuerpos primarios específicos y durante 1h con los anticuerpos conjugados a HRP secundarios necesarios en cada caso. La detección se realizó con reactivos quimioluminiscentes con diferente sensibilidad dependiendo de la proteína de interés. En análisis densitométrico de las bandas se realizó con el software Bio1D, relativizándolo con un control interno.

Los genes y proteínas que se analizaron eran específicos de cada ruta analizada, como la UPR (GRP78, PERK, ATF6, CHOP), autofagia (Beclina-1, LC3, SQSTM/p62), fusión y fisión mitocondrial (MFN1, MFN2, OPA1, DRP1 y FIS1) e inflamación (NFκB).

Análisis estadístico:

Se analizó la distribución de la población para establecer el tipo de análisis estadístico más adecuado para comparar los resultados entre sujetos sanos y pacientes diabéticos con o sin tratamiento de metformina. En el caso de poblaciones con distribución normal, las comparaciones de dos grupos se realizaron con test T y entre 3 grupos se comparó mediante ANOVA con post-test de Bonferroni, Tukey o Newman-Keuls. En poblaciones con distribución no normal se compararon dos poblaciones con test de Mann-Whitney y tres con test de Kruskal-Wallis. En aquellos casos en los que la edad y el IMC diferían significativamente entre las poblaciones de estudio, se incluyeron como covariables y se ajustó mediante análisis de la covarianza las variables de estudio.

Las correlaciones se calcularon mediante coeficientes de Pearson o Spearman dependiendo del tamaño de la muestra analizada. Toda la estadística se calculó en el programa SPSS 17.0 y los gráficos se realizaron con GraphPad Prism 6.0. Las diferencias se consideraron significativas cuando $p<0.05$ en todos los casos, con un intervalo de confianza del 95%.

Resultados y discusión:

Las primeras diferencias entre las poblaciones de estudio se obtuvieron en los parámetros antropométricos, observándose que en los T2D hay un aumento de IMC y circunferencia de cintura. Los parámetros bioquímicos de metabolismo de la glucosa también reflejaron diferencias notables en los niveles de glucosa en ayunas, insulina, en el índice HOMA-IR, y en la HbA_{1C}, que lógicamente aumentaron en los pacientes diabéticos. En el estudio en el cual dividimos la población T2D en función de sus niveles de HbA_{1C}, con un umbral de 6,5%, los pacientes con peor control glucémico presentaban un peor perfil metabólico general, demostrando la importancia de esta aproximación terapéutica en la T2D. En cuanto a los

parámetros de metabolismo lipídico, observamos que en pacientes T2D hay una bajada en el colesterol HDL y un aumento de los triglicéridos y el colesterol VLDL. Sorprendentemente, el colesterol total y el LDL no aumentan y en la mayor parte de los casos disminuyen, posiblemente por el tratamiento con estatinas de gran parte de la cohorte. Las alteraciones mencionadas confirman que en los pacientes T2D existe una alteración metabólica con un aumento de la glucosa y de los lípidos, característica de ésta enfermedad.

La presencia de IR se confirmó mediante el aumento del índice HOMA-IR en todas las cohortes, que se encuentran en el rango considerado clínicamente como IR. Observamos además que los pacientes con peor control glucémico presentan un aumento de la IR comparado con los pacientes con una HbA_{1C} inferior a 6,5%. La relación entre la IR y el control glucémico se explica por el exceso de glucosa, que produce un aumento de AGE, como la HbA_{1c}, y en paralelo generan IR. De hecho, existe evidencia experimental que apoya la relación bidireccional entre estas alteraciones metabólicas.

Posteriormente, realizamos los experimentos con leucocitos humanos para poder esclarecer cómo afecta la patología a este tipo celular. Elegimos este tipo celular por diferentes motivos: la facilidad de su obtención y aislamiento, su representatividad de estado general del paciente y su exposición a las alteraciones metabólicas. Además, en una enfermedad con base inflamatoria, es relevante estudiar el tipo celular más implicado en las respuestas inflamatorias. Estudios previos han determinado que en los pacientes diabéticos hay una mayor activación de éstas células, que muestran alteraciones a nivel mitocondrial y activación de rutas proinflamatorias y apoptóticas. Además, son células muy sensibles a estrés oxidativo, y en el ambiente molecular de la T2D muestran afectación en la respuesta antioxidante y en las correspondientes rutas de rescate.

Los leucocitos generan y modulan la respuesta inmunitaria del organismo que, como se ha explicado anteriormente, en la T2D está activada. Esto se refleja por un aumento circulante de mediadores proinflamatorios entre los que se incluyen TNFα, hsCRP e IL-6, como hemos observado en la presente tesis. Dicho aumento se ha propuesto en diferentes investigaciones como marcador temprano de desarrollo de T2D. Además, el TNFα y la IL-6 son moléculas que predisponen a un estado de IR mediante inhibición de la señalización a través del receptor de insulina. Dichas citoquinas también afectan a los niveles de HbA_{1C}, ya que en situaciones de riesgo metabólico hay un aumento en sus niveles. En este sentido, hemos podido confirmar esta relación, observando aumentos significativos en el grupo de T2D con una mayor HbA_{1C}.

También hemos observado un aumento en las moléculas de adhesión ICAM-1 y VCAM-1 en los pacientes T2D, relacionadas tanto con inflamación generalizada como con un estado de activación endotelial y riesgo cardiometabólico. Además, hemos constatado un aumento en ambas citoquinas en el grupo T2D con un peor control glucémico, confirmando que estas moléculas de adhesión aumentan en estados de riesgo metabólico. Además, este aumento indica que hay cierto nivel de activación endotelial, que puede favorecer la infiltración leucocitaria y predispone al desarrollo de lesiones ateroscleróticas. Por todo ello, se han propuesto como marcadores de riesgo de desarrollo de aterosclerosis junto con otras moléculas, como adipoquinas o moléculas de inflamación.

Un aumento de la expresión de moléculas proinflamatorias y de adhesión refleja una activación endotelial y, posiblemente, un aumento en las interacciones entre los leucocitos y el endotelio. Todas estas modificaciones, se originan como consecuencia de las alteraciones metabólicas típicas en T2D entre las que se incluye la hiperglucemia y la hiperlipidemia. En este sentido, hemos observado que los leucocitos de T2D interaccionan más con el endotelio que los

de los sujetos sanos, y que estas interacciones son también mayores en el grupo de T2D con un peor control glucémico. Resultados similares se han obtenido en modelos *in vitro* e *in vivo* que también se asocian a un peor estado metabólico causado por la T2D y al incremento de las interacciones y por lo tanto a una peor función vascular, apoyando de esta manera nuestros resultados. La explicación a nivel molecular de estos resultados se basa en que la hiperglucemia y la hiperlipidemia pueden causar activación del endotelio a través de PKC y de la bajada de producción de NO, entre otras vías celulares.

Otra manera de evaluar el riesgo cardiovascular en T2D, además de analizar las moléculas proinflamatorias y las interacciones leucocito-endotelio, es determinar el CIMT. Esta determinación es útil como marcador temprano de lesión aterosclerótica, ya que es poco invasiva para el paciente, rápida y relativamente sencilla. Además, se ha demostrado que tiene valor pronóstico de futuras lesiones ateroscleróticas, lo que constituye el inicio de las complicaciones macrovasculares. En el análisis que hemos realizado, observamos que los pacientes T2D mostraron un mayor CIMT, especialmente en la carótida izquierda. En el caso de los pacientes T2D con una glucemia peor controlada, el aumento solamente se mantuvo en la carótida izquierda. Al correlacionar los datos de CIMT con el perfil metabólico y antropométrico de los sujetos reclutados, observamos que había una correlación positiva con el IMC, los parámetros de metabolismo lipídico (excepto para el HDL, en el cual la correlación fue negativa) y glucémico. Curiosamente, en todos los casos, los datos mostraron más significatividad para las medidas de la carótida izquierda que para las de la derecha. Los datos obtenidos apoyan las observaciones previas acerca de la relación de la medida de CIMT con el estado de alteración metabólica. Precisamente, el aumento de CIMT izquierdo en pacientes diabéticos mal controlados refuerza la utilización de esta determinación como marcador temprano de futuras complicaciones macrovasculares.

Parte del origen de la activación endotelial y de las alteraciones celulares de la T2D se encuentra en el exceso de ROS. Se producen en muchos casos por el estrés metabólico y mitocondrial asociado a la hiperlipidemia, la hiperglucemia y la IR. Por ello, analizamos la producción de ROS en los leucocitos de los pacientes T2D y de sujetos sanos. Hemos observado que los leucocitos de pacientes T2D mostraron mayores niveles de ROS, tanto totales como mitocondriales, que los observados en leucocitos de sujetos sanos. Además, los pacientes T2D con un peor control glucémico mostraron mayores niveles de ROS que los bien controlados. El aumento de ROS no solamente altera el balance oxidativo de la célula sino que además activa vías de señalización proinflamatorias y/o apoptóticas que perjudican a la función celular. Dicha afectación se ha confirmado en otras enfermedades cardiovasculares, donde el exceso de ROS perjudica al funcionamiento de las células endoteliales, los cardiomiocitos y a otros tipos celulares involucrados. En cuanto a la relación con el aumento de la HbA_{1C}, es una consecuencia directa del estrés oxidativo y el exceso de glucosa, tal y como se ha explicado anteriormente. Diferentes estudios han profundizado sobre este tema, encontrando que el aumento en la HbA_{1C} se relaciona no solamente con un aumento de ROS sino también con una bajada de las defensas antioxidantes de la célula.

Tal y como hemos observado, hay un aumento de producción de ROS mitocondriales que nos indica que existe disfunción mitocondrial en las cohortes de T2D analizadas. Para medir esta disfunción, analizamos algunos marcadores de función mitocondrial como el consumo de O_2 mitocondrial, el potencial de membrana y el contenido en Ca^{2+}. Observamos que en pacientes T2D hay un menor potencial de membrana, un menor consumo de O_2 y mayores niveles de Ca^{2+} citosólico. Todo ello apunta a una disfunción mitocondrial, que se manifiesta principalmente por un desacoplamiento de la cadena de transporte electrónico y el consiguiente descenso en los niveles de ATP. Estas observaciones se han confirmado con resultados de estudios previos que

demuestran que en modelos celulares y animales de T2D o de IR existe una disfunción mitocondrial. En este sentido, algunos estudios han observado una menor función de los complejos mitocondriales y menor síntesis de ATP, mientras que otros han descrito la ausencia de metabolitos clave en las rutas metabólicas que dependen de la mitocondria como el ciclo de Krebs o la β-oxidación. En conjunto, podemos concluir que en leucocitos de T2D existe una marcada disfunción mitocondrial.

La célula tiene diferentes mecanismos para poder modular el daño mitocondrial, siendo una de ellas la regulación de la dinámica mitocondrial. Mediante este proceso la célula puede adaptar la función mitocondrial a las necesidades celulares y minimizar las consecuencias de la disfunción mitocondrial. Por ello, en esta tesis analizamos el estado de las moléculas implicadas en los procesos dinámicos de fusión y fisión mitocondrial. La expresión de MFN1, MFN2 y OPA1 disminuye en los leucocitos de los pacientes diabéticos, tanto a nivel proteico como génico, lo que sugiere que hay un defecto en la fusión que podría estar involucrado en los mecanismos de reparación de las mitocondrias dañadas. Además, la expresión de las proteínas de fisión DRP1 y FIS1 es mayor en los pacientes T2D comparado con los controles sanos. Estudios previos de este proceso en modelos experimentales de enfermedad metabólica y T2D han observado un aumento de la fisión que se produce en respuesta al daño celular, aunque otros explican que la falta de fisión es la que genera el daño en las mitocondrias. A pesar de esta falta de consenso, nuestros resultados apoyan la idea de que hay un aumento de disfunción mitocondrial que perjudica el funcionamiento de la célula y que se ve agravado por el exceso de fisión. Estas alteraciones en la dinámica mitocondrial pueden provocar un deterioro en la capacidad de síntesis de ATP y de las rutas metabólicas vitales para la homeostasis celular.

Como se ha comentado anteriormente, los ROS se acumulan en las células afectadas por la inflamación generalizada que está asociada a la T2D. Los ROS son moléculas muy reactivas, pudiendo modificar proteínas, lípidos y otras moléculas complejas, afectando finalmente su función. La acumulación de ROS genera un estrés en la principal maquinaria de síntesis y plegado de proteínas, el ER, activando las vías de rescate frente a proteínas mal plegadas o UPR. Al analizar las proteínas implicadas en dicha respuesta, hemos observado que en los leucocitos de pacientes con T2D hay un aumento de la expresión de las proteínas implicadas en la ruta PERK con respecto a los de sujetos sanos. Otros estudios han observado una activación de las vías de UPR en células β pancreáticas para preservar la función celular en T2D, aunque también se ha confirmado que su inhibición perjudica la función de éstas células.

Otro mecanismo central de rescate celular es la autofagia, cuya activación y respuesta al estrés celular se ha visto alterada en la T2D. En nuestra población, observamos que en los leucocitos de T2D hay una activación de la autofagia reflejada por el aumento de expresión de las moléculas Beclina-1 y LC3, y una disminución de SQSTM/p62. En conjunto, estos resultados sugieren una activación de la autofagia en leucocitos de pacientes con T2D. De manera similar a lo que ocurre con la activación de la UPR, en los estudios previos no se ha observado un comportamiento uniforme de la autofagia en la T2D. Numerosos estudios han observado en diferentes tejidos y tipos celulares una inhibición de la autofagia que deteriora los mecanismos de protección ante el estrés celular. En cambio, otros estudios también en modelos experimentales de T2D han observado una activación de la misma vía de rescate. En este sentido, se ha propuesto que los ROS activan la autofagia a través de AMPK en células β pancreáticas, aunque se ha observado que la activación crónica de la autofagia en tejido cardíaco activa procesos proapoptóticos. Por lo tanto, existen ideas contradictorias en cuanto a

la activación o no de la autofagia puesto que parece depender del tipo de tejido, grado de activación y patología asociada.

Además de analizar la autofagia, hemos analizado su relación con la interacción leucocito endotelio. De hecho, hemos observado que aumentos en los niveles de Beclina-1 correlacionaron positivamente con las interacciones de los leucocitos con el endotelio en pacientes diabéticos; en cambio, en los sanos, la correlación fue negativa. Estos resultados reflejan que el comportamiento de la autofagia puede ser diferencial dependiendo de la situación metabólica del individuo; además, apuntan a una relación directa entre la autofagia y la inflamación. En este sentido, diferentes estudios han observado una relación directa de la Beclina-1 con el factor de transcripción NFκB y, por tanto, con la inducción de la inflamación.

Por último, quisimos explorar el efecto a nivel celular de diferentes tratamientos, en concreto la metformina y el péptido antioxidante con diana mitocondrial SS-31. Hemos observado que los leucocitos de pacientes T2D tratados con 1700mg/día de metformina durante al menos un año tienen una mejor función mitocondrial, reduciendo los niveles de ROS y aumentando la respiración mitocondrial y el potencial de membrana. El tratamiento con metformina también mejora el equilibrio entre fusión y fisión mitocondrial, aumentando las proteínas involucradas en la fusión y reduciendo las implicadas en la fisión, mostrando por tanto un efecto beneficioso de la metformina sobre los mecanismos homeostáticos de la mitocondria. Diferentes estudios han propuesto que la metformina puede actuar a través de AMPK y/o de la inhibición del complejo I de la cadena de transporte electrónico mitocondrial. También se ha observado que es posible que la regulación de los ciclos de fusión-fisión sea a través de las proteínas AMPK o AKT. Por tanto, poder determinar el mecanismo por el cual actúa la

metformina para ejercer estos beneficios será útil para poder ampliar los efectos terapéuticos de dicho fármaco.

En cuanto al tratamiento experimental con el antioxidante SS-31, pudimos constatar que al tratar los leucocitos de pacientes T2D con este antioxidante, se redujo la producción de ROS mitocondrial y la liberación de Ca^{2+}. Este efecto fue equiparable al tratamiento de los mismos leucocitos con catalasa, indicando que el SS-31 ejerce un potente efecto antioxidante. Cuando examinamos las rutas activadas por estrés celular, observamos que el SS-31 reduce la UPR, especialmente sobre la vía iniciada por PERK. El tratamiento también redujo efectivamente la activación de la autofagia. En conjunto, los datos apoyan que la actividad antioxidante del péptido SS-31 ejerce un papel homeostático en los leucocitos de pacientes T2D mientras que el péptido sin el residuo dimetiltirosina con actividad antioxidante (SS-20) no tuvo efecto. En este sentido, existen estudios que confirman el efecto beneficioso del SS-31, e incluso hay ensayos clínicos para su uso terapéutico en complicaciones microvasculares como retinopatía o en enfermedad renal, donde ya se han constatado efectos beneficiosos. Por lo tanto, en la presente tesis, hemos mostrado diferentes tratamientos que pueden mejorar la función mitocondrial y la activación de vías y mecanismos de rescate celular en la T2D, aportándose de esta manera nuevas vías de intervención terapéutica.

Conclusiones:

1. Los leucocitos de pacientes T2D presentan un aumento de los ROS totales y mitocondriales, de los marcadores celulares de autofagia y de los marcadores séricos y celulares de inflamación comparando con leucocitos de sujetos sanos. Esto se refleja en un aumento de las interacciones leucocito-endotelio que se correlaciona con los niveles de Beclina-1.

2. Los pacientes diabéticos con HbA_{1C}>6.5% presentan niveles elevados de citoquinas proinflamatorias y moléculas de adhesión solubles. Además, sus leucocitos producen más ROS mitocondriales e interactúan más con el endotelio comparando con los de pacientes con una HbA_{1C} ≤6.5%. Las medidas de CIMT también son mayores en los pacientes peor controlados, y se correlacionan con el aumento de interacciones leucocito-endotelio y un peor perfil metabólico, en especial para las medidas de carótida izquierda. Por tanto, un correcto control glucémico puede ser una estrategia de prevención de las complicaciones cardiovasculares en la T2D.

3. Los leucocitos de pacientes diabéticos muestran un defecto en la función y la dinámica mitocondrial, que se observa mediante un aumento en la producción de ROS, menor potencial de membrana, menor consumo de O_2 y una tendencia a la fisión mitocondrial. Estos leucocitos interactúan más con el endotelio comparando con los leucocitos de sujetos sanos. La terapia con metformina es beneficiosa a nivel mitocondrial, mejorando su función y su dinámica que se refleja en una menor interacción con el endotelio que en los pacientes diabéticos no tratados.

4. El péptido antioxidante con diana mitocondrial SS-31 reduce la producción de ROS mitocondrial y mejora el potencial de membrana y la distribución de calcio en los leucocitos de pacientes T2D. Estos beneficios implican un mejor control sobre los mecanismos de homeostasis celular a través de la reducción del estrés de ER y los marcadores de autofagia. Además, el tratamiento con SS-31 de los leucocitos de pacientes T2D reduce sus interacciones con el endotelio.

1. INTRODUCTION

1.1. Type 2 diabetes:

Type 2 diabetes (T2D) is a chronic non-communicable disease originating in defects in glucose metabolism. It is defined as “non-insulin dependent diabetes or “adult-onset diabetes”, and it accounts for 90-95% of all diabetic patients. It encompasses individuals with relative insulin deficiency and those with peripheral insulin resistance (IR) [1]. T2D requires continuous monitoring and medical care, given that it varies considerably between patients depending on age, lifestyle and the presence or absence of risk factors. Moreover, T2D needs to be tightly controlled in order to prevent possible macro and microvascular complications [2]. Keeping a healthy lifestyle, having a wholesome diet and doing daily physical exercise helps to control the disease. However, antidiabetic drugs must be prescribed for the correct management of glucose blood levels. Different treatments are available for T2D, which might combinate or not with insulin treatment depending on the therapeutic needs of the patient [3,4].

1.1.1. Definition and diagnosis

Diabetes englobes a group of diseases characterised by an alteration of the physiological response to glucose. There are different known types of diabetes[1]:

- Type 1 diabetes: Due to autoimmune pancreatic β-cell destruction.
- Type 2 diabetes: Progressive loss of adequate pancreatic β-cell function associated to IR.
- Gestational diabetes: It develops during pregnancy in the pregnant mother and usually disappears after giving birth. It can occur at any stage of pregnancy, but is more common in the second or third trimester.
- Specific types: Neonatal diabetes, Maturity Onset Diabetes of the Young (MODY), drug-induced diabetes.

T2D is characterised by hyperglycaemia and hyperlipidaemia, and usually also hyperinsulinemia in the early stages [5]. Diagnosis of T2D is based on the measurement of several analytical parameters: fasting plasma glucose (FPG) values, 2h plasma glucose (PG) in an oral glucose tolerance test (OGTT) and glycated haemoglobin concentrations. The criteria for diagnosing T2D is FPG≥126 mg/dL or 2h PG≥200 mg/dL during OGTT, or glycated hemoglobin≥6.5% or - in patients with symptoms of hyperglycaemia - a random plasma glucose ≥ 200 mg/dL [1].

T2D is usually preceded by a prediabetic stage, characterised by a certain grade of IR, but in the absence of severe glucose intolerance, with high levels of glucose that do not meet the diagnostic threshold. These patients exhibit either impaired fasting glycaemia (FPG levels between 100 and 125 mg/dL), impaired glucose tolerance (2-h PG from 140 to 199 mg/dL) and/or glycated haemoglobin between 5.7 and 6.4% [1]. These parameters should also be monitored in individuals with known risk factors for developing T2D (obesity, first-grade relatives with diabetes, history of cardiovascular disease (CVD), hypertension, hypertriglyceridaemia, polycystic ovary syndrome, AIDS, women with history of gestational diabetes, or age over 45 years old) [6]. Once prediabetes is detected, tests should be repeated every year.

1.1.2. Epidemiology and clinical impact

The global increase in a sedentary lifestyle, energy-dense diets and the obesity that occurs as a consequence of both is leading to a huge rise in the number of cases of T2D diagnosed. In 2019, 463 million people were diagnosed with diabetes, of whom 90% had T2D [5]. Epidemiological studies predict that, by 2045, the number will reach 700 million [7,8]. The distribution of diabetes diagnoses is uneven across the globe. In 2019, the Western Pacific Region presented the highest incidence, with 163 million cases. The region with lowest incidence

was Africa, with 18 million people. However, a better indicator of the severity of the situation is the increment predicted by 2045. While in Europe the predicted rise is 15%, with a baseline of 59 million people, in Africa the rise is expected to be 143%, and 96% in Middle East and North Africa [8]. The rise in developing countries is related to their economic growth, which implies access to processed foods and a reduced need for physical exercise. This increase in T2D is expected to rise from 9.5% in 2019 to 11.8% in 2045. If we examine the data for the countries with higher age-matched prevalence, the top 5 countries are the Marshall Islands (30.5%), Kiribati (22.5%), Sudan (22.1%), Tuvalu (22.1%) and Mauritius (22.0%). This ranking is expected to be maintained, with slight variations, until 2045. All the abovementioned countries are undergoing a process of fast economic development. In relation to economic growth, the incidence of T2D is higher in urban areas (10.8%) than in rural ones (7.2%) [8,9]. Again, globalisation and the tendency to live in urban areas favour a sedentary and a hypercaloric lifestyle, which is a perfect breeding ground for developing T2D.

If we consider gender, more men suffer from T2D than women (9.6% vs 9% respectively), and the increase until 2045 is expected to be slightly higher in women (1.8%) than in men (1.5%) [8,10,11].

Another astonishing figure is the number of undiagnosed cases of T2D worldwide: in Europe, it is estimated that 40.7% of all diabetic patients are not diagnosed. However, a much higher prevalence is estimated for regions such as Africa, South and East Asia or the Western Pacific (59.7%, 56.7% and 55.8% respectively), which highlights the need for early detection and primary medical assistance in those regions [8,12–15].

If T2D is not well controlled and monitored, it can lead to other health problems that compromise the life of the patient [16–18]. Indeed, diabetes-related mortality comprises 11.3% of all-cause-deaths worldwide. Specifically, diabetes-related events cause a high proportion of early

age deaths, understood as deaths before 60 years old [8]. Europe has the lowest early-age death proportion (31.4%), while the highest incidence is found in Africa (73.1%), followed by the Middle East and North Africa (53.3%) [8,17].

T2D is an "expensive" disease for both the public health service and patients [9,19,20]. The direct cost (not distinguishing between public or private) is estimated at about 232 billion USD in 2007, 727 billion USD in 2017, and 760 billion USD in 2019, and is expected to grow steadily, reaching the figure of around 845 billion USD in 2045 [8].

1.1.3. Physiopathology

1.1.3.1. Systemic glucose metabolism

Glucose is one of the main energy sources of the organism. The source of glucose is food intake, during which more complex molecules are digested, resulting in the release of simple carbohydrates. Glucose metabolism, in short, comprises 4 main processes. Glucose catabolism occurs during glycolysis, which generates energy in the form of Adenosine Triphosphate (ATP), Nicotinamide Adenine Dinucleotide (NADH) and pyruvate. If coupled with the Krebs cycle and the respiratory chain, it generates more NADH and ATP. Another catabolic process is glycogenolysis, meaning the breakdown of the glycogen reservoir. It is carried out by glycogen phosphorylase, which releases glucose-1-phosphate, which is in turn isomerized into glucose-6-phosphate [21]. The two main anabolic pathways are gluconeogenesis and glycogenesis. The former refers to the synthesis of glucose as it parts from glycerol, free fatty acids (FFA), aminoacids, pyruvate, or Acetyl-CoA intermediates. This pathway is similar to the inverse glycolysis pathway, and is highly endergonic. Glycogenesis consists of the formation of glycogen stores by glucose-6-phosphate, which is isomerised by phosphoglucomutase to glucose-1-phosphate. It is then metabolised to uridine diphosphate glucose (UDP-glucose) by UDP-glucose-pyrophosphorilase, and in this form is added to short glucose chains and to the main glycogen

molecule by glycogenin and glycogen synthase, respectively. The regulation of these pathways is vital for maintaining steady levels of circulating blood glucose [21].

Normoglycaemia is maintained at a concentration between 4 and 6 mM (70-100 mg/dL) through an interplay between insulin and glucagon action and secretion [22], which regulates the glucose and lipid metabolism pathways. Insulin is produced by pancreatic β cells responding to the physiological demands of the whole organism. It is secreted after meals in response to nutrient availability, enabling the organs to metabolise nutrients. The main effects of insulin secretion are anabolic, such as stimulating lipogenesis and glycogen synthesis, and incorporating aminoacids into the cells. Insulin secretion ceases after meals, giving way to glucagon secretion. Glucagon is synthesized in pancreatic α cells, and has catabolic functions, such as activation of glycogenolysis and gluconeogenesis [22].

Insulin acts on cells that present the insulin receptor, which can autophosphorylate on tyrosine residues once dimerized (Figure 1). This modification is a docking place for the insulin receptor substrate (IRS) that is also phosphorylated on tyrosines. Afterwards, phosphoinositol 3 kinase (PI3K) is recruited by phosphotyrosines on the IRS and activates its lipid kinase activity, rendering phosphatidilinositol-3, 4, 5-triphosphate (PIP_3) at the cellular membrane. Local increases of PIP_3 lead to recruitment of the phosphoinositide–dependent kinase (PDK), which, once bound to PIP_3, phosphorylates protein kinase B (AKT) in the Thr308. This last kinase amplifies the effects of insulin signalling by inhibiting forkhead family box O (FOXO) and activating glycogen synthase kinase 3 β (GSK3β) and rabGAP TBC1 domain family member 4 (TBC1D4), which activates glucose uptake and the tuberous sclerosis complex 2 (TSC2), which in turn activates the mammal target of rapamycin complex (mTORC) [23,24]. All these modifications lead to a complex and coordinated change in the main energy metabolism pathways that contributes to an anabolic situation. Globally, insulin signalling causes an increase in glucose

uptake, lipid synthesis, protein synthesis, and glycogen synthesis. Insulin signalling can also be inhibited in the first steps of the pathway. Specifically, inhibitory phosphorylations of the IR are carried out by protein kinase C (PKC), suppressor of cytokine signalling protein (SOCS) and protein tyrosine phosphatase 1B (PTP1B), which induce IR internalization. Inhibitor of nuclear factor kappa B subunit beta (IKKβ), janus kinase (JNK) or mTOR can inhibit IRS signalling at the PI3K level, establishing a negative autofeedback mechanism; and phosphate and tensin homolog (PTEN) or SH2-containing Inositol Phosphatase 2 (SHIP2) lipid phosphatases turn PIP_3 into other lipid species [23,24]. Coordination among all these signalling pathways modulates the effect of insulin on the target tissue [24].

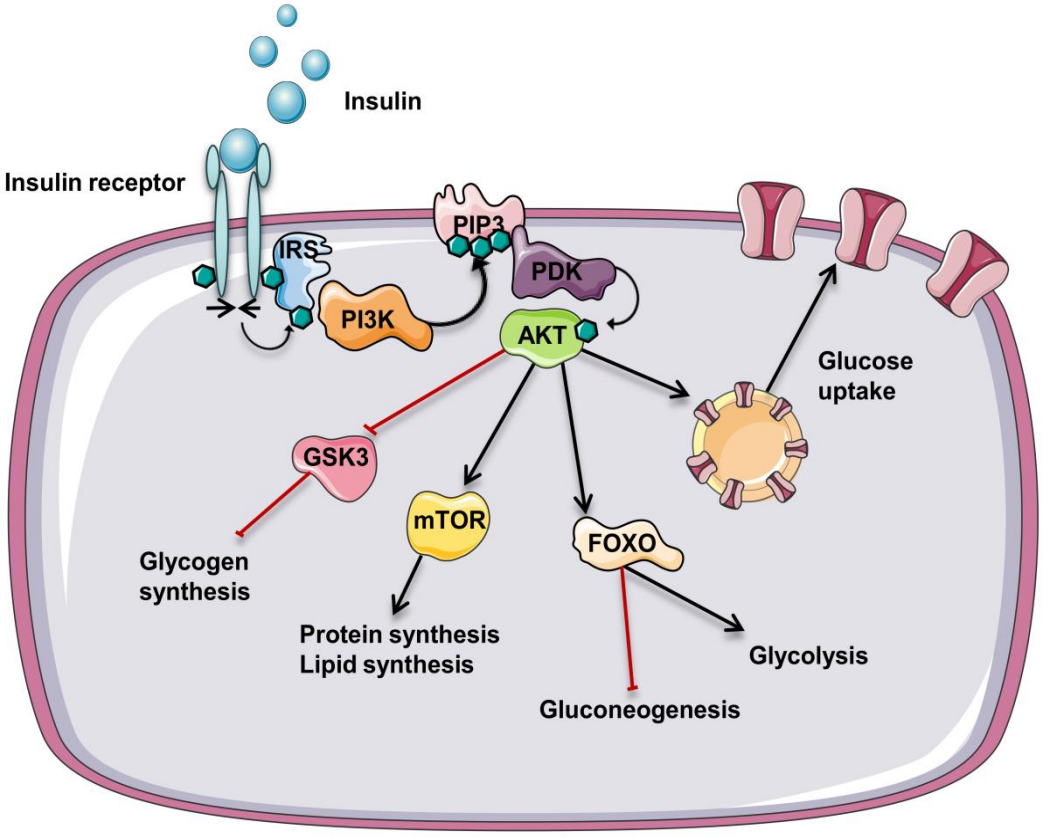

Figure 1: Insulin signalling pathway. Once insulin is bound to insulin receptors, they dimerize and autophosphorylate, recruiting IRS. Insulin receptor phosphorylation of IRS creates a docking domain for PI3K. The PI3K enzyme creates PIP3 rafts in the membrane that enable the binding of PDK. Next, PDK phosphorylates the mediator AKT and amplifies the signalling towards the anabolic use of glucose. IRS=Insulin receptor substrate; PI3K= Phosphoinositol 3 kinase; PIP3= Phosphoinositol 3 phosphate; PDK= Phosphoinositide-dependent kinase D; AKT= a serine/threonine protein kinase; GSK3= glycogen synthase kinase 3; mTOR= mammalian target of rapamycin; FOXO= forkhead box protein 01

Differently to insulin signalling, other manner of modulating glucose concentrations is the central regulation of food intake [25]. A tight coordination between central nervous system signs, peripheral signs from energy stores, or related to hunger and satiety organs gives feedback to the hypothalamus, which eventually regulates appetite, physical activity and body weight. Two of these hormones are the incretins glucagon-like protein 1 (GLP-1) and glucagon inhibitory protein (GIP). They are synthesized by enteroendocrine cells (K-cells and L-cells) when they sense glucose, fructose, aminoacids or FFA. Incretins act on the pancreatic β cells binding to G protein coupled receptors (GPCR), GLP1 receptors (GLP1R) and GIP receptors (GIPR),

stimulating insulin release through adenylate cyclase [26].

The orchestration of these and other hormones, together with the central nervous system (CNS), allows the temporal release of insulin from food intake for storing glucose and building up cellular components, and glucagon when there is need for cellular glucose release for maintaining normoglycaemia.

1.1.3.2. Cellular glucose homeostasis

The main cell types that control glucose homeostasis are pancreatic cells, hepatocytes, myocytes and adipocytes. Pancreatic cells are divided into several cell types depending on their structure and function. The most relevant for glucose regulation are pancreatic α cells and pancreatic β cells. Pancreatic α cells synthesize and release glucagon, while β cells perform the same functions with respect to insulin.

Pancreatic β cells depend on glucose concentration and other hormonal stimuli for the synthesis and release of pre-formed insulin granules. When pancreatic β cells uptake glucose by the low affinity glucose transporter 2 (GLUT-2) receptor, it is released into the cytosol and phosphorylated by glucokinase. Glucose-6-P is then metabolised through glycolysis to form Acetyl-coA and pyruvate, which enter the mitochondria to form ATP. ADP/ATP levels are sensed by sulphonylurea receptor 1 (SUR1), which closes the adjacent potassium channels. This alters the membrane potential, opening the calcium channels and triggering the release of insulin granules (Figure 2). Once glucose ceases to enter, there is a return to the accumulation of insulin granules in the cytoplasm [22,27].

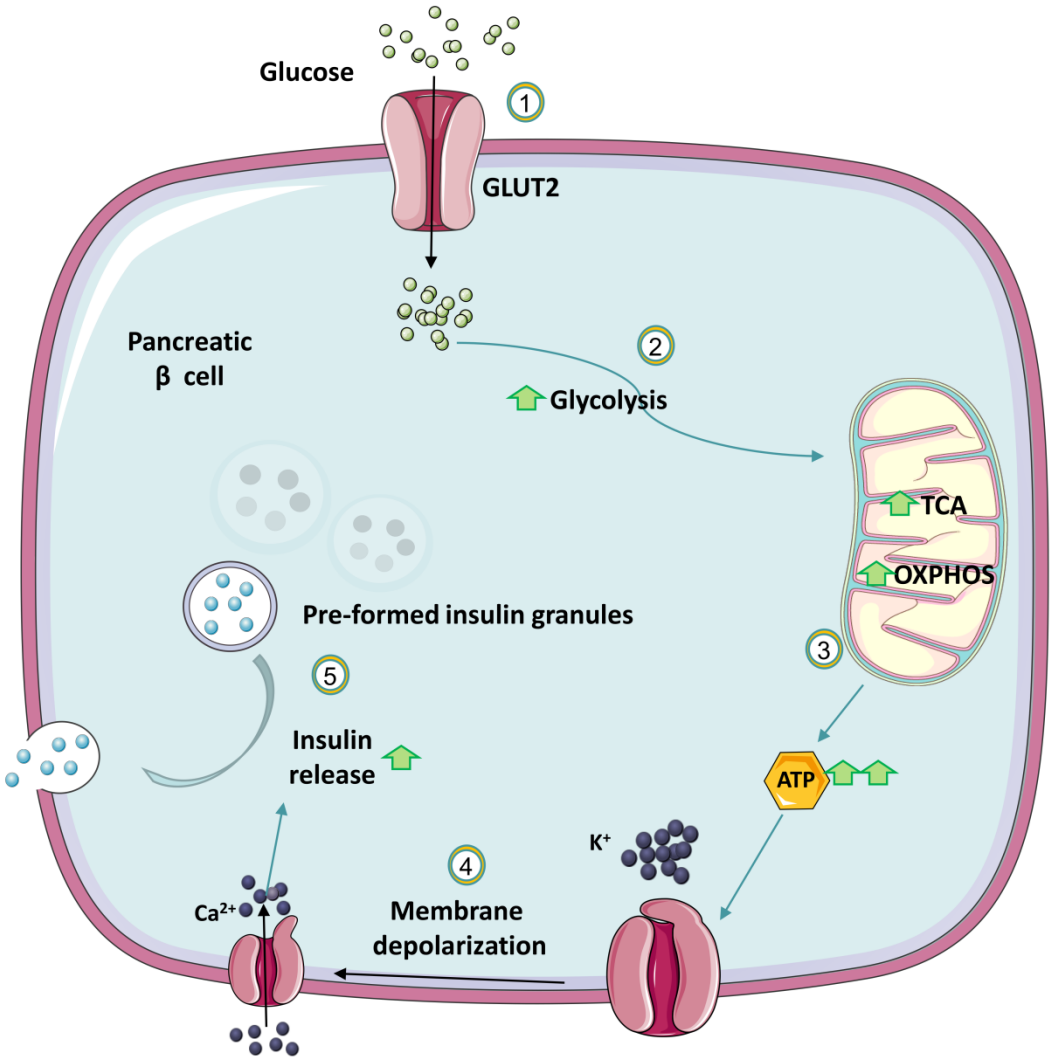

Figure 2: Mechanism of insulin release in pancreatic β cells. Glucose entrance through GLUT2 channels increases intracellular ATP concentrations. ATP-sensitive K^+ channels close in response to this increase, depolarizing the cell membrane. The loss of polarization acts as a trigger for the opening of Ca^{2+} channels and the subsequent increase of cytosolic Ca^{2+} that triggers the release of the preformed insulin granules. GLUT2= glucose transporter 2; TCA= tricarboxilic acid cycle; OXPHOS= oxidative phosphorylation; ATP= adenosine triphosphate.

Hepatocytes are key cell types in the regulation of the release (through glycogenolysis and gluconeogenesis) or the storage (glycogenesis) of glucose in the organism. The main glucose transporter in this cell type is GLUT2. Glucose enters the cell through this transporter and is immediately phosphorylated by glucokinase, resulting in glucose-6-P, which, depending on the systemic needs, will enter the anabolic or catabolic pathways depending on the presence of

insulin or glucagon, respectively [21] [21,28,29].

Myocytes are very specialized and differentiated cells that contain glycogen storages. The glucose channels in myocytes are glucose transporters 1 (GLUT-1) and glucose transporter 4 (GLUT-4), which uptake 80% of the circulating glucose under insulin stimulation [30]. For translocating GLUT4 to the membrane, circulating insulin binds to IR 1 and 2 releasing the insulin receptor substrate (IRS-1) that activates Akt. Akt also activates glycogen synthesis through inhibition of glycogen synthase kinase, an inhibitor of glycogen synthase [31,32].

Adipocytes are the main component of adipose tissue. Their main function is lipid storage and the synthesis of triacylglycerol (TAG) from glycerine and FFA. Adipose tissue only accounts for 10-15% of all the circulating glucose after a meal, despite it sharing GLUT-1 and GLUT-4 channels with myocytes [33]. Glucose in adipocytes is destined for the synthesis of TAGs, which are stored in lipid droplets. When there is no insulin signalling, the stored TAGs are broken down into FFA and released into the bloodstream. Under the action of insulin, Akt activates phosphodiesterase, which inhibits Protein Kinase A (PKA), thus promoting esterification of FFA for its storage [34].

In leukocytes, the main receptors are GLUT1 and Sodium-Glucose Linked transporters (SGLTs). GLUT1 is an insulin-independent glucose channel, which is overexpressed under T-cell activation and induces glucose-dependent ATP synthesis [35,36]. Given its low Km, glucose uptake will depend on circulating concentrations. Hence, it is predictable that under hyperglycaemia, glucose metabolism will be enhanced in this cell type.

1.1.3.3. Insulin resistance and β cell dysfunction

The basis of T2D is hyperglycaemia and hyperinsulinemia; however, which is the origin and which is the primary cause is still under research. Hyperglycaemia is the excess of circulating

glucose, and originates an imbalance between glucose incorporation through food intake and its cellular internalization and usage. The first tissue to sense this abnormality is muscular tissue. Myocytes become insulin-resistant thanks to lipid infiltrates, which increase diacylglycerol (DAG) and PKC, inhibiting IRS activation [37–39]. As a consequence, glycogen synthesis is inhibited and the remnant glucose is redirected to the liver, where glycogen synthesis and *de novo* lipid synthesis takes place. The resulting rise in circulating very low density lipoproteins (VLDL-c) and intrahepatic lipid concentrations increases hepatocyte DAG, which activates PKC, thus decreasing the activation of IR tyrosin kinases [40]. Moreover, hepatic IR leads to activation of gluconeogenesis and glycogen breakdown, thereby increasing circulating glucose levels [41]. Under IR, adipose tissue IRS activity is low, which causes increased lipolysis, implying more circulating FFA and glycerol. Overall, the insulin-resistant situation renders a high level of circulating glucose and lipids and enhanced gluconeogenesis, hepatic lipogenesis and adipose lipolysis [42,43].

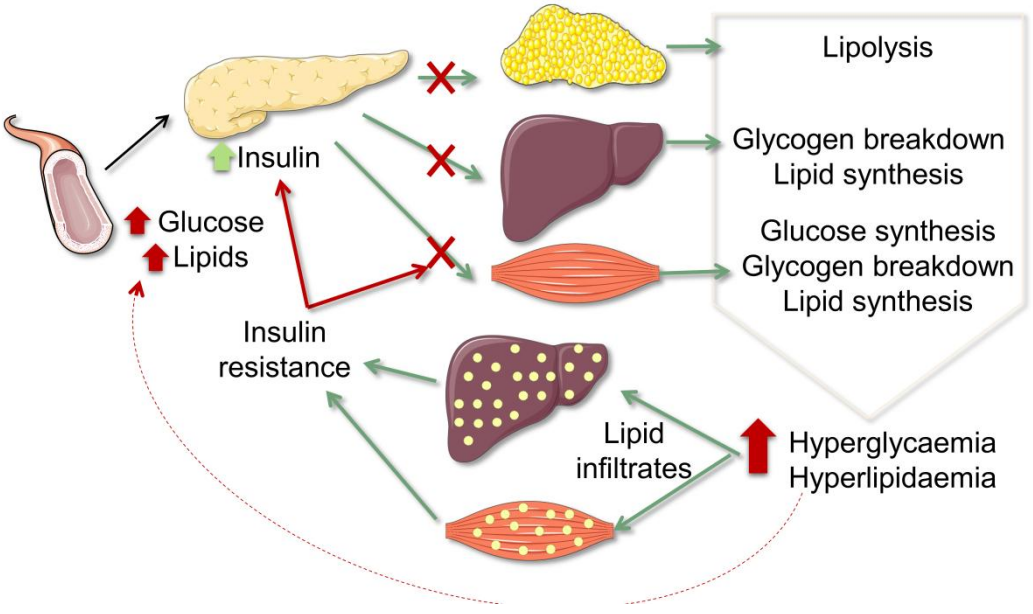

Figure 3: Metabolic alterations of IR. High concentrations of lipids and glucose trigger an increase in the pancreatic production of insulin. Under IR, adipose tissue, liver and muscle are incapable of transducing the insulin signal. As a consequence, lipids are released from adipose tissue and hepatic tissue, and glucose is produced in the liver and muscle. The rise in the circulating concentrations of glucose and lipids leads to tissular lipid infiltration, which inhibits insulin signalling, aggravating the IR. As a compensatory response, the pancreas will continue to produce increasing amounts of insulin until its exhaustion.

Pancreatic cells under hyperglycaemia expand and proliferate in an attempt to achieve euglycaemia by increasing insulin release. Chronic hyperglycaemia leads to hyperinsulinemia and glucotoxicity, ending in the exhaustion and apoptosis of pancreatic β cells. It has been proposed that interleukin-1β (IL-1β) is partly responsible for this failure, activating Fas Ligand (FASL) and its proapoptotic pathway [44]. Hyperglycaemia is also responsible for β cell damage, in combination with hyperlipidaemia, a condition found in T2D and coined glucolipotoxicity, which triggers several prejudicial pathways [45,46]. Pancreatic β cells are particularly sensitive to these aggressions due to the low amount of antioxidant defences and their high metabolic rate [47,48].

In insulin-dependent tissues, IR can occur in response to a reduction in the availability of cell-surface located IR, which is catalyzed by its dephosphorylation by PTP1B or phosphorylation of serine threonine residues by Mitogen-Activated Protein Kinase (MAPK) or Phosphoinositol-3-Kinase related Kinase (PI3KK) [49,50]. Also, SOCS proteins can inhibit IRS activity and target it for proteasomal degradation [51]. The insulin-independent tissues will be affected directly by circulating hyperglycaemia and hyperlipidaemia causing glucolipotoxicity, independently of insulin or glucose intake regulation.

1.1.4. T2D treatments

Treatment for T2D has been always complex given the systemic and widespread effects of this disease. Nonetheless, since T2D pathogenic mechanisms were first described, novel treatments have been developed:

- Sulfonamides were the first pharmacologic group discovered for treating hyperglycaemia. Originally, these antibiotics presented hypoglycaemia as a secondary effect. Subsequently, metformin was discovered, the most prescribed drug against T2D worldwide.
- Thiazolidinediones, namely glitazones, act through activating peroxisome proliferation

activated receptor (PPAR) gamma, reducing hepatic glucose production and improving IR in muscle.

- α-glucosidase inhibitors reduce the breakdown of polysaccharides and thus the rate of absorption of carbohydrates.
- Meglitinides induce insulin production in functional β cells.
- GLP-1 agonists induce increases in insulin release depending on glucose presence, mimicking GLP-1's effect but not its short life.
- Dipeptidyl Peptidase IV (DPP-IV) inhibitors increase the half-life of GLP-1, prolonging the insulinotropic effect of glucose.
- SGLT2 inhibitors antagonize the channel responsible for the reabsorption of glucose in the kidney, increasing glucose excretion.

Of all these, metformin is the most prescribed and the gold standard for complying T2D patients. The mechanisms of action are still under research, but its overall effect is the lowering of circulating glucose through inhibition of liver gluconeogenesis [52]. Metformin enters the liver cells through the organic cation transporter (OCT) and can diffuse into mitochondria. There, it inhibits Complex I of the electron transport chain, possibly by stabilizing a low activity conformation [53]. This reduces the electron flow through the electron transport chain (ETC), subsequently leading to a drop in ATP production. The alteration of adenosine monophosphate (AMP)/ATP and adenosine diphosphate (ADP)/ATP activates AMP-activated kinase (AMPK), which interferes in different cellular processes. Other processes related to the reduction of glucose synthesis are inhibition of fructose biphosphatase, which reduces gluconeogenesis [54] , or inhibition of adenylate cyclase [55]. Metformin also alters lipid storage by inhibiting Acyl-CoA carboxilase (ACC) through AMPK phosphorylation, inhibiting fat synthesis and promoting fat

oxidation [56].

Metformin treatment benefits other cellular processes present in T2D; for example, it reduces oxidative stress [57–59] , possibly by normalizing reactive oxygen species (ROS) production by complex I [60] and reducing mitochondrial dysfunction [61–63].

Metformin is sometimes prescribed together with insulin, which results in better glycaemia management [64] and reductions in the risk of all-cause mortality [65]. However, in young patients with glucose intolerance during the onset of T2D, combination therapy does not generally prevent β cell deterioration [66].

1.2. Molecular mechanisms in T2D

Despite diabetes' origin is a physiological imbalance, many molecular alterations take place before and after it is established. The regulation of these malfunctioning pathways is a wide therapeutic field with many targets yet to be explored.

1.2.1. Oxidative stress

When hyperglycaemia is established, glucose overload increases the metabolic cellular rate in an attempt to consume the nutrient input. As a result, mitochondria, whose main function is to produce energy, generate ROS as a by-product of mitochondrial respiration. In addition, other pathways have been described which also produce ROS, such as the polyol and the hexosamine pathways. While ROS have physiological functions, such as a signal of cellular stress under hypoxia, starvation, pathogen infection or cytokine signalling, its excess can damage cellular components and subsequently activate inflammatory pathways or lead to cell death [67]. In this sense, under hyperglycaemic stress characteristic of T2D there is an excess of DAG that activates PKC and NADPH oxidases (NOX). This enzyme quickly increases ROS concentrations, which will influence autophagy and apoptosis [68]. This is only one general mechanism that relates excessive ROS production to T2D, but there are other mechanisms which imply mitochondrial and cytoplasmic signalling pathways that will be described below. Particularly, understanding the mitochondrial energetic metabolism as a source of ROS is important in T2D pathogenesis.

1.2.1.1. ROS metabolism

1.2.1.1.1. Mitochondrial ROS sources

1.2.1.1.1.1. Oxidative phosphorylation

Mitochondria are double-membrane organelles in which Krebs cycle, β oxidation and ATP synthesis and other vital processes take place [69]. The most important process for ROS generation is mitochondrial respiration. It is the process by which electrons, transferred from

NADH and flavin adenine dinucleotide ($FADH_2$), are transported through protein complexes for ATP synthesis. The ATPase, which is the last protein complex in the ETC, synthesizes ATP depending on the AMP/ATP and ADP/ATP ratios, and only when there is a proper electron transport and proton motive force. The free electrons, once they reach the last protein complex, are bound to free O_2 molecules to generate hydrogen peroxide (H_2O_2) [70].

There are 5 respiratory complexes:

Complex I, also named NADH-ubiquinone oxidoreductase, is a complex of 45 subunits organised in two domains and a flavin mononucleotide (FMN) molecule and an iron-sulphur (FeS) cluster [71] that catalyse the transport of one electron from NADH through CoenzymeQ (CoQ) to complex III. One domain acts as a proton pump, resulting in the transport of one proton to the inner mitochondrial membrane (IMM) space for every two electrons transported.

Complex II, namely succinate dehydrogenase, is part of the Krebs cycle. The electrons flow from succinate to CoQ via FeS clusters transported by $FADH_2$/FAD molecules [72]. This complex has 4 subunits, two of them membrane-anchoring and binding to CoQ, and two on the matrix side [73].

Like complex I, complex III is a proton pump named CoQ-cytochrome reductase and transfers the electrons received by complexes I and II through the coenzyme Q to the cytochrome C (CytC). Complex III is formed by 3 monomers of 11 subunits each. The electron transfer in this complex is carried by these proteins through the Q cycle (122).

Complex IV, also known as CytC oxidase, transfers electrons from CytC to oxygen (O_2) to generate H_2O [75]. It is structured in 13 subunits and 4 metal centers with heme groups and copper ions. The first 4 subunits are coded in the mitochondrial DNA, and are responsible for the main functions (electron transfer and proton pump). The other subunits participate in the allosteric modulation by ATP or in structure maintenance.

Complex V is F_1F_0ATP synthase, whose complex structure utilizes the proton gradient created by the other complexes to synthesize ATP [76]. The F_0 domain is located in the inner mitochondrial membrane, while the F_1 domain is formed by soluble subunits which endow the complex with its catalytic function. The protons previously pumped by complexes I, III and IV pass through F_0 to F_1, causing a conformational change that exposes the catalytic centre, phosphorylating ADP to ATP [77].

1.2.1.1.1.2. ROS generation in oxidative phosphorylation

When ETC is impaired, free electrons react with O_2 molecules and generate superoxide [76,78]. Superoxide is frequently generated in Complex I and is then processed to H_2O_2 by superoxide dismutases 1 or 2 (SOD1 or 2). In mitochondria, superoxide can react with iron and sulphur-containing molecules and produce reactive hydroxyl radicals. These ROS-generating impairments are usually due to two reasons: excess of nutrients and energy, or slow electron transport (Figure 4). Excess of glucose generates high loads of electron donors, promoting electron transfer through the ETC. Thus, the ATP/ADP ratio increases and the mitochondrial membrane becomes hyperpolarized, blocking the electron flow. Electrons remain in the complexes or the transporters and can react with unintended targets or escape the ETC. The best known sources of ROS generation are: Complex I, where NADH transfers its electrons to CoQ [60]; the Q-cycle [74,78] ; and during reverse electron transport [79,80]. Other mitochondrial ROS sources include metabolic enzymes, which can produce a vast amount of ROS under physiological conditions [81,82].

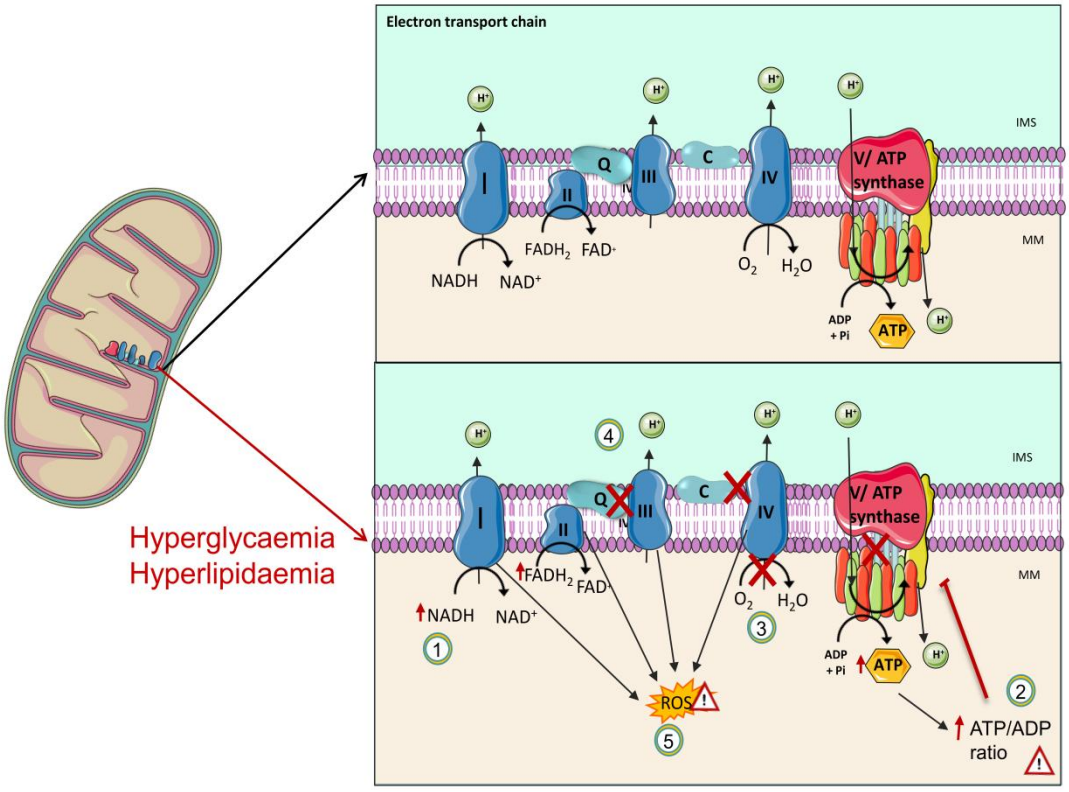

Figure 4: Schematic representation of OXPHOS-related ROS generation. The normal electron flow and ATP generation is depicted in the first scheme. In the second, the mechanism of ROS generation is detailed. (1) Free electrons are transferred by energetic intermediates NADH and $FADH_2$ to complexes I and II respectively. Their excess causes an exaggerated ATP production which blocks ATPase function (2). As a consequence, electron transport is blocked, leading to a reduction in O_2 consumption (3). In addition, the proton pumps continue functioning as the electrons keep on flowing, but eventually, when electron flow does not reach the minimum required they stop, which alters the IMM potential (4). Free electrons react with the proteins, the iron-sulphur clusters and other components of the ETC producing ROS (5). NAD= Nicotinamide adenine dinucleotide; FAD= Flavine adenine dinucleotide; Q= coenzyme Q; C= cytochrome C; I= complex I; II= complex II; III= complex III; IV=complex IV; V= Complex V; ADP= Adenosine diphosphate; ATP= Adenosine Triphosphate; ROS= Reactive Oxygen Species.

1.2.1.1.2. Non mitochondrial ROS sources

1.2.1.1.2.1. Cytoplasmic ROS sources

Some cytoplasmic pathways can produce ROS under certain circumstances. Those pathways are related to management of hyperglycaemia, and can culminate in cellular damage (Figure 5).

The polyol pathway consists in several chemical reactions that use carbonyl compounds, reducing them to their corresponding polyols. The ROS produced by this pathway are relevant in tissues with insulin-independent GLUT channels, deeply affected by changes in glucose concentration [83]. The main carbonyl compound affecting diabetes is the conversion of glucose to sorbitol by the aldose reductase consuming NADPH, and its dehydrogenization to fructose by sorbitol dehydrogenase. Those reactions consume NAD^+, therefore increasing the $NADH/NAD^+$ ratio, which slows down all catabolic reactions and reduces the oxidative potential of the cell. On the other hand, NADPH consumption reduces the regeneration of the vital ROS scavenger and antioxidant glutathione, inducing oxidative stress. Moreover, superoxide production inhibits glyceraldehyde-6-P dehydrogenase, which is the main source of reducing equivalents in the form of NADPH. The result of this inhibition is the accumulation of glycolysis intermediates and a reduction in energy production [83,84].

Accumulated fructose-6-P can also intervene through the hexosamine pathway, increasing the amount of uridyl diphosphate-N-acetylglucosamine (UDP-GlnNAc), a glycosylation substrate. As a consequence, glycosilation reactions are enhanced, including transcriptional activation of proinflammatory genes and other cardiovascular-related molecules such as plasminogen activator inhibitor 1 (PAI-1) [83,85].

Upstream of glyceraldehyde-6-P-dehydrogenase the intermediate glyceraldehyde-3-P accumulates and finally breaks into dihydroxiacetone phosphate and methylglyoxal. This latter

molecule is highly reactive with amino groups, forming advanced glycation end-products (AGEs). AGEs can also be formed through a longer process, which is initiated when glucose and amino groups react to form a Schiff base, which turns into Amadori products. These molecules favour the auto-oxidation of glucose into glyoxal, thus forming AGEs [86,87].

Dihydroxyacetone phosphate can be reduced to glycerol phosphate and then to DAG, which activates PKC [83,84]. Its chronic activation results in the increased production of Platelet-Derived Growth Factor (PDGF) and Vascular Endothelial Growth factor (VEGF), and decreases in the production of Nitric Oxide (NO), PAI-1 synthesis and NFκB activation.

ROS can also be produced by enzymes as a reaction product. Other important ROS sources are NOX1, 2, 4 and 5. They produce NAD^+ through NADPH electron exchange and leave superoxide as a by-product, which increases the glycolytic rate. NOX-dependent ROS production induces GLUT-1 expression through hypoxia-induced factor 1α (HIF1α) and activation of glycolysis [88]. Also, in a proinflammatory scenario, phosphofructokinase 2 (PFK2) colocalizes with NOX2, thus inducing its activation [89].

Another ROS-producing enzyme is NO synthase (NOS), whose 3 isoforms (eNOS, iNOS and nNOS) produce superoxide and NO from L-arginine. Under certain conditions, NO reacts with superoxide to form peroxynitrite. This molecule enhances the polyol pathway, initiating a feedback loop in which NADPH production inhibits glycolysis and stimulates NOX [90].

1.2.1.1.2.2. Endoplasmic reticulum ROS source

The endoplasmic reticulum (ER) also participates in the formation of ROS. The enzyme protein disulfide isomerase (PDI) forms disulphide protein bonds. After the reaction, PDI ends in a reduced state, and is reoxidized by ER oxidase 1α (ERO1α), which produces H_2O_2 as by-product. This enzyme can be also activated under ER stress [91]. ROS are also produced by CYP450, located in the ER membrane, and ER-localized NOX4 [92].

It is believed that mitochondrial and non-mitochondrial sources of ROS are related through the superoxide inhibition of the enzyme glyceraldehyde-3-phosphate dehydrogenase (GAPDH). Mitochondrial ROS (mtROS) cause DNA strand breaks that activate poly-ADP ribose polymerase (PARP), a known inhibitor of GAPDH [93]. GAPDH inhibition leads to accumulation of upstream glycolytic intermediates: glyceraldehyde-3-phosphate activates PKC through DAG and causes methylglyoxal and AGE formation; fructose-6-P increases the flux through the hexosamine pathway; and the glucose accumulation increases the polyol pathway rate [83].

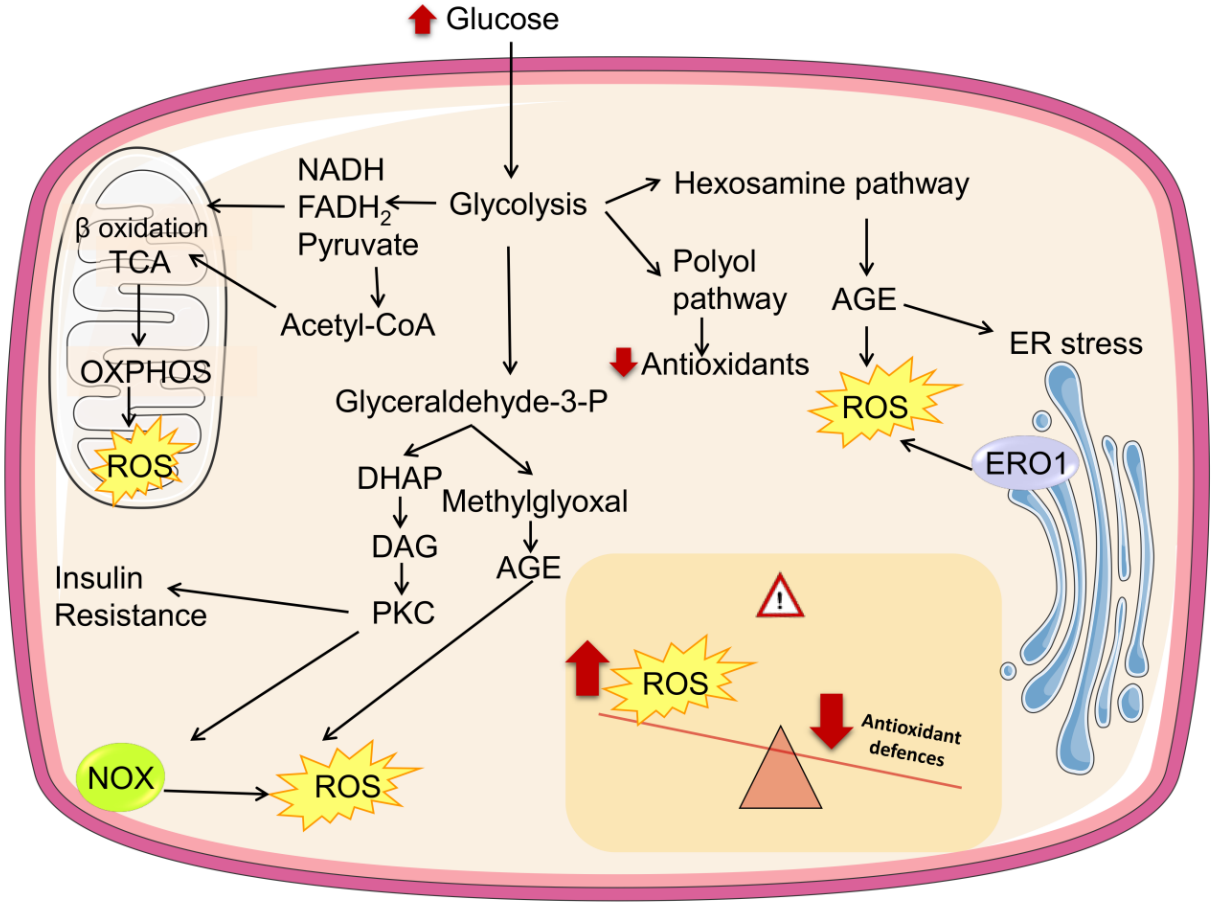

Figure 5: Cellular sources of ROS. ROS generation due to high glucose concentrations is originated by different pathways. Mitochondrial-dependent ROS generation depends on the amount of NADH and $FADH_2$ resulting from glycolysis, β oxidation and TCA. The accumulation of glycolysis intermediates such as Glyceraldehyde-3-phosphate leads to the production of ROS through the formation of AGE and the DAG-dependent activation of PKC. This latter kinase also activates NOX, an important source of ROS. Accumulation of other intermediates facilitates the flow of some metabolites to the polyol and hexosamines pathway, which contributes to oxidative damage. ER stress, partly induced by the presence of AGE, induces ERO1 activation, which also increases ROS. Altogether, excess of ROS concentrations overwhelms antioxidant mechanisms and harms cellular homeostasis. NAD= nicotinamide dinucleotide; FAD= flavin nucleotide; Acetyl-CoA=Acetyl coenzyme A; TCA= tricarboxilic acid cycle; OXPHOS= oxidative phosphorylation; ROS= reactive oxygen species; DHAP= dihydroxyacetone phosphate; DAG= diacylglycerol; PKC= protein kinase C; NOX= NADPH oxidase; AGE= advanced glycation endproducts; ER= endoplasmic reticulum; ERO1= endoplasmic reticulum oxidase 1.

1.2.1.2. ROS and T2D

β cells are especially sensitive to ROS accumulation due to their low levels of antioxidant defences. mtROS damage to the mtDNA has an impact on respiratory efficiency, inducing dependence on glycolysis for ATP production, a reaction that renders less ATP than oxidative phosphorylation (OXPHOS). The reduction in ATP hinders the opening of the ATP channel for insulin release [84]. Other important mechanisms by which mtROS affect β cell function and survival is through the irreversible decrease in levels of the transcription factors pancreatic and duodenal homeobox 1 (PDX-1) and mast cell function-associated antigen (MafA), vital for insulin gene expression and β cell identity and survival [94,95]. Cell survival is also influenced by ROS through inhibition of IRS-1 and induction of the Apoptosis-Signal regulated Kinase ASK/JNK apoptotic pathway [96], and IKK, which phosphorylates IRS in a serine residue, inhibiting its action [97].

In the liver, oxidative stress and AGEs provoke an imbalance in mitochondrial metabolism, OXPHOS, and redox equilibrium. Subsequent lipid accumulation can render the liver prone to developing non-alcoholic fatty liver disease (NAFLD) or non-alcoholic steatohepatitis (NASH) [98]. In a high fat diet (HFD) T2D mice model, higher ROS and lower antioxidant defences have been seen, related to decreased insulin signalling and lower glucose tolerance [99]. Similarly, reduced antioxidants and increased carbonylated proteins and lipid peroxidation has been reported in Zucker diabetic fatty (ZDF) rats, possibly a result of defective OXPHOS [100].

Muscle cells participate in T2D development by producing and accumulating ROS, which harm cellular processes. IR in muscle cells causes IR serine phosphorylation and blocks GLUT4 externalization [101]. Thus, muscle cells internalize and use FFA instead of glucose to produce reducing equivalents for the ETC. Those FFA accumulate in mitochondria and between myocytes, thus increasing ROS production [102,103]. Lipid accumulation reduces the respiratory capacity of the

mitochondria and inhibits β oxidation, thus causing an increase in ROS production [104,105]. Another consequence of lipid infiltration is the rise of DAG concentrations which, as previously mentioned, activate PKC, which in turn directly activates NOX proteins, thereby generating superoxide [106]. ROS accumulation caused by NOX activation and by the other previously mentioned mechanisms contribute to IR through reduction of the hexokinase catalytic capacity [107]. ROS also cause mitochondrial fission and reduced expression of mitochondrial complexes in cardiac myocytes [105].

It has been seen that ROS accumulation in adipocytes triggers similar IR signalling pathways to those in muscle cells or pancreatic cells. The main sources of ROS in adipose tissue are NOX4, polyol pathway and mitochondria [108]. In the early stages of IR there is an activation of glucose-6-phosphate dehydrogenase (G6PD) that enhances the polyol pathway [109] and NOX4 activation [110]. Moreover, the proinflammatory surrounding created by glucolipotoxicity recruits activated macrophages in adipose tissue, which produce ROS via NOX2 [111]. This massive ROS accumulation slows the ETC, which in turn causes accumulation of FFA and contributes to ROS production[112]. In this state, adipocytes produce chemoattractant cytokines that recruit more macrophages, promoting inflammation [113] and leading to adipose tissue hypertrophy [114,115].

Regarding leukocytes, in has been suggested that, in T2D, leukocytes are primed to generate ROS, which renders them prone to apoptosis [116]. Similarly, in Streptozotocin (STZ)-induced T2D rats with retinopathy, ROS causes leukocyte trafficking to the retina, and antioxidant treatment can abolish this effect [117]. In addition, increased levels of superoxide, peroxynitrite and H_2O_2 have been reported in different populations of leukocytes from T2D patients [118].

1.2.1.3. Systemic oxidative stress consequences in T2D

Oxidative stress is a pathologic trait in diseases as varied as liver disease [119], vascular and

atherosclerotic disease [120,121], and metabolic alterations [120,122], and also in the aging process and aging-associated diseases [123,124]. In T2D, as explained above, hyperglycaemia and hyperlipidaemia are the main contributors to ROS production.

AGEs are one of the consequences of ROS abundance, which, once synthesized, can continue to circulate through the bloodstream. AGE distribution causes activation of AGEs receptors (RAGE) in many cell types, activating NFκB dependent inflammatory pathways. This can imply the beginning of the development of microvascular diabetic complications, such as nephropathy, retinopathy and neuropathy [125,126]. AGE-RAGE interactions are responsible for the increased immune vascular adhesion and vascular permeability seen in T2D models [87,127]. AGE serum concentrations correlate with those of glycated haemoglobin, which indicate the severity of the disease and whether it is well managed or not [128]. Moreover, accumulation of AGEs enables metabolic memory. This term was coined for describing the increased cardiovascular risk of T2D patients years after their improvement/disease control [126,129].

Excess ROS interact with lipids to create oxidized LDL (oxLDL), which together boost inflammatory pathways, prime immune cells and activate the endothelium, enhancing the formation of subatherosclerotic lesions [97]. oxLDL can be uptaken by scavenger receptors in the macrophages, contributing to the formation of foam cells inside the intima-media layer of the vasculature, which damage the endothelial tissue [130].

IR is also affected by ROS, as they interfere with normal insulin release and signalling. A clear example is that seen in T2D rats under HFD, in which excessive ROS downregulates glycolysis but enhances oxidation and the pentose pathway, thus favouring IR [131]. Experimental evidence suggests that the mechanisms by which ROS produce IRS inhibition are connected to inflammatory cytokines , AKT signalling [111,132,133] and JNK signalling [134–136].

1.2.1.4. Antioxidant defences

All cell types have enzymatic and non-enzymatic mechanisms to counterbalance ROS production and maintain their levels within a physiological range in which ROS can be beneficial. Among the enzymatic systems, we can find different antioxidante enzymes, such as SOD, catalase or glutathione peroxidases.

SOD are enzymes that transform two superoxide anions into H_2O_2 molecules thanks to reduction and reoxidation of transition metals present at the active site [137]. The enzymatic conversion facilitates some functions that superoxide is not able to: membrane diffusion and metabolic flexibility [138]. SOD1, or also CuZnSOD , is located in the cytosol or secreted (SOD3), whereas MnSOD or SOD2 is located in mitochondria [139] .

SOD1 is present in almost all cytoplasmic compartments and in the mitochondrial intermembrane space. A copper chaperone (CCS) helps to bind the copper atom to the active site and activates SOD1. Its activity is inhibited by high H_2O_2 concentrations [137].

SOD2 or MnSOD is a homotetramer located in the mitochondrial matrix, despite it is synthesized in the cytoplasm, being carried to the mitochondrial matrix by a mitochondria-targeted sequence. It differs from SOD1 in its structure, half life and product inhibition. SOD2 can bind to Mn^{2+} or Fe^{2+} in the active site, but its active form can bind only with Mn^{2+} [137].

SOD3 is the soluble secreted form of the SODs, found as a homotetramer in the plasma or bound to heparan sulphate in the extracellular matrix. It is expressed by blood vessels, lung, kidney, uterus and heart. In the vascular tissue, muscular cells and fibroblasts synthesize and exocyte SOD3, which can be endocyted by endothelial cells. The active center has 50% homology with SOD1, and its activity is regulated by copper availability [137] .

Catalase is present in peroxisomes as tetramers. The active centre turns H_2O_2 into H_2O and molecular O_2, and is formed by a prosthetic group of ferric protoporphyrin IX. It is a

ubiquitous enzyme that ensures the correct control of H_2O_2 concentrations [140].

Polymorphisms or changes in the levels of these antioxidant enzymes can alter their activity. As an example, sequence variations in SOD increase the incidence of T2D [139]. Similarly, low-activity catalase predisposes the organism to the development of diabetes [141,142] or other degenerative diseases [140]. This latter case has been evidenced in T2D patients with low levels of SOD3, as they are predisposed to polyneuropathy [143].

There is a debate surrounding the antioxidant state of the blood in T2D, as in some studies it is enhanced [144] and in others it is decreased [145–147]. In this sense, higher activity of antioxidant enzymes has been seen in newly diagnosed T2D patients [148]. This seems to be the tendency in some cases, as in those shown in a study performed in blood samples from T2D patients with elevated ROS levels and enhanced activity of SOD [146,149]. In other tissues, different behaviours have been observed; for example, hepatic cells from T2D patients have a lower antioxidant activity than healthy individuals [147], but in muscle samples the activity of SOD1 increases in parallel to T2D progression, whereas catalase and SOD2 decreases [150]. Genetically, individuals who carry susceptible variants of antioxidant enzymes have an increased risk of developing T2D [151,152].

These antioxidant enzymes are genetically regulated by oxidative-stress-sensitive pathways. One of the most important pathways is nuclear respiratory factor 2 (NRF2)/kelch like ECH associated protein 1 (KEAP1)/adenylate-uridylate rich elements (ARE). NRF2 is a DNA-binding protein that dimerizes with other proteins in order to regulate the transcription for genes with ARE sequences. KEAP is a protein that inhibits NRF2 by binding to a specific domain and targeting it for proteasomal degradation. Under oxidative stress aggression, NRF2 activators or KEAP1 inhibitors allow NRF2 to enter the nucleus and coactivate ARE-regulated sequences. Some of the genes regulated by ARE are SOD, catalase, glutathione (GSH), NADPH quinone

dehydrogenase 1 (NQO1), heme oxygenase 1 (HMOX1), glutamate-gated chloride channel (GLC), glutathion-S-transferase (GST) and sirtuin 1 (SIRT1) [153,154]. Alternative NRF2 activation can be carried out by AKT, PKC, JNK, PI3K and extracellular-regulated kinase (ERK), which phosphorylate NRF2, difficulting its interaction with KEAP [155].

Inhibition of KEAP1 or induction of NRF2 can delay diabetes onset in diabetic db/db mice, which proves that this antioxidant pathway is vital for T2D prevention [154]. Indeed, in peripheral blood mononuclear cells (PBMCs) from T2D patients lower NRF2 levels, together with a diminished antioxidant capacity, have been reported [156]. Most research has shown that activation of NRF2 or inhibition of KEAP delays or improves T2D and its complications [157,158]

1.2.1.4.1. Antioxidant treatments: SS-31

There are many approaches to tackle oxidative stress, but the most common are activators of endogenous antioxidant mechanisms or molecules with a chemical structure that quench ROS.

The antioxidant NRF2/KEAP1 pathway can be stimulated by some natural or synthetic substances, such as sulphoraphane, methyl bardoxolone, terButylhydroquinone (tHBQ), quercetin, cinnammic acid or curcumin. All of them have been demonstrated to increase the antioxidant production through KEAP1 cysteine residue modification [157,159]. Curcumin is, among other antioxidant molecules, one of the most studied, exerting its effects through NRF2, but also via other molecular pathways that prevent cellular damage by hyperglycaemia [160–162].

Other types of antioxidant molecules, namely targeted antioxidant molecules, quench the reactive radicals thanks to their chemical structure. Among the most important are the mitoquinones, which present a chemical structure that diffuses into mitochondria, where they buffer the excess of superoxide anion. One of these mitoquinones, named MitoQ, is a promising therapy for T2D, endorsed by several studies in which treatment exerted beneficial antioxidant

effects [163–166]. Other mitochondrial superoxide-quenching chemical structures include antioxidant peptides, of which Szeto-Schiller (SS) are the most studied. Those peptides have a characteristic structure based on alternating cationic and aromatic side chains with affinity for cardiolipin and depolarized mitochondrial membranes [167,168]. Once the SS peptide crosses the mitochondrial membrane, it quenches ROS and can accumulate in the mitochondrial matrix without altering mitochondrial function. SS peptides are a promising therapy for diseases in which mitochondrial dysfunction is present, such as T2D. Indeed, studies with SS-31 have been carried out in *in vitro* systems, animal models and human samples, proving the efficacy of SS peptides in reducing oxidative stress and its consequences. Specifically, SS-31 treatment of the ox-LDL challenged macrophage cell line RAW264.7, was shown to prevent their conversion to foam cells, through reduction of ROS concentrations and the inhibition of cholesterol influx. Additionally, SS-31 induced the expression of SOD and reduced that of proinflammatory cytokines.[169]. In addition to improving the metabolism of macrophages, SS-31 treatment also ameliorates the survival and function of transplanted mouse pancreatic islets [170]. Regarding *in vivo* studies, SS-31 or its commercial form, Elamipretide, has been found to improve kidney function and prevent diabetic kidney disease in a T2D mice model by attenuating oxidative damage [171,172]. SS-31 has also been tested in human samples, as shown by previous results from our laboratory, in which leukocytes from T2D patients treated with SS-31 showed a reduction in oxidative stress markers, less inflammation and an increase in SIRT1 levels [173]. All the abovementioned studies highlight the effectiveness of SS-31 in T2D and associated diseases, highlighting the importance of a correct mitochondrial function. The antioxidant effect of this molecule can be attributed to the dimethyltyrosine residue. This has been determined in initial studies in which substitution of dimethyltyrosine residues by phenylalanine, which turned SS-31 into SS-20, eliminated the antioxidant capacity of the peptide [174]. Due to this difference, SS-20 is

employed as a negative control in some studies [175–177].

Despite possible advances with antioxidant treatment, it is not clear whether antioxidant therapy could be totally beneficial in T2D or not. Natural antioxidants, such as vitamins, have shown limited benefits in ameliorating cardiovascular comorbidities in T2D [178], and a possible explanation is that antioxidants tackle ROS generation but allow other stress mechanisms, such as ER stress, to remain active [179]. However, MitoQ and SS-31 have been shown to reduce even ER stress, thanks to mitochondrial targeting and correction of the mitochondrial dysfunction [163,180]. In this context, further research is needed in the field of antioxidant therapies for determining the best antioxidant approach to ameliorate the complications of diabetes.

1.2.2. Mitochondrial dysfunction

Mitochondrial dysfunction is defined as the state in which mitochondria are not able to satisfy the cellular needs of ATP [181,182]. This lack can occur through several mitochondrial function deficiencies: reduced mitochondrial synthesis results in a reduced OXPHOS and defective mitochondrial metabolism. Hence, precursor molecules accumulate and ETC can leak and produce ROS, which further increases the mitochondrial damage [183]. The accumulated precursors can harm other cell processes such as DAG and ceramides, which causes IR [184].

Mitochondrial dysfunction is detected when there are abnormal levels of O_2 consumption and changes in mitochondrial membrane potential. It causes aberrant and excessive production of mtROS, low ATP production and proton leak, which leads to a change in the cellular source of ATP from OXPHOS to glycolysis. In these circumstances, mitochondria can change its shape, reduce or increase its mass, and redistribute in an attempt to fulfil cellular needs of energy and metabolites [185]. Damaged mitochondria can be eliminated by mitophagy, redistributed by fission and fusion events, and replaced by synthesis of new mitochondria [182]. Fusion and fission events are vital complementary mechanisms in preventing mitochondrial

dysfunction, apoptosis and mitochondrial degradation. Fission helps to eliminate damaged fragments of mitochondria and promotes apoptotic cell death, whereas fusion interconnects mitochondria, supporting damaged ones by sharing metabolites from healthy ones. Both mechanisms control mitochondrial biogenesis and localization [186].

1.2.2.1. Mitochondrial dysfunction in T2D

Some studies support the idea that mitochondrial dysfunction is the origin of IR. This process begins when diabetes-related nutrient overload leads to a transient increase in mtROS, which induces mitochondrial fragmentation in order to optimise O_2 consumption rate (OCR), leading to IR [187,188]. The nutrient overload, together with the low NADH/NAD^+ ratio present in diabetes, increases mtROS production and amplifies the damage. Inhibition of reparative mechanisms such as fusion leads to H_2O_2 production and IR [189] , or impaired GLUT4 translocation and calcium uptake, which are also important for insulin signalling [190]. In insulin-sensitive tissues, mtROS, mitochondrial fission, impaired ER-mitochondria contacts and calcium mishandling seem to be a general signature of IR states.

Insulin secretion in pancreatic β cells is closely connected with mitochondrial function. Mitochondrial dysfunction affects pathways related with insulin secretion, such as calcium signalling, mtROS, tricarboxilic Acid (TCA) cycle metabolic intermediates and NADH transport [191,192]. Thus, insulin signalling will depend on a correct mitochondrial function. Scavenging processes like mitophagy or mitochondrial dynamics have also been related to altered insulin release [193–195].

Hepatic cells in T2D also display signs of mitochondrial dysfunction, including mtROS production and altered ETC complexes expression caused by non-esterified FFA, which lead to IR through JNK signalling [135]. Similar results are obtained when hepatocytes are treated with

palmitate, which causes mtROS production, JNK activation and IRS2 serine phosphorylation, thus inhibiting insulin signalling and promoting IR [196].

In muscle cells, adequate mitochondrial function is vital for adequate insulin signalling. Indeed, ROS produced by dysfunctional mitochondria cause lipid accumulation and IR, which can be reversed by mitochondrial catalase treatment [102]. Moreover, dysfunctional mitochondria causes the accumulation of ceramide and carnitine in skeletal muscle cells due to slow β oxidation, membrane depolarization, and low TCA cycle, all of which lead to IR. The authors of the study in question showed that this phenotype could be reversed by mitochondrial transcription factor A (mTFA) overexpression [197].

Adipose tissue is also sensitive to mitochondrial dysfunction, as mTFA inhibition causes mitochondrial dysfunction and leads to IR [198]. An *in vitro* model of IR in 3T3-L1 cells was shown to display low expression of mitochondrial biogenesis genes, mtROS accumulation, loss of membrane potential and decreased mitochondrial calcium [199]. Mitochondrial dysfunction has also been observed in db/db mice, and was improved by treatment with rosiglitazone, an insulin-sensitizing treatment [200]. This indicates that the relationship between mitochondrial function and IR is reciprocal.

Mitochondrial impairments in T2D have also been described in leukocytes. mtROS production was found to be enhanced and antioxidant defences reduced in leukocytes from T2D patients, due to lack of function of Complex I [201]. Likewise, T2D patients under cardiac risk have been shown to display a lower mtDNA copy number and enhanced mtROS production [202].

1.2.2.2. Mitochondrial dynamics

Mitochondria change their morphology, distribution and connectivity through dynamic processes named mitochondrial dynamics. These processes consist of the division of

mitochondria into smaller fragments by fission, or their union by fusion. Mitochondrial dynamics facilitate changes in metabolic activity, from more elongated and metabolically active to a lower rate when fragmented [203]. They also serve as a quality control, by which low quality mitochondria can fuse with functional ones or fragment so as to be eliminated [204,205].

Through fusion, mitochondria dissipate possible imbalances in membrane potential, share harmful metabolites and replace defective enzymes. The fusion process consists of two separate steps: the fusion of the outer membrane and the fusion of the IMM [206,207]. The first is carried out by the proteins mitofusin 1 (MFN1) and mitofusin 2 (MFN2). Both are proteins with GTP-ase activity, bonding in homotypic or heterotypic complexes, the latter being more efficient [208]. Neighbouring mitochondria expressing MFNs can join their outer membranes through GTPase enzymatic activity. The inner mitochondrial membrane proceeds with other proteins and independently of the fusion of the outer mitochondrial membrane, thanks to dynamin-related GTPase protein optic atrophy-1 (OPA1). Its gene encodes a protein with 8 possible isoforms and 3 cleavage sites for the metalloproteases YME-like protein 1 (YmeL1) and OMA1. Cleavage forms give two main isoforms: L-OPA, which retains the N-terminal transmembrane domain, or S-OPA, which is a short soluble form, processed by presenylins-associated rhomboid-like (PARL). L-OPA is situated along the cristae membrane and mediates intercristae tethering. S-OPA may play a role in joining apposing cristae membranes and helping to change cristae shape when needed, although its exact function is still under study [186].

Regarding fission, two main proteins intervene: dynamin-related protein 1 (DRP1) and fission protein 1 (FIS1). The fission process is as follows: first, the fission site is marked; second, DRP1 is assembled around the fission site thanks to FIS1 and other adaptors; and third, the GTPase activity of dynamin constricts and severs the mitochondrion. DRP1 is the main fission GTPase, which can form dimers or tetramers in the cytoplasm, and is recruited by the fission

site. These sites are usually mitochondria-ER contact sites, which are slimmer than the rest of the mitochondria. DRP1 represents one of the proteins that link the cytoplasmic state to mitochondrial events: it is sensitive to calcium concentrations through calcineurin, is inhibited by PKA, and is retained in the cytoplasm during starvation [186,209].

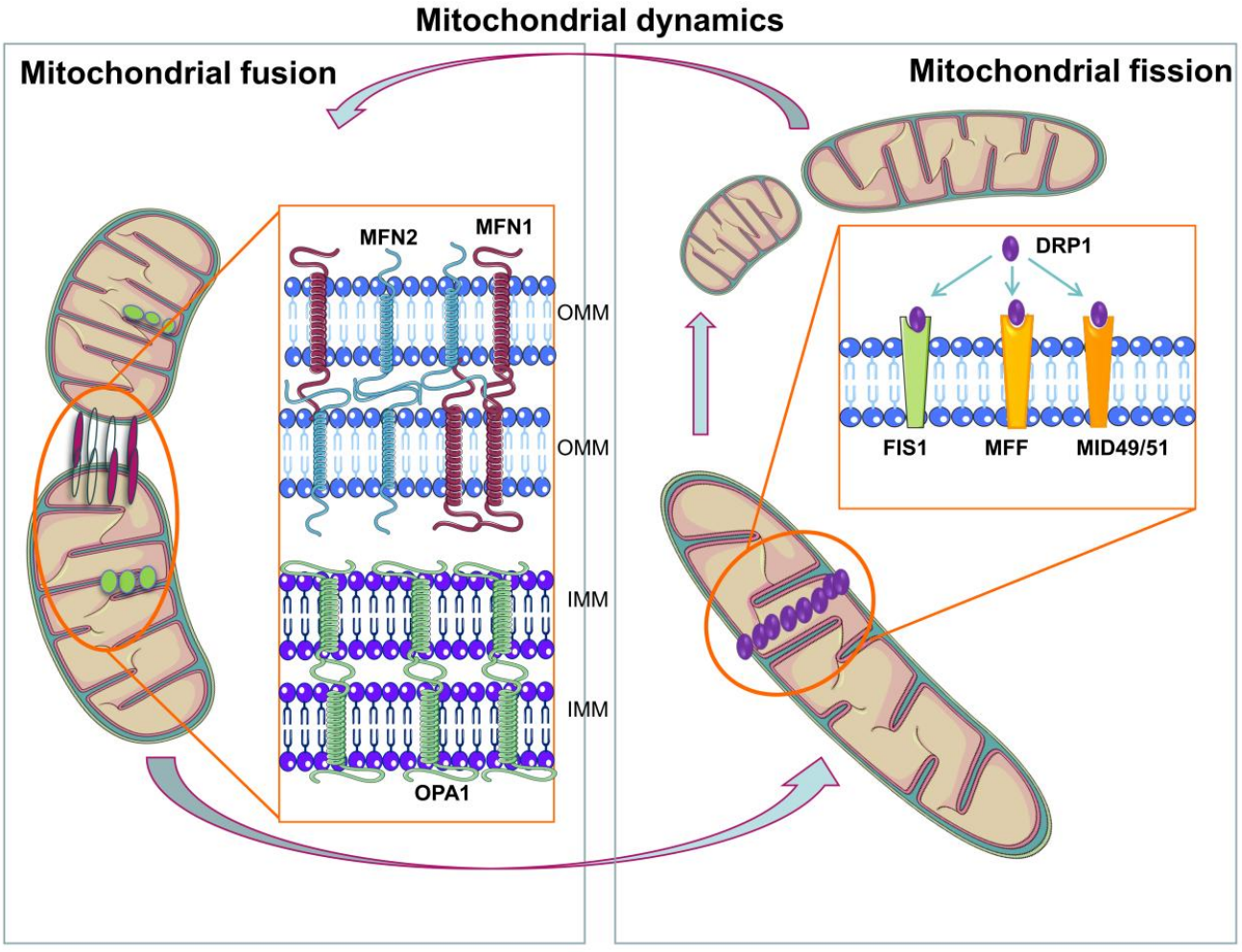

Figure 6: Representation of mitochondrial dynamics. Mitochondrial fusion is carried out by mitofusins 1 and 2 for the outer mitochondrial membrane and by OPA1 for the inner mitochondrial membrane. The fission process depends on the accumulation of FIS1 and DRP-binding proteins at the site of division, and subsequent DRP polimerization. MFN1= mitofusin 1; MFN2= mitofusin 2; IMM= inner mitochondrial membrane; OMM= outer mitocondrial membrane; OPA1= optic atrophy 1 protein; FIS1= fission protein 1; MFF= mitochondrial fusion factor; MID49/51= mitochondrial dynamics protein 49/51; DRP1= dynamin-related protein.

Both processes perform regulating functions depending on the cell's energetic and metabolic needs. Consequently, under starvation, when there is need for more energetic efficiency, ATP synthase complexes dimerize, IMM generate more cristae and mitochondria become more elongated [210]. Moreover, in nutrient deprivation there is an increase in mitochondrial fusion which optimizes respiration [211,212]. Defects in these processes affect cellular metabolic pathways that depend on mitochondrial performance. Among these processes are insulin signalling and ROS production, which are altered upon MFN1 blunting or MFN1 stimulation [213–215]. In the context of T2D, where metabolic imbalances are present, alterations in mitochondrial dynamics have been assessed, particularly reductions in fusion towards a pro-fission metabolism [189,216].

One of the determinants of fusion and fission processes is the balance between ATP need and nutrient supply, which determines the need for more or less efficient mitochondria. Under nutrient excess, respiration increases, despite mitochondria becoming less effective in producing ATP, thus causing mitochondrial fission in order to increase proton conductance [217,218]. Indeed, DRP1 activation by other proteins or by post-transcriptional modifications, such as O-GlcNAcylation (whose production is enhanced in T2D), has been reported [219,220].

1.2.2.3. Mitochondrial dynamics regulation in T2D

In T2D, a decrease in fusion and an increase in fission occur in most cell types, including pancreatic β cells, muscle cells, liver cells and adipocytes, and this may be related to mtROS production and mitochondrial dysfunction [182].

In pancreatic β cells, MFN1 and MFN2 seem to be reduced and FIS1 increased in T2D due, in part, to brain and muscle arnt-like protein-1 (Bmal-1) inhibition [221]. Comparable observations have been reported in a similar model, in which only MFN2 was downregulated,

thus reducing mitochondrial activity and fission [222]. Different studies have been performed regarding fission proteins; for example, it has been demonstrated that β cells from DRP1 KO mice have normal OCR, but diminished insulin secretion [223]. FIS1 findings are scarce but significant, as regular expression of FIS1 is needed for optimal insulin expression and release in β cells, but excessive expression causes loss of glucose responsiveness [224]. Moreover, FIS1 inhibition in β cells reduces respiration and impairs insulin secretion [225].

The liver also undergoes alterations in the mitochondrial dynamic process, as seen in samples of hepatic tissue. In these samples, the metabolite butyrate has been shown to increase mitochondrial function and lipid oxidation and reduced ROS production in HFD mice, which protected against hepatic inflammation [226]. Indeed, fusion was decreased and fission enhanced in a T2D mice model, which was accompanied by increased ROS production, lower ATP generation and higher lipid peroxidation. Inhibiting ROS production with the novel mitochondrial-targeted antioxidant, peptide SS-31, reversed these mitochondrial alterations [227]. Moreover, maintaining a correct fusion process throughout MFN2 expression ensures efficient liver insulin signalling, glucose tolerance and mitochondrial function in T2D, as shown in a MFN2-KO mice model [189].

Regarding muscle cells from T2D subjects, less sarcolemmal mitochondria were found when compared with those of healthy controls. This observation is associated with reduced ETC and lower ATP production *per* mitochondrion [228–230]. In parallel to a lower mitochondria number, OPA1 expression has also been seen to be mitigated in muscle from T2D patients and enhanced by exercise or insulin treatment [231,232]. These alterations could be explained by post-transcriptional modifications seen in T2D, such as O-GlnACylation or proteolitic cleavage, which decrease the activity of OPA1, unstabilizing mitochondrial membrane [105,233]. Additionally, mitofusins play a part in muscle mitochondrial dynamics, as MFN1 is known to improve the

translocation of GLUT4 in muscle cells through a AMPK-dependent mechanism [213]. Moreover, MFN2 overexpression in muscle cells upregulates OXPHOS through expression of its complexes [234], while in T2D its expression is disminished, reducing mitochondrial respiration [235,236]. In relation to fission proteins little is known about FIS1 alterations in T2D, although changes in DRP1 have been well documented. DRP-1 overexpression has not been associated with noticeable changes. In muscle cells [237]; however, DRP1 KO mice display enhanced insulin sensitivity and reduced activity of complexes I and III [209,238]. In cultured C2C12 muscle cells, palmitate treatment was found to enhance FIS1 and DRP1 expression and mitochondrial fission, and was accompanied by mitochondrial depolarization, reduced insulin-induced glucose uptake and ceasing of ATP production [239].

ROS production has been related to DRP1 upregulation and mitochondrial fission in adipose tissue, which contributed to ER stress and NLR-family pyrin-domain containing 3 (NLRP3) activation, and was reversed by AMPK-dependent Ser637 phosphorylation of DRP1 [240]. Pathways governed by overnutrition, such as peroxisome-proliferator-associated receptor γ (PPARγ) transcription factor, govern mitochondrial dynamics through bcl2-interacting protein 3 (BNIP3), establishing a signalling axis that is inhibited by overnutrition, as demonstrated in *in vitro* and *in vivo* models. This results in an increased IR, altered lipid and glucose metabolism and more fused mitochondria [241]. PPARγ also regulates membrane-associated ring-CH-type finger 5 (MARCH5) ubiquitin ligase, which stimulates a pro-fission phenotype and lipid metabolism [242].

Few studies have explored alterations of mitochondrial dynamics in immune cells. However, research has recently revealed that increased fission and reduced fusion exist in leukocytes from T2D patients, together with mitochondrial dysfunction [243]. Recently, a study underlined the importance of MFN2 in adhesion of neutrophils to the endothelium, given that MFN2 assists in ER calcium release [244]

In cellular and murine models of hyperglycaemia or hyperlipidaemia, it is generally established that diabetes-related metabolic alterations produce a pro-fission phenotype with repercussions for mitochondrial performance and insulin signalling. Human samples and animal models show that these processes are highly dependent on cell type, general metabolic state and other regulatory pathways. However, such conclusions should be confirmed in tissue and cell culture.

1.2.3. Endoplasmic reticulum stress

The ER is a large membrane-enclosed organelle involved in folding and modifying the transmembrane and secreted proteins, synthesis of lipids and sterols and storing calcium. Its function is central to cellular anabolism and pathways of cellular exocytosis. It is classified depending on the presence of ribosomes on its surface. The rough ER (RER) has ribosomes that translate the proteins simultaneously to their translocation to the ER lumen. The smooth ER (SER) does not have ribosomes, and is mostly devoted to protein modifications, lipid synthesis and other processes. Conversely, the RER is closer to the nuclear envelope, usually surrounding it, and moves through the cytoplasm towards the cellular membrane as it matures. During this process, RER eventually loses the ribosomes and changes from RER to SER, altering its structure to sheets or tubules [245]. In this compartment, resident ER proteins complete their maturation, but those tagged for exocytosis or those which need further modifications (lipidations, glycosilations) will be traslocated to the Golgi apparatus. [245]

When cells suffer from different types of stress, such as oxidative stress, modified proteins that do not achieve proper folding accumulate and cause ER dysfunction. In response, the ER activates different pathways that sense these unfolded proteins and activate protective pathways. These pathways imply three main processes: attenuation of protein synthesis, activation of ER associated protein degradation (ERAD) or marked enhancement of secreting and

folding capacity by synthesis of folding chaperones, namely the unfolded protein response (UPR) [246]. Simultaneously, proapoptotic and inflammation signalling cascades are activated, which can lead to cell death if ER stress is not resolved by the abovementioned mechanisms [246].

The cell senses the proteostasis imbalance through protein chaperones, especially immunoglobulin heavy chain –binding protein (BiP)/glucose-regulated protein 78 (GRP78) [247,248]. This chaperone binds and inhibits the luminal domain of the transmembrane proteins that triggers UPR rescue pathways or apoptosis, keeping them separate. Once unfolded proteins accumulate, GRP78/BiP dissociates from these proteins and assists with the protein-folding thanks to its ATPase activity. Subsequently, the ER-sensing transmembrane proteins oligomerize and activate the UPR [247]. There are three main ER stress-sensing pathways, all initiated by these ER-sensing proteins located in the ER membrane[249] (Figure 7).

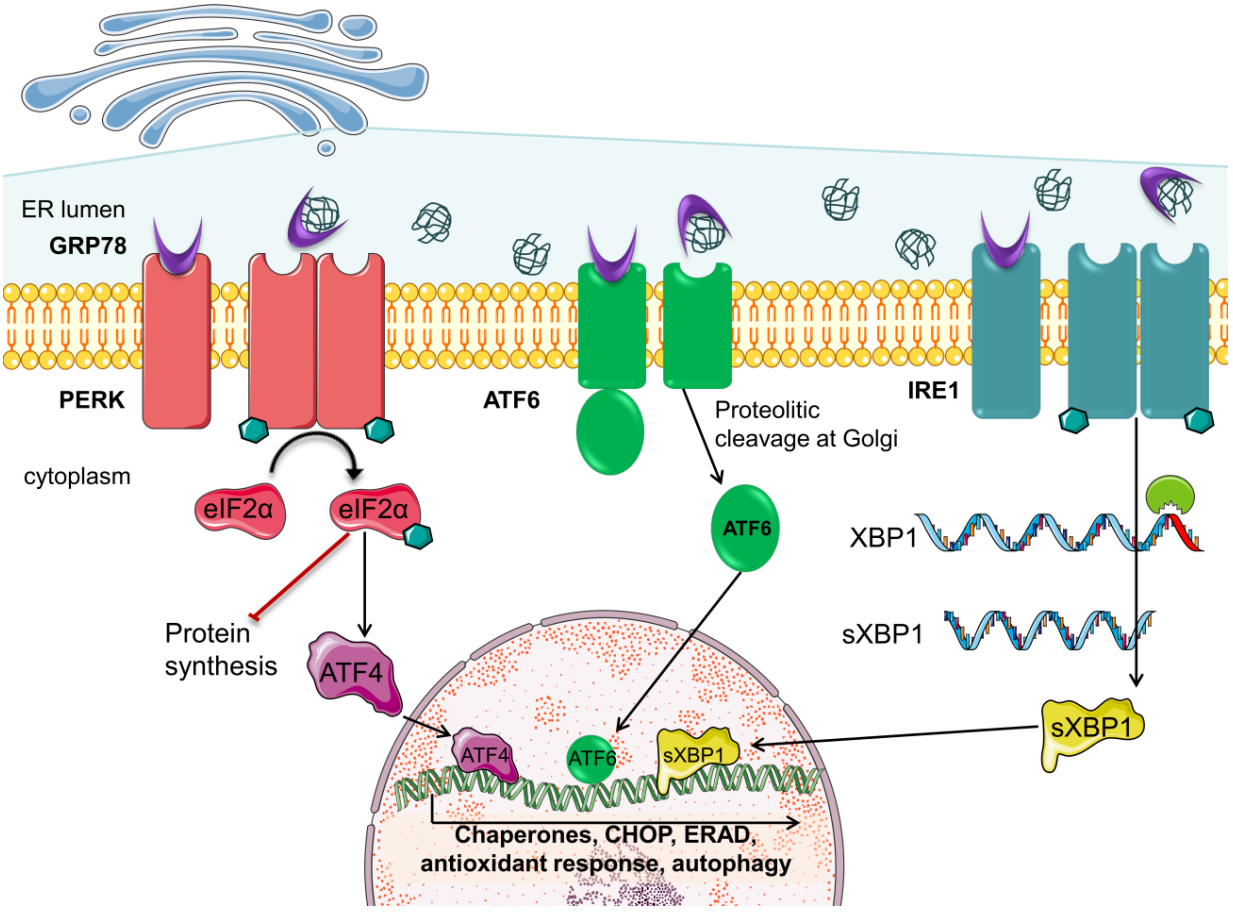

Figure 7: Representation of the three main UPR pathways. Upon ER stress, the protein chaperone GRP78 binds unfolded proteins, activating the intermembrane proteins PERK, ATF6 and IRE1. PERK can dimerize and phosphorylate, activating their kinase activity. This pathway depends on the phosphorylation of eIF2α, which inhibits general protein expression and allows eIF2α-independent genes to be expressed, such as ATF4. ATF6 activation exposes a Golgi location signal, which provokes its translocation and processing, releasing the transcription factor ATF6. Lastly, the IRE1 protein dimerizes, activating its endoribonuclease activity, which processes XBP1 to sXBP1, producing a transcription factor. Globally, the transcription factors in which these pathways culminate activate the transcription of chaperones, CHOP, ERAD, antioxidant defences and autophagic flux. GRP78= glucose-regulated protein 78; PERK= PKR-like endoplasmic reticulum kinase; eIF2α= eukaryotic initiation factor 2 alpha; ATF4= activating transcription factor 4; ATF6= activating transcription factor 6; IRE1= inositol-requiring enzyme 1; XBP1= x-box binding protein 1; CHOP= C/EBP homologous protein; ERAD= endoplasmic reticulum associated protein degradation.

The first of these pathways is initiated by inositol-requiring enzyme 1 (IRE1) (with two isoforms, IRE1α and β), a transmembrane receptor located in the ER membrane that, in presence of unfolded proteins, oligomerices and activates two of its catalytic domains by autophosphorylation: the kinase domain and the endoribonuclease domain [249,250]. The endoribonuclease activity regulates the mRNA splicing of the X-box binding protein 1 (XBP1) gene, activating its transcription. The spliced form of XBP1, namely sXBP1, encodes a basic leucine zipper (B-ZIP) transcription factor from the cAMP responsive element binding protein (CREB)/ATF family that transcribes genes regulated by UPR elements (UPRE) and ER stress elements (ERSE) promoters. The genes in question are protein chaperones that facilitate folding proteins and ERAD proteins which degrade the misfolded ones [249]. The IRE1 kinase domain binds to TNF-associated factor 2 (TRAF2), a scaffold protein that can recruit the kinase ASK. It is phosphorylated by IRE1 and activated, transducing its activation through the JNK and other signalling pathways. TRAF2 can trigger the apoptotic pathway through conversion of procaspase 4 to caspase 4 [251]. Generally, the IRE1 pathway activates ERAD activity and enhances protein folding through chaperone expression [252].

The second pathway also culminates in either apoptosis or ER management of unfolded proteins, and the initiating protein is the transmembrane protein protein kinase RNA-like ER Kinase (PERK). Under ER-stress, PERK oligomerices and activates by autophosphorylation. Its kinase domain phosphorylates the eukaryotic initiation factor 2α (eIF2α) and inhibits its activity. As eIF2α is the only protein that recruits the 80s subunit of the ribosome for initiating protein synthesis, PERK activation slows the *de novo* protein synthesis. In parallel, the protein phosphatase growth arrest and DNA damage-inducible protein (GADD34) is activated by PERK signalling, and it dephosphorylates eIF2α thereby counteracting PERK activation [253]. Only a small subset of genes which have upstream open reading frames (uORFs) in the 5' leader can be

translated without eIF2α. The most relevant one is activating transcription factor 4 (ATF4), a B-ZIP transcription factor from the CREB family, whose targets are aminoacid response elements (AAREs) present in target promoters from ER chaperones (among which is GRP78/BiP), antioxidant defences, protein anabolism and apoptotic transcription factors such as CCAAT-enhancer-binding protein homologous protein (CHOP). CHOP is able to increase the amount of GADD34, thus restoring protein translation, and is also believed to increase oxidative stress through ERO1α expression and apoptosis through inhibition of B cell CLL/Lymphoma 2 (Bcl2) [246,254]. Conversely, it can form heterodimers with CCAAT enhancer binding protein (C/EBP) transcription factors and transcribe genes involved in ER stress response. Other genes with 5' uORFs apart from ATF4, such as C/EBP, activating transcription factor 3 (ATF3), activating transcription factor 5 (ATF5), CHOP, CREB, JUN and FOS, are transcribed under eIF2α phosphorilation [255–258]. Although PERK is the most pro-apoptotic ER stress-related pathway, novel protective mechanisms, such as NRF2 phosphorylation by PERK kinase activity, are also under investigation [259,260].

The third pathway is initiated by a family of transmembrane ER proteins of which the B-ZIP transcription factor activating transcription factor 6 (ATF6) is the most representative [261,262]. This family, unlike PERK and IRE1α, is not ubiquitous, but has analogs in most cell types [263]. ATF6 is itself a transcription factor with a nuclear locating signal masked by GRP68/BiP. Under ER stress, the nuclear-locating sequence (NLS) is exposed, forcing ATF6 translocation to the Golgi [246]. There, specific proteases SP1 and 2 cleave the transmembrane domain by regulated intermembrane processing (RIP) [248,264,265]. The B-ZIP domain of ATF6 is then translocated to the nucleus and binds the transcription factors nuclear transcription factor Y (NFY) and Yin-Yang 1 (YY1) to transcript genes with ERSEI and ERSE II sequences on its promoters. These genes are the same ER-stress protecting genes as ATF4 and the XBP1 transcription factors related to the

protective pathways [261]. Indeed, ATF6 expresses XBP1, acting synergistically with the IRE1α pathway[266,267].Despite ATF6 usually functioning as a rescue pathway, it has been related to apoptotic activation in some cell types, including endothelial cells [268].

All these pathways integrate with transcript specific genes. Most of these proteins are the same ones involved in the UPR, namely PERK, IRE, XBP1, BiP/GRP78, ATF6, CHOP or ATF4 [269]. However, many other proteins involved in other proteostatic processes, such as protein import, trafficking, folding and disulfide bonding, are also stimulated, especially by XBP1 and ATF6 [270] as are transcription factors like C/EBP, or other chaperones, such as microvascular-endothelial differentiation gene 1 protein (MDG1)/ER-localized DnaJ 4 (ERdj4) [271], cysteine-rich with EGF-like domains 2 (CRELD2) and asparagine-linked glycosilaton 12 (ALG12) [272]. Proteins involved in metabolism regulation are also activated by UPR; for example phosphoenolpyruvate carboxykinase (PEPCK) [273]. Regarding apoptotic genes, pro-apoptotic genes such as tribbles homolog 3 (TRB3), keratin 16 (KRT16), hexokinase domain component 1 (HKDC1) and niban-Like protein 2 (NLP2) are stimulated via their specific CHOP response elements (CRE) or ERSE [274,275].

In a situation of ER stress, all UPR pathways become activated in a given sequence to prevent direct apoptosis of the affected cell and to activate rescue mechanisms. Their combined activation initiates survival mechanisms involving ER stress chaperones, reduced protein synthesis and clearance of misfolded proteins. Proapoptotic pathways are also activated to a slight extent, but the protective mechanisms outweigh the cell death ones. If after a time the ER stress is not eventually resolved, the protective mechanisms are attenuated and proapoptotic mechanisms become dominant , leading to cell death [246].

1.2.3.1. Endoplasmic reticulum stress in T2D

ER stress affects cells involved in T2D pathogenesis possibly, by causing apoptotic death. Resolving ER stress through activation of UPR is one of the rescue mechanisms that cells activate

to prevent cell death, and which seem to be overactivated or hampered in T2D. In a ob/ob or HFD diabetic mice model it has been established that ER stress causes IR, and that PERK pathway activation is needed for ER stress alleviation through UPR [276]. Moreover, treatment of diabetic mice with chemical chaperones has been shown to reduce ER stress and improve glucose tolerance and insulin signalling [277]. The cells most affected by ER stress are those with more synthetic and secretory functions, such as adipocytes and β pancreatic cells.

It is believed that ER stress in β cells can increase inflammatory status by accumulation of modified proteins that act as autoantigens [278,279]. A recent review has proposed that ER stress is the most important trigger of β cell apoptosis [280]. In this sense, it is established that the glucose-stimulated IRE2α pathway prevents ER stress through sXBP1-dependent expression of proinsulin biosynthesis proteins[281,282]. This pathway is important for β cell function, as deletion or inhibition of IRE1α causes defects in proinsulin processing and synthesis, which cannot be compensated by PERK or ATF6 signalling. Despite these positive effects, one study demonstrated that sustained production of XBP1 leads to β cell failure and death [283]. PERK is also implicated in this controversial situation, as it seems to have opposing roles: its inhibition in animal models improve insulin sensitivity, secretion and glucose metabolisms in β cells [284,285], while *in vitro* studies have demonstrated that its stimulation promotes insulin release through calcineurin signalling [286]. The ATF6 pathway is necessary for cell survival, even in unstressed cells; if deleted, the JNK pathway is activated, leading to cell death [287]. In addition, it has been demonstrated that the JNK pathway is vital for XBP1 expression in mice islets [288]. Like the other two UPR pathways, ATF6 has controversial roles in pancreatic β cells [289]. Despite the dual role of ER pathways in β cell survival, the consensus is that UPR pathways aid basal insulin synthesis and hyperactivate upon ER stress, but if chronically activated or defective, as occurs in T2D, they can lead to β cell apoptosis [290–292]. Indeed, UPR is activated in PBMCs of T2D patients who do not meet glycaemic

goals, a possible consequence of high oxidative stress, inflammation or hyperglycaemia [293].

ER stress does not affect exclusively pancreatic β cells; indeed, it can affect a variety of cell types, such as adipocytes, muscle or liver, leading to the development or aggravation of IR [294]. It has been proved that UPR pathways are activated in different diabetic or insulin-resistant animal models [295,296]. However, if this stimulus is sustained over time, UPR pathways faint, giving way to apoptotic stimulus initiated by CHOP and JNK, unchaining the apoptotic caspases [297,298]. This can lead to hepatic dysfunction in the form of hepatic inflammation due to the immune infiltration, hepatic steatosis, NAFLD, and other hepatic complications related to diabetes [299,300]

Regarding muscle cells, the PERK pathway is induced by FFA overload or palmitate treatment thus leading to the production of myokines [301,302]. OxLDL also causes PERK activation, which leads to JNK pathway signalling and autophagy in aortic smooth muscle rat cells [303]. Cardiac muscle cells are more related with T2D complications and are also affected by ER stress. Indeed, in cardiac muscle from streptozotozin diabetic mice, palmitic acid was shown to induce all 3 UPR pathways [304]. In this situation, ROS produced by diabetes stimulates PERK, which causes ER stress and apoptosis [305]. Another study of diabetic cardiomyopathy determined that IRE1α is also responsible for cardiac muscle dysfunction and apoptosis through CHOP and JNK signalling [306].

Adipocytes are also altered by ER stress; indeed, PERK and IRE branches are activated in hypoxic 3T3-L1 adipocytes under glucose starvation (a situation typical of IR) [307,308]. Moreover, stimulation of the receptor RAR-related orphan receptor α (RORα), which is involved in inflammation, activates the same UPR pathways as hypoxia, confirming that UPR activates as a rescue mechanism in adipose tissue [309]. In this sense, preconditioning of 3T3-L1 adipocytes with low doses of tunicamycin (ER stimuli) or overexpression of XBP1 has been shown to inhibit inflammation when stimulated with FFA [310].

Another cell type higly affected by ER stress are immune cells, due to their direct contact with generalized hyperglycaemia and hyperlipidaemia. An experimental model of hyperlipidaemia consisting of 5h intravenous lipid infusion caused UPR activation in PBMCs from healthy subjects [311]. The same observation has been made in T2D patients [312–314], who have high circulating lipid levels by default. Immune infiltration of hepatic and adipose tissue also occurs in T2D, aggravating IR through production of cytokines [315,316]. ER stress can lead to more proinflammatory profiles in leukocytes, affecting different tissues.

Considered together, UPR pathways are an effective rescue mechanism when ROS accumulation and cellular stress facilitate unfolded or modified proteins. However, if this stress is sustained, apoptotic activation occurs as a protection mechanism.

1.2.4. Autophagy

Autophagy is defined as a self-eating process activated by certain stimuli and carried out by double-membrane vesicles (autophagosomes), which fuse with lysosomes to digest their content. There are three main types of autophagy: macro-autophagy, micro-autophagy and chaperone-mediated autophagy [317,318]. All three pathways culminate in lysosomal digestion of cellular or extracellular material, but they diverge in the delivery mechanism.

1.2.4.1. Types of autophagy

1.2.4.1.1. Macroautophagy, chaperone-mediated autophagy and microautophagy

Macroautophagy is the best characterized form of autophagy. It involves the formation of large vesicles named autophagosomes that enclose big portions of cytoplasmic material and organelles that end up fusing with lysosomes. Thus, macroautophagy has an important catabolic function [317,319]. The process begins with the formation of the preautophagic structure, about which diverse theories have been raised. There are two main possibilities: the nucleation of the

membrane from other organelles or budding from an already existing membrane.

The first approach has been explored very little; however, it seems that the mechanism is initiated by autophagy-related 17 (ATG17), which acts as a scaffold protein for ATG13p [320] and ATG9-containing vesicles [321]. From this nucleation point, ATG2-ATG18 [322]and ATG8-ATG16-ATG5 complexes generate autophagosomes [323–325]. Subsequently, ATG8 and ATG12 will participate in expanding the membrane and receiving the cargo.

Regarding the second mechanism, 4 sequential steps culminate in the formation of a preautophagosome. The first step is the assembly of the Unc-51 Like autophagy-activating kinase (ULK) complex, composed of ATG13, fak-family interacting protein of 200 KDa (FIP200), ATG101 and ULK, which are recruited to ATG9 or vacuolar protein sorting 34 (Vps34)-containing vesicles [326]. Accumulation of ULK complexes and their activation is the first step in the initiation of autophagosome biogenesis [327,328]. ULK complex activity depends on mTORC and AMPK activity. mTORC inhibits ULK activity through ATG13 phosphorylation [329,330]. AMPK is the best known mTOR best known inhibitor, which is also able to directly activate ULK [331]. ULK accumulation is produced in ER domains enriched in phosphatidilinositol synthase, VAPA and VAPB via FIP200 interaction. This creates a differentiated membrane domain where some autophagic proteins are recruited [332] and phosphorylated [333], such as ATG4B, ATG9, ATG14L, coiled-coil myosin-like BCL2-interacting protein 1 (Beclin-1) or activating molecule in beclin-1-regulated autophagy protein 1 (AMBRA1) [334–338].

The second step begins with ULK phosphorylation of ATG9, resulting in the retention of vesicles with PI3K complexes. These vesicles are needed for expanding the autophagosomal membrane [333,339]. PI3K complex is formed by ATG14L, Beclin-1, VPS34 and nuclear receptor-binding factor 2 (NRBF2), and its function is to synthesize PI3P through VPS34 in the nascent membrane and to expand it, which is the third step [340].

In the fourth step, WD-repeat protein interacting with phosphoinositides (WIPI) proteins are attached to these PI3P-enriched regions and recruit two ubiquitin-like conjugation systems, which leads to ATG16L activation:

- ATG3, ATG7 and ATG16L complex, formed by ATG12, ATG5 and ATG16L1, which conjugates phosphatidiletanolamine to ATG8 isoforms [341,342].
- ATG7 and ATG10, which conjugate ATG5 to ATG12 and together form a complex with ATG16L [343].

ATG16L complexes accumulate in the convex side of the nascent autophagosome, where they activate ATG8 proteins by lipidation. The ATG8 family promotes autophagosome expansion by tethering of membrane-supplying vesicles and recruiting other proteins to the isolation membrane, such as the ULK complex [344]. ULK phosphorylates ATG4 to inhibit its delipidating activity, promoting the expansion of the membrane [345].

ATG8 concentration causes the curving of the nascent membrane, together with actin proteins [346,347] forming the omegasome. This curved region is energetically unstable, finally bending and becoming spontaneously spherical [348]. The small pore that remains after the shape change is closed thanks to the endosomal sorting complex required for transport (ESCRT) machinery [349]. The autophagosome then separates from the original membrane and completes its maturation. Once autophagosomes are formed, they can fuse with late endosomes or lysosomes to form amphisomes or autolysosomes, respectively. The fusion process is carried out by proteins that help to overcome the energetic imbalance, and consists of supposes the breakage of two membranes [350,351]. In the case of autolysosomes, ATG14, lysosome-associated membrane protein 2B (LAMP2B) and a protein of the ATG8 family, Microtubule-associated protein 1A/1B-light chain 3 (LC3), also take part in the process [352–354]. When the autophagolysosome is formed, the acidified lumen of the lysosome degrades the cargo and the

inner autolysosomal membrane [355].

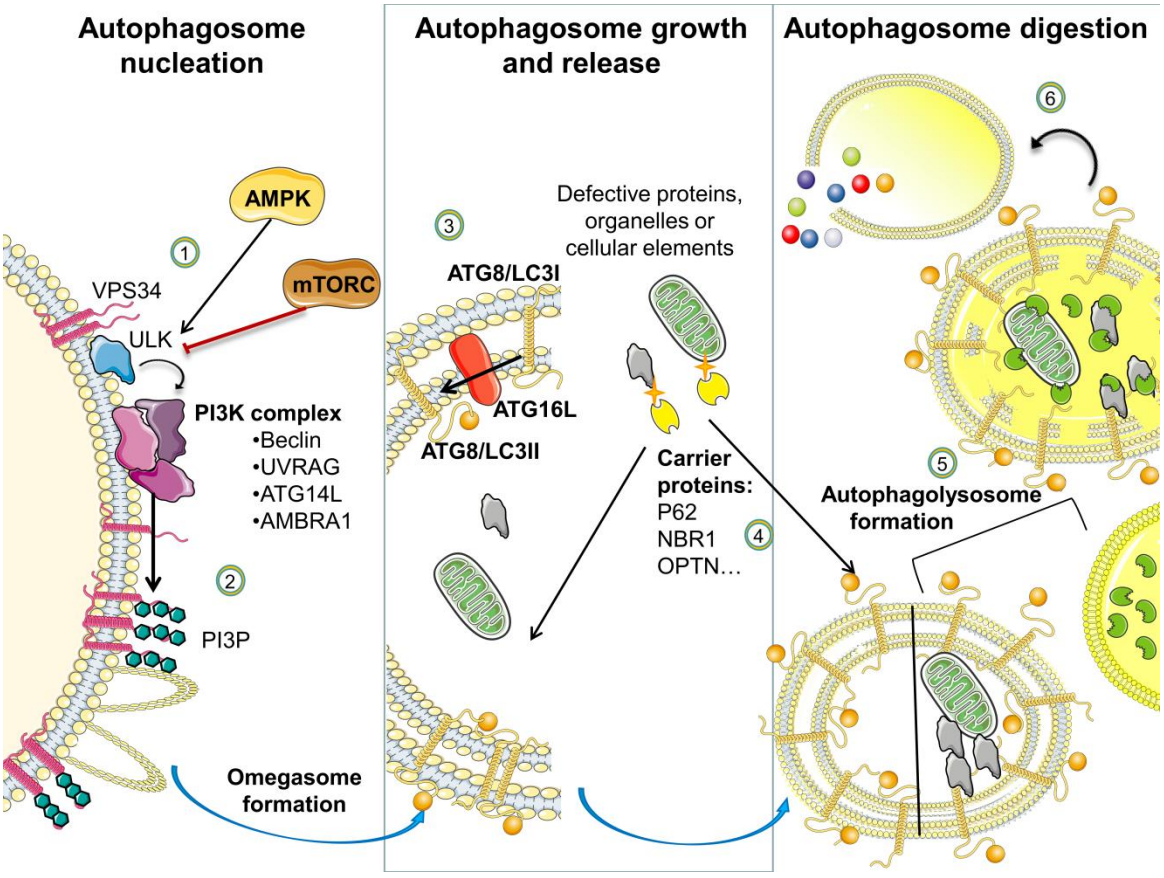

Figure 8: Schematic representation of autophagosome formation, maturation and digestion. The first steps consist of autophagosome nucleation by activation of ULK and PI3K complexes and induces (1) PI3P synthesis (2). Second, accumulation of PI3P creates a domain to recruit ATG16L, which lipidates ATG8, causing the bending of the growing membrane forming the omegasome (3). Meanwhile, defective cellular components are transported by carrier proteins to the nascent autophagosome, or are traslocated to the formed autophagosome (4). Once the autophagosome is closed - including all the elements destinated for degradation - it fuses with a lysosome (5). The autophagolysosome becomes acidified with lytic enzymes that digest the autophagolysosomal content, and it eventually releases the digestion products to the cytoplasm (6). VPS34= vacuolar protein sorting 34; AMPK= AMP-activated protein kinase; ULK= Unc51´like autophagy activating kinase 1; PI3K= phosphoinositol-3 kinase; UVRAG= UV radiation resistance-associated gene protein; ATG14L= autophagy related protein 14L; AMBRA= activating molecule in Beclin-1 regulated autophagy; PI3P= phosphoinositol-3-Phosphate; ATG8/LC3I= autophagy related protein 8/microtubule associated protein 1A /1B light chain; ATG16L= atophagy regulated protein 16 like; p62= ubiquitin binding protein 62; NBR1= neighbor-of-BRCA1-like binding protein 1; OPTN= optineurin;

Over time, it has has been established that the core proteins for correct macroautophagic processes are ATG3, ATG5, ATG7, ATG9, ATG13, ATG16L, ULK, VPS34 and Beclin-1 [356]. However, autophagic pathways independent of these proteins have also been discovered, supporting a high degree of redundancy in protein function and the existence of non-canonical autophagic pathways which rely on other proteins [317,356].

The other best known mechanism of autophagy is chaperone-mediated autophagy (CMA). This involves the direct delivery of proteins targeted for lysosomal degradation [357,358]. CMA only degrades proteins with a KFERQ sequence bound to heat-shock protein A8 (HSPA8)/ heat-shock protein 70 (HSP70) chaperone [359]. The tagged proteins are carried to the LAMP2A complex in the lysosomal membrane. Once in the lysosomal lumen, a pool of heat-shock protein 90 (HSP90) and glial fibrillary acidic protein (GFAP) proteins stabilize the defective proteins, which are later degraded [359,360]. The CMA is regulated by the simultaneous presence of mTORC, AKT and pleckstrin homology domain leucine-rich repeat protein phosphatase (PHLPP1) in the lysosomal membrane [361]. This form of autophagy is vital in physiological and pathological processes such as aging, neurodegeneration, or T-cell activation [357].

Microautophagy is another type of autophagy carried out in yeast and plants through direct invagination of the cytoplasm by the vacuolar membrane. In mammals, a similar process has been seen in late endosomes and has been coined endosomal microautophagy [362,363]. It is able to degrade peroxisomes (micropexophagy), portions of nucleus, damaged mitochondria, lipid droplets and cytosolic proteins with the KFERQ sequence. This last mechanism depends on its recognition by the chaperone HSPA8, also named Hsc70 [364]. Microautophagy does not share the same mechanism for the formation of endosomes. Some require ATG proteins and other require the ESCRT system [362,364,365]. This selective endosomal microautophagy differs from CMA in its independence of LAMP2 [364].

1.2.4.1.2. Selective and non-selective autophagy

Autophagy processes can also be classified depending on the selectivity of the degraded material. Macro and microautophagy can uptake cytoplasmic portions in a non selective way; namely, non-selective autophagy. In contrast, CMA and also macro and microautophagy can operate through selective autophagy, in which determined receptors recognise specific motifs or sequences that deliver the molecules or organelles to the autophagic degradation pathway [366,367].

Selective autophagy depends on a wide range of specific receptors that recognize determined motifs that determine the organelle or molecule to be engulfed.

- Mitophagy can be triggered physiologically in erythrocyte maturation, where it relies on BCL2/adenovirus E1B interacting protein 3-like (BNIP3L/NIX) recognition, or in embryonic development. This latter process depends on the fission and loss of membrane potential, upon which prohibitin 2 (PHB2) and the PTEN-induced kinase (PINK)-PARKIN system tags mitochondria to be recognizable by specific receptors [368,369], including LC3, sequestosome 1 (p62/SQSTM1), Optineurin (OPTN), and Nuclear Dot protein 52 (NDP52) [369–371]. Other specific cases have also been documented: Cardiolipin can also bind to LC3 upon mitochondrial damage, and FUN14 domain containing 1 (FUNDC1) acts as an autophagy receptor under hypoxia [372–375].
- Pexophagy (autophagy of peroxisomes) is carried out by peroxisome biogenesis factor 2 (PEX2) and PEX3-dependent ubiquitination of PEX5 and ATP-binding cassette subfamily D member 3 (ABCD3), which is recognized by p62 and next-to BRC1A autophagy cargo receptor 1 (NBR1) [376,377].
- Nucleophagy has two mechanisms: the first requires nuclear-vacuolar junctions 1 (Nvj1) as an autophagy receptor and Vacuolar protein 8 (Vac8) and oxysterol-binding

protein (OSBP) for forming the invagination; and the second does not require some of the classic ATG nor the autophagy receptor ATG39. In mammals, lamin B1 is responsible for regulating nucleophagy [378,379].

- Reticulophagy consists of the autophagy of ER portions, and there is a debate about its mechanisms. One theory is that it is regulated by Ypt1, a Rab GTPase, while others point to the function of family with sequence similarity 134 member B (FAM134B) or ATG11 [380,381].

- Aggrephagy is the process by which protein aggregates are recognized and degraded, representing an important step in cellular homeostasis. In mammals, it depends on autophagy receptors p62, NBR1, OPTN, toll-interacting protein (TOLLIP) and tectonin β-propeller repeat containing 1 (TECPR1)[382–385].

- Lipophagy is the selective degradation of neutral lipid droplets, and is carried out by the general machinery of macroautophgy when activated through farnesoid X receptor (FXR), PPARα and CREB transcriptional programs [386,387]. Also, CMA-dependent degradation of certain lipid droplet proteins such as perilipin 2 (PLIN2) and 3 precedes and facilitates lipolysis [386,388].

1.2.4.2. Autophagy regulation

Various cellular stresses of different natures can activate autophagy, from hypoxia to proteostatic distress, and from nutrient scarcity or oxidative stress. The primary trigger for activating autophagy is nutrient stress, sensed by rat sarcoma (Ras)-cAMP-PKA and mTOR pathways.

The Ras-cAMP-PKA signalling pathway consists of the activation of adenylyl cyclase by the GTP-binding protein Ras, which leads to the synthesis of cyclic AMP (cAMP). Increases in cAMP activate PKA, which can modulate autophagic proteins. This pathway is activated through

glucose or glycolysis metabolites upon nutrient presence [389,390]. In *Saccharomyces cerevisiae* it has been determined that ablation of this pathway leads to activation of autophagy, while its hyperactivation blocks autophagic flux [391]. Inhibition of autophagy has been also described upon PKA activation in endothelial cells, which marks ATG16L for degradation by phosphorylation [392]. The PKA protein is inhibited by most autophagy activators in *S.cerevisiae*, and is activated by mTOR [393,394]. The interaction between PKA and autophagy was further confirmed in a mammal cell model through the phosphorylation and inhibition of ULK by its transport to the nucleus [395]. The relationship between nutrient intake and PKA was also further confirmed in rat muscle cells, in which neuropeptide signalling inhibited autophagy through PKA-dependent inhibition of LC3 [396]. In conclusion, RAS-cAMP-PKA inhibits autophagy when stimulated by nutrient presence.

mTOR signalling has been widely studied in the nutrient sensing field. This protein belongs to the PI3K family and is only active as a complex (mTORC1 and mTORC2). mTOR complexes are regulated by nutrient and energetic state sensors. Insulin and insulin growth factors activate PI3K, AKT and tuberous sclerosis complex 2 (TSC2), which inhibit Ras homolog enriched in brain (Rheb) and mTOR. Energetic stress signals through high AMP levels and activates AMPK, which phosphorylates TSC, thus inhibiting mTORC1. This is also achieved under GLUT1 inhibition or low O_2 concentrations. Finally, aminoacid starvation also signals for mTORc inhibition mainly through Sestrin2, cytosolic arginine sensor for mTORC1 (CASTOR) and S-adenosyl-methionine sensor upstream of mTORC1 (SAMTOR) [397]. mTOR, when activated, inhibits autophagy by phosphorylating ATG13 and ULK1 [398,399].

An important node for energetic metabolism that influences autophagy through many pathways is insulin signalling. The common trigger is the dimerization and autophosphorylation of IRS1 and 2, which generates a scaffold where many class I PtdIns3K proteins can dock and generate PIP3. These domains recruit PKB and AKT proteins to the membrane, where their

activator phosphoinositide kinase 1 (PDK1) is located. These signals influence autophagy by several approaches: AKT enhances mTORC activity, which inhibits autophagy [400–402]; retrograde signalling has also been observed, by which ATG7 inhibits AKT signalling thanks to c-JUN and PTEN signalling [403], and ATG16L deficiency causes the proteasomal degradation of IRS [404]

One of the main energy-sensing mediators is the AMP-activated protein kinase (AMPK) [405,406]. It activates autophagy only when serine 317 and 377 are phosphorylated. p-AMPK activates the ULK-FIP200-ATG13 complex without affecting the activity of its kinase domain [331]. Moreover, AMPK phosphorylation is necessary for ULK activity and autophagy activation under glucose starvation. AMPK is also necessary for autophagosome maturation and further fusion with the lysosome, as demonstrated in HEK293T AMPK KO cells [407]. Morevoer, it is involved in activating processes that include other autophagy-related proteins, such as WIPIs [408], Beclin-1, or ATG9 [406].

On another level, we can find the transcriptional and post-translational (phosphorylation and acetylation) regulation of autophagy [409,410]. One of these mechanisms is directed by the transcription factor EB (TFEB), a transcription factor retained in the cytosol by mTOR phosphorylation. When mTOR is inhibited, TFEB can translocate to the nucleus and express ATG4, ATG9B, LC3, UV radiation resistance associated gene protein (UVRAG) and WIPI [411,412]. Other modulators are ERK and calcineurin, which can phosphorylate TFEB in response to nutrient availability [413,414]. Conversely, protein phosphatase 2A (PP2A) dephosphorylates TFEB under oxidative stress [415]. Other important regulator of autophagy gene expression is Forkhead box O1 (FOXO). When activated by phosphorylation, FOXO activates the expression of ATG4, ATG5, ATG14, ATG12, BECN1, BNIP3, LC3B, ULK, VPA34 and gamma-aminobutyric acid receptor-associated protein like 1 (GABARAPL1) [416–419]. FOXO1, 2 and 3 are regulated by AKT phosphorylation in response to growth factors and insulin stimulation, producing its cytoplasmic

retention. FOXO1 can be activated and induces autophagy in situations of oxidative stress or serum starvation through binding to ATG7.

At another level of modulation, E2 transcription factor 1 (E2F1) and NFκB regulate autophagy through expression of the carrier protein BNIP3, which activates autophagy by dissociating Beclin-1-BCL2 complex. NFκB constitutively inhibits the binding of E2F to its promoter and impedes BNIP3 expression [420]. E2F itself has a wide range of autophagy-related target genes, such as ULK, ATG5 or LC3 triggered by hypoxia [421].

Lastly, the CREB-FXR and PPAR-FXR transcriptional circuits have recently been described as key players in autophagy regulation [387]. CREB upregulates some autophagy genes in fasting conditions, which are otherwise inhibited by FXR. This transcription factor can also be paired with PPARα, a nutrient sensing regulator, having the same negative feedback loop as CREB and FXR [409,410]. Under nutrient starvation, PPAR and CREB can occupy their promoter regions in LC3 and ATG7 genes to induce their expression [422].

Epigenetic regulation by some proteins is also relevant in the transcriptional regulation of autophagy genes. SIRT1, a histone deacetylase, can induce autophagy directly by deacetylating ATG7, LC3, FOXO1 and FOXO3 [409,423]. It also deacetylates liver kinase B1 (LKB1), thereby activating AMPK and inhibiting mTOR signalling [424].

In conclusion, autophagy is a tightly regulated process at different levels. Almost all cellular stresses can trigger autophagy, leading, or not, to apoptotic activation. However, the objective of autophagy is to prevent cellular death by activating catabolic processes and degrading damaged cellular components.

1.2.4.3. Autophagy and T2D

The autophagic process has been widely studied in T2D subjects, although a firm consensus about its activation or inhibition has not been reached. This is, in part, due to

differences in the recruited cohort and the level of glycaemic control. In pancreatic β cells autophagy seems to be a protective mechanism under a diabetogenic diet [46,425]. Indeed, blocking autophagy leads to the development of β cell failure and subsequent diabetes [426,427]. In human pancreatic islets from T2D donors with ER stress, induction of autophagy resulted in an improvement of the β cell mass survival and insulin secretion, reinforcing the protective role of autophagy in pancreatic β cells [428]. Specifically, the organism has physiological mechanisms to protect β cell mass, such as production of IL-6, which stimulates autophagy in pancreatic islets by signal transducer and activator of transcription 3 (STAT3) signalling [429]. Conversely, liver tissue displays reduced autophagy in T2D, and most treatments prevent liver damage by upregulating this process [430–432]. The inhibiting mechanism could imply inactivation of SIRT 1 [433] or alterations of AMPK and mTOR signalling, as evidenced by some studies [434,435]. Other approaches, such as endocrine signalling through endogenous molecules such as fibroblast growth factor 21 (FGF21) or FGF1, activate autophagy and prevent liver damage and lipid accumulation [433,436]. Furthermore, it has been described that miRNA199a-5p regulates insulin sensitivity through autophagy activation in HFD fed mice [437].

Muscle tissue experiments have not led to a consensus regarding autophagy regulation in T2D. For example, autophagy genes and proteins were reported to downregulated in muscle cells from insulin-resistant T2D patients [438]. However, another study performed in cardiac muscle from T2D and healthy subjects concluded that autophagy is overactivated in T2D samples, specifically by Beclin-1 upregulation, leading to apoptosis [439]. The same effect is produced in vascular smooth muscle cells (VSMC) under high glucose or diabetic conditions, with an increase of some autophagic markers which contributes to VSMC phenotype switching [440]. Furthermore, it was also observed in VSMC that AGEs stimulate autophagy through the RAGE receptor and AKT, JNK and MAPK signalling [441]. Despite these results, one study found no differences in

autophagy between skeletal muscle samples from hyperglycaemic T2D patients and healthy subjects, which could mean that autophagy can adapt to hyperglycaemia [442,443]. Similar results in T2D models of myotubes and mice determined that autophagy was downregulated, even in insulin-resistant hyperinsulinemic states, through mTOR inhibition [444].

Autophagy is also enhanced in adipose tissue from T2D [445,446], metabolic syndrome [447] or obese subjects [448]. A protective mechanism against ER stress and inflammation can be hypothesized, possibly mTOR inhibition [449] or direct interaction of the ER pathway and autophagic machinery [450]. Moreover, inhibition of autophagy in adipocytes can induce IR, mitochondrial mass content, lipid peroxide production and activation of antioxidant response [451].

Few studies have been performed in leukocytes from T2D patients. Some of them have concluded that autophagy is inhibited in T2D leukocytes and is linked to increased inflammation markers [452]. The defect could be at the level of lysosome fusion with the autophagosome [453]. Other research has shown that ROS and RNS induce autophagic activity in dyslipidaemic T2D patients, acting as a rescue mechanism [454]. Indeed, autophagy is hyperactivated in palmitate-treated leukocytes from T2D patients, and if blocked, palmitate causes apoptotic cell death [455]. Hence, autophagy may be activated in a hyperlipidaemic situation to prevent apoptotic death. In general, the results concerning autophagy in leukocytes from T2D patients are controversial.

1.2.5. Interplay between oxidative stress, ER stress and autophagy

Cellular stress can be generated, amplified and signalled by the aforementioned pathways: ROS production, ER stress and autophagy. ROS production can lead to activation of autophagy or ER stress, but, at the same time, ER stress and autophagy can generate ROS. In the following section, the correlation between these 3 processes will be briefly explained.

ROS can be produced in the ER and in mitochondria under cellular stress. In the ER, ERO1α produces H_2O_2 in order to reduce PDI, the main folding protein in the ER [91]. In addition,

NOX4 is located in the ER surface and is activated under extended ER stress [456,457]. The interconnection between ER and mitochondria ROS production is explained by calcium release by the inositol-1,4,5-phosphate receptor (IP3R) channels in the ER [458]. Mitochondrial uptake of the ER-released calcium stimulates OXPHOS and induces the accumulation of H_2O_2, which enhances ROS production. Ca^{2+} release can also be triggered by phospholipase C (PLC) under high lipid content and is accompanied by high ROS production through NOX expression [459,460]. This relationship between ROS and ER stress can be continued when the UPR response triggers CHOP expression, which induces the ERO1α-dependent production of more ROS [461,462]. Conversely, ERO1α also induces IP3R-mediated calcium leakage, activating Ca^{2+}/Calmodulin-dependent protein kinase III (CAMKIII) which can activate apoptosis and NOX2 expression and ROS production [461,463]. The accumulation of ROS can modify proteins that remain unfolded and impairs the folding capacity of the ER and exacerbates the feedback loop [464,465]

Autophagy regulation is also responsive to cellular stresses such as high ROS production or proteostatic dysbalance. However, due to the double-edged nature of autophagy, it is activated to overcome the initial cellular stress, but, if the stress remains, acts as an initiator of apoptotic cell death [466,467]. It is important to highlight certain studies which suggest that autophagy is stimulated by H_2O_2-triggered ER stress *per se* [467] due to signalling through IRE1α/JNK and direct XBP1 induction: JNK phosphorylates BCL2, thus impeding its interaction with Beclin-1 and activating autophagosome formation [468,469]; likewise, sXBP1 induces autophagy by Beclin-1 transcriptional activation [470], while its absence induces FOXO activation and autophagy induction in neurons [471]. The UPR pathway initiated by ATF4/eIF2α and CHOP also stimulates autophagic genes and enhances autophagic flux in order to maintain cellular integrity [472–475]. Although CHOP is induced by autophagy, it performs a dual role by activating autophagy or apoptosis through different genes depending on the duration of the stress [476,477]. Another way

by which ER stress triggers autophagy is through inhibition of AKT phosphorylation by its regulators mTORC and TSC [478–480]. Similarly, AMPK signalling, a well known mTOR inhibitor and autophagy activator, is also induced by ER stress [481–483].

Furthermore, as happens with ROS and ER stress, autophagy is also related with ER stress and UPR through calcium signalling. It has been demonstrated in neurons, in which it has been determined that GRP78 binds to calcium and senses unfolded protein accumulation, but also buffers calcium alterations and mitochondrial function after stress [484]. Other calcium sensing proteins - usually calmodulins or calnexins - can transduce calcium alterations to other molecular pathways. As an example, under loss of calcium homeostasis in the ER due to depletion of luminal ER calcium during ER stress, CaMKKb can trigger AMPK phosphorylation and activation of autophagy [485].

The relation between autophagy and ROS production has also been widely studied, as ROS production and accumulation usually activate autophagy. Under starvation conditions, cells produce ROS, which oxidize Cys81 on the Atg4 protein, which in turn increases the amount of lipidated LC3, thus inducing autophagosome formation [486]. Moreover, starvation stress decreases GSH, which causes an imbalance in oxidized/reduced thiol compounds that activate autophagy [487–489]. AMPK is also stimulated under the same conditions by mtROS production in HeLa cells [490], and this activation might be due to the oxidation of AMPK α subunit seen in HEK293 cells [491]. A possible link between ROS sensing and AMPK is the oxidative stress sensing sestrin family of proteins [492], which are also stimulated by ER stress [483]. They can be activated by nutrient excess, which activates AMPK and NRF2, thus inducing autophagy [493]. LKB1 also transduces the signal between ROS and AMPK to activate autophagy [494], but it is believed that the LKB1 pathway is independent of ER stress [495].

In conclusion, as previously mentioned, oxidative stress modifies DNA and proteins,

causing a proteostatic imbalance and triggering ER stress and, eventually, UPR activation. UPR, cellular stress signalling and calcium signalling converge in autophagy activation with the objective of rescuing cells or leading to apoptotic cell death if the stress is sustained long enough.

1.3. T2D and cardiovascular risk

It is widely established that patients who suffer from T2D also present an increased risk of cardiovascular complications; namely, an approximately 32% greater likelihood of suffering a cardiovascular disease. Moreover, cardiac pathologies are more probable; specifically, 160% in the case of coronary heart disease, 127% in that of ischemic heart disease and 56% in that of haemorrhagic stroke [8]. Most of these diseases have an inflammatory basis involving malfunction of the endothelium and even atherosclerotic events. Indeed, atherosclerosis prevalence in T2D patients is 29.1% [496]. It is important to highlight that the risk of atherosclerotic cardiovascular disease is the same for patients with T2D without a history of myocardial infarction and people who have suffered a previous myocardial infarction [497].

Among all the cell types making up the cardiovascular system, endothelial and immune cells are two of the most important players in vascular risk, together with platelets and VSMC. Endothelial cells cover the inner surface of the vasculature, reacting to circulating blood cells and soluble molecules. Those molecules also influence the activation of circulating immune system cells. Circulating molecules can be produced by any endocrine organ, as well as by the vascular endothelium and immune cells themselves. Hence, the behaviour of endothelial cells and immune cells will depend to a high degree on the overall metabolic state. As in T2D, there is an altered metabolic state characterised by hyperglycaemia and hyperlipidaemia, which trigger the activation of endothelial and immune cells. A consequence is this one of the hallmarks of T2D: chronic generalized low grade inflammation, which is produced by endothelial and immune cell activation and function.

1.3.1. Inflammation and T2D

One of the traits of T2D as a chronic disease is generalised low grade inflammation [498]. This is reflected by elevated levels of inflammation markers and soluble circulating molecules

compared to those of healthy subjects. Research has reported elevated levels of C-reactive protein (CRP), interleukin 1β (IL-1β) or interleukin 6 (IL-6), which are predictive of T2D [499], and levels of interleukin 1 receptor antagonist (IL-1RA) have been shown to peak prior to the onset of T2D [500]. The main contributors of the circulating inflammatory cytokines are liver and adipose tissue their size and metabolic capacity. One of the main proinflammatory cytokines is tumor-necrosis factor α (TNFα), which is believed to be produced mainly by the M1 macrophages recruited by adipose tissue in response to nutrient excess [501,502]. These M1 macrophages produce most of the proinflammatory factors present in high levels in T2D upon TNFα and IL-1β stimulation. Nutrient excess also causes the activation of innate immune cells, which boost the production of the proinflammatory cytokines IL-1β and IL-6 [503–505]. Adaptive immune system cells also participate: CD8+ cells and Th1 cells contribute to IR [506], but Treg and Th2 cells counterbalance it [507,508]. Both types of immune cells contribute to the inflammation observed in T2D. In this sense, macrophage and lymphocyte infiltrates are observed in pancreatic tissue, which also displays fibrosis and amyloid deposits that stimulate the production of IL-1β [509]. This is particularly harming to pancreatic tissue, as it initiates an auto feedback loop that ends in auto-inflammation and β cell apoptosis [510].

Many inflammatory mechanisms have been proposed in T2D. Hypoxia is one of the driving mechanisms, found mainly in hypertrophic adipose tissue. Macrophages accumulate in the hypoxic regions, where they secrete proinflammatory and proangiogenic molecules [511]. If the hypoxia continues it causes cell death, manifested by characteristic crown-like structures consisting of macrophages surrounding an apoptotic adipocyte [512]. Cell death is also common in T2D in pancreatic cells, constituting an early event in T2D that recruits macrophages to the islets[509].

Inflammation at the cellular level is reflected by the activation of proinflammatory signalling cascades such as the NFκB and JNK pathways. FFA and AGEs can activate these pathways through toll-like receptors (TLRs) and RAGE receptors, respectively [126,513]. NFκB is activated by IKKβ, and induces the expression of proinflammatory cytokines such as TNFα, IL-6 or IL-1β [514]. JNK also activates transcription factors such as ETS-like 1 (ELK1), ATF2 and c-JUN, which transcribe proinflammatory genes and phosphorylate IRS, thereby contributing to IR [27]. In T2D, NFκB and JNK pathways are active in adipose tissue, liver [514,515], muscle cells [516], leukocytes [517–519] and pancreatic β cells [27,520].

Another relevant mechanism is IL-1β-mediated inflammation, which is produced by hyperglycaemia [44,521,522] and FFA [523]. The main pathway responsible for IL-1β synthesis is the NLRP3 pathway activated in response to TLR signals [524]. β cells are very sensitive to IL-1β auto stimulation, presumably because of the high expression of IL-1 receptor [510]. Thus, blocking the IL-1 receptor would be a protective mechanism for β cells in T2D [525,526]. Among other proinflammatory cytokines secreted by adipose tissue, immune cells and other tissues, are the chemokine and adipokine families, including C-C chemokines motif ligand 2 (CCL2), CCL3, CCL6, CCL7, CCL8 and CCL9, which participate in monocyte recruitment and are secreted by adipocytes [527]. Proinflammatory cytokines are also produced in the pancreatic islets; e.g., chemokine (C-X-C motif) ligand 8 (CXCL8) and CCL3 [509,523], which have specific receptors that trigger proinflammatory responses.

Globally, T2D implies a generalised immune activation and production of a wide array of proinflammatory molecules that remain in circulation, progressively affecting all tissues. Thus, circulating immune cells and endothelial cells are exposed to these stimuli, rendering immune and endothelial cells sensitized and predisposed to initiating atherosclerotic events.

1.3.2. Endothelial cell activation

In a homeostatic state, endothelial cells maintain the blood flow and fluidity, control vascular permeability and maintain the quiescence of circulating leukocytes [528]. A resting endothelium does not react with immune cells, as adhesion intercellular adhesion molecule 1 (ICAM-1) and vascular cell adhesion molecule 1 (VCAM-1) are not expressed and Weibel-Palade bodies (WPB) are stored. The NO-mediated transcriptional repression of NFκB may be responsible for maintaining this state [529,530]. The release of WPB and the secretion of proinflammatory molecules depend on the activation of endothelial cells. This can be triggered by blood flow disturbances, inflammatory molecules produced mainly by immune cells, or circulating oxLDL presence. This process follows two successive steps: stimulation and activation [528]. The stimulation is triggered by the binding of molecules to GPCR receptors which trigger calcium release through PLC. The rise in cytoplasmic calcium activates rho kinase (ROCK) and PLC, leading to subsequent prostaglandin production [531–533]. Simultaneously, Rho and PLC phosphorylate the myosine light chain (MLC), leading to the contraction of actin filaments, causing the release of WPB [534,535]. These steps are limited in time, as GPCR receptors are quickly desensitized, avoiding reestimulation [536,537]. Afterwards, the activation requires TNFα and IL-1 production by activated leukocytes [538,539]. Both cytokines end up activating NFκB and AP1 transcription factors: in the case of TNFα, by binding to its specific receptor TNFR and the TNFR1-associated death domain protein (TRADD)/TRAF pathway; in the case of IL-1, through the TIR domain containing adaptor protein (TIRAP) receptor and the interleukin associated receptor kinase (IRAK)/TRAF6 pathway [528]. This response also induces increased blood flow, a rise in the leaking of plasma proteins and an increase of leukocyte recruitment. The increase in blood flow is mediated by cyclooxygenase 2 (COX2) induction, which transforms arachidonic acid produced in the stimulation phase into prostaglandins that diffuse into the bloodstream [540,541]. The

filtration of plasma proteins such as fibrinogen is produced by TNFα and IL-1, although the precise mechanisms responsible for this remain elusive [542,543]. Regarding leukocyte recruitment, NFκB mediates the expression of IL-8 that binds to leukocyte E-selectin, which ends in the firm attachment of neutrophils [544]. When the TNFα and IL-1 stimuli are maintained, E-selectin expression decreases, leading to the expression of VCAM-1 and ICAM-1 and other chemokines [544]. Due to this change in the endothelium adhesion molecules, the leukocytes firmly attach to the monolayer. These cells cross the endothelial barrier by diapedesis and remain in the intima-media layer, producing more proinflammatory intermediates. The cell subset that is attracted to the endothelium changes in the activation phase from neutrophils to mononuclear cells [544]. The accumulation of activated leukocytes which produce proinflammatory cytokines such as Interferon γ favours endothelial apoptosis through caspase 8-dependent and -independent pathways [545,546]. Apoptotic endothelial cells can release microparticles with proinflammatory molecules and exposed phosphatidilserines that enhance coagulation and inflammation. In chronic diseases, both stages of activation can be present at the same time, which maintains endothelial inflammation and leads to subsequent endothelial dysfunction [528].

1.3.3. Initial mechanisms of cardiovascular events

The leading mechanisms in these atherosclerotic and cardiovascular events in T2D are varied and include hyperglycaemia, IR, hyperinsulinemia, dyslipidaemia, inflammation, ROS production, endothelial dysfunction, hypercoagulability and vascular calcification.

IR is present in endothelial cells [547], VSMC [548–550] and macrophages [551,552] and promotes the progression of atherosclerotic events and inflammation [553]. Defects in insulin action accelerate atherosclerosis development, as shown in apolipoprotein E (ApoE) -/- mice [547]. IR affects macrophages, one of the main players in atherosclerotic disease, showing a deviance

towards a more inflammatory-prone phenotype [552,554–556]. The precise phenotype of insulin-resistant macrophages is under debate, given that studies have found induction of both M2 and M1 under IR [554–557]. Defects in insulin signalling impact on the barrier function of endothelial cells by a process coined endothelial dysfunction [558,559].

Endothelial dysfunction is defined as the incapability of the endothelium to maintain vascular homeostasis, and is expressed as a reduction in NO bioavailability, enhanced inflammation, prothrombotic phenotype and impaired cell growth in the vascular wall [560]. To regulate the vascular tone, the endothelium produces diverse molecules that help to relax (NO, prostacyclin and endothelium-derived hyperpolarizing factor (EDHF)) or contract (Endothelin-1 (ET-1), angiotensin II (ATII)) the vasculature through smooth muscle cells. Under endothelial dysfunction, vasoconstrictor factors are unopposed, resulting in abnormally high arterial tone and arterial stiffness [561]. In this sense, it has been determined that animal models of T2D have less ET-1 and NO bioavailability than healthy counterparts [562–564]. Moreover, models of diabetes and T2D patients display impaired vasodilation and remodelled vasculature, showing evidence of endothelial dysfunction [565,566]. One of the molecular links between hyperglycaemia, hyperlipidaemia and endothelium dysfunction is PKC. It is activated by ROS and DAG, acting through inhibition of insulin signalling, AKT-dependent eNOS activation, induction of COX2 activity, ET-1 expression and NOX activation [567]. Another factor that influences endothelial function is the interaction with activated immune cells, by regulating their passage through the endothelial monolayer and subsequent infiltration in the tissues [568]. Physiologic endothelium produces NO, which prevents leukocyte adhesion and maintains an anti-inflammatory state, inhibiting ICAM-1 SRC-1-dependent phosphorylation and the expression of other adhesion molecules [569,570]. Moreover, endothelial NO production induces macrophage polarization towards the M2-anti-inflammatory phenotype [571]. In the endothelium, the activation and

adhesion of proinflammatory molecules are produced, altering the circulating blood homeostasis and the VSMC underneath the endothelial layer. These factors are related to an increase of T2D risk, as demonstrated in the MESA study about the relation of soluble adhesion molecules with T2D. [572]. In endothelial cells, the expression of adhesion molecules is induced under circulating TNFα stimulation or by other stimuli such as shear stress, mediated by the NFκB-dependent pathway and epidermal growth factor-like 7 (Egfl7) proteins [573–575].

The activated endothelium also produces prothrombotic molecules, such as PAI-1, thromboxane and von Willebrand factor (vWF), all of which are involved in hypercoagulability. This hypercoagulative state, caused by ROS, NFκB activation, PKC signalling and reduction in NO synthesis is typical of metabolic diseases such as T2D [576–578]. PAI-1 is mainly produced by endothelial cells as a cause of endothelial dysfunction under TNFα or IL-1β stimulation. It represents an independent risk factor for T2D, as demonstrated by several studies in T2D patients [579–582]. The activated endothelium releases both PAI-1 and vWF, and triggers the coagulation cascade, which activates platelets and fibrin formation, as seen in T2D patients compared to healthy subjects [583,584]. Lastly, vascular calcification is the consequence of all the previously mentioned mechanisms working together, and causes blood vessel hardening and dysfunction. Chronic high levels of TNFα or IL-1β, produced by endothelial cells, signal to VSMC, which activate NFκB and classic pathways of bone remodelling [585–587]. This leads to the expression of different types of collagen and an increase of calcium deposits, which reduces its contractility [585,588]. AGEs can be a direct cause of vascular stiffness, as shown in the study by Sanchis *et al* [589]. In T2D patients, circulating osteblasts and myeloid calcifying cells have been found to contribute to vascular calcification [590,591]. These cells abound in T2D patients, and their number rises with poor glycaemic control, but decreases when patients are in range. All these traits are imdysbalanced in T2D, and impede proper endothelial function, thus leading to loss of

vascular homeostasis and contributing to the development of atherosclerotic events [560].

1.3.4. Atherosclerosis

One of the most common cardiovascular complications is the development of atherosclerotic lesions, which develop in a proinflammatory environment accompanied by hyperlipidaemia and a dysfunctional endothelium. Atherosclerosis consists of the formation of atherosclerotic plaques in the vasculature, which are encapsulated deposits of lipids, cholesterol, calcium and apoptotic cells in the intima-media layer of the vasculature. The initial steps of atherosclerosis are endothelial dysfunction and expression of proinflammatory cytokines by the endothelium and smooth muscle cells, which causes the infiltration of immune cells (Figure 9) [592–594]. First, low-density lipoproteins (LDL-c) particles are oxidized by ROS, and AGEs then activate endothelial cells and smooth muscle cells, increasing the vascular permeability [595–597]. Subsequently, the activated endothelium expresses adhesion molecules and chemokines, which recruit immune cells. Monocytes can migrate into the subendothelial compartment, where they recognize oxLDL through its scavenger receptor. The recognition leads to its endocytosis and accumulation in the cytoplasm, thus activating monocytes and transforming them into foam cells [598–600]. Foam cells can secrete proinflammatory cytokines and present oxLDL-derived moieties to recruited T cells, which also involve an adaptive immune response [601,602]. When in excess, other lipids, such as FFA, can be stored as TAG or as intermediate metabolites such as DAG and ceramide. These molecules activate JNK and IKK proinflammatory cascades, as explained previously. Free FFA and LDL-c or oxLDL can also activate macrophages through TLR4 [513,603]. All these steps lead to the forming of the nascent atherosclerotic lesion, which evolves in most cases into a mature atherosclerotic lesion.

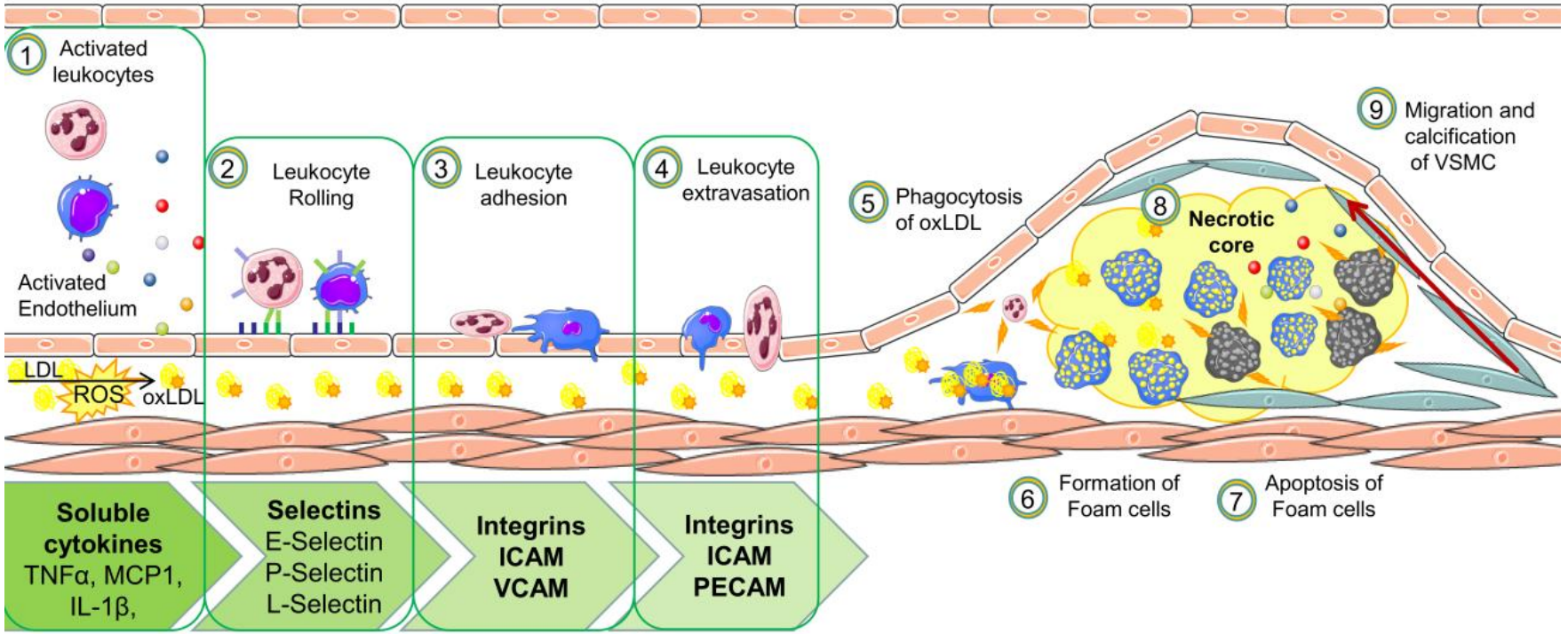

Figure 9: Schematic representation of the formation of the atherosclerotic plaque. Initial leukocyte and endotelial activation produces chemoattractant molecules that attract immune cells to the endothelium (1). Then, leukocytes express selectins that bind to those expressed by the endothelium or platelets, coactivating endotelial cells (2). At this moment, as leukocytes slow down, they firmly interact with the endothelium through intergrins (3). Attached leukocytes eventually migrate to the subendothelial space (4), where they begin to endocyte oxLDL and secrete proinflammatory molecules (5). The excessive endocytosis of oxLDL leads to the formation of foam cells, a term for defining macrophages with massive LDL-c infiltration. Neutrophils in this scenario also secrete proinflammatory cytokines (6). The foam cells eventually become apoptotic, releasing proinflammatory molecules (7). Apoptotic foam cells together with other leukocytes, lipids and cholesterol aggregates form the necrotic core (8). Lastly, the VSMC change their phenotype and migrate from the subendothelial layer to the borders of the necrotic core, stabilizing and calcifying the lesion (9). LDL-c= low density lipoprotein; ROS= reactive oxygen species; oxLDL= oxidatively modified LDL; TNFα= tumor necrosis factor alpha; MCP1= monocyte chemotactic protein 1; IL-1β= interleukin 1 beta; ICAM= intercellular adhesion molecule; VCAM= vascular adhesion molecule; PECAM= platelet-endothelial cell adhesion molecule; VSMC= vascular smooth muscle cells.

Atherosclerotic lesion maturation consists of the formation of a fibrous cap. It begins with the migration and proliferation of VSMCs from the media layer to the intima layer. This is caused by the production of growth factors by macrophages, endothelial cells and T lymphocytes. Once in the intima layer, smooth muscle cells adopt a secretory phenotype, thus releasing collagen, and are able to internalize oxLDL. Eventually, the smooth muscle cells become foam cells and contribute to the necrotic core of the plaque [604–606]. The stable plaque can grow and end up causing ischemic events [594,607]. Otherwise, it evolves into an unstable plaque when macrophages induce the expression of matrix metalloproteinases, which can break the fibrous capsule and form a thrombus [607–609].

In T2D, the presence of activated immune cells, abundance of ROS, the activated endothelium, AGE presence accompanied by IR, hyperlipidaemia and hyperglycaemia creates the perfect background for plaque formation and growth [610–613].

1.3.4.1. Leukocyte-endothelium interactions

This process is one of the initial steps in the formation of the atherosclerotic plaque, subsequent to endothelial activation and dysfunction. Initially, the endothelium produces CCL2/MCP-1 and adhesion molecules such as ICAM-1, VCAM-1 and selectins, which attract and attach to circulating leukocytes. The first expressed adhesion molecules are E-selectin, which binds to ligands in mononuclear cells and polymorphonuclear cells PMNs; and P-Selectin, which binds to platelets [614–616]. Mononuclear cells and PMNs roll along the surface of the endothelium, coactivating endothelial cells, which express and externalize integrins as ICAM-1 and VCAM-1 [617–619]. These molecules mediate the temporal tethering of the immune cells to the endothelium through interactions with lymphocyte function associated antigen 1 (LFA-1) or very late antigen 1 (VLA-1) integrins, respectively. If the interaction persists, it leads to the firm adhesion of the

leukocytes. Later, attached leukocytes and endothelial cells express platelet endothelial cell adhesion molecules (PECAM) that mediate the diapedesis through homotypical interactions [620,621].

1.4. T2D complications

As previously mentioned, the T2D physiopathology predisposes T2D patients to suffer different complications that can be classified according to the root cause. Microvascular complications occur in tissues highly irrigated with insulin-independent glucose channels; on the other hand, macrovascular complications happen in tissues irrigated by arteries that present an atherosclerotic plaque (Figure 10). These different complications reduce the life expectancy and quality of life of T2D patients and increase the private and public costs of T2D. Therefore, it is important to determine the risk factors and the molecular markers of cardiovascular complications in T2D.

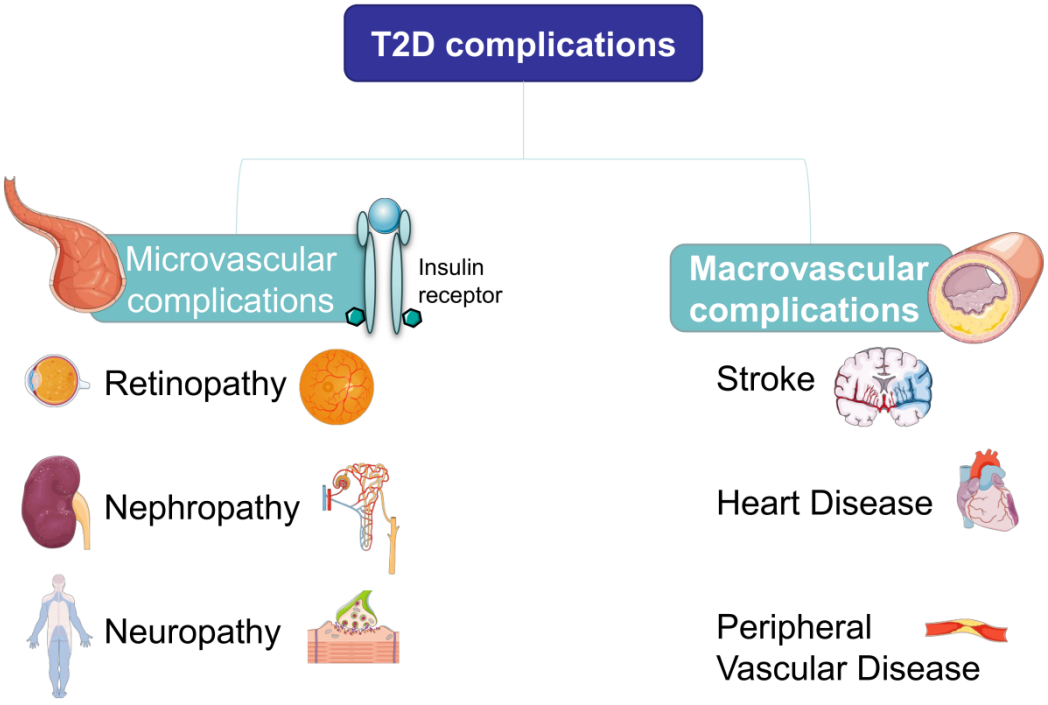

Figure 10: Types of T2D-related complications: Microvascular complications are related to defective insulin signalling in tissues densely irrigated with microvasculature. These include retinopathy, affecting the retina; nephropathy, which undermines kidney function; and neuropathy, which affects neuronal transmission. Macrovascular complications are related to the development of atherosclerotic lesions in the main arteries. They can be classified as stroke events, heart disease and peripheral vascular disease.

1.4.1. Microvascular complications

Chronic hyperglycaemia affects small capillaries from insulin-independent cell types, producing disturbances in the tissues that they irrigate and causing microvascular complications. Overall, they have a high prevalence (17.7%) [622]. All microvascular complications have common pathological mechanisms: loss of pericytes, thickening of the basal membrane and local hypertension. This is caused by high concentration of AGEs, which activate the polyol and PKC pathways, producing oxidative stress and inflammation [623–625].

There are three main forms of microvascular complications: diabetic retinopathy is the most common diabetic microvascular complication, and is related to the severity of the hyperglycaemia and the presence of hypertension. Of particular importance in this case is the production of sorbitol by aldose reductase due to high circulating glucose concentrations [626,627]. This causes local hypertension, microaneurysms and loss of pericytes. It can be classified as background or proliferative retinopathy. The annual incidence of this type of microvascular complication in T2D patients ranges between population studies, from 2.4% in an Indian cohort to 12.7% in a Chinese population [626–628]. The evolution to proliferative retinopathy was found to range between an annual incidence of 0% in Kenya to 1.5% in China [628].

The second type of microvascular complication is diabetic nephropathy, which consists of a thickening of the glomerular basement membrane, podocyte loss and formation of microaneurysms. Those defects lead to glomerular hyperfiltration, causing intraglomerular hypertension and sclerosis. Defective filtration is detected by the excretion of proteins in the form of microalbuminuria (5-299 mg/day) or proteinuria (>500mg/day). The clearest risk factors are elevated glycated haemoglobin and hypertension. Its incidence ranges between 35.3% in sub-Saharian regions to 21.8 in the Chinese population, representing a major complication among T2D patients worldwide [629,630].

Finally, we have diabetic neuropathy, in which pericyte loss and decreased blood flow to the c fibers result in nerve hypoxia [623]. It manifests as ulcerations, pain, numbness and loss of sensitivity to light pressure changes such as vibrations or temperature [631,632]. Its incidence varies widely depending on the years of follow up, glycaemic control and other factors, but is highly representated, reaching 51% incidence among T2D patients [631,632].

1.4.2. Macrovascular complications

Atherosclerosis and endothelial dysfunction are common events to all macrovascular complications. IR enhances platelet aggregation, which, together with the elevated levels of PAI-1 produced by endothelial cells, renders a prothrombotic scenario. Moreover, also in endothelial cells, AGEs and ROS activate PKC, which contributes to a prothrombotic and proinflammatory background through inactivation of eNOS [633]. Globally, there is a hypercoagulative, hypertensive and proinflammatory vasculature that can also present atheroma plaques. This impedes the circulation of blood, resulting in any one of the macrovascular complications: coronary artery disease (infarct, heart failure, myocardial ischaemia), cerebrovascular disease (stroke*),* or peripheral artery disease. Specifically, diabetic patients have a 2-4-fold higher cardiovascular risk compared to non-diabetic subjects [634]. There is an increased risk of suffering coronary artery disease, not only in established T2D, but also in prediabetes [635]. Macrovascular complications have a prevalence of 12.7% worldwide, although a high variation is found depending on the country [622]. The major concern of macrovascular complications is their association with premature death in T2D patients, which can account for up to 50.3% of all T2D-related deaths [634,636]. This risk is preventable, as it is related to diet and intake of excess of lipids and carbohydrates. In this sense, in T2D patients who consumed high levels of fat in their diet presented a 12% higher mortality risk than those consuming a diet of enriched polyunsaturated acids (PUFA) [637]. Worryingly, high BMI and dietary risk habits account for 24.7% and 34.5% of the

disability-adjusted life years (DALY) in Latin-American T2D, representing a high proportion of preventable deaths due to cardiovascular complications [638]. Not only individual nutrients, but dietary patterns that are rich in vitamins, minerals and phytochemicals reduce the incidence of cardiovascular events and associated death in T2D patients [639]. Other controllable parameters, such as glycated haemoglobin, blood pressure, physical activity, and smoking, consistently increase cardiovascular risk and all-cause mortality in T2D [640]. Among all these markers, intensive glycaemic control has been shown to effectively reduce cardiovascular events[641]. Thus, intervention through modifiable lifestyle habits and markers is vital in preventing premature death due to T2D.

Macrovascular complications are rooted in the development of endothelial dysfunction and the atherosclerotic plaque, both of which concepts have been explained above. The atherosclerotic plaque can reduce the blood flow through the arteries as it develops, eventually causing ischaemic events. Indeed, one study showed that the presence of an atherosclerotic plaque with a lipid-rich necrotic core is an independent risk factor of acute cerebral infarct in T2D [642]. According to a recent study in a Spanish cohort, T2D patients had 6% more mortality due to stroke, 15% more due to myocardial infarction, and 6% more for the combination of all cardiovascular events when compared with non-diabetic controls. Moreover, in the same study, women had 6% more mortality for ischaemic stroke than non-diabetic women [643]. A similar study determined that T2D increased the risk of suffering the consequences of atherosclerotic disease, including myocardial infarction, ischaemic stroke, heart failure and aortic valve stenosis [644]. The reported rise of the prevalence of cardiovascular disease and mortality in T2D highlights the importance of the early prevention of these complications. There are useful markers that enable the early detection of plaque development, among which the measurement of carotid intima-media thickness (CIMT) has proven to be of particular interest [645,646] as a reliable

predictor of vascular accidents, and its rise is related to an increase in soluble fibrinogen, E-Selectin and GIP-1 [647,648]. Indeed, it is a more reliable marker of cardiovascular complications than the measurement of coronary artery calcium content, which has been widely used in the past [649]. In recent years, it has been increasingly used and compared or combined with other markers of cardiovascular risk. In this context, CIMT measurement has been demonstrated to increase the accuracy of other previously employed predictors of mortality (presence of plaque, carotid stenosis) and is related to markers of oxidative stress and inflammation (oxLDL and IL-6) [650,651].

2. OBJECTIVES

1. To evaluate the state of autophagy and its relation to mitochondrial function and inflammation in leukocytes from T2D patients.
2. To assess the presence of cardiometabolic risk markers in T2D patients, reflected by soluble cytokine levels, carotid-intima media thickness and leukocyte endothelium interactions, and the influence of strict glycaemic control on these parameters.
3. To evaluate the influence of metformin treatment on mitochondrial dynamics in leukocytes from T2D patients
4. To analyze the effect of the mitochondria-targeted antioxidant SS-31 in endoplasmic reticulum stress, autophagy and oxidative stress.

3.MATERIAL AND METHODS

3.1. Recruitment of study population

For this thesis, we recruited T2D patients and healthy volunteers which attended the Endocrinology and Nutrition Service of the Outpatient unit of the University Hospital Dr Peset from 2017 to 2021. All patients signed a written informed consent with detailed information of the procedure. All collected data was anonimyzed assigning one number and managed according to the data protection law (LOPD). The experimental procedures were approved by the hospital's Ethics Committee of Clinical Investigation, ID: 97/16 or 98/19 (Annex I), in line with the ethical principles of the Helsinki declaration. The diagnosis of T2D was made according to the ADA criteria, and the exclusion requirements were the following: morbid obesity, insulin treatment, and presence of autoimmune, haematological, malignant, infectious, organic or inflammatory diseases.

3.2. Sample collection and laboratory tests

Subjects attended the nursery of the Endocrinology and Nutrition Service where 30 mL of peripheral blood was extracted from the brachial vein, collected in EDTA tubes and a tube for serum isolation. Before the extraction, blood pressure (BP), weight, height, waist circumference and hip circumference were measured. After, BMI (kg/m^2) and hip/waist circumference ratio were calculated. The nurse also collected other relevant information as smoker status or pharmacological treatments. Routine biochemical tubes were also obtained and were analyzed in the biochemistry laboratory of the hospital.

The methods employed in the central biochemistry laboratory of the hospital for the needed determinations were the following: Fasting glucose, total cholesterol, and triglycerides (TG) were determined by an enzymatic method. High density lipoprotein (HDL-c) levels were measured with a Beckman LX-20 autoanalyzer (Beckman Coulter, La Brea, CA, USA) using a direct

method. LDL-c was determined with Friedewald's formula. An immunochemiluminescence assay was employed to determine insulin levels. Glycated haemoglobin % (HbA_{1c}%) was determined with an automatic glycohaemoglobin analyzer (Arkray, Inc., Kyoto, Japan). Apolipoproteins were measured with an electroimmunoassay. hsCRP was analyzed employing an immunonephelometer (Behring Nephelometer II, Dade Behring, Inc., Newark, DE, USA). Afterwards, HOMA-IR index [fasting insulin (μU/mL) × fasting glucose (mg/dl)/405] was calculated to estimate IR.

Serum was isolated from the blood collected in the serum isolation tube by centrifugation for 10 min at 1500g and 4ºC.

3.3. CIMT determination

A subset of all recruited patients was derived to the Cardiology Service in order to determine CIMT. This assay consists in an ecosonocardiographical exploration of the carotid artery performed by trained ecocardiographists following the American Echocardiography Association's guidelines. The evaluation was made by placing the head of the subject at a 45º inclination with respect to the body longitudinal axis. An ultrasound device Aloka 5500 (Hitachi Aloka, Tokyo, Japan) equipped with a 7.5 MHz sector scanner probe was employed for the measurements. Measurements were made in the 1 cm plaque-free segment proximal to the dilation of the carotid bulb. The measurement for each patient corresponded to the mean between three different projections of the far wall (anterior, lateral and posterior). An independent and experimentally blinded observer measured the images. Paired CIMT measurements in the same arteries showed a high degree of reproducibility, with a mean difference in CIMT of 0.020 mm, and an intraclass correlation coefficient of 0.97 ($p < 0.001$).

3.4. Functional assays

3.4.1. Leukocyte isolation

A Ficoll gradient method was employed for isolating PBMCs and PMNs from the samples of whole blood. Initially, the blood is laid over 7mL of a mixture of Ficoll Hystopaque 1119 (Ref 11191) and Hystopaque 1077 (Ref 10771) both from Sigma-Aldrich, St Louis, MO, USA. The blood formed a layer above the ficoll mixture, and the gradient separation will be carried on with a 25-min centrifugation at 650g at room temperature. PBMCs were obtained in the buffy coat and PMNs in the sediment. Both samples were treated with erythrocyte lysis buffer (Red Blood Cell Lysis Solution, Ref. 130-096-941; Miltenyi Biotec, Germany) for 5 min. After, samples were washed with HBSS and stored for subsequent determinations. Cell suspensions with $5x10^6$ cells were centrifuged and the pellet was stored for protein and gene determinations at -80ºC. When needed, a subset of these cells was treated with SS-31 (100 nM, 30 min) or SS-20 (100 nm, 30 min), rotenone (50 µM, 20 min), thapsigargin (1 µM, 20 min), or rapamycin (0.5 µM, 30 min), all purchased in Thermo Fisher Scientific (Waltham, MA, USA) in concentrations that did not alter the cells' viability.

3.4.2. Static cytometry assay

Three hundred thousand PBMCs/well were seeded in 24-well plates in duplicate for each sample. The same amount of seeded Hep3B cells was employed as internal control in each experiment. PBMCs were left for 20 min at room temperature until they attach to the bottom of the plate. Once attached, fluorophores solutions (tetramethylrhodamine (TMRM, 1µM), mitoSOX (5µM), Fluo4 (1µM) and 2'7'dichlorofluorescein diacetate (DCFH-DA, 5µM) and the nuclear staining HOECHST 33342 (1µM), all purchased in Thermo Fisher Scientific (Waltham,

MA, USA), were added to the wells and incubated for 20 min at 37ºC under gentle shaking. Then, wells were washed with warm Ca^{2+} and Mg^{2+} free HBSS. Visualization and measurement of the fluorescence were perfomed with ScanR software coupled to an IX81 Olympus inverted microscope (both from Olympus Corporation, Shinjuku, Tokyo, Japan). Sixteen images were obtained per well in each experiment and the mean fluorescence intensity was calculated and normalized with the internal control.

3.4.3. Flow cytometry assay

Whole blood was processed to detect ROS production thanks to DCFH-DA fluorescent probe. The protocol consisted on three differentiated steps: First, 200µL of whole blood was lysed with erythrocyte lysis buffer (Red Blood Cell Lysis Solution, Ref. 130-096-941; Miltenyi Biotec, Germany) for 15 min and centrifuged for eliminating the supernatant. Second, the pellet was resuspended in a 1µM solution of CD45 antibody (APC Mouse Anti-Human CD45 (BD Biosciences, San Jose, CA, USA) for 20 min to mark the CD45+ cells, which belong to the leukocyte population. Third, once these cells are marked with anti-CD45 APC-coupled antibody, DCFH-DA fluorophore is added at a final concentration of 5µM and incubated in darkness for 10 min. Then cells are analyzed in an Accuri C6 cytometer (BD biosciences, San José, CA, USA), employing the 488 nm laser and the FL1 filter (FITC). Gating of the CD45-positive PMNs and PBMC subpopulations were gated thanks to FSC and SSC parameters. In these subpopulations, the mean intensity of DCFH-DA probe was measured. An internal control (U937 cells) which followed the same experimental procedure was included in all experiments.

3.4.4. Oxygen consumption assay

An aliquot of 500.000 PBMCs/mL was placed in a gas tight chamber from a Clark-Type O_2 electrode (Rank Brothers, Bottisham, United Kingdom) in order to measure O_2 consumption.

An inhibitor of the ETC (Sodium cyanide 1mM) was employed to prove that O_2 consumption was mainly mitochondrial. Data visualization and collection was made with Duo.18 software (WPI, Stevenage, United Kingdom). GraphPad software (GraphPad software, Inc., San Diego, CA) was used to calculate the maximal O_2 consumption rate with endogenous substrates. In order to check the cell viability, a trypan exclusion test was perfomed, showing no significant cell death.

3.4.5. Leukocyte-endothelium interactions analysis

This assay employs two different cell types: 1.2mL of a 10^6 PMNs/mL aliquot and a confluent HUVEC monolayer seeded in a 35mm petri dish (corning, Ref 430165, Chelmsford St Lowell, MA). HUVECs were isolated from fresh umbilical cords whose veins were perfused with a 1mg/mL collagenase solution (Collagenase type IV, GIBCO, Thermo Fisher Scientific Ref 10780004, Waltham, MA, USA). The resultant cell suspension was neutralized with fresh supplemented EGM-2 medium (Lonza, Ref CC-3162, Basel, Switzerland) and seeded until confluence. Cell maintenance was made every two days with fresh medium replacement. The day of the experiment, PMNs are perfused over the HUVEC monolayer thanks to a glycotech parallel-plate flow chamber (Glycotech, ref. 31-001) with the 0.5 width x0.254 mm height flow rubber gasket at a velocity of 0.3 mL/min. A 5 min video was recorded, where afterwards the number of rolling PMNs, its velocity and the adhered ones will be measured. The velocity was measured as the time in which 20 PMNs cover a distance of 200 µm. The adhesion was calculated as the media of adhered PMNs, for at least 30s, in 5 random observation fields.

3.5. Soluble cytokines and adhesion molecules determination

Serum samples stored at -80ºC were selected and employed for measuring the levels of soluble cytokines and adhesion molecules with a Luminex 200 flow analyzer system (Millipore, Austin, TX, USA) and specific Milliplex® MAP Kits (Millipore Corporation, Billerica, MA, USA). This method allows detecting different molecules simultaneously in the same sample and the same assay. The protocol is based in the staining of cells with specific antibodies conjugated to color-coded microbeads, and its detection with biotinylated secondary antibodies with strepatividin-PE conjugates. The fluorescence of each bead color is acquired and analyzed by the Luminex 200 flow analyzer system. The molecules detected and their detection range were the following: TNFα (1750 to 0.43 pg/mL), IL-6 (750 to 0.18 pg/mL), VCAM-1 (500 to 0.122 ng/mL), ICAM-1 (350 to 0.085 ng/mL) and P-selectin (1000 to 0.122 ng/mL). The intra-assay CV is <5% for TNFα and IL-6 and <15% for ICAM-1, VCAM-1, and P-selectin. The interassay CV is <20% for IL-6, ICAM-1, VCAM-1, and P-selectin and <15% for TNFα.

3.6. Protein and gene expression assays

3.6.1. Gene expression

Gene expression was analyzed by RT-PCR method employing frozen samples of PBMCs from healthy and T2D patients. RNA was extracted with a GeneAll Ribospin total RNA extraction kit (GeneAll Biotechnology, Hilden, Germany) and quantified with Nanodrop 2000c (Thermo Fisher Scientific, Waltham, MA). RNA purity was assessed by measuring the optical density ratio between 260nm and 280 nm, which should be comprised between 1.8 and 2. Reverse transcription was made with 1µg RNA from each sample and RevertAid First Strand c-DNA Synthesis kit (Thermo Fisher Scientific, Waltham, MA). 2µg of cDNA were used for analysing gene expression with specific primers (designed specifically for each target in OligoArchitect ^{TM} Online from Sigma Aldrich, Sant Louis, MO, USA), and the KAPA SYBR FAST universal master mix (Biosystems, MA) in a 7500 Fast real-time PCR system (Life Technologies, CA, USA). The methodological details and primers employed are detailed in Table 1. The relative quantification was made with the comparative $2^{-\Delta\Delta Ct}$ method.

Table 1. Protocol details and primers sequences.

qRT-PCR protocol				
Temperature	95ºC	95ºC	60ºC	Melting curve
Time	10 min	10 s	30 s	
Nº of cycles	1	40		

PCR primers		
Target	**Direction**	**5'-3'**
ddit/chop	Forward	AGAACCAGGAAACGGAAACAGA
	Reverse	TCTCCTTCATGCGCTGCTTT
grp78	Forward	AAGAACCAGCTCACCTCCAACCC
	Reverse	TTCAACCACCTTGAACGGCAA
sXBP1	Forward	CTGAGTCCGCAGCAGGTG
	Reverse	AACAGGATATCAGACTCTGAATCTGAA
gapdh	Forward	CGCATCTTCTTTTGCGTCG
	Reverse	TTGAGGTCAATGAAGGGGTCA
mfn1	Forward	CCTCCTCTCCGCCTTTAACT
	Reverse	TATGCTAAGTCTCCGCTCCAAC
mfn2	Forward	CAGCTACACTGGCTCCAACT
	Reverse	TTTCTTGTTCATGGCGGCAA
opa1	Forward	ACCGTTAGCCCTGAGACCATA
	Reverse	GGTAAGTCAACAAGCACCATCC
fis1	Forward	AGAAATTTCAGTCTGAGAAGGCA
	Reverse	CCTCCTTGCTCCCTTTGGG
drp1	Forward	GCTGATGCTTGTGGGCTAATG
	Reverse	TGCCAAAGCACTTGGAACTTT
becn1	Forward	CCCCAGAACAGTATAACGGCA
	Reverse	AGACTGTGTTGCTGCTCCAT
sqstm/p62	Forward	GATTCGCCGCTTCAGCTTCTG
	Reverse	CTGGAAAAGGCAACCAAGTCC

3.6.2. Protein expression

Protein was extracted from PBMCs previously stored at -80ºC by resuspending the pellet in a lysis buffer (20 mM HEPES pH 7.5, 400 mM NaCl, 20% glycerol, 0.1 mM EDTA, 10 µM Na_2MoO_4, 0.5% NP-40) supplemmented with protease inhibitors (10 mM NaF, 1 mM $NaVO_3$, 10 mM PNP, 10 mM β-glycerolphosphate) and dithiothreitol 1 mM. The resuspended pellets were left for 15 min on ice, vigorously mixed for 30 s and centrifuged at 21400 g 15 min at 4ºC. Then, the supernatant was collected and the protein was quantified with the BCA protein assay kit (Thermo Fisher Scientific, Waltham, MA, USA). The isolated and quantified protein was stored at -80ºC for Western blotting assay.

Western blot was perfomed with 25 µg of protein which were separated with 4%-20% gradient or 13% SDS-PAGE gels (Novex Wedge Well 4-20 Tris Glycine Gel, Ref. XP04205B0X; Invitrogen-Life Technology, Carlsbad, CA, USA) and separated at 150V for 60-90 min at RT. After, the resulting protein separation was transferred to a nitrocellulose membrane (BioRad, CA) by a wet transference method, set at 400 mA and constant voltage for 60 min. The membranes then were blocked with 1-5% skimmed milk solution in TBS-T or 5% BSA, depending on the target protein, for 1 h at room temperature. Then, specific blocking buffer-diluted primary antibodies were incubated at 4ºC overnight. The antibodies employed and the dilutions are specified in Table 2. The next day, specific secondary antibodies were added after 3 TBS-T washes, and were incubated for 1 h at room temperature and gentle shaking. Then, after 3 TBST washes, signal was visualized thanks to chemilumiscent reagents ECL plus (GE Healthcare, Amersham Place, Litte Chalfont, UK) or Supersignal West Femto or Pico (Thermo Fisher Scientific, Waltham, MA, USA) in a Fusion FX5 acquisition system (Vilbert Lourmat, Marne La Vallée, France). Densitometric analysis of the images normalized with an internal control and the actin signal was perfomed with Bio1D software (Vilbert Lourmat, Marne La Vallée, France).

Table 2. Primary antibodies, dilutions and specifications employed

Primary antibodies			
Target	**Dilution**	**Source**	**Reference**
NFκB-p65 (phospho S536)	1/1000	Rabbit	ab28856 (Abcam, Cambridge, MA)
TNFα	1/1000	Rabbit	654250-1MG (Sigma-Aldrich, Sant Louis, MO,USA)
SIRT1	1/1000	Rabbit	07-131 (Merck Millipore, Austin, TX, USA)
Beclin-1	1/1000	Rabbit	AB15417 (Merck Millipore, Austin, TX, USA)
LC3	1/1000	Rabbit	L8918 (Merck Millipore, Austin, TX, USA)
SQSTM/p62	1/500	Mouse	H00008878-M01 (Abnova Corp., Taiwan)
Mfn1	1/1000	Rabbit	ABC41, (Merck Millipore, Austin, TX, USA)
Mfn2	1/1000	Rabbit	ABC42, (Merck Millipore, Austin, TX, USA)
Opa1	1/1000	Mouse	MABN737 (Merck Millipore, Austin, TX, USA)
Drp1	1/1000	Mouse	GR3248679-1 (Abcam, Cambridge, UK)
Fis1	1/500	Rabbit	ABC67 (Merck Millipore, Austin, TX, USA)
Actin	1/2000	Rabbit	A2066 (Sigma Aldrich, St. Louis, USA)
Secondary Antibodies			
Rabbit	1/2000	Goat	PI-1000 (Vector Laboratories, Burlingame, CA, USA)
Mouse	1/2000	Goat	31420 (Thermo Fisher Scientific, Waltham, MA, USA)

3.7. Statistical analysis:

Normality analysis was performed in all measured variables with Kolmogorov-Smirnov or Shapiro-Wilk test depending on the simple size. Normally distributed variables present their media and the Standard Deviation (SD), whereas in non-normally distributed data median and 25th-75th quartiles are displayed.

Comparisons were made with two-sided t-test for comparing two populations or one-way ANOVA followed by Bonferroni, Tukey or Newman–Keuls pos-test. In non-normally distributed variables, Mann-Whitney and Kruskal-Wallis tests were applied for two and three group's comparisons, respectively. In the cases when or BMI or age are significantly different between the populations, adjustment of the confounder variables was performed with covariance analysis (univariate or multivariate general linear model). Correlations were calculated with Pearson's or Spearman's correlation coefficient depending on the sample size.

All statistics were calculated with SPSS 17.0 software (SPSS Statistics Inc., Chicago, IL, USA) and graphs were plotted in GraphPad Prism 6.0 (GraphPad, La Jolla, CA, USA). Bar graphs represent the mean and the error bars measure the Standard Error of the Mean (SEM). Differences were considered significant when $p<0.05$ in all cases, applying a confidence interval of 95% in every comparison.

4. RESULTS

4.1. CHAPTER 1

Relationship between PMN-endothelium interactions, ROS production and Beclin-1 in type 2 diabetes

Aranzazu M. De Marañon[a], Francesca Iannantuoni[a], Zaida Abad Jiménez[a], Francisco Canet[a], Pedro Díaz-Pozo[a], Sandra López-Domènech[a], Ana Jover[a], Carlos Morillas[a], Guillermo Mariño[b], Nadezda Apostolova[c], Milagros Rocha[ac], Victor M.Victor[acd].

[a]Service of Endocrinology and Nutrition, University Hospital Doctor Peset, Foundation for the Promotion of Health and Biomedical Research in the Valencian Region (FISABIO), Valencia, Spain

[b]Instituto de Investigación Sanitaria del Principado de Asturias, 33011, Oviedo, Spain

[c]CIBERehd - Department of Pharmacology, University of Valencia, Valencia, Spain

[d]Department of Physiology, University of Valencia, Valencia, Spain

Redox Biology. 2020 Jul;34:101563

DOI: 10.1016/j.redox.2020.101563

ABSTRACT

Type 2 diabetes is closely related to oxidative stress and cardiovascular diseases. In this study, we hypothesized that PMN-endothelium interactions and autophagy are associated. We evaluated PMN-endothelial interactions, ROS production and autophagy parameters in 47 type 2 diabetic patients and 57 control subjects. PMNs from type 2 diabetic patients exhibited slower rolling velocity ($p < 0.001$), higher rolling flux ($p < 0.001$) and adhesion ($p < 0.001$) in parallel to higher levels of total ($p < 0.05$) and mitochondrial ROS ($p < 0.05$). When the protein expression of autophagy markers was analysed, an increase of Beclin-1 ($p < 0.05$), LC3I ($p < 0.05$), LC3II ($p < 0.01$) and LC3II/LC3I ratio ($p< 0.05$) was observed. Several correlations between ROS and leukocyte-endothelium parameters were found. Interestingly, in control subjects, an increase of Beclin-1 levels was accompanied by a decrease in the number of rolling ($r = 0.561$) and adhering PMNs ($r = 0.560$) and a rise in the velocity of the rolling PMNs ($r = 0.593$). In contrast, in the type 2 diabetic population, a rise in Beclin-1 levels was related to an increase in the number of rolling ($r = 0.437$), and adhering PMNs ($r = 0.467$).

These results support the hypothesis that PMN-endothelium interactions, ROS levels and formation of autophagosomes, especially Beclin-1 levels, are enhanced in type 2 diabetes.

1. INTRODUCTION

In recent years, a sustained global increase in the prevalence of obesity and metabolic syndrome has provoked a rise in diseases such as type 2 diabetes [1]. Currently, type 2 diabetes and its comorbidities are among the main health concerns worldwide because of their high prevalence and the associated cost related to public health services. Type 2 diabetes is characterized by hyperglycaemia and IR, which cause chronic subclinical inflammation [2,3]. Hyperglycaemia and inflammation produce cellular alterations, which are the molecular basis of diabetes and cardiometabolic diseases [3–5]. Previous studies have highlighted the relationship between diabetes and inflammation, pointing to circulating hyperlipidaemia and hyperglycaemia as triggers of inflammatory responses [5–7].

One of the consequences of chronic hyperglycaemia is the increased generation of ROS, produced mainly by the mitochondrial respiratory chain [8,9]. This heavy load of ROS overwhelms antioxidant defences and can modify cellular molecules and organelles, disturbing cell homeostasis and inducing inflammation. Furthermore, mitochondrial dysfunction and oxidative stress have been closely related to cardiovascular diseases [10,11]. Hyperglycaemia, together with ROS production, leads to an increased presence of proinflammatory molecules that activate immune cells [8–10]. Moreover, endothelial cells are activated by ROS and proinflammatory cytokines thereby developing endothelial dysfunction [12–15]. This situation enhances a cascade of PMN-endothelium interactions, a process by which immune cells migrate to the site of inflammation [16]. The proinflammatory state and increased ROS content characteristic of type 2 diabetes favour PMN-endothelial interactions throughout the vasculature, not only at the site of inflammation [17]. This process is enhanced in the comorbidities related to type 2 diabetes [17], but the cause and the pathways affected are still being investigated. One of the actions involves the interference of ROS with the proper

functioning of β cells [18], including mechanisms of protein homeostasis, such as protein folding and degradation [19]. It is known that ROS can damage various cellular components, which are degraded and recycled by a process named autophagy. It involves nonselective degradation of proteins, lipids and organelles [20], and occurs in response to internal or external stimuli such as oxidative stress, UPR and malfunctioning of organelles (internal inductors), and growth factors, serum starvation or amino acid deprivation (external stimuli). In this sense, autophagy is a survival mechanism [20] and a strictly regulated process. Two key proteins in this process are LC3 and Beclin-1. The latter, together with other autophagy-related proteins, initiates the formation of the omegasome and the phagophore, thus priming the progression to autophagosome [20]. In parallel, the cytoplasmic form of LC3I is lipidated to LC3II, and, in this form, is recruited to the inner and outer autophagosomal membrane in order to construct the autophagosome. In the case of selective autophagy, altered proteins and organelles are carried to the autophagosome via the ubiquitin- and LC3- binding protein SQSTM1 (p62). Ubiquitinated proteins or organelles are sequestered into the autophagosome for their degradation. When the autophagosome fuses with the lysosome, the autolysosome is created and the material stored in the autophagosome is then digested. If autophagy is impaired, p62 protein accumulates in the autophagosomes [20]; however, p62 is important not only in this process, but it also acts as a scaffold protein that intervenes in cell proliferation and survival/death signalling [21]. Autophagy has been shown to be enhanced and decreased in diabetic patients [22,23]. In fact, insulin influences autophagy regulation, in part through mTOR signalling. Yan et al. [24] described that the adipocytes of obese type 2 diabetic patients display increased autophagy and reduced mTOR signalling. Interestingly, they showed that this state is associated with an undermining of mitochondrial biogenesis and function. Furthermore, several studies have demonstrated that hyperglycaemia induces autophagy as a protective mechanism. For example, autophagy is active

in diabetic mice podocytes with glomerular damage [25–27], a mechanism that may be modulated by HO-1 and AMPK activation [28]. In mice, it has also been observed that defective autophagy in β-cells accelerates the progression from obesity to diabetes through enhancement of UPR, a mechanism also activated by hyperglycaemia [29]. In parallel to these observations, it has been established that the BCL2-Beclin-1 complex is dissociated in response to AMPK activation in cardiac muscle, thus enhancing autophagy and preventing cardiomyocyte death [30]. These observations have been confirmed in other tissues, such as endothelial progenitor cells [31]. Conversely, Qianrong et al. [32] reported that high glucose levels inhibit autophagy in cardiomyocytes, leaving cells unprotected and more prone to apoptosis. In summary, it is thought that autophagy is activated in situations of cellular stress such as hyperglycaemia, but the underlying mechanisms are unknown in most cell types.

In this context, we hypothesized that PMN-endothelium interactions, ROS and autophagy are altered in the PMNs of diabetic patients and that there is an association between all three. In this study, we analyse the link between Beclin-1, ROS production and PMN-endothelium interactions, as well as the varying behaviour of autophagy in diabetic and control conditions.

2. MATERIALS AND METHODS

2.1. Study population

This cross-sectional observational study had a case-control design, and was conducted with 47 diabetic patients and 57 control subjects matched by age and sex. The patients were recruited at the Endocrinology and Nutrition Service of the University Hospital Dr. Peset, Valencia, Spain, and their characteristics are described in Table 1. A diagnosis of type 2 diabetes was determined according to the American Diabetes Association's criteria. Subjects aged 18 or older were eligible for inclusion in the study. The exclusion criteria were having an abnormal haematological profile, suffering any malignant neoplasm or autoimmune disease, consumption of any anti-inflammatory drugs in the two weeks previous to the analysis, and regular consumption of antioxidant nutritional supplements.

The procedures carried out in the study were approved by the Ethics Committee of the Hospital (ID: 97/16) and conducted according to the ethical principles stated in the Declaration of Helsinki. All subjects signed an informed consent document before the interventions. A physical examination was performed in all patients prior to blood extraction, which was conducted in a state of fasting. Body weight and height were recorded and BMI was calculated using the BMI formula (BMI = weight in kg/height in m^2).

2.2. Blood sampling

In order to determine biochemical parameters and obtain PMNs, venous blood was collected from subjects in heparin, EDTA or citrate tubes after 12h overnight fasting. It was then centrifuged (1500g, 10 min, 4 °C) in order to isolate serum and plasma, which were then stored at −80 °C for subsequent analysis, or employed to determine biochemical parameters.

The heparin tubes were used to obtain PMNs.

2.3. Biochemical determinations

All the biochemical parameters were determined by the Hospital's Clinical Analysis Service. An enzymatic method was employed to determine serum concentrations of glucose, total cholesterol, HDL-c and TG levels with a Beckman LX-20 autoanalyzer (Beckman Coulter, La Brea, CA, USA). Low density lipoprotein (LDLc) cholesterol levels were calculated with Friedewald's formula. An immunochemiluminiscent assay was used to determine insulin levels. IR was determined employing the Homeostasis Model, calculated as [fasting glucose in mg/dL x fasting insulin in µUI/mL]/405). HbA_{1c} was assessed with an automatic glycohemoglobin analyser (Arkray, Inc., 73 KYOTO, Japan). Serum concentrations of high-sensitive C-reactive protein (hs-CRP) were determined by immunonephelometry. Atherogenic Index of Plasma (AIP) was calculated using the formula (Total Choresterol (mg/dL))/(HDL-c (mg/dL)).

2.4. PMN-endothelium interaction assay

PMNs were isolated as previously described [33]. We employed a 1.2 mL aliquot of PMNs obtained from the peripheral blood of control and type 2 diabetic subjects with a density of 10^6 cells/mL in complete RPMI (RPMI 1640 medium supplemented with 10% Fetal bovine serum,1% penicillin/streptomycin, 1% glutamine and 1% sodium pyruvate). Prior to this, primary cultures of HUVEC were established. HUVEC were isolated as previously reported [32]. On the day of the experiment, PMNs were monitored through the endothelial monolayer at a speed of 0.3 mL/min during a 5-min period, which was recorded, and the number of rolling PMNs as well as their velocity and adhesion to the endothelial monolayer were determined. The number of rolling

PMNs was measured as those rolling for 1 min, their velocity was assessed by determining the time in which 15 rolling PMNs covered a distance of 100 µm. Adhesion was analysed by counting the number of PMNs adhering to the endothelium for at least 30 s in 5 fields. Protein extraction and quantification PMN pellets were incubated for 15 min on ice with lysis buffer (20 mM HEPES pH 7.5, 400 mM NaCl, 20% glycerol, 0.1 mM EDTA, 10 µM Na MoO, 0.5% NP-40) containing protease inhibitors (10 mM NaF, 1 mM NaVO3, 10 mM PNP, 10 mM β-glycerolphosphate) and dithiothreitol 1 mM. Subsequently, samples were vortexed for 30 s and centrifuged at 21400 g for 15 min at 4 °C. The supernatant was then collected in a new tube and quantified with the BCA protein assay kit (Thermo Scientific, Rockford, USA). The protein extract obtained was stored for subsequent determinations at −80 °C.

2.5. Western blotting

Twenty-five µg protein samples were separated with SDS-PAGE (13% polyacrylamide gels) and transferred to a nitrocellulose membrane. The membranes were then blocked for 1 h at RT with 5% skimmed milk in TBS-T or 5% BSA in TBS-T and incubated with primary antibodies overnight at 4°C: anti-Beclin-1 (Millipore Iberica, Spain, Madrid), anti- LC3 (Millipore Iberica, Spain, Madrid), anti SQSTM/p62 (Abnova Corporation, Taiwan), anti-Actin (Sigma Aldrich, St. Louis, USA). The secondary antibody was HRP-goat anti-rabbit (Millipore Iberica, Spain, Madrid). The protein signal was revealed with SuperSignal West Femto (Thermo Scientific, Rockford, USA) and detected with a Fusion FX5 acquisition system (VilbertLourmat, Marne La Vallée, France). Densitometric quantification of proteins was performed with Bio1D software (VilbertLourmat, Marne La Vallée, France). Data were relativized with the Actin signal for each sample and also to an internal control. Each Western blot was performed and reproved several times, thus, cropped images are represented in Figs. 3 and 4.

2.6. Quantification of total and mitochondrial ROS

Total and mitochondrial ROS were assessed with the fluorescent probes 2'-7' dichlorodihydrofluorescein diacetate (DCFH-DA) and MitoSOX, respectively. Isolated PMNs were seeded in 48-well plates at a density of 150000 cells/well and left to adhere in a 5% CO^2 incubator for 20 min. Cells were subsequently incubated with the specific nuclear stain Hoescht 33342 (4 µM) (Sigma-Aldrich, St. Louis, USA) and the fluorescent probes DCFH-DA (1 µM) or MitoSOX (5 µM) (Thermo Scientific, Rockford, USA) 30 min at 37 °C under gentle shaking. Cells were then washed twice with HBSS and were analysed with the static cytometry software "ScanR" (Olympus) which is coupled to an inverted microscope (lX81; Olympus). 12 fields per well were recorded and quantified. Measurements of fluorescence were referred as % of an external control for each sample.

2.7. Statistical analysis

SPSS was employed to perform statistical analyses. The data in Table 1 are expressed as mean ± standard deviation for parametric data, and median and 25th-75th percentiles for non-parametric data. The bar graphs in figures represent mean ± standard error. An unpaired Student's t-test was performed to compare the control group and type 2 diabetic subjects, and adjustment by BMI was determined by means of a univariate general lineal model. Correlations were calculated with Pearson's correlation coefficient. Differences were considered significant when $p < 0.05$.

3. RESULTS

3.1. Clinical and biochemical characteristics of the study subjects

We analysed 57 type 2 diabetic patients and compared them to 47 healthy control subjects with similar ages and sex distribution. Anthropometric and biochemical parameters were evaluated (Table 1). Type 2 diabetic patients showed higher BMI, fasting glucose, basal insulin, HOMA-IR index and HbA_{1c} compared to control subjects. Lipid metabolism parameters were also significantly enhanced compared to control volunteers, with higher VLDL and TG, and lower HDL-c. Total cholesterol and LDL-c levels showed a slight decrease due to the treatment with statin (90% of patients). Furthermore, type 2 diabetic patients had a higher atherogenic index of plasma (AIP) and higher PCR levels.

Glucose, insulin, HOMA-IR, HbA1c, VLDL, HDL-c, TG and AIP maintained their statistical significance when data were adjusted by BMI, while differences in hsCRP and some lipid profile parameters –including total cholesterol and LDL-c - lost their statistical significance.

Table 1: Biochemical and anthropometrical parameters in control and type 2 diabetic populations. Data are expressed as mean ± SD for parametrical data and as median (25th percentile-75th percentile) for non-parametrical variables. Statistical significance ($P < 0.05$) was compared with T-test following a post-hoc test with BMI as covariate.

	Control	**T2D**	**p-value**	**BMI Adjusted p-value**
N	57	47		
Age	49 ± 10	52 ± 8		
Women	55%	45%		
Men	45%	55%		
BMI (kg/m^2)	24.97 ± 3.32	32.25 ± 4.42	< 0.001	ns
Glucose (mg/dL)	91.15 ± 11.64	137.10 ± 48.93	< 0.001	< 0.001
Insulin (µUI/mL)	5.99 ± 1.87	20.00 ± 12.30	< 0.001	0.04
HOMA-IR	1.60 ± 1.05	6.90 ± 5.10	<0.001	0.004
HbA_{1c} (mmol/mol) (%)	33.84(5.3) ± 0.62	58 (7.3) ± 1.65	< 0.001	< 0.001
Total Cholesterol (mg/dL)	195.06 ± 29.48	172.27 ± 42.28	0.01	ns
Non-HDL-c (mg/dL)	137.00 ± 30.79	127.00 ± 40.89	ns	ns
LDL-c (mg/dL)	121.95 ± 26.02	100.38 ± 36.09	0.006	ns
VLDL-c (mg/dL)	15.33 ± 7.07	28.58 ± 27.41	0.003	0.006
HDL-c (mg/dL)	57.17 ± 12.44	44.64 ± 10.09	< 0.001	0.01
TG (mg/dL)	63 (51–103)	114(89–169.67)	0.002	0.007
AIP	0.11 ± 0.24	0.47 ± 0.29	< 0.001	< 0.001
hs-CRP (mg/L)	1 (0.31–1.87)	3.4 (2.01–7.87)	0.004	ns

3.2. Total and mitochondrial ROS levels

Mitochondria can be severely damaged due to hyperglycaemia by releasing ROS. We measured total and mitochondrial ROS levels in PMNs from type 2 diabetic patients and controls and found an evident enhancement of both total and mitochondrial ROS levels in type 2 diabetic subjects ($p < 0.05$) (Fig. 1) suggesting an oxidative stress condition.

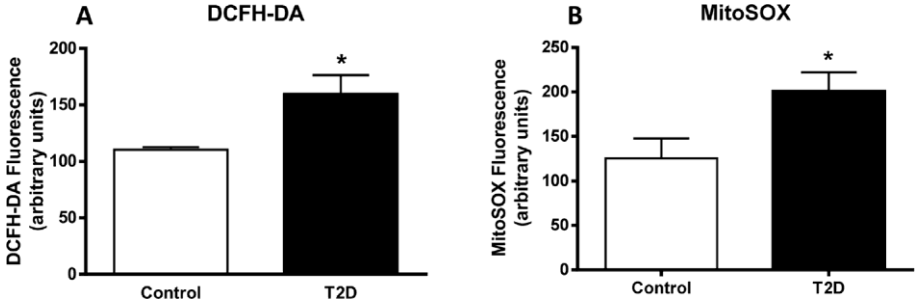

Fig 1. ROS levels in PMNs from control and type2 diabetic populations. (A) Levels of total ROS measured in controls and type 2 diabetic patients with DCFH-DA fluorescence in arbitrary units; (B) Levels of mitochondrial ROS measured in control and type 2 diabetic populations with MitoSOX fluorescence in arbitrary units. Values were expressed as a percentage of an internal experimental control in both populations. *$p < 0.05$ vs Control group.

3.3. PMN-endothelium interactions

Metabolic disorders are associated with increased levels of inflammatory markers. In the present study, we have observed that type 2 diabetic subjects had higher levels of TNFα and IL-6 levels, as well as increased NFκB (p65) protein levels (Supplemmentary figure). This enhanced inflammatory background could be further confirmed analyzing the activation of the PMNs and its interactions with the endothelial cells, using parallel-plate flow chamber experiments. This *in vitro* system reproduces physiological interactions between circulating cells and endothelium, and can quantify the frequency and stability of these interactions. Interestingly, PMNs from type 2 diabetic patients displayed lower rolling velocity through the endothelial monolayer ($p < 0.001$)

(Fig. 2B), greater rolling number ($p < 0.001$) (Fig. 2A) and increased adhesion to the endothelial cells ($p < 0.001$) (Fig. 2C) with respect to those from the control population. This increase in PMN-endothelium interactions is reflected in the representative images obtained before and after the 5-min experimental period (Fig. 2D).

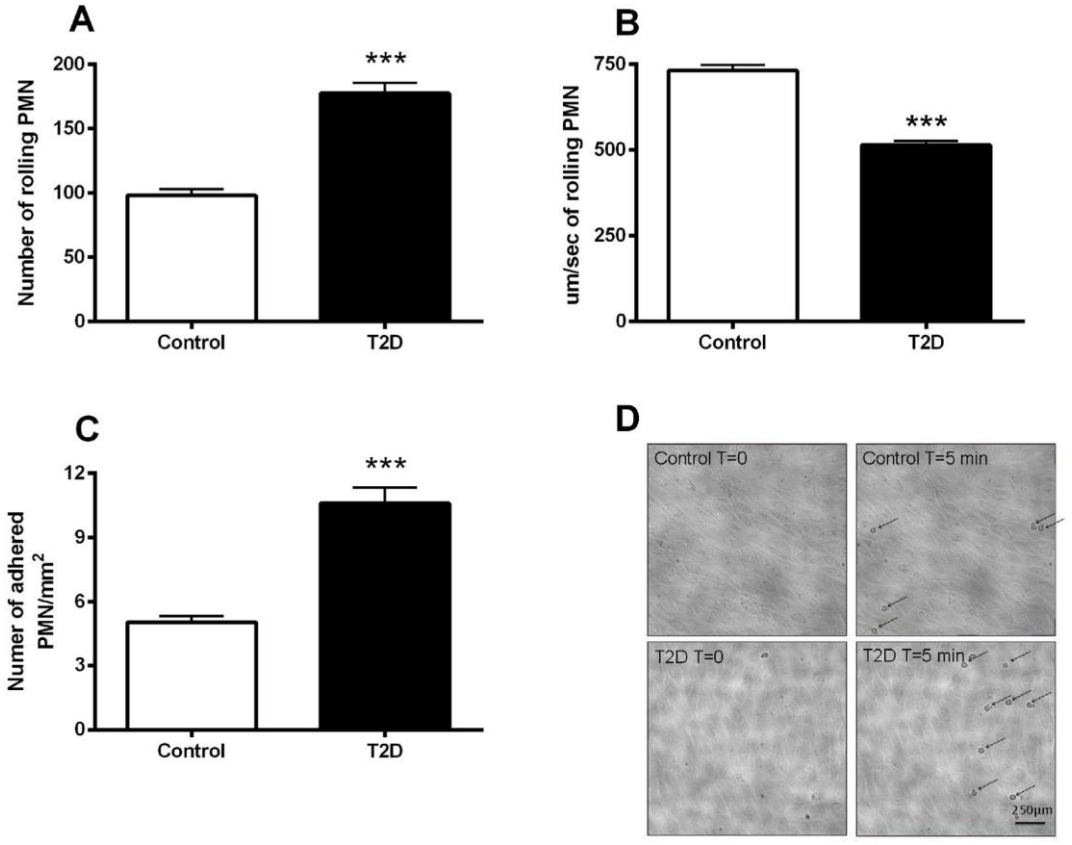

Fig 2 Analysis of PMN-endothelium interactions in control and type 2 diabetic populations: (A) Number of PMNs rolling along the endothelial monolayer during a 1-min period, measured as number of cells/min; (B) Velocity of PMNs measured as µm/sec; (C) Number of adhering PMNs in 1 mm^2, measured as PMN/ mm^2; (D) Representative images of control and type 2 diabetic populations at the start and the end (5 min) of the experiment. ***$p < 0.001$ in type 2 diabetes vs Control.

3.4. LC3I, LC3II, Beclin-1 and p62 protein levels

We examined autophagy, a stress-activated cellular process that might be altered in type 2 diabetic population. PMNs were employed to analyse the protein expression of classical markers such as LC3, Beclin-1 and p62. Type 2 diabetic patients displayed an increased amount of LC3I ($p<0.05$) (Fig.3A and representative WB) and LC3II ($p < 0.05$) (Fig. 3B and representative WB), with a higher LC3II/LC3I ratio ($p < 0.05$) (Fig. 3C and representative WB). In addition, they showed enhanced Beclin-1 and decreased p62 protein levels ($p < 0.05$) compared to control subjects, suggesting an increase in autophagy activation in the type 2 diabetic patient population.

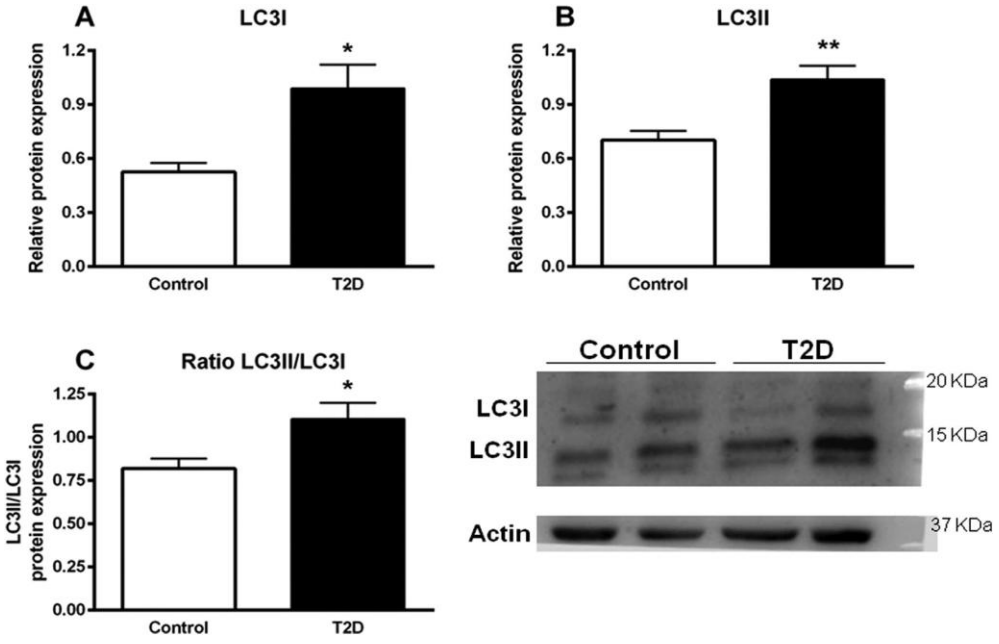

Fig 3 LC3 (I and II) protein expression in controls and type 2 diabetic patients. Protein expression of LC3I (A), LC3II (B) and ratio of LC3II to LC3I (C) in controls and type 2 diabetic patients were assessed by immunoblotting. Quantification was performed in n = 15 samples for each group. Representative image of western blotting of 4 samples (2 controls and 2 type 2 diabetic patients) is displayed. Values represent media ± SD * $p < 0.05$; **$p < 0.01$ vs Control.

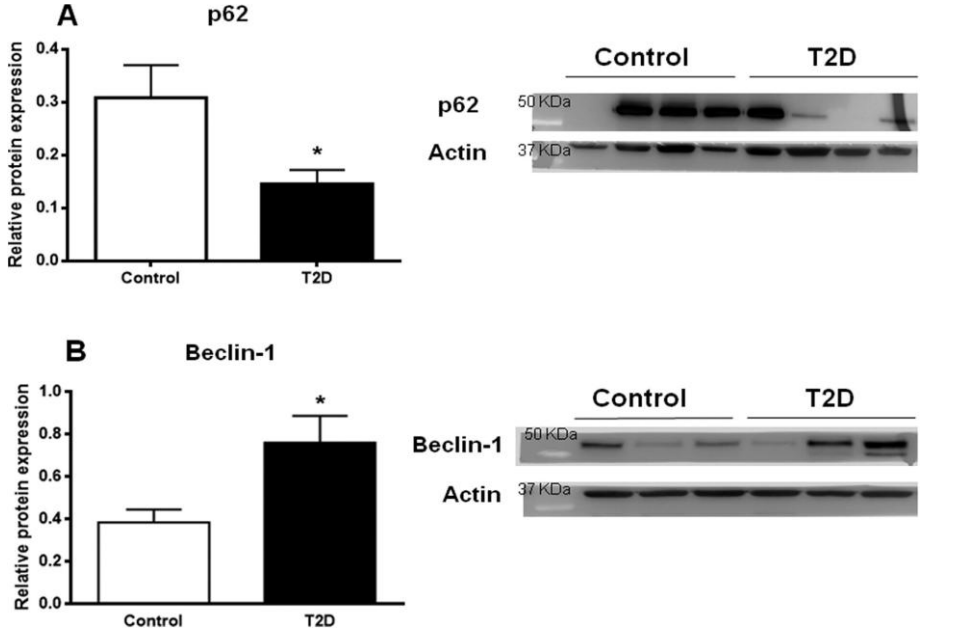

Fig 4 p62 and Beclin-1 protein expression in control and type 2 diabetic populations. Protein expression of p62 (A) and Beclin-1 (B) in control and type 2 diabetic populations was assessed by inmunoblotting. Quantification was performed with n = 15 samples in each group. Representative images of the western blotting are displayed at the side of both graphs. Values represent media ± SD * $p < 0.05$ vs Control.

3.5. Correlations between ROS levels and autophagy markers

As we have mentioned before, excessive production of ROS can generate cellular stress that activates rescue pathways. In the present study, we have tried to highlight the relationship between autophagy and ROS production. We have evaluated correlations between the data obtained for ROS production and autophagic protein expression. We observed that total ROS levels correlated negatively with LC3II/I ratio in the control population ($r = -0.714$, $p = 0.047$) and positively with Beclin-1 levels in type 2 diabetic subjects ($r = 0.911$, $p = 0.001$). On the other hand, mitochondrial ROS was positively correlated with LC3II/LC3I ratio in the type 2 diabetic population ($r=0.416$, $p=0.022$). These data reinforce the hypothesis of a strong relation between autophagy and ROS production in type 2 diabetic patients.

3.6. Correlation between autophagy proteins and PMN-endothelium interaction parameters

Once we had analysed the correlation between ROS and autophagy, we evaluated the correlation between PMN-endothelium interactions and autophagy markers. Interestingly, we observed that Beclin-1 protein levels were differentially correlated with PMN-endothelium interaction parameters (Fig. 5). In the control population, an increase of Beclin-1 was accompanied by a decrease in rolling number, a decrease in the number of adhered PMNs and a rise in the velocity of the rolling PMNs. In contrast, in the type 2 diabetic population, an increase in Beclin-1 was related to an increase in both rolling number and number of adhered PMNs and a trend towards a decrease in rolling velocity (Fig. 5). Additionally, a correlation between PMNs adhesion, and LC3II expression was observed in the type 2 diabetic population ($r=0.386$, $p=0.032$) while the rest of the parameters of PMN-endothelium interactions showed no correlation.

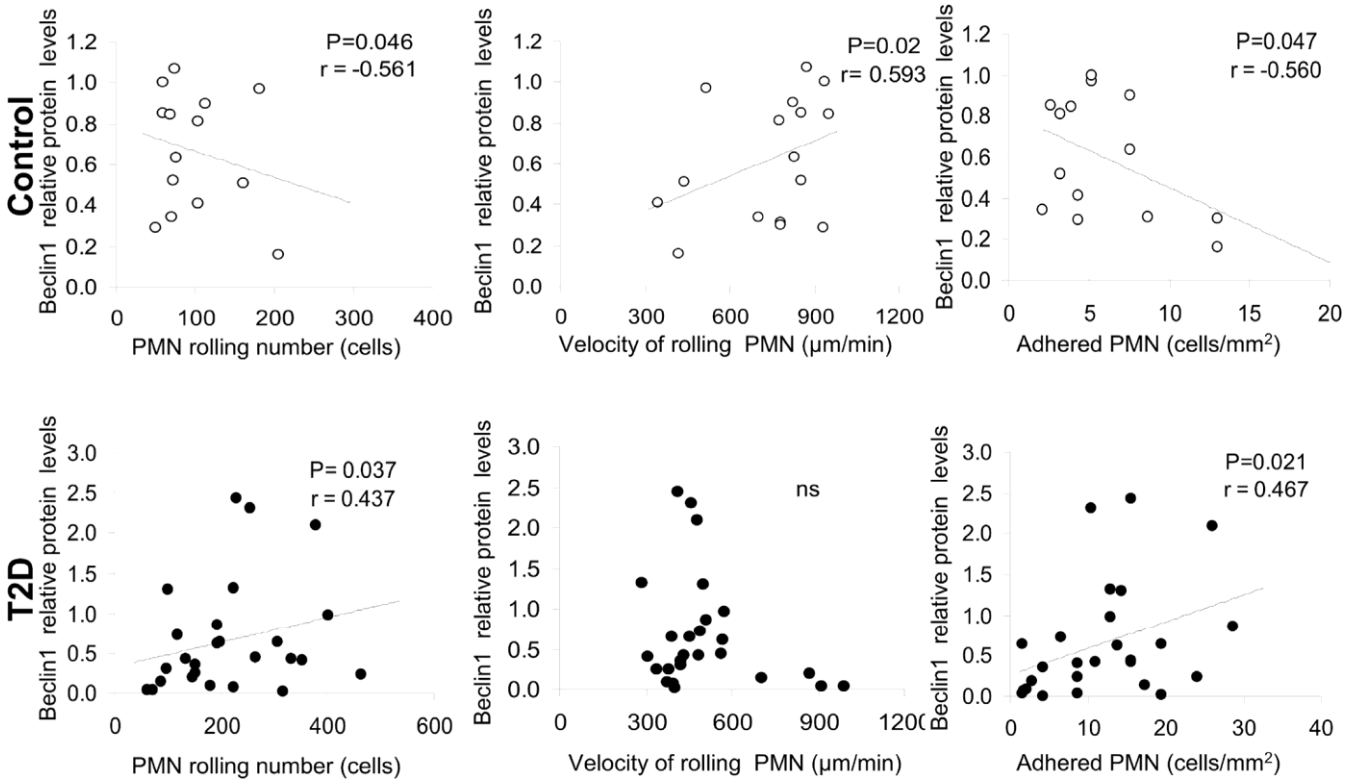

Fig 5 Pearson's correlation between the protein levels of Beclin-1 and PMN-endothelium interaction parameters in control and type 2 diabetic populations. The correlations between Beclin-1 and number of rolling PMNs (5A, D), rolling velocity (5B, E) and adhesion of PMNs (5C, F) are represented.

4. DISCUSSION

In this cross-sectional study, we have shown that diabetic patients display enhanced PMN-endothelium interactions, ROS production, autophagy-related protein expression as well as proinflammatory cytokines TNFα and IL-6, and NFκB activation. Moreover, we demonstrate a differential correlation between PMN-endothelium interactions and Beclin-1 expression in control subjects and type 2 diabetic patients.

With regard to the inflammatory basis of type 2 diabetic, high levels of circulating glucose and lipids increase the expression of adhesion molecules in both the endothelium and PMNs [13,14,16,34,35]. This has been corroborated by several observational studies of type 2 diabetic patients [14,35], but also in interventional studies in patients fitted with hyperglycaemic clamps and undergoing glucose challenge, in whom inflammatory cytokines increase after glucose input [36]. Hyperlipidaemia, another hallmark of type 2 diabetic, is also related to PMNs function [17]; an increase in PMNs ROS production has been described in hyperlipidaemic and hypertensive patients with respect to healthy controls, which can lead to the atherosclerotic complications [37]. Furthermore, it has been observed that PMNs function is altered in patients with diabetic retinopathy; for example, in the case of enhanced extravasation [38]. In this sense, the close relationship between inflammation, ROS production and increase of PMN-endothelium interactions is widely recognised [18,35–37,39–42]. All these studies have concluded that the chronic inflammation characteristic of diabetes and hyperglycaemia promotes the production of inflammatory chemokines and ROS, which in turn alters the functions of the endothelium and PMNs, thus increasing their interaction. Although ROS have an important function as signalling molecules in physiologic processes, their overproduction causes damage of cellular components, which activates the inflammatory response of cells. In the present study, we have observed

higher levels of total and mitochondrial ROS in the type 2 diabetic population compared to healthy controls. The relation between type 2 diabetes and ROS is well documented in the literature [8–10,18,28], and has even been directly related to the regulation of autophagy [19,28]. Interestingly, we have observed a differential pattern in the correlations found between total ROS production and LC3II/ I ratio, suggesting a synergistic effect of ROS and autophagy in type 2 diabetic patients. These results suggest that autophagy is one of the mechanisms that mediate the link between ROS production and the increase of PMN-endothelium interactions in type 2 diabetes versus control conditions.

Several studies point to alterations in autophagy signalling in type 2 diabetic patients [21–23,25,26]. In the present study, type 2 diabetic subjects displayed enhanced protein markers of autophagy, such as LC3I, LC3II, LC3II/LC3I ratio and Beclin-1, which were related to a reduction in p62 protein levels. These results suggest an activation of autophagy in type 2 diabetic patients compared to healthy controls. Activation or alteration of autophagy has been reported in different situations of hyperlipidaemia and hyperglycaemia. For example, previous research has shown mitochondrial dysfunction and altered autophagy in adipocytes from obese type 2 diabetic patients [23], as well as in Goto-Kazikazi (type 2 diabetic) rats [24]. Furthermore, alterations in autophagic parameters in podocytes and leukocytes have been related to diabetic comorbidities such as diabetic nephropathy [26,27,43], cardiac complications [30,31] and neuropathy [31]. Interestingly, in diabetic Wistar rats, insulin exerted different effects on autophagy depending on the origin of the leukocytes [44]. In fact, diabetic M1 bone marrow-derived macrophages (BMM) had their LC3 vesicle-bound content diminished while M2 BMM had enhanced LC3 levels, and insulin treatment failed to rescue autophagy to control levels. In endothelial cells, proinflammatory cytokines have been shown to induce autophagy, which enhances the production of adhesion molecules [45]. In other studies, autophagy has proved to

be a crucial protective mechanism in β cells [28,46].

Our study relates an increase in autophagy-related proteins with an increase of PMN-endothelium interactions in type 2 diabetic patients as well as an increase in NFκB expression. We also show that Beclin-1 protein levels correlate differentially with PMN-endothelium interaction parameters depending on the health status of the subject. While an increase in Beclin-1 was related to a reduction in PMN-endothelium interactions in control subjects, it was associated with an increase in PMN-endothelium interactions in type 2 diabetic patients. This could mean that the increase in PMN-endothelium interactions is strongly influenced by Beclin-1, and that changes in its expression imply different signalling cascades depending on the status of the subject. Furthermore, we have observed a positive correlation between PMNs adhesion and LC3II in type 2 diabetic patients. Beclin-1 is implicated in different biological processes, including cytokinesis, immunity, adaptation to stress, development, ageing, tumorigenesis and cell death [47]. The effects described in the present study may be associated with the ability of Beclin-1 to exert several functions within of the metabolism of the cell; for example, it interacts with BCL2 to form the BCL2-Beclin-1 complex, which is regulated by AMPK, provoking the dissociation of the complex and thus preventing apoptosis [29]. Another possible reason why only this protein is differentially regulated is that Beclin-1 interacts with VMP-1 upstream from all the other regulators of autophagy [48]; thus, variations in regulation could be due to differences at this level of the autophagy signalling.

5. Conclusions

In summary, this study demonstrates enhanced PMN-endothelium interactions, ROS production and autophagy activation in type 2 diabetic patients. Moreover, we show a differential behaviour of autophagy in control and type 2 diabetic subjects regarding ROS levels and PMN endothelium-interactions. These data endorse a connection between these three key mechanisms in type 2 diabetes, and highlights the changes in Beclin-1 as a possible linking mechanism between ROS production and PMN-endothelium interactions. Furthermore, we show that the pattern of autophagy markers differs depending on the presence or not of type 2 diabetes, perhaps pointing to metabolic pathways that need to be elucidated by future research.

Acknowledgements

The authors thank Brian Normanly (University of Valencia/ CIBERehd) for his editorial assistance; and Rosa Falcón for their technical assistance.

Appendix A. Supplementary data:

Supplementary figure 1

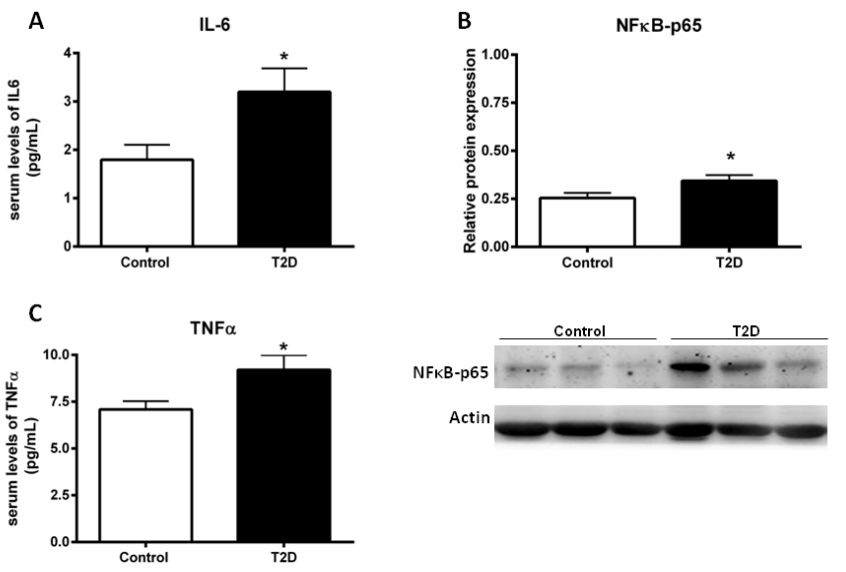

Supplementary Figure 1: Serum and cellular inflammation markers in control and type 2 diabetic patients; Serum levels of IL6 (A) and TNFα (C) in samples obtained from control and type 2 diabetic patients. PMNs protein levels of p-65 NFκB were measured by western blot as shown in the graph (B) and in the representative images.

References

[1] NCD Risk Factor Collaboration, Worldwide trends in diabetes since 1980: a pooled analysis of 751 population-based studies with 4·4 million participants, Lancet 387 (2016) 1513–1530.

[2] American Diabetes Association Diagnosis and Classification of Diabetes Mellitus, Diabetes Care 33 (2009) S62–S69.

[3] V.A. Fonseca, Defining and characterizing the progression of type 2 diabetes, Diabetes Care 32 (2009) S151.

[4] M. Akbari, V. Hassan-Zadeh, Hyperglycemia affects the expression of inflammatory genes in peripheral blood mononuclear cells of patients with type 2 diabetes, Immunol. Invest. (2018) 1–12.

[5] S. Yamagishi, T. Imaizumi, Diabetic vascular complications: pathophysiology, bio-chemical basis and potential therapeutic strategy, Curr. Pharmaceut. Des. 11 (2005) 2279–2299.

[6] N.G. Cruz, L.P. Sousa, M.O. Sousa, N.T. Pietrani, A.P. Fernandes, K.B. Gomes, The linkage between inflammation and Type 2 diabetes mellitus, Diabetes Res. Clin. Pract. 99 (2013) 85–92.

[7] S.E. Kahn, R.L. Hull, K.M. Utzschneider, Mechanisms linking obesity to insulin re-sistance and type 2 diabetes, Nature 444 (2006) 840–846.

[8] S. Bhansali, A. Bhansali, R. Walia, U.N. Saikia, V. Dhawan, Alterations in mi- tochondrial oxidative stress and mitophagy in subjects with prediabetes and type 2 diabetes mellitus, Front. Endocrinol. 8 (2017) 347.

[9] R. Blake, I.A. Trounce, Mitochondrial dysfunction and complications associated with diabetes, BBA 1840 (2014) 1404–1412.

[10] N. Diaz-Morales, S. Rovira-Llopis, I. Escribano-Lopez, C. Bañuls, S. Lopez- Domenech, R. Falcón, A.M. de Marañón, E. Sola, A. Jover, I. Roldan, J.L. Díez, M. Rocha, A. Hernández-Mijares, V.M. Victor, Role of oxidative stress and mi- tochondrial dysfunction in skeletal muscle in type 2 diabetic patients, Curr. Pharmaceut. Des. 22 (2016) 2650–2656.

[11] B. Niemann, S. Rohrbach, M.R. Miller, D.E. Newby, V. Fuster, J.C. Kovacic, Oxidative stress and cardiovascular risk: obesity, diabetes, smoking, and pollution: Part 3 of a 3-Part Series, J. Am. Coll. Cardiol. 70 (2017) 230–251.

[12] M. Morohoshi, K. Fujisawa, I. Uchimura, F. Numano, Glucose-dependent interleukin 6 and tumor necrosis factor production by human peripheral blood monocytes in vitro, Diabetes 45 (1996) 954–959.

[13] C.E. Tabit, W.B. Chung, N.M. Hamburg, J.A. Vita, Endothelial dysfunction in diabetes mellitus: molecular mechanisms and clinical implications, Rev. Endocr. Metab. Disord. 11 (2010) 61–74.

[14] T. McCaffrey, C. Fu, A. Re, H. Bush, A.S. Asch, E. Griffin, N. Hamel, A link between diabetes and atherosclerosis: glucose regulates expression of CD36 at the level of translation, Nat. Med. 7

(2001) 840–846.

[15] F. Kim, K.A. Tysseling, J. Rice, B. Gallis, L. Haji, C.M. Giachelli, E.W. Raines, M.A. Corson, M.W. Schwartz, Activation of IKKbeta by glucose is necessary and sufficient to impair insulin signaling and nitric oxide production in endothelial cells, J. Mol. Cell. Cardiol. 39 (2005) 327–334.

[16] K. Ley, C. Laudanna, M.I. Cybulsky, S. Nourshargh, Getting to the site of inflammation: the leukocyte adhesion cascade updated, Nat. Rev. Immunol. 7 (2007) 678–689.

[17] C. Savoia, E.L. Schiffrin, Vascular inflammation in hypertension and diabetes: molecular mechanisms and therapeutic interventions, Clin. Sci. 112 (2007) 375–384.

[18] R. Robertson, H. Zhou, T. Zhang, J. Harmon, Chronic oxidative stress as a mechanism for glucose toxicity of the beta cell in Type 2 diabetes, Cell Biochem. Biophys. 48 (2007) 139–146.

[19] B. Carroll, E.G. Otten, D. Manni, R. Stefanatos, F.M. Menzies, G.R. Smith, D. Jurk,N. Kenneth, S. Wilkinson, J.F. Passos, J. Attems, E.A. Veal, E. Teyssou, D. Seilhean, S. Millecamps, E.L. Eskelinen, A.K. Bronowska, D.C. Rubinsztein, A. Sanz, V.I. Korolchuk, Oxidation of SQSTM1/p62 mediates the link between redox state and protein homeostasis, Nat. Commun. 9 (2018) 256–272.

[20] Tanida, Autophagosome formation and molecular mechanism of autophagy, Antioxidants Redox Signal. 14 (2011) 2201–2214.

[21] H.S. Jung, Myung-Shik Lee, Role of autophagy in diabetes and mitochondria, Ann. N. Y. Acad. Sci. 1201 (2010) 79–83.

[22] C.D. Gonzalez, M.S. Lee, P. Marchetti, M. Pietropaolo, R. Towns, M.I. Vaccaro, H. Watada, J.W. Wiley, The emerging role of autophagy in the pathophysiology of diabetes mellitus, Autophagy 7 (2011) 2–11.

[23] Ost, K. Svensson, I. Ruishalme, C. Brännmark, N. Franck, H. Krook, P. Sandström, P. Kjolhede, P. Strålfors, Attenuated mTOR signaling and enhanced autophagy in adipocytes from obese patients with type 2 diabetes, Mol. Med. 16 (2010) 235–246.

[24] J. Yan, Z. Feng, J. Liu, J. Liu, W. Shen, Y. Wang, K. Wertz, P. Weber, J. Long, Enhanced autophagy plays a cardinal role in mitochondrial dysfunction in type 2 diabetic Goto–Kakizaki (GK) rats: ameliorating effects of (−)-epigallocatechin-3-gallate, J. Nutr. Biochem. 23 (2012) 716–724.

[25] A.J. Meijer, P. Codogno, Autophagy: a sweet process in diabetes, Cell Metabol. 8 (2008) 275–276.

[26] Li Fang, Yang Zhou, Hongdi Cao, Ping Wen, Lei Jiang, Weichun He, Chunsun Dai, Junwei Yang, Autophagy attenuates diabetic glomerular damage through protec- tion of hyperglycemia-induced podocyte injury, PLoS One 8 (2013) e60546.

[27] C. Dong, H. Zheng, S. Huang, N. You, Q. You, J. Xu, X. Ye, Q. Zhu, Y. Feng, H. Miao, D. Ding, Y. Lu, Heme oxygenase-1 enhances autophagy in podocytes as a protective mechanism against high glucose-induced apoptosis, Exp. Cell Res. 337 (2015) 146–159.

[28] J. Yin, Y. Li, Y. Wang, G. Liu, J. Wang, X. Zhu, S. Pan, The role of autophagy in endoplasmic

reticulum stress-induced pancreatic β cell death, Autophagy 8 (2012) 158–164.

[29] C. He, H. Zhu, H. Li, M. Zou, Z. Xie, Dissociation of Bcl-2-Beclin1 complex by activated AMPK enhances cardiac autophagy and protects against cardiomyocyte apoptosis in diabetes, Diabetes 62 (2013) 1270–1281.

[30] K. Kim, Y. Shin, M. Akram, E. Kim, K. Choi, H. Suh, C. Lee, O. Bae, High glucose condition induces autophagy in endothelial progenitor cells contributing to an- giogenic impairment, Biol. Pharm. Bull. 37 (2014) 1248–1252.

[31] S. Kobayashi, X. Xu, K. Chen, Q. Liang, Suppression of autophagy is protective in high glucose-induced cardiomyocyte injury, Autophagy 8 (2012) 577–592.

[32] Y. Kabeya, S. Hong, J.W. Wiley, T. Yoshimori, R. Towns, D.J. Klionsky, C. Guo, M. Kaplan, Y. Shangguan, Sera from patients with type 2 diabetes and neuropathy induce autophagy and colocalization with mitochondria in SY5Y cells, Autophagy 1 (2005) 163–170.

[33] Escribano-Lopez, N. Diaz-Morales, F. Iannantuoni, S. López-Domènech, A.M. de Marañón, Z. Abad-Jiménez, C. Bañuls, S. Rovira-Llopis, J.R. Herance, M. Rocha, V.M. Víctor, The mitochondrial antioxidant SS-31 increases SIRT1 levels and ameliorates inflammation, oxidative stress and leukocyte-endothelium interactions in type 2 diabetes, Sci. Rep. 1 (2018) 158–162.

[34] D. Howatt, A. Balakrishnan, J. Moorleghen, L. Muniappan, D. Rateri, H. Uchida, J. Takano, T. Saido, A. Chishti, L. Baud, V. Subramanian, Leukocyte calpain defi- ciency reduces angiotensin II–induced inflammation and atherosclerosis but not abdominal aortic aneurysms in mice, ATVB 36 (2016) 835–845.

[35] R. Shurtz-Swirski, S. Sela, A.T. Herskovits, S.M. Shasha, G. Shapiro, L.B.N. Kristal, Involvement of peripheral polymorphonuclear leukocytes in oxidative stress and inflammation in type 2 diabetic patients, Diabetes Care 24 (2001) 104–110.

[36] K. Esposito, F. Nappo, R. Marfella, G. Giugliano, F. Giugliano, M. Ciotola, L. Quagliaro, A. Ceriello, D. Giugliano, Inflammatory cytokine concentrations are acutely increased by hyperglycemia in humans: role of oxidative stress, Circulation 106 (2002) 2067–2072.

[37] R. Mazor, R. Shurtz-Swirski, R. Farah, B. Kristal, G. Shapiro, F. Dorlechter, M. Cohen-Mazor, E. Meilin, S. Tamara, S. Sela, Primed polymorphonuclear leukocytes constitute a possible link between inflammation and oxidative stress in hy- perlipidemic patients, Atherosclerosis 197 (2008) 937–943.

[38] S. Rangasamy, P.G. McGuire, C. Franco Nitta, F. Monickaraj, S.R. Oruganti, A. Das, Chemokine mediated monocyte trafficking into the retina: role of inflammation in alteration of the blood-retinal barrier in diabetic retinopathy, PLoS One 9 (2014) e108508.

[39] R. Farah, R. Shurtz-Swirski, O. Lapin, Intensification of oxidative stress and in- flammation in type 2 diabetes despite antihyperglycemic treatment, Cardiovasc. Diabetol. 7 (2008) 20.

[40] F. Song, W. Jia, Y. Yao, Y. Hu, L. Lei, J. Lin, X. Sun, L. Liu, Oxidative stress, antioxidant status and DNA damage in patients with impaired glucose regulation and newly diagnosed type 2 diabetes, Clin. Sci. 112 (2007) 599–606.

[41] E. Čolak, N. Majkić-Singh, S. Stanković, V. Srecković-Dimitrijević, P.B. Djordjević, K. Lalić, N. Lalić, Parameters of antioxidative defense in type 2 diabetic patients with cardiovascular complications, Ann. Med. 37 (2005) 613–620.

[42] S. Nakanishi, G. Suzuki, Y. Kusunoki, K. Yamane, G. Egusa, N. Kohno, Increasing of oxidative stress from mitochondria in type 2 diabetic patients, Diabetes Metab. Res. Rev. 20 (2004) 399–404.

[43] W. Chen, K. Hung, M.S. Wen, P.Y. Hsu, T.H. Chen, H.D. Wang, J.T. Fang, S.S. Shie, C.Y. Wang, Impaired leukocytes autophagy in chronic kidney disease patients, Cardiorenal Med. 3 (2013) 254–264.

[44] K.K.S. Sunahara, F.P.B. Nunes, M.A.P. Baptista, P. Strell, P. Sannominoya, L.S. Westernberg, J.O. Martins, Insulin influences autophagy response distinctively in macrophages of different compartments, Cell. Physiol. Biochem. 34 (2014) 2017–2026.

[45] L. Chu, Y. Hsueh, H. Cheng, K.K. Wu, Cytokine-induced autophagy promotes long term VCAM-1 but not ICAM-1 expression by degrading late-phase IκBα, Sci. Rep. 7 (2017) 12472.

[46] G. Xia, T. Zhu, X. Li, Y. Jin, J. Zhou, J. Xiao, ROS-mediated autophagy through the AMPK signaling pathway protects INS-1 cells from human islet amyloid polypep- tide-induced cytotoxicity, Mol. Med. Rep. 18 (2018) 2744–2752.

[47] E. Wirawan, S. Lippens, T. Vanden-Berghe, A. Romagnoli, G.A. Fimia, M. Piacentini, P. Vandenabeele, Beclin1: a role in membrane dynamics and beyond, Autophagy 8 (1) (2018) 6–17.

[48] M.I. Molejon, A. Ropolo, A.L. Re, V. Boggio, M.I. Vaccaro, The VMP1-beclin 1 in- teraction regulates autophagy induction, Sci. Rep. 3 (2013) 1055.

4.2. CHAPTER 2

Association between proinflammatory markers, leukocyte–endothelium interactions, and carotid intima–media thickness in type 2 diabetes: role of glycemic control

Aranzazu Martínez de Marañón [1], Francesca Iannantuoni [1], Zaida Abad-Jiménez [1], Francisco Canet [1], Pedro Díaz-Pozo [1], Sandra López-Domènech [1], Ildefonso Roldán-Torres [2], Carlos Morillas [1], Milagros Rocha [1 3], Víctor M Víctor [1 3 4].

[1]Service of Endocrinology and Nutrition, University Hospital Doctor Peset, Foundation for the Promotion of Health and Biomedical Research in the Valencian Region (FISABIO), 46017 Valencia, Spain.

[2]Service of Cardiology, University Hospital Doctor Peset, Foundation for the Promotion of Health and Biomedical Research in the Valencian Region (FISABIO), 46017 Valencia, Spain.

[3]Centro de Investigación Biomédica en Red (CIBERehd)-Department of Pharmacology, University of Valencia, 46010 Valencia, Spain.

[4]Department of Physiology, University of Valencia, 46010 Valencia, Spain.

Journal of Clinical Medicine. 2020 Aug 5;9(8):2522.

DOI: 10.3390/jcm9082522

ABSTRACT

Glycated hemoglobin monitorization could be a tool for maintaining type 2 diabetes (T2D) under control and delaying the appearance of cardiovascular events. This cross-sectional study was designed to assess the role of glycemic control in modulating early-stage markers of cardiovascular complications. One hundred and eight healthy controls and 161 T2D patients were recruited and distributed according to their glycemic control, setting the threshold at 6.5% (good control). Biochemical and anthropometrical parameters were registered during the initial visit, and peripheral blood was extracted to obtain PMNs and analyze inflammatory markers, adhesion molecules, leukocyte–endothelium interactions, and carotid intima–media thickness. Correlations between these parameters were explored. We found that inflammatory markers and adhesion molecules were augmented in T2D subjects with poor glycemic control. PMNs interacted more with the endothelium in the diabetic population, and even more significantly in the poorly controlled subjects. In parallel, carotid intima–media thickness was also increased in the diabetic population, and the difference was greater among poorly controlled subjects. Finally, correlation measurement revealed that carotid intima–media thickness was related to glycemic control and lipid metabolism in diabetic patients. Our results suggest that glycemic control delays the onset of cardiovascular comorbidities in diabetic subjects.

Keywords: type 2 diabetes; glycated hemoglobin; carotid intima–media thickness; inflammation; endothelial function.

1. INTRODUCTION

T2D is currently one of the most prevalent metabolic diseases, affecting around 500 million people. Its incidence has doubled since 1980 [1,2], increasing health expenditure because of T2D itself and due to its derived complications [1–4]. In fact, CVD are the leading cause of death among T2D subjects [2,5], being caused mainly by advanced atherosclerosis, which can be delayed or prevented by early and maintained glycemic control. One of the key markers of glycemic control is HbA_{1c}, and reducing its levels is a primary goal of diabetic treatment [6–8]. In fact, several studies have demonstrated that sustaining HbA_{1c} below 6.5% reduces the incidence of macro- and microvascular comorbidities [7,9–13].

T2D is associated with a proinflammatory background, caused by high circulating glucose, accumulation of advanced glycation end products (AGEs), glycation of haemoglobin, alteration of lipid metabolism in adipose tissue, and other metabolic alterations that favor a proinflammatory state in peripheral blood [14–16]. If sustained for long periods, all of these modifications promote the production by tissue of a wide array of proinflammatory cytokines such as IL-6 and TNFα, as well as ROS [15–20], especially by mitochondria. In short, hyperglycemia and hyperlipidemia trigger NLRP inflammasome activation, TNFα synthesis, and the production of mitochondrial and non mitochondrial ROS [21–23]. This induces NFκB activation and inflammatory cytokine expression, mostly through thioredoxin-related protein action [24–27]. Moreover, lipids can react with ROS and amplify the proinflammatory cascade [28]. This results in a vicious cycle of cell death and greater inflammation [29]. This ROS–inflammation axis has been studied in a wide array of inflammatory-based diseases, such as cardiac alterations [30–32], bone and joint diseases [33–35], neuronal and cerebral dysfunctions [28,29,36], bacterial infection [37], liver diseases [38], respiratory alterations [39,40] and cancer [41]. Furthermore, in T2D, the continuous presence of proinflammatory

molecules causes diverse endocrine effects on the vasculature, and contributes to the development of micro- and macrovascular pathologies such as carotid atherosclerosis [21]. Together, the sustained increase of ROS production and the rise in inflammation have an important effect on the development of diabetic atherosclerosis [22]. Immune cells are also activated in T2D, producing more proinflammatory and adhesion molecules [15,16,42,43]. As explained previously, circulating proinflammatory molecules produced by chronic hyperglycemia and hyperlipidemia can activate leukocytes and the endothelium [44,45]. In this state, immune cells interact with the endothelium, infiltrating the inner layers of tissues and intensifying the inflammation [15,44,45]. There are different epidemiologic studies describing how an increased leukocyte count is a risk factor for the progression of carotid atherosclerosis and cardiovascular events [46–48]. Proinflammatory factors also favor the development of the atherosclerotic plaque, as demonstrated by several studies [49–52]. In fact, atherosclerosis represents the culmination of continued subclinical inflammation, and is one of the main causes of cardiovascular comorbidities [6,23,53–55]. Worryingly, atherosclerosis is often asymptomatic for decades before clinical manifestations appear, and is termed subclinical atherosclerosis during this period [6,56,57]. Carotid intima–media thickness (CIMT) is a biomarker of subclinical atherosclerosis [58,59].

Measurement of the CIMT by B-mode ultrasound has been shown to be suitable for evaluating the early stages of atherosclerosis [57,60,61] and to be an indicator of CVD [62–64]. Different studies have described a rise of CIMT in T2D [63,65,66] and metabolic syndrome [67,68].

The aim of this study was to explore the potential involvement of glycemic control in inflammation, adhesion molecules, leukocyte–endothelium interactions, and the CIMT in T2D patients compared with a healthy control population.

2. EXPERIMENTAL SECTION

2.1. Human Subjects

This study was carried out in 269 subjects, specifically, 161 T2D patients and 108 healthy controls recruited from the Service of Endocrinology and Nutrition of University Hospital Doctor Peset (Valencia, Spain) until June 2019 and adjusted for age and sex. The time that these patients had suffered from T2D, the presence of comorbidities, and their drug prescriptions are specified in Supplementary data (Tables S1–S3). The subjects signed a written informed consent form and protocols were approved by our hospital's Ethics Committee for Clinical Investigation (ID: 98/19), in line with the ethical principles of the Helsinki declaration. T2D patients were diagnosed following the American Diabetes Association (ADA) indications, and presence of morbid obesity, insulin treatment, or any autoimmune, haematological, malignant, infectious, organic, or inflammatory disease represented the exclusion criteria.

2.2. Sample Collection

Venous blood samples were obtained from the antecubital vein in fasting conditions. Weight (kg), height (m), BMI (kg/m^2), SBP/DBP (mmHg), and waist circumference (cm) were assessed previous to the blood extraction.

2.3. Laboratory Tests

Serum was isolated from the blood by centrifugation for 10 min at 1500 g and 4 ºC. Fasting glucose, cholesterol, and TG were determined by an enzymatic method. HDL-c levels

were measured with a Beckman LX-20 autoanalyzer (Beckman Coulter, La Brea, CA, USA) using a direct method. LDL-c was determined with Friedewald's formula. An immunochemiluminescence assay was employed to determine insulin levels. HOMA-IR index [fasting insulin (μU/mL) × fasting glucose (mg/dl)/405] was calculated to estimate IR Percentage of HbA_{1c} was determined with an automatic glycohaemoglobin analyzer (Arkray, Inc., Kyoto, Japan). Apolipoproteins were measured with an electroimmunoassay. hsCRP was analyzed employing an immunonephelometer (Behring Nephelometer II, Dade Behring, Inc., Newark, DE, USA).

2.4. Leukocyte Isolation

In this assay, PMNs were isolated from heparinized whole blood by the following protocol: the blood was mixed with 1:2 volumes of dextran solution (3% in NaCl 0.9%; Sigma Aldrich, MO, USA) and incubated for 45 min. The supernatant was then poured over Ficoll-Hypaque (GE Healthcare, Uppsala, Sweden) and centrifuged at 650× g for 25 min. The resulting pellet was lysed to remove the remaining erythrocytes with lysis buffer (5 min at room temperature) and centrifuged at 240× g. Pellets containing leukocytes were then washed twice and resuspended in Hank's balanced salt solution (HBSS; Sigma Aldrich, MO, USA). This cellular suspension was employed to perform the leukocyte–endothelium interaction assay.

2.5. Soluble Cytokines and Adhesion Molecule Assay

ICAM-1, VCAM-1, P-selectin, IL-6, and TNFα were analyzed in serum samples with a

Luminex 200 flow analyzer system (Millipore, Austin, TX, USA). In brief, specific antibodies covered the color-coded microbead, and detection was performed with biotinylated secondary antibody and streptavidin-PE conjugate. The fluorescence of each individual microbead was analyzed with the Luminex XMap instrument. This method allows multiple cytokines in the same sample to be analyzed with a high specificity ad sensitivity. The TNFα detection range was between 1750 and 0.43 pg/mL; that of IL-6 is 750 to 0.18 pg/mL; that of VCAM-1 is 500 to 0.122 ng/mL; that of ICAM-1 is 350 to 0.085 ng/mL; and that of P-selectin is 1000 to 0.122 ng/mL. The intra-assay %CV is <5% for TNFα and IL-6 and <15% for ICAM-1, VCAM-1, and P-selectin. The interassay %CV is <20% for IL-6, ICAM-1, VCAM-1, and P-selectin and <15% for TNFα.

2.6. Static Cytometry Measurements

Mitochondrial ROS production was evaluated employing a MitoSOX (Thermo Fisher Scientific, Waltham, MA, USA) fluorescent probe. A fluorescence microscope (IX81; Olympus Corporation, Shinjuku-ku, Tokyo, Japan) with automated static cytometry software (ScanR, Olympus, Munich, Germany), which measures the fluorescence emission per individual cell, was also used. In brief, the protocol consisted of seeding PMNs, extracted as previously specified, in 48-well plates and allowing them to adhere to the well surface. MitoSOX and DAPI (Sigma Aldrich, MO, USA) were then added to the well at a final concentration of 0.1 µM, for 20 min. After washing the cells twice with HBSS, fluorescence was measured and MitoSOX emission data relativized to DAPI emission data for each cell. PMNs data were relativized with an internal control for all the experiments. All experiments were performed in duplicate, and 16 images per well were measured.

2.7. PMN–Endothelium Interaction Assay

An aliquot of 1.2 mL PMNs, isolated as previously described [69], with a density of 10^6 cells/mL in complete Roswell Park Memorial Institute medium RPMI, was employed for this assay. Primary cultures of HUVEC were prepared as reported in [69]. In this assay, the PMNs aliquot was perfused across the endothelial monolayer at a speed of 0.3 mL/min over a 5 min period, and the process was recorded. Rolling PMNs were considered to be those rolling for at least 1 min. Velocity was assessed by determining the time in which 15 rolling PMNs covered a distance of 100 µm. Adhesion was analyzed by counting the number of PMNs adhering to the endothelium for at least 30 s in 5 different fields.

2.8. Assessment of Carotid Intima–Media Thickness (CIMT)

Carotid thickness was evaluated following the American Echocardiography Association's guidelines. Healthy subjects and T2D patients were told to attend the Cardiology Service of the Dr. Peset Hospital 7–10 days after the blood extraction in order to evaluate carotid intima–media thickness. This measure has a diagnostic value because of its positive correlation with risk factors and with the prevalence of cardiovascular and cerebrovascular disease. The evaluation was performed by placing the head of the patients at 45º with respect to the body longitudinal axis. Some subjects were dropped from the study due to clinical or schedule reasons.

Carotid sonography was performed with a single ultrasound machine Aloka 5500 (Hitachi Aloka, Tokyo, Japan) equipped with a 7.5 MHz sector scanner probe. Baseline and follow-up studies were performed in a standard fashion by a single specialist physician who

was specifically trained to perform the examination and was blinded to the treatment group. All images were electronically stored. Measurements corresponded with the 1 cm segment proximal to the dilation of the carotid bulb, and were always performed in plaque-free segments. For each patient, three measurements were performed for both sides of the anterior, lateral, and posterior projections of the far wall, and readings were then averaged. An independent observer, who was blinded to the treatment group and trained to interpret the CIMT images, performed an off-line analysis of B-mode ultrasound images. Paired CIMT measurements in the same arteries showed a high degree of reproducibility, with a mean difference in CIMT of 0.020 mm, and an intraclass correlation coefficient of 0.97 ($p < 0.001$). CIMT regression was defined as a decrease of >0.020 mm in mean CIMT at 12 months.

2.9. Statistical Analysis

All data were analyzed with SPSS 17.0 software (SPSS Statistics Inc., Chicago, IL, USA). Values are expressed as mean and standard deviation (SD) for parametric data, while the median (25th–75th percentiles) is presented for nonparametric data. Bar graphs show mean and standard error of the mean (SEM) in the figures. Multivariate lineal analysis was performed to check the influence of BMI and age on the other dependent variables.

Correlation analysis was performed with the Spearman formula, and the linear regression coefficient was also calculated. Graphs were plotted with GraphPad Prism 4.0 (GraphPad, La Jolla, CA, USA).

Multivariate linear analysis was performed in order to eliminate the influence of BMI and age on the variables of interest. Normality of the data sets was assessed by Kolmogorov–Smirnov test. In the case of the variables with normally distributed data, the

groups were compared with a Student's t-test, while a Mann–Whitney U test was employed for non-normally distributed ones, and the Chi-Square test for proportion of frequencies. Study groups were compared using one-way analysis of variance (ANOVA) followed by a Bonferroni post hoc test. Differences were considered to be significant when $p < 0.05$, applying a confidence interval of 95% in every comparison. Graphs were plotted with GraphPad Prism 4.0 (GraphPad, La Jolla, CA, USA).

3. Results

3.1. Anthropometric and Biochemical Parameters

The study population was initially divided into healthy controls (108) and T2D patients (161) following the diagnostic criteria of the ADA. Diabetic patients were divided into two populations depending on their glycemic control, which was represented by their levels of HbA_{1c}. The set threshold was 6.5, in line with ADA criteria [7]. Table 1 confirms that both diabetic populations had typical hallmarks, with significant differences in glucose ($p < 0.01$), HbA_{1c} ($p < 0.01$), and HOMA index ($p < 0.01$). Moreover, significant differences in glucose levels ($p < 0.001$) and HOMA index ($p < 0.001$) were found between the T2D $HbA_{1c} > 6.5$ group and the T2D $HbA_{1c} \leq 6.5$ group. Our T2D populations also displayed features such as greater waist diameter ($p < 0.01$), increased waist-to-hip ratio ($p < 0.01$), higher HOMA index ($p < 0.01$), and altered lipid metabolism parameters, with increased VLDL-c and triglyceride levels ($p < 0.01$), Ct/HDL-c ($p < 0.01$), and AIP ($p < 0.01$) and lower levels of HDL-c ($p < 0.01$). Total cholesterol, LDL-c, and non-HDL-c levels remained unchanged in the T2D $HbA_{1c} \leq 6.5\%$ group. However, total and LDL-c were significantly reduced ($p < 0.01$) in the T2D $HbA_{1c} > 6.5$ group, possibly due to the hypolipemiant treatment. Regarding apolipoproteins, ApoA1 was significantly lower in T2D patients with respect to healthy controls ($p < 0.01$) and the difference was even more significant in the $HbA_{1c} > 6.5\%$ group ($p < 0.001$). ApoB levels did not change. Interestingly, the ApoB/ApoA ratio significantly increased in the T2D $HbA_{1c} > 6.5$ population ($p < 0.01$).

Table 1: Anthropometrical and biochemical parameters.

	Control	T2D	
		HbA_{1c} ≤6.5%	**HbA_{1c} > 6.5%**
N	108	57	104
Age (Years)	57 ± 11	58 ± 8	60 ± 9
%Women	62.2%	43.93%	56.11%
Weight (Kg)	68.51 ± 15.18	85.02 ± 16.07	83.59 ± 15.84 *
BMI (kg/cm2)	24.18 ± 4.11	31.18 ± 4.23 *	30.43 ± 5.13 *
SBP (mmHg)	119.43 ± 18.18	139.82 ± 14.23 *	138.38 ± 17.05 *
DBP (mmHg)	72.35 ± 10.94	82.03 ± 10.97 *	78.25 ± 9.35 *
Waist (cm)	79.81 ± 12.62	106.39 ± 11.46 *	103.99 ± 13.35 *
Hip (cm)	99.09 ± 7.21	108.71 ± 9.53 *	108.48 ± 12.62 *
Waist–Hip ratio	0.80 ± 0.09	0.97 ± 0.08 *	0.95 ± 0.08 *
Glucose (mg/dL)	88.08 ± 10.75	112.37 ± 22.59 *	160.51 ± 55.06 *‡
HOMA	1.69 ± 1.19	3.72 ± 2.00 *	6.57 ± 4.45 *‡
HbA_{1c} (%)	5.18 ± 0,26	5.94 ± 0.30 *	7.85 ± 1.30 *
Total cholesterol (mg/dL)	185.43 ± 35.32	173.67 ± 34.31	167.42 ± 37.67 *
HDL-c (mg/dL)	56.04 ± 13.61	45.10 ± 11.83 *	42.94 ± 10.46 *
LDL-c (mg/dL)	111.38 ± 28.72	102.62 ± 31.33	95.17 ± 31.09 *
VLDL-c (mg/dL)	26.01 ± 10.81	28.63 ± 19.54 *	28.91 ± 22.04 *
Cholesterol/HDL-c	3.46 ± 0.94	4.07 ± 1.18 *	4.06 ± 1.14 *
TG (mg/dL)	87.62 (55.50; 103.00)	130.29 (90.5; 169.00) *	150.75 (92.00; 162.63) *
Non-HDL Cholesterol (mg/dL)	129.39 ± 33.28	129.37 ± 32.51	124.48 ± 36.57
AIP (TG/HDL-c)	0.10 (−0.06; 0.33)	0.47 (0.23; 0.63) *	0.47 (0.29; 0.68) *
APO A1 (mg/dL)	164.02 ± 32.28	151.45 ± 27.21 *	142.72 ± 22.87 *†
APO B (mg/dL)	90.78 ± 26.60	90.33 ± 25.82	94.18 ± 25.27
APO B/APOA1	0.57 ± 0.20	0.64 ± 0.24	0.67 ± 0.19 *
hsCRP (mg/L)	0.75 (0.36; 1.83)	2.64 (1.61; 7.07) †	2.87 (1.31; 6.59) †

Anthropometrical and biochemical parameters obtained from whole peripheral blood from healthy subjects, HbA_{1c} ≤ 6.5% T2D patients and HbA_{1c} > 6.5% T2D patients after 12 h fasting. Kolmogorov–Smirnov normality test was performed in all data sets. Data are shown as mean SD for data with normal distribution, and median and 25th; 75th percentile for non-normal data. The differences were analyzed by a t-test in the case of normal data and a Mann–Whitney test in that of non-normal data. *, $p < 0.01$ vs. control; †, $p < 0.001$ vs. control; ‡, $p < 0.001$ vs. T2D HbA_{1c} ≤ 6.5%.

3.2. Inflammation Markers

A hyperglycemic scenario is usually accompanied by an increase in subclinical inflammation levels. We analyzed some relevant proinflammatory markers in our cohort of patients and their respective controls. The T2D group showed a significant increase in TNFα levels compared to the control group ($p = 0.047$) (Figure 1A). When we distributed the T2D population based on HbA_{1c}, an increase was preserved in the T2D $HbA_{1c} > 6.5$ group ($p = 0.014$) (Figure 1B). Another relevant cytokine, IL-6, was doubled in T2D subjects ($p = 0.019$) (Figure 1C) and, as occurred with TNFα, the increase was associated with T2D HbA_{1c} >6.5% ($p = 0.015$) (Figure 1D).

Moreover, we evaluated mtROS production, and the results showed a significant rise in mtROS in the T2D population ($p = 0.045$) (Figure 1E), which was more pronounced among the poorly controlled population ($p = 0.038$) (Figure 1F). Poorly controlled T2D patients also had significantly higher levels of mtROS than their well-controlled counterparts ($p = 0.041$) (Figure 1F).

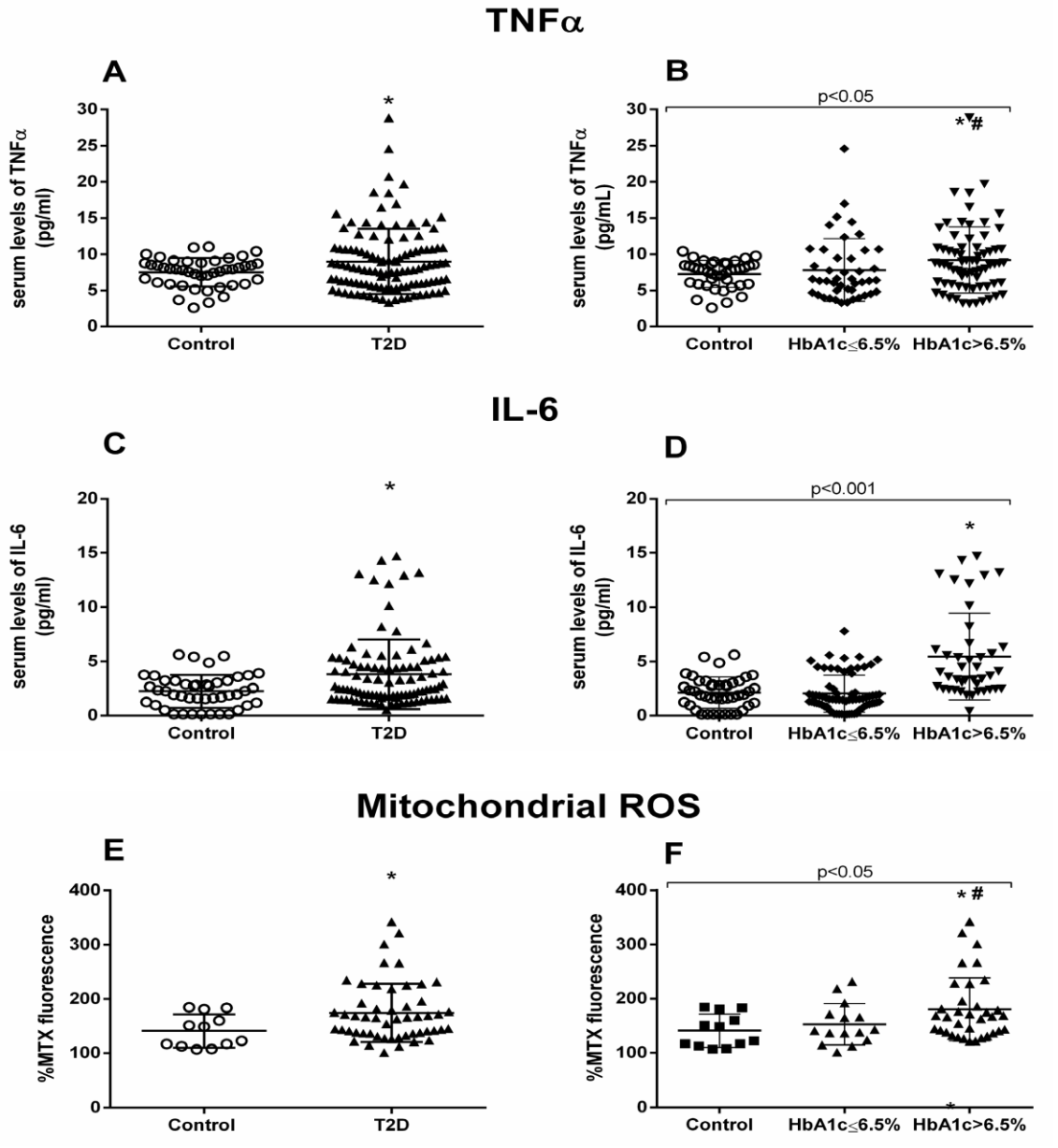

Figure 1: TNF*α*, IL-6, and mtROS measurements. Serum levels of proinflammatory cytokines TNFα (**A**,**B**) and IL-6 (**C**,**D**), and fluorescence levels of mtROS (**E**,**F**). Differences between control and T2D groups (**A**,**C**,**E**) or between control, well-controlled (HbA_{1c} ≤ 6.5%) and poorly controlled diabetic groups (HbA_{1c} > 6.5%) (**B**,**D**,**F**) are shown. Statistical analysis was performed using a t-test to compare two groups, and using ANOVA with Bonferroni post-test for three groups. * $p < 0.05$ vs. control;# $p < 0.05$ vs. T2D HbA1c < 6.5%.

3.3. PMN–Endothelium Interactions

The generalized state of inflammation during T2D entails the activation of immune cells, which, in an active state, are more prone to attach to the endothelium and infiltrate through to the inner layers of the organs. Thus, we analyzed serum levels of adhesion molecules such as ICAM-1, VCAM-1, and P-selectin, some of the main players of leukocyte–endothelium interactions. As can be seen in Figure 2, T2D patients displayed higher levels of ICAM-1 ($p = 0.016$) (Figure 2A) and VCAM-1 ($p = 0.027$) (Figure 2C), but not of P-selectin. The increase in ICAM-1 was already significant in the well-controlled diabetic population ($p = 0.006$) (Figure 2B), and was enhanced in the poorly controlled diabetic population ($p < 0.001$). In addition, VCAM-1 was significantly higher in T2D subjects with $HbA_{1c} > 6.5\%$ ($p = 0.005$) (Figure 2D).

For assessing PMN–endothelium cell interactions directly, we performed an *in vitro* adhesion assay with leukocytes from T2D patients and their respective controls. Leukocyte count was slightly higher but within the normal range in T2D patients. This could reflect the subclinical inflammation level characteristic of T2D (Supplementary Table S4). Rolling number, rolling velocity, and adhesion to the endothelial monolayer were assessed. We obtained a higher number of rolling cells in T2D patients ($p < 0.001$) (Figure 2G), accompanied by a lower velocity of these cells ($p < 0.001$) (Figure 2I) and a higher level of adhesion to the endothelial monolayer ($p < 0.001$) (Figure 2K). These differences remained when we separated the T2D population depending on its glycemic control status ($p < 0.001$) (Figure 2H, J, L). PMN rolling ($p < 0.001$) and adhesion ($p < 0.05$) were increased, while rolling velocity was decreased ($p < 0.001$) in well-controlled diabetic subjects. These significant differences were sustained in poorly controlled diabetic subjects, and were more significant

in the case of cell adhesion ($p< 0.001$). These differences can be assessed in the Supplementary Videos (Supplementary Videos S1–S3), in which representative videos of each experimental group have been attached (Supplementary data).

3.4. Carotid Intima–Media Thickness Measurements

The proinflammatory environment seen in our diabetic patients and the increase in leukocyte–endothelium interactions could represent a rise in the incidence of macro- and microvascular complications. Therefore, we next explored CIMT. All the patients underwent carotid echocardiography at our hospital's Cardiology Service. Diabetic patients showed higher CIMT compared to healthy controls, with this difference being identified in the left carotid ($p < 0.001$) (Figure 3A) and right carotid ($p = 0.003$) (Figure 3C).

We observed that the poorly controlled diabetic population had significantly higher left CIMT than the well-controlled diabetic group ($p = 0.024$) (Figure 3B). On the other hand, right CIMT proved to be significantly higher in the poorly controlled diabetic group than in the control group ($p = 0.001$) (Figure 3D).

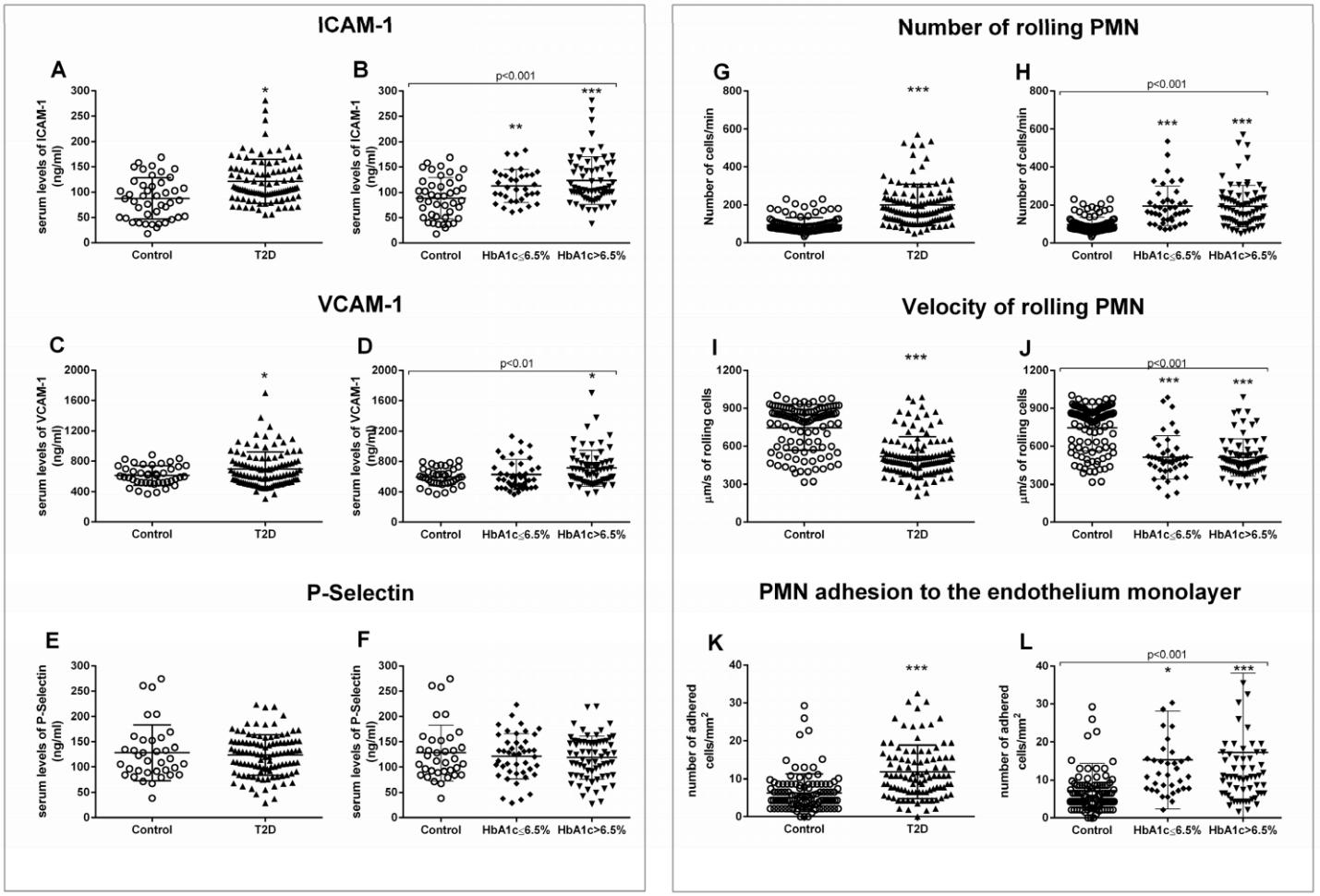

Figure 2: Serum levels of soluble adhesion molecules and measurement of PMN–endothelium interactions. Differences in adhesion molecules between control and T2D groups (**A**,**C**,**E**) or between control, well-controlled diabetics (HbA_{1c} ≤ 6.5%), and poorly controlled diabetics (HbA_{1c} > 6.5%) (**B**,**D**,**F**) are shown. The number of rolling cells (**G**,**H**), their velocity (**I**,**J**), and the adhesion of these cells to the endothelial monolayer (**K**,**L**) were analyzed. Differences between control and T2D groups (**G**,**I**,**K**) or between control, well-controlled diabetics (HbA_{1c} ≤ 6.5%), and poorly controlled diabetic groups (HbA_{1c} > 6.5%) (**H**,**J**,**L**) are shown. Statistical analysis was performed by means of a *t*-test to compare two groups, and using ANOVA with Bonferroni post-test for three groups. * $p < 0.05$;** $p < 0.01$; *** $p < 0.001$ vs. control.

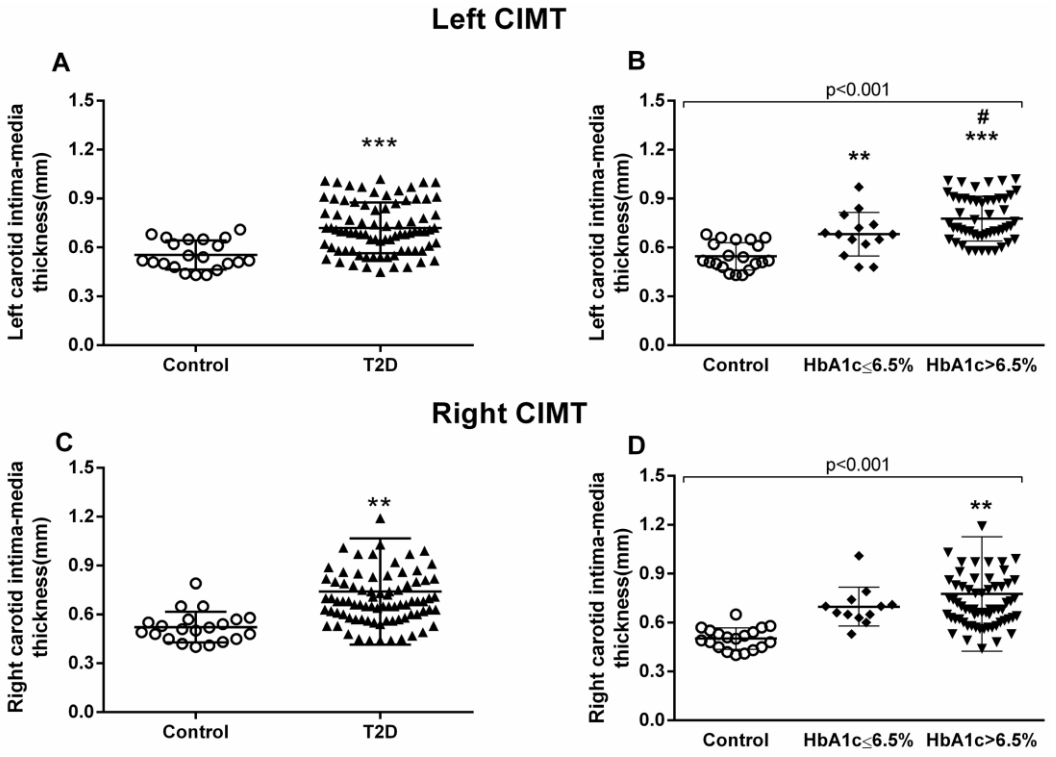

Figure 3. Measurement of carotid intima–media thickness (CIMT). Left carotid (A,B) and right carotid (C,D) were analyzed. Differences between control and T2D groups (A,C) or between control, well-controlled (HbA1c ≤ 6.5%), and poorly controlled diabetic groups (HbA1c > 6.5%) (B,D) are shown in the graphs. Statistical analysis was performed by means of a t-test to compare two groups, and using ANOVA with a Bonferroni post-test for three groups. ** $p < 0.01$; *** $p < 0.001$ vs. control group; # $p < 0.05$ vs HbA1c ≤ 6.5% group.

3.5. Correlation Analysis

We took all these data and performed correlations and linear regression to explore relations between all the analyzed variables. First, we analyzed the relationship between *in vitro* adhesion assay parameters and the left CIMT; we observed positive correlations (rolling number Figure 4A, $p = 0.037$, $r = 0.218$; rolling velocity Figure 4C, $p = 0.021$, $r = 0.252$; adhesion Figure 4E, $p = 0.037$, $r = 0.239$) among the left carotid measures but not among those of the right (Figure 4B,D,F).

Regarding biochemical parameters, we saw that left CIMT measures correlated significantly with glucose ($p = 0.003$, $r = 0.203$) (Figure 5A), HOMA-IR ($p < 0.001$, $r = 0.338$) (Figure 5C), BMI ($p = 0.036$, $r = 0.235$) (Figure 5E), and HbA_{1c} ($p < 0.001$, $r = 0.399$) (Figure 5G). These correlations were similar for the right CIMT, except for BMI correlation, which was not significant (Figure 5B (Glucose), $p < 0.001$, $r = 0.377$; Figure 5D (HOMA-IR), $p < 0.001$, $r = 0.360$; Figure 5F (HbA_{1c}), $p < 0.001$, $r = 0.389$).

When we analyzed the correlation with lipid parameters, we observed that left CIMT was significantly correlated with HDL-c ($p < 0.001$, $r = -0.436$) (Figure 6A), VLDL-c ($p = 0.001$. $r = 0.313$) (Figure 6C), cholesterol/HDL-c index ($p = 0.001$, $r = 0.313$) (Figure 6E), and AIP ($p = 0.001$, $r = 0.402$) (Figure 6G). The data for right CIMT revealed similar correlations (Figure 6B (HDL-c), $p = 0.025$, $r = -0.222$; Figure 6D (VLDL-c), $p = 0.007$, $r = 0.270$; Figure 6H (AIP), $p = 0.002$, $r = 0.307$), with the exception of cholesterol/HDL-c index correlation.

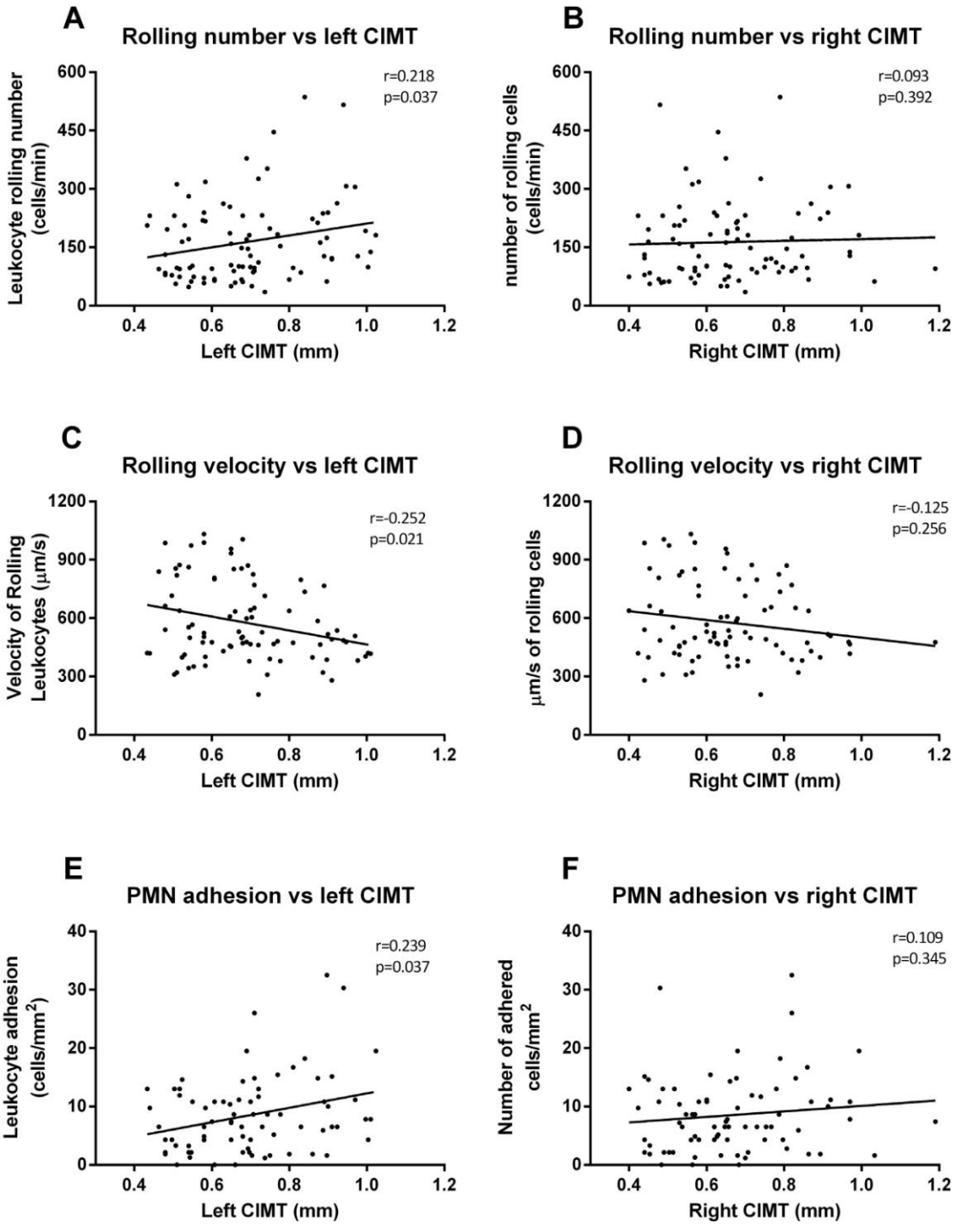

Figure 4. Correlation graphs of adhesion assay vs. CIMT measures. Graphs show correlations between number of rolling PMN and left (**A**) and right CIMT (**B**); rolling velocity and left (**C**) and right CIMT (**D**); and cell adhesion and left (**E**) and right CIMT (**F**). Spearman correlation analysis was performed.

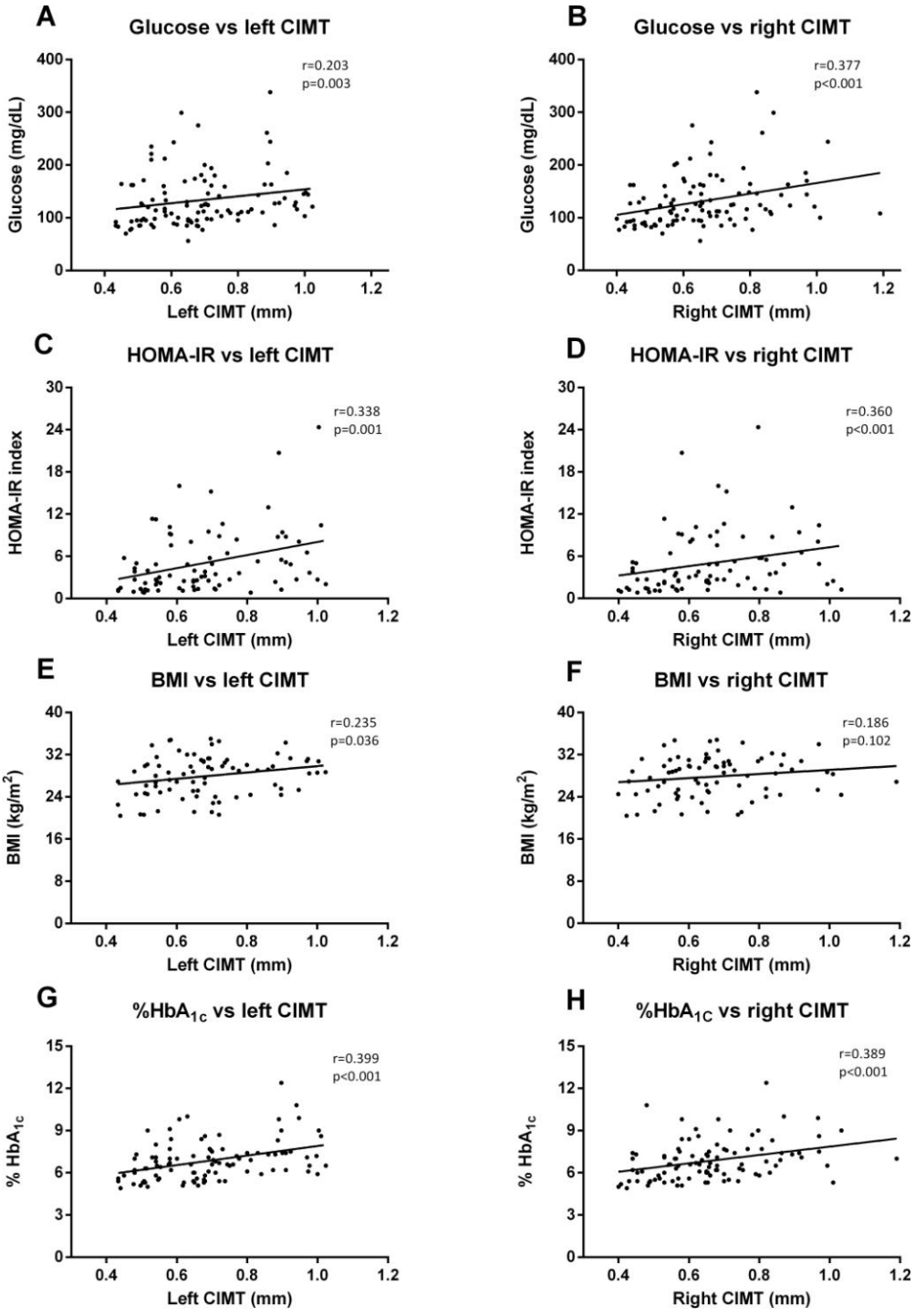

Figure 5. Correlation graphs of biochemical and anthropometrical parameters vs. CIMT measures. Graphs show correlation between glucose levels and left (**A**) and right CIMT (**B**); HOMA index and left (**C**) and right CIMT (**D**); BMI and left (**E**) and right CIMT (**F**); and HbA_{1c} and left (**G**) and right (**H**) CIMT. Spearman correlation analysis was performed.

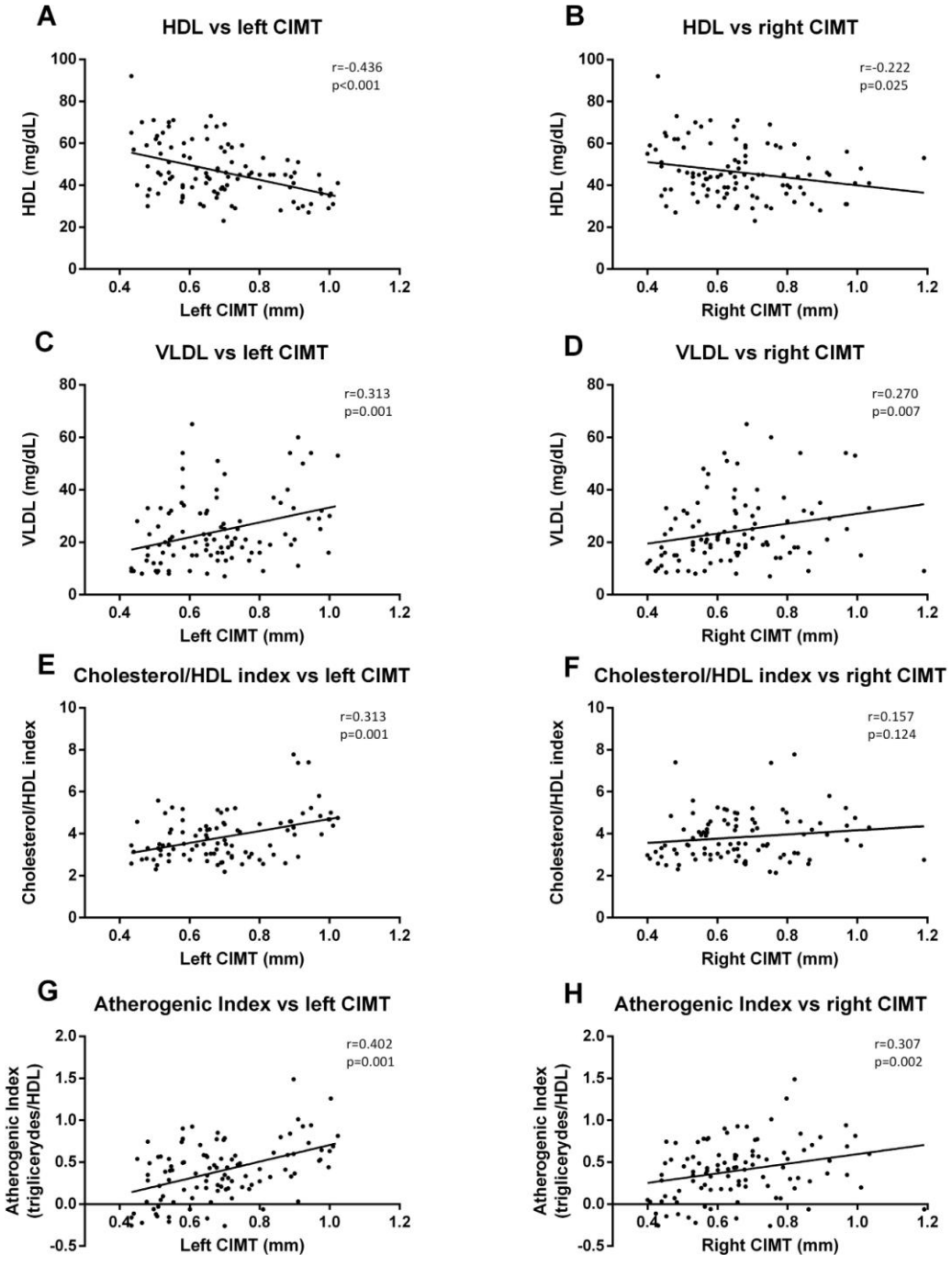

Figure 6. Correlation graphs of lipid metabolism parameters vs. CIMT measurements. Graphs show a correlation of HDL-c with left (**A**) and right CIMT (**B**); of VLDL-c index with left (**C**) and right CIMT (**D**); of cholesterol/HDL-c index with left (**E**) and right CIMT (**F**); and of atherogenic index (AIP) with left (**G**) and right (**H**) CIMT. A Spearman correlation analysis was performed. r coefficient and statistical significance, if any existed, are shown in the graph.

4. Discussion

Cardiovascular complications are a principal concern during diabetes management. The present study gives relevance to the relationship between CIMT, HbA_{1c}, and different hallmarks of T2D (inflammation, ROS production, and leukocyte–endothelium interactions). We have evaluated the involvement of glycemic control in endocrine and anthropometric parameters, inflammatory markers (TNFα, IL-6, and mtROS production), adhesion molecules (ICAM-1, VCAM-1, and P-selectin), leukocyte–endothelium interactions (rolling, rolling velocity, and adhesion) and CIMT in T2D. In addition, we have analyzed their interrelationship by performing correlation studies. T2D patients, and especially those with poor glycemic control (HbA_{1c} > 6.5%), expressed an increase in inflammatory markers, mtROS production, adhesion molecules, leukocyte–endothelium interactions, and CIMT.

Regarding inflammatory intermediates, our study shows a slight but significant increase in TNFα and IL-6 production in T2D patients; it is possible that the difference is not bigger because of the hypolipemiant treatments received by most of the T2D patients. These proinflammatory cytokines are involved in the development of inflammation in T2D. Enhanced levels of TNFα from leukocytes after activation by ROS-induced oxidative stress are thought to impair glucose uptake and inhibit insulin signaling [70,71]. Furthermore, IL-6 is thought to play an important role in atherosclerosis in T2D [56]. We show an increase in mtROS production in leukocytes from T2D patients that was more pronounced in subjects with HbA_{1c} > 6.5%, suggesting that leukocyte mitochondrial function can be altered during chronic hyperglycemia [70,72–74]. Other studies in the field have suggested that good glycemic control reduces ROS production [57,75,76]. These results are in accordance with those of other studies that have demonstrated high mtROS production in T2D related to the development of silent myocardial ischemia [72]. In this sense, it is important to underline

that leukocytes are especially linked to ROS generation and cells that are highly sensitive to the oxidative damage mediated by ROS [77,78].

Different pathophysiological processes, including hypertension and atherosclerosis, are characterized by leukocyte recruitment to the arterial wall. In the present study, we have used an *in vitro* model in which human leukocytes flow over a monolayer of human endothelial cells with a shear stress similar to that observed *in vivo* [72]. This mimics the process that precedes inflammation *in vivo* (rolling and adhesion), and which is critical to homeostasis and vascular cell integrity. Our experimental system has been widely applied to visualize and analyze the multistep recruitment of leukocytes in these diseases, and allows the mechanisms of action implicated in this recruitment to be assessed [79]. Regarding this idea, it has been demonstrated that an inflammatory background favors the increase of leukocyte–endothelium interaction and promotes the early development of atherosclerotic events [80,81]. In the current study, we have observed that T2D enhanced rolling flux and PMNs adhesion and reduced the rolling velocity of PMNs. These effects were more evident in the group with HbA_{1c} > 6.5%. Furthermore, several studies have demonstrated the importance of leukocytes in the atherosclerotic scenario [82–84]. In accordance with these results, an increase in leukocyte–endothelium interactions has been related to oxidative stress in a human model of IR [85]. In addition, Petterson et al. demonstrated that there is increased recruitment but impaired function of leukocytes during inflammation in mouse models of T1D and T2D [86].

Endothelial and immune cell activation can be evaluated by measuring the soluble adhesion molecules VCAM-1, ICAM-1, and P-selectin. In this sense, it has been described that adhesion molecules are enhanced in patients with T2D [87]. In the present study, we show an increase in adhesion molecules, ICAM-1 and VCAM-1, in T2D that was most pronounced

in the case of VCAM-1 in the HbA_{1c} > 6.5% group. These results are compatible with a rise in the number of leukocyte–endothelium interactions, and it has been demonstrated that hyperglycemia in both normal subjects and T2D patients can induce vasoconstriction, adhesion molecules, and inflammation [88,89]. Importantly, there was a slight but significant increase of T2D adhesion molecule levels with respect to the control group, a difference that may have been reduced by the hypolipemiant treatment.

The measurement of CIMT is useful for monitoring the early stages of atherosclerosis [61,90], and CIMT enhancement has been described in T2D [91]. In the present study, we have observed an increase in left and right CIMT, especially in the former case. Furthermore, the increment was more evident in the HbA_{1c} > 6.5% group, suggesting that glycemic control is crucial for leukocyte–endothelium interactions and, therefore, for CIMT. The relevance of these changes in the left CIMT remain to be clarified, though different studies have suggested variations between left and right carotids; for example, Lorentz M. W. et al. revealed that left carotid plaques were vulnerable, whereas right carotid ones were calcified and stable [65]. Luo X et al. studied the factors associated with left and right CIMT and found that changes in biochemical parameters were associated with left carotid measures, while hemodynamic parameters were more related to right carotid measures [92]. The main consequences of CIMT thickening are cerebrovascular events such as stroke, and left carotid stroke is more frequent because of a higher probability of thickening of the left carotid arterial wall [93,94]. The above mentioned authors highlighted that the location of the left carotid renders it more susceptible to hemodynamic stress, thus increasing the probability of arterial wall thickening and rupture. Selwaness M. et al. support this hypothesis; they found that while bilateral plaques were more frequent, 67% of cases of unilateral plaque occurred in the left carotid. This left plaque presented more intraplaque hemorrhage and more

fibrous tissue and was thicker than the left, all of which explain why the left plaque is more vulnerable and prone to stroke. In the same study, right CIMT was found to be more calcified than the left, which would make it more resistant to shear stress [95].

In the present study, we have observed positive correlations between *in vitro* adhesion assay parameters and left CIMT, but not right CIMT. These results confirm the relevance of the enhancement of leukocyte–endothelium interactions in CIMT, especially on the left side. In terms of biochemical parameters, left CIMT measures correlated significantly with glucose, HOMA-IR, BMI, and HbA_{1c}. These correlations were maintained in the right CIMT, except for BMI (which was not significant). In line with these results, a systematic review by Einarson et al. found that individuals with impaired glucose tolerance had slightly (though significantly) higher CIMT values than individuals with normal glucose tolerance [96]. This data, together with leukocyte–endothelium interactions, suggest that poor glycemic control leaves T2D diabetic patients more prone to developing early or subclinical atherosclerotic events due to the rise in the number of leukocytes infiltrating the intima–media layer. Finally, we analyzed correlations between CIMT and lipid parameters, and observed that the left CIMT was significantly correlated with VLDL-c, cholesterol/HDL-c index, and AIP. All these correlations were maintained when we analyzed the right CIMT data, with the exception of the cholesterol/HDL-c index correlation. In this sense, Pillai *et al*., [97] demonstrated that lipid parameters, including total cholesterol, TG, LDL-c, and VLDL-c, were significantly higher in diabetic stroke patients and positively correlated with the risk of stroke. CIMT was significantly higher in diabetic stroke patients, and correlations of lipid parameters (TC, TG, and VLDL-c) with CIMT in said patients were significantly and positively correlated, while lipid parameters (TC, TG, HDL-c, and LDL-c) were negatively correlated in nondiabetic ischemic stroke patients. Although lipidic parameters were differently affected by glycemic

control, it is clear that these parameters increase the risk of developing later cardiovascular complications by increasing CIMT. We did not find any significant correlation with mitochondrial ROS production, adhesion molecules, or cytokine concentrations, though there was a tendency toward a slight correlation.

This study is observational, and so it would be interesting to perform a longitudinal intervention study in which we assess the evolution of CIMT in patients with poor glycemic control that achieve a good glycemic control. Defining the reason why left and right carotids behave and are affected differently is still unclear, and further research focusing on this issue would be useful. Moreover, we have correlated many T2D markers with one indicator of cardiovascular risk; future studies could attempt to find a correlation with other cardiac and endothelium function markers to reinforce our findings.

5. CONCLUSIONS

The current study provides evidence of proinflammatory markers, mtROS production, leukocyte–endothelium interactions, adhesion molecules, and CIMT in T2D. Some of these alterations were more pronounced in patients with HbA_{1c} > 6.5, suggesting that glycemic control is a useful tool for preventing or delaying the onset of subclinical atherosclerotic process. Future research into these aspects will help to clarify the molecular mechanisms involved in glycemic control in T2D, and to modulate and control the atherosclerotic process in T2D.

Acknowledgments: The authors thank Brian Normanly (University of Valencia/CIBERehd) for his editorial assistance; and Rosa Falcón for her technical assistance.

Supplementary Materials: The following are available online at http://www.mdpi.com/2077-0383/9/8/2522/s1, Table S1: Time of T2D evolution on the recruited patients, Table S2: Incidence of most common comorbidities in the recruited T2D patients and in the control population, Table S3: Prescription of the different treatments associated with T2D in all the study subjects, Table S4: Leukocyte composition in healthy subjects and diabetic patients., Video S1: Control, Video S2: $HbA_{1c} > 6.5$, Video S3: $HbA_{1c} \leq 6.5$.

Supplementary Table S1. Time of T2D evolution on the recruited patients. The time was divided in three ranges and the percentages for each of the time ranges were calculated.

Years since T2D diagnosis	T2D	
	HbA_{1c}≤6.5%	HbA_{1c}>6.5%
1-5	57.9%	19%
5-10	17.5%	23%
+10	24.6%	58%

Supplementary Table S2. Incidence of most common comorbidities in the recruited T2D patients and in the control population. Some of the subjects suffered from more than one of the comorbidity.

Comorbidities	Control	T2D	
		HbA_{1c}≤6.5%	HbA_{1c}>6.5%
Hypertension	0	57.9%	47,1%
Hyperlipidaemia	19.5%	19.3%	23.1%
Silent Ischemic Cardiopathy	0	3.5%	5.8%
Retinopathy	0	24.6%	38.4%
Nephropathy	0	15.8%	25%
Neuropathy	0	18%	5.8%

Supplementary Table S3. Prescription of the different treatments associated with T2D in all the study subjects. Some of the subjects were prescribed with more than one treatment or received combined treatment.

Treatments	Control	T2D	
		HbA_{1c}≤6.5%	HbA_{1c}>6.5%
Antihyeperthensive	1.2%	50.9%	50.5%
Antidiabetic	0%	96.5%	93.3%
Metformin	0%	84.2%	76%
DPP-IV Inhibitors	0%	42.1%	39.4%
Insulin	0%	5.3%	42.3%
Sulphonylurea	0%	1.8%	1.9%
Thiazolidinediones	0%	1.8%	3.9%
Meglitinides	0.61%	1.8%	7.7%
GLP-1 agonists	0%	8.8%	16.4%
Hipolipemiant	0.6%	63.2%	68.3%
Statins	0.6%	56.1%	62.5%
Fibrates	0%	14.1%	12.5%
Ezetimibe	0%	3.5%	5.8%

Supplementary Table S4: Leukocyte composition in healthy subjects and diabetic patients. Leukocyte, neutrophil, lymphocyte, monocyte, eosinophil and basophil count was analyzed with the data obtained from the hospital's haematological analysis laboratory. Mean ± SD is shown for all the data, and t-test comparisons determined which differences are statistically significant. * p<0.05 vs Control.

	Control	T2D	
		HbA_{1c}≤6.5%	HbA_{1c}>6.5%
Leukocytes ($x10^9$)/L	6.36±1.68	8.38±1.67*	7.98±2.29*
Neutrophils($x10^9$)/L	3.85±1.95	5.36±1.5*	4.66±1.84*
Lymphocytes($x10^9$)/L	1.95±0.56	2.2±0.56	2.2±0.65*
Monocytes($x10^9$)/L	0.47±0.18	0.87±1.4*	0.58±0.22*
Eosinophils($x10^9$)/L	0.18±0.12	0.31±0.43*	0.25±0.2*
Basophils($x10^9$)/L	0.01±0.03	0.04±0.11*	0.02±0.04*

REFERENCES

1. NCD Risk Factor Collaboration (NCD-RisC). Worldwide trends in diabetes since 1980: A pooled analysis of 751 population-based studies with 4.4 million participants. *Lancet* **2016**, *387*, 1513–1530. [CrossRef]
2. Zheng, Y.; Ley, S.H.; Hu, F.B. Global aetiology and epidemiology of type 2 diabetes mellitus and its complications. *Nat. Rev. Endocrinol.* **2018**, *14*, 88–98. [CrossRef]
3. Zhang, Y.-B.; Pan, X.-F.; Chen, J.; Xia, L.; Cao, A.; Zhang, Y.; Wang, J.; Li, H.; Yang, K.; Guo, K.; et al. Combined lifestyle factors and risk of incident type 2 diabetes and prognosis among individuals with type 2diabetes: A systematic review and meta-analysis of prospective cohort studies. *Diabetologia* **2020**, *63*, 21–33.[CrossRef]
4. Stirban, A.O.; Tschoepe, D. Cardiovascular complications in diabetes: Targets and interventions. *Diabetes Care* **2008**, *31* (Suppl. 2), S215–S221. [CrossRef]
5. Ley, S.H.; Hamdy, O.; Mohan, V.; Hu, F.B. Prevention and Management of Type 2 Diabetes: Dietary Components and Nutritional Strategies. *Lancet* **2014**, *383*, 1999–2007. [CrossRef]
6. Cosentino, F.; Grant, P.J.; Aboyans, V.; Bailey, C.J.; Ceriello, A.; Delgado, V.; Federici, M.; Filippatos, G.; E Grobbee, D.; Hansen, T.B.; et al. 2019 ESC Guidelines on diabetes, pre-diabetes, and cardiovascular diseases developed in collaboration with the EASD. *Eur. Heart J.* **2020**, *41*, 255–323. [CrossRef]
7. American Diabetes Association. 6. Glycemic Targets: Standards of Medical Care in Diabetes—2018. *Diabetes Care* **2018**, *41* (Suppl. 1), S55–S64. [CrossRef]
8. Laiteerapong, N.; A Ham, S.; Gao, Y.; Moffet, H.H.; Liu, J.Y.; Huang, E.S.; Karter, A.J. The Legacy Effect in Type 2 Diabetes: Impact of Early Glycemic Control on Future Complications (The Diabetes & Aging Study). *Diabetes Care* **2019**, *42*, 416–426.
9. Moodahadu, L.S.; Dhall, R.; Zargar, A.H.; Bangera, S.; Ramani, L.; Katipally, R. Tight Glycemic Control andCardiovascular Effects in Type 2 Diabetic Patients. *Heart Views* **2014**, *15*, 111–120. [CrossRef]
10. Hill, D.; Fisher, M. The effect of intensive glycaemic control on cardiovascular outcomes. *Diabetes Obes. Metab.* **2010**, *12*, 641–647. [CrossRef]
11. Punthakee, Z.; Miller, M.E.; Simmons, D.L.; Riddle, M.C.; Ismail-Beigi, F.; Brillon, D.J.; Bergenstal, R.M.; Savage, P.J.; Hramiak, I.; Largay, J.F.; et al. Durable change in glycaemic control following intensive management of type 2 diabetes in the ACCORD clinical trial. *Diabetologia* **2014**, *57*, 2030–2037. [CrossRef]
12. Boussageon, R.; Bejan-Angoulvant, T.; Saadatian-Elahi, M.; Lafont, S.; Bergeonneau, C.; Kassaï, B.; Erpeldinger, S.; Wright, J.M.; Gueyffier, F.; Cornu, C. Effect of intensive glucose lowering treatment on all cause mortality, cardiovascular death, and microvascular events in type 2 diabetes: Meta-analysis ofrandomised controlled trials. *BMJ* **2011**, *343*, d4169. [CrossRef]
13. ADVANCE Collaborative Group; Patel, A.; MacMahon, S.; Chalmers, J.; Neal, B.; Billot, L.; Woodward, M.;Marre, M.; Cooper, M.; Glasziou, P.; et al. Intensive blood glucose control and vascular outcomes in patients with type 2 diabetes. *N. Engl. J. Med.* **2008**, *358*, 2560–2572. [CrossRef]
14. Donath, M.Y.; Shoelson, S.E. Type 2 diabetes as an inflammatory disease. *Nat. Rev. Immunol.* **2011**, *11*, 98–107. [CrossRef]
15. Lontchi-Yimagou, E.; Sobngwi, E.; Matsha, T.E.; Kengne, A.P. Diabetes mellitus and inflammation. *Curr. Diabetes Rep.* **2013**, *13*, 435–444. [CrossRef]
16. Cruz, N.G.; Sousa, L.P.; Sousa, M.O.; Pietrani, N.T.; Fernandes, A.P.; Gomes, K.B. The linkage between inflammation and Type 2 diabetes mellitus. *Diabetes Res. Clin. Pract.* **2013**, *99*, 85–92. [CrossRef]
17. Valentine, W.; Palmer, A.; Nicklasson, L.; Cobden, D.; Roze, S. Improving life expectancy and decreasing the incidence of complications associated with type 2 diabetes: A modelling study of HbA1c targets. *Int. J.Clin. Pract.* **2006**, *60*, 1138–1145. [CrossRef]
18. Lainampetch, J.; Panprathip, P.; Phosat, C.; Chumpathat, N.; Prangthip, P.; Soonthornworasiri, N.;

Puduang, S.; Wechjakwen, N.; Kwanbunjan, K. Association of Tumor Necrosis Factor Alpha, Interleukin 6, and C-Reactive Protein with the Risk of Developing Type 2 Diabetes: A Retrospective Cohort Study of Rural Thais. *J. Diabetes Res.* **2019**, *2019*, 9051929. [CrossRef]

19. Fadaei, R.; Bagheri, N.; Heidarian, E.; Nouri, A.; Hesari, Z.; Moradi, N.; Ahmadi, A.; Ahmadi, R. Serum levels of IL-32 in patients with type 2 diabetes mellitus and its relationship with TNF-α and IL-6. *Cytokine***2020**, *125*, 154832. [CrossRef]
20. Donath, M.Y.; Dinarello, C.A.; Mandrup-Poulsen, T. Targeting innate immune mediators in type 1 and type 2 diabetes. *Nat. Rev. Immunol.* **2019**, *19*, 734–746. [CrossRef]
21. Burgos-Morón, E.; Abad-Jiménez, Z.; De Marañon, A.M.; Iannantuoni, F.; Escribano-López, I.; López-Domènech, S.; Salom, C.; Jover, A.; Llabata, V.; Torres, I.R.; et al. Relationship between Oxidative Stress, ER Stress, and Inflammation in Type 2 Diabetes: The Battle Continues. *J. Clin. Med.* **2019**, *8*, 1385. [CrossRef]
22. Forrester, S.J.; Kikuchi, D.S.; Hernandes, M.S.; Xu, Q.; Griendling, K.K. Reactive Oxygen Species in Metabolic and Inflammatory Signaling. *Circ. Res.* **2018**, *122*, 877–902. [CrossRef]
23. Zhou, R.; Yazdi, A.S.; Menu, P.; Tschopp, J. A role for mitochondria in NLRP3 inflammasome activation. *Nature* **2011**, *469*, 221–225. [CrossRef]
24. Bulua, A.C.; Simon, A.; Maddipati, R.; Pelletier, M.; Park, H.; Kim, K.-Y.; Sack, M.N.; Kastner, D.L.; Siegel, R.M. Mitochondrial reactive oxygen species promote production of proinflammatory cytokines and are elevated in TNFR1-associated periodic syndrome (TRAPS). *J. Exp. Med.* **2011**, *208*, 519–533. [CrossRef]
25. Ungvari, Z.; Orosz, Z.; Labinskyy, N.; Rivera, A.; Xiangmin, Z.; Smith, K.; Csiszar, A. Increased mitochondrial H2O2 production promotes endothelial NF-kappaB activation in aged rat arteries. *Am. J. Physiol. Heart Circ. Physiol.* **2007**, *293*, H37–H47. [CrossRef]
26. Shah, A.; Xia, L.; Goldberg, H.; Lee, K.W.; Quaggin, S.E.; Fantus, I.G. Thioredoxin-interacting protein mediates high glucose-induced reactive oxygen species generation by mitochondria and the NADPH oxidase, Nox4, in mesangial cells. *J. Biol. Chem.* **2013**, *288*, 6835–6848. [CrossRef]
27. Zhou, R.; Tardivel, A.; Thorens, B.; Choi, I.; Tschopp, J. Thioredoxin-interacting protein links oxidative stressto inflammasome activation. *Nat. Immunol.* **2010**, *11*, 136–140. [CrossRef]
28. Yang, B.; Fritsche, K.L.; Beversdorf, D.Q.; Gu, Z.; Lee, J.C.; Folk, W.R.; Greenlief, C.M.; Sun, G.Y. Yin-YangMechanisms Regulating Lipid Peroxidation of Docosahexaenoic Acid and Arachidonic Acid in the CentralNervous System. *Front. Neurol.* **2019**, *10*, 642. [CrossRef]
29. Fischer, R.; Maier, O. Interrelation of Oxidative Stress and Inflammation in Neurodegenerative Disease: Role of TNF. *Oxid. Med. Cell. Longev.* **2015**, *2015*, 610813. [CrossRef]
30. Guo, Y.; Zhuang, X.; Huang, Z.; Zou, J.; Yang, D.; Hu, X.; Du, Z.; Wang, L.; Liao, X. Klotho protects the heart from hyperglycemia-induced injury by inactivating ROS and NF-κB-mediated inflammation both in vitroand in vivo. *Biochim. Biophys. Acta Mol. Basis Dis.* **2018**, *1864*, 238–251. [CrossRef]
31. Luo, B.; Li, B.; Wang, W.; Liu, X.; Xia, Y.; Zhang, C.; Zhang, M.; Zhang, Y.; An, F. NLRP3 gene silencing ameliorates diabetic cardiomyopathy in a type 2 diabetes rat model. *PLoS ONE* **2014**, *9*, e104771. [CrossRef]
32. Zhang, H.-L.; Chen, X.; Zong, B.; Yuan, H.; Wang, Z.; Wei, Y.; Wang, X.; Liu, G.; Zhang, J.; Li, S.; et al. Gypenosides improve diabetic cardiomyopathy by inhibiting ROS-mediated NLRP3 inflammasome activation. *J. Cell. Mol. Med.* **2018**, *22*, 4437–4448. [CrossRef]
33. Le Rossignol, S.; Ketheesan, N.; Haleagrahara, N. Redox-sensitive transcription factors play a significant role in the development of rheumatoid arthritis. *Int. Rev. Immunol.* **2018**, *37*, 129–143. [CrossRef]
34. Lepetsos, P.; Papavassiliou, K.A.; Papavassiliou, A.G. Redox and NF-κB signaling in osteoarthritis. *Free Radic. Biol. Med.* **2019**, *132*, 90–100. [CrossRef]
35. Pradhan, A.; Bagchi, A.; De, S.; Mitra, S.; Mukherjee, S.; Ghosh, P.; Ghosh, A.; Chatterjee, M. Role of redoximbalance and cytokines in mediating oxidative damage and disease progression of patients with rheumatoid arthritis. *Free Radic. Res.* **2019**, *53*, 768–779. [CrossRef]

36. Duecker, R.; Baer, P.C.; Eickmeier, O.; Strecker, M.; Kurz, J.; Schaible, A.; Henrich, D.; Zielen, S.; Schubert, R. Oxidative stress-driven pulmonary inflammation and fibrosis in a mouse model of human ataxia-telangiectasia. *Redox Biol.* **2018**, *14*, 645–655. [CrossRef]
37. Nandi, A.; Bishayi, B. CCR-2 neutralization augments murine fresh BMC activation by Staphylococcus aureus via two distinct mechanisms: At the level of ROS production and cytokine response. *Innate Immun.***2017**, *23*, 345–372. [CrossRef]
38. Diehl, A.M. Cytokine regulation of liver injury and repair. *Immunol. Rev.* **2000**, *174*, 160–171. [CrossRef]
39. Han, S.; Cai, W.; Yang, X.; Jia, Y.; Zheng, Z.; Wang, H.; Li, J.; Li, Y.; Gao, J.; Fan, L.; et al. ROS-Mediated NLRP3 Inflammasome Activity Is Essential for Burn-Induced Acute Lung Injury. *Mediat. Inflamm.* **2015**, *2015*, 720457. [CrossRef]
40. Lee, I.-T.; Yang, C.-M. Role of NADPH oxidase/ROS in pro-inflammatory mediators-induced airway and pulmonary diseases. *Biochem. Pharmacol.* **2012**, *84*, 581–590. [CrossRef]
41. Zuo, L.; Prather, E.R.; Stetskiv, M.; Garrison, D.E.; Meade, J.R.; Peace, T.I.; Zhou, T. Inflammaging and Oxidative Stress in Human Diseases: From Molecular Mechanisms to Novel Treatments. *Int. J. Mol. Sci.* **2019**, *20*, 4472. [CrossRef]
42. Ouedraogo, R.; Gong, Y.; Berzins, B.; Wu, X.; Mahadev, K.; Hough, K.; Chan, L.; Goldstein, B.J.; Scalia, R. Adiponectin deficiency increases leukocyte-endothelium interactions via upregulation of endothelial cell adhesion molecules in vivo. *J. Clin. Investig.* **2007**, *117*, 1718–1726. [CrossRef]
43. Yan, Y.; Li, S.; Liu, Y.; Bazzano, L.; He, J.; Mi, J.; Chen, W. Temporal relationship between inflammation and insulin resistance and their joint effect on hyperglycemia: The Bogalusa Heart Study. *Cardiovasc. Diabetol.* **2019**, *18*, 109. [CrossRef]
44. Galkina, E.; Ley, K. Immune and Inflammatory Mechanisms of Atherosclerosis. *Annu. Rev. Immunol.***2009**, *27*, 165–197. [CrossRef]
45. Legein, B.; Temmerman, L.; Biessen, E.A.L.; Lutgens, E. Inflammation and immune system interactions in atherosclerosis. *Cell. Mol. Life Sci.* **2013**, *70*, 3847–3869. [CrossRef]
46. Kavousi, M.; Elias-Smale, S.; Rutten, J.H.; Leening, M.J.G.; Vliegenthart, R.; Verwoert, G.C.; Krestin, G.P.; Oudkerk, M.; De Maat, M.P.; Leebeek, F.W.; et al. Evaluation of newer risk markers for coronary heart disease risk classification: A cohort study. *Ann. Intern. Med.* **2012**, *156*, 438–444. [CrossRef]
47. Lau, K.K.; Wong, Y.-K.; Chan, Y.-H.; Yiu, K.-H.; Teo, K.C.; Li, L.S.-W.; Ho, S.-L.; Chan, K.H.; Siu, C.-W.; Tse, H.-F. Prognostic implications of surrogate markers of atherosclerosis in low to intermediate risk patients with type 2 diabetes. *Cardiovasc. Diabetol.* **2012**, *11*, 101. [CrossRef]
48. Ortega, E.; Gilabert, R.; Núñez, I.; Cofán, M.; Sala-Vila, A.; De Groot, E.; Ros, E. White blood cell count is associated with carotid and femoral atherosclerosis. *Atherosclerosis* **2012**, *221*, 275–281. [CrossRef]
49. Blüher, M.; Unger, R.; Rassoul, F.; Richter, V.; Paschke, R. Relation between glycaemic control, hyperinsulinaemia and plasma concentrations of soluble adhesion molecules in patients with impaired glucose tolerance or Type II diabetes. *Diabetologia* **2002**, *45*, 210–216. [CrossRef]
50. Jude, E.B.; Douglas, J.T.; Anderson, S.G.; Young, M.J.; Boulton, A.J.M. Circulating cellular adhesion molecules ICAM-1, VCAM-1, P- and E-selectin in the prediction of cardiovascular disease in diabetes mellitus. *Eur. J.Intern. Med.* **2002**, *13*, 185–189. [CrossRef]
51. Pankow, J.S.; Decker, P.A.; Berardi, C.; Hanson, N.Q.; Sale, M.; Tang, W.; Kanaya, A.M.; Larson, N.B.; Tsai, M.; Wassel, C.L.; et al. Circulating cellular adhesion molecules and risk of diabetes: The Multi-Ethnic Study ofAtherosclerosis (MESA). *Diabet. Med.* **2016**, *33*, 985–991. [CrossRef]
52. Qiu, S.; Cai, X.; Liu, J.; Yang, B.; Zügel, M.; Steinacker, J.M.; Sun, Z.; Schumann, U. Association between circulating cell adhesion molecules and risk of type 2 diabetes: A meta-analysis. *Atherosclerosis* **2019**, *287*, 147–154. [CrossRef]
53. Nguyen, P.A.; Won, J.S.; Rahman, M.K.; Bae, E.J.; Cho, M.K. Modulation of Sirt1/NF-κB interaction of evogliptin is attributed to inhibition of vascular inflammatory response leading to attenuation of atherosclerotic plaque formation. *Biochem. Pharmacol.* **2019**, *168*, 452–464.

[CrossRef]

54. Sardu, C.; De Lucia, C.; Wallner, M.; Santulli, G. Diabetes Mellitus and Its Cardiovascular Complications: New Insights into an Old Disease. *J. Diabetes Res.* **2019**, *2019*, 1905194. [CrossRef]
55. Rangel, É.B.; Rodrigues, C.O.; de Sá, J.R. Micro- and Macrovascular Complications in Diabetes Mellitus: Preclinical and Clinical Studies. *J Diabetes Res.* **2019**, *2019*, 2161085. [CrossRef]
56. Golden, S.H.; Folsom, A.R.; Coresh, J.; Sharrett, A.R.; Szklo, M.; Brancati, F. Risk factor groupings related to insulin resistance and their synergistic effects on subclinical atherosclerosis: The atherosclerosis risk in communities study. *Diabetes* **2002**, *51*, 3069–3076. [CrossRef]
57. Tabatabaei-Malazy, O.; Fakhrzadeh, H.; Sharifi, F.; Mirarefin, M.; Arzaghi, S.M.; Badamchizadeh, Z.; Alizadeh-Khoei, M.; Larijani, B. Effect of metabolic control on oxidative stress, subclinical atherosclerosis and peripheral artery disease in diabetic patients. *J. Diabetes Metab. Disord.* **2015**, *14*, 84. [CrossRef]
58. Alharby, H.; Abdelati, T.; Rizk, M.; Youssef, E.; Moghazy, K.; Gaber, N.; Yafei, S. Association of lipid peroxidation and interleukin-6 with carotid atherosclerosis in type 2 diabetes. *Cardiovasc. Endocrinol. Metab.***2019**, *8*, 73–76. [CrossRef]
59. Bauer, M.; Caviezel, S.; Teynor, A.; Erbel, R.; Mahabadi, A.A.; Schmidt-Trucksäss, A. Carotid intima-media thickness as a biomarker of subclinical atherosclerosis. *Swiss Med. Wkly.* **2012**, *142*, w13705. [CrossRef]
60. Abd El Dayem, S.M.; Battah, A.A.; El Bohy, A.E.M. Assessment of Increase in Aortic and Carotid Intimal Medial Thickness in Type 1 Diabetic Patients. *Open Access Maced. J. Med. Sci.* **2016**, *4*, 630. [CrossRef]
61. Pignoli, P.; Tremoli, E.; Poli, A.; Oreste, P.; Paoletti, R. Intimal plus medial thickness of the arterial wall: A direct measurement with ultrasound imaging. *Circulation* **1986**, *74*, 1399–1406. [CrossRef]
62. Santos, I.S.; Bittencourt, M.S.; Goulart, A.C.; Schmidt, M.I.; Diniz, M.D.F.H.S.; Lotufo, P.A.; Benseñor, I.M. Insulin resistance is associated with carotid intima-media thickness in non-diabetic subjects. A cross-sectional analysis of the ELSA-Brasil cohort baseline. *Atherosclerosis* **2017**, *260*, 34–40. [CrossRef]
63. Jeevarethinam, A.; Venuraju, S.; Dumo, A.; Ruano, S.; Mehta, V.S.; Rosenthal, M.; Nair, D.; Cohen, M.; Darko, D.; Lahiri, A.; et al. Relationship between carotid atherosclerosis and coronary artery calcification inasymptomatic diabetic patients: A prospective multicenter study. *Clin. Cardiol.* **2017**, *40*, 752–758. [CrossRef] [PubMed]
64. O'Leary, D.H.; Polak, J.F.; Kronmal, R.A.; Manolio, T.A.; Burke, G.L.; Wolfson, S.K. Carotid-Artery Intima and Media Thickness as a Risk Factor for Myocardial Infarction and Stroke in Older Adults. *N. Engl. J. Med.***1999**, *340*, 14–22. [CrossRef] [PubMed]
65. Lorenz, M.W.; Price, J.F.; Robertson, C.; Bots, M.L.; Polak, J.F.; Poppert, H.; Kavousi, M.; Dorr, M.; Stensland, E.; Ducimetiere, P.; et al. Carotid intima-media thickness progression and risk of vascular events in people with diabetes: Results from the PROG-IMT collaboration. *Diabetes Care* **2015**, *38*, 1921–1929. [CrossRef] [PubMed]
66. Tenjin, A.; Nagai, Y.; Yuji, S.; Ishii, S.; Kato, H.; Ohta, A.; Tanaka, Y. Short-term change of carotid intima-media thickness after treatment of hyperglycemia in patients with diabetes: A cross-sectional study. *BMC Res. Notes* **2016**, *9*, 281. [CrossRef]
67. Asemi, Z.; Raygan, F.; Bahmani, F.; Rezavandi, Z.; Talari, H.R.; Rafiee, M.; Poladchang, S.; Mofrad, M.D.; Taheri, S.; Mohammadi, A.A.; et al. The effects of vitamin D, K and calcium co-supplementation on carotid intima-media thickness and metabolic status in overweight type 2 diabetic patients with CHD. *Br. J. Nutr.* **2016**, *116*, 286–293. [CrossRef]
68. Herder, M.; Arntzen, K.; Johnsen, S.; Mathiesen, E. The metabolic syndrome and progression of carotid atherosclerosis over 13 years. The Tromsø Study. *Cardiovasc. Diabetol.* **2012**, *11*, 77. [CrossRef]
69. Escribano-López, I.; De Marañon, A.M.; Iannantuoni, F.; López-Domènech, S.; Abad-Jiménez, Z.; Díaz-

Pozo, P.; Sola, E.; Apostolova, N.; Rocha, M.; Víctor, V.M. The Mitochondrial Antioxidant SS-31 Modulates Oxidative Stress, Endoplasmic Reticulum Stress, and Autophagy in Type 2 Diabetes. *J. Clin. Med.* **2019**, *8*, 1322. [CrossRef]

70. González, F.; Rote, N.S.; Minium, J.; Kirwan, J.P. Reactive oxygen species-induced oxidative stress in the development of insulin resistance and hyperandrogenism in polycystic ovary syndrome. *J. Clin. Endocrinol. Metab.* **2006**, *91*, 336–340. [CrossRef]
71. Bajpai, A.; Tilley, D.G. The Role of Leukocytes in Diabetic Cardiomyopathy. *Front. Physiol.* **2018**, *9*, 1547. [CrossRef] [PubMed]
72. Mijares, A.H.; Rocha, M.; Rovira-Llopis, S.; Bañuls, C.; Bellod, L.; De Pablo, C.; Alvarez, A.; Roldán, I.; Sola-Izquierdo, E.; Victor, V.M. Human Leukocyte/Endothelial Cell Interactions and Mitochondrial Dysfunction in Type 2 Diabetic Patients and Their Association with Silent Myocardial Ischemia. *Diabetes Care* **2013**, *36*, 1695–1702. [CrossRef]
73. Alcántar-Fernández, J.; González-Maciel, A.; Reynoso-Robles, R.; Andrade, M.E.P.; Hernández-Vázquez, A.D.J.; Velázquez-Arellano, A.; Miranda-Ríos, J. High-glucose diets induce mitochondrial dysfunction in Caenorhabditis elegans. *PLoS ONE* **2019**, *14*, e0226652. [CrossRef]
74. Lin, H.-Y.; Weng, S.-W.; Chang, Y.-H.; Su, B.Y.-J.; Chang, C.-M.; Tsai, C.-J.; Shen, F.-C.; Chuang, J.-H.; Lin, T.-K.; Liou, C.-W.; et al. The Causal Role of Mitochondrial Dynamics in Regulating Insulin Resistance in Diabetes: Link through Mitochondrial Reactive Oxygen Species. *Oxid. Med. Cell. Longev.* **2018**, *2018*, 7514383. [CrossRef]
75. Rehman, K.; Akash, M.S.H. Mechanism of Generation of Oxidative Stress and Pathophysiology of Type 2 Diabetes Mellitus: How Are They Interlinked? *J. Cell. Biochem.* **2017**, *118*, 3577–3585. [CrossRef]
76. Luc, K.; Schramm-Luc, A.; Guzik, T.J.; Mikolajczyk, T.P. Oxidative stress and inflammatory markers in prediabetes and diabetes. *J. Physiol. Pharmacol.* **2019**, *70*, 809–824.
77. Diao, F.-Y.; Xu, M.; Hu, Y.; Li, J.; Xu, Z.; Lin, M.; Wang, L.; Zhou, Y.; Zhou, Z.; Liu, J.; et al. The molecular characteristics of polycystic ovary syndrome (PCOS) ovary defined by human ovary cDNA microarray. *J. Mol. Endocrinol.* **2004**, *33*, 59–72. [CrossRef]
78. Dupré-Crochet, S.; Erard, M.; Nüβe, O. ROS production in phagocytes: Why, when, and where? J. Leukoc. Biol. 2013, 94, 657–670. [CrossRef]
79. Rao, K.M.K. MAP kinase activation in macrophages. *J. Leukoc. Biol.* **2001**, *69*, 3–10.
80. Okazaki, S.; Sakaguchi, M.; Miwa, K.; Furukado, S.; Yamagami, H.; Yagita, Y.; Mochizuki, H.; Kitagawa, K. Association of interleukin-6 with the progression of carotid atherosclerosis: A 9-year follow-up study. *Stroke***2014**, *45*, 2924–2929. [CrossRef]
81. Skoog, T.; Dichtl, W.; Boquist, S.; Skoglund-Andersson, C.; Karpe, F.; Tang, R.; Bond, M.; De Faire, U.; Nilsson, J.; Eriksson, P.; et al. Plasma tumour necrosis factor-alpha and early carotid atherosclerosis in healthy middle-aged men. *Eur. Heart J.* **2002**, *23*, 376–383. [CrossRef]
82. Ijsselmuiden, A.J.; Musters, R.J.; De Ruiter, G.; Van Heerebeek, L.; Alderse-Baas, F.; Van Schilfgaarde, M.; Leyte, A.; Tangelder, G.-J.; Laarman, G.J.; Paulus, W.J. Circulating white blood cells and platelets amplify oxidative stress in heart failure. *Nat. Clin. Pract. Cardiovasc. Med.* **2008**, *5*, 811–820. [CrossRef]
83. Bárány, T.; Simon, A.; Szabó, G.; Benkő, R.; Mezei, Z.; Molnár, L.; Becker, D.; Merkely, B.; Zima, E.; Horváth, E.M. Oxidative Stress-Related Parthanatos of Circulating Mononuclear Leukocytes in Heart Failure. *Oxid. Med. Cell. Longev.* **2017**, *2017*, 1249614. [CrossRef]
84. Tiyerili, V.; Camara, B.; Becher, M.U.; Schrickel, J.W.; Lütjohann, D.; Mollenhauer, M.; Baldus, S.; Nickenig, G.; Andrié, R.P. Neutrophil-derived myeloperoxidase promotes atherogenesis and neointima formation in mice. *Int. J. Cardiol.* **2016**, *204*, 29–36. [CrossRef]
85. Victor, V.M.; Rocha, M.; Sola, E.; Banuls, C.; Garcia-Malpartida, K.; Hernandez-Mijares, A. Oxidative Stress, Endothelial Dysfunction and Atherosclerosis. *Curr. Pharm. Des.* **2009**, *15*, 2988–3002. [CrossRef]

86. Pettersson, U.S.; Christoffersson, G.; Massena, S.; Ahl, D.; Jansson, L.; Henriksnäs, J.; Phillipson, M. Increased Recruitment but Impaired Function of Leukocytes during Inflammation in Mouse Models of Type 1 and Type 2 Diabetes. *PLoS ONE* **2011**, *6*, e22480. [CrossRef]
87. Novak, V.; Zhao, P.; Manor, B.; Sejdić, E.; Alsop, D.; Abduljalil, A.; Roberson, P.K.; Munshi, M.; Novak, P. Adhesion molecules, altered vasoreactivity, and brain atrophy in type 2 diabetes. *Diabetes Care* **2011**, *34*, 2438–2441. [CrossRef]
88. Giugliano, D.; Marfella, R.; Coppola, L.; Verrazzo, G.; Acampora, R.; Giunta, R.; Nappo, F.; Lucarelli, C.; D'Onofrio, F. Vascular Effects of Acute Hyperglycemia in Humans Are Reversed by l-Arginine. *Circulation* **1997**, *95*, 1783–1790. [CrossRef]
89. Kolluru, G.K.; Bir, S.C.; Kevil, C.G. Endothelial dysfunction and diabetes: Effects on angiogenesis, vascularremodeling, and wound healing. *Int. J. Vasc. Med.* **2012**, *2012*, 918267. [CrossRef]
90. Nezu, T.; Hosomi, N.; Aoki, S.; Matsumoto, M. Carotid Intima-Media Thickness for Atherosclerosis. *J. Atheroscler. Thromb.* **2016**, *23*, 18–31. [CrossRef]
91. Zhao, B.; Liu, Y.; Zhang, Y.; Chen, Y.; Yang, Z.-F.; Zhu, Y.; Xu, S. Gender difference in carotid intima-mediathickness in type 2 diabetic patients: A 4-year follow-up study. *Cardiovasc. Diabetol.* **2012**, *11*, 51. [CrossRef]
92. Luo, X.; Yang, Y.; Cao, T.; Li, Z. Differences in left and right carotid intima-media thickness and the associated risk factors. *Clin. Radiol.* **2011**, *66*, 393–398. [CrossRef]
93. Hedna, V.S.; Bodhit, A.N.; Ansari, S.; Falchook, A.D.; Stead, L.; Heilman, K.M.; Waters, M.F. Hemispheric Differences in Ischemic Stroke: Is Left-Hemisphere Stroke More Common? *J. Clin. Neurol.* **2013**, *9*, 97–102. [CrossRef]
94. Hernaández, S.A.R.; Kroon, A.A.; Van Boxtel, M.P.; Mess, W.H.; Lodder, J.; Jolles, J.; De Leeuw, P.W. Is there a side predilection for cerebrovascular disease? *Hypertension* **2003**, *42*, 56–60. [CrossRef]
95. Selwaness, M.; Bouwhuijsen, Q.V.D.; Van Onkelen, R.S.; Hofman, A.; Franco, O.H.; Van Der Lugt, A.; Wentzel, J.J.; Vernooij, M.W. Atherosclerotic plaque in the left carotid artery is more vulnerable than in theright. *Stroke* **2014**, *45*, 3226–3230. [CrossRef]
96. Einarson, T.R.; Hunchuck, J.; Hemels, M. Relationship between blood glucose and carotid intima media thickness: A meta-analysis. *Cardiovasc. Diabetol.* **2010**, *9*, 37. [CrossRef]
97. Pillai, P.R.; Tiwari, D.; Jatav, O.P.; Rai, H. Lipid profile and carotid artery intima-media thickness in diabeticand non-diabetic ischaemic stroke. *Int. J. Adv. Med.* **2017**, *4*, 471. [CrossRef]

4.3. CHAPTER 3:

Does metformin modulate mitochondrial dynamics and function in type 2 diabetic patients?

Aranzazu M. de Marañón [1], Francisco Canet [1], Zaida Abad-Jiménez [1], Ana Jover [1], Carlos Morillas [1], Milagros Rocha [1 2], Victor M. Victor [1 2 3]

[1]Service of Endocrinology and Nutrition, University Hospital Doctor Peset, Foundation for the Promotion of Health and Biomedical Research in the Valencian Region (FISABIO), Valencia, Spain.

[2]Department of Physiology, University of Valencia, Valencia, Spain.

[3]CIBERehd - Department of Pharmacology, University of Valencia, Valencia, Spain.

Antioxidants and Redox Signalling. 2021 Aug 10;35(5):377-385.

DOI: 10.1089/ars.2021.0019

ABSTRACT

Metformin is an effective drug against type 2 diabetes (T2D), a pathogenesis in which mitochondrial dysfunction is one of the main players. Thus, our first aim was to describe the effect of metformin on mitochondrial function in an outpatient population with T2D. For analyzing this hypothesis, we performed a preliminary cross-sectional study complying with the STROBE requirements. We studied leukocytes from 139 healthy controls, 39 T2D patients without metformin treatment, and 81 T2D patients who had been on said treatment for at least 1 year. Leukocytes from T2D patients displayed higher total and mitochondrial reactive oxygen species levels, lower mitochondrial membrane potential, and lower oxygen consumption. Moreover, their mitochondria expressed lower mRNA and protein levels of fusion proteins MFN1, MFN2, OPA1, and higher protein and gene expression levels of mitochondrial FIS1 and DRP1. In addition, we observed enhanced leukocyte-endothelial interactions in T2D patients. Metformin reversed most of these effects, ameliorating mitochondrial function and dynamics, and reducing the leukocyte/endothelial interactions observed in T2D patients. These results raise the question of whether metformin tackles T2D by improving mitochondrial dysfunction and regulating mitochondrial dynamics. Furthermore, it would seem that metformin modulates the alteration of interactions between leukocytes and the endothelium, a subclinical marker of early atherosclerosis.

Keywords: inflammation, metformin, mitochondrial dysfunction, mitochondrial dynamics, type 2 diabetes

1. INTRODUCTION

T2D is a chronic inflammatory disease characterized by hyperglycemia and hyperinsulinemia. Accumulating evidence suggests that mitochondrial dysfunction is one of the main contributors to diabetic disease (7). However, there are controversies about whether mitochondrial dysfunction is the trigger or a consequence of metabolic deregulation.

Mitochondria are essential double-membrane organelles involved in different cell processes such as ATP synthesis, apoptosis, stress regulation, and lipid and carbohydrate metabolism, among others (7). They are responsible for meeting the enormous energy demands of vital tissues by facilitating cellular respiration, which is carried out in the mitochondrial cristae through ETC and the electrons obtained mainly as a result of glycolysis and fatty acid oxidation. Thus, ETC- mediated electron transport pumps protons to the intermembrane space to maintain the protonmotive force. Once the electrons reach the ATP synthase, ATP is synthesized, but only if there is an adequate protonmotive force.

It is now widely accepted that cellular energy demand affects mitochondria by causing changes to their shape, location, and/or mitochondrial mass (5). These processes are known as mitochondrial dynamics and are facilitated by mitochondrial transport through microtubules, and mitochondrial fusion and fission.

Fusion is carried away by three GTPases: MFN1, MFN2, OPA1. Although MFN1 and MFN2 share similar sequences and functions, slight but critical differences have been identified: while MFN1 exerts its function in the outer membrane, MFN2 regulates mainly endoplasmic reticulum/mitochondria contact. Similarly, OPA1, a dynamin- related protein associated with inner mitochondrial membrane fusion and maintenance of the structure of respiratory supercomplexes, helps to regulate the shape of mitochondria through the fusion process (5).

On the contrary, fission machinery is mediated by DRP1, a GTPase protein located in the cytosol as a dimer or tetramer (5) that is recruited to the outer mitochondrial membrane by FIS1

and other receptor proteins in response to specific cellular cues (5).

Defects in these mitochondrial dynamics can lead to a substantial production of ROS, which, in turn, leak into the cytosol and affect the cellular environment and molecular signaling. Subsequently, these stress stimuli expedite recruitment of the immune cells to the activated vascular endothelium, thus promoting further atherosclerotic changes and the development of macrovascular complications (2, 6). In particular, the activation of leukocytes, mediated by chemokine-dependent and chemokine-independent mechanisms, leads to leukocyte/endothelial cell adhesion. During this process, adhesion molecules on rolling leukocytes bind to their counter-receptors on endothelial cells, thus promoting their firm adhesion to the wall. This persistent condition contributes to the initiation and progression of atherosclerotic lesion development (2, 9).

To date, many different treatments have been used to ameliorate T2D. However, since its discovery in 1950, metformin has remained the first-line treatment. Although the exact mechanisms by which metformin exerts its actions are unknown, a wide range of theories have been put forward (3). Of note, metformin seems to alleviate cell activation, thus palliating the inflammatory response (2). However, this aspect has not been assessed in primary leukocytes, and so, the precise effect of metformin is still unclear.

In light of the research described above, we hypothesized that mitochondrial function and dynamics are altered in T2D, thus affecting leukocyte/endothelial interactions, and that metformin can mitigate these alterations.

Innovation

Alterations in mitochondrial function and dynamics and the inflammatory events, which take place as a consequence, are key to the diabetic pathology, but the nature of the effects exerted by metformin on these parameters is unclear. Thus, it is relevant to study them in primary T2D leukocytes, which are central to the immune response. Our results suggest that metformin effectively palliates alterations of leukocyte mitochondrial function and dynamics due to T2D and reduces their activation. Our results contribute to the knowledge of the mechanisms that explain the deregulated immune function in T2D. Future research will need to detangle the precise molecular pathways at work and the exact target of metformin in this scenario.

2. BIOCHEMICAL AND ANTHROPOMETRICAL PARAMETERS

Table 1 shows the results obtained when we analyzed the anthropometrical and biochemical data in our study population. One hundred thirty-five healthy subjects and 120 T2D patients were recruited from the Endocrinology Outpatients Service of the University Hospital Doctor Peset (Valencia, Spain). The T2D group was divided into patients with meformin treatment (81) or without treatment (39). In relation to anthropometrical parameters, T2D patients presented higher weight ($p < 0.05$), body mass index (BMI; $p < 0.05$), waist circumference ($p < 0.05$), and DBP and SBP ($p < 0.05$).

Metformin had a significant effect on SBP ($p < 0.05$), while DBP showed non-significant differences with respect to the control group. Insulin concentrations and homeostatic model HOMA-IR were higher in T2D patients (both $p < 0.05$), with no influence of metformin treatment being observed. HbA_{1c}% and glucose were significantly increased in the T2D group ($p < 0.05$) and lower among patients receiving metformin treatment ($p < 0.05$). Regarding lipid metabolism parameters, we found that cholesterol, HDL-c, and LDL-c were reduced in T2D patients ($p < 0.05$) due to the effect of the hypolipemiant treatment (50% of patients in the T2D group and 63.8% of

metformin-treated patients). VLDL-c, cholesterol/HDL-c ratio, and TG were increased in T2D patients, and were not modified by metformin treatment.

Table 1. Biochemical and anthropometrical profile of control subjects and type 2 diabetes patients with or without metformin treatment

	Control	***T2D***	***T2D+Metformin***
n	135	39	81
Male%	43.70	50.97	59.90
Age (years)	45.22±12.06	58.97±10.05	58.76±12.12
Weight (kg)	67.55±12.30	73.69±10.97[a]	74.53±12.24[a]
BMI (kg/m2)	23.49±2.96	26.92±2.47[a]	26.66±3.14[a]
Waist circumference (cm)	79.67±12.83	95.57±10.32[a]	95.42±11.40[a]
SBP (mm Hg)	118.00±17.95	148.26±25.15[a]	139.80±16.68[a,b]
DBP (mm Hg)	72.07±10.91	82.09±12.56[a]	77.49±10.76[a]
Insulin (lUI/mL)	7.16±3.40	14.51±8.22[a]	15.44±10.63[a]
HOMA-IR	1.65±1.08	4.69±3.39[a]	4.68±5.25[a]
HbA_{1c} (%)	5.29±0.53	7.31±1.17[a]	6.72±1.04[a,b]
Glucose (mg/dL)	90.59±21.57	152.29±44.99[a]	111.94±27.54[a,b]
Cholesterol (mg/dL)	185.74±35.23	173.61±42.30[a]	165.94±35.03[a]
HDL-c (mg/dL)	56.60±13.56	45.91±13.28[a]	43.50±10.07[a]
LDL-c (mg/dL)	111.60±28.49	101.76±33.93	93.22±10.07[a]
VLDL-c (mg/dL)	13 (11–19)	20.5 (14.25–29.75)	25.75 (18–36.5)[a]
CT/HDL-c	3.42 ±0.92	4.04±1.26[a]	4.00±1.14[a]
TG (mg/dL)	67 (55–99)	104 (70.75–149.25)	129.88 (92–185.5)[a]
Non-HDL-c	129.14±33.02	128.97±40.35	122.44±34.61

Kolmogorov/Smirnov or Shapiro/Wilk normality tests were carried out depending on the sample size. For normally distributed data, mean – SD shown, and for non-normally distributed data, the median is shown (first and third quartile). Analysis of variance and Tukey post-test were performed to outline statistically significant differences between groups. [a]$p < 0.05$ *versus* control group. [b]$p < 0.05$ *versus* T2D group.BMI, body mass index; CT, cholesterol; DBP, diastolic blood pressure; HbA_{1c}, glycated hemoglobin; HDL-c, high-density lipoproteins; HOMA-IR, homeostatic model assessment of insulin resistance; LDL-c, low-density lipoproteins; SBP, systolic blood pressure; T2D, type 2 diabetes; VLDL-c, very low-density lipoproteins.

3. ROS CONTENT AND MITOCHONDRIAL FUNCTION

First, we aimed to determine if T2D induced a change in mitochondrial integrity and functionality, and whether metformin was capable of reducing its effects. Figure 1A depicts how T2D leukocytes exhibited higher total ROS content ($p< 0.05$), and how this content was diminished by metformin treatment ($p< 0.05$). Moreover, the results shown in Figure 1B reflect a similar behavior of mitochondrial ROS ($p< 0.01$ in T2D vs. control samples, and $p<0.05$ for T2D + metformin vs.T2D).

In this respect, metformin tempered the rise in ROS production induced by T2D in leukocytes. Figure 1C shows the reduced mitochondrial membrane potential of T2D leukocytes ($p< 0.05$), and illustrates that treatment with metformin returned membrane potential to normal levels ($p<0.05$). Moreover, as shown in Figure 1D, T2D leukocytes exhibited decreased O_2 consumption ($p<0.05$), while mitochondria of patients receiving metformin showed normal O_2 consumption ($p< 0.05$).

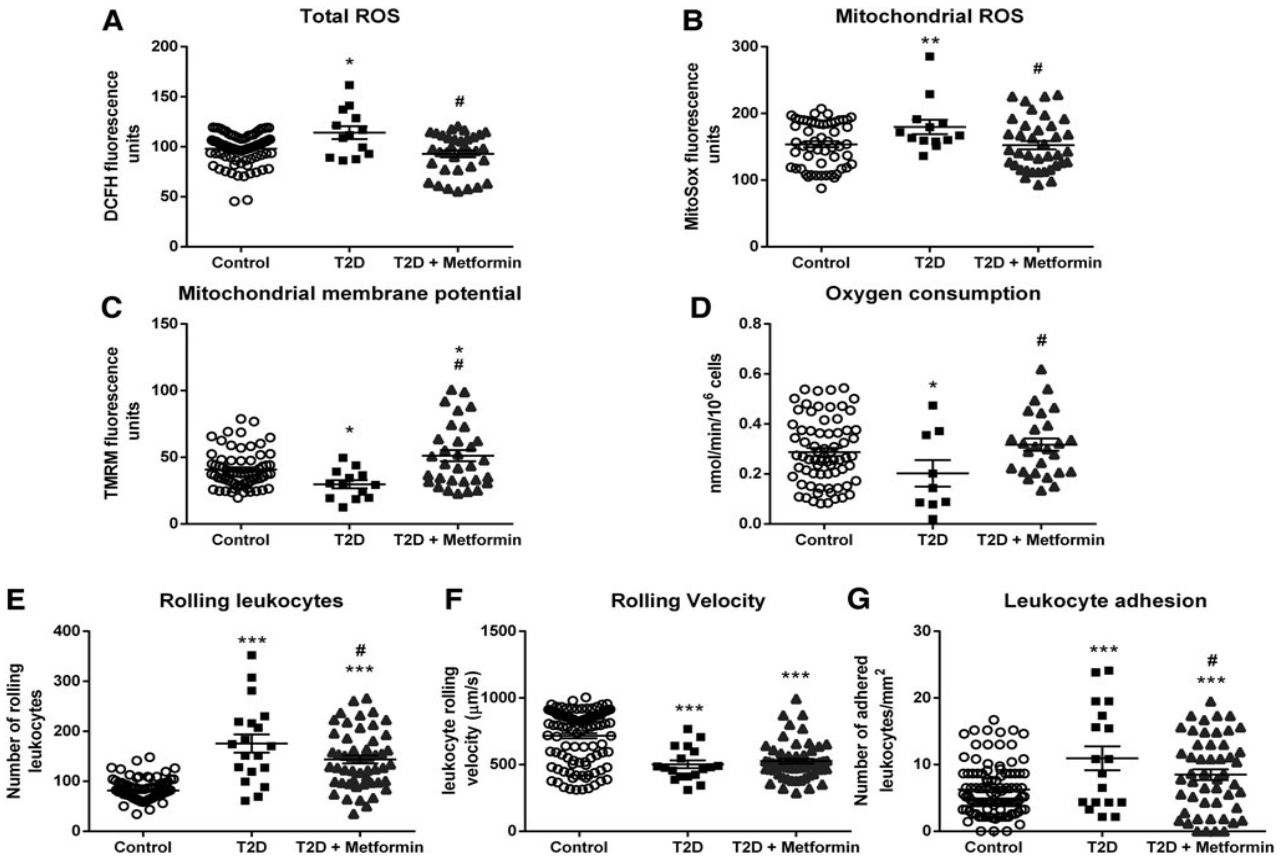

FIG. 1. Mitochondrial ROS production and function parameters and leukocyte/endothelial interaction analysis. (A) Total ROS concentration, measured as relative DCFH fluorescence by static cytometry. (B) Mitochondrial ROS concentrations, measured as relative MitoSOX fluorescence by static cytometry. (C) Mitochondrial membrane potential, measured as relative TMRM fluorescence by static cytometry. (D) O_2 consumption rate of leukocytes, measured by means of a Clark- type oxygen electrode. (E–G) Show the three parameters measured in the parallel plate flow chamber experiments. *$p < 0.05$, **$p < 0.01$, and ***$p < 0.001$ *versus* control; $^{\#}p < 0.05$ *versus* T2D. DCFH, 2'7'-dichlorofluorescein; ROS, reactive oxygen species; T2D, type 2 diabetes; TMRM, tetramethylrhodamine.

4. LEUKOCYTE/ENDOTHELIAL INTERACTIONS

Figure 1E–G describes how diabetes altered the leukocyte/ endothelial interactions and whether metformin restores this phenotype to control levels. T2D leukocyte/endothelial interactions were increased by enhancing rolling ($p< 0.001$) and adhesion ($p< 0.001$) and by decreasing rolling velocity ($p<0.001$). Metformin treatment reduced leukocyte rolling ($p<0.05$) and adhesion ($p<0.05$), highlighting the antiinflammatory effect exerted by metformin.

5. MITOCHONDRIAL DYNAMICS

Figure 2 displays how T2D alters mitochondrial dynamics and how metformin treatment modulates it. The analysis of mRNA expression of fusion genes was diminished in T2D leukocytes (Fig. 2A–E) (p <0.05 for *mfn1*, p <0.001 for *mfn2*, and p <0.05 for *opa1*), and metformin treatment enhanced their expression (p <0.05 for *mfn1* and p <0.01 for *mfn2*), with the exception of *OPA1* ($p< 0.05$ *vs*. control subjects). Furthermore, T2D leukocytes displayed lower levels of fission gene expression than controls (p <0.01 for *fis1* and p<0.001 for *drp1*). *fis1* expression levels were not modified by metformin treatment (p<0.05 *vs*. control subjects), while *drp1* levels returned to normal values (p <0.001 *vs*. T2D samples).

Regarding protein expression, mitochondrial fusion (Fig. 2F–J), orchestrated by MFN1, MFN2, and OPA1, was diminished in leukocytes from T2D patients (p <0.01, p<0.05, and p<0.01, respectively). Metformin treatment increased the levels of these proteins significantly ($p< 0.05$ in all cases). Furthermore, fission protein FIS1 and DRP1 levels were elevated in T2D leukocytes (p<0.01 in both cases), and metformin treatment reversed this increase (p<0.05 in both cases), highlighting the beneficial effect of this drug.

Metformin is the gold standard in the management of T2D, thanks mainly to its hypoglycemiant effect (3, 8, 9). Indeed, previous research has shown the remarkable benefits of metformin uptake on some analytical parameters (8). Our T2D patient cohort displayed

alterations in classic clinical parameters used to identify the diabetic state; namely, higher weight, BMI, waist circumference, glucose, HbA_{1c}%, SBP, DBP, HOMA-IR, and insulin with respect to controls. Metformin treatment reduced glucose and HbA_{1c}%, which is in accordance with the study by van Stee *et al.* (8).

In the case of lipid parameters, T2D patients displayed increased VLDL-c and triglyceride levels, but reduced cholesterol, HDL-c, and LDL-c levels. Research has shown that this is a result of the hypolipemiant treatment of diabetic dyslipidemia, regardless of whether or not there is metformin treatment (8).

In addition to the biochemical alterations described, we have observed altered mitochondrial function. First, leukocytes from T2D patients expressed increased levels of total and mitochondrial ROS. Although ROS can act as cellular signals, an excess is a signal of cellular stress and can lead to the activation of inflammatory pathways (2). Second, oxygen consumption and mitochondrial potential were altered, suggesting that mitochondrial function was compromised. The loss of membrane potential can be attributed to a leaking mitochondrial membrane, which reduces the electron transport complex's efficiency, thus altering oxygen consumption by leukocytes (4, 7). Such alterations are a sign of mitochondrial dysfunction in T2D leukocytes (1, 7). However, whether it is a cause or a consequence of the pathology of diabetes is still unknown, and future research should address this topic.

In a T2D scenario, the triggers of these mitochondrial alterations are chronic hyperglycemia and hyperlipidemia (2, 7). Therefore, we hypothesized that if metformin can alleviate hyperglycemia, it can also be beneficial for mitochondrial dysfunction. Several previous studies have demonstrated that metformin is beneficial for mitochondrial function and can alleviate the alterations that characterize a diabetic organism. The present study supports this, showing that metformin restores total and mitochondrial reactive oxygen species, mitochondrial membrane potential, and O_2 consumption to control levels.

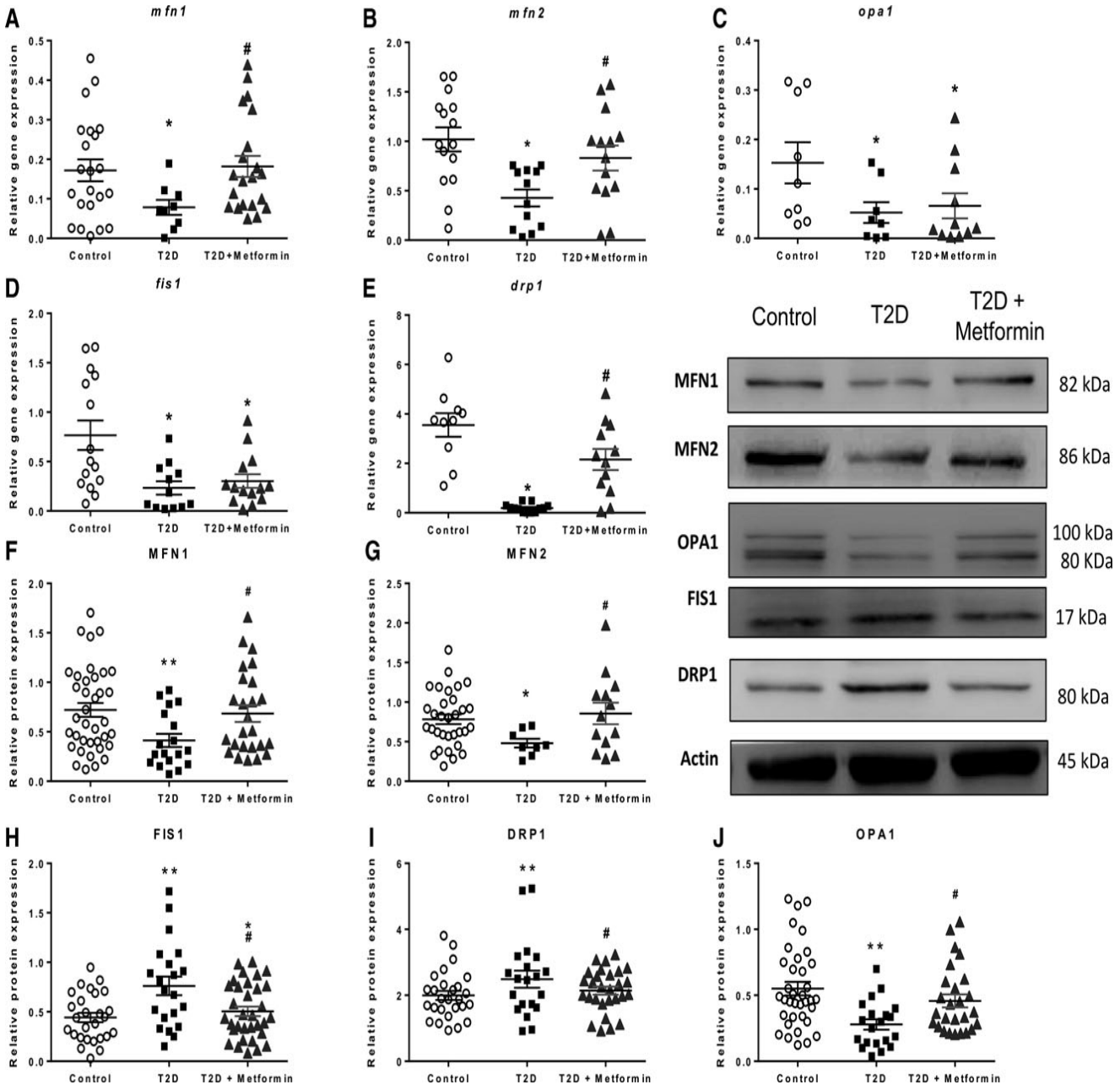

FIG. 2. Fusion and fission gene and protein expression in leukocytes from T2D patients treated (or not) with metformin and from controls. Gene expression in leukocytes from healthy subjects and T2D patients with or without treatment was measured with qRT-PCR. The fusion genes *mfn1* (**A**), *mfn2* (**B**), *opa1* (**C**), *fis1* (**D**), and *drp1* **(E**) were determined. Protein expression of the corresponding proteins was also measured (fusion proteins MFN1 (**F**), MFN2 (**G**), and OPA1 (**J**) and the fission proteins FIS1 (H) and DRP1 (**I**)). Representative images of each protein are displayed. In all graphs, n (control) = 12, n (T2D) = 9, and n (T2D + metformin) = 10. *p < 0.05 and **p < 0.01 versus control; #p < 0.05 versus T2D. DRP1, dynamin-related protein 1; FIS1, fission protein 1; MFN1, mitofusin 1; MFN2, mitofusin 2; OPA1, optic atrophy 1; qRT-PCR, quantitative real time polymerase chain reaction.

Mitochondrial dysfunction is closely related to inflammation, as a cause or a consequence (2, 4). Excessive ROS production activates key pathways in inflammation, and reduces the antioxidant capacity of the cell. In immune and endothelial cells, this leads to their overactivation and a non-physiological activity, both of which contribute to the activation of the endothelial/leukocyte interaction pathway and a subatherosclerotic scenario.

It has previously been reported that altered mitochondrial dynamics increases the endothelial dysfunction in venous endothelial cells from T2D patients and a T2D model of human aortic ring culture (6). Moreover, inhibition of fission has been shown to reduce endothelial impairment, suggesting that mitochondrial dysfunction plays a causative role in T2D. Bearing this in mind, we analyzed the functional repercussions of mitochondrial dysfunction on leukocyte biology in our samples. Our procedure involved us examining leukocyte/endothelial interactions, which were enhanced in T2D patients.

The metformin-treated group displayed less rolling and adhering cells, but velocity remained similar to that in the untreated group. These results suggest that metformin has the capacity to reduce generalized low-grade inflammation. The literature backs our results, confirming that metformin has an anti-inflammatory effect at many different levels (7). The precise mechanism through which the drug acts is yet to be deciphered, although several candidates have been proposed.

Mitochondrial dysfunction involves the deregulation of mitochondrial dynamics. Several *in vitro* and *in vivo* studies have highlighted hampered mitochondrial dynamics in T2D (2, 4, 9). Altogether, T2D seems to promote a profission phenotype and the inhibition of fusion, resulting in the deregulation of mitochondrial dynamics. Conversely, our data show that metformin treatment induces an increase in MFN1, MFN2, and OPA1, and a decrease in FIS1 and DRP1 at the protein level. An increase in mRNA was detected in *mfn1* and *mfn2*, but we did not observe a recovery of *opa-1* mRNA levels in metformin-treated patients, which warrants further research. The inner mitochondrial membrane location of OPA-1 could explain this varying mRNA

expression (7).

In the context of these remaining questions, a previous study determined that metformin reduces fission phenotype in diabetic APOE$^{-/-}$ mice and prevents atherosclerotic lesions (9). Based on the present results, we can affirm that metformin restores mitochondrial dynamics in T2D, although we have not identified the exact underlying mechanism. Research to date implicates AMPK, which can be effectively activated by metformin (3, 6); whether or not this is the elusive mechanism in question is an object for future research.

6. CONCLUSION

In the present study, an improvement in mitochondrial function and dynamics was observed in T2D patients on metformin. Moreover, leukocyte/endothelial cell interactions in the treated subjects were significantly reduced, thus indicating a decrease in inflammation and T2D-related cardiovascular events. Our findings reinforce the idea that metformin plays an important role in modulating the inflammation that occurs in T2D patients. At the same time, it highlights the beneficial effects of this drug, by which it prevents mitochondrial dysfunction and deregulation of mitochondrial dynamics and, in turn, their clinical implications.

7. NOTES

7.1. Materials and methods

7.1.1. Subjects.

One hundred thirty-five healthy subjects and 120 T2D patients were recruited from the Endocrinology and Nutrition Outpatient's Service of University Hospital Doctor Peset, in Valencia (Spain). Of the 120 T2D patients, 81 had been under 1700 mg/day metformin treatment for at least 1 year. All subjects provided written informed consent to participate in the study. The hospital's Ethics Committee for Clinical Investigation approved the study (ID: 98/19), which was

in line with the Helsinki Declaration. T2D was diagnosed following the ADA criteria. Exclusion criteria were BMI>35, history of cardiovascular disease, and the presence of autoimmune, infectious, hematological, or malignant disease.

7.1.2. Sample collection and laboratory tests.

Subjects attended the Endocrinology Service (Hospital Dr Peset) after 12-h fasting and not having taken any anti-inflammatory drug in the previous 24 h. Peripheral blood was extracted from the brachial vein after measuring blood pressure, weight, height, and waist circumference. Anthropometric parameters were measured as follows: weight and height were measured on a graded scale; SBP and DBP were evaluated with an automatic sphygmomanometer; and waist circumference was evaluated with a measuring tape. BMI was calculated as weight (kg)/height (m^2). Insulin was measured with an immunoassay using an Architect Insulin Reagent Kit. Glucose was measured in serum by an automated enzymatic method with a Beckman Synchron LX20 Pro analyzer (Beckman Coulter, Brea, CA). HbA_{1c} was analyzed with an automated glycohemoglobin analyzer (Arkray, Inc., Kyoto, Japan). HOMA-IR index was calculated as follows: (Fasting Insulin [lUI/mL] Fasting Glucose [mg/dL])/405. Cholesterol, HDL-c, and triglyceride levels were analyzed by means of an enzymatic assay (Beckman Coulter). Friedewald's formula was used to calculate LDL-c.

7.1.3. Leukocyte isolation.

Leukocytes were isolated by means of the Ficoll gradient method. The blood was laid over 7 mL of Ficoll (Hystopaque-1119 Ref. 11191 and Hystopaque-1077 Ref. 10771; both from Sigma-Aldrich, St. Louis, MO) and centrifuged for 25 min at room temperature. Leukocytes were subsequently collected and lysed with erythrocyte lysis buffer (Red Blood Cell Lysis Solution, Ref. 130-096-941; Miltenyi Biotec, Germany) for 5 min. Cells were then washed with Hank's balanced saline solution (HBSS) and stored for future experiments.

7.1.4. Static cytometry assay.

Three hundred thousand leukocytes/well were seeded in duplicate in 24-well plates for

each sample. An internal control (Hep3b cells) was also seeded at the same density in each plate. After 20 min, when cells were attached to the bottom of the plate, 250 µL tetramethylrhodamine (1 µ*M*) MitoSOX (1 µ*M*), 2'7'dichlorofluorescein (DCFH; 1 µ*M*), and nuclear staining HOECHST 33342 (1 µ*M*), all purchased in Thermo Fisher Scientific, were added to each well and incubated for 20 min at 37°C under gentle shaking. The wells were then washed twice with warm HBSS. Static cytometry visualization was performed using ScanR software coupled to a IX81 Olympus microscope (both from Olympus Corporation, Shinjuku, Tokyo, Japan). Each experiment was performed in duplicate, with 16 images obtained per well in each experiment and calculating the mean fluorescence intensity. The resulting mean was normalized according to the cell number and internal control.

7.1.5. Oxygen consumption assay.

Once leukocytes had been isolated, an aliquot of $5x10^6$ cells/mL was placed in a gas-tight chamber. A Clark-Type O_2 electrode (Rank Brothers, Bottisham, United Kingdom) was used to measure O_2 consumption. Sodium cyanide (1 m*M*), an inhibitor of the electron transport chain, was used to confirm that O_2 consumption was mainly mitochondrial (95%–99%). Duo.18 software (WPI, Stevenage, United Kingdom) was used to visualize and collect the data. The maximal O_2 consumption rate with endogenous substrates was calculated using GraphPad software (GraphPad software, Inc., San Diego, CA). A trypan blue exclusion test was performed after each experiment to determine cell viability, and revealed no significant cell death.

7.1.6. Leukocyte/endothelial interaction assay.

An aliquot of $1.2x10^6$ leukocytes resuspended in RPMI medium was used for this experiment. Previously, HUVECs isolated from fresh umbilical cords were seeded and grown until a 95% confluent monolayer formed. On the day of the experiment, the leukocyte suspension was perfused over the surface of HUVECs at 0.3 mL/min using a parallel plate flow system, all of which was observed through an inverted microscope. While interacting, cells were recorded with a microscope-coupled camera for 5 min, and, during the last minute, different

fields were observed to count the number of adhered leukocytes. The following data were obtained from the videos: number of leukocytes that crossed a 200 µ*M* surface in 1 min (rolling); the time these leukocytes took to cover this distance (rolling velocity); and the number of leukocytes stably adhering to the HUVEC monolayer (adhesion).

7.1.7. Gene and protein expression analysis.

To measure gene expression, a GeneAll Ribospin Total RNA extraction kit (GeneAll Biotechnology, Hilden, Germany) was used to isolate RNA from leukocyte samples, following the manufacturers' protocol. We measured gene expression by means of a qRT-PCR using a FastStart universal SYBR Green Master (Sigma Aldrich, St. Louis, MO) and a 7500 Fast RT-PCR system (Life Technologies, Carlsbad, CA). RNA was quantified in a NanoDrop 200c spectrophotometer (Life Technologies, Thermo Fisher Scientific), and purity was confirmed with the 260 nm/280 nm absorbance ratio (A260/280). Next, cDNA was determined with a RevertAid first-strand cDNA synthesis kit (Life Technologies, Thermo Fisher Scientific).

Quantification was performed by means of the comparative $2^{-\Delta\Delta Ct}$ method, and a sample was used as an internal control and *gapdh* expression as an endogenous control in all experiments. Data were analyzed with Expression Suite software (Life Technologies, Thermo Fisher Scientific). Table 2 shows the primers used in the study.

Table 2. Forward and Reverse Sequences of the Specific Primers Used in This Study

Target	***Forward***	***Reverse***
Mfn1	CCTCCTCTCCGCCTTTAACT	TATGCTAAGTCTCCGCTCCAAC
Mfn2	CAGCTACACTGGCTCCAACT	TTTCTTGTTCATGGCGGCAA
Opa1	ACCGTTAGCCCTGAGACCATA	GGTAAGTCAACAAGCACCATCC
Fis1	AGAAATTTCAGTCTGAGAAGGCA	CCTCCTTGCTCCCTTTGGG
Drp1	GCTGATGCTTGTGGGCTAATG	TGCCAAAGCACTTGGAACTTT

Regarding protein analysis, previously isolated leukocytes were lysed with RIPA buffer, homogenized, and sonicated in an ultrasound bath for 30 s, three times. Samples were then left for 15 min on ice and centrifuged for 15 min at 21400 g at 4°C. The supernatant was collected and quantified following the bicinchoninic acid protein quantification assay (Thermo Fisher Scientific, Waltham, MA, USA). Twenty-five micrograms of protein were loaded onto 4%–20% gradient sodium dodecyl sulfate/ polyacrylamide gels (Novex Wedge Well 4-20 Tris Glycine Gel, Ref. XP04205B0X; Invitrogen-Life Technology, Carlsbad, CA) and separated at 150 V for 90 min at room temperature. Transference to nitrocellulose membranes (BioRad, CA) was carried out by the wet transference method, running for 60 min at constant amperage (400 mA). Membranes were then blocked with 5% bovine serum albumin or 5% skimmed milk (depending on the protein of interest) for 1 h at room temperature. Specific antibodies against MFN1, MFN2, OPA1, DRP1, and FIS1 were diluted in blocking buffer. Specific antibody dilutions were incubated with the membranes overnight at 4°C under gentle shaking: rabbit polyclonal anti- MFN1 (Ref. ABC41), rabbit polyclonal anti-MFN2 (Ref. ABC42), mouse monoclonal anti-OPA-1 (Ref. MABN737), rabbit polyclonal anti-FIS-1 (Ref. ABC67), all purchased from Merck-Millipore (Burlington, MA), and mouse monoclonal anti DRP-1 (Ref. GR3248679-1; Abcam, Cambridge, United Kingdom). The following day, specific secondary antibodies (goat anti-rabbit antibody [Ref. PI-1000] from Vector Laboratories, Burlingame, CA, and goat anti-mouse antibody [Ref. 31420] from Thermo Fisher Scientific, Waltham, MA) were incubated for 60 min at room temperature. Images of the resulting proteins were obtained using SuperSignal West Pico Plus (Ref. 34580) or Femto (Ref. 34095) chemiluminescent substrate (Thermo-Fisher Scientific) and the Fusion FX5 (Vilber Lourmat, Marne-La Valleé, France) imaging system. Densitometric quantification of the images was performed with Bio1D software (Vilber Lourmat). Each membrane was checked several times by cutting different fragments following the guide of the molecular size marker and also with homemade glycine stripping buffer to maximize the results for each sample. Whole-membrane fragments used for the images in Figure 2 are included in

Supplementary Figure S1.

7.1.8. Statistical analysis.

Normality was confirmed with the Kolmogorov/Smirnov test or the Shapiro/Wilk test depending on the size of the sample. Values are expressed as mean - SD for normally distributed data, and the median – (25th–75th percentiles) is presented for non-normally distributed data. One-way analysis of variance with a Tukey *post-hoc* test was used to compare the three groups. When two groups were compared, a *t*-test was used for normally distributed data, while a Mann/Whitney *U* test was used for non-normal distribution. The influence of sex and BMI was corrected with a covariance analysis (univariate general linear model). Significance was confirmed in all comparisons when $p<0.05$, with a confidence interval of 95%. SPSS 17.0 (SPSS Statistics, Inc., Chicago, IL) was used in all the tests, and GraphPad (GraphPad, La Jolla, CA) was used to plot the data with bar graphs, representing the media and the standard error of the mean.

Acknowledgments

The authors thank Brian Normanly (University of Valencia/CIBERehd) for his editorial assistance and Rosa Falcon for her technical assistance.

Supplementary Material

Supplementary figure 1

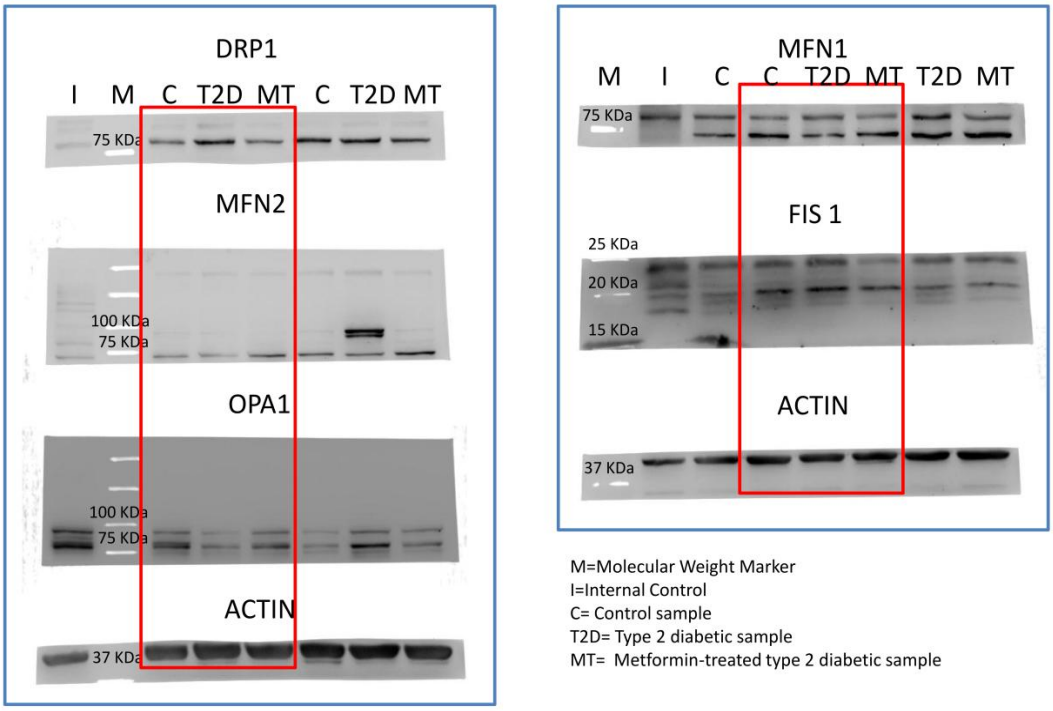

Supplementary figure 1: Uncropped raw images of all blots included in Figure 2. The membranes were cut for maximizing the number of proteins obtained for each experiment.

REFERENCES

1. Adeshara KA, Bangar NS, Doshi PR, Diwan A, and Tupe RS. Action of metformin therapy against advanced glycation, oxidative stress and inflammation in type 2 diabetes patients: 3 months follow-up study. Diabetes Metab Syndr 14: 1449–1458, 2020.
2. Apostolova N, Iannantuoni F, Gruevska A, Muntane J, Rocha M, and Victor VM. Mechanisms of action of metformin in type 2 diabetes: effects on mitochondria and leukocyteendothelium interactions. Redox Biol 34: 101517, 2020.
3. Foretz M, Guigas B, and Viollet B. Understanding the glucoregulatory mechanisms of metformin in type 2 diabetes mellitus. Nat Rev Endocrinol 15: 569–589, 2019.
4. Geto Z, Molla MD, Challa F, Belay Y, and Getahun T. Mitochondrial dynamic dysfunction as a main triggering factor for inflammation associated chronic noncommunicable diseases. J Inflamm Res 13: 97–107, 2020.
5. Pernas L and Scorrano L. Mito-morphosis: mitochondrial fusion, fission, and cristae remodeling as key mediators of cellular function. Annu Rev Physiol 78: 505–531, 2016.
6. Shenouda SM, Widlansky ME, Chen K, Xu G, Holbrook M, Tabit CE, Hamburg NM, Frame AA, Caiano TL, Kluge MA, Duess M-A, Levit A, Kim B, Hartman M-L, Joseph L, Shirihai OS, and Vita JA. Altered mitochondrial dynamics contributes to endothelial dysfunction in diabetes mellitus. Circulation 124: 444–453, 2011.
7. Sivitz WI and Yorek MA. Mitochondrial dysfunction in diabetes: from Molecular mechanisms to functional significance and therapeutic opportunities. Antioxid Redox Signal 12: 537–577, 2010.
8. van Stee MF, de Graaf AA, and Groen AK. Actions of metformin and statins on lipid and glucose metabolism and possible benefit of combination therapy. Cardiovasc Diabetol 17: 94, 2018.
9. Wang Q, Zhang M, Torres G, Wu S, Ouyang C, Xie Z, and Zou M-H. Metformin suppresses diabetes-accelerated atherosclerosis via the inhibition of Drp1-mediated mitochondrial fission. Diabetes 66: 193–205, 2017.

4.4. CHAPTER 4

The mitochondrial antioxidant SS-31 modulates oxidative Stress, endoplasmic reticulum stress, and autophagy in type 2 diabetes

Irene Escribano-López [1†], Aranzazu M. de Marañon [1†], Francesca Iannantuoni [1], Sandra López-Domènech [1], Zaida Abad-Jiménez [1], Pedro Díaz [1], Eva Solá [1], Nadezda Apostolova [2], Milagros Rocha [3 4], Víctor M. Víctor [5 6 7]

[1]Service of Endocrinology, University Hospital Doctor Peset, Foundation for the Promotion of Health and Biomedical Research in the Valencian Region (FISABIO), 46017 Valencia, Spain.

[2]CIBERehd-Department of Pharmacology, University of Valencia, 46010 Valencia, Spain.

[3]Service of Endocrinology, University Hospital Doctor Peset, Foundation for the Promotion of Health and Biomedical Research in the Valencian Region (FISABIO), 46017 Valencia, Spain.

[4]CIBERehd-Department of Pharmacology, University of Valencia, 46010 Valencia, Spain.

[5]Service of Endocrinology, University Hospital Doctor Peset, Foundation for the Promotion of Health and Biomedical Research in the Valencian Region (FISABIO), 46017 Valencia, Spain.

[6]CIBERehd-Department of Pharmacology, University of Valencia, 46010 Valencia, Spain.

[7]Department of Physiology, University of Valencia, 46010 Valencia, Spain.

[†]These authors contributed equally to this work.

Journal of Clinical Medicine, 2019 Aug 28;8(9):1322.

DOI: 10.3390/jcm8091322.

ABSTRACT

Mitochondrial dysfunction has been shown to play a central role in the pathophysiology of T2D, and mitochondria-targeted agents such as SS-31 are emerging as a promising strategy for its treatment. We aimed to study the effects of SS-31 on leukocytes from T2D patients by evaluating oxidative stress, ER stress and autophagy. Sixty-one T2D patients and 53 controls were included. Anthropometric and analytical measurements were performed. We also assessed ROS production, calcium content, the expression of ER stress markers GRP78, CHOP, P-eIF2α, and autophagy-related proteins Beclin-1, LC3 II/I, and p62 in leukocytes from T2D and control subjects treated or not with SS-31. Furthermore, we have evaluated the action of SS-31 on leukocyte-endothelium interactions. T2D patients exhibited elevated ROS concentration, calcium levels and presence of ER markers (*GRP78* and *CHOP* gene expression, and GRP78 and P-eIF2α protein expression), all of which were reduced by SS-31 treatment. SS-31 also led to a drop in *BECN1* gene expression, and Beclin-1 and LC3 II/I protein expression in T2D patients. In contrast, the T2D group displayed reduced p62 protein levels that were restored by SS-31. SS-20 (with non-antioxidant activity) did not change any analyzed parameter. In addition, SS-31 decreased rolling flux and leukocyte adhesion, and increased rolling velocity in T2D patients. Our findings suggest that SS-31 exerts potentially beneficial effects on leukocytes of T2D patients modulating oxidative stress and autophagy, and ameliorating ER stress.

Keywords: Mitochondria; oxidative stress; type 2 diabetes; endoplasmic reticulum stress; autophagy; SS-31.

1. INTRODUCTION

T2D represents a serious global problem with a worryingly high rate worldwide, constituting one of the main public health challenges of the 21st century. T2D is a metabolic disruption characterized by IR and β cell failure. In those affected, the persistent exposure to a hyperglycemic environment promotes excessive generation of ROS and it leads to the imbalance of antioxidant defenses [1], inducing oxidative stress, which contributes to IR and the activation of pro-inflammatory signaling pathways [2], both thought to play key roles in the complications associated with T2D.

Oxidative stress and ER stress are closely linked. Indeed, an altered redox balance has a major impact on ER folding capacity. Under pathological conditions such as T2D, ER homeostasis is disturbed due to an accumulation of misfolded proteins [3,4], in response to which the UPR is activated in order to (i) upregulate the expression of chaperones and aid the folding of ER proteins (ii) and degradation of proteins, and (iii) to prevent protein synthesis [5,6]. It is known that antioxidant production is one of the restorative functions of the UPR, which coordinates the activation of the trans-membrane ER resident protein (PERK) signalling pathway, thus allowing the cell to adapt to oxidative and ER stress [7,8]. The ER stress response also includes mechanisms of autophagy induction, and it has been demonstrated that low-grade autophagy reduces ER stress by destruction of the ubiquitinated unfolded/misfolded dysfunctional proteins and damaged organelles that result from said stress [9]. The onset of autophagy involves the formation of an autophagosome, a process in which several autophagy-related genes coordinate to engulf the defective material in a double membrane. This process is initiated when the complex formed by Beclin-1/Vps34/VPs15/UVRAG—known as PI3K complex III—nucleates the formation of the autophagosome. In parallel, the cytosolic protein microtubule-associated to LC3 I is conjugated to a phosphatidylethanolamine to form LC3 II. In this form, LC3 II migrates to the growing autophagosome and helps to build the double membrane. The ubiquitinated

protein and defective organelles are detected by SQSTM1—also known as the p62 protein—which associates itself to membrane-bound LC3 II. The autophagosome then fuses with a lysosome, which pours its hydrolytic enzymes into the inner space of the autophagosome, thereby degrading its content [10,11]. This is usually a rescue mechanism in situations of stress. However, when ER stress is prolonged, the autophagy activated as a result can lead to severe cell damage and, eventually, to apoptosis [12,13]. Incipient insult has serious consequences for the balance of pro- and anti-survival signals. Therefore, the mechanisms of oxidative stress, ER stress and autophagy are closely related to each other and are considered key targets for understanding the development of T2D. In the present work, we have studied these processes by analyzing general markers for their activation.

Mitochondria are essential to the control of cellular homeostasis, cell death and apoptosis. Furthermore, overproduction of ROS occurs mainly in mitochondria, through the electron transport chain [14,15], thus attributing these organelles a key role in the development and control of metabolic diseases such as T2D. For the aforementioned reasons, the identification of novel mitoprotective therapies may lead to the prevention and successful treatment of the complications associated with this disease.

One of the molecules that might be beneficial in mitochondria-based diseases is the mitochondria-targeted antioxidant SS-31 (D-Arg-2'6'-dimethylTyr-Lys-Phe-NH_2), a member of the SS peptide family, aromatic-cationic tetrapeptides targeted to cardiolipin on the inner mitochondrial membrane via hydrophobic and electrostatic interactions. There, they increase ATP production, thus restoring cellular function and preserving vital ATP-dependent processes [16, 18]. Their antioxidant action is due to two actions, the dimethyltyrosine residue, scavenging H_2O_2 and $ONOO^-$ and inhibiting lipid peroxidation. In addition, preclinical studies support their potential use in neurodegenerative disorders and ischaemia-reperfusion injury [19]. Our group has already demonstrated that SS-31 increases SIRT1 levels in leukocytes and ameliorates inflammation, oxidative stress and leukocyte-endothelium interactions in T2D [20].

In the present study, we set out to explore the effects of SS-31 on leukocytes of T2D patients by evaluating different key pathways including oxidative stress, ER stress and autophagy. We have used peripheral blood leukocytes as surrogate model for the general/systemic oxidative stress and its consequences present in T2D. Actually, T2D has been widely related with leukocyte dysfunction [21–25]. Peripheral blood leukocytes are the primary sensors of the alterations in the presence of different soluble molecules in the bloodstream [26–30]. More precisely, we have employed PMNs, which present higher vulnerability to oxidative damage in T2D compared to mononuclear cells [21]. Numerous studies suggest that the continuous exposure of leukocytes to high circulating levels of glucose, lipids, insulin, and proinflammatory cytokines (known as the T2D environment) alters the cell metabolism and affect the cell ability to manage stress situations. These alterations have a direct impact on the leukocytes' function and main pathways such as oxidative stress regulation, ER stress, autophagy, and mitochondrial homeostasis [31–35]. Previous research stated that different molecules, drugs or antioxidants can relieve the stress response [36–39]. Taken into account these facts, we consider that PMNs are a readily available, representative and valid model to evaluate the influence of ROS on the different pathways related to T2D [21].

2. EXPERIMENTAL SECTION

2.1. Human Subjects

A total of 114 subjects were included in the study population, specifically 61 T2D patients and 53 healthy controls recruited from the Service of Endocrinology and Nutrition of University Hospital Doctor Peset (Valencia, Spain) and adjusted for age and sex. All subjects gave their written informed consent to participate in the study and the protocols followed were approved by our hospital's Ethics Committee for Clinical Investigation (ID: 97/16), in line with the ethical principles of the Helsinki declaration. All T2D patients in this study have suffered from

T2D for at least 5 years, which ensures that they display a chronic phenotype.

The ADA criteria were used for T2D diagnosis, and exclusion criteria were history of CVD, presence of morbid obesity or autoimmune, hematological, malignant, infectious, organic, or inflammatory disease, and insulin treatment.

2.2. Sample Collection

Venous blood samples were taken from the antecubital vein and collected in Vacutainer® tubes in fasting conditions, between 8 AM and 10 AM. Anthropometric parameters—weight (kg), height (m), BMI (kg/m^2), SBP and DBP (mmHg), and waist circumference (cm)—were assessed.

2.3. Laboratory Tests

Fresh blood samples were centrifuged for 10 min at 1500 g at a temperature of 4 ◦C in order to separate serum from the blood. Serum levels of fasting glucose, total cholesterol and TG were determined by enzymatic method, HDL-c was recorded employing a Beckman LX-20 autoanalyzer (Beckman Coulter, La Brea, CA, USA) using a direct method and LDL-c content was quantified with Friedewald's formula. Insulin levels were obtained by an immunochemiluminescence assay, and HOMA-IR index (fasting insulin (µU/mL) × fasting glucose (mg/dL)/405) was calculated to estimate IR. The percentage of HbA_{1c} was determined with an automatic glycohemoglobin analyzer (Arkray, Inc., Kyoto, Japan) and an immunonephelometric assay was used to measure hsCRP levels.

2.4. Leukocyte Isolation

Human PMNs were isolated from heparinized blood samples incubated for 45 min with 1:2 volumes of dextran solution (3% in NaCl 0.9%; Sigma Aldrich, MO, USA). The supernatant was centrifuged over Fycoll-Hypaque (GE Healthcare, Uppsala, Sweden) at 650 g for 25 min and the pellet lysed to remove the remaining erythrocytes. It was then incubated with lysis buffer (5 min

at room temperature) and centrifuged at 240 g. Pellets containing leukocytes were then washed twice and resuspended in Hank's balanced salt solution (HBSS; Sigma Aldrich, MO, USA). A Scepter 2.0 device (Millipore Iberica, Madrid, Spain) was employed for the cell count. The cellular suspension was split into two samples, which were treated under the same conditions with concentrations that did not affect the cells' viability; one was incubated with SS-31 (100 nM, 30 min), and the other with SS-20 (100 nm, 30 min, without antioxidant activity).

2.5. PMN-Endothelium Interaction Assay

PMNs were isolated as previously described by our group [20]. In this assay, we employed a 1.2 mL aliquot of PMNs obtained from the peripheral blood of control and T2D subjects with a density of 10^6 cells/mL in complete RPMI. Prior to this, primary cultures of HUVEC were established. HUVEC were isolated as previously reported [20]. On the day of the experiment, the PMNs aliquot was passed through the endothelial monolayer at a speed of 0.3 mL/min during a 5-min period, which was recorded. Next, the number of rolling PMNs, as well as their velocity and adhesion to the endothelial monolayer were recorded. The number of rolling PMNs was measured as those rolling for 1 min (recorded on video). Velocity was assessed by determining the time in which 15 rolling PMNs covered a distance of 100 µm. Adhesion was analyzed by counting the number of PMNs adhering to the endothelium for at least 30 s in 5 fields.

2.6. Quantitative Fluorescence Microscopy

Fluorescence probes 2',7'-dichlorodihydrofluorescein diacetate (DCFH-DA; 5×10^{-6} mol/L), MitoSOX (5×10^{-6} mol/L) and (acetyloxy)methyl ester (Fluo-4 AM; 1×10^{-6} mol/L) were used to assess total ROS, mitochondrial ROS and calcium levels, respectively. DCFH-DA is routinely used in intact cells, being taken up and deacetylated by endogenous hydrolases to a form (DCFH) that is then oxidized by peroxides to fluorescent 2,7-Dichlorofluorescein (DCF).

MitoSOX, a mitochondria-targeted dihydroethidium (by addition of a triphenylphosphonium group) is a probe widely used to detect mitochondrial superoxide. To perform these assays, isolated leukocytes were placed in 48-well plates and incubated for 30 min at 37 ◦C with the appropriate fluorochrome, diluted in phosphate-buffered saline (PBS; Sigma Aldrich, MO, USA). Fluorescence intensity was then recorded with a fluorescence microscope (IX81; Olympus Corporation, Shinjuku-ku, Tokyo, Japan) coupled to the static cytometry software "ScanR" (Olympus). Fluorescence units of these measurements were normalized with respect to the control group, in which the mean fluorescence units were considered 100%, and the data were relativized to that fluorescence value. Experiments were performed in duplicate and 16 images per well were obtained and analyzed obtaining a mean fluorescence value. The mean value of these two replicates of each sample was used for data representation and statistical analysis. Nuclei were detected with Hoechst 33342. All fluorochromes were supplied by Thermo Fisher Scientific, Waltham, MA, USA.

2.7. Flow Cytometry

ROS generation in human leukocytes was analyzed using whole blood by flow cytometry using DCFH-DA (5×10^{-6} mol/L) as marker dye. The distribution of different leukocyte subsets was analyzed in peripheral blood using a single staining (CD45), no-lyse no-wash method. CD45 positive cells (marked with the fluorescent probe APC Mouse Anti-Human CD45, BD Biosciences, San Jose, CA, USA) and the morphological characteristics of the cells (FSC and SSC parameters) were used for determining the PMNs cellular subset as shown in previous work [40,41]. Briefly, 200 µL of heparinized blood were incubated with 4 µL of CD45 monoclonal antibody for 20 min at room temperature in darkness, in the presence and absence of several treatments. For this assay, 500 µL of stained blood diluted 20-fold in PBS was incubated for 30 min at 37 ◦C with the fluorochrome DCFH-DA. Samples were acquired for 10,000 individual cells by BD AccuriTM C6 Plus Flow Cytometer (BD Biosciences, San Jose, CA, USA) and ROS production was quantified by

median fluorescence intensities.

2.8. Western Blotting (WB)

Leukocyte pellets were homogenized and incubated on ice in cell lysis buffer for 15 min (10 mM HEPES pH 7.5, 10 mM NaCl, 2 mM MgCl2, 1 mM EDTA, 1 mM EGTA, 0.5% Nonidet P-40, 1 mM DTT, 'Complete Mini' and 'Pefabloc' protease inhibitor cocktail from Roche Diagnostics and phosphatase inhibitor mixture: 10 mM NaF and 0.1 mM Na3VO4); tubes were vortexed to disrupt the cell membranes and centrifuged at 4 ◦C for 10 min. The supernatants were stored at −70 ◦C till further use as cytoplasmic extracts. The pelleted nuclei were resuspended in the nuclear extraction buffer (25 mM HEPES pH 7.5, 500 mM NaCl, 9 % glycerol (v/v), 5 mM $MgCl_2$, 0.5 % Nonidet P-40, 1 mM DTT) supplemented with protease inhibitors ('Complete Mini' protease inhibitor cocktail, and 'Pefabloc', both from Roche Diagnostics) and 10 mM NaF as a phosphatase inhibitor, and were incubated on ice for 10 min under sonication. Nuclear extracts were collected by centrifugation for 10 min at 4 ◦C, and were either immediately used or stored at −70 ◦C. Protein concentration was determined with a BCA protein assay kit (Thermo Fisher Scientific, Waltham, MA, USA). Next, 25 µg proteins per sample were loaded onto SDS-polyacrilamide gels. Gel electrophoresis was performed at 120 V, 90 min, followed by transfer to nitrocellulose membranes (Bio-Rad, Hercules, CA, USA) at 400 mA, for 1 h. After blocking at room temperature for 1 h in 5% non-fat milk in TBST buffer containing 25 mM Tris, 150 mM sodium chloride and 0.1% Tween20, at pH 7.5, membranes were incubated overnight at 4 ◦C with anti-GRP78 rabbit polyclonal antibody (Abcam, Cambridge, UK), anti- P-eIF2α (pS52) rabbit polyclonal antibody (Life Technologies, Carlsbad, CA USA), anti-Beclin-1 rabbit polyclonal antibody (Abcam, Cambridge, UK), anti-LC3 rabbit polyclonal antibody (Millipore Iberica, Madrid, Spain), anti-SQSTM1/p62 mouse monoclonal antibody (Abnova, Taipei, Taiwan) or anti-Actin rabbit polyclonal antibody (Sigma Aldrich, St Louis, MO, USA), followed by horseradish peroxidase (HRP) goat anti-rabbit (Millipore Iberica, Madrid, Spain) or HRP goat anti-mouse

(Thermo Fisher Scientific, Waltham, MA, USA) secondary antibodies as appropriate, for 1 h at RT. Protein expression was assessed with ECL plus reagent (GE Healthcare, Amersham Place, Litte Chalfont, UK) or Supersignal West Femto (Thermo Fisher Scientific, Waltham, MA, USA). A Fusion FX5 acquisition system (Vilbert Lourmat, Marne La Vallée, France) was employed for chemiluminescence signal detection, which was analyzed by densitometry using Bio1D software (Vilbert Lourmat, Marne La Vallée, France). For quantification of the expression level of the studied protein, an internal control was included in each blot and the expression was normalized to that of actin in the same sample.

2.9. Quantitative RT-PCR (qRT-PCR)

Total RNA was isolated from leukocytes with the GeneAll® RibospinTM kit following the manufacturer's instructions (GeneAll Biotechnology, Hilden, Germany). RNA concentrations were measured using Nanodrop 2000c (Thermo Fisher Scientific, Waltham, MA, USA), and 1 µg of the extracted RNA was employed in the following steps. To detect the expression of genes involved in autophagy and ER stress, the RevertAid First Strand c-DNA Synthesis kit (Thermo Fisher Scientific) and KAPA SYBR FAST universal master mix (Applied Biosystems-Thermo Fisher Scientific, Walthman, MA, USA) were used. RT-qPCR analysis was performed with a 7500 Fast real-time PCR system (Life Technologies, Carlsbad, CA, USA) (Table 1). Fold changes were calculated by the $2^{-\Delta\Delta Ct}$ method through Expression Suite software (Life Technologies) and relative gene expression of GRP78, DDIT3/CHOP, BECN1 and SQSTM/p62 was calculated using GAPDH as a housekeeping control.

Table1: Protocol details and primer sequences.

qRT-PCR protocol				
Temperature	95ºC	95ºC	60ºC	Melting
Time	10 min	10 s	30 s	curve
Nº cycles	1	40		
PCR primers				
Target	**Direction**	**5'-3'**		
BECN1	Forward	CCCCAGAACAGTATAACGGCA		
	Reverse	AGACTGTGTTGCTGCTCCAT		
GRP78	Forward	AAGAACCAGCTCACCTCCAACCC		
	Reverse	TTCAACCACCTTGAACGGCAA		
DDIT/CHOP	Forward	AGAACCAGGAAACGGAAACAGA		
	Reverse	TCTCCTTCATGCGCTGCTTT		
GAPDH	Forward	CGCATCTTCTTTTGCGTCG		
	Reverse	TTGAGGTCAATGAAGGGGTCA		
SQSTM/p62	Forward	GATTCGCCGCTTCAGCTTCTG		
	Reverse	CTGGAAAAGGCAACCAAGTCC		

2.10. Statistical Analysis

All data were analyzed with SPSS 17.0 software (SPSS Statistics Inc., Chicago, IL, USA). Values are expressed as mean and standard deviation (SD) for parametric data; while the median (25th–75th percentiles) is presented for non-parametric data. Bar graphs show mean and standard error of the mean (SEM) in the figures.

In the case of the variables with normally distributed data, groups were compared with a Student's t-test, while a Mann–Whitney U test was employed for non-normally distributed ones, and the chi-square test for proportion of frequencies. To examine the main effects of the treatment, the study groups were compared with one-way analysis of variance (ANOVA) followed by a Newman–Keuls post hoc test. In addition, the prominent influence of BMI was reduced by means of an analysis of covariance with a univariate general linear model. Differences were considered to be significant when $p < 0.05$, applying a confidence interval of 95% in every comparison. Graphs were plotted with GraphPad Prism 4.0 (GraphPad, La Jolla, CA, USA).

3. RESULTS

3.1. Clinical and Endocrine Parameters

Our study was carried out in a population of 53 healthy volunteers (mean age 51.7 ± 9.3) and 61 T2D patients (mean age 55.1 ± 10.2), both of which groups had a similar gender distribution. The results of the anthropometric and analytical evaluations are shown in Table 2. As expected, an altered carbohydrate metabolism was observed in T2D patients in comparison with the control group, with glucose, HOMA-IR and HbA_{1c} being significantly higher ($p < 0.001$). Moreover, the T2D group showed higher values for upper waist circumference ($p < 0.01$), SBP, weight, BMI, insulin and hsCRP levels ($p < 0.001$) than control subjects. Regarding lipid profile, a higher triglyceride concentration ($p < 0.01$) and lower HDL-c ($p < 0.001$) were characteristics of the T2D patients. However, due to lipid-lowering medication received, total cholesterol and LDL-c levels were lower in the diabetic group than in healthy controls ($p < 0.001$) (56.9% were taking statins, 10.3% fibrates, and 3.4% ezetimibe). Given that BMI was significantly different in T2D patients, data were adjusted for this variable, but statistical differences remained similar.

3.2. Leukocyte Function

For assessing the influence of T2D and SS-31 treatment on one of the main functions of PMNs, which is interaction with the endothelial monolayer, we performed a parallel plate flux chamber assay. As stated in methods, PMNs were perfused through a monolayer of confluent endothelial cells for assessing those interactions. As shown in Figure S1, T2D enhanced the flux of leukocytes (Figure S1A), reduced its velocity (Figure S1B) which allowed them to adhere more to the endothelial monolayer (Figure S1C). When treated with SS-31, those interactions were significantly reduced. This result shows that leukocyte function is positively affected by SS-31 in T2D PMNs. SS-20 did not alter those parameters in any of the analyzed samples.

Table 2: Anthropometric and analytical parameters.

	Control	Type 2 Diabetes	p-Value	BMI-Adjusted p-Value
N	53	61	-	-
Male (%)	47.2	52.5	ns	ns
Age (years)	51.7 ± 9.3	55.1 ± 10.2	ns	ns
Weight (Kg)	72.9 ± 18.8	85.6 ± 15.5	$p < 0.001$	$p < 0.001$
BMI (kg/m^2)	25.8 ± 5.4	31.4 ± 5.6	$p < 0.001$	-
Waist circumference (cm)	85.8 ± 13.2	104.0 ± 11.9	$p < 0.001$	$p < 0.01$
SBP (mmHg)	23.3 ± 19.7	145.8 ± 14.8	$p < 0.001$	$p < 0.001$
DBP (mmHg)	73.6 ± 10.9	74.2 ± 25.6	ns	ns
Glucose (mg/dL)	95.6 ± 13.6	154.0 ± 49.8	$p < 0.001$	$p < 0.001$
Insulin (µUI/mL)	7.5 ± 3.6	16.3 ± 9.09	$p < 0.001$	$p < 0.01$
HOMA-IR	1.7 ± 0.9	6.2 ± 4.6	$p < 0.001$	$p < 0.001$
HbA_{1c} (%)	5.3 ± 0.4	7.4 ± 1.6	$p < 0.001$	$p < 0.001$
Total cholesterol (mg/dL)	198.8 ± 35.5	168.0 ± 37.7	$p < 0.001$	$p < 0.001$
HDL-c (mg/dL)	57.3 ± 19.9	43.1 ± 9.2	$p < 0.001$	$p < 0.001$
LDL-c (mg/dL)	122.1 ± 28.9	93.7 ± 30.6	$p < 0.001$	$p < 0.001$
TG (mg/dL)	93.0 (26.5–150.5)	133.0 (94.0–170.0)	$p < 0.01$	$p < 0.01$
hsCRP (mg/L)	1.17 (0.46–2.40)	2.92 (1.88–6.39)	$p < 0.001$	$p < 0.001$

Data are shown as mean SD ± and were compared by a Student's t test for parametric variables, while they are shown as median and were compared by a Mann–Whitney U test (25th and 75th percentiles) for non-parametric variables. A univariate general linear model was used to adjust changes for BMI. A Chi-Square test was used to compare proportions among groups. ns: not significant.

3.3. Oxidative Stress: ROS Production

Total (DCFH-DA fluorescence) and mitochondrial (MitoSOX fluorescence) ROS were considerably increased in leukocytes of T2D patients in comparison with control subjects (Figure 1A,B; $p < 0.001$), and these effects were reversed by SS-31 (Figure 1A,B; $p < 0.001$, $p < 0.01$ respectively) in leukocytes of T2D patients, while no differences were observed in controls. The SS-20 compound did not alter these oxidative stress parameters. The specificity of the observed response was corroborated by cytometry analysis of the effect of a positive control, rotenone, a well-known inhibitor of Complex I of the electron transport chain whose action induces mitochondrial superoxide production [42]. Incubation with whole blood from control subjects with rotenone (50 µM, 20 min) led to a major increase in total cellular ROS (detected by DCFH-DA) and this effect was reversed with the treatment of both SS-31 and catalase (Figure 1D; $p < 0.05$). Thus, our data show that SS-31 exerts an antioxidant action by reducing total and mitochondrial ROS production.

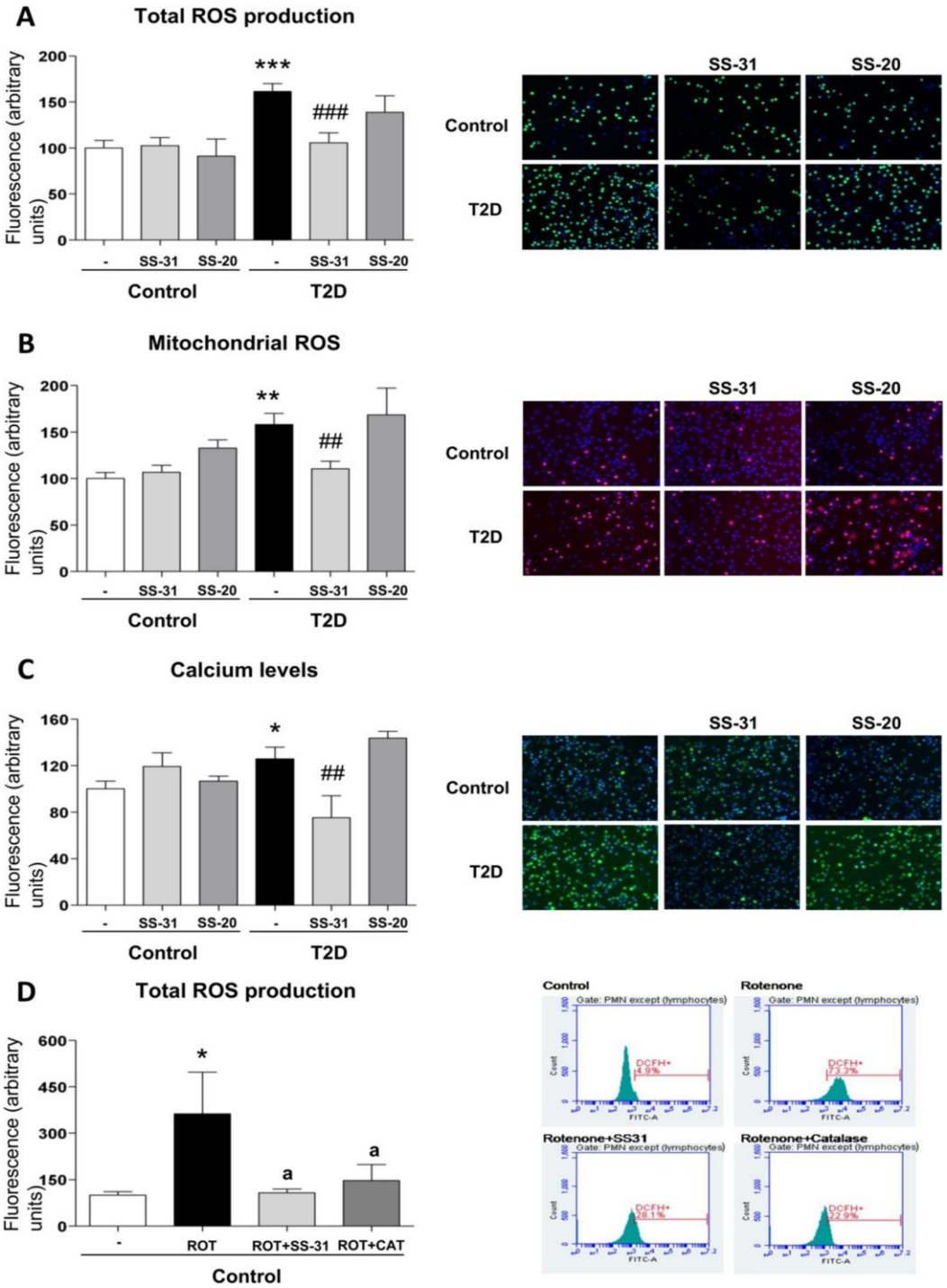

Figure 1. Effects of Szeto–Schiller (SS)-31 (30 min, 100 nM) on total and mitochondrial ROS production, and calcium levels in leukocytes from type 2 diabetes (T2D) patients and healthy subjects. (**A**) Reactive oxygen species (ROS) production, measured as deacetylated by endogenous hydrolases to a form (DCFH)-DA fluorescence. (**B**) Mitochondrial ROS production, assessed as MitoSOX fluorescence. (**C**) Calcium levels, determined as Fluo-4 fluorescence. Representative fluorescence microscopy images are also shown. (**D**) Analysis of total ROS levels, measured as DCFH-DA fluorescence in leukocytes from healthy subjects upon a positive control treatment (rotenone, ROT) in the presence or absence of SS-31 or catalase (CAT) and representative cytograms of the 4 groups stained with APC-CD45 and DCFH-DA. 10,000 cells were analyzed in each experiment. n = 6. * $p < 0.05$, ** $p < 0.01$ and *** $p < 0.001$ with regard to control group; ## $p < 0.01$ ### $p < 0.001$ vs. non-treated T2D group; a $p < 0.05$ vs. rotenone treatment

3.4. Calcium Levels

In the T2D study population, intracellular calcium content—measured as Fluo4-AM fluorescence—was higher than in the control group (Figure 1C; $p < 0.05$), while under treatment with SS-31, calcium levels in T2D patients reached similar values to those in healthy subjects (Figure 1C; $p < 0.01$). The marked decrease of calcium content in the SS-31-treated T2D group in comparison with healthy volunteers may indicate an attenuation of ER stress in these patients given the fact that ER stress is often related to an increase in cytosolic calcium content SS-20 treatment did not modify calcium content in any condition.

3.5. Regulation of UPR Signalling

ER stress markers were determined in order to analyze UPR activation in leukocytes from T2D patients and control subjects. A higher peak in GRP78 expression was observed in the T2D vs. control group (Figure 2A; $p < 0.05$); similarly, DDIT3/CHOP expression was augmented in T2D patients (Figure 2B; $p < 0.05$). Interestingly, SS-31 treatment reduced mRNA levels of both genes in leukocytes from T2D patients (Figure 2A, B; $p < 0.05$). Furthermore, the treatment with the mitochondria-targeted antioxidant SS-31 had no effect about protein levels of GRP78 and P-eIF2α on leukocytes of control subjects (Figure 2C, D) while a reduction in these ER stress parameters was observed in leukocytes from T2D patients with T2D (Figure 2C, D; $p < 0.05$). None of these markers were altered by treatment with SS-20.

These findings suggest that SS-31 can attenuate ER stress in the leukocytes of T2D patients.

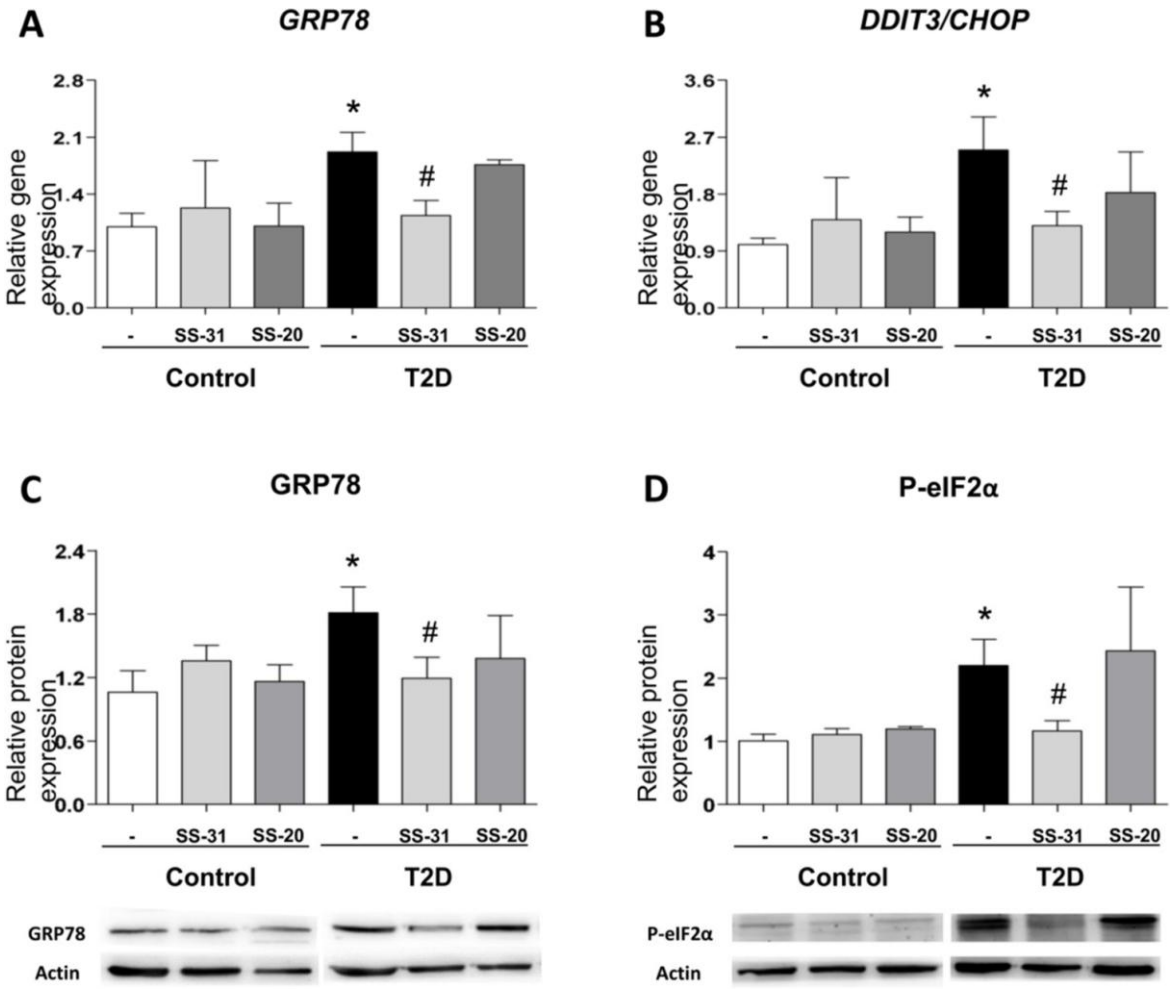

Figure 2. Evaluation of endoplasmic reticulum (ER) stress parameters in leukocytes from T2D patients and controls in the absence and presence of SS-31 (30 min, 100 nM) (**A**) *GRP78* expression. (**B**) *DDIT3/CHOP* expression. (**C**) GRP78 protein levels and representative western blotting (WB) images. (**D**) P-eIF2α protein levels and representative WB images. * $p < 0.05$ with regard to control group # $p < 0.05$ vs. non-treated T2D group

3.6. Autophagy Assessment

BECN1 gene expression were enhanced in leukocytes from T2D patients with respect to those of healthy controls (Figure 3A; $p < 0.05$), a trend that was reversed by treatment with SS-31 (Figure 3A; $p < 0.05$). In leukocytes from T2D patients treated with SS-31, this trend was also accompanied by a significant reduction of protein expression of distinct markers of autophagy such as Beclin-1 and the ratio of LC3 II/I (Figure 3B, C; $p < 0.05$). p62 protein level was significantly lower in leukocytes from diabetic patients compared to controls, however its mRNA levels were more abundant in T2D patients which is indicative of enhanced autophagy. Treatment of leukocytes from T2D patients with SS-31 reversed the protein level of p62 (Figure 3D; $p < 0.05$), while no changes were seen in the gene expression of SQSTM1/p62 suggesting that SS-31 can modify autophagy at protein level. On the other hand, no significant differences were observed in control group or with SS-20 treatment. These results provide some evidence that the mitochondria-targeted antioxidant SS-31 reduces parameters of autophagy in leukocytes from T2D patients.

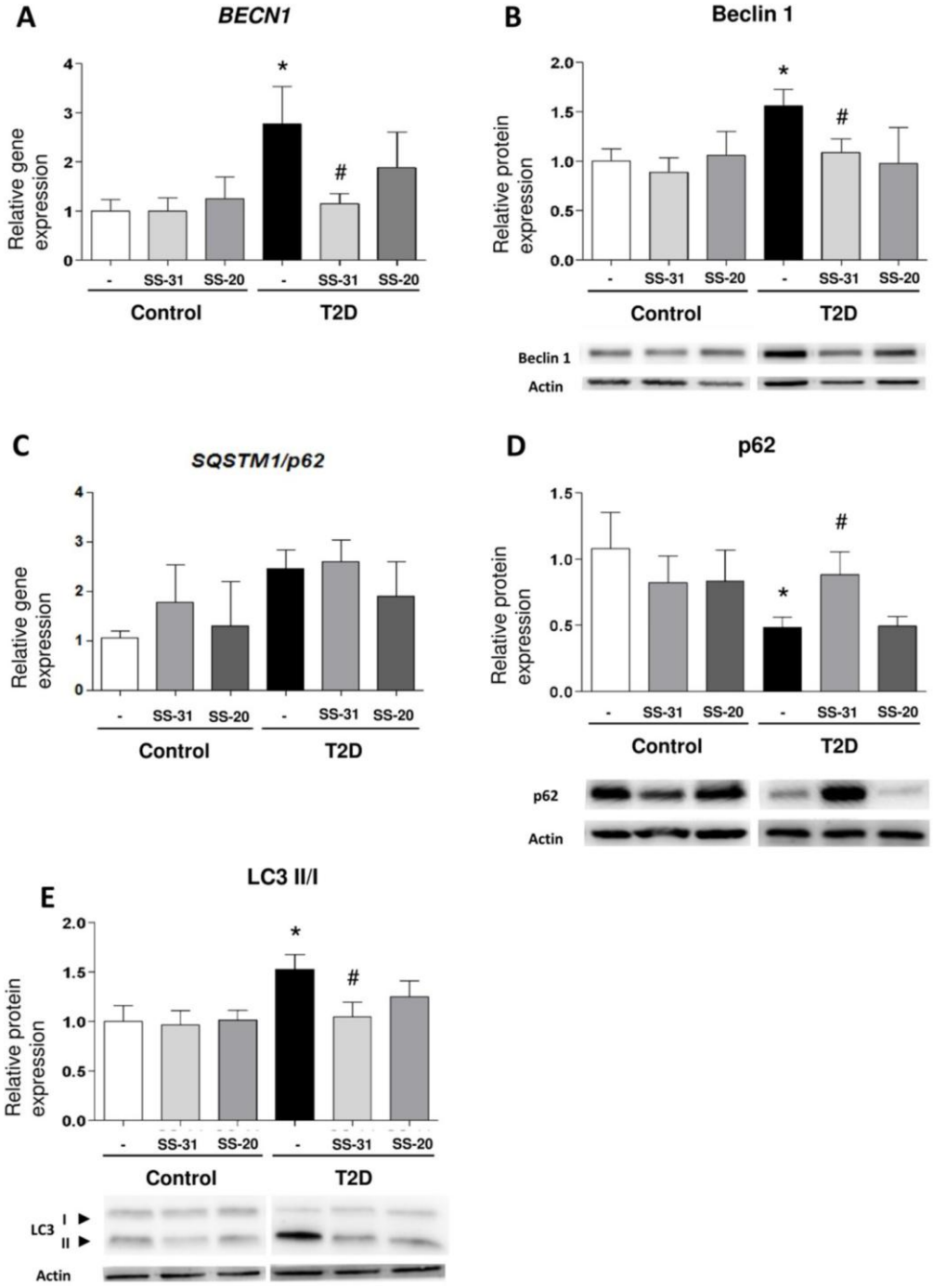

Figure 3. Study of autophagy-related parameters in leukocytes from control subjects and T2D patients in the presence and absence of SS-31 (30 min, 100 nM). (A) BECN1 expression. (B) Beclin-1 protein expression and representative WB images. (C) SQSTM1/p62 expression (D) p62 protein expression and representative WB images (E) LC3 II/I ratio of protein expression and representative WB images. * $p < 0.05$ with regard to control group, # $p < 0.05$ vs. non-treated T2D group.

3.7. Analysis of Pharmacologically Induced ER Stress and Autophagy

Given that leukocytes from T2D display markers of ER stress and activated autophagy, and the observation that both effects can be alleviated with SS-31 treatment, we set to explore the connection between these processes. For this, we evaluated the capacity of SS-31 to interfere with pharmacologically induced ER stress (thapsigargin) and autophagy (rapamycin). Treatment with thapsigargin (1 μM, 20 min) produced a significant increase in the protein content of P-eIF2α and a slight increase in GRP78, however these effects were not impaired if cells were co-treated with SS-31 (Figure 4A, B). The sesquiterpene alkaloid thapsigargin, a highly selective inhibitor of sarcoplasmic/endoplasmic reticulum Ca^{2+} ATPase (SERCA) prevents Ca^{2+} transport into the ER lumen, which leads to its subsequent increase in the cytosol, and promotes accumulation of unfolded proteins and perturbation of intracellular Ca^{2+} homeostasis [42]. On the contrary, SS-31 was able to prevent the increase in GRP78 protein content when it was induced by the mitochondrial inhibitor rotenone (Figure 4A), a finding that reinforces the ability of SS-31 to act as an antioxidant. Regarding autophagy, as expected, leukocytes from healthy subjects exposed to the pharmacological inducer rapamycin (0.5 μM, 30 min) displayed enhanced autophagy as evidenced by the incremented Beclin-1 and LC3 II levels (Figure 4C, D), and the diminished p62 protein content (Figure 4E). Rapamycin inhibits the mTOR complex, a central negative regulator of autophagy in the mammalian cell, thus triggering a strong autophagic response [42,43]. Importantly, SS-31 treatment had no effect on these alterations (Figure 4C–E), a finding that once more underscores the specificity of SS-31 action in the complex metabolic disturbances in leukocytes of T2D patients. We also evaluated autophagy induction in the cells exposed to rotenone and observed no increase in Beclin-1 and LC3 II levels. The protein levels of p62 were diminished; however, given the lack of changes in the LC3 II/I ratio the effect may be evidence of an autophagy-independent regulation.

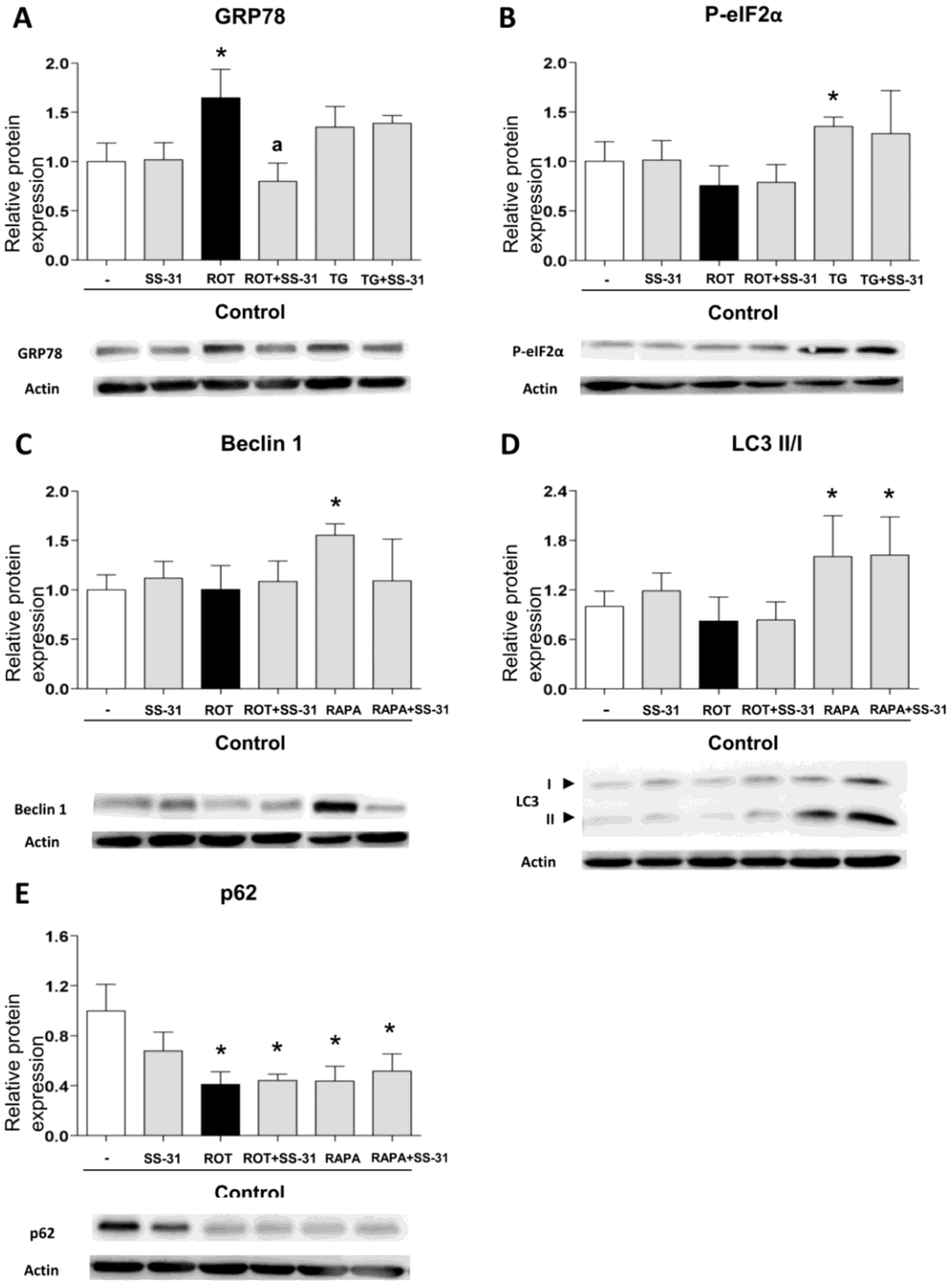

Figure 4. Study of the expression of protein markers of ER stress and autophagy, induced pharmacologically in leukocytes from healthy controls, in the presence and absence of SS-31 (30 min, 100 nM). (**A**) GRP78, (**B**) P-eIF2α, (**C**) Beclin1, (**D**) LC3 II/I ratio, and (E) p62. Representative WB images are also shown. * $p < 0.05$ with regard to control group; a $p < 0.05$ vs. rotenone-treated group. n = 6. ROT, rotenone (50 µM, 20 min); TG, thapsigargin (1 µM, 20 min); RAPA, rapamycin (0.5 µM, 30 min).

4. DISCUSSION

Based on renewed concepts of T2D pathogenesis, the targets of a potential therapy for this chronic progressive disease include, not only glucose homeostasis correction, but also modulation of cellular stress and mitochondrial function in highly metabolic tissues, with the aim of attenuating IR and low-grade inflammation and ameliorating β cell function and mass, thus preventing the development of macro- and microvascular complications.

In this sense, the mitochondrial antioxidant SS-31 has been described to exert protective effects in several disease models. Indeed, SS-31 has previously been reported to attenuate renal injury in diabetic nephropathy through an antioxidant effect [44]. Furthermore, Zhu et al. have demonstrated that SS-31 attenuates the severity of lung damage by modulating mitochondrial dysfunction in a mouse model of spinal cord injury [45]. However, the exact pathophysiological mechanism involved in the protective effects of SS-31 on leukocytes in T2D is not fully understood. For this reason, the present study was designed to evaluate whether SS-31 can modulate oxidative stress, ER stress and autophagy in leukocytes of T2D patients, three important pathways involved in the development of T2D.

The pathophysiology of T2D is associated with an impairment of β cell function and, consequently, IR, a hallmark of this disease [46]. Nevertheless, whether cell failure is a primary cause of T2D or secondary to associated long-term metabolic abnormalities is yet to be confirmed, though increased oxidative stress, ER stress and autophagy are thought to be involved [47]. In fact, previous studies have suggested that alterations in ΔΨm disturb mitochondrial dynamics, eventually promoting a failure in glucose-stimulated insulin secretion [48]. Moreover, our group has previously demonstrated oxidative stress and mitochondrial dysfunction in leukocytes from T2D patients [49]. In this sense, SS-peptides can scavenge ROS, and these molecules have been shown to exert beneficial effects against mitochondrial dysfunction [19,50]. SS-31 protects mitochondria against oxidative damage by accumulating in

the inner mitochondrial membrane, a location close to the site of ROS production. In fact, after crossing the mitochondrial outer membrane, SS-31 associates with cardiolipin, an anionic phospholipid expressed exclusively in the inner mitochondrial membrane. Furthermore, SS-31 seems to protect cristae architecture by alleviating mitochondrial oxidative stress and preventing cytochrome c peroxidase activity [17,19].

In the present study, we have found that the leukocytes of T2D patients have functional alterations compared to those of control individuals, as shown in Figure S1. SS-31 is able to rescue the parameters of leucocyte–endothelial interactions, which confirms that SS-31 can modulate leukocyte function. The fact that the effects can be ameliorated with SS-31 but not with SS-20 shows that the alterations of the leukocyte function in T2D leukocytes can be due to the high levels of total and mitochondrial ROS levels compared to controls. Fluorescent probes are widely used for ROS detection in biological systems; DCFH–DA has been suggested as a relatively specific probe for H_2O_2, while dihydroethidium seems to be more suitable for superoxide. However, abundant evidence over the past years has shown that all fluorescent probes for ROS detection suffer a lack of selectivity given that they react with various types of ROS, and therefore in living cells or tissues they are generally used for detecting total oxidative activity. In order to reaffirm our findings, we have employed two fluorescent probes and verified the specificity of the detection by studying a positive control of mitochondrial ROS generation, rotenone. One of the leading hypotheses regarding the onset of IR is that enhanced ROS production triggers ER stress, which leads to activation of the UPR. In relation to this, ER stress is considered a target mechanism under IR conditions. An association between IR and mitochondrial abnormalities, such as lower numbers of mitochondria, reduction in mitochondrial oxidative enzyme activity or mitochondrial dysfunction, have been reported in human studies [51,52]. Furthermore, it has been described that ER stress is related to apoptosis in leukocytes from T2D patients [53]. In addition, a study by Sage et al. demonstrated that levels of ER stress markers such as GRP78, sXBP1 and CHOP correlated positively with glucose levels in

leukocytes from patients with metabolic syndrome [54]. In line with such data, we have shown in previous studies that leukocytes from T2D patients exhibit increased ER stress markers which display enhanced GRP78, P-eIF2α and ATF6 protein levels [35]. Interestingly, the present study shows that SS-31 treatment in leukocytes from T2D patients reduces GRP78 and P-eIF2α protein levels, and GRP78 and CHOP mRNA levels, suggesting that this molecule could promote the restoration of cell homeostasis to battle ER stress. The reduction of intracellular calcium levels under treatment with SS-31 described in the present study could also be indicative of lower ER stress compared to untreated T2D leukocytes, but these data need to be considered with caution given that with our methodology we cannot determine the subcellular source of increased calcium. This idea is further enforced by the fact that SS-31 did not alleviate ER stress triggered by other types of stimuli such as thapsigargin, an ER stressor with a direct effect on ER calcium homeostasis.

ER stress can also induce autophagy, and in this sense Gonzalez et al. have described that cleavage and lipidation of microtubule-associated protein LC3 I into LC3 II is mediated by the phosphorylation of PERK/eIF2α [55]. Importantly, we have previously demonstrated in leukocytes from T2D patients that UPR activation occurs in parallel with autophagy [35]. The present study describes an increase in Beclin-1 and LC3-II levels in T2D patients compared to controls which is indicative of increased generation of autophagosomes. As this occurs concomitantly with a decrease in p62 protein levels, we believe that it may suggest an increase in the autophagic clearance. Nevertheless, the results presented are not sufficient as to state that autophagy is not only induced but also active/functional in T2D patients.

The expression levels of autophagy-related parameters are significantly decreased in leukocytes of T2D patients under SS-31 therapy. In contrast, p62 protein expression, which is involved in aggresome formation and is itself degraded through autophagy, was increased in leukocytes from T2D patients by addition of SS-31. Of note, this was not due to changes in the gene expression of SQSTM1/p62 suggesting rather a SS-31 effect on autophagy. Our results

support the existence of cross-talk between oxidative stress and autophagy in T2D [56], as SS-31 treatment of leukocytes of T2D patients reduces mitochondrial ROS production, which seems to prevent the increase induced by autophagic biomarkers. The specificity of this effect was shown by the fact SS-31 lacked the capacity to prevent the autophagic process induced by the pharmacological inducer of autophagy, rapamycin. As shown in many reports, rapamycin does not increase intracellular ROS levels (or can even diminish them) which is in keeping with our conclusion of SS-31 interfering with the autophagy observed in leukocytes from T2D patients through its capacity to scavenge mitochondrial ROS.

A link between ER stress, ROS production and autophagy could also be established considering the implication of cardiolipin in mitochondrial function including calcium buffering and mitophagy [57–60]. Given that in this work intracellular calcium levels in leukocytes from diabetics are enhanced concomitantly with increased presence of total and mitochondrial ROS, we could speculate that cardiolipin might be altered. With this and considering that SS-31 is a ROS scavenger that binds cardiolipin, we can speculate that cardiolipin may be involved in the effects exerted by SS-31. It could act as a regulator of mitophagy, explaining the reducing effect on autophagy seen in our work and could also affect calcium handling by mitochondria. It is widely known that calcium levels influence leukocyte function [61,62] and this occurs through NLRP3 signaling and the regulation of calmodulins and GTPases which participate in crucial processes in leukocytes such as innate defense and transmigration. Both aspects could reinforce SS-31 as a mitoprotective molecule that prevents leukocyte dysfunction. The effect of SS-31 on cardiolipin in this model and its relation to mitophagy seems a promising idea that needs to be explored in future studies.

It is important to mention that a possible limitation of this study are the potential interactions, synergisms, or detriments that may arise when studying or implementing novel drugs like SS-31 in a background affected by other medications such as statins. In this sense, previous research has stated that statins can have both detrimental [63–66] and beneficial

effects [67–77], often unrelated to their lipid-lowering effect and rather associated with their pleiotropic actions. The variation of the effect is explained by the type of statin, the dose, the combination with other treatments and the experimental model. However, to our knowledge, there are no reports about the interference of statins with SS-31 when applied in combination, in patients or in animal studies.

5. **CONCLUSIONS**

In summary, our findings reveal a potential protective effect of novel SS-31 therapy in diseases with increased oxidative and an ER stress state such as T2D. It is important to highlight that mitochondrial accumulation of SS-peptides does not depend on alterations of ΔΨm, which represents a major advantage to respect to other antioxidants [78–80]. The discovery of novel potential therapeutic strategies based on mitochondrial biology is key to future treatments, but further research is essential. The SS-31 peptide in particular represents a possible approach, through targeted delivery of antioxidants to mitochondria. In fact, in the present study we have demonstrated that SS-31 reduces ROS and could modulate ER stress and autophagy, key molecular pathways in cellular homeostasis, suggesting that this compound may exert beneficial effects that can be channeled for the treatment of T2D. Further investigations including clinical trials are required to elucidate these and other important mechanisms underlying the actions of SS-31 in treatment of T2D.

Acknowledgments:

The authors give special thanks to Brian Normanly (University of Valencia-CIBERehd) for his editorial assistance, and Rosa Falcon and Carmen Ramirez (FISABIO) for their technical assistance.

Supplementary Materials:

The following are available online at http://www.mdpi.com/2077-0383/8/9/1322/s1,

Figure S1: Leukocyte-enfothelium interaction evaluation under SS-31 and SS-20 treatment.

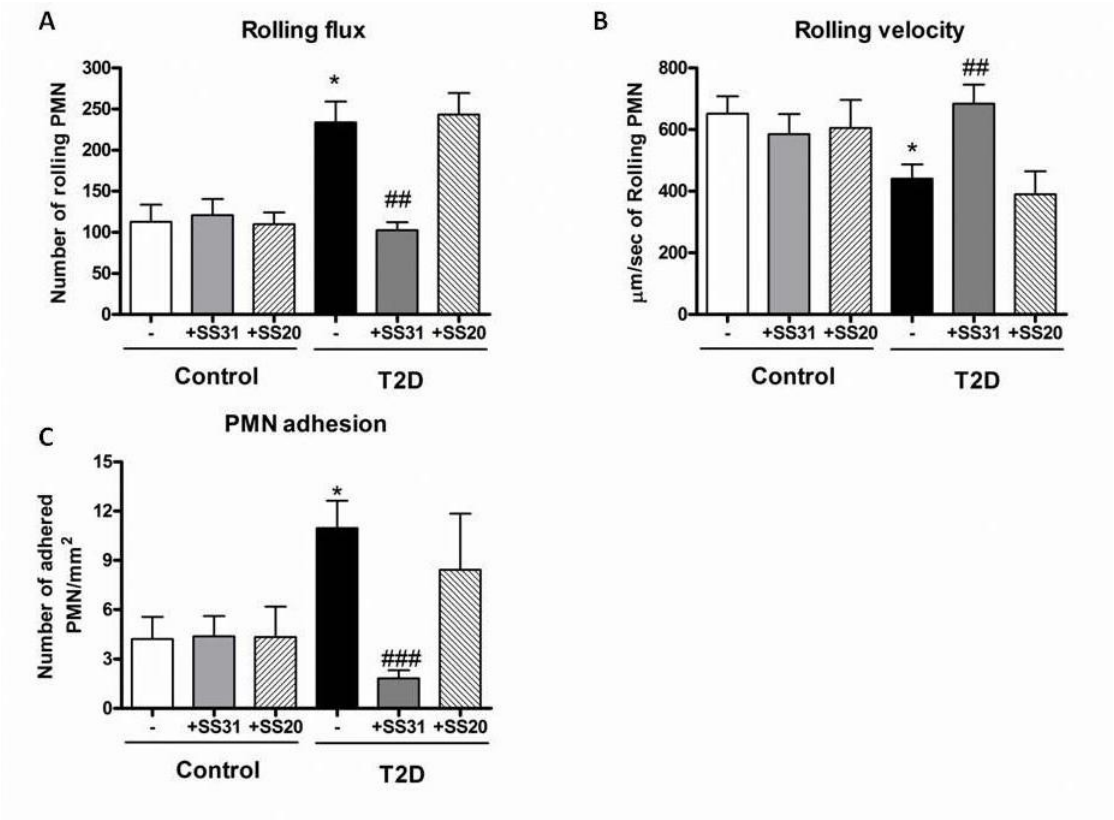

Figure S1. Leukocyte-enfothelium interaction evaluation under SS-31 and SS-20 treatment.
(A) Number of rolling PMNs in 1 min, (**B**) velocity of this rolling PMNs and (**C**) PMNs adhesion to the endothelial monolayer. * $p < 0.05$ with regard to control group; ## $p < 0.01$ ### $p < 0.001$ vs. non- treated T2D group.

REFERENCES

1. Giacco, F.; Brownlee, M. Oxidative stress and diabetic complications. *Circ. Res.* **2010**, *107*, 1058–1070. [CrossRef] [PubMed]
2. Akash, M.S.; Rehman, K.; Chen, S. Role of inflammatory mechanisms in pathogenesis of type 2 diabetes mellitus. *J. Cell. Biochem.* **2013**, *114*, 525–531. [CrossRef] [PubMed]
3. Higa, A.; Chevet, E. Redox signaling loops in the unfolded protein response. *Cell. Signal.* **2012**, *24*, 1548–1555. [CrossRef] [PubMed]
4. Klausner, R.D.; Sitia, R. Protein degradation in the endoplasmic reticulum. *Cell* **1990**, *62*, 611–614. [CrossRef]
5. Shamu, C.E.; Cox, J.S.; Walter, P. The unfolded-protein-response pathway in yeast. *Trends Cell Biol.* **1994**, *4*, 56–60. [CrossRef]
6. Hotamisligil, G.S. Inflammation and endoplasmic reticulum stress in obesity and diabetes. *Int. J. Obes.* **2008**, *32*, 52. [CrossRef] [PubMed]
7. Ron, D.; Walter, P. Signal integration in the endoplasmic reticulum unfolded protein response. *Nat. Rev. Mol. Cell Biol.* **2007**, *8*, 519–529. [CrossRef] [PubMed]
8. Wang, S.; Kaufman, R.J. The impact of the unfolded protein response on human disease. *J. Cell. Biol.* **2012**, *197*, 857–867. [CrossRef] [PubMed]
9. Meusser, B.; Hirsch, C.; Jarosch, E.; Sommer, T. ERAD: The long road to destruction. *Nat. Cell Biol.* **2005**, *7*, 766–772. [CrossRef] [PubMed]
10. Tanida, I. Autophagosome formation and molecular mechanism of autophagy. *Antioxid. Redox. Signal.* **2011**, *14*, 2201–2214. [CrossRef]
11. Yin, J.J.; Li, Y.B.; Wang, Y.; Liu, G.D.; Wang, J.; Zhu, X.O.; Pan, S.H. The role of autophagy in endoplasmic reticulum stress-induced pancreatic beta cell death. *Autophagy* **2012**, *8*, 158–164. [CrossRef] [PubMed]
12. Su, J.; Zhou, L.; Kong, X.; Yang, X.; Xiang, X.; Zhang, Y.; Li, X.; Sun, L. Endoplasmic reticulum is atthe crossroads of autophagy, inflammation, and apoptosis signaling pathways and participates in the pathogenesis of diabetes mellitus. *J. Diabetes Res.* **2013**, *2013*, 193461. [CrossRef] [PubMed]
13. Demirtas, L.; Guclu, A.; Erdur, F.M.; Akbas, E.M.; Ozcicek, A.; Onk, D.; Turkmen, K. Apoptosis, autophagy& endoplasmic reticulum stress in diabetes mellitus. *Indian J. Med. Res.* **2016**, *144*, 515–524. [CrossRef] [PubMed]
14. Cadenas, E.; Davies, K.J. Mitochondrial free radical generation, oxidative stress, and aging. *Free Radic. Biol. Med.* **2000**, *29*, 222–230. [CrossRef]
15. Murphy, M.P. How mitochondria produce reactive oxygen species. *Biochem. J.* **2009**, *417*, 1–13. [CrossRef]
16. Szeto, H.H. First-in-class cardiolipin-protective compound as a therapeutic agent to restore mitochondrial bioenergetics. *Br. J. Pharmacol.* **2014**, *171*, 2029–2050. [CrossRef]
17. Birk, A.V.; Liu, S.; Soong, Y.; Mills, W.; Singh, P.; Warren, J.D.; Seshan, S.V.; Pardee, J.D.; Szeto, H.H. The mitochondrial-targeted compound SS-31 re-energizes ischemic mitochondria by interacting with cardiolipin.*J. Am. Soc. Nephrol.* **2013**, *24*, 1250–1261. [CrossRef]
18. Szeto, H.H.; Liu, S.; Soong, Y.; Wu, D.; Darrah, S.F.; Cheng, F.Y.; Zhao, Z.; Ganger, M.; Tow, C.Y.; Seshan, S.V. Mitochondria-targeted peptide accelerates ATP recovery and reduces ischemic kidney injury. *J. Am. Soc. Nephrol.* **2011**, *22*, 1041–1052. [CrossRef]
19. Zhao, K.; Zhao, G.M.; Wu, D.; Soong, Y.; Birk, A.V.; Schiller, P.W.; Szeto, H.H. Cell-permeable peptide antioxidants targeted to inner mitochondrial membrane inhibit mitochondrial swelling, oxidative cell death, and reperfusion injury. *J. Biol. Chem.* **2004**, *279*, 34682–34690. [CrossRef]
20. Escribano-López, I.; Díaz-Morales, N.; Iannantuoni, F.; López-Domènech, S.; de Marañón, A.M.; Abad-Jiménez, Z.; Bañuls, C.; Rovira-Llopis, S.; Herance, J.R.; Rocha, M.; et al. The mitochondrial antioxidant SS-31 increases Sirt-1 levels and ameliorates inflammation, oxidative stress and leukocyte-endothelium interactions in type 2 diabetes. *Sci. Rep.* **2018**, *8*, 15862. [CrossRef]
21. Pitozzi, V.; Giovanelli, L.; Bardini, G.; Rotella, C.M.; Dolara, P. Oxidative DNA damage in peripheral blood cells in type 2 diabetes mellitus; higher vulnerability of polymorphonuclear leukocytes. *Mutat. Res.* **2003**, *529*, 129–133. [CrossRef]
22. Bir, S.C.; Kevil, C.G. Diabetic neutrophil mitochondrial dysfunction: an inflammatory situation? *Free Radic. Biol. Med.* **2011**, *50*, 1213–1214. [CrossRef] [PubMed]
23. Zozulinska, D.; Wierusz-Wysocka, B. Type 2 diabetes mellitus as inflammatory disease. *Diabetes Res. Clin. Pract.* **2006**, *74*, S12–S16. [CrossRef]
24. Shurtz-Swirski, R.; Sela, S.; Herskovits, A.T.; Shasha, S.M.; Shapiro, G.; Nasser, L.; Kristal, B. Involvement of Peripheral Polymorphonuclear Leukocytes in Oxidative Stress and Inflammation in Type 2 Diabetic Patients. *Diabetes Care* **2001**, *24*, 104–110. [CrossRef] [PubMed]
25. Pettersson, U.S.; Christoffersson, G.; Massena, S.; Ahl, D.; Jansson, L.; Henriksnäs, J.; Phillipson, M. Increased Recruitment but Impaired Function of Leukocytes during Inflammation in Mouse Models of Type 1 and Type

2 Diabetes. *PLoS ONE* **2011**, *6*, e22480. [CrossRef] [PubMed]
26. Guan, Y.; Zhou, L.; Zhang, Y.; Tian, H.; Li, A.; Han, X. Effects of PP2A/Nrf2 on experimental diabetes mellitus-related cardiomyopathy by regulation of autophagy and apoptosis through ROS dependent pathway. *Cell. Signal.* **2019**, *62*, 109339. [CrossRef] [PubMed]
27. Tampakakis, E.; Tabit, C.E.; Holbrook, M.; Linder, E.A.; Berk, B.D.; Frame, A.A.; Bretón-Romero, R.; Fetterman, J.L.; Gokce, N.; Vita, J.A.; et al. Intravenous lipid infusion induces endoplasmic reticulum stress in endothelial cells and blood mononuclear cells of healthy adults. *J. Am. Heart Assoc.* **2016**, *5*, e002574. [CrossRef]
28. RostamiRad, A.; Ebrahimi, S.S.S.; Sadeghi, A.; Taghikhani, M.; Meshkani, R. Palmitate-induced impairmentof autophagy turnover leads to increased apoptosis and inflammation in peripheral blood mononuclear cells. *Immunobiology* **2018**, *223*, 269–278. [CrossRef]
29. Mozzini, C.; Garbin, U.; Stranieri, C.; Pasini, A.; Solani, E.; Tinelli, I.A.; Cominacini, L.; Fratta-Pasini, A.M. Endoplasmic reticulum stress and Nrf2 repression in circulating cells of type 2 diabetic patients without the recommended glycemic goals. *Free Radic. Res.* **2015**, *49*, 244–252. [CrossRef]
30. Rovira-Llopis, S.; Bañuls, C.; Apostolova, N.; Morillas, C.; Hernandez-Mijares, A.; Rocha, M.; Victor, V.M. Is glycemic control modulating endoplasmic reticulum stress in leukocytes of type2 diabetic patients? *Antioxid. Redox. Signal.* **2014**, *21*, 1759–1765. [CrossRef]
31. Szpigel, A.; Hainault, I.; Carlier, A.; Venteclef, N.; Batto, A.F.; Hajduch, E.; Bernard, C.; Ktorza, A.; Gautier, J.F.; Ferré, P.; et al. Lipid environment induces ER stress, TXNIP expression and inflammation in immune cells of individuals with type 2 diabetes. *Diabetologia* **2018**, *61*, 399–412. [CrossRef] [PubMed]
32. Sindhu, S.; Akhter, N.; Kochumon, S.; Thomas, R.; Wilson, A.; Shenouda, S.; Tuomilehto, J.; Ahmad, R. Increased expression of the innate immune receptor TLR10 in obesity and type-2 diabetes: Association with ROS-mediated oxidative stress. *Cell. Physiol. Biochem.* **2018**, *45*, 572–590. [CrossRef] [PubMed]
33. Bañuls, C.; Rovira-Llopis, S.; Lopez-Domenech, S.; Diaz-Morales, N.; Blas-Garcia, A.; Veses, S.; Morillas, C.; Victor, V.M.; Rocha, M.; Hernandez-Mijares, A. Oxidative and endoplasmic reticulum stress is impaired in leukocytes from metabolically unhealthy vs healthy obese individuals. *Int. J. Obes.* **2017**, *41*, 1556–1563.
34. Restaino, R.M.; Deo, S.H.; Parrish, A.R.; Fadel, P.J.; Padilla, J. Increased monocyte-derived reactive oxygen species in type 2 diabetes: Role of endoplasmic reticulum stress. *Exp. Physiol.* **2017**, *102*, 139–153. [CrossRef] [PubMed]
35. Rovira-Llopis, S.; Díaz-Morales, N.; Bañuls, C.; Blas-García, A.; Polo, M.; López-Domenech, S.; Jover, A.; Rocha, M.; Hernández-Mijares, A.; Víctor, V.M. Is Autophagy Altered in the Leukocytes of Type 2 Diabetic Patients? *Antioxid. Redox. Signal.* **2015**, *23*, 1050–1056. [CrossRef]
36. Riek, A.; Oh, J.; Sprague, J.; Timpson, A.; de las Fuentes, L.; Bernal-Mizrachi, L.; Schechtman, K.; Bernal-Mizrachi, C. Vitamin D Suppression of Endoplasmic Reticulum Stress Promotes an Antiatherogenic Monocyte/Macrophage Phenotype in Type 2 Diabetic Patients. *J. Biol. Chem.* **2012**, *287*, 38482–38484. [CrossRef] [PubMed]
37. Lenin, R.; Maria, M.S.; Agrawal, M.; Balasubramanyam, J.; Mohan, V.; Balasubramanyam, M. Ameliorationof glucolipotoxicity-induced endoplasmic reticulum stress by a "chemical chaperone" in human THP-1 monocytes. *Exp. Diabetes Res.* **2012**, 356487. [CrossRef]
38. Mehrzadi, S.; Yousefi, B.; Hosseinzadeh, A.; Reiter, R.J.; Safa, M.; Ghaznavi, H.; Naseripour, M. Diabetic retinopathy pathogenesis and the ameliorating effects of melatonin; involvement of autophagy, inflammation and oxidative stress. *Life Sci.* **2018**, *193*, 20–33. [CrossRef]
39. Diaz-Morales, N.; Iannantuoni, F.; Escribano-Lopez, I.; Bañuls, C.; Rovira-Llopis, S.; Sola, E.; Rocha, M.; Hernandez-Mijares, A.; Victor, V.M. Does Metformin Modulate Endoplasmic Reticulum Stress and Autophagy in Type 2 Diabetic Peripheral Blood Mononuclear Cells? *Antioxid. Redox. Signal.* **2018**, *28*, 1562–1569. [CrossRef]
40. Streitz, M.; Miloud, T.; Kapinsky, M.; Reed, M.R.; Magari, R.; Geissler, E.K.; Hutchinson, J.A.; Vogt, K.; Schickeisler, S.; Kverneland, A.H.; et al. Standarization of whole blood immune phenotype monitoring for clinical trials: Panels and methods for the ONE study. *Transplant. Res.* **2013**, *2*, 17. [CrossRef]
41. Fujimoto, H.; Sakata, T.; Hamaguchi, Y.; Shiga, S.; Tohyama, K.; Ichiyama, S.; Wang, F.S.; Houwen, B. Flow cytometric method for enumeration and classification of reactive immature granulocyte populations. *Cytommetry* **2000**, *42*, 371–378. [CrossRef]
42. Fato, R.; Bergamini, C.; Bortolus, M.; Maniero, A.L.; Leoni, S.; Ohnishi, T.; Lenaz, G. Differential effects of mitochondrial Complex I inhibitors on production of reactive oxygen species. *Biochim. Biophys. Acta* **2009**, *1787*, 384–392. [CrossRef]
43. Lytton, J.; Westlin, M.; Hanley, M.R. Thapsigargin inhibits the sarcoplasmic or endoplasmic reticulum Ca-ATPase family of calcium pumps. *J. Biol. Chem.* **1991**, *266*, 17067–17071.
44. Hou, Y.; Li, S.; Wu, M.; Wei, J.; Ren, Y.; Du, C.; Wu, H.; Han, C.; Duan, H.; Shi, Y. Mitochondria-targeted peptide SS-31 attenuates renal injury via an antioxidant effect in diabetic nephropathy. *Am. J. Physiol. Renal Physiol.* **2016**, *310*, 547. [CrossRef]

45. Zhu, L.L.; Li, M.Q.; He, F.; Zhou, S.B.; Jiang, W. Mitochondria Targeted Peptide Attenuates Mitochondrial Dysfunction, Controls Inflammation and Protects Against Spinal Cord Injury-Induced Lung Injury. *Cell. Physiol. Biochem.* **2017**, *44*, 388–400. [CrossRef] [PubMed]
46. Leahy, J.L. Pathogenesis of type 2 diabetes mellitus. *Arch. Med. Res.* **2005**, *36*, 197–209.
47. Mizukami, H.; Takahashi, K.; Inaba, W.; Tsuboi, K.; Osonoi, S.; Yoshida, T.; Yagihashi, S. Involvement of oxidative stress-induced DNA damage, endoplasmic reticulum stress, and autophagy deficits in the declineof beta-cell mass in Japanese type 2 diabetic patients. *Diabetes Care* **2014**, *37*, 1966–1974. [CrossRef] [PubMed]
48. Lo, M.C.; Chen, M.H.; Lee, W.S.; Lu, C.I.; Chang, C.R.; Kao, S.H.; Lee, H.M. Nepsilon-(carboxymethyl) lysine-induced mitochondrial fission and mitophagy cause decreased insulin secretion from beta-cells. *Am.J. Physiol. Endocrinol. Metab.* **2015**, *309*, 829. [CrossRef] [PubMed]
49. Hernandez-Mijares, A.; Rocha, M.; Rovira-Llopis, S.; Bañuls, C.; Bellod, L.; de Pablo, C.; Alvarez, A.; Roldan-Torres, I.; Sola-Izquierdo, E.; Victor, V.M. Human leukocyte/endothelial cell interactions and mitochondrial dysfunction in type 2 diabetic patients and their association with silent myocardial ischemia.*Diabetes Care* **2013**, *36*, 1695–1702. [CrossRef] [PubMed]
50. Whiteman, M.; Spencer, J.P.; Szeto, H.H.; Armstrong, J.S. Do mitochondriotropic antioxidants prevent chlorinative stress-induced mitochondrial and cellular injury? *Antioxid. Redox. Signal.* **2008**, *10*, 641–650. [CrossRef] [PubMed]
51. Petersen, K.F.; Dufour, S.; Befroy, D.; Garcia, R.; Shulman, G.I. Impaired mitochondrial activity in the insulin-resistant offspring of patients with type 2 diabetes. *N. Engl. J. Med.* **2004**, *350*, 664–671. [CrossRef] [PubMed]
52. Kelley, D.E.; He, J.; Menshikova, E.V.; Ritov, V.B. Dysfunction of mitochondria in human skeletal muscle intype 2 diabetes. *Diabetes* **2002**, *51*, 2944–2950. [CrossRef] [PubMed]
53. Komura, T.; Sakai, Y.; Honda, M.; Takamura, T.; Matsushima, K.; Kaneko, S. CD14+ monocytes are vulnerable and functionally impaired under endoplasmic reticulum stress in patients with type 2 diabetes. *Diabetes* **2010**, *59*, 634–643. [CrossRef] [PubMed]
54. Sage, A.T.; Holtby-Ottenhof, S.; Shi, Y.; Damjanovic, S.; Sharma, A.M.; Werstuck, G.H. Metabolic syndromeand acute hyperglycemia are associated with endoplasmic reticulum stress in human mononuclear cells. *Obesity* **2012**, *20*, 748–755. [CrossRef] [PubMed]
55. Gonzalez, C.D.; Lee, M.S.; Marchetti, P.; Pietropaolo, M.; Towns, R.; Vaccaro, M.I.; Watada, H.; Wiley, J.W. The emerging role of autophagy in the pathophysiology of diabetes mellitus. *Autophagy* **2011**, *7*, 2–11. [CrossRef] [PubMed]
56. Liu, H.; Yin, J.J.; Cao, M.M.; Liu, G.D.; Su, Y.; Li, Y.B. Endoplasmic reticulum stress induced by lipopolysaccharide is involved in the association between inflammation and autophagy in INS1 cells. *Mol. Med. Rep.* **2017**, *16*, 5787–5792. [CrossRef] [PubMed]
57. Dudek, J. Role of Cardiolipin in Mitochodnrial signaling pathways. *Front. Cell Dev. Biol.* **2017**, *5*, 90. [CrossRef] [PubMed]
58. Hwang, M.S.; Schwall, C.T.; Pazarentzos, E.; Datler, C.; Alder, N.N.; Grimm, S. Mitochondrial calcium ibnflux targets cardiolipin to disintegrate respiratory chain complex II for cell death induction. *Cell Death Differ.* **2014**, *21*, 1733–1745. [CrossRef] [PubMed]
59. Paradies, G.; Petrosillo, G.; Paradies, V.; Ruggiero, F.M. Role of cardiolipin peroxidation and calcium in mitochondrial dysfunction and disease. *Cell Calcium* **2009**, *45*, 643–650. [CrossRef] [PubMed]
60. Petrosillo, G.; Ruggiero, F.M.; Pistolese, M.; Paradies, G. Calcium-induced Reactive Oxigen Species production promotes Cytocrome C release from rat liver mitochodnria via Mitochondrial Permeability Transition (MPT)-dependent and MPT-independent mechanisms. *J. Biol. Chem.* **2004**, *279*, 53103–53108. [CrossRef] [PubMed]
61. Martinvalet, D. The role of the mitochondria and the rendoplasmic reticulum contact sites in the development of the immune responses. *Cell Death Dis.* **2018**, *9*, 336. [CrossRef] [PubMed]
62. Prahrtana, J.D.; Sullivan, D.P.; Muller, W.A. Exploring the role of calmodulin and calcium signaling in leukocyte transmigration. *FASEB J.* **2018**, *32*, 280.
63. Pal, S.; Ghosh, M.; Ghosh, S.; Bhattacharyya, S.; Sil, P.C. Atorvastatin induced hepatic oxidative stress and apoptotic damage via MAPKs, mitochondria, calpain and caspase 12 dependent pathways. *Food Chem. Toxicol.* **2015**, *83*, 36–47. [CrossRef] [PubMed]
64. Godoy, J.C.; Niesman, I.R.; Busija, A.R.; Kassan, A.; Schilling, J.M.; Schwarz, A.; Alvarez, E.A.; Dalton, N.D.; Drummond, J.C.; Roth, D.M.; et al. Atorvastatin, but not pravastatin, inhibits cardiac Akt/mTOR signalingand disturbs mitochondrial ultrastructure in cardiac myocytes. *FASEB J.* **2019**, *33*, 1209–1225. [CrossRef] [PubMed]
65. Ghavami, S.; Sharma, P.; Yeganeh, B.; Ojo, O.O.; Jha, A.; Mutawe, M.M.; Kashani, H.H.; Los, M.J.; Klonisch, T.; Unruh, H.; et al. Airway mesenchymal cell death by mevalonate cascade inhibition: Integration of autophagy, unfolded protein response and apoptosis focusing on Bcl2 family proteins. *Biochim. Biophys. Acta* **2014**, *1843*, 1259–1271. [CrossRef] [PubMed]

66. Schirris, T.J.; Renkema, G.H.; Ritschel, T.; Voermans, N.C.; Bilos, A.; van Engelen, B.G.; Brandt, U.; Koopman, W.J.; Beyrath, J.D.; Rodenburg, R.J.; et al. Statin-Induced Myopathy Is Associated with Mitochondrial Complex III Inhibition. *Cell Metab.* **2015**, *22*, 399–407.
67. Costa, S.; Reina-Couto, M.; Albino-Teixeira, A.; Sousa, T. Statins and oxidative stress in chronic heart failure. *Rev. Port. Cardiol.* **2016**, *35*, 41–57. [CrossRef] [PubMed]
68. Escudero, P.; Martinez de Marañón, A.; Collado, A.; Gonzalez-Navarro, H.; Hermenegildo, C.; Peiró, C.; Piqueras, L.; Sanz, M.J. Combined sub-optimal doses of rosuvastatin and bexarotene impair angiotensin II-induced arterial mononuclear cell adhesion through inhibition of Nox5 signaling pathways and increased RXR/PPARα and RXR/PPARγ interactions. *Antiox. Redox. Sign.* **2015**, *22*, 901–920. [CrossRef]
69. Whitehead, N.P. Enhanced autophagy as a potential mechanism for the improved physiological function by simvastatin in muscular dystrophy. *Autophagy* **2016**, *12*, 705–706. [CrossRef]
70. Chen, Y.H.; Chen, Y.C.; Liu, C.S.; Hsieh, M.C. The Different Effects of Atorvastatin and Pravastatin on Cell Death and PARP Activity in Pancreatic NIT-1 Cells. *J. Diabetes Res.* **2016**, 1828071. [CrossRef]
71. Zhang, T.; Lu, D.; Yang, W.; Shi, C.; Zang, J.; Shen, L.; Mai, H.; Xu, A. HMG-CoA Reductase Inhibitors Relieve Endoplasmic Reticulum Stress by Autophagy Inhibition in Rats With Permanent Brain Ischemia. *Front. Neurosci.* **2018**, *12*, 405. [CrossRef] [PubMed]
72. Xu, J.Z.; Chai, Y.L.; Zhang, Y.L. Effect of rosuvastatin on high glucose-induced endoplasmic reticulum stressin human umbilical vein endothelial cells. *Genet. Mol. Res.* **2016**, *15*. [CrossRef] [PubMed]
73. Li, Y.; Lu, G.; Sun, D.; Zuo, H.; Wang, D.W.; Yan, J. Inhibition of endoplasmic reticulum stress signaling pathway: A new mechanism of statins to suppress the development of abdominal aortic aneurysm. *PloS ONE* **2017**, *12*, e0174821. [CrossRef] [PubMed]
74. Kojanian, H.; Szafran-Swietlik, A.; Onstead-Haas, L.M.; Haas, M.J.; Mooradian, A.D. Statins prevent dextrose-induced endoplasmic reticulum stress and oxidative stress in endothelial and HepG2 cells. *Am. J.Ther.* **2016**, *23*, e1456–e1463. [CrossRef] [PubMed]
75. Wu, Z.H.; Chen, Y.Q.; Zhao, S.P. Simvastatin inhibits ox-LDL-induced inflammatory adipokines secretion via amelioration of ER stress in 3T3-L1 adipocyte. *Biochem. Biophys. Res. Commun.* **2013**, *432*, 365–369. [CrossRef] [PubMed]
76. Li, L.; Wang, Y.; Xu, Y.; Chen, L.; Fang, Q.; Yan, X. Atorvastatin inhibits CD68 expression in aortic root through a GRP78-involved pathway. *Cardiovasc. Drugs Ther.* **2014**, *28*, 523–532. [CrossRef] [PubMed]
77. Alaarg, A.; Zheng, K.H.; van der Valk, F.M.; da Silva, A.E.; Versloot, M.; van Ufford, L.C.; Schulte, D.M.; Storm, G.; Metselaar, J.M.; Stroes, E.S.; et al. Multiple pathway assessment to predict anti-atherogenic efficacy of drugs targeting macrophages in atherosclerotic plaques. *Vascul. Pharmacol.* **2016**, *82*, 51–59. [CrossRef] [PubMed]
78. Szeto, H.H.; Schiller, P.W. Novel therapies targeting inner mitochondrial membrane—From discovery to clinical development. *Pharm. Res.* **2011**, *28*, 2669–2679. [CrossRef] [PubMed]
79. Szeto, H.H. Cell-permeable, mitochondrial-targeted, peptide antioxidants. *AAPS J.* **2006**, *8*, 277. [CrossRef]
80. Kelso, G.F.; Porteous, C.M.; Coulter, C.V.; Hughes, G.; Porteous, W.K.; Ledgerwood, E.C.; Smith, R.A.; Murphy, M.P. Selective targeting of a redox-active ubiquinone to mitochondria within cells: Antioxidant and antiapoptotic properties. *J. Biol. Chem.* **2001**, *276*, 4588–4596

5. DISCUSSION

Recent lifestyle changes have led our society towards more sedentary habits and unhealthy nutrition patterns. Hence, overweight and obesity have become a worldwide pandemic, raising the prevalence of metabolic alterations as T2D. These alterations have a striking impact on overall health and increase the risk of cardiovascular disease and premature death. Therefore, understanding the mechanisms that underlie the development of T2D and its subsequent complications is vital for preventing their evolution. In addition, determining the therapeutic effects of antidiabetic treatments at the cellular level might help to develop new therapeutic strategies or improve those that already exist.

1. Anthropometrical data analysis of T2D and healthy subjects

In general, the recruited T2D patients were around 60 years-old with an average T2D duration of 10 years since diagnosis. All patients were under nutrition and lifestyle supervision to prevent sedentarism and malnutrition. Most were being treated with antidiabetic treatments, metformin being the most common; however, statins and antihypertensives were also prescribed frequently, and can be consulted in the supplementary table in chapter 2.

It is relevant to outline that T2D patients presented high BP. Hypertension is part of the aggravating factors that cause the increased cardiovascular risk associated with T2D [652]. The influence of high BP on cardiovascular risk is not limited to T2D, as rises in BP have been related to a increase in the CIMT, not only in T2D, but also in healthy subjects [653]. However, the impact of hypertension is greater in T2D, as analyzed in a retrospective work studying the Framingham cohort and its offspring. The research in question showed that T2D hypertensive subjects had a 57% greater chance of having any cardiovascular event than normotensive T2D subjects [654]. Although high BP and T2D are related, it is difficult to determine what the trigger of each is. Nevertheless, it is known that a positive feedback loop exists between T2D and hypertension,

and that the triggering mechanisms for both of them are similar. Vascular calcification, activation of the renin-angiotesin system, and vascular remodelling are common consequences of T2D and hypertension, which culminate in microvascular and macrovascular damage [655]. However, lifestyle intervention can have a striking impact on lowering BP, which significantly reduces the risk of future complications [656]. Thus, reducing hypertension is a relatively easy approach for lowering cardiovascular risk in T2D.

T2D is also characterised by overweight and obesity, as indicated by the significantly increased BMI and waist circumference we observed in our patients with respect to the healthy subjects. The increases in BMI and waist circumference were associated with alterations in lipid metabolism. In order to explain whether the differences in inflammation and lipid metabolism were due to the increased BMI, we adjusted the significance for BMI. As a result, most of these alterations lost their statistical significance, meaning that weight increase explained most of the differences. This suggests that the changes in inflammation and lipid are not detectable or that lipid-lowering treatments were masking increased inflammation, an aspect that needs further research.

2. Characteristic T2D alterations in glucose metabolism markers

The biochemical data obtained from the samples isolated from T2D patients and healthy volunteers reflected alterations in glucose homeostasis in the T2D patients. The main alterations were increased fasting glucose levels and a rise in HbA_{1c}%, which were significantly higher than levels in the healthy population. Moreover, hyperinsulinemia and IR was also reflected by the high HOMA index. These alterations reflect the classic metabolic imbalances in T2D populations, namely hyperglycaemia and hyperinsulinemia, which confirms that the analyzed cohorts had the diagnostic traits of T2D.

Hyperglycaemia has been studied as a cause of the cardiovascular alterations that can

lead to later complications, with AGEs being one of the most important factors [86,125,128]. Hence, maintaining a good glycaemic control by monitoring HbA_{1c}% levels is of vital importance to prevent future cardiovascular complications [657–659]. In chapter 2 of the present thesis, we established a HbA_{1c}% threshold of 6.5%, as recommended by clinical guidelines and the criteria for diagnosis for T2D, as it is a turning point in the development of T2D cardiovascular complications [6,660–662]. In line with the results obtained in chapter 2, which showed that HbA_{1c}%>6.5% is related to a higher CIMT and inflammation, several studies confirm that high HbA_{1c}% or/and a poor glycaemic control lead to more vascular complications and debilitated endogenous antioxidant defences [663,664]. Monitoring glycaemic levels has other benefits, such as regulating cellular stress processes including mitochondrial dysfunction, ER stress and inflammation, as shown by previous research by our group [243,313,665]. All these data confirm that controlling HbA_{1c}% is a useful tool and an easy approach to prevent T2D-related cellular alterations, which can lead to a reduction of T2D complications [666] and therefore improve the patient´s quality of life .

3. Assessment of T2D lipid metabolism parameters

Overweight-related biochemical and anthropometrical dysbalances are rooted in the cellular alterations found in T2D or obese patients. The origin is found in adipocytes, which, in a hypercaloric situation, internalize circulating lipids and store them in the lipid droplets until they become hypertrophic. Under IR, adipocytes enter into a catabolic metabolism that involves lipolysis, increasing plasmatic lipid concentrations and leading to hyperlipidaemia [43]. This positive feedback loop between lipids and IR will continue to cause adipose hypertrophy until one of these factors is limited by pharmacological or lifestyle interventions.

It has been demonstrated that increased circulating lipids can activate endothelial cells, thus leaving the endothelium prone to develop atherosclerotic lesions [667,668]. Furthermore, in a

hyperlipidemic environment, another factor that results in atherosclerotic lesions is the presence of atherogenic dyslipidaemia, a term which comprises a rise in small and dense LDL-c particles, high TG and decreased HDL-c levels. Indeed, we observed some of these alterations (elevated TG and low HDL-c) when there was a rise in LDL-c. These alterations were correlated to an enhanced CIMT, which suggests increased cardiovascular risk in such patients. In agreement with this idea, the EURIKA cross-sectional analysis found that most T2D patients presented atherogenic dyslipidaemia, despite most of them being undiagnosed and untreated [669]. Atherogenic dyslipidaemia, especially the undiagnosed subset, can lead to more cardiovascular complications and premature death, so proper monitoring and treatment of T2D patients is important. The most common therapeutic approach for tackling atherogenic dislipidaemia is a combination of lifestyle changes and pharmacological treatment with statins (for lowering cholesterol synthesis), ezetimibe or fenofibrates [670]. The high statin prescription in our study cohorts may explain, in part, our results showing that lipid profile was unaltered or even improved with respect to the control group. Specifically, the analyzed patients presented lower total cholesterol and less LDL-c, despite displaying traits of atherogenic dislipidaemia such as higher TG and lower HDL-c. The results remained unaltered regardless of the metformin treatment referred to in chapter 4 or the glycaemic control administered in chapter 3, suggesting that there is a metabolic change which needs sustained lifestyle changes and pharmacological treatment in order to be reversed. Despite our results, obtained in a relatively small number of patients without follow up, most studies confirm that a correct and strict glycaemic control, weight control, lifestyle supervision and specific lipid-lowering treatment are vital approaches for preventing T2D complications [671].

4. Presence of IR in T2D subjects

The metabolic consequence of chronic hyperglycaemia and hyperlipidaemia is the development of IR [43]. Insulin-dependent and -independent tissues present imbalances in insulin signalling and nutrient intake, which induce more profound cellular alterations, such as energetic imbalances and ROS production [43,672,673]. A useful index for measuring IR is the Homeostatic assessment model of IR (HOMA-IR) which takes into account insulin and glucose levels to calculate the presence of IR and its degree [674]. The cut-off values vary depending on the population, and also on whether the patient presents T2D or not, ranging between 1.6 to 3.8 in the healthy population and from 2 to 3.8 in T2D patients [675–679]. In our studied cohorts, the healthy volunteers presented a HOMA-IR ranging from 1.6 to 1.71; and in T2D, from 3.72 to 6.9. These levels corroborate that all our study cohorts presented established IR. Glycaemic control also seemed to influence IR, as poorly controlled patients had higher a HOMA-IR index than the closely controlled ones, indicating a possible relationship between glycaemic control and HOMA-IR, as already proposed [680]. The relationship between IR and glycaemic control is deeply rooted in the cellular alterations underlying the physiopathology of T2D [43]. Initially, nutrient excess can lead to mtROS production and blunting of insulin signalling [132]. The proposed mechanism for this alteration is the mtROS-dependent inhibition of Akt/IRS insulin signalling through PKC [102]. Therapeutic approaches to reduce ROS have shown improvements in IR in different experimental models. One approach is to reduce mtROS with mitochondria-targeted catalase (mCAT) , which was shown to improve insulin sensitivity and glucose tolerance [102]. Similarly, inhibition of NOX4 in adipose tissue from mice on a high fat and high sucrose diet reduced IR and inflammation [110]. Regarding inflammation, it is important to highlight, as previously mentioned, that numerous studies link it to IR and demonstrate its capacity to blunt IR signalling [681,682]. Such evidence shows that IR is triggered and maintained by an altered cellular environment like that present in T2D, and is characterized by hyperglycaemia, hyperlipidaemia, hyperinsulinemia and

inflammation.

5. Leukocytes as a cell model in T2D research

Among all the hallmarks of T2D, one of the most studied is inflammation in the form of chronic low grade inflammation. Given this background, we decided to study leukocytes, the main cell type mediating the inflammatory response. In this context, immune cells sense T2D metabolic alterations, as they are exposed to the chronic hyperglycaemia and hyperlipidaemia, and in response they produce proinflammatory cytokines. Simultaneously, they are also exposed to the proinflammatory background produced by alterations in metabolically active tissues (adipose tissue, muscle or liver). Hence, leukocytes are highly exposed, sensitized and responsive to the plethora of metabolic changes in T2D. This has been demonstrated in different studies that have demonstrated leukocyte activation by hyperglycaemia, such as the clinical trial carried out by de Vries et al [683]. Specifically, in PBMCs from T2D patients, the production of proinflammatory cytokines and the expression of the key inflammatory transcription factor NFκB are enhanced [517]. When these cells are under conditions of hyperglycaemia, the JNK pathway and OXPHOS complex expression are altered, which could explain the increase in the inflammation related to ROS production [519]. Other proinflammatory signalling pathways activated under hyperglycaemic damage, such as PKC-p66shc, are associated with macrovascular complications in T2D [684].

Far from affecting only PBMCs or specific leukocyte subpopulations, activation caused by T2D-related insults is seen in all hematopoietic lineages, and affects neutrophils, macrophages and lymphocytes [685]. In paticular, hyperglycaemia-dependent activation of neutrophils promotes the appearance of thrombotic events through hepatic production of coagulation factors and proinflammatory cytokines [686]. As we have mentioned previously, the most studied proinflammatory cytokines in the context of T2D are TNFα, IL-6 and IL-1β, which accumulate in the bloodstream and trigger inflammatory responses in the neighbouring tissues. Endothelial

cells are deeply affected by them and, in a hyperglycaemic state, they are activated producing adhesion molecules as selectins, ICAM-1 and VCAM-1. This generalised activation causes the interaction of leukocytes with the endothelium, which is enhanced under hyperglycaemic states [687].

Leukocytes from T2D patients are very sensitive cells and, apart from inflammation, display enhanced oxidative stress, ER stress and an altered antioxidant response [293]. All this evidence, together with the easy isolation method and almost non-invasive method for obtaining the sample, make leukocytes a suitable model for studying T2D and related molecular alterations.

6. Chronic low grade inflammation and early markers of atherosclerosis

In the T2D background, adipocytes secrete proinflammatory cytokines and chemokines that recruit macrophages, which favour the proinflammatory environment [512,688,689]. Previous studies have outlined the value of proinflammatory molecules (TNFα, CRP, IL-6) as predictors of either development of T2D, a worse prognosis, [690] or atherosclerosis [691]. The progressive increase in the levels of tissular and circulating proinflammatory molecules causes a generalised state of low-grade inflammation that predisposes metabolically active organs to develop IR.

Some studies suggest that low-grade inflammation, assessed by the markers CRP and IL-6, begins before T2D onset and can be employed as T2D risk markers. These markers were assessed, together with TNFα, during a 2-year retrospective analysis, demonstrating themselves to be good predictors of T2D onset [690] [692,693]. At the cellular level, those cytokines activate proinflammatory pathways such as JNK and NFκB, which inhibit insulin signalling and contribute to IR [694]. For instance, IL-6 impairs the vasodilator properties of endothelial cells by JNK and ERK inhibition of insulin signalling to eNOS [695]. Similarly, the proinflammatory cytokines TNFα and IL-1β promote apoptosis in pancreatic β cells by triggering NFκB signalling [520]. The existing

knowledge of the proinflammatory background in T2D led us to analyse whether these proinflammatory molecules were present in the analyzed cohorts of T2D patients.

In our results, levels of hsCRP were higher in the serum samples from T2D patients. Although in our study the changes in hsCRP seem to be caused by T2D, other research has suggested that overweight is the common cause of the hsCRP rise in both metabolic syndrome and T2D [696,697].

Given that hsCRP confirmed that the analyzed patients presented increased inflammation, we continued our analysis by testing the molecules related with chronic inflammation. Therefore, we measured serum concentrations of TNFα and IL-6 in healthy and T2D patients. As expected, we observed that T2D patients had higher levels of both cytokines. In this sense, recent research found that those higher levels could be explained by the induction of TNFα and IL-6 expression exerted by IL-32, a proinflammatory cytokine secreted by leukocytes in situations of chronic inflammation and whose secretion peaks when there is cardiometabolic risk [698,699]. This observation would explain the increase in the levels of TNFα and IL-6 observed in poorly controlled T2D patients with respect to those with a correct glycaemic control.

Focusing our attention on TNFα, it is one of the most studied cytokines because of its presence in inflammation-based diseases. TNFα signals through TNRF, which inhibits JNK and activates NFκB, resulting in the inhibition of insulin signalling and increased inflammation in a T2D setting. Additionally to affecting insulin signalling, TNFα reduces the externalization of GLUT4 channels in insulin-sensitive tissues, hindering the regulation of glucose intake [681]. TNFα does not only play an important role in IR, but also predisposes to and aggravates T2D cardiovascular complications. Indeed, the T2D patients with poorer glycaemic control analyzed in chapter 2 had higher levels of TNFα, as observed in a previous correlation study [682]. Furthermore, it was observed in a small cohort study that TNFα correlated with several markers of cardiometabolic risk, leading to this cytokine being proposed as a marker for preventing diabetic complications [700]. An alternative approach - measuring sTNFR – was found to be useful

as a marker of diabetic kidney disease in the CARDIPP study, which analyzed a cohort of T2D subjects [701]. All these pieces of evidence allow us to conclude that assessing TNFα serum concentrations might be a good marker of inflammation-related diseases with cardiovascular risk, as suggested by our data.

Regarding IL-6, its function as a T2D marker is almost established; however, there is still debate surrounding the different reported effects of IL-6 in cellular and animal models [504]. Indeed, a study has shown two different behaviours of this cytokine depending on the cell type: IL-6 secreted by myeloid cells from adipose tissue induces accumulation of macrophages through classic IL-6 receptor signalling; but if secreted by muscle or adipocytes, IL-6 induces macrophage accumulation through a non-canonical pathway in which soluble IL-6 receptor is involved [702]. This cytokine also has been seen to have influence in the insulin signalling pathway, as observed in endothelial cells and hepatocytes, where IL-6 stimulates JNK signalling, thus inducing IR [695,703]. In contrast, IL-6 has a protective function in pancreatic β cells, preserving its capacity of secreting insulin through activation of autophagy and induction of proliferation [429,704]. The protective mechanism of IL-6 in pancreatic β cells might imply the transcription factor STAT3, through a signalling pathway which is hampered in T2D [429]. We observed that IL-6 serum concentrations rise in T2D patients, and that the difference is even more marked in those that are poorly controlled. The relationship between IL-6 and poor glycaemic control is still under debate, despite a recent metaanalysis showing that IL-6 levels and glycaemic control were positively associated [705]. Regarding the contribution or association of IL-6 to cardiovascular events, increases in IL-6 levels are related to increased coronary artery disease risk, but a direct causal relationship has not been established [706]. Based on all these data, the contribution of IL-6 would seem to be limited; however, it can act as a marker of cardiovascular risk, as assessed in the previously mentioned studies, and reflected by the increased HbA_{1c}% in our samples.

The proinflammatory state and previously discussed alterations have an impact on the function of whole organs and tissues [707,708]. The most damaged tissues are those independent of

insulin-dependent glucose uptake, such as the peripheral nervous system, kidney and retina; and those originating in the malfunction of the vascular wall, due to the presence of the atherosclerotic plaque. Based on this classification, T2D causes microvascular and macrovascular complications [707].

In this thesis, macrovascular complications were assessed using three different approaches: analysis of vascular inflammation, assessment of leukocyte-endothelium interactions, and measurement of the CIMT. The first analysis that we performed was to examine the inflammatory state of the patients' vasculature by measuring serum levels of proinflammatory cytokines (already discussed) and the adhesion molecules ICAM-1, VCAM-1 and P-Selectin. In this sense, we observed an increase of both integrins (VCAM-1 and ICAM-1) in T2D vs control subjects, but no differences were found with respect to P-selectin. When we divided the T2D group depending on its glycaemic control, poorly controlled patients had higher levels than their properly controlled counterparts, whereas only VCAM-1 levels from poorly controlled patients were significantly higher than those from healthy or properly controlled subjects. This result indicates that, when established for at least 5 years, TD2 causes a relatively high level of inflammation, reflected by an increase in VCAM-1 and ICAM-1 serum concentrations. Moreover, patients who do not achieve glycaemic goals had higher concentrations of serum VCAM-1 and ICAM-1 than those with an adequate HbA_{1c}%.

ICAM1 has been endorsed as a reliable marker of subclinical atherosclerotic risk assessment in T2D [709]. Its reduction diminishes the incidence of atherosclerotic lesions in ApoE-/- mice fed a HFD, underlining the relevance of this adhesion molecule in the atherosclerotic process [710,711]. Indeed, ICAM-1 inhibition is an effective approach for reducing atherosclerotic lesion development, as observed in different studies for determining the mechanisms behind resveratrol protective effect. [712,713]. However, ICAM-1 might also be important in the early stages of T2D development, as Odegaard et al. showed that rises of ICAM-1 and other proinflammatory cytokines precedes the onset of T2D [714]. Our results might reflect this early increase in the levels

of ICAM-1 in well-controlled patients, while those of VCAM-1 showed no differences. T2D pathogenic mechanisms other than atherosclerotic lesion formation can also upregulate ICAM-1 expression in endothelial cells, namely: AGEs, [715] ROS, [714] ER stress [716] and autophagy [717]. Collectively, these data lead us to suspect that ICAM-1 expression begins with the first metabolic alterations before the development of T2D, and progressively contributes to the incremented cardiovascular risk in T2D.

VCAM-1 has been suggested as a good marker of cardiovascular complications in T2D [718]. In T2D patients, higher levels of VCAM-1 were found to be present in patients with worse glycaemic control, who might have been at risk of cardiovascular complications. Similar findings were determined in a small case-control study in which poorly controlled patients displayed higher VCAM-1 serum levels [719]. In this sense , VCAM-1 has been proposed as a novel biomarker of cardiovascular risk, specifically as a predictor of atherosclerotic lesion formation in T2D patients [720]. The same finding was observed in a study performed by Hegazy et al. in which cardiovascular risk in T2D patients was associated with VCAM-1, but not with ICAM-1 or E-selectin [721]. The increase of VCAM-1 associated with an increment in cardiovascular risk can be explained by endothelial cell activation. As explained in the introduction, the second phase of endothelial activation induces the expression of integrins that facilitate the attachment of immune cells. As ICAM-1 and VCAM-1 are both integrins, it is feasible that these molecules are expressed simultaneously, so that a similar risk is predicted with both molecules. The differences observed in this thesis could be attributed to particularities in the expression of each of the two adhesion molecules in the different vascular tissues, as previously suggested by Kanda et al., who reported that VCAM-1 was more expressed in arteries [722]. This could be the reason why another study found an overexpression of VCAM-1 but not ICAM-1 in arterial tissue from atherosclerotic T2D patients [723]. Similar results were observed in LDLR -/- mice under HFD, a model of atherosclerosis lesion development; under impairment of the immunoglobulin domain of VCAM-1, the animals did not develop an atherosclerotic lesion, in contrast to their control

littermates [724]. This effect was not accomplished with ICAM-1 impairment, proving that VCAM-1 has a much greater influence on atherosclerotic event development than ICAM-1 [724]. VCAM-1 has not only been associated with macrovascular complications, but also with microvascular complications such as nephropathy [725] or retinopathy [726]. Indeed, VCAM-1 has been established as an independent risk factor for cardiovascular mortality, and is slightly associated with the presence of T2D [727]. Altogether, these data support our results showing increased levels of soluble inflammation markers characteristic of T2D patients, which were higher even in poorly controlled patients.

In the second approach, we evaluated the interactions of leukocytes from T2D and healthy subjects with a cultured monolayer of HUVECs seeded until confluence. This system is known as as parallel-plate flow chamber, and has been employed as an *in vitro* approach of analyzing the different steps of the immune infiltration or the formation of the atherosclerotic plaque [728–730]. With this system, we evaluated how leukocytes interacted through their adhesion molecules with those on the endothelium, thus allowing interaction, rolling or adhesion. The analysis of these intercellular interactions is relevant due to their implication in the formation of the atherosclerotic plaque. In a pro-inflammatory hyperlipidaemic and hyperglycaemic background, endothelial cells are activated and promote the malfunctioning of the vascular wall. Those dysfunctional endothelial cells will secrete prothrombotic, vasoconstricting and hypertensive cytokines and molecules, thus leading to a dysfunctional leukocyte circulation [731]. Moreover, as these cells have active proinflammatory pathways, such as NFκB, they express adhesion molecules as selectins and integrins [732]. On the other hand, immune cells are primed by the hyperglycaemia and hyperlipidaemia and by the proinflammatory cytokines secreted by metabolically active tissues, such as adhesion molecules [683,685].

These enhanced levels of adhesion molecules seem to lead to an increment in the adhesiveness of immune cells to the activated endothelium, which we assessed with the parallel-plate flow chamber model. We observed an increase in the interactions of the samples

isolated from T2D patients, in which there were more rolling and adhering leukocytes that flowed more slowly than in healthy samples. In this sense, our group had previously observed the same rise in interactions with T2D leukocytes [164,243], but we associated a worse glycaemic control to an increase in the number of rolling leukocytes [243]. This could be attributed to differences in the characteristics of the cohort recruited for the different studies, whose biochemical profile or baseline characteristics might have differed slightly. However, our results are in line with those of an *in vitro* study which employed oxLDL-stimulated THP1 and analysed their interaction with HUVECs [733]. The results were contrasted in *in vivo* mice models of T2D – namely, adiponectin deficient mice - in which it was revealed that adiponectin deficiency induced an increase in leukocyte-endothelium interactions [734]. This deficiency is also present in T2D subjects; therefore, it is possible that a lack of adiponectin contributes to the increment in the interactions that we assessed. The mechanism behind increased leukocyte adhesiveness is based on the endothelial dysfunction that creates a prothrombotic, pro-inflammatory and proatherogenic scenario. Precise mechanisms of endothelial dysfunction in a T2D endothelium might involve PKC activation [491,735,736], the NFκB pathway and NO production [569,570,575]. In this thesis, and in previous work, we have witnessed an increase of NFκB in leukocytes from T2D [173]. However, the state of PKC and NO production have not been described in detail, and might be an interesting research topic for future investigations. Among the triggering mechanisms of leukocyte-endothelium interactions, the simultaneous activation of leukocytes and endothelium due to loss of vascular homeostasis is central. This activation is usually triggered by pathological situations which cause metabolic deregulations, such as overweight [737], inflammation [687,738] and glucolipotoxicity [739,740]. Overweight and inflammation are present in T2D patients, and glucolipotoxicity is also likely to be present due to the high lipid and glucose concentrations. Hence, some degree of endothelial dysfunction might be present, reflected by enhanced leukocyte-endothelial interactions.

The third approach to cardiovascular risk in T2D that we evaluated is measurement of the thickness of the intima-media layer of the carotid artery. Measurement was conducted in an accessible and vital artery with a high blood flow, where the atherosclerotic plaque can be usually easily visualized. As demonstrated, measuring wall thickness has prognostic value for atherosclerotic events [645,646]. Taking into account its relevance in atherosclerosis, we assessed CIMT in healthy and T2D patients in which leukocyte-endothelium interactions and biochemical profile were measured. We observed an increase in right and left CIMT in T2D patients compared to healthy subjects; when glycaemic control was considered, only left CIMT increased significantly in poorly controlled patients. Right CIMT was slightly higher in these poorly controlled subjects, though the difference was not statistically significant, possibly due to differences between right and left carotids or the size of the analysed population. When we correlated the CIMT measurements with our leukocyte-interaction results, we found significant correlations for left CIMT only, which was positively correlated with rolling number and adhesion, and negatively correlated with rolling velocity. These results confirmed that CIMT is related to leukocyte-endothelium interactions, and supported previous evidence of left CIMT being more implicated in atherosclerotic lesion development. We studied the correlation of our CIMT data with glucose metabolism parameters and BMI in order to assess the possible correlation of CIMT measurements with biochemical and anthropometrical changes in T2D, and found significant positive correlations in all cases except for BMI vs right CIMT. A similar pattern was revealed by the correlation analysis of CIMT measurements and lipid metabolism data, which showed significant correlations that pointed to a dyslipidaemic profile that were more significant for left CIMT than for right CIMT.

All these data underline the importance of assessing CIMT measurements in T2D without clinical signs of plaque development as a tool for preventing future cardiovascular events. This technique is useful and affords great benefit to T2D patients regarding the early detection and prevention of macrovascular complications. In this sense, previous research has highlighted

greater CIMT in T2D patients, thus proving its value as a cardiovascular risk biomarker [646,647,649,709]. Indeed, other markers of disease progression of T2D, such as glycaemic control, have also been related to higher CIMT, and their combination can be useful for assessing cardiovascular risk [659]. Some therapies that pursue the improvement of T2D could also help to reduce CIMT and, in turn, cardiovascular risk. As an example, interventional lifestyle approaches to reduce T2D, such as diet, do not reduce CIMT, despite them positively affecting glycated haemoglobin [741]. However, CIMT has been shown to be effectively reduced by pharmacological intervention, which indicates that CIMT reduction requires intensive treatment together with lifestyle intervention if clinical relevance is to be achieved [742–744].

Apparently, left CIMT is more influenced by T2D alterations that right CIMT, which could be explained by the different haemodynamic properties of both carotid arteries. This fact was examined in the study performed by Luo et al., who determined that, while plaques in the left carotid were more influenced by hydrostatic pressure and changes in biochemical parameters, the right carotid was exposed to hemodynamic changes [745]. This might be explained by the different anatomical origin of both carotid arteries, which render a more vulnerable plaque on the left side which will break more easily than that on the right side [745,746]. Indeed, one study determined that cerebrovascular disease was more prevalent on the left side, possibly due to the high shear stress observed [747]. Selwaness et al. corroborated these findings; they reported that, despite bilateral plaques being more frequent, 67% of unilateral ones were located in the left carotid. Moreover, the left plaque suffered more intraplaque haemorrhage and was thicker than the right, which was more calcified and resistant to shear stress [748]. All these studies support our observations and help to explain why the left carotid is more affected than the right. Furthermore, it is important to highlight that prevention through glycaemic control might be the key to reducing macrovascular complications.

7. Oxidative stress and ROS production in leukocytes from T2D subjects

Hyperglycaemia and hyperlipidaemia are characteristic of T2D, and cause several cellular alterations, among which one of the most important is ROS production. The main explanation for the hyperglycaemia-dependent generation of oxidative stress is that hyperglycaemia activates the cellular pathways that generate energy. This energetic excess causes an imbalance in the AMP/ATP and ADP/ATP ratios, leading to slowing down of the ETC in the mitochondria. Despite this slow electronic transport, the hyperactivation of the catabolism continues to render energetic intermediates in the form of NADH and $FADH_2$. This reduces the availability of NAD^+ equivalents in the cell, which alters other redox cellular processes. Moreover, these energetic intermediates continue providing free electrons to the ETC, which in turn produce ROS. ROS accumulation modifies mtDNA, lipids and, eventually, circulating lipids and glucose, thus creating oxLDL and AGEs. In parallel, energy excess causes the accumulation of glucose, which leads to the activation of the polyol pathway and hexosamine pathway. Consequently, the energy imbalance favours ROS, and so AGE production further increases [86,130]. AGEs can activate leukocytes through the RAGE receptor, leading to an auto-feedback which generates an unsustainable situation involving inflammation and ROS production [686,749]. Evidence suggests that ROS production in leukocytes is relevant in cardiovascular diseases, although little research has been done in T2D [750]. This is why we considered it relevant to evaluate whether leukocytes from T2D patients present enhanced ROS production. Knowledge of ROS production by leukocytes in a T2D setting is limited, but pathways which promote the generation of ROS or proteins that mediate its production seem to be active agents. As an example, thioredoxin interacting protein (TXNIP) (a cytoplasmic ROS-producing enzyme), is strongly upregulated in PBMCs from T2D patients and its activation is related to ER stress [314]. In parallel, one study determined low expression of OXPHOS complexes in leukocytes from T2D, which led to production of high amounts of ROS. Their accumulation activates the JNK pathway, which

promotes further ROS production and apoptosis [519]. In this sense, mitochondrial alterations might be deeply implicated in ROS production, as complex I is defective in leukocytes from T2D patients, and is accompanied by impaired oxygen consumption [201].

In this context, we determined that PBMCs from T2D patients presented higher levels of mitochondrial and total ROS, observing an increase in mtROS and total ROS. Interestingly, T2D patients with poor glycaemic control presented more ROS than the strictly controlled ones. Several studies reinforce the relevance of our results; for example, experiments carried out in leukocytes exposed to an IR background revealed that leukocytes produce ROS and cause cellular stress [751] and inflammation [752]. ROS production has been further confirmed in leukocytes from T2D patients [312] and in a leukocyte subpopulation (granulocytes) [118]. The source of ROS production is thought to be rooted in impaired mitochondria with slow OXPHOS due to the excess of nutrients. Hence, examining OXPHOS could be an interesting objective of future research.

Regarding the relationship between HbA_{1c} and ROS production, some evidence points to the glycated protein causing ROS production in cardiac muscle cells through NOX2 [753]. In leukocytes from T2D patients, it was also demonstrated that those from poorly controlled patients had more total and mitochondrial ROS production [665]. Regardless of whether there is a direct causal relationship or not, several investigations have found that poorly controlled T2D (which usually have macrovascular or microvascular comorbidities) have less antioxidant defences and more oxidative stress markers. This was the case in cardiac autonomic neuropathy T2D patients, among whom those with a worse glycaemic control had less catalase and SOD [664]. Similarly, cardiovascular risk measurements and total antioxidant capacity were measured in T2D patients with different grades of glycaemic control. Those with poor glycaemic control had more cardiovascular risk markers and less total antioxidant capacity, though a direct correlation was not found [659]. An alternative approach evaluated circulating concentrations of sRAGE (which antagonizes the effect of AGEs) that were found to be lower in poorly controlled patients

compared to properly controlled and healthy subjects [719]. Therefore, ROS excess and antioxidant scarcity could be a hallmark of T2D patients with poor glycaemic control. All this evidence supports our results, which shown that leukocytes from T2D patients with poor glycaemic control produce more total and mtROS.

8. Assessment of mitochondrial function and dynamics in leukocytes from T2D subjects

To further explain the origin of this T2D-related ROS alteration, we set out to determine the source of ROS in the leukocytes under evaluation. Given that one of the main known sources of ROS is dysfunctional mitochondria, we measured markers of mitochondrial dysfunction. Mitochondrial dysfunction consists of the inability of mitochondria to adapt to energetic and metabolic cellular demands. It comprises different alterations which impede the correct mitochondrial metabolism and renders high amounts of ROS and lack of mitochondrial-synthesized metabolites [754]. The phenotype of dysfunctional mitochondria usually include altered membrane potential, defective O_2 consumption and ATP production, and decreased Ca^{2+} content [182,185]. Many non-communicable diseases present this type of mitochondrial damage due to genetic and environmental or behavioural factors. Among these, high caloric intake and sedentary lifestyle are more related to mitochondrial dysfunction, as these habits alter the energy balance upon which their function depends [754]. The resulting mitochondrial alterations affect all the cell types in different manners depending on their function and dependence on mitochondrial performance. One of the most affected cell types is pancreatic β cell mass, due to its low antioxidant capacity, in which high ROS concentrations impedes adequate insulin release. In fact, a study carried out in pancreatic islets isolated from T2D patients challenged with glucose and arginine showed that altered insulin secretion was related to high expression of OXPHOS complexes I and V, overexpression of uncoupling protein 2 expression (possibly due to

fuel overload) and lower ATP production [755]. Moreover, ROS produced by dysfunctional mitochondria can directly cause IR through activation of ROS-sensing kinases such as JNK, p38MAPK, IKKβ or PKC [95]. In particular, JNK is able to dephosphorylate the IRS protein, thus reducing insulin signalling [756]. Similarly, under stimulation by DAG or ceramides, other kinases that regulate insulin signalling, such as PKC, phosphorylate and inhibit the insulin receptor, thus contributing to a positive auto-feedback loop that aggravates IR [40,102,106]. Hence, a correct mitochondrial function is decisive for preventing IR and contributes to the correct management of fuel disposal and energy production for the whole cell.

As our patients displayed classic T2D alterations including IR, high circulating lipids and high fasting glucose, we considered that their leukocytes might display markers of mitochondrial dysfunction. We measured different parameters, such as membrane potential, O_2 consumption, or Ca^{2+} concentrations, as surrogate markers of mitochondrial function. Our results demonstrated that leukocytes had more cytosolic Ca^{2+}, which implied dysregulated mitochondrial Ca^{2+} storage. Additionally, we confirmed that leukocytes from T2D patients have altered mitochondrial function, reflected by loss of membrane potential and lower O_2 production. Together, these results depict a situation of mitochondrial alterations reflected in the previously discussed rise in mtROS production. In this sense, our results are supported by abundant evidence of malfunctioning mitochondria in different tissues in a T2D setting. As an example, in muscle fibres isolated from obese diabetic patients, mitochondria presented a lower respiratory capacity than healthy ones [757] and ATP synthesis was attenuated [758]. The same finding was observed in liver tissue from mice fed a HFD [759]. Following on from the idea of mitochondrial alterations in T2D, other studies measured metabolite flow through metabolic pathways such as the Krebs cycle in T2D models – for example, Goto-kazikazi rats - demonstrating that the key enzyme aconitase was reduced in key metabolic tissues [59]. This finding demonstrated that mitochondrial dysfunction also affects the fundamental pathways of mitochondrial metabolism.

Another trait of T2D that affects mitochondrial function is IR, as illustrated by a study in which muscle with IR displayed impaired respiration and enhanced production of H_2O_2 [188]. Glucolipotoxicity has also been demonstrated to induce mitochondrial dysfunction in 3T3-L1 adipocytes, reflected by ROS production, loss of membrane potential and less intramitochondrial Ca^{2+} [199]. This contributes to the idea that glucose and lipid excess affects all metabolically active tissues (liver, adipose tissue, and muscle). Collectively, our results and those of previous studies are in accordance in that they show a marked mitochondrial dysfunction in T2D that is triggered by glucolipotoxicity and IR. Thus, tackling mitochondrial function would appear to be a promising target for future antidiabetic therapies.

An adequate mitochondrial function requires the establishment of a mitochondrial network which enables metabolite and energy diffusion throughout the whole cell. The deregulation of this mitochondrial structure may be involved in the pathogenic mechanisms of metabolic diseases. The mitochondrial network is maintained by a tight dynamic process named mitochondrial dynamics, which is responsible for changing mitochondrial morphology in response to cellular metabolic needs and maintaining a healthy mitochondrial population. Given that there is mitochondrial dysfunction in T2D, it can be hypothesized that mitochondrial dynamics are altered. Although an imbalance occurs in those processes in T2D, there is debate about which process is undermined. In this sense, one study of muscle cells described that T2D causes a defect in fusion and alterations in fission [760], which could be due to a hampered mitochondrial dynamics regulation. Despite this conclusion, other studies have not found such differences in muscle from T2D patients, or the differences that existed were limited to DRP1 and MFN2 proteins with a tendency towards fission [227,231]. However, most studies agree about the beneficial function of mitochondrial fusion, as confirmed by recent research showing that insulin is able to activate OPA1 through AKT-mTOR-NFκB signalling [232]. Surprisingly, insulin signalling can also induce mitochondrial fission in C2C12 myotubes, reflecting the influence of the different effects of insulin on mitochondrial dynamics processes depending on the signalling

pathway and the studied tissue or cell type [239]. These examples illustrate the lack of consensus regarding the alteration in mitochondrial dysfunction and its relevance in T2D. A reason might be that most studies have analyzed muscle cells because of the importance of mitochondrial function surveillance in this energy-consuming tissue. Examining mitochondrial dynamics in other cell types and tissues affected by or influencing T2D pathogenesis might shed light on the overall relevance of this process.

Our group has previously described that poor glycaemic control in leukocytes from T2D subjects is related to an increase in fission and a reduction in fusion proteins [243]. In the present thesis, similar results have been obtained, showing that fusion proteins and genes (MFN1, MFN2 and OPA1) are reduced and fission ones (FIS1 and DRP1) are increased. Although we have measured the key molecules regulating these processes, the contribution of each protein to said phenomenon has not yet been determined. Specifically, we have reported the same behaviour for the three analyzed fusion molecules (decreased levels of OPA1, MFN1 and 2) and for both fission molecules (an increase of FIS1 and DRP1). However, given the slightly different functions of these molecules, a significant variability between the results can be expected. In this regard, different levels of the fusion proteins MFN1 and MFN2 could suggest that the altered process is not mitochondrial fussion. Other functions in which MFN2 can participate are the interaction between ER and mitochondria or the regulation of Ca^{2+} release. Indeed, it has been described that MFN2 in macrophages perform roles as different as inflammatory response, autophagy, apoptosis and antigen processing [761]. Besides these particular functions in macrophages, MFN2 also interacts with AMPK under energy stress to form mitochondria-associated ER membranes [762]. This particular function of MFN2 also participates in ER stress-triggered apoptosis by translocating ER Ca^{2+} to the mitochondria, a situation in which inhibition of MFN2 could be beneficial [214]. Given that we did not find differing behaviour between MFN1 and MFN2 in control *vs* T2D patients, our results are consistent with mitochondrial fussion being one of the main alterations in T2D, and not other related processes.

This might suggest a reduction of IMM fusion and reorganization, which is decisive for proper mitochondrial function. It is important to highlight that we did not detect L-OPA1 and S-OPA1 isoforms, an experimental approach that could have shed light about the processes of IMM and outer mitochondrial membrane (OMM) fusion. Other studies have obtained similar results by employing other experimental approaches and T2D models. For example, in a study performed in muscle from a HFD OPA1KO mice model, OPA1 expression induced FGF21 expression, which was abolished in OPA1 KO and HFD mice [763]. This finding leads us to think that OPA1 downregulation in T2D is accompanied by decreases in the myokine FGF21, beneficial in IR states. However, the same authors showed that OPA1 KO in adipose tissue ameliorated IR [764]. Therefore, in adipose tissue OPA1 expression would contribute to IR, possibly by reducing FGF21 concentrations. These observations suggest that the effect of OPA1 depends on the tissue or the cell type. In addition, it has been demonstrated that OPA1-driven fusion inhibits chemotaxis in leukocytes [765]. The function of OPA1 in leukocyte populations might exist beyond chemotaxis, as neutrophils depend on OPA1 for the formation of neutrophils extracellular traps (NETs), and T memory lymphocytes need OPA1 for reprogramming [766,767]. Thus, OPA1 expression can have a positive or negative impact on cellular metabolism depending on the process and cell type. However, there is much evidence of the beneficial effect of OPA1 in T2D in different experimental settings [227,768,769]. Our analysis of OPA1 in T2D and healthy leukocytes presented in chapter 3 are in line with the beneficial effects of OPA1 in T2D at gene and protein level.

Furthermore, there is a broad consensus among studies examining the fission process, which has been shown to be enhanced in T2D. However, it is not known whether this is a cause or a consequence of T2D. The results presented in this thesis show an increase in the protein levels of FIS1 and DRP1, but a decrease in their gene expression. Previous results back our data, as a pro-fission phenotype has been previously assessed in T2D heart, driven by DRP-1 and reverted through the SIRT1- PPAR γ coactivator 1 (PGC1) pathway [770,771]. Similar results were

observed in a model of hyperglycaemic damage in retinal endothelial cells, and was mediated by DRP1 [772]. Despite fission being generally prejudicial and related to metabolic dysbalances, in cardiomyocytes DRP-1 has a protective effect against oxidative stress [773]. FIS1 also performs divergent functions as a protective or harmful protein depending on the tissue or cell type. As an example, hyperglycaemia causes an increase in FIS1 and DRP1 in retinal endothelial cells, while their inhibition prevents hyperglycaemia-triggered apoptosis [772]. In pancreatic β cells, which are characterized by a high sensitivity to glucose fluctuations and ROS, FIS1 expression is needed for an adequate insulin release as it helps the mitochondrial network to adapt [224]. Hence, as in the previous mitochondrial dynamics-related proteins, the regulation depends highly on the cell type, the stimuli and the cellular environment. Our results reflect an increase of DRP1 and FIS1 protein expression, which could be a compensatory response to glucolipotoxicity or a consequence of mitochondrial dysfunction.

Globally, the results of our analysis of mitochondrial dynamics suggest that there is a deregulation of fusion and fission in T2D. Further research in this direction needs to be carried out to determine the precise mechanisms at work in T2D leukocytes.

9. Evaluation of the UPR pathways in T2D leukocytes

Usually, ROS accumulation caused by hyperglycaemia, hyperlipidaemia and/or IR implies molecular modifications, as occurs with the previously discussed AGEs. But other modifications also take place, such as lipid peroxidation, protein glycation and protein lipidations, which end up causing accumulation of defective and misfolded proteins [463,464]. During the folding process, large loads of ROS are synthesized by ERO1α, the enzyme that assists PDI in creating disulphide bonds [91,774]. Apart from ROS produced by ERO1 isoforms, other ROS sources trigger ER stress by different direct and indirect mechanisms [465]. As an example, oxLDL activates UPR pathways, mainly the PERK pathway, which in turn activates autophagy [303]. Similarly, ROS induces PERK pathway in an animal model of diabetic cardiomyopathy, leading to apoptotic death [305].

With this information in mind, we aimed to explore whether there is ER stress reflected by activation of the UPR pathways in leukocytes from T2D patients. These pathways comprise a complex and coordinated cellular reaction to ER stress, and are activated in order to compensate for the loss of homeostasis [463,775]. By focusing on immune cells, a vast amount of research has shed light on the relevance of UPR in leukocyte homeostasis and activation [776–779]. Leukocytes in T2D display traits of ER stress, as observed in a previous study by our group, in which we reported that leukocytes from T2D patients with poor glycaemic control presented enhanced UPR markers. In the same study we determined that those patients with a good glycaemic control displayed increased rescue pathways, such as sXBP1 processing; but those with poor glycaemic control showed a peak in the pathways triggered by chronic ER stress and which culminate in apoptosis, marked by ATF6 and CHOP [313].

In this context, we show in this thesis that CHOP and GRP78 gene expression were upregulated in leukocytes from T2D patients with poor glycaemic control, while protein expression revealed a peak in GRP78 and in P-eIF2. We did not observe differences in other UPR activation markers, such as ATF6 or IRE1α. The data we present is in accordance with the

aforementioned studies, confirming that the PERK branch of the UPR is active in poorly controlled patients, and is reflected by enhanced gene expression of GRP78 and CHOP. Those genes are expressed regadless of eIF2α repression of protein translation and assist to overcome the proteostatic stress [256,269]. Regarding GRP78, its expression is upregulated during UPR through ATF4 independently of ERSE sequences, initiating a positive feedback loop that can help to resolve ER stress [254,780]. On the other hand, CHOP expression is upregulated by ATF4, but can exert protective or proapoptotic effects, as widely documented [254,476]. Not only those proteins, but the activation of the whole PERK-eIF2α-CHOP axis that occurs in T2D has been demonstrated in liver tissue, where an increase in ROS and a decrease in antioxidant enzymes were also assessed [298,781]. Among all T2D-affected tissues, pancreatic β cells are among the most affected by ER stress because of their secretory nature. This was confirmed by a study carried out in STZ T2D rats, which showed that activation of the PERK-CHOP axis leads to apoptosis in pancreatic β cells [782]. Nevertheless, the rescue function of the UPR, particularly the PERK pathway, has proven to be necessary in these cells, which have impaired insulin release and alter tissue structure under ER stress [428,783]. This rescue function can also be activated by the transcription factor CHOP through the transcription of autophagy genes, leading to the degradation of the altered or misfolded proteins that cause ER stress [472,476]. This constitutes the most accepted model by which CHOP expression by mild ER stress activates rescue mechanisms, but under chronic ER stress CHOP adopts a proapoptotic function. The results presented herein are in accordance with those previously observed in T2D, and contribute to the evidence that the UPR pathway, specifically PERK, is activated in leukocytes from T2D patients.

10. Activation of autophagy in T2D leukocytes

T2D damages cells through the mechanisms already discussed, namely ROS production, hypoglycaemia or hyperlipidaemia. In this context, rescue mechanisms such as UPR are vital for maintaining cellular homeostasis. One of these vital mechanisms is autophagy, which can be triggered by several cellular insults, such as nutrient deprivation or excess, oxidative stress or proteostatic stress. These stressors activate different cellular pathways that tightly modulate autophagy in its three stages: formation of the autophagosome, delivery of cargo, and fusion with the lysosome [351,410,784]. Many studies have explored the possible alterations of autophagy and their regulation in metabolic diseases, as they alter the energetic balance of the cell. Specifically, the tissues implied in T2D pathogenesis have been shown to display deep alterations in their autophagic machinery. Pancreatic tissue, and more precisely pancreatic β cells, depend on a functioning autophagy in order to resolve the high ER stress induced by glucolipotoxic aggressions [426]. β cells can induce autophagy in order to avoid apoptotic cell death, which can be caused after chronic exposure to hyperglycaemia and hyperlipidaemia and under IR. This was observed in a study in which mice models of high-fat or high glucose diet or a combination of both demonstrated that the combination of both diets or only HFD caused an increase in autophagic flux, greater β cell mass and increased proliferation for compensating the reduction of insulin production [46]. In the same research work, it was demonstrated that hampering autophagy caused damage in the pancreatic islets due to apoptotic β cell death, thus underlining the relevance of autophagy in rescuing cells under stress [46]. Moreover, this study demonstrated that autophagy also promotes β cell proliferation to assure the secretion of insulin and a proper pancreatic function. A similar model employed islets from healthy or T2D donors treated with palmitate and combinations of brefeldin, rapamycin or concanamycin A, and came to the conclusion that autophagy activation is beneficial for preventing apoptosis after activation of ER stress [428].

Despite the vast literature comcerning autophagy in pancreatic tissue from T2D patients or T2D models, knowledge about the regulation of autophagy in leukocytes in a T2D background is scarce. One study examined the inflammatory status of leukocytes from T2D patients and autophagy proteins and genes, observing that Beclin-1, LAMP2 and LC3II expression levels were reduced, p62 was increased, and no changes in ATG5 or ATG8 were detected. Moreover, the expression of proinflammatory molecules was markedly enhanced, and was related to the suppression of autophagy signalling. [452] A similar study determined that leukocytes from T2D patients displayed defective autophagy, reflected by reduced AMPK and LAMP2 and increased mTOR and p62, and a flawed fusion between the autophagosome and the lysosome [453]. In the same sense, a study carried out in leukocytes suggested that impairments in autophagy, reflected by accumulation of LC3II and p62 despite autophagy activation, are the reason for the increased inflammation and autophagy observed after palmitate treatment [455]. The alterations in these autophagy markers indicate that the defective autophagy is owing to a defective autophagosome degradation, which could be reverted with adequate autophagy regulation. All these studies carried out in leukocytes from T2D patients or leukocyte T2D models point to the hypothesis that chronic inflammation impairs autophagy in leukocytes from T2D patients, causing apoptosis and altered proinflammatory response.

Taking into account this information, we evaluated the expression of key autophagic molecules in leukocytes from T2D patients and healthy subjects. We observed a rise in Beclin-1 gene and protein expression, as well as in the LC3II/I ratio and a decrease of p62, which pointed to the activation of autophagy in T2D leukocytes. Furthermore, we observed that the impairment of the ETC by rotenone in healthy leukocytes reduce the expression of p62, similarly to the effect exerted with rapamycin treatment. This treatment did not alter other autophagic markers, meaning that ROS could induce autophagosome degradation or inhibit autophagy. Globally, we observed that leukocytes from T2D patients activated autophagy as a response to the hyperglycaemic and hyperlipidemic surroundings. To further confirm this phenotype, other

autophagic proteins should be examined, such as ATG5, 7 or AMPK and mTOR.

As explained before, most studies are in accordance that autophagy is downregulated in T2D, leaving cells unprotected against T2D-related stresses. Although this could be the case for some tissues, we observed that autophagy was correctly activated in response to the cellular stress. Compelling evidence backs our data and the activation of autophagy in different cell types and experimental models of T2D. One of the studies in question observed AMPK-dependent activation of autophagy in INS-1 pancreatic β cells treated with human islet amyloid peptide (hIAPP, a by-product of insulin synthesis that can accumulate and form deposits) [785]. hIAPP induced ROS production, which activated AMPK and autophagy, possibly to degrade the amyloid deposits that damage the cell. A similar phenomenon has been reported in human explants from pancreatic islets which displayed enhanced autophagy markers, and its blockage led to apoptotic cell death and defects in insulin production [46]. A steep rise in the autophagy markers Beclin-1, LC3II and p62 expression was found in heart tissue donated by non-T2D and T2D patients, and inhibition of Beclin-1 caused an increase of apoptotic cell death due to loss of autophagic rescue [439]. On the other hand, autophagy was activated in parallel to apoptosis in visceral adipose tissue but not in subcutaneous adipose tissue, highlighting that autophagy might be regulated differently in diverse tissues [445]. Likewise, activation of autophagy caused by mTOR inhibition was observed in biopsies of adipose tissue donated by obese T2D patients [446]. All this evidence suggests that autophagy regulation differs strikingly depending on the tissue and the environment, and that both inhibition and activation of autophagy could be mechanisms at work in T2D. Previous results from our laboratory have revealed an upregulation of autophagy in leukocytes from T2D patients, in line with our present results [312,786]. Hence, our findings support a protective effect of autophagy in leukocytes from T2D patients. However, the influence of the different treatments prescribed to T2D patients should be assessed and taken into account, as they may modify the regulation of autophagy and its upstream modulators.

In addition to the previously mentioned markers, we set out to explore the relation

between autophagy activation and the interaction between the leukocyte and the endothelium, for which we performed a statistical analysis of correlation. We observed that only Beclin-1 protein expression levels correlated with the different parameters of leukocyte-endothelium interactions, but that, curiously, the behaviour differed depending on the presence or not of T2D. Beclin-1 expression correlated with a lower number of rolling leukocytes, less leukocyte adhesion and higher leukocyte velocity in healthy subjects. This could lead us to think that, in the absence of pathology, defects in autophagy are related with inflammatory molecules involved in the leukocytary adhesion process, a hypothesis which would require further study. On the other hand, Beclin-1 was related to higher leukocyte rolling and adhesion in T2D leukocytes. These results could point to autophagy stimulation after or in parallel to leukocyte activation. A possible hypothesis is that the additional stress of leukocyte activation is buffered by autophagy activation, thus ensuring a correct cellular function in a T2D setting. In fact, it has been argued that excess ROS triggers autophagy to maintain cellular homeostasis, but also to limit exaggerated inflammation [454]. Furthermore, the relationship between autophagy and inflammation has been reinforced in a study in which an increase of autophagy markers was achieved by treating HUVEC with TNFα and IL-1β. The inverse relationship was also observed, as autophagy induced the adhesion of Jurkat cells to the HUVEC monolayer through autophagic degradation of IKβα, which allows NFκB translocation to the nucleus and transcription of VCAM-1 [787]. Beclin-1 has also been linked to autophagic degradation of the NLRP3 inflammasome for limiting IL-1β and IL-18 release in glia cells, establishing another link between this protein and inflammation [788]. Interestingly, Beclin-1 responds to thrombin by aiding inflammatory cytokine expression, NFκB activation and membrane permeabilization in endothelial cells [789]. However, the most promising pathway relating inflammation and Beclin-1 depends on the interaction with NFκB signalling through TGFβ-activated kinase 1 (TAK1) and their binding molecules TBK1 and 2. TBK1 and 2 can bind either Beclin-1 or TAK: under autophagy stimulation, they sequester TAK1, impeding NFκB translocation to the nucleus; however, under autophagy inhibition, these

molecules bind Beclin-1 and allow TAK1 to transport NFκB [790,791]. In this context, many possible theories could be raised about the function of Beclin-1 or autophagy in inflammation, but much further research is needed. Globally, our results support autophagy as a protective mechanism that is active in leukocytes in T2D, and which might have some influence on their response to inflammation.

11. T2D treatments: Metformin and SS-31

T2D has many therapeutic approaches, as stated in the introduction. However, metformin is the most prescribed drug due to its effectiveness in lowering hyperglycaemia, its mild side effects and easy administration for patients [792]. This drug can be combined with other antidiabetic treatments that bring specific clinical benefits and/or reduce side effects [793]. Its benefit is reflected not only in diabetic symptoms, but also in the improvement of inflammation [794,795], ER stress [61], mitochondrial function [796] and pancreatic β cell performance [428,797]. Hence, in this thesis we sought to determine if metformin treatment influences aspects of the metabolism of leukocytes.

To this end, we assessed leukocytes from patients who had been under metformin treatment at a dose of 1700 mg/day for at least 1 year. We compared their leukocyte-endothelium interactions, parameters of mitochondrial function and dynamics to those of healthy and non-treated T2D subjects. The results regarding mitochondrial function showed that, despite mitochondrial impairment and enhanced ROS production in T2D leukocytes, metformin was able to return the measured parameters to those of healthy subjects. More precisely, O_2 consumption and the membrane potential increased and ROS production dropped significantly in leukocytes from metformin-treated T2D patients. This could be attributable to metformin's nature as a homeostatic and antioxidant molecule, although the precise mechanism is still under debate. In this regard, some authors have suggested that the inhibitory effect of

metformin on complex I is dose-dependent and that it can exert an inhibitory function only at suprapharmacologic concentrations. However, an alternative mechanism has been proposed, which involves the inhibition of ROS production by induction of reverse electron transport in complex I. Experimental evidence has demonstrated that this precise mechanism is effective *in vitro* [79,798] and *in vivo* [799]; however, more research is needed to determine the precise mechanism by which metformin directly reduces ROS production.

Regarding the improvement in mitochondrial function, AMPK activation and G3PD inhibition are the most studied of the proposed mechanisms to date [52,800]. The mechanism behind AMPK activation involves the protection of mitochondrial function by boosting fission and protecting healthy mitochondria, as observed in HFD-fed mice [801]. This protein complex also increases mitochondrial biogenesis in response to metformin treatment, as assessed in endothelial cells [802] and cardiomyocytes [803,804]. A different AMPK-dependent mechanism for preventing ROS formation and mitochondrial damage has been observed in mice models; namely, DRP1 inhibition by AMPK [240,805]. AMPK can also regulate central metabolism pathways located in the mitochondria, inducing metabolic changes to increase energy expenditure, including the activation of β oxidation, the reduction of IR and lipid accumulation [806]. Hence, AMPK-dependent metformin mechanisms are pleiotropic, but most of them end in the improvement of mitochondrial function and, therefore, a reduction in ROS concentrations. Our work has yet to assess AMPK function in leukocytes from T2D patients, but we believe it could be an interesting approach for future works.

An aspect that seems to be modified by metformin and AMPK is mitochondrial dynamics, as set out by the aforementioned studies. Regardless of an AMPK-dependent or –independent mechanism, metformin treatment alters mitochondrial dynamics; however, little research has been done in this regard. Among the proposed mechanisms, re-establishing fusion and fission cycles through an AMPK-dependent mechanism has been shown to restore the respiratory capacity of damaged mitochondria in HFD-fed mice [801]. Similarly, it has been

determined that metformin treatment increases MFN2 expression and reduces mitochondrial dysfunction in oxLDL challenges RAW264.7 macrophages, possibly by AKT signalling [807]. Mitochondrial dynamics deregulation is a hallmark of some syndromes such as Rett syndrome or Down syndrome, in which metformin treatment has been seen to be beneficial by increasing mitochondrial fusion [63,808]. Due to the limited knowledge about the effect of metformin on mitochondrial dynamics, our results in leukocytes from T2D patients imply a significant contribution to the field. We have described that leukocytes from metformin-treated T2D patients display improved mitochondrial dynamics compared to non-treated T2D subjects. More precisely, metformin-treated patients displayed significantly higher protein expression of fusion molecules MFN1, MFN2 and OPA1, and reduced fission proteins DRP1 and FIS1. At the gene expression level, we observed that OPA1 did not recover its expression in metformin-treated patients, and this might have been due to the particular function of this protein in IMM fusion and reorganization. Similar discordances were seen in the gene expression of the fission genes FIS-1 and DRP-1 in metformin-treated patients: FIS-1 continued to be reduced, as in T2D patients, but DRP1 expression peaked and almost reached levels in the healthy population. These differences could be attributed to specific regulation of the translation of DRP1 and FIS1 genes or to the unusually long life of their translated mRNAs. Although this phenomenon is not well understood, we can affirm that metformin increases mitochondrial fusion and decreases fission at the protein level, therefore improving mitochondrial function. The mechanism behind this improvement is still unclear, at least in leukocytes, but it might be explained by AMPK signalling or a reduction in ROS production. Either way, future research is needed to bring clarity to the subject.

Although numerous T2D treatments have already been discovered, research continues to determine other therapeutic avenues and targets against T2D. A novel therapeutic mechanism tackles the imbalance between antioxidant capacity and pro-oxidant molecule accumulation in T2D. Boosting the antioxidant capacity of the cell is under debate, given the

limited efficacy of some experimental therapies. Among the different vitamin supplementation therapies available, a recent metaanalysis determined that only Vitamin E can help to prevent diabetic complications [809]. The antioxidant properties of already prescribed drugs have been studied, and most of them have been found to strongly induce the cellular antioxidant response [810]. For example, metformin, glibenclamide and repaglinide were shown to boost antioxidant enzymes SOD, CAT and glutathione (GSH) in alloxan-induced diabetic rats [811] and in STZ-induced diabetic mice [812]. Indeed, previous research by our group showed how 24-week treatment with empaglifozin increased the antioxidant response in leukocytes from T2D patients [813]. Until now, the antioxidant-inducing properties of the classic T2D treatments have been researched thoroughly and have been confirmed to effectively prevent cardiovascular complications [810,814]. As a consequence of the effectiveness of antioxidant-boosting therapies, finding new antioxidant strategies is now a growing field in antidiabetic treatment.

Among all the possible pathways for reducing oxidative stress or increasing antioxidant response, the most intuitive approach given the physiopathology of T2D is to reduce mitochondria-generated ROS by specifically targeting this organelle. Mitochondria-targeted antioxidants are a wide area of current research that has so far rendered many chemical structures with the following special ability: to quench ROS production without hindering mitochondrial function [815–817]. Among all the researched chemical structures, those with a better profile - and therefore the most studied - are lipophilic-cation linked structures, such as MitoQ, SkQ1, Mito-E and Mito-TEMPO, and peptide-based mitochondria antioxidants, such as SS peptides or mitochondria-penetrating peptides (MPPs). Among these, our group has described the beneficial properties of MitoQ in a T2D model of INS-1E cells, and also in leukocytes from T2D patients [163,164]. As we observed in previous studies that MitoQ improved mitochondrial function, reduced inflammation and diminished the cellular stress caused by hyperglycaemia and hyperlipidaemia, we decided to explore whether other therapeutic approaches would give similar benefits in T2D. Thus, we devoted part of this thesis to studying another antioxidant

strategy; namely, the effect of the peptide-based mitochondria antioxidant SS-31 on leukocytes from T2D patients. It is important to highlight that previous results from our laboratory determined that the treatment of leukocytes from T2D patients with the SS-31 peptide decreased oxidative stress, inflammation and increased SIRT1 levels [173]. Thus, we continued this line of research by assessing whether or not SS-31 was able to reduce the cellular stress provoked by T2D.

In chapter 4 we have demonstrated that SS-31 treatment reduces mtROS production and Ca^{2+} efflux in leukocytes from T2D patients. Moreover, these reductions are comparable to the effect of treating the leukocytes with catalase, an important antioxidant enzyme. We continued analysing the activation of cellular stress pathways caused by ROS accumulation, such as UPR activation and autophagy. We observed that SS-31 effectively reduced the UPR response by reducing GRP78 and CHOP gene expression, besides GRP78 and P-eIF2α protein levels, which points to a particular effect exerted on the PERK pathway. SS-31 treatment of T2D leukocytes also diminished the activation of autophagy, as shown by a reduction of protein levels of Beclin-1 and LC3, and a rise in p62 protein levels; and a parallel alteration of gene expression, reflected by a reduction in the expression of Beclin-1. Therefore, it could be deduced that SS-31 exerts a homeostatic effect in the leukocytes of T2D patients. We explored whether SS-31 could reduce the pharmacological induction of ROS production, ER-stress and autophagy by treating the leukocytes with rotenone, thapsigargin and rapamycin, respectively. We observed that SS-31 reduced thapsigargin-induced UPR activation and rotenone-induced GRP78 increase. Regarding autophagy, rapamycin-treated leukocytes displayed enhanced autophagy flux, which was not reduced by SS-31. These results reflect that SS-31 does not target one specific cellular process, but instead acts through the reduction of ROS cellular concentrations, thus contributing to cellular homeostasis. In all cases, we also used the negative control SS-20, which does not have the dimethyltyrosine residue responsible for ROS quenching. The null influence of this peptide reinforced the idea that its chemical structure *per se* does not alter cellular processes and that

its antioxidant property was responsible for the observed benefits. Globally, these results highlight the influence that a mitochondrial ROS scavenger strategy can exert on the cellular stress pathways activated by T2D conditions, and endorse such a strategy as a therapeutic tool for T2D treatment.

Other studies have obtained similar results in *in vivo* and *in vitro* models, underlining the therapeutic properties of this peptide with respect to T2D cellular consequences and cardiovascular complications [169,171,172,818]. In this sense, oral administration of a commercial form of the SS-31 peptide was demonstrated to prevent kidney complications in db/db mice by protecting mitochondrial function thanks to cardiolipin synthesis [172]. The benefit of SS-31 in T2D-associated renal disease was proved in STZ diabetic mice, where the peptide reduced renal cell fibrosis and apoptosis through inhibition of ROS production. SS-31 treatment also reduced the activity of key ROS-producing enzymes and normalized membrane potential and ATP production as observed in renal anfd mesangial cells analyzed in the same study [171]. SS-31 also has benefits for cardiac tissue, as illustrated by a study in which old mice displaying cardiac dysfunction were treated with SS-31 supplied by means of a minipump. The mitochondrial-targeted treatment improved the contractility of the cardiomyocytes due to restoration of the electron flux in the ETC and a reduction of the proton leak [818]. SS-31 also protected against the development of foam cell formation in a macrophage cell line treated with oxLDL. In the work in question it was found that SS-31 not only reduced ROS and upregulated SOD, but also downregulated the scavenger receptors CD36 and LOX-1 and diminished the expression of some inflammation markers [169]. This promising antioxidant therapy has also been shown to protect the liver tissue from Tallyho/JngJ mice, restoring mitochondrial function and promoting mitochondrial biogenesis and dynamics [227]. Taking all this knowledge into account, our work endorses existing discoveries, as it demonstrates that the SS-31 peptide has a remarkable biological relevance in the leukocytes of T2D patients by protecting mitochondria from glucolipotoxicity. Clinical trials have begun with the commercial forms of SS-31 (Elamipretide and Bendavia) with the objective

of evaluating the its security, tolerability and efficacy in different diseases, such as Barth syndrome [819–822], retinal diseases [823,824] and cardiovascular disease [825,826]. More assays in T2D patients or in human tissues are needed to fully disclose the function of SS-31 in different backgrounds and to possibly develop a new and effective drug against cardiovascular complications of T2D.

Globally, the results presented in this doctoral thesis underline the importance of mitochondrial function, dynamics and homeostatic pathways such as the UPR and autophagy in the leukocytes of T2D patients. Moreover, we believe that all these mechanisms are linked to the inflammation and development of atherosclerosis and the subsequent cardiovascular complications. We underline the relevance of studying these processes as a path for discovering new targets for T2D treatment. Nevertheless, we also endorse the benefits of metformin and SS-31 treatments for mitochondrial homeostasis and the cell by helping to overcome stress by downregulating stress-activated cellular pathways. Eventually, this cellular protection reduces leukocyte activation and promotes a less proinflammatory surrounding with fewer cardiovascular repercussions. The present thesis explores some of the pathways that explain the pathological mechanisms of T2D, but further research is needed to fully understand them.

6. CONCLUSIONS

1. Leukocytes from T2D patients display increased total and mitochondrial ROS production and a rise in cellular markers of autophagy and serum and cellular markers of inflammation compared to leukocytes from healthy subjects. This is reflected by an enhanced interaction with the endothelium that correlates with the autophagy marker Beclin-1. These findings suggest that autophagy and inflammation are related through a mechanism involving Beclin-1.
2. T2D patients with HbA_{1C}>6.5% display elevated levels of proinflammatory cytokines and soluble adhesion molecules. Accordingly, their leukocytes produce mitochondrial ROS and interact more with the endothelium compared with those with HbA_{1C}≤6.5%. Carotid intima-media thickness measurements are also higher in poorly controlled patients, which correlate with increased leukocyte interactions and a worse metabolic profile, especially in the case of left carotid measurements. Hence, sufficient glycemic control might be an effective approach to prevent the cardiovascular complications of T2D.
3. Mitochondrial function and dynamics are hampered in leukocytes from T2D patients, which show increased ROS production, lower membrane potential and less O_2 consumption and an imbalance towards mitochondrial fission. These leukocytes also interact more with the endothelium compared to those from healthy subjects. Sustained therapy with metformin exerts a beneficial effect at the mitochondrial level, ameliorating the mitochondrion's function and dynamics, evident in fewer leukocyte interactions with the endothelium than those of untreated T2D patients.
4. The mitochondria-targeted peptide with antioxidant action SS-31 reduces ROS production and ameliorates mitochondrial membrane potential and Ca^{2+} distribution in leukocytes from T2D patients. These benefits are reflected by cellular homeostatic processes in the reduction of ER stress and autophagy markers. Additionally, SS-31 treatment of leukocytes from T2D patients reduces their interaction with the endothelium.

7. BIBLIOGRAPHY

1. Association, A. D. 2. Classification and Diagnosis of Diabetes: Standards of Medical Care in Diabetes—2021. *Diabetes Care* **44**, S15–S33 (2021).

2. Association, A. D. 6. Glycemic Targets: Standards of Medical Care in Diabetes—2018. *Diabetes Care* **41**, S55–S64 (2018).

3. Association, A. D. 3. Prevention or Delay of Type 2 Diabetes: Standards of Medical Care in Diabetes—2021. *Diabetes Care* **44**, S34–S39 (2021).

4. Association, A. D. 9. Pharmacologic Approaches to Glycemic Treatment: Standards of Medical Care in Diabetes—2021. *Diabetes Care* **44**, S111–S124 (2021).

5. Chatterjee, S., Khunti, K. & Davies, M. J. Type 2 diabetes. *The Lancet* **389**, 2239–2251 (2017).

6. Association, A. D. 6. Glycemic Targets: Standards of Medical Care in Diabetes—2021. *Diabetes Care* **44**, S73–S84 (2021).

7. Fazeli Farsani, S., van der Aa, M. P., van der Vorst, M. M. J., Knibbe, C. A. J. & de Boer, A. Global trends in the incidence and prevalence of type 2 diabetes in children and adolescents: a systematic review and evaluation of methodological approaches. *Diabetologia* **56**, 1471–1488 (2013).

8. Saeedi, P. *et al.* Global and regional diabetes prevalence estimates for 2019 and projections for 2030 and 2045: Results from the International Diabetes Federation Diabetes Atlas, 9th edition. *Diabetes Res. Clin. Pract.* **157**, 107843 (2019).

9. Bommer, C. *et al.* The global economic burden of diabetes in adults aged 20-79 years: a cost-of-illness study. *Lancet Diabetes Endocrinol.* **5**, 423–430 (2017).

10. Kautzky-Willer, A., Harreiter, J. & Pacini, G. Sex and Gender Differences in Risk, Pathophysiology and Complications of Type 2 Diabetes Mellitus. *Endocr. Rev.* **37**, 278–316 (2016).

11. Singh, S. S. *et al.* Sex difference in the incidence of microvascular complications in patients with type 2 diabetes mellitus: a prospective cohort study. *Acta Diabetol.* **57**, 725–732 (2020).

12. Lim, H. M., Chia, Y. C. & Koay, Z. L. Performance of the Finnish Diabetes Risk Score (FINDRISC) and Modified Asian FINDRISC (ModAsian FINDRISC) for screening of undiagnosed type 2 diabetes mellitus and dysglycaemia in primary care. *Prim. Care Diabetes* **14**, 494–500 (2020).

13. Mao, T. *et al.* The Efficacy of New Chinese Diabetes Risk Score in Screening Undiagnosed Type 2 Diabetes and Prediabetes: A Community-Based Cross-Sectional Study in Eastern China. *J. Diabetes Res.* **2020**, 7463082 (2020).

14. Mavrogianni, C. *et al.* Evaluation of the Finnish Diabetes Risk Score as a screening tool for undiagnosed type 2 diabetes and dysglycaemia among early middle-aged adults in a large-scale European cohort. The Feel4Diabetes-study. *Diabetes Res. Clin. Pract.* **150**, 99–110

(2019).

15. Mirahmadizadeh, A. *et al.* The prevalence of undiagnosed type 2 diabetes and prediabetes in Eastern Mediterranean region (EMRO): A systematic review and meta-analysis. *Diabetes Res. Clin. Pract.* **160**, 107931 (2020).

16. Andersson, T. *et al.* Mortality trends and cause of death in patients with new-onset type 2 diabetes and controls: A 24-year follow-up prospective cohort study. *Diabetes Res. Clin. Pract.* **138**, 81–89 (2018).

17. Lawson, C. A. *et al.* Association Between Type 2 Diabetes and All-Cause Hospitalization and Mortality in the UK General Heart Failure Population: Stratification by Diabetic Glycemic Control and Medication Intensification. *JACC Heart Fail.* **6**, 18–26 (2018).

18. Zghebi, S. S. *et al.* Examining trends in type 2 diabetes incidence, prevalence and mortality in the UK between 2004 and 2014. *Diabetes Obes. Metab.* **19**, 1537–1545 (2017).

19. Association, A. D. Economic Costs of Diabetes in the U.S. in 2017. *Diabetes Care* **41**, 917–928 (2018).

20. Bommer, C. *et al.* Global Economic Burden of Diabetes in Adults: Projections From 2015 to 2030. *Diabetes Care* **41**, 963–970 (2018).

21. Han, H.-S., Kang, G., Kim, J. S., Choi, B. H. & Koo, S.-H. Regulation of glucose metabolism from a liver-centric perspective. *Exp. Mol. Med.* **48**, e218–e218 (2016).

22. Röder, P. V., Wu, B., Liu, Y. & Han, W. Pancreatic regulation of glucose homeostasis. *Exp. Mol. Med.* **48**, e219 (2016).

23. Copps, K. D. & White, M. F. Regulation of insulin sensitivity by serine/threonine phosphorylation of insulin receptor substrate proteins IRS1 and IRS2. *Diabetologia* **55**, 2565–2582 (2012).

24. Haeusler, R. A., McGraw, T. E. & Accili, D. Biochemical and cellular properties of insulin receptor signalling. *Nat. Rev. Mol. Cell Biol.* **19**, 31–44 (2018).

25. Nolan, C. J., Damm, P. & Prentki, M. Type 2 diabetes across generations: from pathophysiology to prevention and management. *The Lancet* **378**, 169–181 (2011).

26. Nauck, M. A. & Meier, J. J. Incretin hormones: Their role in health and disease. *Diabetes Obes. Metab.* **20**, 5–21 (2018).

27. Lanuza-Masdeu, J. *et al.* In Vivo JNK Activation in Pancreatic β-Cells Leads to Glucose Intolerance Caused by Insulin Resistance in Pancreas. *Diabetes* **62**, 2308–2317 (2013).

28. Kim, S.-Y. *et al.* SREBP-1c Mediates the Insulin-dependent Hepatic Glucokinase Expression*. *J. Biol. Chem.* **279**, 30823–30829 (2004).

29. Miller, R. A. & Birnbaum, M. J. Glucagon: acute actions on hepatic metabolism. *Diabetologia* **59**, 1376–1381 (2016).

30. Beg, M., Abdullah, N., Thowfeik, F. S., Altorki, N. K. & McGraw, T. E. Distinct Akt

phosphorylation states are required for insulin regulated Glut4 and Glut1-mediated glucose uptake. *eLife* **6**, e26896 (2017).

31. Meng, Z.-X. *et al.* Glucose sensing by skeletal myocytes couples nutrient signaling to systemic homeostasis. *Mol. Cell* **66**, 332-344.e4 (2017).

32. Montessuit, C. & Lerch, R. Regulation and dysregulation of glucose transport in cardiomyocytes. *Biochim. Biophys. Acta BBA - Mol. Cell Res.* **1833**, 848–856 (2013).

33. Minokoshi, Y., Kahn, C. R. & Kahn, B. B. Tissue-specific Ablation of the GLUT4 Glucose Transporter or the Insulin Receptor Challenges Assumptions about Insulin Action and Glucose Homeostasis *. *J. Biol. Chem.* **278**, 33609–33612 (2003).

34. Morigny, P., Boucher, J., Arner, P. & Langin, D. Lipid and glucose metabolism in white adipocytes: pathways, dysfunction and therapeutics. *Nat. Rev. Endocrinol.* **17**, 276–295 (2021).

35. Cretenet, G. *et al.* Cell surface Glut1 levels distinguish human CD4 and CD8 T lymphocyte subsets with distinct effector functions. *Sci. Rep.* **6**, 24129 (2016).

36. Palmer, C. S., Ostrowski, M., Balderson, B., Christian, N. & Crowe, S. M. Glucose Metabolism Regulates T Cell Activation, Differentiation, and Functions. *Front. Immunol.* **6**, 1 (2015).

37. DeFronzo, R. A. & Tripathy, D. Skeletal Muscle Insulin Resistance Is the Primary Defect in Type 2 Diabetes. *Diabetes Care* **32**, S157–S163 (2009).

38. Kitessa, S. M. & Abeywardena, M. Y. Lipid-Induced Insulin Resistance in Skeletal Muscle: The Chase for the Culprit Goes from Total Intramuscular Fat to Lipid Intermediates, and Finally to Species of Lipid Intermediates. *Nutrients* **8**, 466 (2016).

39. Li, Y., Xu, S., Zhang, X., Yi, Z. & Cichello, S. Skeletal intramyocellular lipid metabolism and insulin resistance. *Biophys. Rep.* **1**, 90–98 (2015).

40. Lyu, K. *et al.* A Membrane-Bound Diacylglycerol Species Induces PKCε-Mediated Hepatic Insulin Resistance. *Cell Metab.* **32**, 654-664.e5 (2020).

41. Petersen, M. C., Vatner, D. F. & Shulman, G. I. Regulation of hepatic glucose metabolism in health and disease. *Nat. Rev. Endocrinol.* **13**, 572–587 (2017).

42. Saini, V. Molecular mechanisms of insulin resistance in type 2 diabetes mellitus. *World J. Diabetes* **1**, 68–75 (2010).

43. Samuel, V. T. & Shulman, G. I. The pathogenesis of insulin resistance: integrating signaling pathways and substrate flux. *J. Clin. Invest.* **126**, 12–22 (2016).

44. Maedler, K. *et al.* Glucose-induced β cell production of IL-1β contributes to glucotoxicity in human pancreatic islets. *J. Clin. Invest.* **110**, 851–860 (2002).

45. El-Assaad, W. *et al.* Saturated fatty acids synergize with elevated glucose to cause pancreatic beta-cell death. *Endocrinology* **144**, 4154–4163 (2003).

46. Sheng, Q. *et al.* Autophagy protects pancreatic beta cell mass and function in the setting of a high-fat and high-glucose diet. *Sci. Rep.* **7**, 16348 (2017).

47. Gurgul-Convey, E., Mehmeti, I., Plötz, T., Jörns, A. & Lenzen, S. Sensitivity profile of the human EndoC-βH1 beta cell line to proinflammatory cytokines. *Diabetologia* **59**, 2125–2133 (2016).

48. Newsholme, P., Cruzat, V. F., Keane, K. N., Carlessi, R. & de Bittencourt, P. I. H. Molecular mechanisms of ROS production and oxidative stress in diabetes. *Biochem. J.* **473**, 4527–4550 (2016).

49. Lori, G. *et al.* Honey extracts inhibit PTP1B, upregulate insulin receptor expression, and enhance glucose uptake in human HepG2 cells. *Biomed. Pharmacother.* **113**, 108752 (2019).

50. Pirola, L. *et al.* Phosphoinositide 3-kinase-mediated reduction of insulin receptor substrate-1/2 protein expression via different mechanisms contributes to the insulin-induced desensitization of its signaling pathways in L6 muscle cells. *J. Biol. Chem.* **278**, 15641–15651 (2003).

51. Wang, Y., Nishina, P. M. & Naggert, J. K. Degradation of IRS1 leads to impaired glucose uptake in adipose tissue of the type 2 diabetes mouse model TALLYHO/Jng. *J. Endocrinol.* **203**, 65–74 (2009).

52. Rena, G., Hardie, D. G. & Pearson, E. R. The mechanisms of action of metformin. *Diabetologia* **60**, 1577–1585 (2017).

53. Fontaine, E. Metformin-Induced Mitochondrial Complex I Inhibition: Facts, Uncertainties, and Consequences. *Front. Endocrinol.* **9**, (2018).

54. Hunter, R. W. *et al.* Metformin reduces liver glucose production by inhibition of fructose-1-6-bisphosphatase. *Nat. Med.* **24**, 1395–1406 (2018).

55. Miller, R. A. *et al.* Biguanides suppress hepatic glucagon signaling by decreasing production of cyclic AMP. *Nature* **494**, 256–260 (2013).

56. Lee, M. *et al.* Phosphorylation of Acetyl-CoA Carboxylase by AMPK Reduces Renal Fibrosis and Is Essential for the Anti-Fibrotic Effect of Metformin. *J. Am. Soc. Nephrol.* **29**, 2326–2336 (2018).

57. Bułdak, Ł. *et al.* Metformin affects macrophages' phenotype and improves the activity of glutathione peroxidase, superoxide dismutase, catalase and decreases malondialdehyde concentration in a partially AMPK-independent manner in LPS-stimulated human monocytes/macrophages. *Pharmacol. Rep.* **66**, 418–429 (2014).

58. Ouslimani, N. *et al.* Metformin decreases intracellular production of reactive oxygen species in aortic endothelial cells. *Metabolism.* **54**, 829–834 (2005).

59. Rösen, P. & Wiernsperger, N. F. Metformin delays the manifestation of diabetes and vascular dysfunction in Goto–Kakizaki rats by reduction of mitochondrial oxidative stress.

Diabetes Metab. Res. Rev. **22**, 323–330 (2006).

60. Wu, J. *et al.* Pancreatic mitochondrial complex I exhibits aberrant hyperactivity in diabetes. *Biochem. Biophys. Rep.* **11**, 119–129 (2017).

61. Docrat, T. F. *et al.* The protective effect of metformin on mitochondrial dysfunction and endoplasmic reticulum stress in diabetic mice brain. *Eur. J. Pharmacol.* **875**, 173059 (2020).

62. García-Puga, M., Saenz-Antoñanzas, A., Fernández-Torrón, R., de Munain, A. L. & Matheu, A. Myotonic Dystrophy type 1 cells display impaired metabolism and mitochondrial dysfunction that are reversed by metformin. *Aging* **12**, 6260–6275 (2020).

63. Izzo, A. *et al.* Metformin restores the mitochondrial network and reverses mitochondrial dysfunction in Down syndrome cells. *Hum. Mol. Genet.* **26**, 1056–1069 (2017).

64. Wulffelé, M. G. *et al.* Combination of Insulin and Metformin in the Treatment of Type 2 Diabetes. *Diabetes Care* **25**, 2133–2140 (2002).

65. Holden, S. E., Jenkins-Jones, S. & Currie, C. J. Association between Insulin Monotherapy versus Insulin plus Metformin and the Risk of All-Cause Mortality and Other Serious Outcomes: A Retrospective Cohort Study. *PLOS ONE* **11**, e0153594 (2016).

66. Consortium, T. R. Impact of Insulin and Metformin Versus Metformin Alone on β-Cell Function in Youth With Impaired Glucose Tolerance or Recently Diagnosed Type 2 Diabetes. *Diabetes Care* **41**, 1717–1725 (2018).

67. Sena, L. A. & Chandel, N. S. Physiological roles of mitochondrial reactive oxygen species. *Mol. Cell* **48**, 158–167 (2012).

68. Volpe, C. M. O., Villar-Delfino, P. H., dos Anjos, P. M. F. & Nogueira-Machado, J. A. Cellular death, reactive oxygen species (ROS) and diabetic complications. *Cell Death Dis.* **9**, 1–9 (2018).

69. Kwak, S. H., Park, K. S., Lee, K. & Lee, H. K. Mitochondrial metabolism and diabetes. *J. Diabetes Investig.* **1**, 161–169 (2010).

70. Guo, R., Gu, J., Zong, S., Wu, M. & Yang, M. Structure and mechanism of mitochondrial electron transport chain. *Biomed. J.* **41**, 9–20 (2018).

71. Hunte, C., Zickermann, V. & Brandt, U. Functional Modules and Structural Basis of Conformational Coupling in Mitochondrial Complex I. *Science* **329**, 448–451 (2010).

72. Sun, F. *et al.* Crystal Structure of Mitochondrial Respiratory Membrane Protein Complex II. *Cell* **121**, 1043–1057 (2005).

73. Iverson, T. M. “Catalytic mechanisms of Complex II enzymes: A structural perspective”. *Biochim. Biophys. Acta* **1827**, 648–657 (2013).

74. Cramer, W. A., Hasan, S. S. & Yamashita, E. The Q Cycle of Cytochrome bc Complexes: a Structure Perspective. *Biochim. Biophys. Acta* **1807**, 788–802 (2011).

75. Shimada, S. *et al.* Complex structure of cytochrome c–cytochrome c oxidase reveals a novel

protein–protein interaction mode. *EMBO J.* **36**, 291–300 (2017).

76. Zhao, R.-Z., Jiang, S., Zhang, L. & Yu, Z.-B. Mitochondrial electron transport chain, ROS generation and uncoupling (Review). *Int. J. Mol. Med.* **44**, 3–15 (2019).

77. Jonckheere, A. I., Smeitink, J. A. M. & Rodenburg, R. J. T. Mitochondrial ATP synthase: architecture, function and pathology. *J. Inherit. Metab. Dis.* **35**, 211–225 (2012).

78. Murphy, M. P. How mitochondria produce reactive oxygen species. *Biochem. J.* **417**, 1–13 (2009).

79. Batandier, C. *et al.* The ROS Production Induced by a Reverse-Electron Flux at Respiratory-Chain Complex 1 is Hampered by Metformin. *J. Bioenerg. Biomembr.* **38**, 33–42 (2006).

80. Robb, E. L. *et al.* Control of mitochondrial superoxide production by reverse electron transport at complex I. *J. Biol. Chem.* **293**, 9869–9879 (2018).

81. Starkov, A. A. An update on the role of mitochondrial α-ketoglutarate dehydrogenase in oxidative stress. *Mol. Cell. Neurosci.* **55**, 13–16 (2013).

82. Tretter, L. Generation of Reactive Oxygen Species in the Reaction Catalyzed by -Ketoglutarate Dehydrogenase. *J. Neurosci.* **24**, 7771–7778 (2004).

83. Giacco Ferdinando, Brownlee Michael, & Schmidt Ann Marie. Oxidative Stress and Diabetic Complications. *Circ. Res.* **107**, 1058–1070 (2010).

84. Rolo, A. P. & Palmeira, C. M. Diabetes and mitochondrial function: Role of hyperglycemia and oxidative stress. *Toxicol. Appl. Pharmacol.* **212**, 167–178 (2006).

85. Buse, M. G. Hexosamines, insulin resistance and the complications of diabetes: current status. *Am. J. Physiol. Endocrinol. Metab.* **290**, E1–E8 (2006).

86. Singh, V. P., Bali, A., Singh, N. & Jaggi, A. S. Advanced Glycation End Products and Diabetic Complications. *Korean J. Physiol. Pharmacol. Off. J. Korean Physiol. Soc. Korean Soc. Pharmacol.* **18**, 1–14 (2014).

87. Stirban, A., Gawlowski, T. & Roden, M. Vascular effects of advanced glycation endproducts: Clinical effects and molecular mechanisms. *Mol. Metab.* **3**, 94–108 (2013).

88. Biswas, S., Gupta, M. K., Chattopadhyay, D. & Mukhopadhyay, C. K. Insulin-induced activation of hypoxia-inducible factor-1 requires generation of reactive oxygen species by NADPH oxidase. *Am. J. Physiol.-Heart Circ. Physiol.* **292**, H758–H766 (2007).

89. Baillet, A. *et al.* Unexpected function of the phagocyte NADPH oxidase in supporting hyperglycolysis in stimulated neutrophils: key role of 6-phosphofructo-2-kinase. *FASEB J.* **31**, 663–673 (2017).

90. García-Nogales, P., Almeida, A. & Bolaños, J. P. Peroxynitrite protects neurons against nitric oxide-mediated apoptosis. A key role for glucose-6-phosphate dehydrogenase activity in neuroprotection. *J. Biol. Chem.* **278**, 864–874 (2003).

91. Araki, K. *et al.* Ero1-α and PDIs constitute a hierarchical electron transfer network of

endoplasmic reticulum oxidoreductases. *J. Cell Biol.* **202**, 861–874 (2013).

92. Forrester, S. J., Kikuchi, D. S., Hernandes, M. S., Xu, Q. & Griendling, K. K. Reactive Oxygen Species in Metabolic and Inflammatory Signaling. *Circ. Res.* **122**, 877–902 (2018).

93. Nishikawa, T. & Araki, E. Impact of Mitochondrial ROS Production in the Pathogenesis of Diabetes Mellitus and Its Complications. *Antioxid. Redox Signal.* **9**, 343–353 (2007).

94. Guo, S. *et al.* Inactivation of specific β cell transcription factors in type 2 diabetes. *J. Clin. Invest.* **123**, 3305–3316 (2013).

95. Newsholme, P., Keane, K. N., Carlessi, R. & Cruzat, V. Oxidative stress pathways in pancreatic β-cells and insulin-sensitive cells and tissues: importance to cell metabolism, function, and dysfunction. *Am. J. Physiol.-Cell Physiol.* **317**, C420–C433 (2019).

96. Yung, J. H. M. & Giacca, A. Role of c-Jun N-terminal Kinase (JNK) in Obesity and Type 2 Diabetes. *Cells* **9**, 706 (2020).

97. Kaneto, H., Katakami, N., Matsuhisa, M. & Matsuoka, T. Role of reactive oxygen species in the progression of type 2 diabetes and atherosclerosis. *Mediators Inflamm.* **2010**, 453892 (2010).

98. Patche, J. *et al.* Diabetes-induced hepatic oxidative stress: a new pathogenic role for glycated albumin. *Free Radic. Biol. Med.* **102**, 133–148 (2017).

99. Ren, C. *et al.* A polysaccharide extract of mulberry leaf ameliorates hepatic glucose metabolism and insulin signaling in rats with type 2 diabetes induced by high fat-diet and streptozotocin. *Int. J. Biol. Macromol.* **72**, 951–959 (2015).

100. Raza, H., John, A. & Howarth, F. C. Increased Oxidative Stress and Mitochondrial Dysfunction in Zucker Diabetic Rat Liver and Brain. *Cell. Physiol. Biochem.* **35**, 1241–1251 (2015).

101. Ding, H. *et al.* Chronic reactive oxygen species exposure inhibits glucose uptake and causes insulin resistance in C2C12 myotubes. *Biochem. Biophys. Res. Commun.* **478**, 798–803 (2016).

102. Lee, H.-Y. *et al.* Mitochondrial-Targeted Catalase Protects Against High-Fat Diet–Induced Muscle Insulin Resistance by Decreasing Intramuscular Lipid Accumulation. *Diabetes* **66**, 2072–2081 (2017).

103. Peluso, G. *et al.* Decreased mitochondrial carnitine translocase in skeletal muscles impairs utilization of fatty acids in insulin-resistant patients. *Front. Biosci. J. Virtual Libr.* **7**, a109-116 (2002).

104. Haffar, T., Akoumi, A. & Bousette, N. Lipotoxic Palmitate Impairs the Rate of β-Oxidation and Citric Acid Cycle Flux in Rat Neonatal Cardiomyocytes. *Cell. Physiol. Biochem.* **40**, 969–981 (2016).

105. Tsushima, K. *et al.* Mitochondrial Reactive Oxygen Species in Lipotoxic Hearts Induce Post-Translational Modifications of AKAP121, DRP1, and OPA1 That Promote Mitochondrial

Fission. *Circ. Res.* **122**, 58–73 (2018).

106. Szendroedi, J. *et al.* Role of diacylglycerol activation of PKCθ in lipid-induced muscle insulin resistance in humans. *Proc. Natl. Acad. Sci. U. S. A.* **111**, 9597–9602 (2014).

107. Di Meo, S., Iossa, S. & Venditti, P. Skeletal muscle insulin resistance: role of mitochondria and other ROS sources. *J. Endocrinol.* **233**, R15–R42 (2017).

108. Han, C. Y. Roles of Reactive Oxygen Species on Insulin Resistance in Adipose Tissue. *Diabetes Metab. J.* **40**, 272 (2016).

109. Park, Y. J., Choe, S. S., Sohn, J. H. & Kim, J. B. The role of glucose-6-phosphate dehydrogenase in adipose tissue inflammation in obesity. *Adipocyte* **6**, 147–153 (2017).

110. Den Hartigh, L. J. *et al.* Adipocyte-Specific Deficiency of NADPH Oxidase 4 Delays the Onset of Insulin Resistance and Attenuates Adipose Tissue Inflammation in Obesity. *Arterioscler. Thromb. Vasc. Biol.* **37**, 466–475 (2017).

111. Kim, S. Y. *et al.* Pro-inflammatory hepatic macrophages generate ROS through NADPH oxidase 2 via endocytosis of monomeric TLR4–MD2 complex. *Nat. Commun.* **8**, 2247 (2017).

112. Castro, J. P., Grune, T. & Speckmann, B. The two faces of reactive oxygen species (ROS) in adipocyte function and dysfunction. *Biol. Chem.* **397**, 709–724 (2016).

113. Kaplan, J. L. *et al.* Adipocyte progenitor cells initiate monocyte chemoattractant protein-1-mediated macrophage accumulation in visceral adipose tissue. *Mol. Metab.* **4**, 779–794 (2015).

114. Cusi, K. The Role of Adipose Tissue and Lipotoxicity in the Pathogenesis of Type 2 Diabetes. *Curr. Diab. Rep.* **10**, 306–315 (2010).

115. Eckel-Mahan, K., Ribas Latre, A. & Kolonin, M. G. Adipose Stromal Cell Expansion and Exhaustion: Mechanisms and Consequences. *Cells* **9**, 863 (2020).

116. Shurtz-Swirski, R. *et al.* Involvement of Peripheral Polymorphonuclear Leukocytes in Oxidative Stress and Inflammation in Type 2 Diabetic Patients. *Diabetes Care* **24**, 104–110 (2001).

117. Chen, P., Thandra, V. R., Scicli, G. M., Edwards, P. A. & Scicli, A. G. Role of Reactive Oxygen Species in Retinal Leukostasis of Diabetic Rats. *Invest. Ophthalmol. Vis. Sci.* **47**, 1711–1711 (2006).

118. Eid, H. M., Lyberg, T., Larsen, J., Arnesen, H. & Seljeflot, I. Reactive oxygen species generation by leukocytes in populations at risk for atherosclerotic disease. *Scand. J. Clin. Lab. Invest.* **62**, 431–439 (2002).

119. Jadeja, R. N., Devkar, R. V. & Nammi, S. Oxidative Stress in Liver Diseases: Pathogenesis, Prevention, and Therapeutics. *Oxid. Med. Cell. Longev.* **2017**, 8341286 (2017).

120. Incalza, M. A. *et al.* Oxidative stress and reactive oxygen species in endothelial dysfunction

associated with cardiovascular and metabolic diseases. *Vascul. Pharmacol.* **100**, 1–19 (2018).

121. Steven, S. *et al.* Vascular Inflammation and Oxidative Stress: Major Triggers for Cardiovascular Disease. *Oxid. Med. Cell. Longev.* **2019**, 7092151 (2019).

122. Vona, R., Gambardella, L., Cittadini, C., Straface, E. & Pietraforte, D. Biomarkers of Oxidative Stress in Metabolic Syndrome and Associated Diseases. *Oxid. Med. Cell. Longev.* **2019**, 8267234 (2019).

123. Luo, J., Mills, K., le Cessie, S., Noordam, R. & van Heemst, D. Ageing, age-related diseases and oxidative stress: What to do next? *Ageing Res. Rev.* **57**, 100982 (2020).

124. Papaconstantinou, J. The Role of Signaling Pathways of Inflammation and Oxidative Stress in Development of Senescence and Aging Phenotypes in Cardiovascular Disease. *Cells* **8**, (2019).

125. Rhee, S. Y. & Kim, Y. S. The Role of Advanced Glycation End Products in Diabetic Vascular Complications. *Diabetes Metab. J.* **42**, 188–195 (2018).

126. Yamagishi, S. Role of advanced glycation end products (AGEs) and receptor for AGEs (RAGE) in vascular damage in diabetes. *Exp. Gerontol.* **46**, 217–224 (2011).

127. Hirose, A., Tanikawa, T., Mori, H., Okada, Y. & Tanaka, Y. Advanced glycation end products increase endothelial permeability through the RAGE/Rho signaling pathway. *FEBS Lett.* **584**, 61–66 (2010).

128. Greifenhagen, U., Frolov, A., Blüher, M. & Hoffmann, R. Plasma Proteins Modified by Advanced Glycation End Products (AGEs) Reveal Site-specific Susceptibilities to Glycemic Control in Patients with Type 2 Diabetes *. *J. Biol. Chem.* **291**, 9610–9616 (2016).

129. Ceriello, A., Ihnat, M. A. & Thorpe, J. E. The "Metabolic Memory": Is More Than Just Tight Glucose Control Necessary to Prevent Diabetic Complications? *J. Clin. Endocrinol. Metab.* **94**, 410–415 (2009).

130. Yuan, T. *et al.* New insights into oxidative stress and inflammation during diabetes mellitus-accelerated atherosclerosis. *Redox Biol.* **20**, 247–260 (2019).

131. Dong, K. *et al.* ROS-mediated glucose metabolic reprogram induces insulin resistance in type 2 diabetes. *Biochem. Biophys. Res. Commun.* **476**, 204–211 (2016).

132. Calvo-Ochoa, E., Sánchez-Alegría, K., Gómez-Inclán, C., Ferrera, P. & Arias, C. Palmitic acid stimulates energy metabolism and inhibits insulin/PI3K/AKT signaling in differentiated human neuroblastoma cells: The role of mTOR activation and mitochondrial ROS production. *Neurochem. Int.* **110**, 75–83 (2017).

133. Wang, K., Liang, Y., Su, Y. & Wang, L. DhHP-6 ameliorates hepatic oxidative stress and insulin resistance in type 2 diabetes mellitus through the PI3K/AKT and AMPK pathway. *Biochem. J.* **477**, 2363–2381 (2020).

134. Gao, D. *et al.* The effects of palmitate on hepatic insulin resistance are mediated by NADPH

Oxidase 3-derived reactive oxygen species through JNK and p38MAPK pathways. *J. Biol. Chem.* **285**, 29965–29973 (2010).

135. Gao, W. *et al.* NEFA-induced ROS impaired insulin signalling through the JNK and p38MAPK pathways in non-alcoholic steatohepatitis. *J. Cell. Mol. Med.* **22**, 3408–3422 (2018).

136. Zhang, D. *et al.* Kakkalide ameliorates endothelial insulin resistance by suppressing reactive oxygen species-associated inflammation. *J. Diabetes* **5**, 13–24 (2013).

137. Fukai, T. & Ushio-Fukai, M. Superoxide Dismutases: Role in Redox Signaling, Vascular Function, and Diseases. *Antioxid. Redox Signal.* **15**, 1583–1606 (2011).

138. Wang, Y., Branicky, R., Noë, A. & Hekimi, S. Superoxide dismutases: Dual roles in controlling ROS damage and regulating ROS signaling. *J. Cell Biol.* **217**, 1915–1928 (2018).

139. Flekac, M., Skrha, J., Hilgertova, J., Lacinova, Z. & Jarolimkova, M. Gene polymorphisms of superoxide dismutases and catalase in diabetes mellitus. *BMC Med. Genet.* **9**, 30 (2008).

140. Nandi, A., Yan, L.-J., Jana, C. K. & Das, N. Role of Catalase in Oxidative Stress- and Age-Associated Degenerative Diseases. *Oxidative Medicine and Cellular Longevity* vol. 2019 e9613090 (2019).

141. Góth, L. Catalase Deficiency and Type 2 Diabetes. *Diabetes Care* **31**, e93–e93 (2008).

142. Goth, L. & Eaton, J. W. Hereditary catalase deficiencies and increased risk of diabetes. *The Lancet* **356**, 1820–1821 (2000).

143. Strom, A. *et al.* Lower serum extracellular superoxide dismutase levels are associated with polyneuropathy in recent-onset diabetes. *Exp. Mol. Med.* **49**, e394 (2017).

144. Atli, T. *et al.* Oxidative stress and antioxidant status in elderly diabetes mellitus and glucose intolerance patients. *Arch. Gerontol. Geriatr.* **39**, 269–275 (2004).

145. Neelofar, K., Arif, Z., Arafat, M. Y., Alam, K. & Ahmad, J. A study on correlation between oxidative stress parameters and inflammatory markers in type 2 diabetic patients with kidney dysfunction in north Indian population. *J. Cell. Biochem.* **120**, 4892–4902 (2019).

146. Siemianowicz, K. *et al.* Blood antioxidant parameters in patients with diabetic retinopathy. *Int. J. Mol. Med.* **14**, 433–437 (2004).

147. Sindhu, R. K., Koo, J.-R., Roberts, C. K. & Vaziri, N. D. Dysregulation of hepatic superoxide dismutase, catalase and glutathione peroxidase in diabetes: response to insulin and antioxidant therapies. *Clin. Exp. Hypertens. N. Y. N 1993* **26**, 43–53 (2004).

148. Siddiqui, A. *et al.* Association of oxidative stress and inflammatory markers with chronic stress in patients with newly diagnosed type 2 diabetes. *Diabetes Metab. Res. Rev.* **35**, e3147 (2019).

149. Bandeira, S. de M. *et al.* Characterization of blood oxidative stress in type 2 diabetes mellitus patients: increase in lipid peroxidation and SOD activity. *Oxid. Med. Cell. Longev.* **2012**, 819310 (2012).

150. Ivanović-Matić, S. *et al.* The absence of cardiomyopathy is accompanied by increased activities of CAT, MnSOD and GST in long-term diabetes in rats. *J. Physiol. Sci. JPS* **60**, 259–266 (2010).

151. Banerjee, M. & Vats, P. Reactive metabolites and antioxidant gene polymorphisms in Type 2 diabetes mellitus. *Redox Biol.* **2**, 170–177 (2013).

152. Banerjee, M., Vats, P., Kushwah, A. S. & Srivastava, N. Interaction of antioxidant gene variants and susceptibility to type 2 diabetes mellitus. *Br. J. Biomed. Sci.* **76**, 166–171 (2019).

153. Adelusi, T. I. *et al.* Keap1/Nrf2/ARE signaling unfolds therapeutic targets for redox imbalanced-mediated diseases and diabetic nephropathy. *Biomed. Pharmacother.* **123**, 109732 (2020).

154. Uruno, A. *et al.* The Keap1-Nrf2 System Prevents Onset of Diabetes Mellitus. *Mol. Cell. Biol.* **33**, 2996–3010 (2013).

155. Bhakkiyalakshmi, E., Sireesh, D., Rajaguru, P., Paulmurugan, R. & Ramkumar, K. M. The emerging role of redox-sensitive Nrf2–Keap1 pathway in diabetes. *Pharmacol. Res.* **91**, 104–114 (2015).

156. Jiménez-Osorio, A. S. *et al.* Nrf2 and redox status in prediabetic and diabetic patients. *Int. J. Mol. Sci.* **15**, 20290–20305 (2014).

157. Jiang, Z. *et al.* MicroRNA-200a improves diabetic endothelial dysfunction by targeting KEAP1/NRF2. *J. Endocrinol.* **245**, 129–140 (2020).

158. Slocum, S. L. *et al.* Keap1/Nrf2 pathway activation leads to a repressed hepatic gluconeogenic and lipogenic program in mice on a high-fat diet. *Arch. Biochem. Biophys.* **591**, 57–65 (2016).

159. David, J. A., Rifkin, W. J., Rabbani, P. S. & Ceradini, D. J. The Nrf2/Keap1/ARE Pathway and Oxidative Stress as a Therapeutic Target in Type II Diabetes Mellitus. *J. Diabetes Res.* **2017**, (2017).

160. Ashrafizadeh, M., Ahmadi, Z., Mohammadinejad, R., Farkhondeh, T. & Samarghandian, S. Curcumin Activates the Nrf2 Pathway and Induces Cellular Protection Against Oxidative Injury. *Curr. Mol. Med.* **20**, 116–133 (2020).

161. Pugazhenthi, S., Akhov, L., Selvaraj, G., Wang, M. & Alam, J. Regulation of heme oxygenase-1 expression by demethoxy curcuminoids through Nrf2 by a PI3-kinase/Akt-mediated pathway in mouse beta-cells. *Am. J. Physiol. Endocrinol. Metab.* **293**, E645-655 (2007).

162. Rashid, K. & Sil, P. C. Curcumin enhances recovery of pancreatic islets from cellular stress induced inflammation and apoptosis in diabetic rats. *Toxicol. Appl. Pharmacol.* **282**, 297–310 (2015).

163. Escribano-Lopez, I. *et al.* The Mitochondria-Targeted Antioxidant MitoQ Modulates Mitochondrial Function and Endoplasmic Reticulum Stress in Pancreatic β Cells Exposed to

Hyperglycaemia. *Cell. Physiol. Biochem. Int. J. Exp. Cell. Physiol. Biochem. Pharmacol.* **52**, 186–197 (2019).

164. Escribano-Lopez, I. *et al.* The mitochondria-targeted antioxidant MitoQ modulates oxidative stress, inflammation and leukocyte-endothelium interactions in leukocytes isolated from type 2 diabetic patients. *Redox Biol.* **10**, 200–205 (2016).

165. Lim, S. *et al.* Mitochondria-targeted antioxidants protect pancreatic β-cells against oxidative stress and improve insulin secretion in glucotoxicity and glucolipotoxicity. *Cell. Physiol. Biochem. Int. J. Exp. Cell. Physiol. Biochem. Pharmacol.* **28**, 873–886 (2011).

166. Yang, M.-Y., Fan, Z., Zhang, Z. & Fan, J. MitoQ protects against high glucose-induced brain microvascular endothelial cells injury via the Nrf2/HO-1 pathway. *J. Pharmacol. Sci.* **145**, 105–114 (2021).

167. Mitchell, W. *et al.* The mitochondria-targeted peptide SS-31 binds lipid bilayers and modulates surface electrostatics as a key component of its mechanism of action. *J. Biol. Chem.* **295**, 7452–7469 (2020).

168. Szeto, H. H. First-in-class cardiolipin-protective compound as a therapeutic agent to restore mitochondrial bioenergetics. *Br. J. Pharmacol.* **171**, 2029–2050 (2014).

169. Hao, S. *et al.* Mitochondrion-Targeted Peptide SS-31 Inhibited Oxidized Low-Density Lipoproteins-Induced Foam Cell Formation through both ROS Scavenging and Inhibition of Cholesterol Influx in RAW264.7 Cells. *Mol. Basel Switz.* **20**, 21287–21297 (2015).

170. Thomas, D. A. *et al.* Mitochondrial targeting with antioxidant peptide SS-31 prevents mitochondrial depolarization, reduces islet cell apoptosis, increases islet cell yield, and improves posttransplantation function. *J. Am. Soc. Nephrol. JASN* **18**, 213–222 (2007).

171. Hou, Y. *et al.* Mitochondria-targeted peptide SS-31 attenuates renal injury via an antioxidant effect in diabetic nephropathy. *Am. J. Physiol. Renal Physiol.* **310**, F547-559 (2016).

172. Miyamoto, S. *et al.* Restoring mitochondrial superoxide levels with elamipretide (MTP-131) protects db/db mice against progression of diabetic kidney disease. *J. Biol. Chem.* **295**, 7249–7260 (2020).

173. Escribano-Lopez, I. *et al.* The mitochondrial antioxidant SS-31 increases SIRT1 levels and ameliorates inflammation, oxidative stress and leukocyte-endothelium interactions in type 2 diabetes. *Sci. Rep.* **8**, 15862 (2018).

174. Zhao, K. *et al.* Cell-permeable Peptide Antioxidants Targeted to Inner Mitochondrial Membrane inhibit Mitochondrial Swelling, Oxidative Cell Death, and Reperfusion Injury *. *J. Biol. Chem.* **279**, 34682–34690 (2004).

175. Carter, E. A. *et al.* Evaluation of the antioxidant peptide SS31 for treatment of burn-induced insulin resistance. *Int. J. Mol. Med.* **28**, 589–594 (2011).

176. Dai, D.-F. *et al.* Global proteomics and pathway analysis of pressure-overload-induced

heart failure and its attenuation by mitochondrial-targeted peptides. *Circ. Heart Fail.* **6**, 1067–1076 (2013).

177. Dridi, H. *et al.* Mitochondrial oxidative stress induces leaky ryanodine receptor during mechanical ventilation. *Free Radic. Biol. Med.* **146**, 383–391 (2020).

178. Sheikh-Ali, M., Chehade, J. M. & Mooradian, A. D. The Antioxidant Paradox in Diabetes Mellitus. *Am. J. Ther.* **18**, 266–278 (2011).

179. Mooradian, A. D. & Haas, M. J. Glucose-induced endoplasmic reticulum stress is independent of oxidative stress: A mechanistic explanation for the failure of antioxidant therapy in diabetes. *Free Radic. Biol. Med.* **50**, 1140–1143 (2011).

180. Escribano-López, I. *et al.* The Mitochondrial Antioxidant SS-31 Modulates Oxidative Stress, Endoplasmic Reticulum Stress, and Autophagy in Type 2 Diabetes. *J. Clin. Med.* **8**, 1322 (2019).

181. Fisher-Wellman, K. H. *et al.* Mitochondrial Diagnostics: A Multiplexed Assay Platform for Comprehensive Assessment of Mitochondrial Energy Fluxes. *Cell Rep.* **24**, 3593-3606.e10 (2018).

182. Sivitz, W. I. & Yorek, M. A. Mitochondrial Dysfunction in Diabetes: From Molecular Mechanisms to Functional Significance and Therapeutic Opportunities. *Antioxid. Redox Signal.* **12**, 537–577 (2010).

183. Montgomery, M. K. & Turner, N. Mitochondrial dysfunction and insulin resistance: an update. *Endocr. Connect.* **4**, R1–R15 (2015).

184. Sergi, D. *et al.* Mitochondrial (Dys)function and Insulin Resistance: From Pathophysiological Molecular Mechanisms to the Impact of Diet. *Front. Physiol.* **10**, (2019).

185. Brand, M. D. & Nicholls, D. G. Assessing mitochondrial dysfunction in cells. *Biochem. J.* **435**, 297–312 (2011).

186. Pernas, L. & Scorrano, L. Mito-Morphosis: Mitochondrial Fusion, Fission, and Cristae Remodeling as Key Mediators of Cellular Function. *Annu. Rev. Physiol.* **78**, 505–531 (2016).

187. Yu, T., Robotham, J. L. & Yoon, Y. Increased production of reactive oxygen species in hyperglycemic conditions requires dynamic change of mitochondrial morphology. *Proc. Natl. Acad. Sci. U. S. A.* **103**, 2653–2658 (2006).

188. Anderson, E. J. *et al.* Mitochondrial H2O2 emission and cellular redox state link excess fat intake to insulin resistance in both rodents and humans. *J. Clin. Invest.* **119**, 573–581 (2009).

189. Sebastián, D. *et al.* Mitofusin 2 (Mfn2) links mitochondrial and endoplasmic reticulum function with insulin signaling and is essential for normal glucose homeostasis. *Proc. Natl. Acad. Sci. U. S. A.* **109**, 5523–5528 (2012).

190. del Campo, A. *et al.* Mitochondrial fragmentation impairs insulin-dependent glucose uptake by modulating Akt activity through mitochondrial Ca2+ uptake. *Am. J. Physiol.*

Endocrinol. Metab. **306**, E1–E13 (2014).

191. Jitrapakdee, S., Wutthisathapornchai, A., Wallace, J. C. & MacDonald, M. J. Regulation of insulin secretion: role of mitochondrial signalling. *Diabetologia* **53**, 1019–1032 (2010).

192. Maechler, P. Mitochondrial function and insulin secretion. *Mol. Cell. Endocrinol.* **379**, 12–18 (2013).

193. Hoshino, A. *et al.* Inhibition of p53 preserves Parkin-mediated mitophagy and pancreatic β-cell function in diabetes. *Proc. Natl. Acad. Sci.* **111**, 3116–3121 (2014).

194. Schultz, J., Warkus, J., Wolke, C., Waterstradt, R. & Baltrusch, S. MiD51 Is Important for Maintaining Mitochondrial Health in Pancreatic Islet and MIN6 Cells. *Front. Endocrinol.* **11**, (2020).

195. Sidarala, V. *et al.* Mitophagy protects **β** cells from inflammatory damage in diabetes. *JCI Insight* **5**, (2020).

196. Nakamura, S. *et al.* Palmitate induces insulin resistance in H4IIEC3 hepatocytes through reactive oxygen species produced by mitochondria. *J. Biol. Chem.* **284**, 14809–14818 (2009).

197. Koh, J.-H. *et al.* TFAM Enhances Fat Oxidation and Attenuates High-Fat Diet–Induced Insulin Resistance in Skeletal Muscle. *Diabetes* **68**, 1552–1564 (2019).

198. Vernochet, C. *et al.* Adipose tissue mitochondrial dysfunction triggers a lipodystrophic syndrome with insulin resistance, hepatosteatosis, and cardiovascular complications. *FASEB J.* **28**, 4408–4419 (2014).

199. Gao, C.-L. *et al.* Mitochondrial dysfunction is induced by high levels of glucose and free fatty acids in 3T3-L1 adipocytes. *Mol. Cell. Endocrinol.* **320**, 25–33 (2010).

200. Choo, H.-J. *et al.* Mitochondria are impaired in the adipocytes of type 2 diabetic mice. *Diabetologia* **49**, 784–791 (2006).

201. Hernandez-Mijares, A. *et al.* Mitochondrial complex I impairment in leukocytes from type 2 diabetic patients. *Free Radic. Biol. Med.* **50**, 1215–1221 (2011).

202. Lien Li-Ming *et al.* Significant Association Between Low Mitochondrial DNA Content in Peripheral Blood Leukocytes and Ischemic Stroke. *J. Am. Heart Assoc.* **6**, e006157.

203. Chan, D. C. Mitochondrial fusion and fission in mammals. *Annu. Rev. Cell Dev. Biol.* **22**, 79–99 (2006).

204. Liesa, M. & Shirihai, O. S. Mitochondrial dynamics in the regulation of nutrient utilization and energy expenditure. *Cell Metab.* **17**, 491–506 (2013).

205. Liesa, M., Van der Bliek, A. & Shirihai, O. S. To Fis or not to Fuse? This is the question! *EMBO J.* **38**, (2019).

206. Giacomello, M. & Scorrano, L. The INs and OUTs of mitofusins. *J. Cell Biol.* **217**, 439–440 (2018).

207. Song, Z., Ghochani, M., McCaffery, J. M., Frey, T. G. & Chan, D. C. Mitofusins and OPA1 mediate sequential steps in mitochondrial membrane fusion. *Mol. Biol. Cell* **20**, 3525–3532 (2009).

208. Hoppins, S. *et al.* The soluble form of Bax regulates mitochondrial fusion via MFN2 homotypic complexes. *Mol. Cell* **41**, 150–160 (2011).

209. Favaro, G. *et al.* DRP1-mediated mitochondrial shape controls calcium homeostasis and muscle mass. *Nat. Commun.* **10**, 2576 (2019).

210. Gomes, L. C., Di Benedetto, G. & Scorrano, L. During autophagy mitochondria elongate, are spared from degradation and sustain cell viability. *Nat. Cell Biol.* **13**, 589–598 (2011).

211. Rambold, A. S., Kostelecky, B., Elia, N. & Lippincott-Schwartz, J. Tubular network formation protects mitochondria from autophagosomal degradation during nutrient starvation. *Proc. Natl. Acad. Sci. U. S. A.* **108**, 10190–10195 (2011).

212. Zhang, H. *et al.* Ubl4A is critical for mitochondrial fusion process under nutrient deprivation stress. *PLOS ONE* **15**, e0242700 (2020).

213. Kong, D. *et al.* Overexpression of mitofusin 2 improves translocation of glucose transporter 4 in skeletal muscle of high-fat diet-fed rats through AMP-activated protein kinase signaling. *Mol. Med. Rep.* **8**, 205–210 (2013).

214. Yuan, M. *et al.* Hyperglycemia Induces Endoplasmic Reticulum Stress in Atrial Cardiomyocytes, and Mitofusin-2 Downregulation Prevents Mitochondrial Dysfunction and Subsequent Cell Death. *Oxid. Med. Cell. Longev.* **2020**, 6569728 (2020).

215. Zhang, Y. *et al.* MicroRNA-106b induces mitochondrial dysfunction and insulin resistance in C2C12 myotubes by targeting mitofusin-2. *Mol. Cell. Endocrinol.* **381**, 230–240 (2013).

216. Hernández-Alvarez, M. I. *et al.* Subjects with early-onset type 2 diabetes show defective activation of the skeletal muscle PGC-1{alpha}/Mitofusin-2 regulatory pathway in response to physical activity. *Diabetes Care* **33**, 645–651 (2010).

217. Gasier, H. G., Dohl, J., Suliman, H. B., Piantadosi, C. A. & Yu, T. Skeletal muscle mitochondrial fragmentation and impaired bioenergetics from nutrient overload are prevented by carbon monoxide. *Am. J. Physiol.-Cell Physiol.* **319**, C746–C756 (2020).

218. Nisr, R. B., Shah, D. S., Ganley, I. G. & Hundal, H. S. Proinflammatory NFkB signalling promotes mitochondrial dysfunction in skeletal muscle in response to cellular fuel overloading. *Cell. Mol. Life Sci. CMLS* **76**, 4887–4904 (2019).

219. Morita, M. *et al.* mTOR Controls Mitochondrial Dynamics and Cell Survival via MTFP1. *Mol. Cell* **67**, 922-935.e5 (2017).

220. Park, S. J. *et al.* Increased O-GlcNAcylation of Drp1 by amyloid-beta promotes mitochondrial fission and dysfunction in neuronal cells. *Mol. Brain* **14**, 6 (2021).

221. Ye, L., Wu, H. & Xu, W. Deletion of Bmal1 Impairs Pancreatic β-Cell Function via Mitochondrial Signaling Pathway. *BioMed Res. Int.* **2020**, 9803024 (2020).

222. Hong, Y. *et al.* RNA binding protein HuD contributes to β-cell dysfunction by impairing mitochondria dynamics. *Cell Death Differ.* **27**, 1633–1643 (2020).

223. Hennings, T. G. *et al.* In Vivo Deletion of β-Cell Drp1 Impairs Insulin Secretion Without Affecting Islet Oxygen Consumption. *Endocrinology* **159**, 3245–3256 (2018).

224. Schultz, J. *et al.* Precise expression of Fis1 is important for glucose responsiveness of beta cells. *J. Endocrinol.* **230**, 81–91 (2016).

225. Twig, G. *et al.* Fission and selective fusion govern mitochondrial segregation and elimination by autophagy. *EMBO J.* **27**, 433–446 (2008).

226. Mollica, M. P. *et al.* Butyrate Regulates Liver Mitochondrial Function, Efficiency, and Dynamics in Insulin-Resistant Obese Mice. *Diabetes* **66**, 1405–1418 (2017).

227. Bhatti, J. S. *et al.* Protective effects of a mitochondria-targeted small peptide SS31 against hyperglycemia-induced mitochondrial abnormalities in the liver tissues of diabetic mice, Tallyho/JngJ mice. *Mitochondrion* **58**, 49–58 (2021).

228. Croston, T. L. *et al.* Functional deficiencies of subsarcolemmal mitochondria in the type 2 diabetic human heart. *Am. J. Physiol. - Heart Circ. Physiol.* **307**, H54–H65 (2014).

229. Lai, N., Kummitha, C. & Hoppel, C. Defects in skeletal muscle subsarcolemmal mitochondria in a non-obese model of type 2 diabetes mellitus. *PloS One* **12**, e0183978 (2017).

230. Mogensen, M. *et al.* Mitochondrial Respiration Is Decreased in Skeletal Muscle of Patients With Type 2 Diabetes. *Diabetes* **56**, 1592–1599 (2007).

231. Houzelle, A. *et al.* Human skeletal muscle mitochondrial dynamics in relation to oxidative capacity and insulin sensitivity. *Diabetologia* **64**, 424–436 (2021).

232. Parra, V. *et al.* Insulin stimulates mitochondrial fusion and function in cardiomyocytes via the Akt-mTOR-NFκB-Opa-1 signaling pathway. *Diabetes* **63**, 75–88 (2014).

233. Makino, A. *et al.* Regulation of mitochondrial morphology and function by O-GlcNAcylation in neonatal cardiac myocytes. *Am. J. Physiol. Regul. Integr. Comp. Physiol.* **300**, R1296-1302 (2011).

234. Pich, S. *et al.* The Charcot-Marie-Tooth type 2A gene product, Mfn2, up-regulates fuel oxidation through expression of OXPHOS system. *Hum. Mol. Genet.* **14**, 1405–1415 (2005).

235. Bach, D. *et al.* Expression of Mfn2, the Charcot-Marie-Tooth Neuropathy Type 2A Gene, in Human Skeletal Muscle : Effects of Type 2 Diabetes, Obesity, Weight Loss, and the Regulatory Role of Tumor Necrosis Factor α and Interleukin-6. *Diabetes* **54**, 2685–2693 (2005).

236. Zorzano, A., Liesa, M. & Palacín, M. Mitochondrial dynamics as a bridge between mitochondrial dysfunction and insulin resistance. *Arch. Physiol. Biochem.* **115**, 1–12 (2009).

237. Touvier, T. *et al.* Muscle-specific Drp1 overexpression impairs skeletal muscle growth via translational attenuation. *Cell Death Dis.* **6**, e1663 (2015).

238. Moore, T. M. *et al.* The impact of exercise on mitochondrial dynamics and the role of Drp1 in exercise performance and training adaptations in skeletal muscle. *Mol. Metab.* **21**, 51–67 (2019).

239. Jheng, H.-F. *et al.* Mitochondrial Fission Contributes to Mitochondrial Dysfunction and Insulin Resistance in Skeletal Muscle. *Mol. Cell. Biol.* **32**, 309–319 (2012).

240. Li, A. *et al.* Metformin and resveratrol inhibit Drp1-mediated mitochondrial fission and prevent ER stress-associated NLRP3 inflammasome activation in the adipose tissue of diabetic mice. *Mol. Cell. Endocrinol.* **434**, 36–47 (2016).

241. Tol, M. J. *et al.* A PPARγ-Bnip3 Axis Couples Adipose Mitochondrial Fusion-Fission Balance to Systemic Insulin Sensitivity. *Diabetes* **65**, 2591–2605 (2016).

242. Bond, S. T. *et al.* The E3 ligase MARCH5 is a PPARγ target gene that regulates mitochondria and metabolism in adipocytes. *Am. J. Physiol. - Endocrinol. Metab.* **316**, E293–E304 (2019).

243. Diaz-Morales, N. *et al.* Are Mitochondrial Fusion and Fission Impaired in Leukocytes of Type 2 Diabetic Patients? *Antioxid. Redox Signal.* **25**, 108–115 (2016).

244. Zhou, W. *et al.* Mitofusin 2 regulates neutrophil adhesive migration and the actin cytoskeleton. *J. Cell Sci.* **133**, (2020).

245. Schwarz, D. S. & Blower, M. D. The endoplasmic reticulum: structure, function and response to cellular signaling. *Cell. Mol. Life Sci.* **73**, 79–94 (2016).

246. Boyce, M. & Yuan, J. Cellular response to endoplasmic reticulum stress: a matter of life or death. *Cell Death Differ.* **13**, 363–373 (2006).

247. Kopp, M. C., Larburu, N., Durairaj, V., Adams, C. J. & Ali, M. M. U. UPR proteins IRE1 and PERK switch BiP from chaperone to ER stress sensor. *Nat. Struct. Mol. Biol.* **26**, 1053–1062 (2019).

248. Shen, J., Chen, X., Hendershot, L. & Prywes, R. ER stress regulation of ATF6 localization by dissociation of BiP/GRP78 binding and unmasking of Golgi localization signals. *Dev. Cell* **3**, 99–111 (2002).

249. Lin, J. H., Walter, P. & Yen, T. S. B. Endoplasmic Reticulum Stress in Disease Pathogenesis. *Annu. Rev. Pathol.* **3**, 399–425 (2008).

250. Rainbolt, T. K. & Frydman, J. Dynamics and clustering of IRE1α during ER stress. *Proc. Natl. Acad. Sci.* **117**, 3352–3354 (2020).

251. Chen, Y. & Brandizzi, F. IRE1: ER stress sensor and cell fate executor. *Trends Cell Biol.* **23**, (2013).

252. Lee, A.-H., Iwakoshi, N. N. & Glimcher, L. H. XBP-1 Regulates a Subset of Endoplasmic Reticulum Resident Chaperone Genes in the Unfolded Protein Response. *Mol. Cell. Biol.* **23**, 7448–7459 (2003).

253. Liu, Z., Lv, Y., Zhao, N., Guan, G. & Wang, J. Protein kinase R-like ER kinase and its role in

endoplasmic reticulum stress-decided cell fate. *Cell Death Dis.* **6**, e1822–e1822 (2015).

254. Arensdorf, A., Diedrichs, D. & Rutkowski, T. Regulation of the transcriptome by ER stress: non-canonical mechanisms and physiological consequences. *Front. Genet.* **4**, (2013).

255. Alasiri, G. *et al.* Reciprocal regulation between GCN2 (eIF2AK4) and PERK (eIF2AK3) through the JNK-FOXO3 axis to modulate cancer drug resistance and clonal survival. *Mol. Cell. Endocrinol.* **515**, 110932 (2020).

256. Baird, T. D. & Wek, R. C. Eukaryotic Initiation Factor 2 Phosphorylation and Translational Control in Metabolism12. *Adv. Nutr.* **3**, 307–321 (2012).

257. Liang, S.-H., Zhang, W., Mcgrath, B. C., Zhang, P. & Cavener, D. R. PERK (eIF2α kinase) is required to activate the stress-activated MAPKs and induce the expression of immediate-early genes upon disruption of ER calcium homoeostasis. *Biochem. J.* **393**, 201–209 (2005).

258. Ventoso, I., Kochetov, A., Montaner, D., Dopazo, J. & Santoyo, J. Extensive Translatome Remodeling during ER Stress Response in Mammalian Cells. *PLOS ONE* **7**, e35915 (2012).

259. Cullinan, S. B. & Diehl, J. A. Coordination of ER and oxidative stress signaling: The PERK/Nrf2 signaling pathway. *Int. J. Biochem. Cell Biol.* **38**, 317–332 (2006).

260. Tao, T. *et al.* The PERK/Nrf2 pathway mediates endoplasmic reticulum stress-induced injury by upregulating endoplasmic reticulophagy in H9c2 cardiomyoblasts. *Life Sci.* **237**, 116944 (2019).

261. Glembotski, C. C., Arrieta, A., Blackwood, E. A. & Stauffer, W. T. ATF6 as a Nodal Regulator of Proteostasis in the Heart. *Front. Physiol.* **11**, (2020).

262. Hillary, R. F. & FitzGerald, U. A lifetime of stress: ATF6 in development and homeostasis. *J. Biomed. Sci.* **25**, 48 (2018).

263. Bailey, D. & O'Hare, P. Transmembrane bZIP Transcription Factors in ER Stress Signaling and the Unfolded Protein Response. *Antioxid. Redox Signal.* **9**, 2305–2322 (2007).

264. Blackwood, E. A. *et al.* Pharmacologic ATF6 activation confers global protection in widespread disease models by reprograming cellular proteostasis. *Nat. Commun.* **10**, 187 (2019).

265. Tam, A. B. *et al.* The UPR Activator ATF6 Responds to Proteotoxic and Lipotoxic Stress by Distinct Mechanisms. *Dev. Cell* **46**, 327-343.e7 (2018).

266. Guo, F.-J. *et al.* ATF6 upregulates XBP1S and inhibits ER stress-mediated apoptosis in osteoarthritis cartilage. *Cell. Signal.* **26**, 332–342 (2014).

267. Yoshida, H., Matsui, T., Yamamoto, A., Okada, T. & Mori, K. XBP1 mRNA Is Induced by ATF6 and Spliced by IRE1 in Response to ER Stress to Produce a Highly Active Transcription Factor. *Cell* **107**, 881–891 (2001).

268. Huang, J., Wan, L., Lu, H. & Li, X. High expression of active ATF6 aggravates endoplasmic reticulum stress-induced vascular endothelial cell apoptosis through the mitochondrial

apoptotic pathway. *Mol. Med. Rep.* **17**, 6483–6489 (2018).

269. Takayanagi, S., Fukuda, R., Takeuchi, Y., Tsukada, S. & Yoshida, K. Gene regulatory network of unfolded protein response genes in endoplasmic reticulum stress. *Cell Stress Chaperones* **18**, 11–23 (2013).

270. Shoulders, M. D. *et al.* Stress-Independent Activation of XBP1s and/or ATF6 Reveals Three Functionally Diverse ER Proteostasis Environments. *Cell Rep.* **3**, 1279–1292 (2013).

271. Kanemoto, S. *et al.* XBP1 activates the transcription of its target genes via an ACGT core sequence under ER stress. *Biochem. Biophys. Res. Commun.* **331**, 1146–1153 (2005).

272. Oh-Hashi, K. *et al.* Role of an ER stress response element in regulating the bidirectional promoter of the mouse CRELD2 - ALG12 gene pair. *BMC Genomics* **11**, 664 (2010).

273. Choudhury, M. *et al.* C/EBPβ is AMP kinase sensitive and up-regulates PEPCK in response to ER stress in hepatoma cells. *Mol. Cell. Endocrinol.* **331**, 102–108 (2011).

274. Evstafieva, A. G., Kovaleva, I. E., Shoshinova, M. S., Budanov, A. V. & Chumakov, P. M. Implication of KRT16, FAM129A and HKDC1 genes as ATF4 regulated components of the integrated stress response. *PLoS ONE* **13**, e0191107. (2018).

275. Ohoka, N., Yoshii, S., Hattori, T., Onozaki, K. & Hayashi, H. TRB3, a novel ER stress-inducible gene, is induced via ATF4–CHOP pathway and is involved in cell death. *EMBO J.* **24**, 1243–1255 (2005).

276. Ozcan, U. *et al.* Endoplasmic reticulum stress links obesity, insulin action, and type 2 diabetes. *Science* **306**, 457–461 (2004).

277. Ozcan, U. *et al.* Chemical chaperones reduce ER stress and restore glucose homeostasis in a mouse model of type 2 diabetes. *Science* **313**, 1137–1140 (2006).

278. Brooks-Worrell, B. M. & Palmer, J. P. Setting the Stage for Islet Autoimmunity in Type 2 Diabetes: Obesity-Associated Chronic Systemic Inflammation and Endoplasmic Reticulum (ER) Stress. *Diabetes Care* **42**, 2338–2346 (2019).

279. James, E. A., Pietropaolo, M. & Mamula, M. J. Immune Recognition of β-Cells: Neoepitopes as Key Players in the Loss of Tolerance. *Diabetes* **67**, 1035–1042 (2018).

280. Fonseca, S. G., Gromada, J. & Urano, F. Endoplasmic reticulum stress and pancreatic beta cell death. *Trends Endocrinol. Metab. TEM* **22**, 266–274 (2011).

281. Hassler, J. R. *et al.* The IRE1α/XBP1s Pathway Is Essential for the Glucose Response and Protection of β Cells. *PLOS Biol.* **13**, e1002277 (2015).

282. Tsuchiya, Y. *et al.* IRE1–XBP1 pathway regulates oxidative proinsulin folding in pancreatic β cells. *J. Cell Biol.* **217**, 1287–1301 (2018).

283. Allagnat, F. *et al.* Sustained production of spliced X-box binding protein 1 (XBP1) induces pancreatic beta cell dysfunction and apoptosis. *Diabetologia* **53**, 1120–1130 (2010).

284. Kim, M. J. *et al.* Specific PERK inhibitors enhanced glucose-stimulated insulin secretion in a

mouse model of type 2 diabetes. *Metabolism.* **97**, 87–91 (2019).

285. Kim, M. J. *et al.* Attenuation of PERK enhances glucose-stimulated insulin secretion in islets. *J. Endocrinol.* **236**, 125–136 (2018).

286. Wang, R. *et al.* Insulin Secretion and Ca2+ Dynamics in β-Cells Are Regulated by PERK (EIF2AK3) in Concert with Calcineurin *. *J. Biol. Chem.* **288**, 33824–33836 (2013).

287. Teodoro, T., Odisho, T., Sidorova, E. & Volchuk, A. Pancreatic β-cells depend on basal expression of active ATF6α-p50 for cell survival even under nonstress conditions. *Am. J. Physiol.-Cell Physiol.* **302**, C992–C1003 (2012).

288. Sharma, R. B., Darko, C. & Alonso, L. C. Intersection of the ATF6 and XBP1 ER stress pathways in mouse islet cells. *J. Biol. Chem.* **295**, 14164–14177 (2020).

289. Usui, M. *et al.* Atf6α-null mice are glucose intolerant due to pancreatic β-cell failure on a high-fat diet but partially resistant to diet-induced insulin resistance. *Metabolism.* **61**, 1118–1128 (2012).

290. Engin, F., Nguyen, T., Yermalovich, A. & Hotamisligil, G. S. Aberrant islet unfolded protein response in type 2 diabetes. *Sci. Rep.* **4**, 4054 (2014).

291. Herbert, T. P. & Laybutt, D. R. A Reevaluation of the Role of the Unfolded Protein Response in Islet Dysfunction: Maladaptation or a Failure to Adapt? *Diabetes* **65**, 1472–1480 (2016).

292. Lenin, R., Sankaramoorthy, A., Mohan, V. & Balasubramanyam, M. Altered immunometabolism at the interface of increased endoplasmic reticulum (ER) stress in patients with type 2 diabetes. *J. Leukoc. Biol.* **98**, 615–622 (2015).

293. Mozzini, C. *et al.* Endoplasmic reticulum stress and Nrf2 repression in circulating cells of type 2 diabetic patients without the recommended glycemic goals. *Free Radic. Res.* **49**, 244–252 (2015).

294. Villalobos-Labra, R., Subiabre, M., Toledo, F., Pardo, F. & Sobrevia, L. Endoplasmic reticulum stress and development of insulin resistance in adipose, skeletal, liver, and foetoplacental tissue in diabesity. *Mol. Aspects Med.* **66**, 49–61 (2019).

295. Balakumar, M. *et al.* High-fructose diet is as detrimental as high-fat diet in the induction of insulin resistance and diabetes mediated by hepatic/pancreatic endoplasmic reticulum (ER) stress. *Mol. Cell. Biochem.* **423**, 93–104 (2016).

296. Shi, C.-X. *et al.* β-aminoisobutyric acid attenuates hepatic endoplasmic reticulum stress and glucose/lipid metabolic disturbance in mice with type 2 diabetes. *Sci. Rep.* **6**, 21924 (2016).

297. Jamalat, Y. *et al.* Phosphocreatine attenuates endoplasmic reticulum stress-mediated hepatocellular apoptosis ameliorates insulin resistance in diabetes model. *Biochem. Biophys. Res. Commun.* **506**, 611–618 (2018).

298. Pandey, V. K., Mathur, A., Khan, M. F. & Kakkar, P. Activation of PERK-eIF2α-ATF4 pathway contributes to diabetic hepatotoxicity: Attenuation of ER stress by Morin. *Cell. Signal.* **59**, 41–52 (2019).

299. Radaelli, M. G. *et al.* NAFLD/NASH in patients with type 2 diabetes and related treatment options. *J. Endocrinol. Invest.* **41**, 509–521 (2018).

300. Targher, G., Lonardo, A. & Byrne, C. D. Nonalcoholic fatty liver disease and chronic vascular complications of diabetes mellitus. *Nat. Rev. Endocrinol.* **14**, 99–114 (2018).

301. Gu, N. *et al.* Palmitate increases musclin gene expression through activation of PERK signaling pathway in C2C12 myotubes. *Biochem. Biophys. Res. Commun.* **467**, 521–526 (2015).

302. Guo, Q. *et al.* C/EBPβ mediates palmitate-induced musclin expression via the regulation of PERK/ATF4 pathways in myotubes. *Am. J. Physiol. Endocrinol. Metab.* **316**, E1081–E1092 (2019).

303. Haberzettl, P. & Hill, B. G. Oxidized lipids activate autophagy in a JNK-dependent manner by stimulating the endoplasmic reticulum stress response. *Redox Biol.* **1**, 56–64 (2013).

304. He, Y., Zhou, L., Fan, Z., Liu, S. & Fang, W. Palmitic acid, but not high-glucose, induced myocardial apoptosis is alleviated by N-acetylcysteine due to attenuated mitochondrial-derived ROS accumulation-induced endoplasmic reticulum stress. *Cell Death Dis.* **9**, 568 (2018).

305. Liu, Z.-W. *et al.* Protein kinase RNA-like endoplasmic reticulum kinase (PERK) signaling pathway plays a major role in reactive oxygen species (ROS)-mediated endoplasmic reticulum stress-induced apoptosis in diabetic cardiomyopathy. *Cardiovasc. Diabetol.* **12**, 158 (2013).

306. Ji, Y., Zhao, Z., Cai, T., Yang, P. & Cheng, M. Liraglutide alleviates diabetic cardiomyopathy by blocking CHOP-triggered apoptosis via the inhibition of the IRE-α pathway. *Mol. Med. Rep.* **9**, 1254–1258 (2014).

307. Guo, Q. *et al.* Hypoxia in 3T3-L1 adipocytes suppresses adiponectin expression via the PERK and IRE1 unfolded protein response. *Biochem. Biophys. Res. Commun.* **493**, 346–351 (2017).

308. Mihai, A. D. & Schröder, M. Glucose starvation and hypoxia, but not the saturated fatty acid palmitic acid or cholesterol, activate the unfolded protein response in 3T3-F442A and 3T3-L1 adipocytes. *Adipocyte* **4**, 188–202 (2015).

309. Liu, Y. *et al.* Retinoic acid receptor-related orphan receptor α stimulates adipose tissue inflammation by modulating endoplasmic reticulum stress. *J. Biol. Chem.* **292**, 13959–13969 (2017).

310. Wang, M. *et al.* Beneficial effect of ER stress preconditioning in protection against FFA-induced adipocyte inflammation via XBP1 in 3T3-L1 adipocytes. *Mol. Cell. Biochem.* **463**, 45–55 (2020).

311. Tampakakis, E. *et al.* Intravenous Lipid Infusion Induces Endoplasmic Reticulum Stress in Endothelial Cells and Blood Mononuclear Cells of Healthy Adults. *J. Am. Heart Assoc.* **5**, e002574 (2016).

312. Diaz-Morales, N. *et al.* Does Metformin Modulate Endoplasmic Reticulum Stress and Autophagy in Type 2 Diabetic Peripheral Blood Mononuclear Cells? *Antioxid. Redox Signal.* **28**, 1562–1569 (2018).

313. Rovira-Llopis, S. *et al.* Is glycemic control modulating endoplasmic reticulum stress in leukocytes of type 2 diabetic patients? *Antioxid. Redox Signal.* **21**, 1759–1765 (2014).

314. Szpigel, A. *et al.* Lipid environment induces ER stress, TXNIP expression and inflammation in immune cells of individuals with type 2 diabetes. *Diabetologia* **61**, 399–412 (2018).

315. Suzuki, T. *et al.* ER Stress Protein CHOP Mediates Insulin Resistance by Modulating Adipose Tissue Macrophage Polarity. *Cell Rep.* **18**, 2045–2057 (2017).

316. Wu, J. *et al.* NK cells induce hepatic ER stress to promote insulin resistance in obesity through osteopontin production. *J. Leukoc. Biol.* **107**, 589–596 (2020).

317. Galluzzi, L. *et al.* Molecular definitions of autophagy and related processes. *EMBO J.* **36**, 1811–1836 (2017).

318. Glick, D., Barth, S. & Macleod, K. F. Autophagy: cellular and molecular mechanisms. *J. Pathol.* **221**, 3–12 (2010).

319. Feng, Y., He, D., Yao, Z. & Klionsky, D. J. The machinery of macroautophagy. *Cell Res.* **24**, 24–41 (2014).

320. Kumar, S. *et al.* Phosphorylation of Syntaxin 17 by TBK1 Controls Autophagy Initiation. *Dev. Cell* **49**, 130-144.e6 (2019).

321. Mattera, R., Park, S. Y., De Pace, R., Guardia, C. M. & Bonifacino, J. S. AP-4 mediates export of ATG9A from the trans-Golgi network to promote autophagosome formation. *Proc. Natl. Acad. Sci. U. S. A.* **114**, E10697–E10706 (2017).

322. Kotani, T., Kirisako, H., Koizumi, M., Ohsumi, Y. & Nakatogawa, H. The Atg2-Atg18 complex tethers pre-autophagosomal membranes to the endoplasmic reticulum for autophagosome formation. *Proc. Natl. Acad. Sci. U. S. A.* **115**, 10363–10368 (2018).

323. Shibutani, S. T. & Yoshimori, T. A current perspective of autophagosome biogenesis. *Cell Res.* **24**, 58–68 (2014).

324. Suzuki, H., Osawa, T., Fujioka, Y. & Noda, N. N. Structural biology of the core autophagy machinery. *Curr. Opin. Struct. Biol.* **43**, 10–17 (2017).

325. Yamamoto, H. *et al.* Atg9 vesicles are an important membrane source during early steps of autophagosome formation. *J. Cell Biol.* **198**, 219–233 (2012).

326. Karanasios, E. *et al.* Dynamic association of the ULK1 complex with omegasomes during autophagy induction. *J. Cell Sci.* **126**, 5224–5238 (2013).

327. Itakura, E. & Mizushima, N. Characterization of autophagosome formation site by a hierarchical analysis of mammalian Atg proteins. *Autophagy* **6**, 764–776 (2010).

328. Koyama-Honda, I., Itakura, E., Fujiwara, T. K. & Mizushima, N. Temporal analysis of

recruitment of mammalian ATG proteins to the autophagosome formation site. *Autophagy* **9**, 1491–1499 (2013).

329. Jung, C. H. *et al.* ULK-Atg13-FIP200 complexes mediate mTOR signaling to the autophagy machinery. *Mol. Biol. Cell* **20**, 1992–2003 (2009).

330. Puente, C., Hendrickson, R. C. & Jiang, X. Nutrient-regulated Phosphorylation of ATG13 Inhibits Starvation-induced Autophagy. *J. Biol. Chem.* **291**, 6026–6035 (2016).

331. Kim, J., Kundu, M., Viollet, B. & Guan, K.-L. AMPK and mTOR regulate autophagy through direct phosphorylation of Ulk1. *Nat. Cell Biol.* **13**, 132–141 (2011).

332. Axe, E. L. *et al.* Autophagosome formation from membrane compartments enriched in phosphatidylinositol 3-phosphate and dynamically connected to the endoplasmic reticulum. *J. Cell Biol.* **182**, 685–701 (2008).

333. Karanasios, E. *et al.* Autophagy initiation by ULK complex assembly on ER tubulovesicular regions marked by ATG9 vesicles. *Nat. Commun.* **7**, 12420 (2016).

334. Park, J.-M. *et al.* The ULK1 complex mediates MTORC1 signaling to the autophagy initiation machinery via binding and phosphorylating ATG14. *Autophagy* **12**, 547–564 (2016).

335. Pengo, N., Agrotis, A., Prak, K., Jones, J. & Ketteler, R. A reversible phospho-switch mediated by ULK1 regulates the activity of autophagy protease ATG4B. *Nat. Commun.* **8**, (2017).

336. Russell, R. C. *et al.* ULK1 induces autophagy by phosphorylating Beclin-1 and activating VPS34 lipid kinase. *Nat. Cell Biol.* **15**, 741–750 (2013).

337. Wold, M. S., Lim, J., Lachance, V., Deng, Z. & Yue, Z. ULK1-mediated phosphorylation of ATG14 promotes autophagy and is impaired in Huntington's disease models. *Mol. Neurodegener.* **11**, 76 (2016).

338. Zhou, C. *et al.* Regulation of mATG9 trafficking by Src- and ULK1-mediated phosphorylation in basal and starvation-induced autophagy. *Cell Res.* **27**, 184–201 (2017).

339. Judith, D. *et al.* ATG9A shapes the forming autophagosome through Arfaptin 2 and phosphatidylinositol 4-kinase IIIβ. *J. Cell Biol.* **218**, 1634–1652 (2019).

340. Nishimura, T. *et al.* Autophagosome formation is initiated at phosphatidylinositol synthase-enriched ER subdomains. *EMBO J.* **36**, 1719–1735 (2017).

341. Dooley, H. C. *et al.* WIPI2 links LC3 conjugation with PI3P, autophagosome formation, and pathogen clearance by recruiting Atg12-5-16L1. *Mol. Cell* **55**, 238–252 (2014).

342. Fujita, N. *et al.* The Atg16L Complex Specifies the Site of LC3 Lipidation for Membrane Biogenesis in Autophagy. *Mol. Biol. Cell* **19**, 2092–2100 (2008).

343. Noda, N. N. & Inagaki, F. Mechanisms of Autophagy. *Annu. Rev. Biophys.* **44**, 101–122 (2015).

344. Kraft, C. *et al.* Binding of the Atg1/ULK1 kinase to the ubiquitin-like protein Atg8 regulates

autophagy. *EMBO J.* **31**, 3691–3703 (2012).

345. Sánchez-Wandelmer, J. *et al.* Atg4 proteolytic activity can be inhibited by Atg1 phosphorylation. *Nat. Commun.* **8**, 295 (2017).

346. Mi, N. *et al.* CapZ regulates autophagosomal membrane shaping by promoting actin assembly inside the isolation membrane. *Nat. Cell Biol.* **17**, 1112–1123 (2015).

347. Nath, S. *et al.* Lipidation of the LC3/GABARAP family of autophagy proteins relies on a membrane-curvature-sensing domain in Atg3. *Nat. Cell Biol.* **16**, 415–424 (2014).

348. Knorr, R. L., Dimova, R. & Lipowsky, R. Curvature of Double-Membrane Organelles Generated by Changes in Membrane Size and Composition. *PLOS ONE* **7**, e32753 (2012).

349. Takahashi, Y. *et al.* An autophagy assay reveals the ESCRT-III component CHMP2A as a regulator of phagophore closure. *Nat. Commun.* **9**, 2855 (2018).

350. Amaya, C., Fader, C. M. & Colombo, M. I. Autophagy and proteins involved in vesicular trafficking. *FEBS Lett.* **589**, 3343–3353 (2015).

351. Antonioli, M., Rienzo, M. D., Piacentini, M. & Fimia, G. M. Emerging Mechanisms in Initiating and Terminating Autophagy. *Trends Biochem. Sci.* **42**, 28–41 (2017).

352. Chi, C. *et al.* LAMP-2B regulates human cardiomyocyte function by mediating autophagosome–lysosome fusion. *Proc. Natl. Acad. Sci.* **116**, 556–565 (2019).

353. Diao, J. *et al.* ATG14 promotes membrane tethering and fusion of autophagosomes to endolysosomes. *Nature* **520**, 563–566 (2015).

354. Nguyen, T. N. *et al.* Atg8 family LC3/GABARAP proteins are crucial for autophagosome-lysosome fusion but not autophagosome formation during PINK1/Parkin mitophagy and starvation. *J. Cell Biol.* **215**, 857–874 (2016).

355. Tsuboyama, K. *et al.* The ATG conjugation systems are important for degradation of the inner autophagosomal membrane. *Science* **354**, 1036–1041 (2016).

356. Codogno, P., Mehrpour, M. & Proikas-Cezanne, T. Canonical and non-canonical autophagy: variations on a common theme of self-eating? *Nat. Rev. Mol. Cell Biol.* **13**, 7–12 (2011).

357. Cuervo, A. M. & Wong, E. Chaperone-mediated autophagy: roles in disease and aging. *Cell Res.* **24**, 92–104 (2014).

358. Kaushik, S. & Cuervo, A. M. Chaperone-mediated autophagy: a unique way to enter the lysosome world. *Trends Cell Biol.* **22**, 407–417 (2012).

359. Bandyopadhyay, U., Kaushik, S., Varticovski, L. & Cuervo, A. M. The chaperone-mediated autophagy receptor organizes in dynamic protein complexes at the lysosomal membrane. *Mol. Cell. Biol.* **28**, 5747–5763 (2008).

360. Bandyopadhyay, U., Sridhar, S., Kaushik, S., Kiffin, R. & Cuervo, A. M. Identification of Regulators of Chaperone-Mediated Autophagy. *Mol. Cell* **39**, 535–547 (2010).

361. Arias, E. *et al.* Lysosomal mTORC2/PHLPP1/Akt Regulate Chaperone-Mediated Autophagy. *Mol. Cell* **59**, 270–284 (2015).

362. Mukherjee, A., Patel, B., Koga, H., Cuervo, A. M. & Jenny, A. Selective endosomal microautophagy is starvation-inducible in Drosophila. *Autophagy* **12**, 1984–1999 (2016).

363. Schuck, S. Microautophagy – distinct molecular mechanisms handle cargoes of many sizes. *J. Cell Sci.* **133**, jcs246322 (2020).

364. Tekirdag, K. & Cuervo, A. M. Chaperone-mediated autophagy and endosomal microautophagy: Joint by a chaperone. *J. Biol. Chem.* **293**, 5414–5424 (2018).

365. Krick, R. *et al.* Piecemeal microautophagy of the nucleus requires the core macroautophagy genes. *Mol. Biol. Cell* **19**, 4492–4505 (2008).

366. Kirkin, V. History of the Selective Autophagy Research: How Did It Begin and Where Does It Stand Today? *J. Mol. Biol.* **432**, 3–27 (2020).

367. Johansen, T. & Lamark, T. Selective Autophagy: ATG8 Family Proteins, LIR Motifs and Cargo Receptors. *J. Mol. Biol.* **432**, 80–103 (2020).

368. Lahiri, V. & Klionsky, D. J. PHB2/prohibitin 2: An inner membrane mitophagy receptor. *Cell Res.* **27**, 311–312 (2017).

369. Wei, Y., Chiang, W.-C., Sumpter, R., Mishra, P. & Levine, B. Prohibitin 2 Is an Inner Mitochondrial Membrane Mitophagy Receptor. *Cell* **168**, 224-238.e10 (2017).

370. Furuya, N. *et al.* NDP52 interacts with mitochondrial RNA poly(A) polymerase to promote mitophagy. *EMBO Rep.* **19**, e46363 (2018).

371. Wong, Y. C. & Holzbaur, E. L. F. Optineurin is an autophagy receptor for damaged mitochondria in parkin-mediated mitophagy that is disrupted by an ALS-linked mutation. *Proc. Natl. Acad. Sci. U. S. A.* **111**, E4439-4448 (2014).

372. Chen, Z. *et al.* Mitochondrial E3 ligase MARCH5 regulates FUNDC1 to fine-tune hypoxic mitophagy. *EMBO Rep.* **18**, 495–509 (2017).

373. Paradies, G., Paradies, V., Ruggiero, F. M. & Petrosillo, G. Role of Cardiolipin in Mitochondrial Function and Dynamics in Health and Disease: Molecular and Pharmacological Aspects. *Cells* **8**, 728 (2019).

374. Shen, Z., Li, Y., Gasparski, A. N., Abeliovich, H. & Greenberg, M. L. Cardiolipin Regulates Mitophagy through the Protein Kinase C Pathway *. *J. Biol. Chem.* **292**, 2916–2923 (2017).

375. Wu, H. *et al.* Deficiency of mitophagy receptor FUNDC1 impairs mitochondrial quality and aggravates dietary-induced obesity and metabolic syndrome. *Autophagy* **15**, 1882–1898 (2019).

376. Germain, K. & Kim, P. K. Pexophagy: A Model for Selective Autophagy. *Int. J. Mol. Sci.* **21**, 578 (2020).

377. Subramani, S. A mammalian pexophagy target. *Nat. Cell Biol.* **17**, 1371–1373 (2015).

378. Bo Otto, F. & Thumm, M. Nucleophagy—Implications for Microautophagy and Health. *Int. J. Mol. Sci.* **21**, 4506 (2020).

379. Kvam, E. & Goldfarb, D. S. Nvj1p is the outer-nuclear-membrane receptor for oxysterol-binding protein homolog Osh1p in Saccharomyces cerevisiae. *J. Cell Sci.* **117**, 4959–4968 (2004).

380. Chino, H. & Mizushima, N. ER-Phagy: Quality Control and Turnover of Endoplasmic Reticulum. *Trends Cell Biol.* **30**, 384–398 (2020).

381. Mochida, K. *et al.* Receptor-mediated selective autophagy degrades the endoplasmic reticulum and the nucleus. *Nature* **522**, 359–362 (2015).

382. Kirkin, V., Lamark, T., Johansen, T. & Dikic, I. NBR1 cooperates with p62 in selective autophagy of ubiquitinated targets. *Autophagy* **5**, 732–733 (2009).

383. Korac, J. *et al.* Ubiquitin-independent function of optineurin in autophagic clearance of protein aggregates. *J. Cell Sci.* **126**, 580–592 (2013).

384. Lu, K., Psakhye, I. & Jentsch, S. Autophagic clearance of polyQ proteins mediated by ubiquitin-Atg8 adaptors of the conserved CUET protein family. *Cell* **158**, 549–563 (2014).

385. Wetzel, L. *et al.* TECPR1 promotes aggrephagy by direct recruitment of LC3C autophagosomes to lysosomes. *Nat. Commun.* **11**, 2993 (2020).

386. Schulze, R. J., Sathyanarayan, A. & Mashek, D. G. Breaking fat: the regulation and mechanisms of lipophagy. *Biochim. Biophys. Acta* **1862**, 1178–1187 (2017).

387. Seok, S. *et al.* Transcriptional regulation of autophagy by an FXR/CREB axis. *Nature* **516**, 108–111 (2014).

388. Mardani, I. *et al.* Plin2-deficiency reduces lipophagy and results in increased lipid accumulation in the heart. *Sci. Rep.* **9**, 6909 (2019).

389. Kunkel, J., Luo, X. & Capaldi, A. P. Integrated TORC1 and PKA signaling control the temporal activation of glucose-induced gene expression in yeast. *Nat. Commun.* **10**, 3558 (2019).

390. Peeters, K. *et al.* Fructose-1,6-bisphosphate couples glycolytic flux to activation of Ras. *Nat. Commun.* **8**, 922 (2017).

391. Budovskaya, Y. V., Stephan, J. S., Reggiori, F., Klionsky, D. J. & Herman, P. K. The Ras/cAMP-dependent protein kinase signaling pathway regulates an early step of the autophagy process in Saccharomyces cerevisiae. *J. Biol. Chem.* **279**, 20663–20671 (2004).

392. Zhao, X. *et al.* Endothelial PKA activity regulates angiogenesis by limiting autophagy through phosphorylation of ATG16L1. *eLife* **8**, e58195 (2019).

393. Filteau, M. *et al.* Systematic identification of signal integration by protein kinase A. *Proc. Natl. Acad. Sci. U. S. A.* **112**, 4501–4506 (2015).

394. Torres-Quiroz, F., Filteau, M. & Landry, C. R. Feedback regulation between autophagy and PKA. *Autophagy* **11**, 1181–1183 (2015).

395. Shin, S. H., Lee, E. J., Chun, J., Hyun, S. & Kang, S. S. ULK2 Ser 1027 Phosphorylation by PKA Regulates Its Nuclear Localization Occurring through Karyopherin Beta 2 Recognition of a PY-NLS Motif. *PloS One* **10**, e0127784 (2015).

396. Machado, J. *et al.* Calcitonin gene-related peptide inhibits autophagic-lysosomal proteolysis through cAMP/PKA signaling in rat skeletal muscles. *Int. J. Biochem. Cell Biol.* **72**, 40–50 (2016).

397. Condon, K. J. & Sabatini, D. M. Nutrient regulation of mTORC1 at a glance. *J. Cell Sci.* **132**, jcs222570 (2019).

398. Hosokawa, N. *et al.* Nutrient-dependent mTORC1 association with the ULK1-Atg13-FIP200 complex required for autophagy. *Mol. Biol. Cell* **20**, 1981–1991 (2009).

399. Jung, C. H., Ro, S.-H., Cao, J., Otto, N. M. & Kim, D.-H. mTOR regulation of autophagy. *FEBS Lett.* **584**, 1287–1295 (2010).

400. He, C. & Klionsky, D. J. Regulation Mechanisms and Signaling Pathways of Autophagy. *Annu. Rev. Genet.* **43**, 67–93 (2009).

401. Wu, Y.-T., Tan, H.-L., Huang, Q., Ong, C.-N. & Shen, H.-M. Activation of the PI3K-Akt-mTOR signaling pathway promotes necrotic cell death via suppression of autophagy. *Autophagy* **5**, 824–834 (2009).

402. Yamamoto, A., Cremona, M. L. & Rothman, J. E. Autophagy-mediated clearance of huntingtin aggregates triggered by the insulin-signaling pathway. *J. Cell Biol.* **172**, 719–731 (2006).

403. Zhao, D. *et al.* ATG7 regulates hepatic Akt phosphorylation through the c-JUN/PTEN pathway in high fat diet-induced metabolic disorder. *FASEB J.* **33**, 14296–14306 (2019).

404. Frendo-Cumbo, S. *et al.* Deficiency of the autophagy gene ATG16L1 induces insulin resistance through KLHL9/KLHL13/CUL3-mediated IRS1 degradation. *J. Biol. Chem.* **294**, 16172–16185 (2019).

405. Ha, J., Guan, K.-L. & Kim, J. AMPK and autophagy in glucose/glycogen metabolism. *Mol. Aspects Med.* **46**, 46–62 (2015).

406. Tamargo-Gómez, I. & Mariño, G. AMPK: Regulation of Metabolic Dynamics in the Context of Autophagy. *Int. J. Mol. Sci.* **19**, 3812 (2018).

407. Jang, M. *et al.* AMPK contributes to autophagosome maturation and lysosomal fusion. *Sci. Rep.* **8**, 12637 (2018).

408. Bakula, D. *et al.* WIPI3 and WIPI4 β-propellers are scaffolds for LKB1-AMPK-TSC signalling circuits in the control of autophagy. *Nat. Commun.* **8**, 15637 (2017).

409. Di Malta, C., Cinque, L. & Settembre, C. Transcriptional Regulation of Autophagy: Mechanisms and Diseases. *Front. Cell Dev. Biol.* **7**, 114 (2019).

410. Füllgrabe, J., Ghislat, G., Cho, D.-H. & Rubinsztein, D. C. Transcriptional regulation of

mammalian autophagy at a glance. *J. Cell Sci.* **129**, 3059–3066 (2016).

411. Martina, J. A., Chen, Y., Gucek, M. & Puertollano, R. MTORC1 functions as a transcriptional regulator of autophagy by preventing nuclear transport of TFEB. *Autophagy* **8**, 903–914 (2012).

412. Napolitano, G. *et al.* mTOR-dependent phosphorylation controls TFEB nuclear export. *Nat. Commun.* **9**, 3312 (2018).

413. Pan, B. *et al.* The Calcineurin-TFEB-p62 Pathway Mediates the Activation of Cardiac Macroautophagy by Proteasomal Malfunction. *Circ. Res.* **127**, 502–518 (2020).

414. Settembre, C. *et al.* TFEB Links Autophagy to Lysosomal Biogenesis. *Science* **332**, 1429–1433 (2011).

415. Martina, J. A. & Puertollano, R. Protein phosphatase 2A stimulates activation of TFEB and TFE3 transcription factors in response to oxidative stress. *J. Biol. Chem.* **293**, 12525–12534 (2018).

416. Audesse, A. J. *et al.* FOXO3 directly regulates an autophagy network to functionally regulate proteostasis in adult neural stem cells. *PLOS Genet.* **15**, e1008097 (2019).

417. Mammucari, C. *et al.* FoxO3 Controls Autophagy in Skeletal Muscle In Vivo. *Cell Metab.* **6**, 458–471 (2007).

418. Milan, G. *et al.* Regulation of autophagy and the ubiquitin–proteasome system by the FoxO transcriptional network during muscle atrophy. *Nat. Commun.* **6**, 6670 (2015).

419. Sengupta, A., Molkentin, J. D. & Yutzey, K. E. FoxO Transcription Factors Promote Autophagy in Cardiomyocytes. *J. Biol. Chem.* **284**, 28319–28331 (2009).

420. Shaw, J. *et al.* Antagonism of E2F-1 regulated Bnip3 transcription by NF-κB is essential for basal cell survival. *Proc. Natl. Acad. Sci.* **105**, 20734–20739 (2008).

421. Wang, P. *et al.* Hypoxia inducible factor-1α regulates autophagy via the p27-E2F1 signaling pathway. *Mol. Med. Rep.* **16**, 2107–2112 (2017).

422. Kim, H. *et al.* Regulation of hepatic autophagy by stress-sensing transcription factor CREBH. *FASEB J.* **33**, 7896–7914 (2019).

423. Lee, I. H. *et al.* A role for the NAD-dependent deacetylase Sirt1 in the regulation of autophagy. *Proc. Natl. Acad. Sci.* **105**, 3374–3379 (2008).

424. Zhang, H. *et al.* Genistein protects against ox-LDL-induced senescence through enhancing SIRT1/LKB1/AMPK-mediated autophagy flux in HUVECs. *Mol. Cell. Biochem.* **455**, 127–134 (2019).

425. Ebato, C. *et al.* Autophagy Is Important in Islet Homeostasis and Compensatory Increase of Beta Cell Mass in Response to High-Fat Diet. *Cell Metab.* **8**, 325–332 (2008).

426. Lee, Y.-H., Kim, J., Park, K. & Lee, M.-S. β-cell autophagy: Mechanism and role in β-cell dysfunction. *Mol. Metab.* **27S**, S92–S103 (2019).

427. Mir, S. U. R. *et al.* Inhibition of Autophagic Turnover in β-Cells by Fatty Acids and Glucose Leads to Apoptotic Cell Death. *J. Biol. Chem.* **290**, 6071–6085 (2015).

428. Bugliani, M. *et al.* Modulation of Autophagy Influences the Function and Survival of Human Pancreatic Beta Cells Under Endoplasmic Reticulum Stress Conditions and in Type 2 Diabetes. *Front. Endocrinol.* **10**, (2019).

429. Linnemann, A. K. *et al.* Interleukin 6 protects pancreatic β cells from apoptosis by stimulation of autophagy. *FASEB J. Off. Publ. Fed. Am. Soc. Exp. Biol.* **31**, 4140–4152 (2017).

430. He, Q. *et al.* Mesenchymal stem cell-derived exosomes exert ameliorative effects in type 2 diabetes by improving hepatic glucose and lipid metabolism via enhancing autophagy. *Stem Cell Res. Ther.* **11**, 223 (2020).

431. Zhou, W. & Ye, S. Rapamycin improves insulin resistance and hepatic steatosis in type 2 diabetes rats through activation of autophagy. *Cell Biol. Int.* **42**, 1282–1291 (2018).

432. Zhu, Y. *et al.* Astragaloside IV alleviates liver injury in type 2 diabetes due to promotion of AMPK/mTOR-mediated autophagy. *Mol. Med. Rep.* **23**, 1–12 (2021).

433. Sun, Y. *et al.* Berberine attenuates hepatic steatosis and enhances energy expenditure in mice by inducing autophagy and fibroblast growth factor 21. *Br. J. Pharmacol.* **175**, 374–387 (2018).

434. He, Y. *et al.* The preventive effect of liraglutide on the lipotoxic liver injury via increasing autophagy. *Ann. Hepatol.* **19**, 44–52 (2020).

435. Zhong, J. *et al.* Irbesartan ameliorates hyperlipidemia and liver steatosis in type 2 diabetic db/db mice via stimulating PPAR-γ, AMPK/Akt/mTOR signaling and autophagy. *Int. Immunopharmacol.* **42**, 176–184 (2017).

436. Xu, Z. *et al.* Fibroblast Growth Factor 1 Ameliorates Diabetes-Induced Liver Injury by Reducing Cellular Stress and Restoring Autophagy. *Front. Pharmacol.* **11**, 52 (2020).

437. Li, B. *et al.* miR199a-5p inhibits hepatic insulin sensitivity via suppression of ATG14-mediated autophagy. *Cell Death Dis.* **9**, 405 (2018).

438. Møller, A. B. *et al.* Altered gene expression and repressed markers of autophagy in skeletal muscle of insulin resistant patients with type 2 diabetes. *Sci. Rep.* **7**, 43775 (2017).

439. Munasinghe, P. E. *et al.* Type-2 diabetes increases autophagy in the human heart through promotion of Beclin-1 mediated pathway. *Int. J. Cardiol.* **202**, 13–20 (2016).

440. An, X.-R., Li, X., Wei, W., Li, X.-X. & Xu, M. Prostaglandin E1 Inhibited Diabetes-Induced Phenotypic Switching of Vascular Smooth Muscle Cells Through Activating Autophagy. *Cell. Physiol. Biochem.* **50**, 745–756 (2018).

441. Hu, P., Lai, D., Lu, P., Gao, J. & He, H. ERK and Akt signaling pathways are involved in advanced glycation end product-induced autophagy in rat vascular smooth muscle cells. *Int. J. Mol. Med.* **29**, 613–618 (2012).

442. Kruse, R., Vind, B. F., Petersson, S. J., Kristensen, J. M. & Højlund, K. Markers of autophagy are adapted to hyperglycaemia in skeletal muscle in type 2 diabetes. *Diabetologia* **58**, 2087–2095 (2015).

443. Kruse, R. *et al.* Intact initiation of autophagy and mitochondrial fission by acute exercise in skeletal muscle of patients with Type 2 diabetes. *Clin. Sci.* **131**, 37–47 (2016).

444. Ehrlicher, S. E., Stierwalt, H. D., Newsom, S. A. & Robinson, M. M. Skeletal muscle autophagy remains responsive to hyperinsulinemia and hyperglycemia at higher plasma insulin concentrations in insulin-resistant mice. *Physiol. Rep.* **6**, e13810 (2018).

445. Kosacka, J. *et al.* Autophagy in adipose tissue of patients with obesity and type 2 diabetes. *Mol. Cell. Endocrinol.* **409**, 21–32 (2015).

446. Öst, A. *et al.* Attenuated mTOR Signaling and Enhanced Autophagy in Adipocytes from Obese Patients with Type 2 Diabetes. *Mol. Med.* **16**, 235–246 (2010).

447. Kosacka, J. *et al.* Up-regulated autophagy: as a protective factor in adipose tissue of WOKW rats with metabolic syndrome. *Diabetol. Metab. Syndr.* **10**, 13 (2018).

448. Nuñez, C. E. *et al.* Defective regulation of adipose tissue autophagy in obesity. *Int. J. Obes. 2005* **37**, 1473–1480 (2013).

449. Stienstra, R. *et al.* Autophagy in adipose tissue and the beta cell: implications for obesity and diabetes. *Diabetologia* **57**, 1505–1516 (2014).

450. Li, H. *et al.* The reciprocal interaction between autophagic dysfunction and ER stress in adipose insulin resistance. *Cell Cycle Georget. Tex* **13**, 565–579 (2014).

451. Cai, J. *et al.* Autophagy Ablation in Adipocytes Induces Insulin Resistance and Reveals Roles for Lipid Peroxide and Nrf2 Signaling in Adipose-Liver Crosstalk. *Cell Rep.* **25**, 1708-1717.e5 (2018).

452. Alizadeh, S. *et al.* Evidence for the link between defective autophagy and inflammation in peripheral blood mononuclear cells of type 2 diabetic patients. *J. Physiol. Biochem.* **74**, 369–379 (2018).

453. Bhattacharya, D. *et al.* The protective role of metformin in autophagic status in peripheral blood mononuclear cells of type 2 diabetic patients. *Cell Biol. Int.* **44**, 1628–1639 (2020).

454. Chatterjee, T., Pattanayak, R., Ukil, A., Chowdhury, S. & Bhattacharyya, M. Autophagy protects peripheral blood mononuclear cells against inflammation, oxidative and nitrosative stress in diabetic dyslipidemia. *Free Radic. Biol. Med.* **143**, 309–323 (2019).

455. RostamiRad, A., Ebrahimi, S. S. S., Sadeghi, A., Taghikhani, M. & Meshkani, R. Palmitate-induced impairment of autophagy turnover leads to increased apoptosis and inflammation in peripheral blood mononuclear cells. *Immunobiology* **223**, 269–278 (2018).

456. Sciarretta, S. *et al.* Activation of Nox4 in the Endoplasmic Reticulum Promotes Cardiomyocyte Autophagy and Survival during Energy Stress through the PERK/eIF-2α/ATF4 pathway. *Circ. Res.* **113**, 1253–1264 (2013).

457. Wu, R.-F., Ma, Z., Liu, Z. & Terada, L. S. Nox4-Derived H2O2 Mediates Endoplasmic Reticulum Signaling through Local Ras Activation. *Mol. Cell. Biol.* **30**, 3553–3568 (2010).

458. Booth, D. M., Enyedi, B., Geiszt, M., Várnai, P. & Hajnóczky, G. Redox Nanodomains Are Induced by and Control Calcium Signaling at the ER-Mitochondrial Interface. *Mol. Cell* **63**, 240–248 (2016).

459. Ly, L. D. *et al.* Oxidative stress and calcium dysregulation by palmitate in type 2 diabetes. *Exp. Mol. Med.* **49**, e291 (2017).

460. Ochoa, C. D., Wu, R. F. & Terada, L. S. ROS signaling and ER stress in cardiovascular disease. *Mol. Aspects Med.* **63**, 18–29 (2018).

461. Li, G. *et al.* Role of ERO1-alpha-mediated stimulation of inositol 1,4,5-triphosphate receptor activity in endoplasmic reticulum stress-induced apoptosis. *J. Cell Biol.* **186**, 783–792 (2009).

462. Nishitoh, H. CHOP is a multifunctional transcription factor in the ER stress response. *J. Biochem. (Tokyo)* **151**, 217–219 (2012).

463. Zhang, Z. *et al.* Redox signaling and unfolded protein response coordinate cell fate decisions under ER stress. *Redox Biol.* **25**, 101047 (2019).

464. Bhandary, B., Marahatta, A., Kim, H.-R. & Chae, H.-J. An Involvement of Oxidative Stress in Endoplasmic Reticulum Stress and Its Associated Diseases. *Int. J. Mol. Sci.* **14**, 434–456 (2013).

465. Malhotra, J. D. & Kaufman, R. J. Endoplasmic reticulum stress and oxidative stress: a vicious cycle or a double-edged sword? *Antioxid. Redox Signal.* **9**, 2277–2293 (2007).

466. Rojas, J. *et al.* Pancreatic Beta Cell Death: Novel Potential Mechanisms in Diabetes Therapy. *J. Diabetes Res.* **2018**, 9601801 (2018).

467. Wu, Z., Wang, H., Fang, S. & Xu, C. Roles of endoplasmic reticulum stress and autophagy on H2O2-induced oxidative stress injury in HepG2 cells. *Mol. Med. Rep.* **18**, 4163–4174 (2018).

468. Wei, Y., Pattingre, S., Sinha, S., Bassik, M. & Levine, B. JNK1-Mediated Phosphorylation of Bcl-2 Regulates Starvation-Induced Autophagy. *Mol. Cell* **30**, 678–688 (2008).

469. Zhang, M.-Z., Wang, Y., Paueksakon, P. & Harris, R. C. Epidermal Growth Factor Receptor Inhibition Slows Progression of Diabetic Nephropathy in Association With a Decrease in Endoplasmic Reticulum Stress and an Increase in Autophagy. *Diabetes* **63**, 2063–2072 (2014).

470. Margariti, A. *et al.* XBP1 mRNA splicing triggers an autophagic response in endothelial cells through BECLIN-1 transcriptional activation. *J. Biol. Chem.* **288**, 859–872 (2013).

471. Vidal, R. L. *et al.* Targeting the UPR transcription factor XBP1 protects against Huntington's disease through the regulation of FoxO1 and autophagy. *Hum. Mol. Genet.* **21**, 2245–2262 (2012).

472. B'chir, W. *et al.* The eIF2α/ATF4 pathway is essential for stress-induced autophagy gene expression. *Nucleic Acids Res.* **41**, 7683–7699 (2013).

473. Kouroku, Y. *et al.* ER stress (PERK/eIF2 α phosphorylation) mediates the polyglutamine-induced LC3 conversion, an essential step for autophagy formation. *Cell Death Differ.* **14**, 230–239 (2007).

474. Rouschop, K. M. A. *et al.* The unfolded protein response protects human tumor cells during hypoxia through regulation of the autophagy genes MAP1LC3B and ATG5. *J. Clin. Invest.* **120**, 127–141 (2010).

475. Wang, J. *et al.* Hepatitis C virus core protein activates autophagy through EIF2AK3 and ATF6 UPR pathway-mediated MAP1LC3B and ATG12 expression. *Autophagy* **10**, 766–784 (2014).

476. B'chir, W. *et al.* Dual role for CHOP in the crosstalk between autophagy and apoptosis to determine cell fate in response to amino acid deprivation. *Cell. Signal.* **26**, 1385–1391 (2014).

477. Puthalakath, H. *et al.* ER stress triggers apoptosis by activating BH3-only protein Bim. *Cell* **129**, 1337–1349 (2007).

478. Chen, C.-H. *et al.* ER Stress Inhibits mTORC2 and Akt Signaling Through GSK-3β–Mediated Phosphorylation of Rictor. *Sci. Signal.* **4**, ra10–ra10 (2011).

479. Winnay, J. N., Solheim, M. H., Sakaguchi, M., Njølstad, P. R. & Kahn, C. R. Inhibition of the PI 3-kinase pathway disrupts the unfolded protein response and reduces sensitivity to ER stress-dependent apoptosis. *FASEB J.* **34**, 12521–12532 (2020).

480. Yung, H. W., Charnock-Jones, D. S. & Burton, G. J. Regulation of AKT Phosphorylation at Ser473 and Thr308 by Endoplasmic Reticulum Stress Modulates Substrate Specificity in a Severity Dependent Manner. *PLOS ONE* **6**, e17894 (2011).

481. Han, M. *et al.* Hispidulin induces ER stress-mediated apoptosis in human hepatocellular carcinoma cells in vitro and in vivo by activating AMPK signaling pathway. *Acta Pharmacol. Sin.* **40**, 666–676 (2019).

482. Hwang, S.-L. *et al.* Inhibitory cross-talk between the AMPK and ERK pathways mediates endoplasmic reticulum stress-induced insulin resistance in skeletal muscle. *Br. J. Pharmacol.* **169**, 69–81 (2013).

483. Jin, H. R., Du, C. H., Wang, C.-Z., Yuan, C.-S. & Du, W. Ginseng metabolite Protopanaxadiol induces Sestrin2 expression and AMPK activation through GCN2 and PERK. *Cell Death Dis.* **10**, 1–9 (2019).

484. Ouyang, Y.-B., Xu, L.-J., Emery, J. F., Lee, A. S. & Giffard, R. G. Overexpressing GRP78 influences Ca2+ handling and function of mitochondria in astrocytes after ischemia-like stress. *Mitochondrion* **11**, 279–286 (2011).

485. Høyer-Hansen, M. *et al.* Control of Macroautophagy by Calcium, Calmodulin-Dependent

Kinase Kinase-β, and Bcl-2. *Mol. Cell* **25**, 193–205 (2007).

486. Scherz-Shouval, R. *et al.* Reactive oxygen species are essential for autophagy and specifically regulate the activity of Atg4. *EMBO J.* **26**, 1749–1760 (2007).

487. Desideri, E., Filomeni, G. & Ciriolo, M. R. Glutathione participates in the modulation of starvation-induced autophagy in carcinoma cells. *Autophagy* **8**, 1769–1781 (2012).

488. Filomeni, G., De Zio, D. & Cecconi, F. Oxidative stress and autophagy: the clash between damage and metabolic needs. *Cell Death Differ.* **22**, 377–388 (2015).

489. Filomeni, G., Desideri, E., Cardaci, S., Rotilio, G. & Ciriolo, M. R. Under the ROS: Thiol network is the principal suspect for autophagy commitment. *Autophagy* **6**, 999–1005 (2010).

490. Li, L., Chen, Y. & Gibson, S. B. Starvation-induced autophagy is regulated by mitochondrial reactive oxygen species leading to AMPK activation. *Cell. Signal.* **25**, 50–65 (2013).

491. Zmijewski, J. W. *et al.* Exposure to Hydrogen Peroxide Induces Oxidation and Activation of AMP-activated Protein Kinase *. *J. Biol. Chem.* **285**, 33154–33164 (2010).

492. Cordani, M., Sánchez-Álvarez, M., Strippoli, R., Bazhin, A. V. & Donadelli, M. Sestrins at the Interface of ROS Control and Autophagy Regulation in Health and Disease. *Oxid. Med. Cell. Longev.* **2019**, 1283075 (2019).

493. Lee, J. H. *et al.* Maintenance of Metabolic Homeostasis by Sestrin2 and Sestrin3. *Cell Metab.* **16**, 311–321 (2012).

494. Li, G.-H. *et al.* Ox-Lp(a) transiently induces HUVEC autophagy via an ROS-dependent PAPR-1-LKB1-AMPK-mTOR pathway. *Atherosclerosis* **243**, 223–235 (2015).

495. Kim, D.-Y., Lim, S.-G., Suk, K. & Lee, W.-H. Mitochondrial dysfunction regulates the JAK-STAT pathway via LKB1-mediated AMPK activation ER-stress-independent manner. *Biochem. Cell Biol. Biochim. Biol. Cell.* **98**, 137–144 (2020).

496. Einarson, T. R., Acs, A., Ludwig, C. & Panton, U. H. Prevalence of cardiovascular disease in type 2 diabetes: a systematic literature review of scientific evidence from across the world in 2007–2017. *Cardiovasc. Diabetol.* **17**, 83 (2018).

497. Low Wang Cecilia C., Hess Connie N., Hiatt William R., & Goldfine Allison B. Clinical Update: Cardiovascular Disease in Diabetes Mellitus. *Circulation* **133**, 2459–2502 (2016).

498. Donath, M. Y. & Shoelson, S. E. Type 2 diabetes as an inflammatory disease. *Nat. Rev. Immunol.* **11**, 98–107 (2011).

499. Spranger, J. *et al.* Inflammatory cytokines and the risk to develop type 2 diabetes: results of the prospective population-based European Prospective Investigation into Cancer and Nutrition (EPIC)-Potsdam Study. *Diabetes* **52**, 812–817 (2003).

500. Herder, C. *et al.* Elevated levels of the anti-inflammatory interleukin-1 receptor antagonist precede the onset of type 2 diabetes: the Whitehall II study. *Diabetes Care* **32**, 421–423

(2009).

501. Appari, M., Channon, K. M. & McNeill, E. Metabolic Regulation of Adipose Tissue Macrophage Function in Obesity and Diabetes. *Antioxid. Redox Signal.* **29**, 297–312 (2018).

502. Lumeng, C. N., DeYoung, S. M., Bodzin, J. L. & Saltiel, A. R. Increased Inflammatory Properties of Adipose Tissue Macrophages Recruited During Diet-Induced Obesity. *Diabetes* **56**, 16–23 (2007).

503. Herder, C., Dalmas, E., Böni-Schnetzler, M. & Donath, M. Y. The IL-1 Pathway in Type 2 Diabetes and Cardiovascular Complications. *Trends Endocrinol. Metab.* **26**, 551–563 (2015).

504. Kristiansen, O. P. & Mandrup-Poulsen, T. Interleukin-6 and Diabetes: The Good, the Bad, or the Indifferent? *Diabetes* **54**, S114–S124 (2005).

505. Ridker Paul M. From C-Reactive Protein to Interleukin-6 to Interleukin-1. *Circ. Res.* **118**, 145–156 (2016).

506. Wu, H. *et al.* T-cell accumulation and regulated on activation, normal T cell expressed and secreted upregulation in adipose tissue in obesity. *Circulation* **115**, 1029–1038 (2007).

507. Feuerer, M. *et al.* Lean, but not obese, fat is enriched for a unique population of regulatory T cells that affect metabolic parameters. *Nat. Med.* **15**, 930–939 (2009).

508. Ilan, Y. *et al.* Induction of regulatory T cells decreases adipose inflammation and alleviates insulin resistance in ob/ob mice. *Proc. Natl. Acad. Sci. U. S. A.* **107**, 9765–9770 (2010).

509. Ehses, J. A. *et al.* Increased Number of Islet-Associated Macrophages in Type 2 Diabetes. *Diabetes* **56**, 2356–2370 (2007).

510. Böni-Schnetzler, M. *et al.* Increased interleukin (IL)-1beta messenger ribonucleic acid expression in beta -cells of individuals with type 2 diabetes and regulation of IL-1beta in human islets by glucose and autostimulation. *J. Clin. Endocrinol. Metab.* **93**, 4065–4074 (2008).

511. Burke, B. *et al.* Hypoxia-induced gene expression in human macrophages: implications for ischemic tissues and hypoxia-regulated gene therapy. *Am. J. Pathol.* **163**, 1233–1243 (2003).

512. Cinti, S. *et al.* Adipocyte death defines macrophage localization and function in adipose tissue of obese mice and humans. *J. Lipid Res.* **46**, 2347–2355 (2005).

513. Shi, H. *et al.* TLR4 links innate immunity and fatty acid-induced insulin resistance. *J. Clin. Invest.* **116**, 3015–3025 (2006).

514. Cai, D. *et al.* Local and systemic insulin resistance resulting from hepatic activation of IKK-β and NF-κB. *Nat. Med.* **11**, 183–190 (2005).

515. Tuncman, G. *et al.* Functional in vivo interactions between JNK1 and JNK2 isoforms in obesity and insulin resistance. *Proc. Natl. Acad. Sci. U. S. A.* **103**, 10741–10746 (2006).

516. Andreasen, A. S., Kelly, M., Berg, R. M. G., Møller, K. & Pedersen, B. K. Type 2 Diabetes Is

Associated with Altered NF-κB DNA Binding Activity, JNK Phosphorylation, and AMPK Phosphorylation in Skeletal Muscle after LPS. *PLOS ONE* **6**, e23999 (2011).

517. Inayat, H., Azim, M. K. & Baloch, A. A. Analysis of Inflammatory Gene Expression Profile of Peripheral Blood Leukocytes in Type 2 Diabetes. *Immunol. Invest.* **48**, 618–631 (2019).

518. Liu, F. *et al.* The expression of GPR109A, NF-kB and IL-1β in peripheral blood leukocytes from patients with type 2 diabetes. *Ann. Clin. Lab. Sci.* **44**, 443–448 (2014).

519. Takamura, T. *et al.* Gene expression profiles in peripheral blood mononuclear cells reflect the pathophysiology of type 2 diabetes. *Biochem. Biophys. Res. Commun.* **361**, 379–384 (2007).

520. Ortis, F. *et al.* Induction of nuclear factor-κB and its downstream genes by TNF-α and IL-1β has a pro-apoptotic role in pancreatic beta cells. *Diabetologia* **51**, 1213 (2008).

521. Maedler, K. *et al.* Glucose-induced β cell production of IL-1β contributes to glucotoxicity in human pancreatic islets. *J. Clin. Invest.* **110**, 851–860 (2002).

522. Maedler, K. *et al.* Glucose- and Interleukin-1β-Induced β-Cell Apoptosis Requires Ca2+ Influx and Extracellular Signal-Regulated Kinase (ERK) 1/2 Activation and Is Prevented by a Sulfonylurea Receptor 1/Inwardly Rectifying K+ Channel 6.2 (SUR/Kir6.2) Selective Potassium Channel Opener in Human Islets. *Diabetes* **53**, 1706–1713 (2004).

523. Böni-Schnetzler, M. *et al.* Free fatty acids induce a proinflammatory response in islets via the abundantly expressed interleukin-1 receptor I. *Endocrinology* **150**, 5218–5229 (2009).

524. Zhou, R., Tardivel, A., Thorens, B., Choi, I. & Tschopp, J. Thioredoxin-interacting protein links oxidative stress to inflammasome activation. *Nat. Immunol.* **11**, 136–140 (2010).

525. Böni-Schnetzler, M. *et al.* β Cell-Specific Deletion of the IL-1 Receptor Antagonist Impairs β Cell Proliferation and Insulin Secretion. *Cell Rep.* **22**, 1774–1786 (2018).

526. Larsen, C. M. *et al.* Interleukin-1-receptor antagonist in type 2 diabetes mellitus. *N. Engl. J. Med.* **356**, 1517–1526 (2007).

527. Jiao, P. *et al.* Obesity-related upregulation of monocyte chemotactic factors in adipocytes: involvement of nuclear factor-kappaB and c-Jun NH2-terminal kinase pathways. *Diabetes* **58**, 104–115 (2009).

528. Pober, J. S. & Sessa, W. C. Evolving functions of endothelial cells in inflammation. *Nat. Rev. Immunol.* **7**, 803–815 (2007).

529. Kuhlencordt, P. J. *et al.* Role of endothelial nitric oxide synthase in endothelial activation: insights from eNOS knockout endothelial cells. *Am. J. Physiol.-Cell Physiol.* **286**, C1195–C1202 (2004).

530. Lowenstein, C. J., Morrell, C. N. & Yamakuchi, M. Regulation of Weibel–Palade Body Exocytosis. *Trends Cardiovasc. Med.* **15**, 302–308 (2005).

531. Bijli, K. M. *et al.* Phospholipase C-ε signaling mediates endothelial cell inflammation and

barrier disruption in acute lung injury. *Am. J. Physiol. - Lung Cell. Mol. Physiol.* **311**, L517–L524 (2016).

532. Niu Jiaxin, Profirovic Jasmina, Pan Haiyun, Vaiskunaite Rita, & Voyno-Yasenetskaya Tatyana. G Protein βγ Subunits Stimulate p114RhoGEF, a Guanine Nucleotide Exchange Factor for RhoA and Rac1. *Circ. Res.* **93**, 848–856 (2003).

533. Shimokawa, H. & Godo, S. Nitric oxide and endothelium-dependent hyperpolarization mediated by hydrogen peroxide in health and disease. *Basic Clin. Pharmacol. Toxicol.* **127**, 92–101 (2020).

534. Erent, M. *et al.* Rate, extent and concentration dependence of histamine-evoked Weibel-Palade body exocytosis determined from individual fusion events in human endothelial cells. *J. Physiol.* **583**, 195–212 (2007).

535. Nightingale, T. D. *et al.* Actomyosin II contractility expels von Willebrand factor from Weibel-Palade bodies during exocytosis. *J. Cell Biol.* **194**, 613–629 (2011).

536. Morris, G. E., Nelson, C. P., Standen, N. B., Challiss, R. A. J. & Willets, J. M. Endothelin signalling in arterial smooth muscle is tightly regulated by G protein-coupled receptor kinase 2. *Cardiovasc. Res.* **85**, 424–433 (2010).

537. Oyama, J. & Node, K. Is GRK2 a new target for cardiovascular disease? *Hypertens. Res.* **41**, 575–577 (2018).

538. Pober, J. S. & Cotran, R. S. The role of endothelial cells in inflammation. *Transplantation* **50**, 537–544 (1990).

539. Pober, J. S. Endothelial activation: intracellular signaling pathways. *Arthritis Res. Ther.* **4**, S109 (2002).

540. Caughey, G. E., Cleland, L. G., Penglis, P. S., Gamble, J. R. & James, M. J. Roles of Cyclooxygenase (COX)-1 and COX-2 in Prostanoid Production by Human Endothelial Cells: Selective Up-Regulation of Prostacyclin Synthesis by COX-2. *J. Immunol.* **167**, 2831–2838 (2001).

541. Tang, S. Y. *et al.* Cyclooxygenase-2 in Endothelial and Vascular Smooth Muscle Cells Restrains Atherogenesis in Hyperlipidemic Mice. *Circulation* **129**, 1761–1769 (2014).

542. Lominadze, D., Dean, W. L., Tyagi, S. C. & Roberts, A. M. Mechanisms of fibrinogen-induced microvascular dysfunction during cardiovascular disease. *Acta Physiol. Oxf. Engl.* **198**, 1–13 (2010).

543. Tyagi, N., Roberts, A. M., Dean, W. L., Tyagi, S. C. & Lominadze, D. Fibrinogen induces endothelial cell permeability. *Mol. Cell. Biochem.* **307**, 13–22 (2008).

544. Langer, H. F. & Chavakis, T. Leukocyte – endothelial interactions in inflammation. *J. Cell. Mol. Med.* **13**, 1211–1220 (2009).

545. Li, J. H. & Pober, J. S. The Cathepsin B Death Pathway Contributes to TNF Plus IFN-γ-Mediated Human Endothelial Injury. *J. Immunol.* **175**, 1858–1866 (2005).

546. Yamaoka, J., Kabashima, K., Kawanishi, M., Toda, K.-I. & Miyachi, Y. Cytotoxicity of IFN-γ and TNF-α for Vascular Endothelial Cell Is Mediated by Nitric Oxide. *Biochem. Biophys. Res. Commun.* **291**, 780–786 (2002).

547. Rask-Madsen, C. *et al.* Loss of Insulin Signaling in Vascular Endothelial Cells Accelerates Atherosclerosis in Apolipoprotein E Null Mice. *Cell Metab.* **11**, 379–389 (2010).

548. Doronzo, G. *et al.* Insulin activates hypoxia-inducible factor-1alpha in human and rat vascular smooth muscle cells via phosphatidylinositol-3 kinase and mitogen-activated protein kinase pathways: impairment in insulin resistance owing to defects in insulin signalling. *Diabetologia* **49**, 1049–1063 (2006).

549. Li, Q. *et al.* Homozygous receptors for insulin and not IGF-1 accelerate intimal hyperplasia in insulin resistance and diabetes. *Nat. Commun.* **10**, 4427 (2019).

550. Martínez-Hervás, S. *et al.* Insulin resistance aggravates atherosclerosis by reducing vascular smooth muscle cell survival and increasing CX3CL1/CX3CR1 axis. *Cardiovasc. Res.* **103**, 324–336 (2014).

551. Ieronymaki, E., Daskalaki, M. G., Lyroni, K. & Tsatsanis, C. Insulin Signaling and Insulin Resistance Facilitate Trained Immunity in Macrophages Through Metabolic and Epigenetic Changes. *Front. Immunol.* **10**, (2019).

552. Orliaguet, L., Dalmas, E., Drareni, K., Venteclef, N. & Alzaid, F. Mechanisms of Macrophage Polarization in Insulin Signaling and Sensitivity. *Front. Endocrinol.* **11**, (2020).

553. Bornfeldt Karin E. 2013 Russell Ross Memorial Lecture in Vascular Biology. *Arterioscler. Thromb. Vasc. Biol.* **34**, 705–714 (2014).

554. Ieronymaki, E. *et al.* Insulin Resistance in Macrophages Alters Their Metabolism and Promotes an M2-Like Phenotype. *J. Immunol.* **202**, 1786–1797 (2019).

555. Kubota, T. *et al.* Downregulation of macrophage Irs2 by hyperinsulinemia impairs IL-4-indeuced M2a-subtype macrophage activation in obesity. *Nat. Commun.* **9**, (2018).

556. Song, M. *et al.* Adipocyte-Derived Exosomes Carrying Sonic Hedgehog Mediate M1 Macrophage Polarization-Induced Insulin Resistance via Ptch and PI3K Pathways. *Cell. Physiol. Biochem.* **48**, 1416–1432 (2018).

557. Song, L. *et al.* GRP94 regulates M1 macrophage polarization and insulin resistance. *Am. J. Physiol.-Endocrinol. Metab.* **318**, E1004–E1013 (2020).

558. De Nigris, V. *et al.* Short-term high glucose exposure impairs insulin signaling in endothelial cells. *Cardiovasc. Diabetol.* **14**, 114 (2015).

559. Kim Jeong-a, Montagnani Monica, Koh Kwang Kon, & Quon Michael J. Reciprocal Relationships Between Insulin Resistance and Endothelial Dysfunction. *Circulation* **113**, 1888–1904 (2006).

560. Tabit, C. E., Chung, W. B., Hamburg, N. M. & Vita, J. A. Endothelial dysfunction in diabetes mellitus: Molecular mechanisms and clinical implications. *Rev. Endocr. Metab. Disord.* **11**,

61–74 (2010).

561. Krüger-Genge, A., Blocki, A., Franke, R.-P. & Jung, F. Vascular Endothelial Cell Biology: An Update. *Int. J. Mol. Sci.* **20**, 4411(2019).

562. Idris-Khodja, N. *et al.* Endothelin-1 Overexpression Exaggerates Diabetes-Induced Endothelial Dysfunction by Altering Oxidative Stress. *Am. J. Hypertens.* **29**, 1245–1251 (2016).

563. Park, S.-H. *et al.* Empagliflozin improved systolic blood pressure, endothelial dysfunction and heart remodeling in the metabolic syndrome ZSF1 rat. *Cardiovasc. Diabetol.* **19**, 19 (2020).

564. Tang, S.-T. *et al.* Sitagliptin inhibits endothelin-1 expression in the aortic endothelium of rats with streptozotocin-induced diabetes by suppressing the nuclear factor-κB/IκBα system through the activation of AMP-activated protein kinase. *Int. J. Mol. Med.* **37**, 1558–1566 (2016).

565. Beck, L. *et al.* Endothelial Dysfunction and Passive Changes in the Aorta and Coronary Arteries of Diabetic db/db Mice. *Front. Physiol.* **11**, 667 (2020).

566. Ghardashi Afousi, A. *et al.* Improved brachial artery shear patterns and increased flow-mediated dilatation after low-volume high-intensity interval training in type 2 diabetes. *Exp. Physiol.* **103**, 1264–1276 (2018).

567. Kizub, I. V., Klymenko, K. I. & Soloviev, A. I. Protein kinase C in enhanced vascular tone in diabetes mellitus. *Int. J. Cardiol.* **174**, 230–242 (2014).

568. Muller, W. A. Leukocyte-Endothelial Cell Interactions in the Inflammatory Response. *Lab. Invest.* **82**, 521–534 (2002).

569. Gao, F. *et al.* Reduction of Endothelial Nitric Oxide Increases the Adhesiveness of Constitutive Endothelial Membrane ICAM-1 through Src-Mediated Phosphorylation. *Front. Physiol.* **8**, 1124 (2018).

570. Xu, S., Zhou, X., Yuan, D., Xu, Y. & He, P. Caveolin-1 scaffolding domain promotes leukocyte adhesion by reduced basal endothelial nitric oxide-mediated ICAM-1 phosphorylation in rat mesenteric venules. *Am. J. Physiol. Heart Circ. Physiol.* **305**, H1484-1493 (2013).

571. Lee, W. J. *et al.* M2 Macrophage Polarization Mediates Anti-inflammatory Effects of Endothelial Nitric Oxide Signaling. *Diabetes* **64**, 2836–2846 (2015).

572. Pankow, J. S. *et al.* Circulating cellular adhesion molecules and risk of diabetes: the Multi-Ethnic Study of Atherosclerosis (MESA). *Diabet. Med. J. Br. Diabet. Assoc.* **33**, 985–991 (2016).

573. Chiu Jeng-Jiann *et al.* Shear Stress Increases ICAM-1 and Decreases VCAM-1 and E-selectin Expressions Induced by Tumor Necrosis Factor-α in Endothelial Cells. *Arterioscler. Thromb. Vasc. Biol.* **24**, 73–79 (2004).

574. Pinte, S. *et al.* Endothelial Cell Activation Is Regulated by Epidermal Growth Factor-like

Domain 7 (Egfl7) during Inflammation. *J. Biol. Chem.* **291**, 24017–24028 (2016).

575. Sawa, Y. *et al.* Effects of TNF-α on Leukocyte Adhesion Molecule Expressions in Cultured Human Lymphatic Endothelium. *J. Histochem. Cytochem.* **55**, 721–733 (2007).

576. Domingueti, C. P. *et al.* Diabetes mellitus: The linkage between oxidative stress, inflammation, hypercoagulability and vascular complications. *J. Diabetes Complications* **30**, 738–745 (2016).

577. Kubisz, P., Stančiaková, L., Staško, J., Galajda, P. & Mokáň, M. Endothelial and platelet markers in diabetes mellitus type 2. *World J. Diabetes* **6**, 423–431 (2015).

578. Nieuwdorp, M., Stroes, E. S., Meijers, J. C. & Büller, H. Hypercoagulability in the metabolic syndrome. *Curr. Opin. Pharmacol.* **5**, 155–159 (2005).

579. Fan, Q. *et al.* Association of SERPINE1 rs6092 with type 2 diabetes and related metabolic traits in a Chinese population. *Gene* **661**, 176–181 (2018).

580. Li, L., Shi, Z., Ma, L. & Lu, Y. Analysis of the correlation between plasma coagulation factor VII, PAI-1, and uric acid with insulin resistance and macrovascular complications in elderly patients with type 2 diabetes. *Ann. Palliat. Med.* **10**, 664–671 (2021).

581. Sakurai, S. *et al.* Empagliflozin decreases the plasma concentration of plasminogen activator inhibitor-1 (PAI-1) in patients with type 2 diabetes: Association with improvement of fibrinolysis. *J. Diabetes Complications* **34**, 107703 (2020).

582. Yarmolinsky, J. *et al.* Plasminogen activator inhibitor-1 and type 2 diabetes: a systematic review and meta-analysis of observational studies. *Sci. Rep.* **6**, 17714 (2016).

583. Pretorius, L. *et al.* Platelet activity and hypercoagulation in type 2 diabetes. *Cardiovasc. Diabetol.* **17**, 141 (2018).

584. Tripodi, A. *et al.* Hypercoagulability in patients with type 2 diabetes mellitus detected by a thrombin generation assay. *J. Thromb. Thrombolysis* **31**, 165–172 (2011).

585. Bessueille, L. & Magne, D. Inflammation: a culprit for vascular calcification in atherosclerosis and diabetes. *Cell. Mol. Life Sci.* **72**, 2475–2489 (2015).

586. Harper, E. *et al.* Vascular calcification in type-2 diabetes and cardiovascular disease: Integrative roles for OPG, RANKL and TRAIL. *Vascul. Pharmacol.* **82**, 30–40 (2016).

587. Raaz Uwe *et al.* Transcription Factor Runx2 Promotes Aortic Fibrosis and Stiffness in Type 2 Diabetes Mellitus. *Circ. Res.* **117**, 513–524 (2015).

588. Stabley John N. & Towler Dwight A. Arterial Calcification in Diabetes Mellitus. *Arterioscler. Thromb. Vasc. Biol.* **37**, 205–217 (2017).

589. Sanchis, P. *et al.* Role of Advanced Glycation End Products on Aortic Calcification in Patients with Type 2 Diabetes Mellitus. *J. Clin. Med.* **9**, 1751 (2020).

590. Eghbali-Fatourechi, G. Z. *et al.* Circulating Osteoblast-Lineage Cells in Humans. *N. Engl. J. Med.* **352**, 1959–1966 (2005).

591. Fadini Gian Paolo *et al.* Widespread Increase in Myeloid Calcifying Cells Contributes to Ectopic Vascular Calcification in Type 2 Diabetes. *Circ. Res.* **108**, 1112–1121 (2011).

592. Hansson, G. K. & Hermansson, A. The immune system in atherosclerosis. *Nat. Immunol.* **12**, 204–212 (2011).

593. Rocha, V. Z. & Libby, P. Obesity, inflammation, and atherosclerosis. *Nat. Rev. Cardiol.* **6**, 399–409 (2009).

594. Wolf Dennis & Ley Klaus. Immunity and Inflammation in Atherosclerosis. *Circ. Res.* **124**, 315–327 (2019).

595. Chen, C. & Khismatullin, D. B. Oxidized Low-Density Lipoprotein Contributes to Atherogenesis via Co-activation of Macrophages and Mast Cells. *PLOS ONE* **10**, e0123088 (2015).

596. Singh, P. *et al.* Reduced oxidized LDL in T2D plaques is associated with a greater statin usage but not with future cardiovascular events. *Cardiovasc. Diabetol.* **19**, 214 (2020).

597. Takahashi, T. *et al.* The endocytosis of oxidized LDL via the activation of the angiotensin II type 1 receptor. *iScience* **24**, 102076 (2021).

598. Chistiakov, D. A., Melnichenko, A. A., Myasoedova, V. A., Grechko, A. V. & Orekhov, A. N. Mechanisms of foam cell formation in atherosclerosis. *J. Mol. Med.* **95**, 1153–1165 (2017).

599. Luo, Y. *et al.* Macrophagic CD146 promotes foam cell formation and retention during atherosclerosis. *Cell Res.* **27**, 352–372 (2017).

600. Poznyak, A. V. *et al.* Signaling Pathways and Key Genes Involved in Regulation of foam Cell Formation in Atherosclerosis. *Cells* **9**, 584 (2020).

601. Bartlett, B., Ludewick, H. P., Misra, A., Lee, S. & Dwivedi, G. Macrophages and T cells in atherosclerosis: a translational perspective. *Am. J. Physiol.-Heart Circ. Physiol.* **317**, H375–H386 (2019).

602. van Dijk R. A. *et al.* A Change in Inflammatory Footprint Precedes Plaque Instability: A Systematic Evaluation of Cellular Aspects of the Adaptive Immune Response in Human Atherosclerosis. *J. Am. Heart Assoc.* **4**, e001403 (2015).

603. Singh Rajesh K. *et al.* TLR4 (Toll-Like Receptor 4)-Dependent Signaling Drives Extracellular Catabolism of LDL (Low-Density Lipoprotein) Aggregates. *Arterioscler. Thromb. Vasc. Biol.* **40**, 86–102 (2020).

604. Allahverdian, S., Chaabane, C., Boukais, K., Francis, G. A. & Bochaton-Piallat, M.-L. Smooth muscle cell fate and plasticity in atherosclerosis. *Cardiovasc. Res.* **114**, 540–550 (2018).

605. Chappell, J. *et al.* Extensive Proliferation of a Subset of Differentiated, yet Plastic, Medial Vascular Smooth Muscle Cells Contributes to Neointimal Formation in Mouse Injury and Atherosclerosis Models. *Circ. Res.* **119**, 1313–1323 (2016).

606. Pan, J. *et al.* AIM2 regulates vascular smooth muscle cell migration in atherosclerosis.

Biochem. Biophys. Res. Commun. **497**, 401–409 (2018).

607. Abdolmaleki, F., Gheibi Hayat, S. M., Bianconi, V., Johnston, T. P. & Sahebkar, A. Atherosclerosis and immunity: A perspective. *Trends Cardiovasc. Med.* **29**, 363–371 (2019).

608. Banerjee Chirantan & Chimowitz Marc I. Stroke Caused by Atherosclerosis of the Major Intracranial Arteries. *Circ. Res.* **120**, 502–513 (2017).

609. Howard Dominic P.J. *et al.* Symptomatic Carotid Atherosclerotic Disease. *Stroke* **46**, 182–189 (2015).

610. Aronson, D. & Rayfield, E. J. How hyperglycemia promotes atherosclerosis: molecular mechanisms. *Cardiovasc. Diabetol.* **1**, 1 (2002).

611. Bornfeldt, K. E. & Tabas, I. Insulin Resistance, Hyperglycemia, and Atherosclerosis. *Cell Metab.* **14**, 575–585 (2011).

612. Chait, A. & Bornfeldt, K. E. Diabetes and atherosclerosis: is there a role for hyperglycemia? *J. Lipid Res.* **50**, S335–S339 (2009).

613. Poznyak, A. *et al.* The Diabetes Mellitus–Atherosclerosis Connection: The Role of Lipid and Glucose Metabolism and Chronic Inflammation. *Int. J. Mol. Sci.* **21**, 1835 (2020).

614. de Almeida-Pititto, B. *et al.* Usefulness of circulating E-selectin to early detection of the atherosclerotic process in the Brazilian Longitudinal Study of Adult Health (ELSA-Brasil). *Diabetol. Metab. Syndr.* **8**, 19 (2016).

615. Yoshida Masayuki, Takano Yoshio, Sasaoka Taishi, Izumi Toru, & Kimura Akinori. E-Selectin Polymorphism Associated With Myocardial Infarction Causes Enhanced Leukocyte-Endothelial Interactions Under Flow Conditions. *Arterioscler. Thromb. Vasc. Biol.* **23**, 783–788 (2003).

616. Yu, G., Rux, A. H., Ma, P., Bdeir, K. & Sachais, B. S. Endothelial expression of E-selectin is induced by the platelet-specific chemokine platelet factor 4 through LRP in an NF-κB–dependent manner. *Blood* **105**, 3545–3551 (2005).

617. Bozic, M. *et al.* Impaired Vitamin D Signaling in Endothelial Cell Leads to an Enhanced Leukocyte-Endothelium Interplay: Implications for Atherosclerosis Development. *PloS One* **10**, e0136863 (2015).

618. Habas, K. & Shang, L. Alterations in intercellular adhesion molecule 1 (ICAM-1) and vascular cell adhesion molecule 1 (VCAM-1) in human endothelial cells. *Tissue Cell* **54**, 139–143 (2018).

619. Xu, K., Liu, X., Yin, D., Ren, G. & Zhao, Y. PP2A alleviates oxidized LDL-induced endothelial dysfunction by regulating LOX-1/ROS/MAPK axis. *Life Sci.* **243**, 117270 (2020).

620. Packard, R. R. S. & Libby, P. Inflammation in Atherosclerosis: From Vascular Biology to Biomarker Discovery and Risk Prediction. *Clin. Chem.* **54**, 24–38 (2008).

621. Tavares, J. C. & Muscará, M. N. Chapter 14 - Adhesion Molecules and Endothelium. in

Endothelium and Cardiovascular Diseases (eds. Da Luz, P. L., Libby, P., Chagas, A. C. P. & Laurindo, F. R. M.) 189–201 (Academic Press, 2018). doi:10.1016/B978-0-12-812348-5.00014-3.

622. Kosiborod, M. *et al.* Vascular complications in patients with type 2 diabetes: prevalence and associated factors in 38 countries (the DISCOVER study program). *Cardiovasc. Diabetol.* **17**, 150 (2018).

623. Dewanjee, S. *et al.* Molecular mechanism of diabetic neuropathy and its pharmacotherapeutic targets. *Eur. J. Pharmacol.* **833**, 472–523 (2018).

624. Rodríguez, M. L., Pérez, S., Mena-Mollá, S., Desco, M. C. & Ortega, Á. L. Oxidative Stress and Microvascular Alterations in Diabetic Retinopathy: Future Therapies. *Oxid. Med. Cell. Longev.* **2019**, (2019).

625. Wada, J. & Makino, H. Inflammation and the pathogenesis of diabetic nephropathy. *Clin. Sci. Lond. Engl. 1979* **124**, 139–152 (2013).

626. Li, W., Chen, S., Mei, Z., Zhao, F. & Xiang, Y. Polymorphisms in Sorbitol-Aldose Reductase (Polyol) Pathway Genes and Their Influence on Risk of Diabetic Retinopathy Among Han Chinese. *Med. Sci. Monit. Int. Med. J. Exp. Clin. Res.* **25**, 7073–7078 (2019).

627. Lin, S. *et al.* Association between Aldose Reductase Gene C(-106)T Polymorphism and Diabetic Retinopathy: A Systematic Review and Meta-Analysis. *Ophthalmic Res.* **63**, 224–233 (2020).

628. Sabanayagam, C. *et al.* Incidence and progression of diabetic retinopathy: a systematic review. *Lancet Diabetes Endocrinol.* **7**, 140–149 (2019).

629. Wagnew, F. *et al.* Diabetic nephropathy and hypertension in diabetes patients of sub-Saharan countries: a systematic review and meta-analysis. *BMC Res. Notes* **11**, (2018).

630. Zhang, X.-X., Kong, J. & Yun, K. Prevalence of Diabetic Nephropathy among Patients with Type 2 Diabetes Mellitus in China: A Meta-Analysis of Observational Studies. *J. Diabetes Res.* **2020**, 2315607 (2020).

631. Feldman, E. L. *et al.* Diabetic neuropathy. *Nat. Rev. Dis. Primer* **5**, 41 (2019).

632. Iqbal, Z. *et al.* Diabetic Peripheral Neuropathy: Epidemiology, Diagnosis, and Pharmacotherapy. *Clin. Ther.* **40**, 828–849 (2018).

633. Carrizzo, A. *et al.* The Main Determinants of Diabetes Mellitus Vascular Complications: Endothelial Dysfunction and Platelet Hyperaggregation. *Int. J. Mol. Sci.* **19**, 2968 (2018).

634. Dal Canto, E. *et al.* Diabetes as a cardiovascular risk factor: An overview of global trends of macro and micro vascular complications. *Eur. J. Prev. Cardiol.* **26**, 25–32 (2019).

635. Mutie, P. M. *et al.* An investigation of causal relationships between prediabetes and vascular complications. *Nat. Commun.* **11**, 4592 (2020).

636. Cusick, M. *et al.* Associations of Mortality and Diabetes Complications in Patients With

Type 1 and Type 2 Diabetes: Early Treatment Diabetic Retinopathy Study report no. 27. *Diabetes Care* **28**, 617–625 (2005).

637. Jiao, J. *et al.* Dietary fats and mortality among patients with type 2 diabetes: analysis in two population based cohort studies. *The BMJ* **366**, 14009 (2019).

638. Lin, X. *et al.* Global, regional, and national burden and trend of diabetes in 195 countries and territories: an analysis from 1990 to 2025. *Sci. Rep.* **10**, 14790 (2020).

639. Archundia Herrera, M. C., Subhan, F. B. & Chan, C. B. Dietary Patterns and Cardiovascular Disease Risk in People with Type 2 Diabetes. *Curr. Obes. Rep.* **6**, 405–413 (2017).

640. Rawshani, A. *et al.* Risk Factors, Mortality, and Cardiovascular Outcomes in Patients with Type 2 Diabetes. *N. Engl. J. Med.* **379**, 633–644 (2018).

641. Reaven, P. D. *et al.* Intensive Glucose Control in Patients with Type 2 Diabetes — 15-Year Follow-up. *N. Engl. J. Med.* **380**, 2215–2224 (2019).

642. Sun, B. *et al.* Association between carotid plaque characteristics and acute cerebral infarction determined by MRI in patients with type 2 diabetes mellitus. *Cardiovasc. Diabetol.* **16**, 111 (2017).

643. de Miguel-Yanes, J. M. *et al.* Impact of type 2 diabetes mellitus on in-hospital-mortality after major cardiovascular events in Spain (2002–2014). *Cardiovasc. Diabetol.* **16**, 126 (2017).

644. Larsson, S. C. *et al.* Type 1 and type 2 diabetes mellitus and incidence of seven cardiovascular diseases. *Int. J. Cardiol.* **262**, 66–70 (2018).

645. Cardoso, C. R. L., Salles, G. C., Leite, N. C. & Salles, G. F. Prognostic impact of carotid intima-media thickness and carotid plaques on the development of micro- and macrovascular complications in individuals with type 2 diabetes: the Rio de Janeiro type 2 diabetes cohort study. *Cardiovasc. Diabetol.* **18**, 2 (2019).

646. Dalan, R., Sx, S. C., Seneviratna, A. & Ek, D. C. Carotid Artery Intima-Media Thickness Is Associated With Cardiometabolic Risk Factors In Diabetes. *Atherosclerosis* **287**, e126 (2019).

647. Jujić, A. *et al.* Glucose-Dependent Insulinotropic Peptide in the High-Normal Range Is Associated With Increased Carotid Intima-Media Thickness. *Diabetes Care* **44**, 224–230 (2021).

648. Lopes-Virella, M. F. *et al.* Risk Factors Related to Inflammation and Endothelial Dysfunction in the DCCT/EDIC Cohort and Their Relationship With Nephropathy and Macrovascular Complications. *Diabetes Care* **31**, 2006–2012 (2008).

649. Joseph, T. P. *et al.* Coronary artery calcification, carotid intima-media thickness and cardiac dysfunction in young adults with type 2 diabetes mellitus. *J. Diabetes Complications* **34**, 107609 (2020).

650. Yang, C.-W. *et al.* Subclinical Atherosclerosis Markers of Carotid Intima-Media Thickness,

Carotid Plaques, Carotid Stenosis, and Mortality in Community-Dwelling Adults. *Int. J. Environ. Res. Public. Health* **17**, 4745 (2020).

651. Alharby, H. *et al.* Association of lipid peroxidation and interleukin-6 with carotid atherosclerosis in type 2 diabetes. *Cardiovasc. Endocrinol. Metab.* **8**, 73–76 (2019).

652. Petrie, J. R., Guzik, T. J. & Touyz, R. M. Diabetes, Hypertension, and Cardiovascular Disease: Clinical Insights and Vascular Mechanisms. *Can. J. Cardiol.* **34**, 575–584 (2018).

653. Wu, D. *et al.* Influence of blood pressure variability on early carotid atherosclerosis in hypertension with and without diabetes. *Medicine (Baltimore)* **95**, e3864 (2016).

654. Chen, G., McAlister, F. A., Walker, R. L., Hemmelgarn, B. R. & Campbell, N. R. Cardiovascular outcomes in framingham participants with diabetes: the importance of blood pressure. *Hypertension* **57**, 891–897 (2011).

655. Climie Rachel E. *et al.* Macrovasculature and Microvasculature at the Crossroads Between Type 2 Diabetes Mellitus and Hypertension. *Hypertension* **73**, 1138–1149 (2019).

656. Rizvi, A. A. ADDRESSING HYPERTENSION IN THE PATIENT WITH TYPE 2 DIABETES MELLITUS: PATHOGENESIS, GOALS, AND THERAPEUTIC APPROACH. *Eur. Med. J. Diabetes* **5**, 84–92 (2017).

657. Prasad, K. Does HbA1cc Play a Role in the Development of Cardiovascular Diseases? *Curr. Pharm. Des.* **24**, 2876–2882 (2018).

658. Selvin, E. *et al.* Glycaemia (haemoglobin A1c) and incident ischaemic stroke: the Atherosclerosis Risk in Communities (ARIC) Study. *Lancet Neurol.* **4**, 821–826 (2005).

659. Tabatabaei-Malazy, O. *et al.* Effect of metabolic control on oxidative stress, subclinical atherosclerosis and peripheral artery disease in diabetic patients. *J. Diabetes Metab. Disord.* **14**, 84 (2015).

660. ADVANCE Collaborative Group *et al.* Intensive blood glucose control and vascular outcomes in patients with type 2 diabetes. *N. Engl. J. Med.* **358**, 2560–2572 (2008).

661. Association, A. D. 10. Cardiovascular Disease and Risk Management: Standards of Medical Care in Diabetes—2020. *Diabetes Care* **43**, S111–S134 (2020).

662. Skyler, J. S. *et al.* Intensive glycemic control and the prevention of cardiovascular events: implications of the ACCORD, ADVANCE, and VA diabetes trials: a position statement of the American Diabetes Association and a scientific statement of the American College of Cardiology Foundation and the American Heart Association. *Circulation* **119**, 351–357 (2009).

663. Laiteerapong, N. *et al.* The Legacy Effect in Type 2 Diabetes: Impact of Early Glycemic Control on Future Complications (The Diabetes & Aging Study). *Diabetes Care* **42**, 416–426 (2019).

664. Verma, S. *et al.* Effect of glycemic control and disease duration on cardiac autonomic function and oxidative stress in type 2 diabetes mellitus. *J. Diabetes Metab. Disord.* **17**,

149–158 (2018).

665. Iannantuoni, F. *et al.* Does Glycemic Control Modulate the Impairment of NLRP3 Inflammasome Activation in Type 2 Diabetes? *Antioxid. Redox Signal.* **30**, 232–240 (2018).

666. Punthakee, Z. *et al.* Durable change in glycaemic control following intensive management of type 2 diabetes in the ACCORD clinical trial. *Diabetologia* **57**, 2030–2037 (2014).

667. Tao, Y. *et al.* SIRT4 suppresses the PI3K/Akt/NF-κB signaling pathway and attenuates HUVEC injury induced by oxLDL. *Mol. Med. Rep.* **19**, 4973–4979 (2019).

668. Zhang, G. *et al.* OxLDL/β2GPI/anti-β2GPI Ab complex induces inflammatory activation via the TLR4/NF-κB pathway in HUVECs. *Mol. Med. Rep.* **23**, 1–1 (2021).

669. Halcox, J. P. *et al.* Prevalence and treatment of atherogenic dyslipidemia in the primary prevention of cardiovascular disease in Europe: EURIKA, a cross-sectional observational study. *BMC Cardiovasc. Disord.* **17**, 160 (2017).

670. Dias, S., Paredes, S. & Ribeiro, L. Drugs Involved in Dyslipidemia and Obesity Treatment: Focus on Adipose Tissue. *Int. J. Endocrinol.* **2018**, e2637418 (2018).

671. Zhang, Y. *et al.* Combined lifestyle factors and risk of incident type 2 diabetes and prognosis among individuals with type 2 diabetes: a systematic review and meta-analysis of prospective cohort studies. *Diabetologia* **63**, 21–33 (2020).

672. Petersen, M. C. & Shulman, G. I. Mechanisms of Insulin Action and Insulin Resistance. *Physiol. Rev.* **98**, 2133–2223 (2018).

673. Szendroedi, J., Phielix, E. & Roden, M. The role of mitochondria in insulin resistance and type 2 diabetes mellitus. *Nat. Rev. Endocrinol.* **8**, 92–103 (2012).

674. Katsuki, A. *et al.* Homeostasis Model Assessment Is a Reliable Indicator of Insulin Resistance During Follow-up of Patients With Type 2 Diabetes. *Diabetes Care* **24**, 362–365 (2001).

675. Burrows, R. *et al.* Healthy Chilean Adolescents with HOMA-IR ≥ 2.6 Have Increased Cardiometabolic Risk: Association with Genetic, Biological, and Environmental Factors. *J. Diabetes Res.* **2015**, 783296 (2015).

676. Chissini, R. de B. C., Kuschnir, M. C., de Oliveira, C. L., Giannini, D. T. & Santos, B. Cutoff values for HOMA-IR associated with metabolic syndrome in the Study of Cardiovascular Risk in Adolescents (ERICA Study). *Nutrition* **71**, 110608 (2020).

677. Esteghamati, A. *et al.* Optimal cut-off of homeostasis model assessment of insulin resistance (HOMA-IR) for the diagnosis of metabolic syndrome: third national surveillance of risk factors of non-communicable diseases in Iran (SuRFNCD-2007). *Nutr. Metab.* **7**, 26 (2010).

678. Gayoso-Diz, P. *et al.* Insulin resistance (HOMA-IR) cut-off values and the metabolic syndrome in a general adult population: effect of gender and age: EPIRCE cross-sectional study. *BMC Endocr. Disord.* **13**, 47 (2013).

679. Kim, B. *et al.* The cut-off values of surrogate measures for insulin resistance in the Korean population according to the Korean Genome and Epidemiology Study (KOGES). *PLOS ONE* **13**, e0206994 (2018).

680. Hirata, T. *et al.* HOMA-IR Values are Associated With Glycemic Control in Japanese Subjects Without Diabetes or Obesity: The KOBE Study. *J. Epidemiol.* **25**, 407–414 (2015).

681. Akash, M. S. H., Rehman, K. & Liaqat, A. Tumor Necrosis Factor-Alpha: Role in Development of Insulin Resistance and Pathogenesis of Type 2 Diabetes Mellitus. *J. Cell. Biochem.* **119**, 105–110 (2018).

682. Alzamil, H. Elevated Serum TNF-α Is Related to Obesity in Type 2 Diabetes Mellitus and Is Associated with Glycemic Control and Insulin Resistance. *J. Obes.* **2020**, e5076858 (2020).

683. de Vries, M. A. *et al.* Glucose-dependent leukocyte activation in patients with type 2 diabetes mellitus, familial combined hyperlipidemia and healthy controls. *Metabolism.* **64**, 213–217 (2015).

684. Fadini, G. P. *et al.* p66Shc gene expression in peripheral blood mononuclear cells and progression of diabetic complications. *Cardiovasc. Diabetol.* **17**, 16 (2018).

685. Swirski, F. K. & Nahrendorf, M. Leukocyte Behavior in Atherosclerosis, Myocardial Infarction, and Heart Failure. *Science* **339**, 161–166 (2013).

686. Lee, R. H. & Bergmeier, W. Sugar makes neutrophils RAGE: linking diabetes-associated hyperglycemia to thrombocytosis and platelet reactivity. *J. Clin. Invest.* **127**, 2040–2043 (2017).

687. Pettersson, U. S. *et al.* Increased Recruitment but Impaired Function of Leukocytes during Inflammation in Mouse Models of Type 1 and Type 2 Diabetes. *PLoS ONE* **6**, e22480 (2011).

688. Elkhatib, M. A. W. *et al.* Amelioration of perivascular adipose inflammation reverses vascular dysfunction in a model of nonobese prediabetic metabolic challenge: potential role of antidiabetic drugs. *Transl. Res.* **214**, 121–143 (2019).

689. Verboven, K. *et al.* Abdominal subcutaneous and visceral adipocyte size, lipolysis and inflammation relate to insulin resistance in male obese humans. *Sci. Rep.* **8**, 4677 (2018).

690. Lainampetch, J. *et al.* Association of Tumor Necrosis Factor Alpha, Interleukin 6, and C-Reactive Protein with the Risk of Developing Type 2 Diabetes: A Retrospective Cohort Study of Rural Thais. *J. Diabetes Res.* **2019**, 9051929 (2019).

691. Okazaki, S. *et al.* Association of interleukin-6 with the progression of carotid atherosclerosis: a 9-year follow-up study. *Stroke* **45**, 2924–2929 (2014).

692. Pradhan, A. D., Manson, J. E., Rifai, N., Buring, J. E. & Ridker, P. M. C-reactive protein, interleukin 6, and risk of developing type 2 diabetes mellitus. *JAMA* **286**, 327–334 (2001).

693. Wang, X. *et al.* Inflammatory markers and risk of type 2 diabetes: a systematic review and meta-analysis. *Diabetes Care* **36**, 166–175 (2013).

694. Lontchi-Yimagou, E., Sobngwi, E., Matsha, T. E. & Kengne, A. P. Diabetes mellitus and inflammation. *Curr. Diab. Rep.* **13**, 435–444 (2013).

695. Andreozzi, F. *et al.* Interleukin-6 Impairs the Insulin Signaling Pathway, Promoting Production of Nitric Oxide in Human Umbilical Vein Endothelial Cells. *Mol. Cell. Biol.* **27**, 2372–2383 (2007).

696. Aronson, D. *et al.* Obesity is the major determinant of elevated C-reactive protein in subjects with the metabolic syndrome. *Int. J. Obes. Relat. Metab. Disord. J. Int. Assoc. Study Obes.* **28**, 674–679 (2004).

697. Kahn, S. E. *et al.* Obesity Is a Major Determinant of the Association of C-Reactive Protein Levels and the Metabolic Syndrome in Type 2 Diabetes. *Diabetes* **55**, 2357–2364 (2006).

698. Damen, M. S. M. A., Popa, C. D., Netea, M. G., Dinarello, C. A. & Joosten, L. A. B. Interleukin-32 in chronic inflammatory conditions is associated with a higher risk of cardiovascular diseases. *Atherosclerosis* **264**, 83–91 (2017).

699. Fadaei, R. *et al.* Serum levels of IL-32 in patients with type 2 diabetes mellitus and its relationship with TNF-α and IL-6. *Cytokine* **125**, 154832 (2020).

700. Barakat, L. A. A., Shora, H. A., El-Deen, I. M. & El-Sayed, E.-S. A. E.-S. Inflammatory Biomarkers of Cardiometabolic Risk in Obese Egyptian Type 2 Diabetics. *Med. Sci. Basel Switz.* **5**, (2017).

701. Carlsson, A. C. *et al.* Association of soluble tumor necrosis factor receptors 1 and 2 with nephropathy, cardiovascular events, and total mortality in type 2 diabetes. *Cardiovasc. Diabetol.* **15**, 40 (2016).

702. Han, M. S. *et al.* Regulation of adipose tissue inflammation by interleukin 6. *Proc. Natl. Acad. Sci.* **117**, 2751–2760 (2020).

703. Senn, J. J., Klover, P. J., Nowak, I. A. & Mooney, R. A. Interleukin-6 Induces Cellular Insulin Resistance in Hepatocytes. *Diabetes* **51**, 3391–3399 (2002).

704. Ellingsgaard, H. *et al.* Interleukin-6 regulates pancreatic α-cell mass expansion. *Proc. Natl. Acad. Sci.* **105**, 13163–13168 (2008).

705. Bowker, N. *et al.* Meta-analysis investigating the role of interleukin-6 mediated inflammation in type 2 diabetes. *EBioMedicine* **61**, (2020).

706. Danesh, J. *et al.* Long-Term Interleukin-6 Levels and Subsequent Risk of Coronary Heart Disease: Two New Prospective Studies and a Systematic Review. *PLOS Med.* **5**, e78 (2008).

707. Beckman Joshua A. & Creager Mark A. Vascular Complications of Diabetes. *Circ. Res.* **118**, 1771–1785 (2016).

708. Sardu, C., De Lucia, C., Wallner, M. & Santulli, G. Diabetes Mellitus and Its Cardiovascular Complications: New Insights into an Old Disease. *J. Diabetes Res.* **eCollection 2019**, 1905194 (2019).

709. Sasikala, T., M Manohar, S., RR Bitla, A., Sarala, S. & Vaikkakara, S. Intercellular adhesion molecule-1 is a surrogate biomarker for subclinical atherosclerosis in Type 2 diabetes mellitus. *Biomark. Med.* **15**, 123–134 (2021).

710. Bourdillon, M.-C. *et al.* ICAM-1 Deficiency Reduces Atherosclerotic Lesions in Double-Knockout Mice (ApoE−/−/ICAM-1−/−) Fed a Fat or a Chow Diet. Arterioscler Thromb Vasc Biol.**20,** 2630-2635 (2000)

711. Collins, R. G. *et al.* P-Selectin or Intercellular Adhesion Molecule (Icam)-1 Deficiency Substantially Protects against Atherosclerosis in Apolipoprotein E–Deficient Mice. *J. Exp. Med.* **191**, 189–194 (2000).

712. Liu, C.-W. *et al.* Resveratrol attenuates ICAM-1 expression and monocyte adhesiveness to TNF-α-treated endothelial cells: evidence for an anti-inflammatory cascade mediated by the miR-221/222/AMPK/p38/NF-κB pathway. *Sci. Rep.* **7**, 44689 (2017).

713. Seo, Y. *et al.* Antiatherogenic Effect of Resveratrol Attributed to Decreased Expression of ICAM-1 (Intercellular Adhesion Molecule-1). *Arterioscler. Thromb. Vasc. Biol.* **39**, 675–684 (2019).

714. Odegaard, A. O. *et al.* Oxidative stress, inflammation, endothelial dysfunction and incidence of type 2 diabetes. *Cardiovasc. Diabetol.* **15**, 51 (2016).

715. Nonaka, K. *et al.* Advanced glycation end-products increase IL-6 and ICAM-1 expression via RAGE, MAPK and NF-κB pathways in human gingival fibroblasts. *J. Periodontal Res.* **53**, 334–344 (2018).

716. Riek, A. E. *et al.* Vitamin D Suppression of Endoplasmic Reticulum Stress Promotes an Antiatherogenic Monocyte/Macrophage Phenotype in Type 2 Diabetic Patients. *J. Biol. Chem.* **287**, 38482–38494 (2012).

717. Wang, C.-Y. *et al.* Autophagy facilitates cytokine-induced ICAM-1 expression. *Innate Immun.* **20**, 200–213 (2014).

718. Matsumoto, K. *et al.* Comparison of serum concentrations of soluble adhesion molecules in diabetic microangiopathy and macroangiopathy. *Diabet. Med. J. Br. Diabet. Assoc.* **19**, 822–826 (2002).

719. Motawi, T. M., Abou-Seif, M. A., Bader, A. M. & Mahmoud, M. O. Effect of glycemic control on soluble RAGE and oxidative stress in type 2 diabetic patients. *BMC Endocr. Disord.* **13**, 32 (2013).

720. Néri, A. K. *et al.* Cardiovascular risk assessment and association with novel biomarkers in patients with Type 2 diabetes mellitus. *Biomark. Med.* **15,** 8 (2021)

721. Hegazy, G. A., Awan, Z., Hashem, E., Al-Ama, N. & Abunaji, A. B. Levels of soluble cell adhesion molecules in type 2 diabetes mellitus patients with macrovascular complications. *J. Int. Med. Res.* **48**, 0300060519893858 (2020).

722. Kanda, K., Hayman, G. T., Silverman, M. D. & Lelkes, P. I. Comparison of ICAM-1 and VCAM-

1 expression in various human endothelial cell types and smooth muscle cells. *Endothel. J. Endothel. Cell Res.* **6**, 33–44 (1998).

723. Mu, W., Chen, M., Gong, Z., Zheng, F. & Xing, Q. Expression of vascular cell adhesion molecule-1 in the aortic tissues of atherosclerotic patients and the associated clinical implications. *Exp. Ther. Med.* **10**, 423–428 (2015).

724. Cybulsky, M. I. *et al.* A major role for VCAM-1, but not ICAM-1, in early atherosclerosis. *J. Clin. Invest.* **107**, 1255–1262 (2001).

725. Liu, J.-J. *et al.* Vascular cell adhesion molecule-1, but not intercellular adhesion molecule-1, is associated with diabetic kidney disease in Asians with type 2 diabetes. *J. Diabetes Complications* **29**, 707–712 (2015).

726. Yan, Z. *et al.* CTRP3 is a novel biomarker for diabetic retinopathy and inhibits HGHL-induced VCAM-1 expression in an AMPK-dependent manner. *PLOS ONE* **12**, e0178253 (2017).

727. Jager, A. *et al.* Increased levels of soluble vascular cell adhesion molecule 1 are associated with risk of cardiovascular mortality in type 2 diabetes: the Hoorn study. *Diabetes* **49**, 485–491 (2000).

728. Kaur, H., Carriveau, R. & Mutus, B. A Simple Parallel Plate Flow Chamber to Study Effects of Shear Stress on Endothelial Cells. *Am. J. Biomed. Sci.***4***,* 70–78 (2012)

729. Wang, Y.-X. *et al.* A multi-component parallel-plate flow chamber system for studying the effect of exercise-induced wall shear stress on endothelial cells. *Biomed. Eng. OnLine* **15**, 154 (2016).

730. Zhang, Y. & Neelamegham, S. An analysis tool to quantify the efficiency of cell tethering and firm-adhesion in the parallel-plate flow chamber. *J. Immunol. Methods* **278**, 305–317 (2003).

731. Kaur, R., Kaur, M. & Singh, J. Endothelial dysfunction and platelet hyperactivity in type 2 diabetes mellitus: molecular insights and therapeutic strategies. *Cardiovasc. Diabetol.* **17**, 121 (2018).

732. Marchio, P. *et al.* Targeting Early Atherosclerosis: A Focus on Oxidative Stress and Inflammation. *Oxid. Med. Cell. Longev.* **2019**, 8563845 (2019).

733. Chang, W. *et al.* Glucagon-like peptide-1 receptor agonist dulaglutide prevents ox-LDL-induced adhesion of monocytes to human endothelial cells: An implication in the treatment of atherosclerosis. *Mol. Immunol.* **116**, 73–79 (2019).

734. Ouedraogo, R. *et al.* Adiponectin deficiency increases leukocyte-endothelium interactions via upregulation of endothelial cell adhesion molecules in vivo. *J. Clin. Invest.* **117**, 1718–1726 (2007).

735. Smolock, A. R., Mishra, G., Eguchi, K., Eguchi, S. & Scalia, R. Protein Kinase C Upregulates Intercellular Adhesion Molecule-1 and Leukocyte-Endothelium Interactions in

Hyperglycemia via Activation of Endothelial Expressed Calpain. *Arterioscler. Thromb. Vasc. Biol.* **31**, 289–296 (2011).

736. Tabit Corey E. *et al.* Protein Kinase C-β Contributes to Impaired Endothelial Insulin Signaling in Humans With Diabetes Mellitus. *Circulation* **127**, 86–95 (2013).

737. Martí-Masanet, M. *et al.* Leukocyte–Endothelium Interaction Is Associated with Fat Mass in Children. *J. Pediatr.* **221**, 181-187.e1 (2020).

738. Azcutia, V. *et al.* Inflammation Determines the Pro-Adhesive Properties of High Extracellular D-Glucose in Human Endothelial Cells In Vitro and Rat Microvessels In Vivo. *PLOS ONE* **5**, e10091 (2010).

739. Bakker, W., Eringa, E. C., Sipkema, P. & van Hinsbergh, V. W. M. Endothelial dysfunction and diabetes: roles of hyperglycemia, impaired insulin signaling and obesity. *Cell Tissue Res.* **335**, 165 (2008).

740. Galkina, E. & Ley, K. Immune and Inflammatory Mechanisms of Atherosclerosis. *Annu. Rev. Immunol.* **27**, 165–197 (2009).

741. Yuan, C. *et al.* The effect of diabetes self-management education on body weight, glycemic control, and other metabolic markers in patients with type 2 diabetes mellitus. *J. Diabetes Res.* **2014**, 789761 (2014).

742. Mita, T. *et al.* Nateglinide reduces carotid intima-media thickening in type 2 diabetic patients under good glycemic control. *Arterioscler. Thromb. Vasc. Biol.* **27**, 2456–2462 (2007).

743. Patti, A. M. *et al.* Exenatide once-weekly improves metabolic parameters, endothelial dysfunction and carotid intima-media thickness in patients with type-2 diabetes: An 8-month prospective study. *Diabetes Res. Clin. Pract.* **149**, 163–169 (2019).

744. Tenjin, A. *et al.* Short-term change of carotid intima-media thickness after treatment of hyperglycemia in patients with diabetes: a cross-sectional study. *BMC Res. Notes* **9**, 281 (2016).

745. Luo, X., Yang, Y., Cao, T. & Li, Z. Differences in left and right carotid intima-media thickness and the associated risk factors. *Clin. Radiol.* **66**, 393–398 (2011).

746. Hedna, V. S. *et al.* Hemispheric Differences in Ischemic Stroke: Is Left-Hemisphere Stroke More Common? *J. Clin. Neurol. Seoul Korea* **9**, 97–102 (2013).

747. Rodríguez Hernández, S. A. *et al.* Is there a side predilection for cerebrovascular disease? *Hypertens. Dallas Tex 1979* **42**, 56–60 (2003).

748. Selwaness, M. *et al.* Atherosclerotic plaque in the left carotid artery is more vulnerable than in the right. *Stroke* **45**, 3226–3230 (2014).

749. Fishman, S. L., Sonmez, H., Basman, C., Singh, V. & Poretsky, L. The role of advanced glycation end-products in the development of coronary artery disease in patients with and without diabetes mellitus: a review. *Mol. Med.* **24**, 59 (2018).

750. Rubattu, S., Forte, M. & Raffa, S. Circulating Leukocytes and Oxidative Stress in Cardiovascular Diseases: A State of the Art. *Oxid. Med. Cell. Longev.* **2019**, 2650429 (2019).

751. González, F., Rote, N. S., Minium, J. & Kirwan, J. P. Reactive oxygen species-induced oxidative stress in the development of insulin resistance and hyperandrogenism in polycystic ovary syndrome. *J. Clin. Endocrinol. Metab.* **91**, 336–340 (2006).

752. Bhansali, S., Bhansali, A., Dutta, P., Walia, R. & Dhawan, V. Metformin upregulates mitophagy in patients with T2DM: A randomized placebo-controlled study. *J. Cell. Mol. Med.* **24**, 2832–2846 (2020).

753. Zhang Min *et al.* Glycated Proteins Stimulate Reactive Oxygen Species Production in Cardiac Myocytes. *Circulation* **113**, 1235–1243 (2006).

754. Diaz-Vegas, A. *et al.* Is Mitochondrial Dysfunction a Common Root of Noncommunicable Chronic Diseases? *Endocr. Rev.* **41**, 491–517 (2020).

755. Anello, M. *et al.* Functional and morphological alterations of mitochondria in pancreatic beta cells from type 2 diabetic patients. *Diabetologia* **48**, 282–289 (2005).

756. Kaneto, H. *et al.* Oxidative stress, ER stress, and the JNK pathway in type 2 diabetes. *J. Mol. Med.* **83**, 429–439 (2005).

757. Boudina, S. *et al.* Mitochondrial Energetics in the Heart in Obesity-Related Diabetes: Direct Evidence for Increased Uncoupled Respiration and Activation of Uncoupling Proteins. *Diabetes* **56**, 2457–2466 (2007).

758. Phielix, E. *et al.* Lower Intrinsic ADP-Stimulated Mitochondrial Respiration Underlies In Vivo Mitochondrial Dysfunction in Muscle of Male Type 2 Diabetic Patients. *Diabetes* **57**, 2943–2949 (2008).

759. Mantena, S. K. *et al.* High fat diet induces dysregulation of hepatic oxygen gradients and mitochondrial function in vivo. *Biochem. J.* **417**, 183–193 (2009).

760. Liu, R. *et al.* Impaired Mitochondrial Dynamics and Bioenergetics in Diabetic Skeletal Muscle. *PLOS ONE* **9**, e92810 (2014).

761. Tur, J. *et al.* Mitofusin 2 in Macrophages Links Mitochondrial ROS Production, Cytokine Release, Phagocytosis, Autophagy, and Bactericidal Activity. *Cell Rep.* **32**, 108079 (2020).

762. Hu, Y. *et al.* The AMPK-MFN2 axis regulates MAM dynamics and autophagy induced by energy stresses. *Autophagy* **17,** 1142-1156 (2020)

763. Pereira, R. O. *et al.* OPA1 deficiency promotes secretion of FGF21 from muscle that prevents obesity and insulin resistance. *EMBO J.* **36**, 2126–2145 (2017).

764. Pereira Renata O *et al.* Abstract 18105: Mice Lacking OPA1 in Adipose Tissue Are Resistant to Diet-Induced Obesity and Insulin Resistance. *Circulation* **136**, A18105–A18105 (2017).

765. Campello, S. *et al.* Orchestration of lymphocyte chemotaxis by mitochondrial dynamics. *J. Exp. Med.* **203**, 2879–2886 (2006).

766. Amini, P. *et al.* Neutrophil extracellular trap formation requires OPA1-dependent glycolytic ATP production. *Nat. Commun.* **9**, 2958 (2018).

767. Buck, M. D. *et al.* Mitochondrial Dynamics Controls T Cell Fate Through Metabolic Programming. *Cell* **166**, 63–76 (2016).

768. Raffaele, M. *et al.* Cold Press Pomegranate Seed Oil Attenuates Dietary-Obesity Induced Hepatic Steatosis and Fibrosis through Antioxidant and Mitochondrial Pathways in Obese Mice. *Int. J. Mol. Sci.* **21**, (2020).

769. Rovira-Llopis, S. *et al.* Mitochondrial dynamics in type 2 diabetes: Pathophysiological implications. *Redox Biol.* **11**, 637–645 (2017).

770. Ding, M. *et al.* Melatonin prevents Drp1-mediated mitochondrial fission in diabetic hearts through SIRT1-PGC1α pathway. *J. Pineal Res.* **65**, e12491 (2018).

771. Tao, A. *et al.* Experimental diabetes mellitus exacerbates ischemia/reperfusion-induced myocardial injury by promoting mitochondrial fission: Role of down-regulation of myocardial Sirt1 and subsequent Akt/Drp1 interaction. *Int. J. Biochem. Cell Biol.* **105**, 94–103 (2018).

772. Kim, D., Sankaramoorthy, A. & Roy, S. Downregulation of Drp1 and Fis1 Inhibits Mitochondrial Fission and Prevents High Glucose-Induced Apoptosis in Retinal Endothelial Cells. *Cells* **9**, 1662 (2020).

773. Brand, C. S., Tan, V. P., Brown, J. H. & Miyamoto, S. RhoA regulates Drp1 mediated mitochondrial fission through ROCK to protect cardiomyocytes. *Cell. Signal.* **50**, 48–57 (2018).

774. Tavender, T. J. & Bulleid, N. J. Molecular mechanisms regulating oxidative activity of the Ero1 family in the endoplasmic reticulum. *Antioxid. Redox Signal.* **13**, 1177–1187 (2010).

775. Back, S. H. & Kaufman, R. J. Endoplasmic reticulum stress and type 2 diabetes. *Annu. Rev. Biochem.* **81**, 767–793 (2012).

776. Li, A., Song, N.-J., Riesenberg, B. P. & Li, Z. The Emerging Roles of Endoplasmic Reticulum Stress in Balancing Immunity and Tolerance in Health and Diseases: Mechanisms and Opportunities. *Front. Immunol.* **10**, (2020).

777. Martins, A. S., Alves, I., Helguero, L., Domingues, M. R. & Neves, B. M. The Unfolded Protein Response in Homeostasis and Modulation of Mammalian Immune Cells. *Int. Rev. Immunol.* **35**, 457–476 (2016).

778. Smith, J. A. Regulation of Cytokine Production by the Unfolded Protein Response; Implications for Infection and Autoimmunity. *Front. Immunol.* **9**, (2018).

779. So, J.-S. Roles of Endoplasmic Reticulum Stress in Immune Responses. *Mol. Cells* **41**, 705–716 (2018).

780. Luo, S., Baumeister, P., Yang, S., Abcouwer, S. F. & Lee, A. S. Induction of Grp78/BiP by translational block: activation of the Grp78 promoter by ATF4 through and upstream

ATF/CRE site independent of the endoplasmic reticulum stress elements. *J. Biol. Chem.* **278**, 37375–37385 (2003).

781. Dong, Y. *et al.* Baicalein Alleviates Liver Oxidative Stress and Apoptosis Induced by High-Level Glucose through the Activation of the PERK/Nrf2 Signaling Pathway. *Mol. Basel Switz.* **25**, (2020).

782. Hu, Y. *et al.* Sodium butyrate mitigates type 2 diabetes by inhibiting PERK-CHOP pathway of endoplasmic reticulum stress. *Environ. Toxicol. Pharmacol.* **64**, 112–121 (2018).

783. Cnop, M., Toivonen, S., Igoillo-Esteve, M. & Salpea, P. Endoplasmic reticulum stress and eIF2α phosphorylation: The Achilles heel of pancreatic β cells. *Mol. Metab.* **6**, 1024–1039 (2017).

784. Corona Velazquez, A. F. & Jackson, W. T. So Many Roads: the Multifaceted Regulation of Autophagy Induction. *Mol. Cell. Biol.* **38**, (2018).

785. Xia, G. *et al.* ROS-mediated autophagy through the AMPK signaling pathway protects INS-1 cells from human islet amyloid polypeptide-induced cytotoxicity. *Mol. Med. Rep.* **18**, 2744–2752 (2018).

786. Rovira-Llopis, S. *et al.* Is Autophagy Altered in the Leukocytes of Type 2 Diabetic Patients? *Antioxid. Redox Signal.* **23**, 1050–1056 (2015).

787. Chu, L.-Y., Hsueh, Y.-C., Cheng, H.-L. & Wu, K. K. Cytokine-induced autophagy promotes long-term VCAM-1 but not ICAM-1 expression by degrading late-phase IκBα. *Sci. Rep.* **7**, 12472 (2017).

788. Houtman, J. *et al.* Beclin1-driven autophagy modulates the inflammatory response of microglia via NLRP3. *EMBO J.* **38**, e99430 (2019).

789. Leonard, A. *et al.* Critical role of autophagy regulator Beclin1 in endothelial cell inflammation and barrier disruption. *Cell. Signal.* **61**, 120–129 (2019).

790. Kroemer, G. Autophagy and the Integrated Stress Response. *Mol. Cell* **40**, 280-293 (2010)

791. Niso-Santano, M. *et al.* Direct molecular interactions between Beclin 1 and the canonical NFκB activation pathway. **8**, 268-270 (2012)

792. Flory, J. & Lipska, K. Metformin in 2019. *JAMA* **321**, 1926–1927 (2019).

793. Sanchez-Rangel, E. & Inzucchi, S. E. Metformin: clinical use in type 2 diabetes. *Diabetologia* **60**, 1586–1593 (2017).

794. Adeshara, K. A., Bangar, N. S., Doshi, P. R., Diwan, A. & Tupe, R. S. Action of metformin therapy against advanced glycation, oxidative stress and inflammation in type 2 diabetes patients: 3 months follow-up study. *Diabetes Metab. Syndr.* **14**, 1449–1458 (2020).

795. Jing, Y. *et al.* Metformin improves obesity-associated inflammation by altering macrophages polarization. *Mol. Cell. Endocrinol.* **461**, 256–264 (2018).

796. Apostolova, N. *et al.* Mechanisms of action of metformin in type 2 diabetes: Effects on

mitochondria and leukocyte-endothelium interactions. *Redox Biol.* **34**, 101517 (2020).

797. Cen, J., Sargsyan, E., Forslund, A. & Bergsten, P. Mechanisms of beneficial effects of metformin on fatty acid-treated human islets. *J. Mol. Endocrinol.* **61**, 91–99 (2018).

798. Kelly, B., Tannahill, G. M., Murphy, M. P. & O'Neill, L. A. J. Metformin Inhibits the Production of Reactive Oxygen Species from NADH:Ubiquinone Oxidoreductase to Limit Induction of Interleukin-1β (IL-1β) and Boosts Interleukin-10 (IL-10) in Lipopolysaccharide (LPS)-activated Macrophages *. *J. Biol. Chem.* **290**, 20348–20359 (2015).

799. Kane, D. A. *et al.* Metformin selectively attenuates mitochondrial H2O2 emission without affecting respiratory capacity in skeletal muscle of obese rats. *Free Radic. Biol. Med.* **49**, 1082–1087 (2010).

800. He, L. & Wondisford, F. E. Metformin Action: Concentrations Matter. *Cell Metab.* **21**, 159–162 (2015).

801. Wang, Y. *et al.* Metformin Improves Mitochondrial Respiratory Activity through Activation of AMPK. *Cell Rep.* **29**, 1511-1523.e5 (2019).

802. Karnewar, S. *et al.* Metformin regulates mitochondrial biogenesis and senescence through AMPK mediated H3K79 methylation: Relevance in age-associated vascular dysfunction. *Biochim. Biophys. Acta Mol. Basis Dis.* **1864**, 1115–1128 (2018).

803. Hu, M., Ye, P., Liao, H., Chen, M. & Yang, F. Metformin Protects H9C2 Cardiomyocytes from High-Glucose and Hypoxia/Reoxygenation Injury via Inhibition of Reactive Oxygen Species Generation and Inflammatory Responses: Role of AMPK and JNK. *J. Diabetes Res.* **2016**, 2961954 (2016).

804. Liu, X.-D. *et al.* Metformin protects high glucose-cultured cardiomyocytes from oxidative stress by promoting NDUFA13 expression and mitochondrial biogenesis via the AMPK signaling pathway. *Mol. Med. Rep.* **22**, 5262–5270 (2020).

805. Wang, Q. *et al.* Metformin Suppresses Diabetes-Accelerated Atherosclerosis via the Inhibition of Drp1-Mediated Mitochondrial Fission. *Diabetes* **66**, 193–205 (2017).

806. Fullerton, M. D. *et al.* Single phosphorylation sites in Acc1 and Acc2 regulate lipid homeostasis and the insulin-sensitizing effects of metformin. *Nat. Med.* **19**, 1649–1654 (2013).

807. He, X. *et al.* Metformin improved oxidized low-density lipoprotein-impaired mitochondrial function and increased glucose uptake involving Akt-AS160 pathway in raw264.7 macrophages. *Chin. Med. J. (Engl.)* **132**, 1713–1722 (2019).

808. Zuliani, I. *et al.* The Anti-Diabetic Drug Metformin Rescues Aberrant Mitochondrial Activity and Restrains Oxidative Stress in a Female Mouse Model of Rett Syndrome. *J. Clin. Med.* **9**, 1669 (2020).

809. Balbi, M. E. *et al.* Antioxidant effects of vitamins in type 2 diabetes: a meta-analysis of randomized controlled trials. *Diabetol. Metab. Syndr.* **10**, 18 (2018).

810. Choi, S. W. & Ho, C. K. Antioxidant properties of drugs used in Type 2 diabetes management: could they contribute to, confound or conceal effects of antioxidant therapy? *Redox Rep.* **23**, 1–24 (2018).

811. Chukwunonso Obi, B., Chinwuba Okoye, T., Okpashi, V. E., Nonye Igwe, C. & Olisah Alumanah, E. Comparative Study of the Antioxidant Effects of Metformin, Glibenclamide, and Repaglinide in Alloxan-Induced Diabetic Rats. *J. Diabetes Res.* **2016**, 1635361 (2016).

812. Diniz Vilela, D. *et al.* The Role of Metformin in Controlling Oxidative Stress in Muscle of Diabetic Rats. *Oxid. Med. Cell. Longev.* **2016**, e6978625 (2016).

813. Iannantuoni, F. *et al.* The SGLT2 Inhibitor Empagliflozin Ameliorates the Inflammatory Profile in Type 2 Diabetic Patients and Promotes an Antioxidant Response in Leukocytes. *J. Clin. Med.* **8**, (2019).

814. Teodoro, J. S., Nunes, S., Rolo, A. P., Reis, F. & Palmeira, C. M. Therapeutic Options Targeting Oxidative Stress, Mitochondrial Dysfunction and Inflammation to Hinder the Progression of Vascular Complications of Diabetes. *Front. Physiol.* **9**, (2019).

815. Jiang, Q. *et al.* Mitochondria-Targeted Antioxidants: A Step towards Disease Treatment. *Oxid. Med. Cell. Longev.* **2020**, e8837893 (2020).

816. Plecitá-Hlavatá, L. *et al.* Potential of Mitochondria-Targeted Antioxidants to Prevent Oxidative Stress in Pancreatic β-cells. *Oxid. Med. Cell. Longev.* **2019**, e1826303 (2019).

817. Rocha, M. *et al.* Perspectives and Potential Applications of Mitochondria-Targeted Antioxidants in Cardiometabolic Diseases and Type 2 Diabetes. *Med. Res. Rev.* **34**, 160–189 (2014).

818. Chiao, Y. A. *et al.* Late-life restoration of mitochondrial function reverses cardiac dysfunction in old mice. *eLife* **9**, 1857 (2020).

819. Karaa, A., Haas, R., Goldstein, A., Vockley, J. & Cohen, B. H. A randomized crossover trial of elamipretide in adults with primary mitochondrial myopathy. *J. Cachexia Sarcopenia Muscle* **11**, 909–918 (2020).

820. Karaa, A. *et al.* Randomized dose-escalation trial of elamipretide in adults with primary mitochondrial myopathy. *Neurology* **90**, e1212–e1221 (2018).

821. Reid Thompson, W. *et al.* A phase 2/3 randomized clinical trial followed by an open-label extension to evaluate the effectiveness of elamipretide in Barth syndrome, a genetic disorder of mitochondrial cardiolipin metabolism. *Genet. Med.* **1**, 8 (2020).

822. Sabbah, H. N. Barth syndrome cardiomyopathy: targeting the mitochondria with elamipretide. *Heart Fail. Rev.* (2020) doi:10.1007/s10741-020-10031-3.

823. Stealth BioTherapeutics Inc. *Part A: a prospective, randomized, double-masked, vehicle controlled, paired-eye phase 1/2 clinical study to evaluate the safety, tolerability and efficacy of elamipretide topical ophthalmic solution in subjects with fced presenting with mild to moderate corneal edema part b: a prospective, randomized, double-masked, vehicle*

controlled, phase 1/2 clinical study to evaluate the safety, tolerability, and efficacy of Elamipretide topical ophthalmic solution in subjects with fced presenting with mild to moderate corneal edema. https://clinicaltrials.gov/ct2/show/NCT02653391 (2019).

824. Stealth BioTherapeutics Inc. *An Open-Label, Phase 1 Clinical Study to Evaluate the Safety and Tolerability of Subcutaneous Elamipretide in Subjects With Intermediate Age-Related Macular Degeneration*. https://clinicaltrials.gov/ct2/show/NCT02848313 (2020).

825. Butler, J. *et al.* Effects of Elamipretide on Left Ventricular Function in Patients With Heart Failure With Reduced Ejection Fraction: The PROGRESS-HF Phase 2 Trial. *J. Card. Fail.* **26**, 429–437 (2020).

826. Saad, A. *et al.* Phase 2a Clinical Trial of Mitochondrial Protection (Elamipretide) During Stent Revascularization in Patients With Atherosclerotic Renal Artery Stenosis. *Circ. Cardiovasc. Interv.* **10**, (2017).

8. ANNEXES

8.1. Annex I

GENERALITAT VALENCIANA
CONSELLERIA DE SANITAT UNIVERSAL I SALUT PÚBLICA

DEPARTAMENT DE SALUT DE VALÈNCIA
DOCTOR PESET

A/A.: Dr. Victor Manuel Victor
Servicio de Endocrino

Dña. Pilar Codoñer Franch, Presidenta del Comité Ético de Investigación Clínica del Hospital Universitario Dr. Peset.

CERTIFICA:

Que este comité en su reunión celebrada el día 26 de Octubre de 2016 ha evaluado y ha aprobado el estudio titulado: Estudio de la dinámica y la función mitocondrial, el inflamasoma y su relación con las complicaciones cardiovasculares en la diabetes tipo 2: Implicaciones fisiopatológicas y clínicas.
Proyecto de investigación. FIS
Código Ceic: 97/16

Valencia 28 de Octubre de 2016

CONSELLERIA DE SANITAT UNIVERSAL I SALUT PÚBLICA - VALÈNCIA
Hospital "Dr. Peset" COMITÉ ÉTICO DE INVESTIGACIÓ CLÍNICA

Fdo.: Pilar Codoñer Franch

Comité Ético de Investigación clínica. Hospital Universitario Doctor Peset de Valencia.
C/ San Lázaro s/n. Edificio CIPS 1ª Planta. Valencia 46017. Teléfono 96.3131652
Correo electrónico ceic_peset@gva.es.

GENERALITAT VALENCIANA
CONSELLERIA DE SANITAT UNIVERSAL I SALUT PÚBLICA

DEPARTAMENT DE SALUT DE VALÈNCIA
DOCTOR PESET

A/A.: Dr. Victor M. Victor
Unidad investigación Endocrino

Dña. Pilar Codoñer Franch, Presidenta del Comité Ético de Investigación con Medicamentos del Hospital Universitario Dr. Peset.

CERTIFICA:

Que este comité en su reunión celebrada el día 30 de octubre de 2019 ha evaluado y ha aprobado el estudio titulado: "Estudio de la función mitocondrial, la autofagia y la mitofagia en la diabetes tipo 2: relación con las complicaciones cardiovasculares e implicaciones clínicas"
Proyecto de investigación
Código CEIm: 98/19

Valencia 12 de noviembre de 2019

CONSELLERIA DE SANITAT UNIVERSAL I SALUT PÚBLICA - VALÈNCIA
Hospital "Dr. Peset"
COMITÉ ÉTICO DE INVESTIGACIÓ CLÍNICA

Fdo.: Dra. Pilar Codoñer Franch

8.2. Annex II: Articles

Redox Biology 34 (2020) 101563

Contents lists available at ScienceDirect

Redox Biology

journal homepage: www.elsevier.com/locate/redox

Research Paper

Relationship between PMN-endothelium interactions, ROS production and Beclin-1 in type 2 diabetes

Aranzazu M. De Marañon[a], Francesca Iannantuoni[a], Zaida Abad-Jiménez[a], Francisco Canet[a], Pedro Díaz-Pozo[a], Sandra López-Domènech[a], Ana Jover[a], Carlos Morillas[a], Guillermo Mariño[b], Nadezda Apostolova[c], Milagros Rocha[a,c,**], Victor M. Victor[a,c,d,*]

[a] Service of Endocrinology and Nutrition, University Hospital Doctor Peset, Foundation for the Promotion of Health and Biomedical Research in the Valencian Region (FISABIO), Valencia, Spain
[b] Instituto de Investigación Sanitaria del Principado de Asturias, 33011, Oviedo, Spain
[c] CIBERehd - Department of Pharmacology, University of Valencia, Valencia, Spain
[d] Department of Physiology, University of Valencia, Valencia, Spain

ARTICLE INFO

Keywords:
Type 2 diabetes
Autophagy
Mitochondria
PMN-Endothelium interactions
Oxidative stress
ROS

ABSTRACT

Type 2 diabetes is closely related to oxidative stress and cardiovascular diseases. In this study, we hypothesized that polymorphonuclear leukocytes (PMN)-endothelium interactions and autophagy are associated. We evaluated PMN-endothelial interactions, ROS production and autophagy parameters in 47 type 2 diabetic patients and 57 control subjects. PMNs from type 2 diabetic patients exhibited slower rolling velocity ($p < 0.001$), higher rolling flux ($p < 0.001$) and adhesion ($p < 0.001$) in parallel to higher levels of total ($p < 0.05$) and mitochondrial ROS ($p < 0.05$). When the protein expression of autophagy markers was analysed, an increase of Beclin-1 ($p < 0.05$), LC3I ($p < 0.05$), LC3II ($p < 0.01$) and LC3II/LC3I ratio ($p < 0.05$) was observed. Several correlations between ROS and leukocyte-endothelium parameters were found. Interestingly, in control subjects, an increase of Beclin-1 levels was accompanied by a decrease in the number of rolling ($r = 0.561$) and adhering PMNs ($r = 0.560$) and a rise in the velocity of the rolling PMNs ($r = 0.593$). In contrast, in the type 2 diabetic population, a rise in Beclin-1 levels was related to an increase in the number of rolling ($r = 0.437$), and adhering PMNs ($r = 0.467$).

These results support the hypothesis that PMN-endothelium interactions, ROS levels and formation of autophagosomes, especially Beclin-1 levels, are enhanced in type 2 diabetes.

1. Introduction

In recent years, a sustained global increase in the prevalence of obesity and metabolic syndrome [1] has provoked a rise in diseases such as type 2 diabetes. Currently, type 2 diabetes and its comorbidities are among the main health concerns worldwide because of their high prevalence and the associated cost related to public health services. Type 2 diabetes is characterized by hyperglycaemia and insulin resistance, which cause chronic subclinical inflammation [2,3]. Hyperglycaemia and inflammation produce cellular alterations, which are the molecular basis of diabetes and cardiometabolic diseases [3–5]. Previous studies have highlighted the relationship between diabetes and inflammation, pointing to circulating hyperlipidaemia and hyperglycaemia as triggers of inflammatory responses [5–7].

One of the consequences of chronic hyperglycaemia is the increased generation of reactive oxygen species (ROS), produced mainly by the mitochondrial respiratory chain [8,9]. This heavy load of ROS overwhelms antioxidant defences and can modify cellular molecules and organelles, disturbing cell homeostasis and inducing inflammation. Furthermore, mitochondrial dysfunction and oxidative stress have been closely related to cardiovascular diseases [10,11].

Hyperglycaemia, together with ROS production, leads to an increased presence of proinflammatory molecules that activate immune cells [8–10]. Moreover, endothelial cells are activated by ROS and proinflammatory cytokines thereby developing endothelial dysfunction [12–15]. This situation enhances a cascade of PMN-endothelium interactions, a process by which immune cells migrate to the site of inflammation [16]. The proinflammatory state and increased ROS content

* Corresponding author. FISABIO- University Hospital Doctor Peset, Avda Gaspar Aguilar 90, 46017, Valencia, Spain.
** Corresponding author. FISABIO- University Hospital Doctor Peset, Avda Gaspar Aguilar 90, 46017, Valencia, Spain.
E-mail addresses: milagros.rocha@uv.es (M. Rocha), victor.victor@uv.es (V.M. Victor).

https://doi.org/10.1016/j.redox.2020.101563
Received 31 March 2020; Accepted 27 April 2020
Available online 04 May 2020

Abbreviations

AIP	Atherogenic Index of Plasma
AMPK	AMP-activated protein kinase
BCA	Bicinchonic acid
BMI	Body mass index
DCFH-DA	2′,7′-Dichlorofluorescin diacetate
EDTA	Ethylenediamine tetraacetic acid
HbA1c	Glycated haemoglobin
HDL	High density lipoprotein
HO-1	Heme oxygenase 1 protein
HOMA	Homeostatic Model Assessment
hs-CRP	High sensitivity C-Reactive Protein
IL-6	Interleukin 6
LC3	Microtubule associated protein 1A/1B light chain 3 protein
LDL	Low density lipoprotein
PMN	Polymorphonuclear cells
ROS	Reactive Oxygen Species
RPMI	Roswell Park Memorial Institute medium
SDS-PAGE	Sodium dodecylsulphate-polyacrylamide gel electrophoresis
SQSTM1/p62	Sequestosome protein 1/p62
TNFα	Tumor necrosis factor alpha
UPR	Unfolded protein response
VLDL	Very low density lipoprotein

characteristic of type 2 diabetes favour PMN-endothelial interactions throughout the vasculature, not only at the site of inflammation [17]. This process is enhanced in the comorbidities related to type 2 diabetes [17], but the cause and the pathways affected are still being investigated. One of the actions involves the interference of ROS with the proper functioning of β-cells [18], including mechanisms of protein homeostasis, such as protein folding and degradation [19]. It is known that ROS can damage various cellular components, which are degraded and recycled by a process named autophagy. It involves nonselective degradation of proteins, lipids and organelles [20], and occurs in response to internal or external stimuli such as oxidative stress, unfolded protein response (UPR) and malfunctioning of organelles (internal inductors), and growth factors, serum starvation or amino acid deprivation (external stimuli). In this sense, autophagy is a survival mechanism [20] and a strictly regulated process. Two key proteins in this process are microtubule-associated protein light chain 3 (LC3) and Beclin-1. The latter, together with other autophagy-related proteins, initiates the formation of the omegasome and the phagophore, thus priming the progression to autophagosome ([20]). In parallel, the cytoplasmic form of LC3I is lipidated to LC3II, and, in this form, is recruited to the inner and outer autophagosomal membrane in order to construct the autophagosome. In the case of selective autophagy, altered proteins and organelles are carried to the autophagosome via the ubiquitin- and LC3-binding protein SQSTM1 (p62). Ubiquitinated proteins or organelles are sequestered into the autophagosome for their degradation. When the autophagosome fuses with the lysosome, the autolysosome is created and the material stored in the autophagosome is then digested. If autophagy is impaired, p62 protein accumulates in the autophagosomes [20]; however, p62 is important not only in this process, but it also acts as a scaffold protein that intervenes in cell proliferation and survival/death signalling [21]. Autophagy has been shown to be enhanced and decreased in diabetic patients [22,23]. In fact, insulin influences autophagy regulation, in part through mTOR signalling. Yan *et al.* [24] described that the adipocytes of obese type 2 diabetic patients display increased autophagy and reduced mTOR signalling. Interestingly, they showed that this state leads is associated with an undermining of mitochondrial biogenesis and function. Furthermore, several studies have demonstrated that hyperglycaemia induces autophagy as a protective mechanism. For example, autophagy is active in diabetic mice podocytes with glomerular damage [25–27], a mechanism that may be modulated by heme oxygenase 1 (HO-1) and AMPK activation [28]. In mice, it has also been observed that defective autophagy in β-cells accelerates the progression from obesity to diabetes through enhancement of UPR, a mechanism also activated by hyperglycaemia [29]. In parallel to these observations, it has been established that the BCL2-Beclin-1 complex is dissociated in response to AMPK activation in cardiac muscle, thus enhancing autophagy and preventing cardiomyocyte death [30]. These observations have been confirmed in other tissues, such as endothelial progenitor cells [31]. Conversely, Qianrong *et al.* [32] reported that high glucose levels inhibit autophagy in cardiomyocytes, leaving cells unprotected and more prone to apoptosis. In summary, it is thought that autophagy is activated in situations of cellular stress such as hyperglycaemia, but the underlying mechanisms are unknown in most cell types.

In this context, we hypothesized that PMN-endothelium interactions, ROS and autophagy are altered in the PMNs of diabetic patients and that there is an association between all three. In this study, we analyse the link between Beclin-1, ROS production and PMN-

Table 1
Biochemical and anthropometrical parameters in control and type 2 diabetic populations. Data are expressed as mean ± SD for parametrical data and as median (25th percentile-75th percentile) for non-parametrical variables. Statistical significance ($P < 0.05$) was compared with T-test following a post-hoc test with BMI as covariate.

	Control	T2D	p-value	BMI Adjusted p-value
N	57	47		
Age	49 ± 10	52 ± 8		
Women	55%	45%		
Men	45%	55%		
BMI (kg/m^2)	24.97 ± 3.32	32.25 ± 4.42	< 0.001	ns
Glucose (mg/dL)	91.15 ± 11.64	137.1 ± 48.93	< 0.001	< 0.001
Insulin (μUI/mL)	5.99 ± 1.87	20 ± 12.3	< 0.001	0.04
HOMA-IR	1.6 ± 1,05	6.9 ± 5.10	< 0.001	0.004
HbA1c (mmol/mol) (%)	33.84(5.3) ± 0.62	58 (7.3) ± 1.65	< 0.001	< 0.001
Total Cholesterol (mg/dL)	195.06 ± 29.48	172.27 ± 42.28	0.01	ns
Non-HDL-C (mg/dL)	137 ± 30.79	127 ± 40.89	ns	ns
LDL-C (mg/dL)	121.95 ± 26.02	100.38 ± 36.09	0.006	ns
VLDL-C (mg/dL)	15.33 ± 7.07	28.58 ± 27.41	0.003	0.006
HDL-C (mg/dL)	57.17 ± 12.44	44.64 ± 10.09	< 0.001	0.01
Triglycerides (mg/dL)	63 (51–103)	114(89–169.67)	0.002	0.007
AIP	0.11 ± 0.24	0.47 ± 0.29	< 0.001	< 0.001
hs-CRP (mg/L)	1 (0.31–1.87)	3.4 (2.01–7.87)	0.004	ns

endothelium interactions, as well as the varying behaviour of autophagy in diabetic and control conditions.

2. Materials and methods

2.1. Study population

This cross-sectional observational study had a case-control design, and was conducted with 47 diabetic patients and 57 control subjects matched by age and sex. The patients were recruited at the Endocrinology and Nutrition Service of the University Hospital Dr. Peset, Valencia, Spain, and their characteristics are described in Table 1. A diagnosis of type 2 diabetes was determined according to the American Diabetes Association's criteria. Subjects aged 18 or older were eligible for inclusion in the study. The exclusion criteria were having an abnormal haematological profile, suffering any malignant neoplasm or autoimmune disease, consumption of any anti-inflammatory drugs in the two weeks previous to the analysis, and regular consumption of antioxidant nutritional supplements.

The procedures carried out in the study were approved by the Ethics Committee of the Hospital (ID: 97/16) and conducted according to the ethical principles stated in the Declaration of Helsinki. All subjects signed an informed consent document before the interventions. A physical examination was performed in all patients prior to blood extraction, which was conducted in a state of fasting. Body weight and height were recorded and body mass index (BMI) was calculated using the BMI formula (BMI = weight in kg/(height in m) 2^2).

2.2. Blood sampling

In order to determine biochemical parameters and obtain PMN, venous blood was collected from subjects in heparin, EDTA or citrate tubes after 12h overnight fasting. It was then centrifuged (1500g, 10 min, 4 °C) in order to isolate serum and plasma, which were then stored at −80 °C for subsequent analysis, or employed to determine biochemical parameters. The heparin tubes were used to obtain PMNs.

2.3. Biochemical determinations

All the biochemical parameters were determined by the Hospital's Clinical Analysis Service. An enzymatic method was employed to determine serum concentrations of glucose, total cholesterol, HDL-cholesterol and triglyceride levels with a Beckman LX-20 autoanalyzer (Beckman Coulter, La Brea, CA, USA). Low density lipoprotein (LDL) cholesterol levels were calculated with Friedewald's formula. An immunochemiluminiscent assay was used to determine insulin levels. Insulin resistance was determined employing the Homeostasis Model, calculated as [fasting glucose in mg/dL x fasting insulin in μUI/mL]/405). Glycated haemoglobin (HbA1c) was assessed with an automatic glycohemoglobin analyser (Arkray, Inc., 73 KYOTO, Japan). Serum concentrations of high-sensitive C-reactive protein (hs-CRP) were determined by immunonephelometry. Atherogenic Index of Plasma (AIP) was calculated using the formula (Total Choresterol(mg/dL))/(HDL-Cholesterol (mg/dL)).

2.4. PMN-endothelium interaction assay

PMNs were isolated as previously described [33]. We employed a 1.2 mL aliquot of PMNs obtained from the peripheral blood of control and type 2 diabetic subjects with a density of 10^6 cells/mL in complete RPMI (RPMI 1640 medium supplemented with 10% Fetal bovine serum,1% penicillin/streptomycin, 1% glutamine and 1% sodium pyruvate). Prior to this, primary cultures of human umbilical cord endothelial cells (HUVEC) were established. HUVEC were isolated as previously reported [32]. On the day of the experiment, PMNs were monitored through the endothelial monolayer at a speed of 0.3 mL/min during a 5-min period, which was recorded, and the number of rolling PMNs as well as their velocity and adhesion to the endothelial monolayer were determined. The number of rolling PMNs was measured as those rolling for 1 min, their velocity was assessed by determining the time in which 15 rolling PMNs covered a distance of 100 μm. Adhesion was analysed by counting the number of PMNs adhering to the endothelium for at least 30 s in 5 fields.

2.5. Protein extraction and quantification

PMN pellets were incubated for 15 min on ice with lysis buffer (20 mM HEPES pH 7.5, 400 mM NaCl, 20% glycerol, 0.1 mM EDTA, 10 μM Na_2MoO_4, 0.5% NP-40) containing protease inhibitors (10 mM NaF, 1 mM $NaVO_3$, 10 mM PNP, 10 mM β-glycerolphosphate) and dithiothreitol 1 mM. Subsequently, samples were vortexed for 30 s and centrifuged at 13200 rpm for 15 min at 4 °C. The supernatant was then collected in a new tube and quantified with the *BCA protein assay kit* (Thermo Scientific, Rockford, USA). The protein extract obtained was stored for subsequent determinations at −80 °C.

2.6. Western blotting

25 μg protein samples were separated with SDS-PAGE (13% polyacrylamide gels) and transferred to a nitrocellulose membrane. The membranes were then blocked for 1h at RT with 5% skimmed milk in TBS-T or 5% BSA in TBS-T and incubated with primary antibodies overnight at 4°C- anti-Beclin-1 (Millipore Iberica, Spain, Madrid), anti-LC3 (Millipore Iberica, Spain, Madrid), anti SQSTM/p62 (Abnova Corporation, Taiwan), anti-Actin (Sigma Aldrich, St. Louis, USA). The secondary antibody was HRP-goat anti-rabbit (Millipore Iberica, Spain, Madrid). The protein signal was revealed with SuperSignal West Femto (Thermo Scientific, Rockford, USA) and detected with a Fusion FX5 acquisition system (VilbertLourmat, Marne La Vallée, France). Densitometric quantification of proteins was performed with Bio1D software (VilbertLourmat, Marne La Vallée, France). Data were relativized with the Actin signal for each sample and also to an internal control. Each Western blot was performed and reproved several times, thus, cropped images are represented in Figs. 3 and 4.

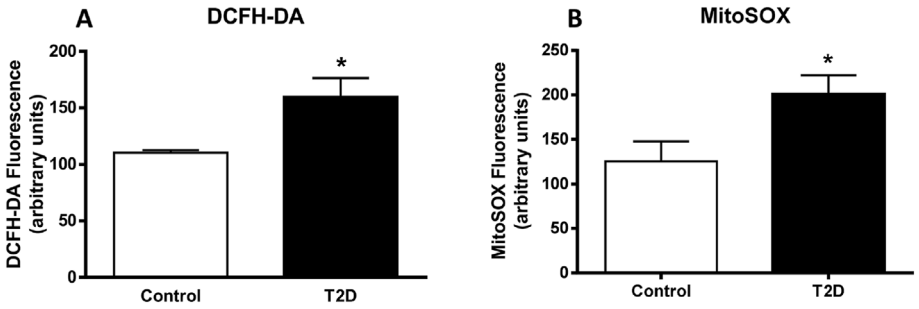

Fig. 1. ROS levels in PMNs from control and type 2 diabetic populations. (A) Levels of total ROS measured in controls and type 2 diabetic patients with DCFH-DA fluorescence in arbitrary units; (B) Levels of mitochondrial ROS measured in control and type 2 diabetic populations with MitoSOX fluorescence in arbitrary units. Values were expressed as a percentage of an internal experimental control in both populations. *p < 0.05 vs Control group.

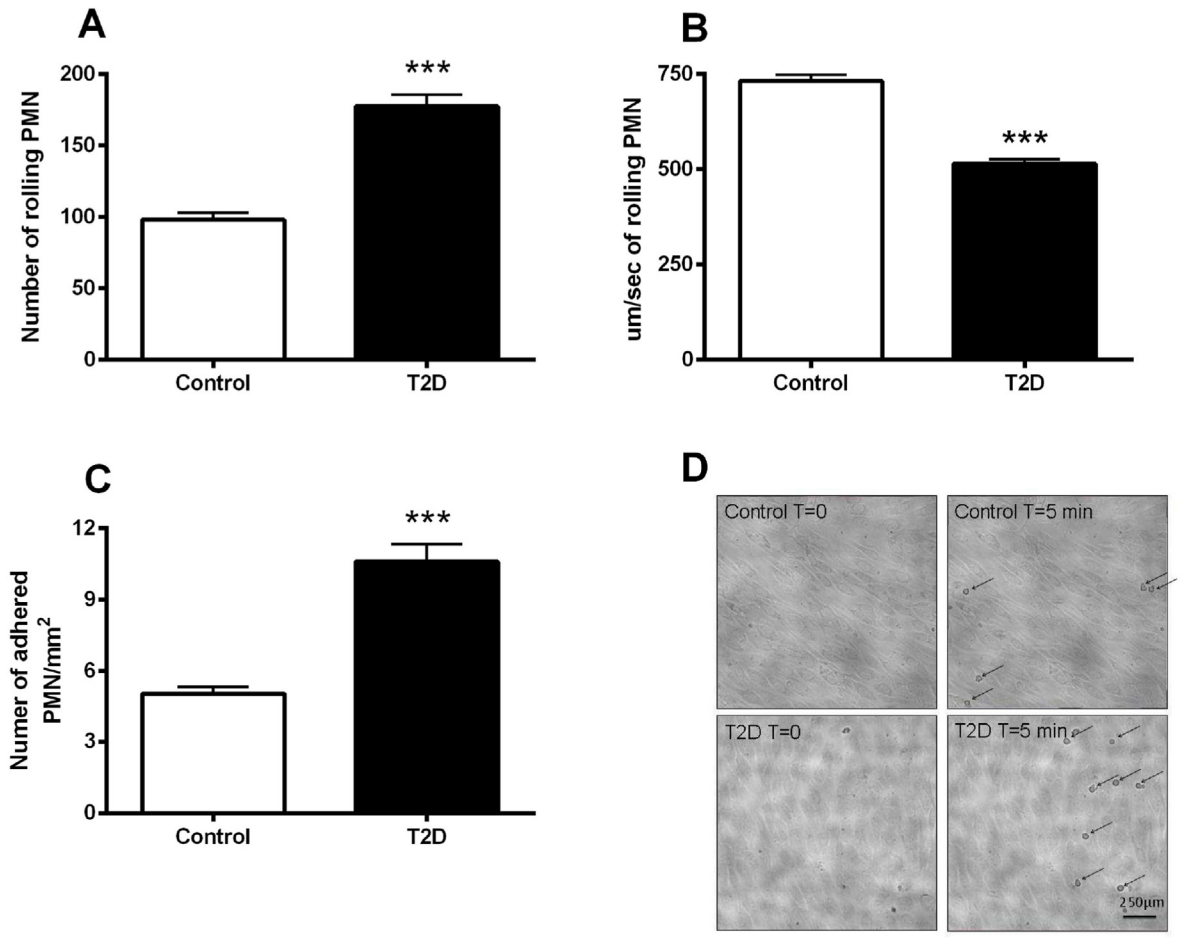

Fig. 2. Analysis of PMN-endothelium interactions in control and type 2 diabetic populations: (A) Number of PMNs rolling along the endothelial monolayer during a 1-min period, measured as number of cells/min; (B) Velocity of PMNs measured as µm/sec; (C) Number of adhering PMNs in 1 mm^2, measured as PMN/mm^2; (D) Representative images of control and type 2 diabetic populations at the start and the end (5 min) of the experiment. ***$p < 0.001$ in type 2 diabetes vs Control.

2.7. Quantification of total and mitochondrial ROS

Total and mitochondrial ROS were assessed with the fluorescent probes 2′-7′ dichlorodihydrofluorescein diacetate (DCFH-DA) and MitoSOX, respectively. Isolated PMNs were seeded in 48-well plates at a density of 150000 cells/well and left to adhere in a 5% CO_2 incubator for 20 min. Cells were subsequently incubated with the specific nuclear stain Hoescht 33342 (4 µM) (Sigma-Aldrich, St. Louis, USA) and the fluorescent probes DCFH-DA (1 µM) or MitoSOX (5 µM) (Thermo Scientific, Rockford, USA) 30 min at 37 °C under gentle shaking. Cells were then washed twice with HBSS and were analysed with the static cytometry software "ScanR" (Olympus) which is coupled to an inverted microscope (lX81; Olympus). 12 fields per well were recorded and quantified. Measurements of fluorescence were referred as % of an external control for each sample.

2.8. Statistical analysis

SPSS was employed to perform statistical analyses. The data in Table 1 are expressed as mean ± standard deviation for parametric data, and median and 25th-75th percentiles for non-parametric data. The bar graphs in figures represent mean ± standard error. An unpaired Student's t-test was performed to compare the control group and type 2 diabetic subjects, and adjustment by BMI was determined by means of a univariate general lineal model. Correlations were calculated with Pearson's correlation coefficient. Differences were considered significant when $p < 0.05$.

3. Results

3.1. Clinical and biochemical characteristics of the study subjects

We analysed 57 type 2 diabetic patients and compared them to 47 healthy control subjects with similar ages and sex distribution. Anthropometric and biochemical parameters were evaluated (Table 1). Type 2 diabetic patients showed higher BMI, fasting glucose, basal insulin, HOMA-IR index and glycated haemoglobin (HbA1c) compared to control subjects. Lipid metabolism parameters were also significantly enhanced compared to control volunteers, with higher VLDL and triglycerides, and lower HDL. Total cholesterol and LDL levels showed a slight decrease due to the treatment with statin (90% of patients). Furthermore, type 2 diabetic patients had a higher atherogenic index of plasma (AIP) and higher PCR levels.

Glucose, insulin, HOMA-IR, HbA1c, VLDL, HDL triglycerides and AIP maintained their statistical significance when data were adjusted by BMI, while differences in hsPCR and some lipid profile parameters – including total cholesterol and LDL - lost their statistical significance.

3.2. Total and mitochondrial ROS levels

Mitochondria can be severely damaged due to hyperglycaemia by releasing ROS. We measured total and mitochondrial ROS levels in

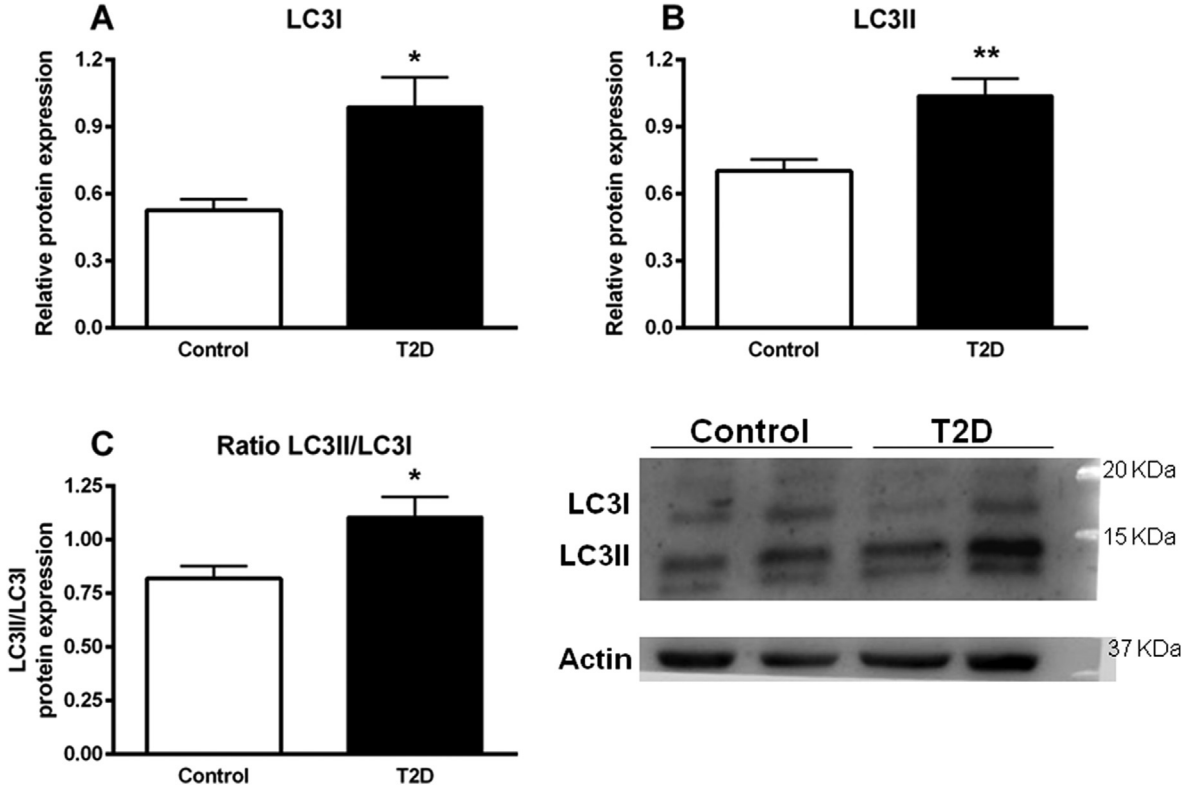

Fig. 3. LC3 (I and II) protein expression in controls and type 2 diabetic patients. Protein expression of LC3I (A), LC3II (B) and ratio of LC3II to LC3I (C) in controls and type 2 diabetic patients were assessed by immunoblotting. Quantification was performed in n = 15 samples for each group. Representative image of western blotting of 4 samples (2 controls and 2 type 2 diabetic patients) is displayed. Values represent media ± SD * $p < 0.05$; **$p < 0.01$ vs Control.

PMNs from type 2 diabetic patients and controls and found an evident enhancement of both total and mitochondrial ROS levels in type 2 diabetic subjects ($p < 0.05$) (Fig. 1) suggesting an oxidative stress condition.

3.3. PMN-endothelium interactions

Metabolic disorders are associated with increased levels of inflammatory markers. In the present study, we have observed that type 2 diabetic subjects had higher levels of TNFα and IL-6 levels, as well as increased NF-κB (p65) protein levels (Supplemmentary figure). This enhanced inflammatory background could be further confirmed analyzing the activation of the PMN cells and its interactions with the endothelial cells, using parallel-plate flow chamber experiments. This *in vitro* system reproduces physiological interactions between circulating cells and endothelium, and can quantify the frequency and stability of these interactions. Interestingly, PMNs from type 2 diabetic patients displayed lower rolling velocity through the endothelial monolayer ($p < 0.001$) (Fig. 2B), greater rolling number ($p < 0.001$) (Fig. 2A) and increased adhesion to the endothelial cells ($p < 0.001$) (Fig. 2C) with respect to those from the control population. This increase in PMN-endothelium interactions is reflected in the representative images obtained before and after the 5-min experimental period (Fig. 2D).

3.4. LC3I, LC3II, Beclin-1 and p62 protein levels

We examined autophagy, a stress-activated cellular process that might be altered in type 2 diabetic population. PMNs were employed to analyse the protein expression of classical markers such as LC3, Beclin-1 and p62. Type 2 diabetic patients displayed an increased amount of LC3I ($p < 0.05$) (Fig. 3A and representative WB) and LC3II ($p < 0.05$) (Fig. 3B and representative WB), with a higher LC3II/LC3I ratio ($p < 0.05$) (Fig. 3C and representative WB). In addition, they showed enhanced Beclin-1 and decreased p62 protein levels ($p < 0.05$) compared to control subjects (Fig. 4), suggesting an increase in autophagy activation in the type 2 diabetic patient population.

3.5. Correlations between ROS levels and autophagy markers

As we have mentioned before, excessive production of ROS can generate cellular stress that activates rescue pathways. In the present study, we have tried to highlight the relationship between autophagy and ROS production. We have evaluated correlations between the data obtained for ROS production and autophagic protein expression. We observed that total ROS levels correlated negatively with LC3II/I ratio in the control population ($r = -0.714$, $p = 0.047$) and positively with Beclin-1 levels in type 2 diabetic subjects ($r = 0.911$, $p = 0.001$). On the other hand, mitochondrial ROS was positively correlated with LC3II/LC3I ratio in the type 2 diabetic population ($r = 0.416$, $p = 0.022$). These data reinforce the hypothesis of a strong relation between autophagy and ROS production in type 2 diabetic patients.

3.6. Correlation between autophagy proteins and PMN-endothelium interaction parameters

Once we had analysed the correlation between ROS and autophagy, we evaluated the correlation between PMN-endothelium interactions and autophagy markers. Interestingly, we observed that Beclin-1 protein levels were differentially correlated with PMN-endothelium interaction parameters (Fig. 5). In the control population, an increase of Beclin-1 was accompanied by a decrease in rolling number, a decrease in the number of adhered PMNs and a rise in the velocity of the rolling PMNs. In contrast, in the type 2 diabetic population, an increase in Beclin-1 was related to an increase in both rolling number and number of adhered PMNs and a trend towards a decrease in rolling velocity (Fig. 5). Additionally, a correlation between PMN adhesion, and LC3II

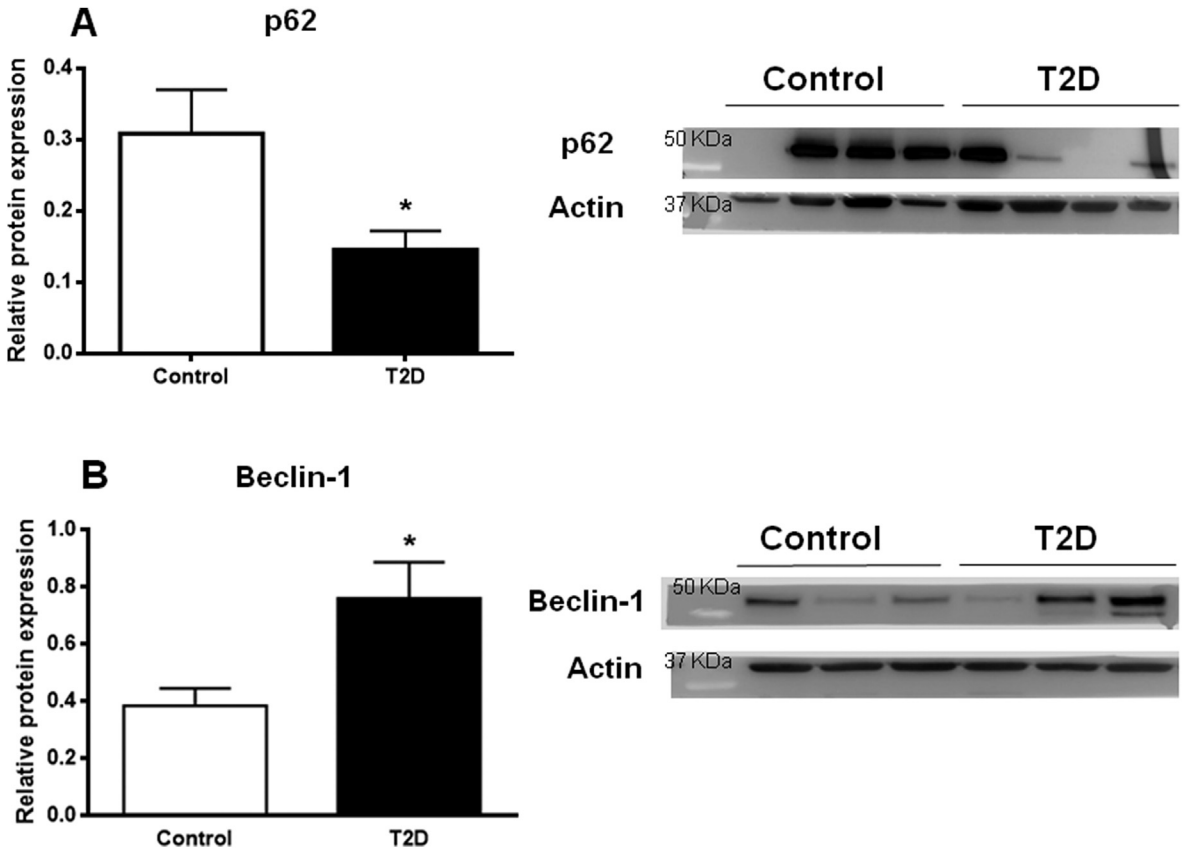

Fig. 4. p62 and Beclin-1 protein expression in control and type 2 diabetic populations. Protein expression of p62 (A) and Beclin-1 (B) in control and type 2 diabetic populations was assessed by inmunoblotting. Quantification was performed with n = 15 samples in each group. Representative images of the western blotting are displayed at the side of both graphs. Values represent media ± SD * $p < 0.05$ vs Control.

expression was observed in the type 2 diabetic population ($r = 0.386$, $p = 0.032$) while the rest of the parameters of PMN-endothelium interactions showed no correlation.

4. Discussion

In this cross-sectional study, we have shown that diabetic patients display enhanced PMN-endothelium interactions, ROS production, autophagy-related protein expression as well as proinflammatory cytokines TNFα and IL-6, and NF-κB activation. Moreover, we demonstrate a differential correlation between PMN-endothelium interactions and Beclin-1 expression in control subjects and type 2 diabetic patients.

With regard to the inflammatory basis of type 2 diabetic, high levels of circulating glucose and lipids increase the expression of adhesion molecules in both the endothelium and PMNs [13,14,16,34,35]. This has been corroborated by several observational studies of type 2 diabetic patients [14,35], but also in interventional studies in patients fitted with hyperglycaemic clamps and undergoing glucose challenge, in whom inflammatory cytokines increase after glucose input [36]. Hyperlipidaemia, another hallmark of type 2 diabetic, is also related to PMN function [17]; an increase in PMN ROS production has been described in hyperlipidaemic and hypertensive patients with respect to healthy controls, which can lead to the atherosclerotic complications [37]. Furthermore, it has been observed that PMN function is altered in patients with diabetic retinopathy; for example, in the case of enhanced extravasation [38]. In this sense, the close relationship between inflammation, ROS production and increase of PMN-endothelium interactions is widely recognised [18,35–37,39–42]. All these studies have concluded that the chronic inflammation characteristic of diabetes and hyperglycaemia promotes the production of inflammatory chemokines and ROS, which in turn alters the functions of the endothelium and PMNs, thus increasing their interaction. Although ROS have an important function as signalling molecules in physiologic processes, their overproduction causes damage of cellular components, which activates the inflammatory response of cells. In the present study, we have observed higher levels of total and mitochondrial ROS in the type 2 diabetic population compared to healthy controls. The relation between type 2 diabetes and ROS is well documented in the literature [8–10,18,28], and has even been directly related to the regulation of autophagy [19,28]. Interestingly, we have observed a differential pattern in the correlations found between total ROS production and LC3II/I ratio, suggesting a synergistic effect of ROS and autophagy in type 2 diabetic patients. These results suggest that autophagy is one of the mechanisms that mediate the link between ROS production and the increase of PMN-endothelium interactions in type 2 diabetes versus control conditions.

Several studies point to alterations in autophagy signalling in type 2 diabetic patients [21–23,25,26]. In the present study, type 2 diabetic subjects displayed enhanced protein markers of autophagy, such as LC3I, LC3II, LC3II/LC3I ratio and Beclin-1, which were related to a reduction in p62 protein levels. These results suggest an activation of autophagy in type 2 diabetic patients compared to healthy controls. Activation or alteration of autophagy has been reported in different situations of hyperlipidaemia and hyperglycaemia. For example, previous research has shown mitochondrial dysfunction and altered autophagy in adipocytes from obese type 2 diabetic patients [23], as well as in Goto-Kazikazi (type 2 diabetic) rats [24]. Furthermore, alterations in autophagic parameters in podocytes and leukocytes have been related to diabetic comorbidities such as diabetic nephropathy [26,27,43], cardiac complications [30,31] and neuropathy [31]. Interestingly, in diabetic Wistar rats, insulin exerted different effects on autophagy depending on the origin of the leukocytes [44]. In fact,

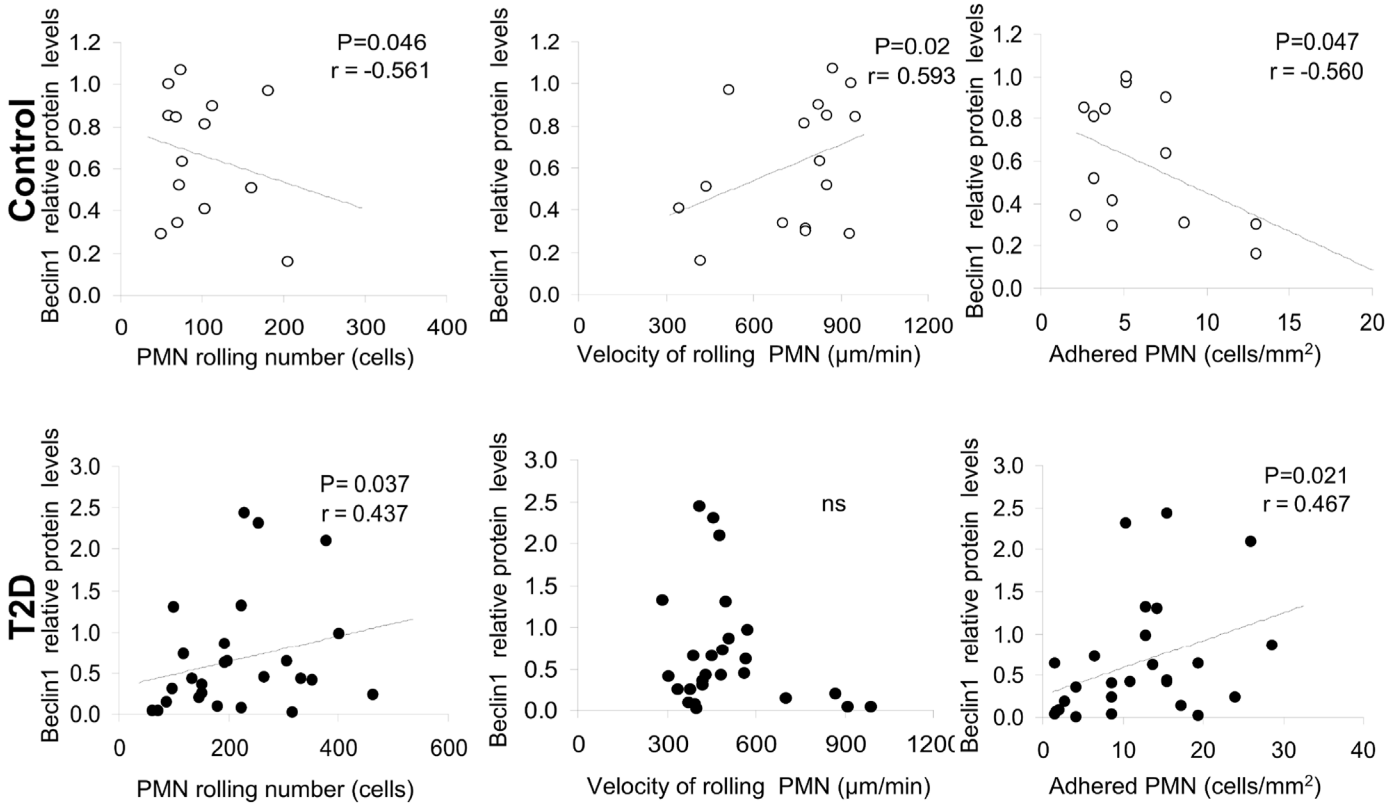

Fig. 5. Pearson's correlation between the protein levels of Beclin-1 and PMN-endothelium interaction parameters in control and type 2 diabetic populations. The correlations between Beclin-1 and number of rolling PMNs (5A, D), rolling velocity (5B, E) and adhesion of PMNs (5C, F) are represented.

diabetic M1 bone marrow-derived macrophages (BMM) had their LC3 vesicle-bound content diminished while M2 BMM had enhanced LC3 levels, and insulin treatment failed to rescue autophagy to control levels. In endothelial cells, proinflammatory cytokines have been shown to induce autophagy, which enhances the production of adhesion molecules [45]. In other studies, autophagy has proved to be a crucial protective mechanism in beta cells [28,46].

Our study relates an increase in autophagy-related proteins with an increase of PMN-endothelium interactions in type 2 diabetic patients as well as an increase in NF-κB expression. We also show that Beclin-1 protein levels correlate differentially with PMN-endothelium interaction parameters depending on the health status of the subject. While an increase in Beclin-1 was related to a reduction in PMN-endothelium interactions in control subjects, it was associated with an increase in PMN-endothelium interactions in type 2 diabetic patients. This could mean that the increase in PMN-endothelium interactions is strongly influenced by Beclin-1, and that changes in its expression imply different signalling cascades depending on the status of the subject. Furthermore, we have observed a positive correlation between PMNs adhesion and LC3II in type 2 diabetic patients. Beclin-1 is implicated in different biological processes, including cytokinesis, immunity, adaptation to stress, development, ageing, tumorigenesis and cell death [47]. The effects described in the present study may be associated with the ability of Beclin-1 to exert several functions within of the metabolism of the cell; for example, it interacts with BCL2 to form the BCL2-Beclin-1 complex, which is regulated by AMPK, provoking the dissociation of the complex and thus preventing apoptosis [29]. Another possible reason why only this protein is differentially regulated is that Beclin-1 interacts with VMP-1 upstream from all the other regulators of autophagy [48]; thus, variations in regulation could be due to differences at this level of the autophagy signalling.

5. Conclusions

In summary, this study demonstrates enhanced PMN-endothelium interactions, ROS production and autophagy activation in type 2 diabetic patients. Moreover, we show a differential behaviour of autophagy in control and type 2 diabetic subjects regarding ROS levels and PMN endothelium-interactions. These data endorse a connection between these three key mechanisms in type 2 diabetes, and highlights the changes in Beclin-1 as a possible linking mechanism between ROS production and PMN-endothelium interactions. Furthermore, we show that the pattern of autophagy markers differs depending on the presence or not of type 2 diabetes, perhaps pointing to metabolic pathways that need to be elucidated by future research.

Author contributions

Conceptualization: V.M.V, A.N., G.M. and R.M.; Methodology, A.M.M, A-J. Z, L-D.S, C.F and D-P.P; Resources: A.J, C. M., V.M.V and R.M; Data curation: A.M.M, F.I, V.M.V.; Writing-Original Draft: A.M.M and C.F; Writing-Review and Editing: V.M.V, L-D.S, A.N. and R.M.; Visualization: A.M.M and F.I; Supervision: C.M., A.N., V.M.V and R.M; Project administration: V.M.V and R.M.; Funding acquisition: V.M.V and R.M.

Funding

This study was financed by grants PI19/00838, PI19/0437, and CIBERehd CB06/04/0071 by Carlos III Health Institute and by the European Regional Development Fund (ERDF "A way to build Europe"); by PROMETEO/2019/027 by Ministry of Education of the Valencian Regional Government, UGP-15-220 by FISABIO and by an unrestricted grant from Menarini S.A. A.M. and Z. A-J. are recipients of PFIS contracts from Carlos III Health Institute (FI17/00126 and FI17/

00144 respectively). F.C is recipient of a Santiago Grisolía contract from the Valencian Regional Government (GRISOLIAP/2019/091). V.M.V is recipient of CES/10/030 contract and R.M. is recipient of CPII16/00037 contract, both from the Ministry of Health of the Valencian Regional Government and Carlos III Health Institute.

Declaration of competing interest

The authors declare no conflict of interest.

Acknowledgements

The authors thank Brian Normanly (University of Valencia/CIBERehd) for his editorial assistance; and Rosa Falcón for their technical assistance.

Appendix A. Supplementary data

Supplementary data to this article can be found online at https://doi.org/10.1016/j.redox.2020.101563.

References

[1] NCD Risk Factor Collaboration, Worldwide trends in diabetes since 1980: a pooled analysis of 751 population-based studies with 4·4 million participants, Lancet 387 (2016) 1513–1530.
[2] American Diabetes Association Diagnosis and Classification of Diabetes Mellitus, Diabetes Care 33 (2009) S62–S69.
[3] V.A. Fonseca, Defining and characterizing the progression of type 2 diabetes, Diabetes Care 32 (2009) S151.
[4] M. Akbari, V. Hassan-Zadeh, Hyperglycemia affects the expression of inflammatory genes in peripheral blood mononuclear cells of patients with type 2 diabetes, Immunol. Invest. (2018) 1–12.
[5] S. Yamagishi, T. Imaizumi, Diabetic vascular complications: pathophysiology, biochemical basis and potential therapeutic strategy, Curr. Pharmaceut. Des. 11 (2005) 2279–2299.
[6] N.G. Cruz, L.P. Sousa, M.O. Sousa, N.T. Pietrani, A.P. Fernandes, K.B. Gomes, The linkage between inflammation and Type 2 diabetes mellitus, Diabetes Res. Clin. Pract. 99 (2013) 85–92.
[7] S.E. Kahn, R.L. Hull, K.M. Utzschneider, Mechanisms linking obesity to insulin resistance and type 2 diabetes, Nature 444 (2006) 840–846.
[8] S. Bhansali, A. Bhansali, R. Walia, U.N. Saikia, V. Dhawan, Alterations in mitochondrial oxidative stress and mitophagy in subjects with prediabetes and type 2 diabetes mellitus, Front. Endocrinol. 8 (2017) 347.
[9] R. Blake, I.A. Trounce, Mitochondrial dysfunction and complications associated with diabetes, BBA 1840 (2014) 1404–1412.
[10] N. Diaz-Morales, S. Rovira-Llopis, I. Escribano-Lopez, C. Bañuls, S. Lopez-Domenech, R. Falcón, A.M. de Marañón, E. Sola, A. Jover, I. Roldan, J.L. Díez, M. Rocha, A. Hernández-Mijares, V.M. Victor, Role of oxidative stress and mitochondrial dysfunction in skeletal muscle in type 2 diabetic patients, Curr. Pharmaceut. Des. 22 (2016) 2650–2656.
[11] B. Niemann, S. Rohrbach, M.R. Miller, D.E. Newby, V. Fuster, J.C. Kovacic, Oxidative stress and cardiovascular risk: obesity, diabetes, smoking, and pollution: Part 3 of a 3-Part Series, J. Am. Coll. Cardiol. 70 (2017) 230–251.
[12] M. Morohoshi, K. Fujisawa, I. Uchimura, F. Numano, Glucose-dependent interleukin 6 and tumor necrosis factor production by human peripheral blood monocytes in vitro, Diabetes 45 (1996) 954–959.
[13] C.E. Tabit, W.B. Chung, N.M. Hamburg, J.A. Vita, Endothelial dysfunction in diabetes mellitus: molecular mechanisms and clinical implications, Rev. Endocr. Metab. Disord. 11 (2010) 61–74.
[14] T. McCaffrey, C. Fu, A. Re, H. Bush, A.S. Asch, E. Griffin, N. Hamel, A link between diabetes and atherosclerosis: glucose regulates expression of CD36 at the level of translation, Nat. Med. 7 (2001) 840–846.
[15] F. Kim, K.A. Tysseling, J. Rice, B. Gallis, L. Haji, C.M. Giachelli, E.W. Raines, M.A. Corson, M.W. Schwartz, Activation of IKKbeta by glucose is necessary and sufficient to impair insulin signaling and nitric oxide production in endothelial cells, J. Mol. Cell. Cardiol. 39 (2005) 327–334.
[16] K. Ley, C. Laudanna, M.I. Cybulsky, S. Nourshargh, Getting to the site of inflammation: the leukocyte adhesion cascade updated, Nat. Rev. Immunol. 7 (2007) 678–689.
[17] C. Savoia, E.L. Schiffrin, Vascular inflammation in hypertension and diabetes: molecular mechanisms and therapeutic interventions, Clin. Sci. 112 (2007) 375–384.
[18] R. Robertson, H. Zhou, T. Zhang, J. Harmon, Chronic oxidative stress as a mechanism for glucose toxicity of the beta cell in Type 2 diabetes, Cell Biochem. Biophys. 48 (2007) 139–146.
[19] B. Carroll, E.G. Otten, D. Manni, R. Stefanatos, F.M. Menzies, G.R. Smith, D. Jurk, N. Kenneth, S. Wilkinson, J.F. Passos, J. Attems, E.A. Veal, E. Teyssou, D. Seilhean, S. Millecamps, E.L. Eskelinen, A.K. Bronowska, D.C. Rubinsztein, A. Sanz, V.I. Korolchuk, Oxidation of SQSTM1/p62 mediates the link between redox state and protein homeostasis, Nat. Commun. 9 (2018) 256–272.
[20] I. Tanida, Autophagosome formation and molecular mechanism of autophagy, Antioxidants Redox Signal. 14 (2011) 2201–2214.
[21] H.S. Jung, Myung-Shik Lee, Role of autophagy in diabetes and mitochondria, Ann. N. Y. Acad. Sci. 1201 (2010) 79–83.
[22] C.D. Gonzalez, M.S. Lee, P. Marchetti, M. Pietropaolo, R. Towns, M.I. Vaccaro, H. Watada, J.W. Wiley, The emerging role of autophagy in the pathophysiology of diabetes mellitus, Autophagy 7 (2011) 2–11.
[23] A. Ost, K. Svensson, I. Ruishalme, C. Brännmark, N. Franck, H. Krook, P. Sandström, P. Kjolhede, P. Strålfors, Attenuated mTOR signaling and enhanced autophagy in adipocytes from obese patients with type 2 diabetes, Mol. Med. 16 (2010) 235–246.
[24] J. Yan, Z. Feng, J. Liu, J. Liu, W. Shen, Y. Wang, K. Wertz, P. Weber, J. Long, Enhanced autophagy plays a cardinal role in mitochondrial dysfunction in type 2 diabetic Goto–Kakizaki (GK) rats: ameliorating effects of (−)-epigallocatechin-3-gallate, J. Nutr. Biochem. 23 (2012) 716–724.
[25] A.J. Meijer, P. Codogno, Autophagy: a sweet process in diabetes, Cell Metabol. 8 (2008) 275–276.
[26] Li Fang, Yang Zhou, Hongdi Cao, Ping Wen, Lei Jiang, Weichun He, Chunsun Dai, Junwei Yang, Autophagy attenuates diabetic glomerular damage through protection of hyperglycemia-induced podocyte injury, PLoS One 8 (2013) e60546.
[27] C. Dong, H. Zheng, S. Huang, N. You, Q. You, J. Xu, X. Ye, Q. Zhu, Y. Feng, H. Miao, D. Ding, Y. Lu, Heme oxygenase-1 enhances autophagy in podocytes as a protective mechanism against high glucose-induced apoptosis, Exp. Cell Res. 337 (2015) 146–159.
[28] J. Yin, Y. Li, Y. Wang, G. Liu, J. Wang, X. Zhu, S. Pan, The role of autophagy in endoplasmic reticulum stress-induced pancreatic β cell death, Autophagy 8 (2012) 158–164.
[29] C. He, H. Zhu, H. Li, M. Zou, Z. Xie, Dissociation of Bcl-2-Beclin1 complex by activated AMPK enhances cardiac autophagy and protects against cardiomyocyte apoptosis in diabetes, Diabetes 62 (2013) 1270–1281.
[30] K. Kim, Y. Shin, M. Akram, E. Kim, K. Choi, H. Suh, C. Lee, O. Bae, High glucose condition induces autophagy in endothelial progenitor cells contributing to angiogenic impairment, Biol. Pharm. Bull. 37 (2014) 1248–1252.
[31] S. Kobayashi, X. Xu, K. Chen, Q. Liang, Suppression of autophagy is protective in high glucose-induced cardiomyocyte injury, Autophagy 8 (2012) 577–592.
[32] Y. Kabeya, S. Hong, J.W. Wiley, T. Yoshimori, R. Towns, D.J. Klionsky, C. Guo, M. Kaplan, Y. Shangguan, Sera from patients with type 2 diabetes and neuropathy induce autophagy and colocalization with mitochondria in SY5Y cells, Autophagy 1 (2005) 163–170.
[33] I. Escribano-Lopez, N. Diaz-Morales, F. Iannantuoni, S. López-Domènech, A.M. de Marañón, Z. Abad-Jiménez, C. Bañuls, S. Rovira-Llopis, J.R. Herance, M. Rocha, V.M. Víctor, The mitochondrial antioxidant SS-31 increases SIRT1 levels and ameliorates inflammation, oxidative stress and leukocyte-endothelium interactions in type 2 diabetes, Sci. Rep. 1 (2018) 158–162.
[34] D. Howatt, A. Balakrishnan, J. Moorleghen, L. Muniappan, D. Rateri, H. Uchida, J. Takano, T. Saido, A. Chishti, L. Baud, V. Subramanian, Leukocyte calpain deficiency reduces angiotensin II–induced inflammation and atherosclerosis but not abdominal aortic aneurysms in mice, ATVB 36 (2016) 835–845.
[35] R. Shurtz-Swirski, S. Sela, A.T. Herskovits, S.M. Shasha, G. Shapiro, L.B.N. Kristal, Involvement of peripheral polymorphonuclear leukocytes in oxidative stress and inflammation in type 2 diabetic patients, Diabetes Care 24 (2001) 104–110.
[36] K. Esposito, F. Nappo, R. Marfella, G. Giugliano, F. Giugliano, M. Ciotola, L. Quagliaro, A. Ceriello, D. Giugliano, Inflammatory cytokine concentrations are acutely increased by hyperglycemia in humans: role of oxidative stress, Circulation 106 (2002) 2067–2072.
[37] R. Mazor, R. Shurtz-Swirski, R. Farah, B. Kristal, G. Shapiro, F. Dorlechter, M. Cohen-Mazor, E. Meilin, S. Tamara, S. Sela, Primed polymorphonuclear leukocytes constitute a possible link between inflammation and oxidative stress in hyperlipidemic patients, Atherosclerosis 197 (2008) 937–943.
[38] S. Rangasamy, P.G. McGuire, C. Franco Nitta, F. Monickaraj, S.R. Oruganti, A. Das, Chemokine mediated monocyte trafficking into the retina: role of inflammation in alteration of the blood-retinal barrier in diabetic retinopathy, PLoS One 9 (2014) e108508.
[39] R. Farah, R. Shurtz-Swirski, O. Lapin, Intensification of oxidative stress and inflammation in type 2 diabetes despite antihyperglycemic treatment, Cardiovasc. Diabetol. 7 (2008) 20.
[40] F. Song, W. Jia, Y. Yao, Y. Hu, L. Lei, J. Lin, X. Sun, L. Liu, Oxidative stress, antioxidant status and DNA damage in patients with impaired glucose regulation and newly diagnosed type 2 diabetes, Clin. Sci. 112 (2007) 599–606.
[41] E. Čolak, N. Majkić-Singh, S. Stanković, V. Srecković-Dimitrijević, P.B. Djordjević, K. Lalić, N. Lalić, Parameters of antioxidative defense in type 2 diabetic patients with cardiovascular complications, Ann. Med. 37 (2005) 613–620.
[42] S. Nakanishi, G. Suzuki, Y. Kusunoki, K. Yamane, G. Egusa, N. Kohno, Increasing of oxidative stress from mitochondria in type 2 diabetic patients, Diabetes Metab. Res. Rev. 20 (2004) 399–404.
[43] W. Chen, K. Hung, M.S. Wen, P.Y. Hsu, T.H. Chen, H.D. Wang, J.T. Fang, S.S. Shie, C.Y. Wang, Impaired leukocytes autophagy in chronic kidney disease patients, Cardiorenal Med. 3 (2013) 254–264.
[44] K.K.S. Sunahara, F.P.B. Nunes, M.A.P. Baptista, P. Strell, P. Sannominoya, L.S. Westernberg, J.O. Martins, Insulin influences autophagy response distinctively in macrophages of different compartments, Cell. Physiol. Biochem. 34 (2014) 2017–2026.
[45] L. Chu, Y. Hsueh, H. Cheng, K.K. Wu, Cytokine-induced autophagy promotes long-term VCAM-1 but not ICAM-1 expression by degrading late-phase IκBα, Sci. Rep. 7

(2017) 12472.
[46] G. Xia, T. Zhu, X. Li, Y. Jin, J. Zhou, J. Xiao, ROS-mediated autophagy through the AMPK signaling pathway protects INS-1 cells from human islet amyloid polypeptide-induced cytotoxicity, Mol. Med. Rep. 18 (2018) 2744–2752.
[47] E. Wirawan, S. Lippens, T. Vanden-Berghe, A. Romagnoli, G.A. Fimia, M. Piacentini, P. Vandenabeele, Beclin1: a role in membrane dynamics and beyond, Autophagy 8 (1) (2018) 6–17.
[48] M.I. Molejon, A. Ropolo, A.L. Re, V. Boggio, M.I. Vaccaro, The VMP1-beclin 1 interaction regulates autophagy induction, Sci. Rep. 3 (2013) 1055.

Journal of
Clinical Medicine

MDPI

Article

Association between Proinflammatory Markers, Leukocyte–Endothelium Interactions, and Carotid Intima–Media Thickness in Type 2 Diabetes: Role of Glycemic Control

Aranzazu Martinez de Marañón [1], Francesca Iannantuoni [1], Zaida Abad-Jiménez [1], Francisco Canet [1], Pedro Díaz-Pozo [1], Sandra López-Domènech [1], Ildefonso Roldán-Torres [2], Carlos Morillas [1], Milagros Rocha [1,3,*] and Víctor M. Víctor [1,3,4,*]

1 Service of Endocrinology and Nutrition, University Hospital Doctor Peset, Foundation for the Promotion of Health and Biomedical Research in the Valencian Region (FISABIO), 46017 Valencia, Spain; amardema@alumni.uv.es (A.M.d.M.); franian@alumni.uv.es (F.I.); zaiaji@alumni.uv.es (Z.A.-J.); francisco.canet.1994@gmail.com (F.C.); pedrodpas2@gmail.com (P.D.-P.); Sandra.Lopez@uv.es (S.L.-D.); carlos.morillas@uv.es (C.M.)

2 Service of Cardiology, University Hospital Doctor Peset, Foundation for the Promotion of Health and Biomedical Research in the Valencian Region (FISABIO), 46017 Valencia, Spain; il.roldant@comv.es

3 Centro de Investigación Biomédica en Red (CIBERehd)—Department of Pharmacology, University of Valencia, 46010 Valencia, Spain

4 Department of Physiology, University of Valencia, 46010 Valencia, Spain

* Correspondence: milagros.rocha@uv.es (M.R.); victor.victor@uv.es (V.M.V.); Tel.: +34-963189132 (M.R. & V.M.V.)

Received: 4 June 2020; Accepted: 29 July 2020; Published: 5 August 2020

Abstract: Glycated hemoglobin monitorization could be a tool for maintaining type 2 diabetes (T2D) under control and delaying the appearance of cardiovascular events. This cross-sectional study was designed to assess the role of glycemic control in modulating early-stage markers of cardiovascular complications. One hundred and eight healthy controls and 161 type 2 diabetic patients were recruited and distributed according to their glycemic control, setting the threshold at 6.5% (good control). Biochemical and anthropometrical parameters were registered during the initial visit, and peripheral blood was extracted to obtain polymorphonuclear cells and analyze inflammatory markers, adhesion molecules, leukocyte–endothelium interactions, and carotid intima–media thickness. Correlations between these parameters were explored. We found that inflammatory markers and adhesion molecules were augmented in type 2 diabetic subjects with poor glycemic control. Polymorphonuclear leukocytes interacted more with the endothelium in the diabetic population, and even more significantly in the poorly controlled subjects. In parallel, carotid intima–media thickness was also increased in the diabetic population, and the difference was greater among poorly controlled subjects. Finally, correlation measurement revealed that carotid intima–media thickness was related to glycemic control and lipid metabolism in diabetic patients. Our results suggest that glycemic control delays the onset of cardiovascular comorbidities in diabetic subjects.

Keywords: type 2 diabetes; glycated hemoglobin; carotid intima–media thickness; inflammation; endothelial function

1. Introduction

Type 2 diabetes (T2D) is currently one of the most prevalent metabolic diseases, affecting around 500 million people. Its incidence has doubled since 1980 [1,2], increasing health expenditure because

of T2D itself and due to its derived complications [1–4]. In fact, cardiovascular diseases (CVD) are the leading cause of death among type 2 diabetic subjects [2,5], being caused mainly by advanced atherosclerosis, which can be delayed or prevented by early and maintained glycemic control. One of the key markers of glycemic control is glycated hemoglobin (HbA_{1c}), and reducing its levels is a primary goal of diabetic treatment [6–8]. In fact, several studies have demonstrated that sustaining HbA_{1c} below 6.5% reduces the incidence of macro- and microvascular comorbidities [7,9–13].

T2D is associated with a proinflammatory background, caused by high circulating glucose, accumulation of advanced glycation end products (AGEs), glycation of hemoglobin, alteration of lipid metabolism in adipose tissue, and other metabolic alterations that favor a proinflammatory state in peripheral blood [14–16]. If sustained for long periods, all of these modifications promote the production by tissue of a wide array of proinflammatory cytokines such as Interleukin-6 (IL6) and Tumor Necrosis Factor alpha (TNFα), as well as reactive oxygen species (ROS) [15–20], specially by mitochondria. In short, hyperglycemia and hyperlipidemia trigger Nod-Like Receptor Protein NLRP inflammasome activation, TNFα synthesis, and the production of mitochondrial and nonmitochondrial ROS [21–23]. This induces Nuclear Factor Kappa B (NFκB) activation and inflammatory cytokine expression, mostly through thioredoxin-related protein action [24–27]. Moreover, lipids can react with ROS and amplify the proinflammatory cascade [28]. This results in a vicious cycle of cell death and greater inflammation [29]. This ROS–inflammation axis has been studied in a wide array of inflammatory-based diseases, such as cardiac alterations [30–32], bone and joint diseases [33–35], neuronal and cerebral dysfunctions [28,29,36], bacterial infection [37], liver diseases [38], respiratory alterations [39,40] and cancer [41]. Furthermore, in T2D, the continuous presence of proinflammatory molecules causes diverse endocrine effects on the vasculature, and contributes to the development of micro- and macrovascular pathologies such as carotid atherosclerosis [21]. Together, the sustained increase of ROS production and the rise in inflammation have an important effect on the development of diabetic atherosclerosis [22].

Immune cells are also activated in T2D, producing more proinflammatory and adhesion molecules [15,16,42,43]. As explained previously, circulating proinflammatory molecules produced by chronic hyperglycemia and hyperlipidemia can activate leukocytes and the endothelium [44,45]. In this state, immune cells interact with the endothelium, infiltrating the inner layers of tissues and intensifying the inflammation [15,44,45]. There are different epidemiologic studies describing how an increased leukocyte count is a risk factor for the progression of carotid atherosclerosis and cardiovascular events [46–48]. Proinflammatory factors also favor the development of the atherosclerotic plaque, as demonstrated by several studies [49–52]. In fact, atherosclerosis represents the culmination of continued subclinical inflammation, and is one of the main causes of cardiovascular comorbidities [6,23,53–55]. Worryingly, atherosclerosis is often asymptomatic for decades before clinical manifestations appear, and is termed subclinical atherosclerosis during this period [6,56,57].

Carotid intima–media thickness (CIMT) is a biomarker of subclinical atherosclerosis [58,59]. Measurement of the CIMT by B-mode ultrasound has been shown to be suitable for evaluating the early stages of atherosclerosis [57,60,61] and to be an indicator of CVD [62–64]. Different studies have described a rise of CIMT in T2D [63,65,66] and metabolic syndrome [67,68].

The aim of this study was to explore the potential involvement of glycemic control in inflammation, adhesion molecules, leukocyte–endothelium interactions, and the CIMT in T2D patients compared with a healthy control population.

2. Experimental Section

2.1. Human Subjects

This study was carried out in 269 subjects, specifically, 161 T2D patients and 108 healthy controls recruited from the Service of Endocrinology and Nutrition of University Hospital Doctor Peset (Valencia, Spain) until June 2019 and adjusted for age and sex. The time that these patients had suffered from T2D, the presence of comorbidities, and their drug prescriptions are specified in

Supplementary data (Tables S1–S3). The subjects signed a written informed consent form and protocols were approved by our hospital's Ethics Committee for Clinical Investigation (ID: 98/19), in line with the ethical principles of the Helsinki declaration. T2D patients were diagnosed following the American Diabetes Association (ADA) indications, and presence of morbid obesity, insulin treatment, or any autoimmune, hematological, malignant, infectious, organic, or inflammatory disease represented the exclusion criteria.

2.2. Sample Collection

Venous blood samples were obtained from the antecubital vein in fasting conditions. Weight (kg), height (m), body mass index (BMI; kg/m^2), systolic and diastolic blood pressure (SBP/DBP; mmHg), and waist circumference (cm) were assessed previous to the blood extraction.

2.3. Laboratory Tests

Serum was isolated from the blood by centrifugation for 10 min at 1500 g and 4 ºC. Fasting glucose, cholesterol, and triglycerides were determined by an enzymatic method. High-density lipoprotein cholesterol (HDL-c) levels were measured with a Beckman LX-20 autoanalyzer (Beckman Coulter, La Brea, CA, USA) using a direct method. Low-density lipoprotein cholesterol (LDL-c) was determined with Friedewald's formula. An immunochemiluminescence assay was employed to determine insulin levels. Homeostatic Model Assessment of insulin resistance HOMA-IR index [fasting insulin (μU/mL) × fasting glucose (mg/dl)/405] was calculated to estimate insulin resistance (IR). Percentage of HbA_{1c} was determined with an automatic glycohemoglobin analyzer (Arkray, Inc., Kyoto, Japan). Apolipoproteins were measured with an electroimmunoassay. High-sensitivity C-reactive protein (hsCRP) was analyzed employing an immunonephelometer (Behring Nephelometer II, Dade Behring, Inc., Newark, DE, USA).

2.4. Leukocyte Isolation

In this assay, polymorphonuclear leukocytes (PMNs) were isolated from heparinized whole blood by the following protocol: the blood was mixed with 1:2 volumes of dextran solution (3% in NaCl 0.9%; Sigma Aldrich, MO, USA) and incubated for 45 min. The supernatant was then poured over Ficoll-Hypaque (GE Healthcare, Uppsala, Sweden) and centrifuged at 650× *g* for 25 min. The resulting pellet was lysed to remove the remaining erythrocytes with lysis buffer (5 min at room temperature) and centrifuged at 240× *g*. Pellets containing leukocytes were then washed twice and resuspended in Hank's balanced salt solution (HBSS; Sigma Aldrich, MO, USA). This cellular suspension was employed to perform the leukocyte–endothelium interaction assay.

2.5. Soluble Cytokines and Adhesion Molecule Assay

Intercellular adhesion molecule 1 (ICAM-1), vascular cell adhesion molecule-1 (VCAM-1), P-selectin, IL-6, and TNFα were analyzed in serum samples with a Luminex 200 flow analyzer system (Millipore, Austin, TX, USA). In brief, specific antibodies covered the color-coded microbead, and detection was performed with biotinylated secondary antibody and streptavidin-PE conjugate. The fluorescence of each individual microbead was analyzed with the Luminex XMap instrument. This method allows multiple cytokines in the same sample to be analyzed with a high specificity ad sensitivity. The TNFα detection range was between 1750 and 0.43 pg/mL; that of IL-6 is 750 to 0.18 pg/mL; that of VCAM-1 is 500 to 0.122 ng/mL; that of ICAM-1 is 350 to 0.085 ng/mL; and that of P-selectin is 1000 to 0.122 ng/mL. The intra-assay %CV is <5% for TNFα and IL-6 and <15% for ICAM-1, VCAM-1, and P-selectin. The interassay %CV is <20% for IL-6, ICAM-1, VCAM-1, and P-selectin and <15% for TNFα.

2.6. Static Cytometry Measurements

Mitochondrial ROS production was evaluated employing a MitoSOX (Thermo Fisher Scientific, Waltham, MA, USA) fluorescent probe. A fluorescence microscope (IX81; Olympus Corporation, Shinjuku-ku, Tokyo, Japan) with automated static cytometry software (ScanR, Olympus, Munich, Germany), which measures the fluorescence emission per individual cell, was also used. In brief, the protocol consisted of seeding PMN, extracted as previously specified, in 48-well plates and allowing them to adhere to the well surface. MitoSOX and DAPI (Sigma Aldrich, MO, USA) were then added to the well at a final concentration of 0.1 μM, for 20 min. After washing the cells twice with HBSS, fluorescence was measured and MitoSOX emission data relativized to DAPI emission data for each cell. PMN data were relativized with an internal control for all the experiments. All experiments were performed in duplicate, and 16 images per well were measured.

2.7. PMN–Endothelium Interaction Assay

An aliquot of 1.2 mL PMNs, isolated as previously described [69], with a density of 10^6 cells/mL in complete Roswell Park Memorial Institute medium RPMI, was employed for this assay. Primary cultures of human umbilical cord endothelial cells (HUVEC) were prepared as reported in [69]. In this assay, the PMN aliquot was perfused across the endothelial monolayer at a speed of 0.3 mL/min over a 5 min period, and the process was recorded. Rolling PMNs were considered to be those rolling for at least 1 min. Velocity was assessed by determining the time in which 15 rolling PMNs covered a distance of 100 μm. Adhesion was analyzed by counting the number of PMNs adhering to the endothelium for at least 30 s in 5 different fields.

2.8. Assessment of Carotid Intima–Media Thickness (CIMT)

Carotid thickness was evaluated following the American Echocardiography Association's guidelines. Healthy subjects and T2D patients were told to attend the Cardiology Service of the Dr. Peset Hospital 7–10 days after the blood extraction in order to evaluate carotid intima–media thickness. This measure has a diagnostic value because of its positive correlation with risk factors and with the prevalence of cardiovascular and cerebrovascular disease. The evaluation was performed by placing the head of the patients at 45º with respect to the body longitudinal axis. Some subjects were dropped from the study due to clinical or schedule reasons.

Carotid sonography was performed with a single ultrasound machine Aloka 5500 (Hitachi Aloka, Tokyo, Japan) equipped with a 7.5 MHz sector scanner probe. Baseline and follow-up studies were performed in a standard fashion by a single specialist physician who was specifically trained to perform the examination and was blinded to the treatment group. All images were electronically stored. Measurements corresponded with the 1 cm segment proximal to the dilation of the carotid bulb, and were always performed in plaque-free segments. For each patient, three measurements were performed for both sides of the anterior, lateral, and posterior projections of the far wall, and readings were then averaged. An independent observer, who was blinded to the treatment group and trained to interpret the CIMT images, performed an off-line analysis of B-mode ultrasound images. Paired CIMT measurements in the same arteries showed a high degree of reproducibility, with a mean difference in CIMT of 0.020 mm, and an intraclass correlation coefficient of 0.97 ($p < 0.001$). CIMT regression was defined as a decrease of >0.020 mm in mean CIMT at 12 months.

2.9. Statistical Analysis

All data were analyzed with SPSS 17.0 software (SPSS Statistics Inc., Chicago, IL, USA). Values are expressed as mean and standard deviation (SD) for parametric data, while the median (25th–75th percentiles) is presented for nonparametric data. Bar graphs show mean and standard error of the mean (SEM) in the figures. Multivariate lineal analysis was performed to check the influence of BMI and age on the other dependent variables.

Correlation analysis was performed with the Spearman formula, and the linear regression coefficient was also calculated. Graphs were plotted with GraphPad Prism 4.0 (GraphPad, La Jolla, CA, USA).

Multivariate linear analysis was performed in order to eliminate the influence of BMI and age on the variables of interest. Normality of the data sets was assessed by Kolmogorov–Smirnov test. In the case of the variables with normally distributed data, the groups were compared with a Student's *t*-test, while a Mann–Whitney U test was employed for non-normally distributed ones, and the Chi-Square test for proportion of frequencies. Study groups were compared using one-way analysis of variance (ANOVA) followed by a Bonferroni post hoc test. Differences were considered to be significant when $p < 0.05$, applying a confidence interval of 95% in every comparison. Graphs were plotted with GraphPad Prism 4.0 (GraphPad, La Jolla, CA, USA).

3. Results

3.1. Anthropometric and Biochemical Parameters

The study population was initially divided into healthy controls (108) and T2D patients (161) following the diagnostic criteria of the ADA. Diabetic patients were divided into two populations depending on their glycemic control, which was represented by their levels of HbA_{1c}. The set threshold was 6.5, in line with ADA criteria [7]. Table 1 confirms that both diabetic populations had typical hallmarks, with significant differences in glucose ($p < 0.01$), HbA1c ($p < 0.01$), and HOMA index ($p < 0.01$). Moreover, significant differences in glucose levels ($p < 0.001$) and HOMA index ($p < 0.001$) were found between the T2D $HbA_{1c} > 6.5$ group and the T2D $HbA_{1c} \leq 6.5$ group. Our T2D populations also displayed features such as greater waist diameter ($p < 0.01$), increased waist-to-hip ratio ($p < 0.01$), higher HOMA index ($p < 0.01$), and altered lipid metabolism parameters, with increased VLDL and triglyceride levels ($p < 0.01$), Ct/HDL ($p < 0.01$), and AIP ($p < 0.01$) and lower levels of HDL-c ($p < 0.01$). Total cholesterol, LDL cholesterol, and non-HDL cholesterol levels remained unchanged in the T2D $HbA_{1c} \leq 6.5\%$ group. However, total and LDL cholesterol were significantly reduced ($p < 0.01$) in the T2D $HbA_{1c} > 6.5$ group, possibly due to the hypolipemiant treatment. Regarding apolipoproteins, ApoA1 was significantly lower in T2D patients with respect to healthy controls ($p < 0.01$) and the difference was even more significant in the $HbA_{1c} > 6.5\%$ group ($p < 0.001$). ApoB levels did not change. Interestingly, the ApoB/ApoA ratio significantly increased in the T2D $HbA_{1c} > 6.5$ population ($p < 0.01$).

3.2. Inflammation Markers

A hyperglycemic scenario is usually accompanied by an increase in subclinical inflammation levels. We analyzed some relevant proinflammatory markers in our cohort of patients and their respective controls. The T2D group showed a significant increase in TNFα levels compared to the control group ($p = 0.047$) (Figure 1A). When we distributed the T2D population based on HbA_{1c}, an increase was preserved in the T2D $HbA_{1c} > 6.5$ group ($p = 0.014$) (Figure 1B). Another relevant cytokine, IL-6, was doubled in T2D subjects ($p = 0.019$) (Figure 1C) and, as occurred with TNFα, the increase was associated with T2D $HbA_{1c} > 6.5\%$ ($p = 0.015$) (Figure 1D).

Moreover, we evaluated mtROS production, and the results showed a significant rise in mtROS in the T2D population ($p = 0.045$) (Figure 1E), which was more pronounced among the poorly controlled population ($p = 0.038$) (Figure 1F). Poorly controlled T2D patients also had significantly higher levels of mtROS than their well-controlled counterparts ($p = 0.041$) (Figure 1F).

3.3. PMN–Endothelium Interactions

The generalized state of inflammation during T2D entails the activation of immune cells, which, in an active state, are more prone to attach to the endothelium and infiltrate through to the inner layers of the organs. Thus, we analyzed serum levels of adhesion molecules such as ICAM-1, VCAM-1,

and P-selectin, some of the main players of leukocyte–endothelium interactions. As can be seen in Figure 2, T2D patients displayed higher levels of ICAM-1 ($p = 0.016$) (Figure 2A) and VCAM-1 ($p = 0.027$) (Figure 2C), but not of P-selectin. The increase in ICAM-1 was already significant in the well-controlled diabetic population ($p = 0.006$) (Figure 2B), and was enhanced in the poorly controlled diabetic population ($p < 0.001$). In addition, VCAM-1 was significantly higher in T2D subjects with $HbA_{1c} > 6.5\%$ ($p = 0.005$) (Figure 2D).

Table 1. Anthropometrical and biochemical parameters.

	Control	T2D	
		$HbA_{1c} \leq 6.5\%$	**$HbA_{1c} > 6.5\%$**
N	108	57	104
Age (Years)	57 ± 11	58 ± 8	60 ± 9
%Women	62.2%	43.93%	56.11%
Weight (kg)	68.51 ± 15.18	85.02 ± 16,07 *	83.59 ± 15.84 *
BMI (kg/cm^2)	24.18 ± 4.11	31.18 ± 4.23 *	30.43 ± 5.13 *
SBP (mmHg)	119.43 ± 18.18	139.82 ± 14.23 *	138.38 ± 17.05 *
DBP (mmHg)	72.35 ± 10.94	82.03 ± 10.97 *	78.25 ± 9.35 *
Waist (cm)	79.81 ± 12.62	106.39 ± 11.46 *	103.99 ± 13.35 *
Hip (cm)	99.09 ± 7.21	108.71 ± 9.53 *	108.48 ± 12.62 *
Waist–Hip ratio	0.80 ± 0.09	0.97 ± 0.08 *	0.95 ± 0.08 *
Glucose (mg/dL)	88.08 ± 10.75	112.37 ± 22.59 *	160.51 ± 55.06 *‡
HOMA	1.69 ± 1.19	3.72 ± 2.00 *	6.57 ± 4.45 *‡
HbA_{1c} (%)	5.18 ± 0,26	5.94 ± 0.30 *	7.85 ± 1.30 *
Total cholesterol (mg/dL)	185.43 ± 35.32	173.67 ± 34.31	167.42 ± 37.67 *
HDL-c (mg/dL)	56.04 ± 13.61	45.10 ± 11.83 *	42.94 ± 10.46 *
LDL-c (mg/dL)	111.38 ± 28.72	102.62 ± 31.33	95.17 ± 31.09 *
VLDL (mg/dL)	26.01 ± 10.81	28.63 ± 19.54 *	28.91 ± 22.04 *
Cholesterol/HDL	3.46 ± 0.94	4.07 ± 1.18 *	4.06 ± 1.14 *
Triglycerides (mg/dL)	87.62 (55.50; 103.00)	130.29 (90.5; 169.00) *	150.75 (92.00; 162.63) *
Non-HDL Cholesterol (mg/dL)	129.39 ± 33.28	129.37 ± 32.51	124.48 ± 36.57
AIP (TG/HDL-c)	0.10 (−0.06; 0.33)	0.47 (0.23; 0.63) *	0.47 (0.29; 0.68) *
APO A1 (mg/dL)	164.02 ± 32.28	151.45 ± 27.21 *	142.72 ± 22.87 *†
APO B (mg/dL)	90.78 ± 26.60	90.33 ± 25.82	94.18 ± 25.27
APOB/APOA1	0.57 ± 0.20	0.64 ± 0.24	0.67 ± 0.19 *
hsCRP (mg/L)	0.75 (0.36; 1.83)	2.64 (1.61; 7.07) †	2.87 (1.31; 6.59) †

Anthropometrical and biochemical parameters obtained from whole peripheral blood from healthy subjects, $HbA_{1c} \leq 6.5\%$ T2D patients and $HbA_{1c} > 6.5\%$ T2D patients after 12 h fasting. Kolmogorov–Smirnov normality test was performed in all data sets. Data are shown as mean ± SD for data with normal distribution, and median and 25th; 75th percentile for non-normal data. The differences were analyzed by a t-test in the case of normal data and a Mann–Whitney test in that of non-normal data. *, $p < 0.01$ vs. control; †, $p < 0.001$ vs. control; ‡, $p < 0.001$ vs. T2D $HbA_{1c} \leq 6.5\%$.

For assessing PMN–endothelium cell interactions directly, we performed an in vitro adhesion assay with leukocytes from T2D patients and their respective controls. Leukocyte count was slightly higher but within the normal range in T2D patients. This could reflect the subclinical inflammation level characteristic of T2D (Supplementary Table S4). Rolling number, rolling velocity, and adhesion to the endothelial monolayer were assessed. We obtained a higher number of rolling cells in T2D patients ($p < 0.001$) (Figure 2G), accompanied by a lower velocity of these cells ($p < 0.001$) (Figure 2I) and a higher level of adhesion to the endothelial monolayer ($p < 0.001$) (Figure 2K). These differences remained when we separated the T2D population depending on its glycemic control status ($p < 0.001$) (Figure 2H,J,L). PMN rolling ($p < 0.001$) and adhesion ($p < 0.05$) were increased, while rolling velocity was decreased ($p < 0.001$) in well-controlled diabetic subjects. These significant differences were sustained in poorly controlled diabetic subjects, and were more significant in the case of cell adhesion (p

< 0.001). These differences can be assessed in the Supplementary Videos (Supplementary Videos S1–S3), in which representative videos of each experimental group have been attached (Supplementary data).

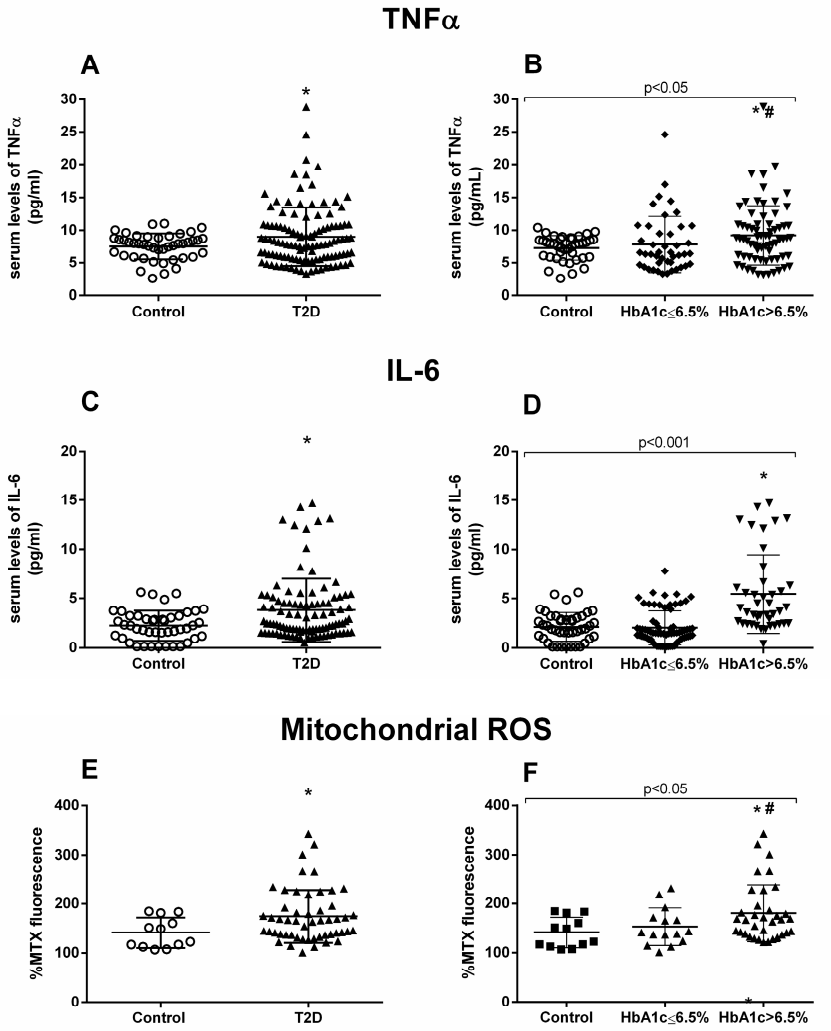

Figure 1. TNFα, IL-6, and mtROS measurements. Serum levels of proinflammatory cytokines TNFα (**A**,**B**) and IL-6 (**C**,**D**), and fluorescence levels of mtROS (**E**,**F**). Differences between control and T2D groups (**A**,**C**,**E**) or between control, well-controlled (HbA_{1c} ≤ 6.5%) and poorly controlled diabetic groups (HbA_{1c} > 6.5%) (**B**,**D**,**F**) are shown. Statistical analysis was performed using a t-test to compare two groups, and using ANOVA with Bonferroni post-test for three groups. * $p < 0.05$ vs. control; # $p < 0.05$ vs. T2D HbA1c < 6.5%.

3.4. Carotid Intima–Media Thickness Measurements

The proinflammatory environment seen in our diabetic patients and the increase in leukocyte–endothelium interactions could represent a rise in the incidence of macro- and microvascular complications. Therefore, we next explored CIMT. All the patients underwent carotid echocardiography at our hospital's Cardiology Service. Diabetic patients showed higher CIMT compared to healthy controls, with this difference being identified in the left carotid ($p < 0.001$) (Figure 3A) and right carotid ($p = 0.003$) (Figure 3C).

We observed that the poorly controlled diabetic population had significantly higher left CIMT than the well-controlled diabetic group ($p = 0.024$) (Figure 3B). On the other hand, right CIMT proved to be significantly higher in the poorly controlled diabetic group than in the control group ($p = 0.001$) (Figure 3D).

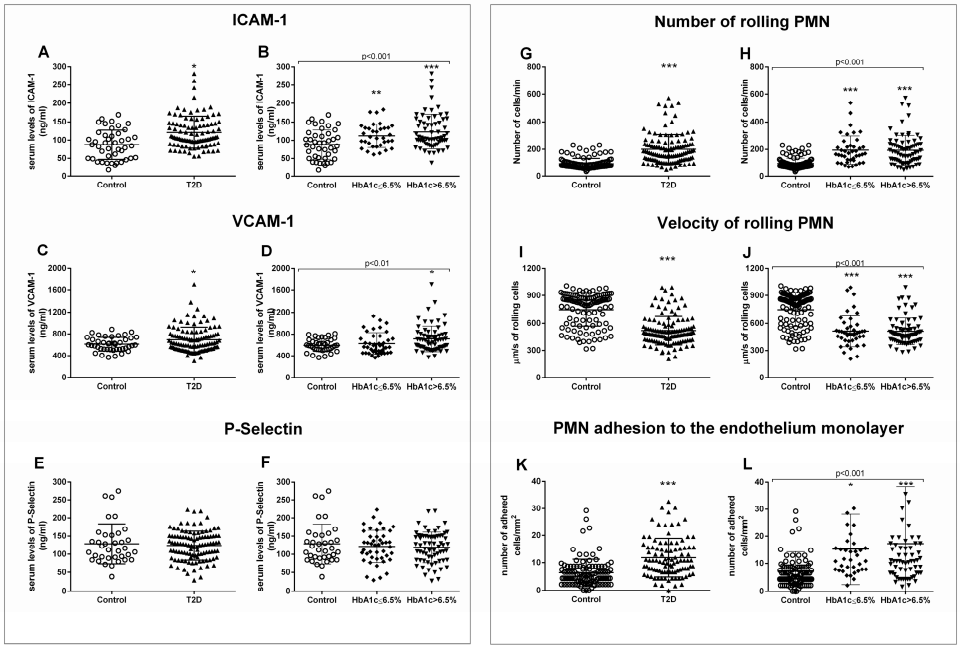

Figure 2. Serum levels of soluble adhesion molecules and measurement of PMN–endothelium interactions. Differences in adhesion molecules between control and T2D groups (**A**,**C**,**E**) or between control, well-controlled diabetics ($HbA_{1c} \leq 6.5\%$), and poorly controlled diabetics ($HbA_{1c} > 6.5\%$) (**B**,**D**,**F**) are shown. The number of rolling cells (**G**,**H**), their velocity (**I**,**J**), and the adhesion of these cells to the endothelial monolayer (**K**,**L**) were analyzed. Differences between control and T2D groups (**G**,**I**,**K**) or between control, well-controlled diabetics ($HbA_{1c} \leq 6.5\%$), and poorly controlled diabetic groups ($HbA_{1c} > 6.5\%$) (**H**,**J**,**L**) are shown. Statistical analysis was performed by means of a *t*-test to compare two groups, and using ANOVA with Bonferroni post-test for three groups. * $p < 0.05$; ** $p < 0.01$; *** $p < 0.001$ vs. control.

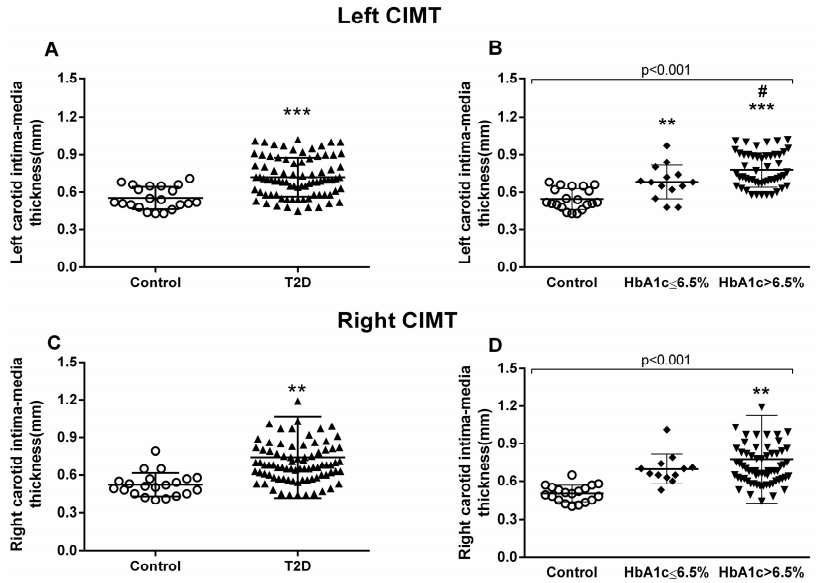

Figure 3. Measurement of carotid intima–media thickness (CIMT). Left carotid (**A**,**B**) and right carotid (**C**,**D**) were analyzed. Differences between control and T2D groups (**A**,**C**) or between control, well-controlled ($HbA_{1c} \leq 6.5\%$), and poorly controlled diabetic groups ($HbA_{1c} > 6.5\%$) (**B**,**D**) are shown in the graphs. Statistical analysis was performed by means of a t-test to compare two groups, and using ANOVA with a Bonferroni post-test for three groups. ** $p < 0.01$; *** $p < 0.001$ vs. control group; # $p < 0.05$ vs $HbA_{1c} \leq 6.5\%$ group.

3.5. Correlation Analysis

We took all these data and performed correlations and linear regression to explore relations between all the analyzed variables. First, we analyzed the relationship between in vitro adhesion assay parameters and the left CIMT; we observed positive correlations (rolling number Figure 4A, $p = 0.037$, r = 0.218; rolling velocity Figure 4C, $p = 0.021$, r = 0.252; adhesion Figure 4E, $p = 0.037$, r = 0.239) among the left carotid measures but not among those of the right (Figure 4B,D,F).

Regarding biochemical parameters, we saw that left CIMT measures correlated significantly with glucose ($p = 0.003$, r = 0.203) (Figure 5A), HOMA-IR ($p < 0.001$, r = 0.338) (Figure 5C), BMI ($p = 0.036$, r = 0.235) (Figure 5E), and HbA1c ($p < 0.001$, r = 0.399) (Figure 5G). These correlations were similar for the right CIMT, except for BMI correlation, which was not significant (Figure 5B (Glucose), $p < 0.001$, r = 0.377; Figure 5D (HOMA-IR), $p < 0.001$, r = 0.360; Figure 5F (HbA1c), $p < 0.001$, r = 0.389).

When we analyzed the correlation with lipid parameters, we observed that left CIMT was significantly correlated with HDL-c ($p < 0.001$, r = −0.436) (Figure 6A), VLDL ($p = 0.001$. r = 0.313) (Figure 6C), cholesterol/HDL index ($p = 0.001$, r = 0.313) (Figure 6E), and AIP ($p = 0.001$, r = 0.402) (Figure 6G). The data for right CIMT revealed similar correlations (Figure 6B (HDL-c), $p = 0.025$, r = −0.222; Figure 6D (VLDL), $p = 0.007$, r = 0.270; Figure 6H (AIP), $p = 0.002$, r = 0.307), with the exception of cholesterol/HDL index correlation.

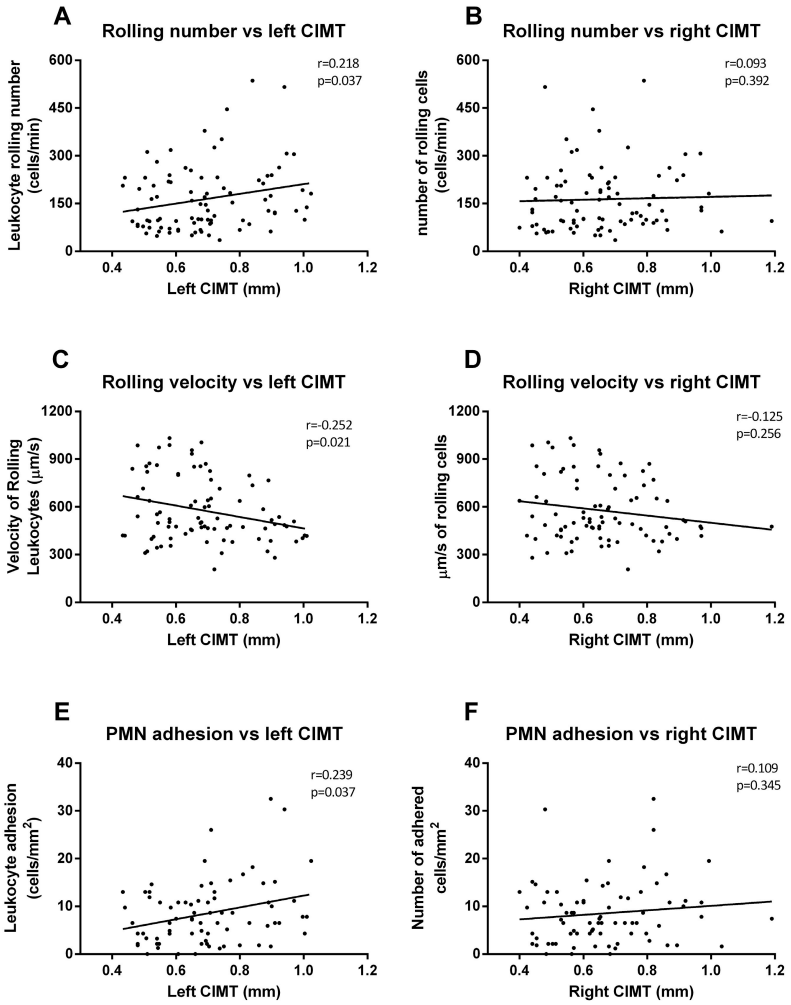

Figure 4. Correlation graphs of adhesion assay vs. CIMT measures. Graphs show correlations between number of rolling PMN and left (**A**) and right CIMT (**B**); rolling velocity and left (**C**) and right CIMT (**D**); and cell adhesion and left (**E**) and right CIMT (**F**). Spearman correlation analysis was performed.

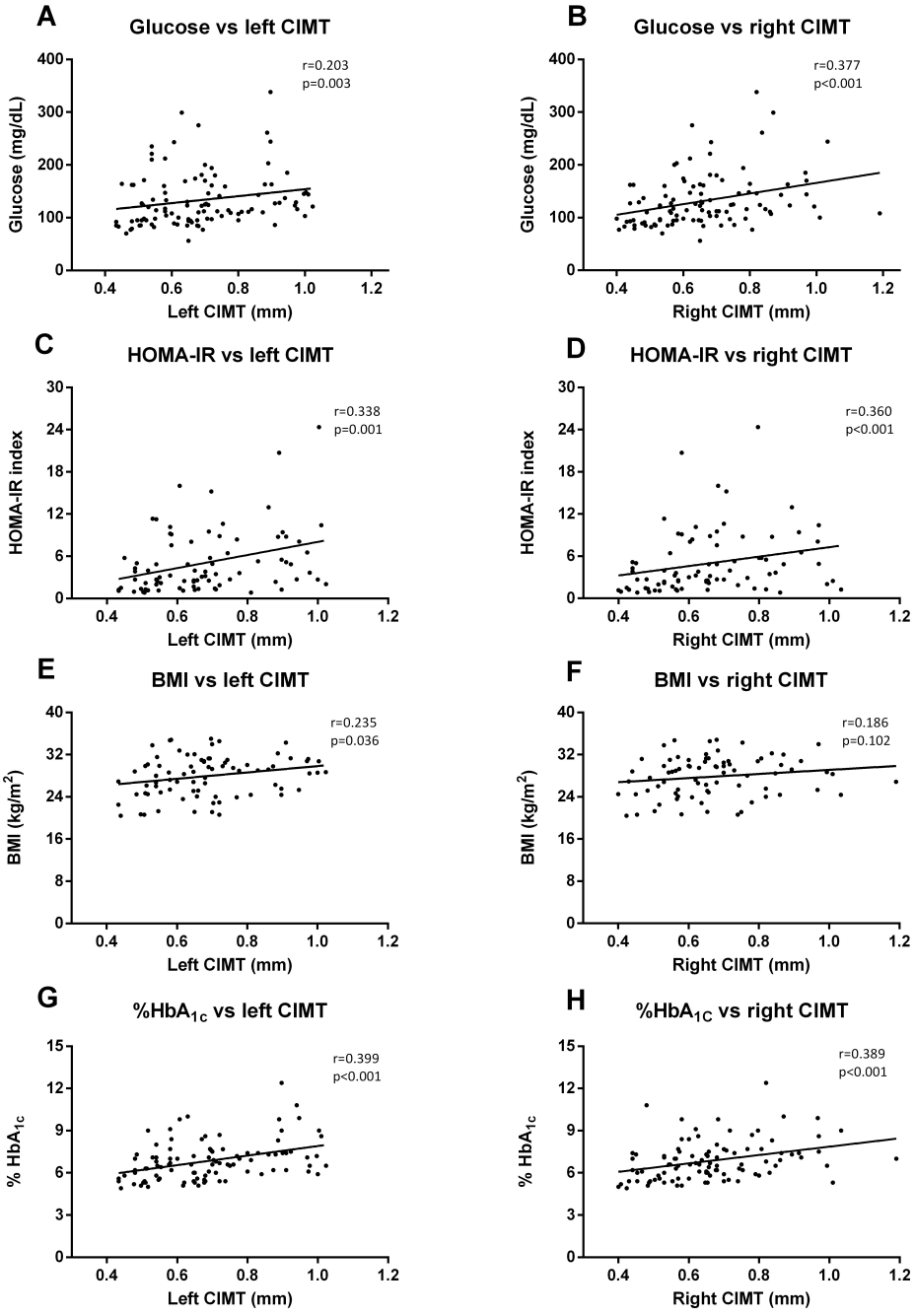

Figure 5. Correlation graphs of biochemical and anthropometrical parameters vs. CIMT measures. Graphs show correlation between glucose levels and left (**A**) and right CIMT (**B**); HOMA index and left (**C**) and right CIMT (**D**); BMI and left (**E**) and right CIMT (**F**); and HbA_{1c} and left (**G**) and right (**H**) CIMT. Spearman correlation analysis was performed.

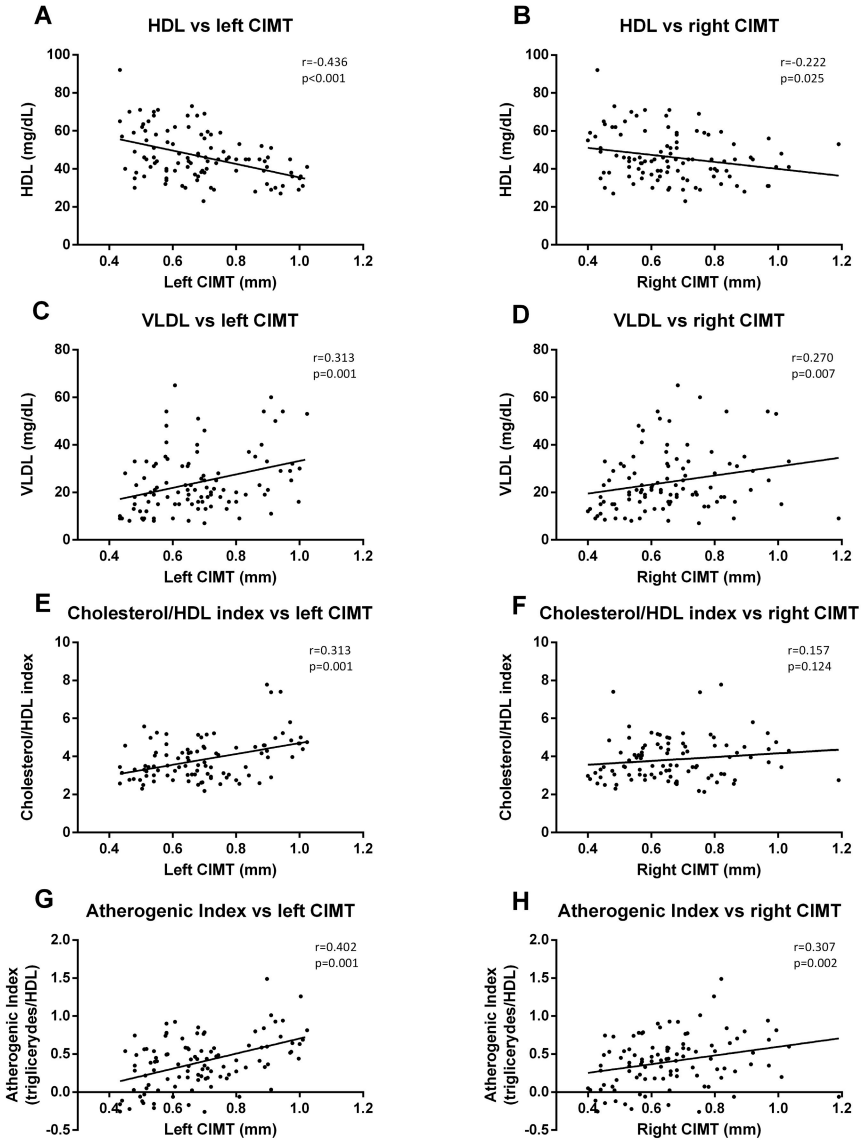

Figure 6. Correlation graphs of lipid metabolism parameters vs. CIMT measurements. Graphs show a correlation of HDL-c with left (**A**) and right CIMT (**B**); of VLDL index with left (**C**) and right CIMT (**D**); of cholesterol/HDL-c index with left (**E**) and right CIMT (**F**); and of atherogenic index (AIP) with left (**G**) and right (**H**) CIMT. A Spearman correlation analysis was performed. r coefficient and statistical significance, if any existed, are shown in the graph.

4. Discussion

Cardiovascular complications are a principal concern during diabetes management. The present study gives relevance to the relationship between CIMT, HbA_{1c}, and different hallmarks of T2D (inflammation, ROS production, and leukocyte–endothelium interactions). We have evaluated the involvement of glycemic control in endocrine and anthropometric parameters, inflammatory markers (TNF-α, IL-6, and mtROS production), adhesion molecules (ICAM-1, VCAM-1, and P-selectin), leukocyte–endothelium interactions (rolling, rolling velocity, and adhesion) and CIMT in T2D. In addition, we have analyzed their interrelationship by performing correlation studies. T2D patients, and especially those with poor glycemic control (HbA_{1c} > 6.5%), expressed an increase in inflammatory markers, mtROS production, adhesion molecules, leukocyte–endothelium interactions, and CIMT.

Regarding inflammatory intermediates, our study shows a slight but significant increase in TNF-α and IL-6 production in T2D patients; it is possible that the difference is not bigger because of the

hypolipemiant treatments received by most of the T2D patients. These proinflammatory cytokines are involved in the development of inflammation in T2D. Enhanced levels of TNF-α from leukocytes after activation by ROS-induced oxidative stress are thought to impair glucose uptake and inhibit insulin signaling [70,71]. Furthermore, IL-6 is thought to play an important role in atherosclerosis in T2D [56]. We show an increase in mtROS production in leukocytes from T2D patients that was more pronounced in subjects with HbA_{1c} > 6.5%, suggesting that leukocyte mitochondrial function can be altered during chronic hyperglycemia [70,72–74]. Other studies in the field have suggested that good glycemic control reduces ROS production [57,75,76]. These results are in accordance with those of other studies that have demonstrated high mtROS production in T2D related to the development of silent myocardial ischemia [72]. In this sense, it is important to underline that leukocytes are especially linked to ROS generation and cells that are highly sensitive to the oxidative damage mediated by ROS [77,78].

Different pathophysiological processes, including hypertension and atherosclerosis, are characterized by leukocyte recruitment to the arterial wall. In the present study, we have used an in vitro model in which human leukocytes flow over a monolayer of human endothelial cells with a shear stress similar to that observed in vivo [72]. This mimics the process that precedes inflammation in vivo (rolling and adhesion), and which is critical to homeostasis and vascular cell integrity. Our experimental system has been widely applied to visualize and analyze the multistep recruitment of leukocytes in these diseases, and allows the mechanisms of action implicated in this recruitment to be assessed [79]. Regarding this idea, it has been demonstrated that an inflammatory background favors the increase of leukocyte–endothelium interaction and promotes the early development of atherosclerotic events [80,81]. In the current study, we have observed that T2D enhanced rolling flux and PMN adhesion and reduced the rolling velocity of PMN. These effects were more evident in the group with HbA_{1c} > 6.5%. Furthermore, several studies have demonstrated the importance of leukocytes in the atherosclerotic scenario [82–84]. In accordance with these results, an increase in leukocyte–endothelium interactions has been related to oxidative stress in a human model of insulin resistance [85]. In addition, Petterson et al. demonstrated that there is increased recruitment but impaired function of leukocytes during inflammation in mouse models of T1D and T2D [86].

Endothelial and immune cell activation can be evaluated by measuring the soluble adhesion molecules VCAM-1, ICAM-1, and P-selectin. In this sense, it has been described that adhesion molecules are enhanced in patients with T2D [87]. In the present study, we show an increase in adhesion molecules, ICAM-1 and VCAM-1, in T2D that was most pronounced in the case of VCAM-1 in the HbA_{1c} > 6.5% group. These results are compatible with a rise in the number of leukocyte–endothelium interactions, and it has been demonstrated that hyperglycemia in both normal subjects and T2D patients can induce vasoconstriction, adhesion molecules, and inflammation [88,89]. Importantly, there was a slight but significant increase of T2D adhesion molecule levels with respect to the control group, a difference that may have been reduced by the hypolipemiant treatment.

The measurement of CIMT is useful for monitoring the early stages of atherosclerosis [61,90], and CIMT enhancement has been described in T2D [91]. In the present study, we have observed an increase in left and right CIMT, especially in the former case. Furthermore, the increment was more evident in the HbA1c > 6.5% group, suggesting that glycemic control is crucial for leukocyte–endothelium interactions and, therefore, for CIMT. The relevance of these changes in the left CIMT remain to be clarified, though different studies have suggested variations between left and right carotids; for example, Lorentz M. W. et al. revealed that left carotid plaques were vulnerable, whereas right carotid ones were calcified and stable [65]. Luo X et al. studied the factors associated with left and right CIMT and found that changes in biochemical parameters were associated with left carotid measures, while hemodynamic parameters were more related to right carotid measures [92]. The main consequences of CIMT thickening are cerebrovascular events such as stroke, and left carotid stroke is more frequent because of a higher probability of thickening of the left carotid arterial wall [93,94]. The above mentioned authors highlighted that the location of the left carotid renders it more susceptible to hemodynamic stress, thus increasing the probability of arterial wall thickening and

rupture. Selwaness M. et al. support this hypothesis; they found that while bilateral plaques were more frequent, 67% of cases of unilateral plaque occurred in the left carotid. This left plaque presented more intraplaque hemorrhage and more fibrous tissue and was thicker than the left, all of which explain why the left plaque is more vulnerable and prone to stroke. In the same study, right CIMT was found to be more calcified than the left, which would make it more resistant to shear stress [95].

In the present study, we have observed positive correlations between in vitro adhesion assay parameters and left CIMT, but not right CIMT. These results confirm the relevance of the enhancement of leukocyte–endothelium interactions in CIMT, especially on the left side. In terms of biochemical parameters, left CIMT measures correlated significantly with glucose, HOMA-IR, BMI, and HbA_{1c}. These correlations were maintained in the right CIMT, except for BMI (which was not significant). In line with these results, a systematic review by Einarson et al. found that individuals with impaired glucose tolerance had slightly (though significantly) higher CIMT values than individuals with normal glucose tolerance [96]. This data, together with leukocyte–endothelium interactions, suggest that poor glycemic control leaves T2D diabetic patients more prone to developing early or subclinical atherosclerotic events due to the rise in the number of leukocytes infiltrating the intima–media layer.

Finally, we analyzed correlations between CIMT and lipid parameters, and observed that the left CIMT was significantly correlated with VLDL, cholesterol/HDL index, and AIP. All these correlations were maintained when we analyzed the right CIMT data, with the exception of the cholesterol/HDL index correlation. In this sense, [97] demonstrated that lipid parameters, including total cholesterol (TC), triglycerides (TG), LDL, and VLDL, were significantly higher in diabetic stroke patients and positively correlated with the risk of stroke. CIMT was significantly higher in diabetic stroke patients, and correlations of lipid parameters (TC, TG, and VLDL) with CIMT in said patients were significantly and positively correlated, while lipid parameters (TC, TG, HDL, and LDL) were negatively correlated in nondiabetic ischemic stroke patients. Although lipidic parameters were differently affected by glycemic control, it is clear that these parameters increase the risk of developing later cardiovascular complications by increasing CIMT. We did not find any significant correlation with mitochondrial ROS production, adhesion molecules, or cytokine concentrations, though there was a tendency toward a slight correlation.

This study is observational, and so it would be interesting to perform a longitudinal intervention study in which we assess the evolution of CIMT in patients with poor glycemic control that achieve a good glycemic control. Defining the reason why left and right carotids behave and are affected differently is still unclear, and further research focusing on this issue would be useful. Moreover, we have correlated many T2D markers with one indicator of cardiovascular risk; future studies could attempt to find a correlation with other cardiac and endothelium function markers to reinforce our findings.

5. Conclusions

The current study provides evidence of proinflammatory markers, mtROS production, leukocyte–endothelium interactions, adhesion molecules, and CIMT in T2D. Some of these alterations were more pronounced in patients with HbA1c > 6.5, suggesting that glycemic control is a useful tool for preventing or delaying the onset of subclinical atherosclerotic process. Future research into these aspects will help to clarify the molecular mechanisms involved in glycemic control in T2D, and to modulate and control the atherosclerotic process in T2D.

Supplementary Materials: The following are available online at http://www.mdpi.com/2077-0383/9/8/2522/s1, Table S1: Time of T2D evolution on the recruited patients, Table S2: Incidence of most common comorbidities in the recruited T2D patients and in the control population, Table S3: Prescription of the different treatments associated with T2D in all the study subjects, Table S4: Leukocyte composition in healthy subjects and diabetic patients., Video S1: Control, Video S2: HbA1c > 6.5, Video S3: HbA1c ≤ 6.5.

Author Contributions: Conceptualization: V.M.V. and M.R.; Methodology, A.M.d.M., Z.A.-J., F.C., P.D.-P., S.L.-D.; Resources: I.R.-T., C.M., V.M.V., M.R.; Data curation: A.M.d.M., F.I., F.C., V.M.V.; Writing—Original Draft: A.M.d.M. and F.I.; Writing—Review and Editing: V.M.V., S.L-D., and M.R.; Visualization: A.M.d.M. and F.I;

Supervision: C.M., V.M.V. and M.R; Project administration: V.M.V., I.R.-T., M.R.; Funding acquisition: V.M.V., M.R. All authors have read and agreed to the published version of the manuscript.

Funding: This study was financed by grants PI19/00838, PI19/0437, and CIBERehd CB06/04/0071 by Carlos III Health Institute and by the European Regional Development Fund (ERDF "A way to build Europe"); UGP-15-220 by FISABIO; PROMETEO/2019/027 by Ministry of Health of the Valencian Regional Government; and by an unrestricted grant from Menarini S.A. A.M. and Z. A-J. are recipients of PFIS contracts from Carlos III Health Institute (FI17/00126 and FI17/00144, respectively). F.C. is recipient of a Santiago Grisolía contract from the Valencian Regional Government (GRISOLIAP/2019/091). V.M.V. is recipient of CES/10/030 contract and R.M. is recipient of CPII16/00037 contract, both from the Ministry of Health of the Valencian Regional Government and Carlos III Health Institute.

Acknowledgments: The authors thank Brian Normanly (University of Valencia/CIBERehd) for his editorial assistance; and Rosa Falcón for her technical assistance.

Conflicts of Interest: The authors declare no conflict of interest.

Abbreviations

ADA	American Diabetes Association
AGE	Advanced glycation end products
AIP	Atherogenic index of plasma
CIMT	Carotid intima–media thickness
CT	Cholesterol
DAPI	4′6′Diamidin-2-fenilindol
DBP	Diastolic blood pressure
HbA_{1c}	Glycated hemoglobin
HBSS	Hanks' Balanced Salt Solution
HDLc	High-density lipoprotein cholesterol
HOMA-IR	Homeostatic model assessment–insulin resistance
HUVEC	Human umbilical cord vein endothelial cell
ICAM-1	Intercellular adhesion molecule 1
IL-6	Interleukin 6
IR	Insulin resistance
LDLc	Low-density lipoprotein cholesterol
PMN	Polymorphonuclear cells
ROS	Radical oxygen species
RPMI	Roswell Park Memorial Institute culture medium
SBP	Systolic blood pressure
TG	Triglycerides
TNFα	Tumor necrosis factor alpha
VCAM-1	Vascular cell adhesion molecule 1
VLDLc	Very low-density lipoprotein cholesterol

References

1. NCD Risk Factor Collaboration (NCD-RisC). Worldwide trends in diabetes since 1980: A pooled analysis of 751 population-based studies with 4.4 million participants. *Lancet* **2016**, *387*, 1513–1530. [CrossRef]
2. Zheng, Y.; Ley, S.H.; Hu, F.B. Global aetiology and epidemiology of type 2 diabetes mellitus and its complications. *Nat. Rev. Endocrinol.* **2018**, *14*, 88–98. [CrossRef]
3. Zhang, Y.-B.; Pan, X.-F.; Chen, J.; Xia, L.; Cao, A.; Zhang, Y.; Wang, J.; Li, H.; Yang, K.; Guo, K.; et al. Combined lifestyle factors and risk of incident type 2 diabetes and prognosis among individuals with type 2 diabetes: A systematic review and meta-analysis of prospective cohort studies. *Diabetologia* **2020**, *63*, 21–33. [CrossRef]
4. Stirban, A.O.; Tschoepe, D. Cardiovascular complications in diabetes: Targets and interventions. *Diabetes Care* **2008**, *31* (Suppl. 2), S215–S221. [CrossRef]
5. Ley, S.H.; Hamdy, O.; Mohan, V.; Hu, F.B. Prevention and Management of Type 2 Diabetes: Dietary Components and Nutritional Strategies. *Lancet* **2014**, *383*, 1999–2007. [CrossRef]

6. Cosentino, F.; Grant, P.J.; Aboyans, V.; Bailey, C.J.; Ceriello, A.; Delgado, V.; Federici, M.; Filippatos, G.; E Grobbee, D.; Hansen, T.B.; et al. 2019 ESC Guidelines on diabetes, pre-diabetes, and cardiovascular diseases developed in collaboration with the EASD. *Eur. Heart J.* **2020**, *41*, 255–323. [CrossRef]
7. American Diabetes Association. 6. Glycemic Targets: Standards of Medical Care in Diabetes—2018. *Diabetes Care* **2018**, *41* (Suppl. 1), S55–S64. [CrossRef]
8. Laiteerapong, N.; A Ham, S.; Gao, Y.; Moffet, H.H.; Liu, J.Y.; Huang, E.S.; Karter, A.J. The Legacy Effect in Type 2 Diabetes: Impact of Early Glycemic Control on Future Complications (The Diabetes & Aging Study). *Diabetes Care* **2019**, *42*, 416–426.
9. Moodahadu, L.S.; Dhall, R.; Zargar, A.H.; Bangera, S.; Ramani, L.; Katipally, R. Tight Glycemic Control and Cardiovascular Effects in Type 2 Diabetic Patients. *Heart Views* **2014**, *15*, 111–120. [CrossRef]
10. Hill, D.; Fisher, M. The effect of intensive glycaemic control on cardiovascular outcomes. *Diabetes Obes. Metab.* **2010**, *12*, 641–647. [CrossRef]
11. Punthakee, Z.; Miller, M.E.; Simmons, D.L.; Riddle, M.C.; Ismail-Beigi, F.; Brillon, D.J.; Bergenstal, R.M.; Savage, P.J.; Hramiak, I.; Largay, J.F.; et al. Durable change in glycaemic control following intensive management of type 2 diabetes in the ACCORD clinical trial. *Diabetologia* **2014**, *57*, 2030–2037. [CrossRef]
12. Boussageon, R.; Bejan-Angoulvant, T.; Saadatian-Elahi, M.; Lafont, S.; Bergeonneau, C.; Kassaï, B.; Erpeldinger, S.; Wright, J.M.; Gueyffier, F.; Cornu, C. Effect of intensive glucose lowering treatment on all cause mortality, cardiovascular death, and microvascular events in type 2 diabetes: Meta-analysis of randomised controlled trials. *BMJ* **2011**, *343*, d4169. [CrossRef]
13. ADVANCE Collaborative Group; Patel, A.; MacMahon, S.; Chalmers, J.; Neal, B.; Billot, L.; Woodward, M.; Marre, M.; Cooper, M.; Glasziou, P.; et al. Intensive blood glucose control and vascular outcomes in patients with type 2 diabetes. *N. Engl. J. Med.* **2008**, *358*, 2560–2572. [CrossRef]
14. Donath, M.Y.; Shoelson, S.E. Type 2 diabetes as an inflammatory disease. *Nat. Rev. Immunol.* **2011**, *11*, 98–107. [CrossRef]
15. Lontchi-Yimagou, E.; Sobngwi, E.; Matsha, T.E.; Kengne, A.P. Diabetes mellitus and inflammation. *Curr. Diabetes Rep.* **2013**, *13*, 435–444. [CrossRef]
16. Cruz, N.G.; Sousa, L.P.; Sousa, M.O.; Pietrani, N.T.; Fernandes, A.P.; Gomes, K.B. The linkage between inflammation and Type 2 diabetes mellitus. *Diabetes Res. Clin. Pract.* **2013**, *99*, 85–92. [CrossRef]
17. Valentine, W.; Palmer, A.; Nicklasson, L.; Cobden, D.; Roze, S. Improving life expectancy and decreasing the incidence of complications associated with type 2 diabetes: A modelling study of HbA1c targets. *Int. J. Clin. Pract.* **2006**, *60*, 1138–1145. [CrossRef]
18. Lainampetch, J.; Panprathip, P.; Phosat, C.; Chumpathat, N.; Prangthip, P.; Soonthornworasiri, N.; Puduang, S.; Wechjakwen, N.; Kwanbunjan, K. Association of Tumor Necrosis Factor Alpha, Interleukin 6, and C-Reactive Protein with the Risk of Developing Type 2 Diabetes: A Retrospective Cohort Study of Rural Thais. *J. Diabetes Res.* **2019**, *2019*, 9051929. [CrossRef]
19. Fadaei, R.; Bagheri, N.; Heidarian, E.; Nouri, A.; Hesari, Z.; Moradi, N.; Ahmadi, A.; Ahmadi, R. Serum levels of IL-32 in patients with type 2 diabetes mellitus and its relationship with TNF-α and IL-6. *Cytokine* **2020**, *125*, 154832. [CrossRef]
20. Donath, M.Y.; Dinarello, C.A.; Mandrup-Poulsen, T. Targeting innate immune mediators in type 1 and type 2 diabetes. *Nat. Rev. Immunol.* **2019**, *19*, 734–746. [CrossRef]
21. Burgos-Morón, E.; Abad-Jiménez, Z.; De Marañon, A.M.; Iannantuoni, F.; Escribano-López, I.; López-Domènech, S.; Salom, C.; Jover, A.; Llabata, V.; Torres, I.R.; et al. Relationship between Oxidative Stress, ER Stress, and Inflammation in Type 2 Diabetes: The Battle Continues. *J. Clin. Med.* **2019**, *8*, 1385. [CrossRef]
22. Forrester, S.J.; Kikuchi, D.S.; Hernandes, M.S.; Xu, Q.; Griendling, K.K. Reactive Oxygen Species in Metabolic and Inflammatory Signaling. *Circ. Res.* **2018**, *122*, 877–902. [CrossRef]
23. Zhou, R.; Yazdi, A.S.; Menu, P.; Tschopp, J. A role for mitochondria in NLRP3 inflammasome activation. *Nature* **2011**, *469*, 221–225. [CrossRef]
24. Bulua, A.C.; Simon, A.; Maddipati, R.; Pelletier, M.; Park, H.; Kim, K.-Y.; Sack, M.N.; Kastner, D.L.; Siegel, R.M. Mitochondrial reactive oxygen species promote production of proinflammatory cytokines and are elevated in TNFR1-associated periodic syndrome (TRAPS). *J. Exp. Med.* **2011**, *208*, 519–533. [CrossRef]

25. Ungvari, Z.; Orosz, Z.; Labinskyy, N.; Rivera, A.; Xiangmin, Z.; Smith, K.; Csiszar, A. Increased mitochondrial H2O2 production promotes endothelial NF-kappaB activation in aged rat arteries. *Am. J. Physiol. Heart Circ. Physiol.* **2007**, *293*, H37–H47. [CrossRef]
26. Shah, A.; Xia, L.; Goldberg, H.; Lee, K.W.; Quaggin, S.E.; Fantus, I.G. Thioredoxin-interacting protein mediates high glucose-induced reactive oxygen species generation by mitochondria and the NADPH oxidase, Nox4, in mesangial cells. *J. Biol. Chem.* **2013**, *288*, 6835–6848. [CrossRef]
27. Zhou, R.; Tardivel, A.; Thorens, B.; Choi, I.; Tschopp, J. Thioredoxin-interacting protein links oxidative stress to inflammasome activation. *Nat. Immunol.* **2010**, *11*, 136–140. [CrossRef]
28. Yang, B.; Fritsche, K.L.; Beversdorf, D.Q.; Gu, Z.; Lee, J.C.; Folk, W.R.; Greenlief, C.M.; Sun, G.Y. Yin-Yang Mechanisms Regulating Lipid Peroxidation of Docosahexaenoic Acid and Arachidonic Acid in the Central Nervous System. *Front. Neurol.* **2019**, *10*, 642. [CrossRef]
29. Fischer, R.; Maier, O. Interrelation of Oxidative Stress and Inflammation in Neurodegenerative Disease: Role of TNF. *Oxid. Med. Cell. Longev.* **2015**, *2015*, 610813. [CrossRef]
30. Guo, Y.; Zhuang, X.; Huang, Z.; Zou, J.; Yang, D.; Hu, X.; Du, Z.; Wang, L.; Liao, X. Klotho protects the heart from hyperglycemia-induced injury by inactivating ROS and NF-κB-mediated inflammation both in vitro and in vivo. *Biochim. Biophys. Acta Mol. Basis Dis.* **2018**, *1864*, 238–251. [CrossRef]
31. Luo, B.; Li, B.; Wang, W.; Liu, X.; Xia, Y.; Zhang, C.; Zhang, M.; Zhang, Y.; An, F. NLRP3 gene silencing ameliorates diabetic cardiomyopathy in a type 2 diabetes rat model. *PLoS ONE* **2014**, *9*, e104771. [CrossRef]
32. Zhang, H.-L.; Chen, X.; Zong, B.; Yuan, H.; Wang, Z.; Wei, Y.; Wang, X.; Liu, G.; Zhang, J.; Li, S.; et al. Gypenosides improve diabetic cardiomyopathy by inhibiting ROS-mediated NLRP3 inflammasome activation. *J. Cell. Mol. Med.* **2018**, *22*, 4437–4448. [CrossRef]
33. Le Rossignol, S.; Ketheesan, N.; Haleagrahara, N. Redox-sensitive transcription factors play a significant role in the development of rheumatoid arthritis. *Int. Rev. Immunol.* **2018**, *37*, 129–143. [CrossRef]
34. Lepetsos, P.; Papavassiliou, K.A.; Papavassiliou, A.G. Redox and NF-κB signaling in osteoarthritis. *Free Radic. Biol. Med.* **2019**, *132*, 90–100. [CrossRef]
35. Pradhan, A.; Bagchi, A.; De, S.; Mitra, S.; Mukherjee, S.; Ghosh, P.; Ghosh, A.; Chatterjee, M. Role of redox imbalance and cytokines in mediating oxidative damage and disease progression of patients with rheumatoid arthritis. *Free Radic. Res.* **2019**, *53*, 768–779. [CrossRef]
36. Duecker, R.; Baer, P.C.; Eickmeier, O.; Strecker, M.; Kurz, J.; Schaible, A.; Henrich, D.; Zielen, S.; Schubert, R. Oxidative stress-driven pulmonary inflammation and fibrosis in a mouse model of human ataxia-telangiectasia. *Redox Biol.* **2018**, *14*, 645–655. [CrossRef]
37. Nandi, A.; Bishayi, B. CCR-2 neutralization augments murine fresh BMC activation by Staphylococcus aureus via two distinct mechanisms: At the level of ROS production and cytokine response. *Innate Immun.* **2017**, *23*, 345–372. [CrossRef]
38. Diehl, A.M. Cytokine regulation of liver injury and repair. *Immunol. Rev.* **2000**, *174*, 160–171. [CrossRef]
39. Han, S.; Cai, W.; Yang, X.; Jia, Y.; Zheng, Z.; Wang, H.; Li, J.; Li, Y.; Gao, J.; Fan, L.; et al. ROS-Mediated NLRP3 Inflammasome Activity Is Essential for Burn-Induced Acute Lung Injury. *Mediat. Inflamm.* **2015**, *2015*, 720457. [CrossRef]
40. Lee, I.-T.; Yang, C.-M. Role of NADPH oxidase/ROS in pro-inflammatory mediators-induced airway and pulmonary diseases. *Biochem. Pharmacol.* **2012**, *84*, 581–590. [CrossRef]
41. Zuo, L.; Prather, E.R.; Stetskiv, M.; Garrison, D.E.; Meade, J.R.; Peace, T.I.; Zhou, T. Inflammaging and Oxidative Stress in Human Diseases: From Molecular Mechanisms to Novel Treatments. *Int. J. Mol. Sci.* **2019**, *20*, 4472. [CrossRef]
42. Ouedraogo, R.; Gong, Y.; Berzins, B.; Wu, X.; Mahadev, K.; Hough, K.; Chan, L.; Goldstein, B.J.; Scalia, R. Adiponectin deficiency increases leukocyte-endothelium interactions via upregulation of endothelial cell adhesion molecules in vivo. *J. Clin. Investig.* **2007**, *117*, 1718–1726. [CrossRef]
43. Yan, Y.; Li, S.; Liu, Y.; Bazzano, L.; He, J.; Mi, J.; Chen, W. Temporal relationship between inflammation and insulin resistance and their joint effect on hyperglycemia: The Bogalusa Heart Study. *Cardiovasc. Diabetol.* **2019**, *18*, 109. [CrossRef]
44. Galkina, E.; Ley, K. Immune and Inflammatory Mechanisms of Atherosclerosis. *Annu. Rev. Immunol.* **2009**, *27*, 165–197. [CrossRef]
45. Legein, B.; Temmerman, L.; Biessen, E.A.L.; Lutgens, E. Inflammation and immune system interactions in atherosclerosis. *Cell. Mol. Life Sci.* **2013**, *70*, 3847–3869. [CrossRef]

46. Kavousi, M.; Elias-Smale, S.; Rutten, J.H.; Leening, M.J.G.; Vliegenthart, R.; Verwoert, G.C.; Krestin, G.P.; Oudkerk, M.; De Maat, M.P.; Leebeek, F.W.; et al. Evaluation of newer risk markers for coronary heart disease risk classification: A cohort study. *Ann. Intern. Med.* **2012**, *156*, 438–444. [CrossRef]
47. Lau, K.K.; Wong, Y.-K.; Chan, Y.-H.; Yiu, K.-H.; Teo, K.C.; Li, L.S.-W.; Ho, S.-L.; Chan, K.H.; Siu, C.-W.; Tse, H.-F. Prognostic implications of surrogate markers of atherosclerosis in low to intermediate risk patients with type 2 diabetes. *Cardiovasc. Diabetol.* **2012**, *11*, 101. [CrossRef]
48. Ortega, E.; Gilabert, R.; Núñez, I.; Cofán, M.; Sala-Vila, A.; De Groot, E.; Ros, E. White blood cell count is associated with carotid and femoral atherosclerosis. *Atherosclerosis* **2012**, *221*, 275–281. [CrossRef]
49. Blüher, M.; Unger, R.; Rassoul, F.; Richter, V.; Paschke, R. Relation between glycaemic control, hyperinsulinaemia and plasma concentrations of soluble adhesion molecules in patients with impaired glucose tolerance or Type II diabetes. *Diabetologia* **2002**, *45*, 210–216. [CrossRef]
50. Jude, E.B.; Douglas, J.T.; Anderson, S.G.; Young, M.J.; Boulton, A.J.M. Circulating cellular adhesion molecules ICAM-1, VCAM-1, P- and E-selectin in the prediction of cardiovascular disease in diabetes mellitus. *Eur. J. Intern. Med.* **2002**, *13*, 185–189. [CrossRef]
51. Pankow, J.S.; Decker, P.A.; Berardi, C.; Hanson, N.Q.; Sale, M.; Tang, W.; Kanaya, A.M.; Larson, N.B.; Tsai, M.; Wassel, C.L.; et al. Circulating cellular adhesion molecules and risk of diabetes: The Multi-Ethnic Study of Atherosclerosis (MESA). *Diabet. Med.* **2016**, *33*, 985–991. [CrossRef]
52. Qiu, S.; Cai, X.; Liu, J.; Yang, B.; Zügel, M.; Steinacker, J.M.; Sun, Z.; Schumann, U. Association between circulating cell adhesion molecules and risk of type 2 diabetes: A meta-analysis. *Atherosclerosis* **2019**, *287*, 147–154. [CrossRef]
53. Nguyen, P.A.; Won, J.S.; Rahman, M.K.; Bae, E.J.; Cho, M.K. Modulation of Sirt1/NF-κB interaction of evogliptin is attributed to inhibition of vascular inflammatory response leading to attenuation of atherosclerotic plaque formation. *Biochem. Pharmacol.* **2019**, *168*, 452–464. [CrossRef]
54. Sardu, C.; De Lucia, C.; Wallner, M.; Santulli, G. Diabetes Mellitus and Its Cardiovascular Complications: New Insights into an Old Disease. *J. Diabetes Res.* **2019**, *2019*, 1905194. [CrossRef]
55. Rangel, É.B.; Rodrigues, C.O.; de Sá, J.R. Micro- and Macrovascular Complications in Diabetes Mellitus: Preclinical and Clinical Studies. *J Diabetes Res.* **2019**, *2019*, 2161085. [CrossRef]
56. Golden, S.H.; Folsom, A.R.; Coresh, J.; Sharrett, A.R.; Szklo, M.; Brancati, F. Risk factor groupings related to insulin resistance and their synergistic effects on subclinical atherosclerosis: The atherosclerosis risk in communities study. *Diabetes* **2002**, *51*, 3069–3076. [CrossRef]
57. Tabatabaei-Malazy, O.; Fakhrzadeh, H.; Sharifi, F.; Mirarefin, M.; Arzaghi, S.M.; Badamchizadeh, Z.; Alizadeh-Khoei, M.; Larijani, B. Effect of metabolic control on oxidative stress, subclinical atherosclerosis and peripheral artery disease in diabetic patients. *J. Diabetes Metab. Disord.* **2015**, *14*, 84. [CrossRef]
58. Alharby, H.; Abdelati, T.; Rizk, M.; Youssef, E.; Moghazy, K.; Gaber, N.; Yafei, S. Association of lipid peroxidation and interleukin-6 with carotid atherosclerosis in type 2 diabetes. *Cardiovasc. Endocrinol. Metab.* **2019**, *8*, 73–76. [CrossRef]
59. Bauer, M.; Caviezel, S.; Teynor, A.; Erbel, R.; Mahabadi, A.A.; Schmidt-Trucksäss, A. Carotid intima-media thickness as a biomarker of subclinical atherosclerosis. *Swiss Med. Wkly.* **2012**, *142*, w13705. [CrossRef]
60. Abd El Dayem, S.M.; Battah, A.A.; El Bohy, A.E.M. Assessment of Increase in Aortic and Carotid Intimal Medial Thickness in Type 1 Diabetic Patients. *Open Access Maced. J. Med. Sci.* **2016**, *4*, 630. [CrossRef]
61. Pignoli, P.; Tremoli, E.; Poli, A.; Oreste, P.; Paoletti, R. Intimal plus medial thickness of the arterial wall: A direct measurement with ultrasound imaging. *Circulation* **1986**, *74*, 1399–1406. [CrossRef]
62. Santos, I.S.; Bittencourt, M.S.; Goulart, A.C.; Schmidt, M.I.; Diniz, M.D.F.H.S.; Lotufo, P.A.; Benseñor, I.M. Insulin resistance is associated with carotid intima-media thickness in non-diabetic subjects. A cross-sectional analysis of the ELSA-Brasil cohort baseline. *Atherosclerosis* **2017**, *260*, 34–40. [CrossRef]
63. Jeevarethinam, A.; Venuraju, S.; Dumo, A.; Ruano, S.; Mehta, V.S.; Rosenthal, M.; Nair, D.; Cohen, M.; Darko, D.; Lahiri, A.; et al. Relationship between carotid atherosclerosis and coronary artery calcification in asymptomatic diabetic patients: A prospective multicenter study. *Clin. Cardiol.* **2017**, *40*, 752–758. [CrossRef] [PubMed]
64. O'Leary, D.H.; Polak, J.F.; Kronmal, R.A.; Manolio, T.A.; Burke, G.L.; Wolfson, S.K. Carotid-Artery Intima and Media Thickness as a Risk Factor for Myocardial Infarction and Stroke in Older Adults. *N. Engl. J. Med.* **1999**, *340*, 14–22. [CrossRef] [PubMed]

65. Lorenz, M.W.; Price, J.F.; Robertson, C.; Bots, M.L.; Polak, J.F.; Poppert, H.; Kavousi, M.; Dorr, M.; Stensland, E.; Ducimetiere, P.; et al. Carotid intima-media thickness progression and risk of vascular events in people with diabetes: Results from the PROG-IMT collaboration. *Diabetes Care* **2015**, *38*, 1921–1929. [CrossRef] [PubMed]
66. Tenjin, A.; Nagai, Y.; Yuji, S.; Ishii, S.; Kato, H.; Ohta, A.; Tanaka, Y. Short-term change of carotid intima-media thickness after treatment of hyperglycemia in patients with diabetes: A cross-sectional study. *BMC Res. Notes* **2016**, *9*, 281. [CrossRef]
67. Asemi, Z.; Raygan, F.; Bahmani, F.; Rezavandi, Z.; Talari, H.R.; Rafiee, M.; Poladchang, S.; Mofrad, M.D.; Taheri, S.; Mohammadi, A.A.; et al. The effects of vitamin D, K and calcium co-supplementation on carotid intima-media thickness and metabolic status in overweight type 2 diabetic patients with CHD. *Br. J. Nutr.* **2016**, *116*, 286–293. [CrossRef]
68. Herder, M.; Arntzen, K.; Johnsen, S.; Mathiesen, E. The metabolic syndrome and progression of carotid atherosclerosis over 13 years. The Tromsø Study. *Cardiovasc. Diabetol.* **2012**, *11*, 77. [CrossRef]
69. Escribano-López, I.; De Marañon, A.M.; Iannantuoni, F.; López-Domènech, S.; Abad-Jiménez, Z.; Díaz-Pozo, P.; Sola, E.; Apostolova, N.; Rocha, M.; Víctor, V.M. The Mitochondrial Antioxidant SS-31 Modulates Oxidative Stress, Endoplasmic Reticulum Stress, and Autophagy in Type 2 Diabetes. *J. Clin. Med.* **2019**, *8*, 1322. [CrossRef]
70. González, F.; Rote, N.S.; Minium, J.; Kirwan, J.P. Reactive oxygen species-induced oxidative stress in the development of insulin resistance and hyperandrogenism in polycystic ovary syndrome. *J. Clin. Endocrinol. Metab.* **2006**, *91*, 336–340. [CrossRef]
71. Bajpai, A.; Tilley, D.G. The Role of Leukocytes in Diabetic Cardiomyopathy. *Front. Physiol.* **2018**, *9*, 1547. [CrossRef] [PubMed]
72. Mijares, A.H.; Rocha, M.; Rovira-Llopis, S.; Bañuls, C.; Bellod, L.; De Pablo, C.; Alvarez, A.; Roldán, I.; Sola-Izquierdo, E.; Victor, V.M. Human Leukocyte/Endothelial Cell Interactions and Mitochondrial Dysfunction in Type 2 Diabetic Patients and Their Association with Silent Myocardial Ischemia. *Diabetes Care* **2013**, *36*, 1695–1702. [CrossRef]
73. Alcántar-Fernández, J.; González-Maciel, A.; Reynoso-Robles, R.; Andrade, M.E.P.; Hernández-Vázquez, A.D.J.; Velázquez-Arellano, A.; Miranda-Ríos, J. High-glucose diets induce mitochondrial dysfunction in Caenorhabditis elegans. *PLoS ONE* **2019**, *14*, e0226652. [CrossRef]
74. Lin, H.-Y.; Weng, S.-W.; Chang, Y.-H.; Su, B.Y.-J.; Chang, C.-M.; Tsai, C.-J.; Shen, F.-C.; Chuang, J.-H.; Lin, T.-K.; Liou, C.-W.; et al. The Causal Role of Mitochondrial Dynamics in Regulating Insulin Resistance in Diabetes: Link through Mitochondrial Reactive Oxygen Species. *Oxid. Med. Cell. Longev.* **2018**, *2018*, 7514383. [CrossRef]
75. Rehman, K.; Akash, M.S.H. Mechanism of Generation of Oxidative Stress and Pathophysiology of Type 2 Diabetes Mellitus: How Are They Interlinked? *J. Cell. Biochem.* **2017**, *118*, 3577–3585. [CrossRef]
76. Luc, K.; Schramm-Luc, A.; Guzik, T.J.; Mikolajczyk, T.P. Oxidative stress and inflammatory markers in prediabetes and diabetes. *J. Physiol. Pharmacol.* **2019**, *70*, 809–824.
77. Diao, F.-Y.; Xu, M.; Hu, Y.; Li, J.; Xu, Z.; Lin, M.; Wang, L.; Zhou, Y.; Zhou, Z.; Liu, J.; et al. The molecular characteristics of polycystic ovary syndrome (PCOS) ovary defined by human ovary cDNA microarray. *J. Mol. Endocrinol.* **2004**, *33*, 59–72. [CrossRef]
78. Dupré-Crochet, S.; Erard, M.; Nüβe, O. ROS production in phagocytes: Why, when, and where? *J. Leukoc. Biol.* **2013**, *94*, 657–670. [CrossRef]
79. Rao, K.M.K. MAP kinase activation in macrophages. *J. Leukoc. Biol.* **2001**, *69*, 3–10.
80. Okazaki, S.; Sakaguchi, M.; Miwa, K.; Furukado, S.; Yamagami, H.; Yagita, Y.; Mochizuki, H.; Kitagawa, K. Association of interleukin-6 with the progression of carotid atherosclerosis: A 9-year follow-up study. *Stroke* **2014**, *45*, 2924–2929. [CrossRef]
81. Skoog, T.; Dichtl, W.; Boquist, S.; Skoglund-Andersson, C.; Karpe, F.; Tang, R.; Bond, M.; De Faire, U.; Nilsson, J.; Eriksson, P.; et al. Plasma tumour necrosis factor-alpha and early carotid atherosclerosis in healthy middle-aged men. *Eur. Heart J.* **2002**, *23*, 376–383. [CrossRef]
82. Ijsselmuiden, A.J.; Musters, R.J.; De Ruiter, G.; Van Heerebeek, L.; Alderse-Baas, F.; Van Schilfgaarde, M.; Leyte, A.; Tangelder, G.-J.; Laarman, G.J.; Paulus, W.J. Circulating white blood cells and platelets amplify oxidative stress in heart failure. *Nat. Clin. Pract. Cardiovasc. Med.* **2008**, *5*, 811–820. [CrossRef]

83. Bárány, T.; Simon, A.; Szabó, G.; Benkő, R.; Mezei, Z.; Molnár, L.; Becker, D.; Merkely, B.; Zima, E.; Horváth, E.M. Oxidative Stress-Related Parthanatos of Circulating Mononuclear Leukocytes in Heart Failure. *Oxid. Med. Cell. Longev.* **2017**, *2017*, 1249614. [CrossRef]
84. Tiyerili, V.; Camara, B.; Becher, M.U.; Schrickel, J.W.; Lütjohann, D.; Mollenhauer, M.; Baldus, S.; Nickenig, G.; Andrié, R.P. Neutrophil-derived myeloperoxidase promotes atherogenesis and neointima formation in mice. *Int. J. Cardiol.* **2016**, *204*, 29–36. [CrossRef]
85. Victor, V.M.; Rocha, M.; Sola, E.; Banuls, C.; Garcia-Malpartida, K.; Hernandez-Mijares, A. Oxidative Stress, Endothelial Dysfunction and Atherosclerosis. *Curr. Pharm. Des.* **2009**, *15*, 2988–3002. [CrossRef]
86. Pettersson, U.S.; Christoffersson, G.; Massena, S.; Ahl, D.; Jansson, L.; Henriksnäs, J.; Phillipson, M. Increased Recruitment but Impaired Function of Leukocytes during Inflammation in Mouse Models of Type 1 and Type 2 Diabetes. *PLoS ONE* **2011**, *6*, e22480. [CrossRef]
87. Novak, V.; Zhao, P.; Manor, B.; Sejdić, E.; Alsop, D.; Abduljalil, A.; Roberson, P.K.; Munshi, M.; Novak, P. Adhesion molecules, altered vasoreactivity, and brain atrophy in type 2 diabetes. *Diabetes Care* **2011**, *34*, 2438–2441. [CrossRef]
88. Giugliano, D.; Marfella, R.; Coppola, L.; Verrazzo, G.; Acampora, R.; Giunta, R.; Nappo, F.; Lucarelli, C.; D'Onofrio, F. Vascular Effects of Acute Hyperglycemia in Humans Are Reversed by l-Arginine. *Circulation* **1997**, *95*, 1783–1790. [CrossRef]
89. Kolluru, G.K.; Bir, S.C.; Kevil, C.G. Endothelial dysfunction and diabetes: Effects on angiogenesis, vascular remodeling, and wound healing. *Int. J. Vasc. Med.* **2012**, *2012*, 918267. [CrossRef]
90. Nezu, T.; Hosomi, N.; Aoki, S.; Matsumoto, M. Carotid Intima-Media Thickness for Atherosclerosis. *J. Atheroscler. Thromb.* **2016**, *23*, 18–31. [CrossRef]
91. Zhao, B.; Liu, Y.; Zhang, Y.; Chen, Y.; Yang, Z.-F.; Zhu, Y.; Xu, S. Gender difference in carotid intima-media thickness in type 2 diabetic patients: A 4-year follow-up study. *Cardiovasc. Diabetol.* **2012**, *11*, 51. [CrossRef]
92. Luo, X.; Yang, Y.; Cao, T.; Li, Z. Differences in left and right carotid intima-media thickness and the associated risk factors. *Clin. Radiol.* **2011**, *66*, 393–398. [CrossRef]
93. Hedna, V.S.; Bodhit, A.N.; Ansari, S.; Falchook, A.D.; Stead, L.; Heilman, K.M.; Waters, M.F. Hemispheric Differences in Ischemic Stroke: Is Left-Hemisphere Stroke More Common? *J. Clin. Neurol.* **2013**, *9*, 97–102. [CrossRef]
94. Hernaández, S.A.R.; Kroon, A.A.; Van Boxtel, M.P.; Mess, W.H.; Lodder, J.; Jolles, J.; De Leeuw, P.W. Is there a side predilection for cerebrovascular disease? *Hypertension* **2003**, *42*, 56–60. [CrossRef]
95. Selwaness, M.; Bouwhuijsen, Q.V.D.; Van Onkelen, R.S.; Hofman, A.; Franco, O.H.; Van Der Lugt, A.; Wentzel, J.J.; Vernooij, M.W. Atherosclerotic plaque in the left carotid artery is more vulnerable than in the right. *Stroke* **2014**, *45*, 3226–3230. [CrossRef]
96. Einarson, T.R.; Hunchuck, J.; Hemels, M. Relationship between blood glucose and carotid intima media thickness: A meta-analysis. *Cardiovasc. Diabetol.* **2010**, *9*, 37. [CrossRef]
97. Pillai, P.R.; Tiwari, D.; Jatav, O.P.; Rai, H. Lipid profile and carotid artery intima-media thickness in diabetic and non-diabetic ischaemic stroke. *Int. J. Adv. Med.* **2017**, *4*, 471. [CrossRef]

VOLUME 35 NUMBER 5 • AUGUST 10, 2021 • ISSN 1523-0864

ARS Therapeutics

Editor-in-Chief
Chandan K. Sen

Antioxidants & Redox Signaling

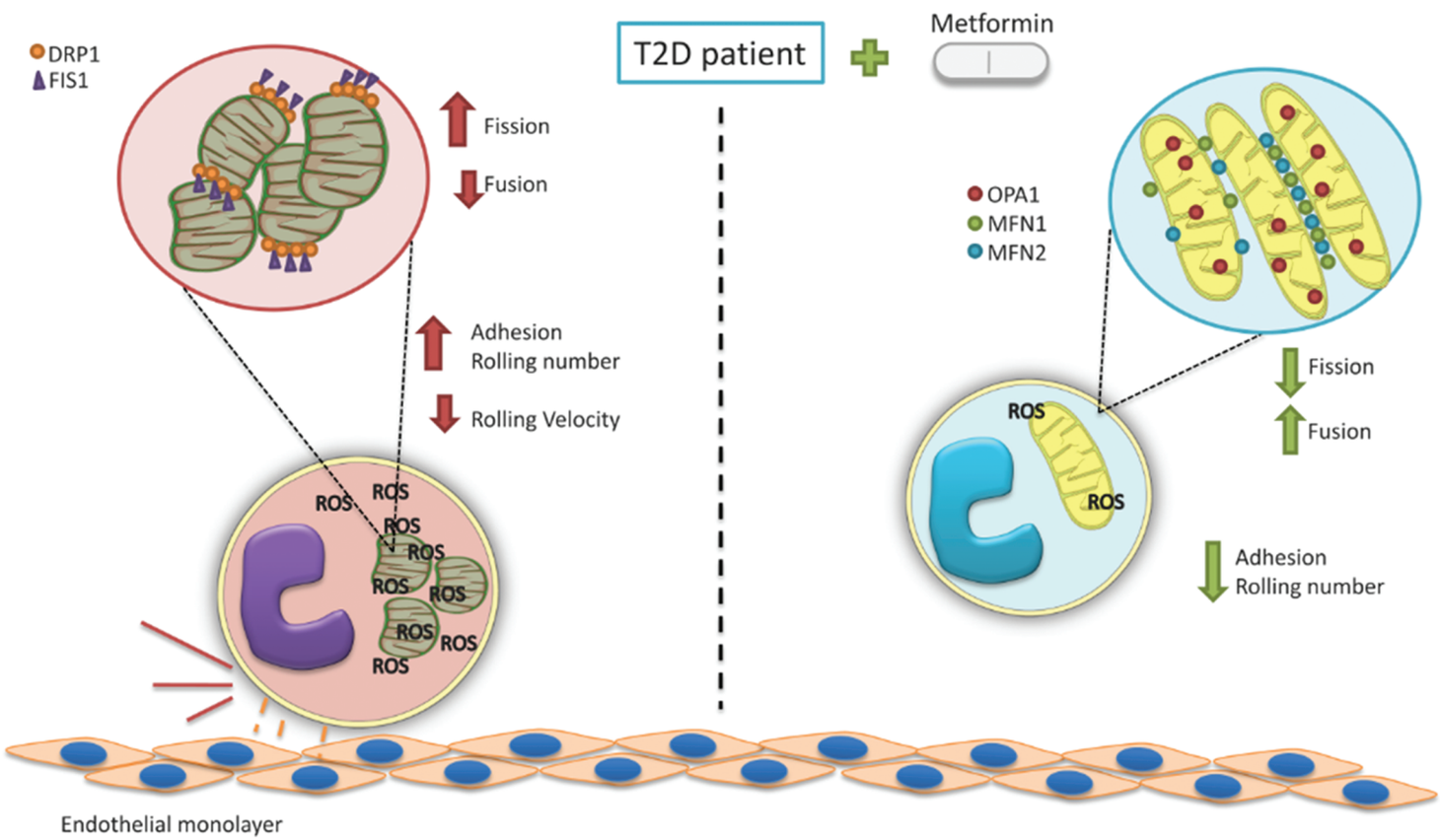

Mary Ann Liebert, Inc. publishers
www.liebertpub.com/ars

ANTIOXIDANTS & REDOX SIGNALING
Volume 35, Number 5, 2021

DOI: 10.1089/ars.2021.0019

Therapeutics

News & Views

Does Metformin Modulate Mitochondrial Dynamics and Function in Type 2 Diabetic Patients?

Aranzazu M. de Marañón,[1] Francisco Canet,[1] Zaida Abad-Jiménez,[1] Ana Jover,[1] Carlos Morillas,[1] Milagros Rocha,[1,2] and Victor M. Victor[1–3]

Abstract

Metformin is an effective drug against type 2 diabetes (T2D), a pathogenesis in which mitochondrial dysfunction is one of the main players. Thus, our first aim was to describe the effect of metformin on mitochondrial function in an outpatient population with T2D. For analyzing this hypothesis, we performed a

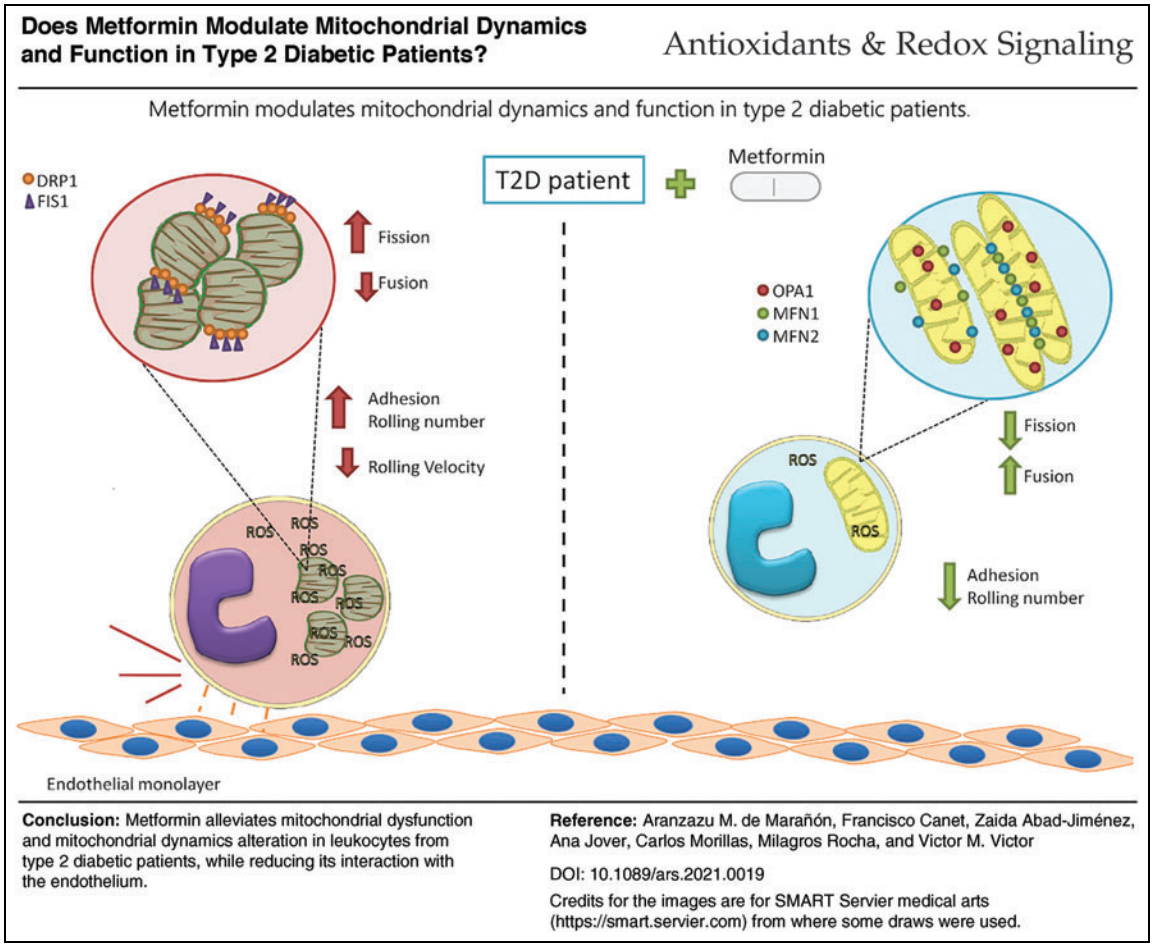

Color images are available online.

[1]Service of Endocrinology and Nutrition, University Hospital Doctor Peset, Foundation for the Promotion of Health and Biomedical Research in the Valencian Region (FISABIO), Valencia, Spain.
[2]Department of Physiology, University of Valencia, Valencia, Spain.
[3]CIBERehd - Department of Pharmacology, University of Valencia, Valencia, Spain.

preliminary cross-sectional study complying with the STROBE requirements. We studied leukocytes from 139 healthy controls, 39 T2D patients without metformin treatment, and 81 T2D patients who had been on said treatment for at least 1 year. Leukocytes from T2D patients displayed higher total and mitochondrial reactive oxygen species levels, lower mitochondrial membrane potential, and lower oxygen consumption. Moreover, their mitochondria expressed lower mRNA and protein levels of fusion proteins mitofusin-1 (MFN1), mitofusin-2 (MFN2), and optic atrophy 1 (OPA1), and higher protein and gene expression levels of mitochondrial fission protein 1 (FIS1) and dynamin-related protein 1 (DRP-1). In addition, we observed enhanced leukocyte/endothelial interactions in T2D patients. Metformin reversed most of these effects, ameliorating mitochondrial function and dynamics, and reducing the leukocyte/endothelial interactions observed in T2D patients. These results raise the question of whether metformin tackles T2D by improving mitochondrial dysfunction and regulating mitochondrial dynamics. Furthermore, it would seem that metformin modulates the alteration of interactions between leukocytes and the endothelium, a subclinical marker of early atherosclerosis. *Antioxid. Redox Signal.* 35, 377–385.

Keywords: inflammation, metformin, mitochondrial dysfunction, mitochondrial dynamics, type 2 diabetes

Introduction

TYPE 2 DIABETES (T2D) is a chronic inflammatory disease characterized by hyperglycemia and hyperinsulinemia. Accumulating evidence suggests that mitochondrial dysfunction is one of the main contributors to diabetic disease (7). However, there are controversies about whether mitochondrial dysfunction is the trigger or a consequence of metabolic deregulation.

Mitochondria are essential double-membrane organelles involved in different cell processes such as adenine triphosphate (ATP) synthesis, apoptosis, stress regulation, and lipid and carbohydrate metabolism, among others (7). They are responsible for meeting the enormous energy demands of vital tissues by facilitating cellular respiration, which is carried out in the mitochondrial cristae through electronic transport complexes (ETC) and the electrons obtained mainly as a result of glycolysis and fatty acid oxidation. Thus, ETC-mediated electron transport pumps protons to the intermembrane space to maintain the protonmotive force. Once the electrons reach the ATP synthase, ATP is synthesized, but only if there is an adequate protonmotive force.

It is now widely accepted that cellular energy demand affects mitochondria by causing changes to their shape, location, and/or mitochondrial mass (5). These processes are known as mitochondrial dynamics and are facilitated by mitochondrial transport through microtubules, and mitochondrial fusion and fission.

Fusion is carried away by three guanylyl triphosphatases (GTPases): mitofusin 1 (MFN1), mitofusin 2 (MFN2), and optic atrophy 1 (OPA1). Although MFN1 and MFN2 share similar sequences and functions, slight but critical differences have been identified: while MFN1 exerts its function in the outer membrane, MFN2 regulates mainly endoplasmic reticulum/mitochondria contact. Similarly, OPA1, a dynamin-related protein associated with inner mitochondrial membrane fusion and maintenance of the structure of respiratory supercomplexes, helps to regulate the shape of mitochondria through the fusion process (5).

On the contrary, fission machinery is mediated by dynamin-related protein 1 (DRP1), a GTPase protein located in the cytosol as a dimer or tetramer (5) that is recruited to the outer mitochondrial membrane by protein fission protein 1 (FIS1) and other receptor proteins in response to specific cellular cues (5).

Defects in these mitochondrial dynamics can lead to a substantial production of reactive oxygen species (ROS), which, in turn, leak into the cytosol and affect the cellular environment and molecular signaling. Subsequently, these stress stimuli expedite recruitment of the immune cells to the activated vascular endothelium, thus promoting further atherosclerotic changes and the development of macrovascular complications (2, 6). In particular, the activation of leukocytes, mediated by chemokine-dependent and chemokine-independent mechanisms, leads to leukocyte/endothelial cell adhesion. During this process, adhesion molecules on rolling leukocytes bind to their counter-receptors on endothelial cells, thus promoting their firm adhesion to the wall. This persistent condition contributes to the initiation and progression of atherosclerotic lesion development (2, 9).

To date, many different treatments have been used to ameliorate T2D. However, since its discovery in 1950, metformin has remained the first-line treatment. Although the exact mechanisms by which metformin exerts its actions are unknown, a wide range of theories have been put forward (3). Of note, metformin seems to alleviate cell activation, thus palliating the inflammatory response (2). However, this aspect has not been assessed in primary leukocytes, and so, the precise effect of metformin is still unclear.

Innovation

Alterations in mitochondrial function and dynamics and the inflammatory events, which take place as a consequence, are key to the diabetic pathology, but the nature of the effects exerted by metformin on these parameters is unclear. Thus, it is relevant to study them in primary type 2 diabetes (T2D) leukocytes, which are central to the immune response. Our results suggest that metformin effectively palliates alterations of leukocyte mitochondrial function and dynamics due to T2D and reduces their activation. Our results contribute to the knowledge of the mechanisms that explain the deregulated immune function in T2D. Future research will need to detangle the precise molecular pathways at work and the exact target of metformin in this scenario.

In light of the research described above, we hypothesized that mitochondrial function and dynamics are altered in T2D, thus affecting leukocyte/endothelial interactions, and that metformin can mitigate these alterations.

Biochemical and anthropometrical parameters

Table 1 shows the results obtained when we analyzed the anthropometrical and biochemical data in our study population. One hundred thirty-five healthy subjects and 120 T2D patients were recruited from the Endocrinology Outpatients Service of the University Hospital Doctor Peset (Valencia, Spain). The T2D group was divided into patients with metformin treatment (81) or without treatment (39). In relation to anthropometrical parameters, T2D patients presented higher weight ($p < 0.05$), body mass index (BMI; $p < 0.05$), waist circumference ($p < 0.05$), and diastolic blood pressure (DBP) and systolic blood pressure (SBP; $p < 0.05$).

Metformin had a significant effect on SBP ($p < 0.05$), while DBP showed nonsignificant differences with respect to the control group. Insulin concentrations and homeostatic model assessment (HOMA) index were higher in T2D patients (both $p < 0.05$), with no influence of metformin treatment being observed. HbA_{1c}% and glucose were significantly increased in the T2D group ($p < 0.05$) and lower among patients receiving metformin treatment ($p < 0.05$). Regarding lipid metabolism parameters, we found that cholesterol, high-density lipoproteins (HDL), and low-density lipoproteins (LDL) were reduced in T2D patients ($p < 0.05$) due to the effect of the hypolipemiant treatment (50% of patients in the T2D group and 63.8% of metformin-treated patients). Very low-density lipoproteins (VLDL), cholesterol/HDL ratio, and triglycerides were increased in T2D patients, and were not modified by metformin treatment.

ROS content and mitochondrial function

First, we aimed to determine if T2D induced a change in mitochondrial integrity and functionality, and whether metformin was capable of reducing its effects. Figure 1A depicts how T2D leukocytes exhibited higher total ROS content ($p < 0.05$), and how this content was diminished by metformin treatment ($p < 0.05$). Moreover, the results shown in Figure 1B reflect a similar behavior of mitochondrial ROS ($p < 0.01$ in T2D *vs.* control samples, and $p < 0.05$ for T2D + metformin *vs.*T2D).

In this respect, metformin tempered the rise in ROS production induced by T2D in leukocytes. Figure 1C shows the reduced mitochondrial membrane potential of T2D leukocytes ($p < 0.05$), and illustrates that treatment with metformin returned membrane potential to normal levels ($p < 0.05$). Moreover, as shown in Figure 1D, T2D leukocytes exhibited decreased O_2 consumption ($p < 0.05$), while mitochondria of patients receiving metformin showed normal O_2 consumption ($p < 0.05$).

Leukocyte/endothelial interactions

Figure 1E–G describes how diabetes altered the leukocyte/endothelial interactions and whether metformin restores this phenotype to control levels. T2D leukocyte/endothelial interactions were increased by enhancing rolling ($p < 0.001$) and adhesion ($p < 0.001$) and by decreasing rolling velocity

Table 1. Biochemical and Anthropometrical Profile of Control Subjects and Type 2 Diabetes Patients With or Without Metformin Treatment

	Control	*T2D*	*T2D + metformin*
n	135	39	81
Male%	43.70	50.97	59.90
Age (years)	45.22 ± 12.06	58.97 ± 10.05	58.76 ± 12.12
Weight (kg)	67.55 ± 12.30	73.69 ± 10.97[a]	74.53 ± 12.24[a]
BMI (kg/m^2)	23.49 ± 2.96	26.92 ± 2.47[a]	26.66 ± 3.14[a]
Waist circumference (cm)	79.67 ± 12.83	95.57 ± 10.32[a]	95.42 ± 11.40[a]
SBP (mm Hg)	118 ± 17.95	148.26 ± 25.15[a]	139.80 ± 16.68[a,b]
DBP (mm Hg)	72.07 ± 10.91	82.09 ± 12.56[a]	77.49 ± 10.76[a]
Insulin (μUI/mL)	7.16 ± 3.40	14.51 ± 8.22[a]	15.44 ± 10.63[a]
HOMA-IR	1.65 ± 1.08	4.69 ± 3.39[a]	4.68 ± 5.25[a]
HbA_{1c} (%)	5.29 ± 0.53	7.31 ± 1.17[a]	6.72 ± 1.04[a,b]
Glucose (mg/dL)	90.59 ± 21.57	152.29 ± 44.99[a]	111.94 ± 27.54[a,b]
Cholesterol (mg/dL)	185.74 ± 35.23	173.61 ± 42.30[a]	165.94 ± 35.03[a]
HDL (mg/dL)	56.60 ± 13.56	45.91 ± 13.28[a]	43.50 ± 10.07[a]
LDL (mg/dL)	111.60 ± 28.49	101.76 ± 33.93	93.22 ± 10.07[a]
VLDL (mg/dL)	13 (11–19)	20.5 (14.25–29.75)	25.75 (18–36.5)[a]
CT/HDL	3.42 ± 0.92	4.04 ± 1.26[a]	4.00 ± 1.14[a]
Triglycerides (mg/dL)	67 (55–99)	104 (70.75–149.25)	129.88 (92–185.5)[a]
Non-HDL cholesterol	129.14 ± 33.02	128.97 ± 40.35	122.44 ± 34.61

Kolmogorov/Smirnov or Shapiro/Wilk normality tests were carried out depending on the sample size. For normally distributed data, mean ± SD shown, and for non-normally distributed data, the median is shown (first and third quartile). Analysis of variance and Tukey post-test were performed to outline statistically significant differences between groups.

[a] $p < 0.05$ *versus* control group.

[b] $p < 0.05$ *versus* T2D group.

BMI, body mass index; CT, cholesterol; DBP, diastolic blood pressure; HbA_{1c}, glycated hemoglobin; HDL, high-density lipoproteins; HOMA-IR, homeostatic model assessment of insulin resistance; LDL, low-density lipoproteins; SBP, systolic blood pressure; T2D, type 2 diabetes; VLDL, very low-density lipoproteins.

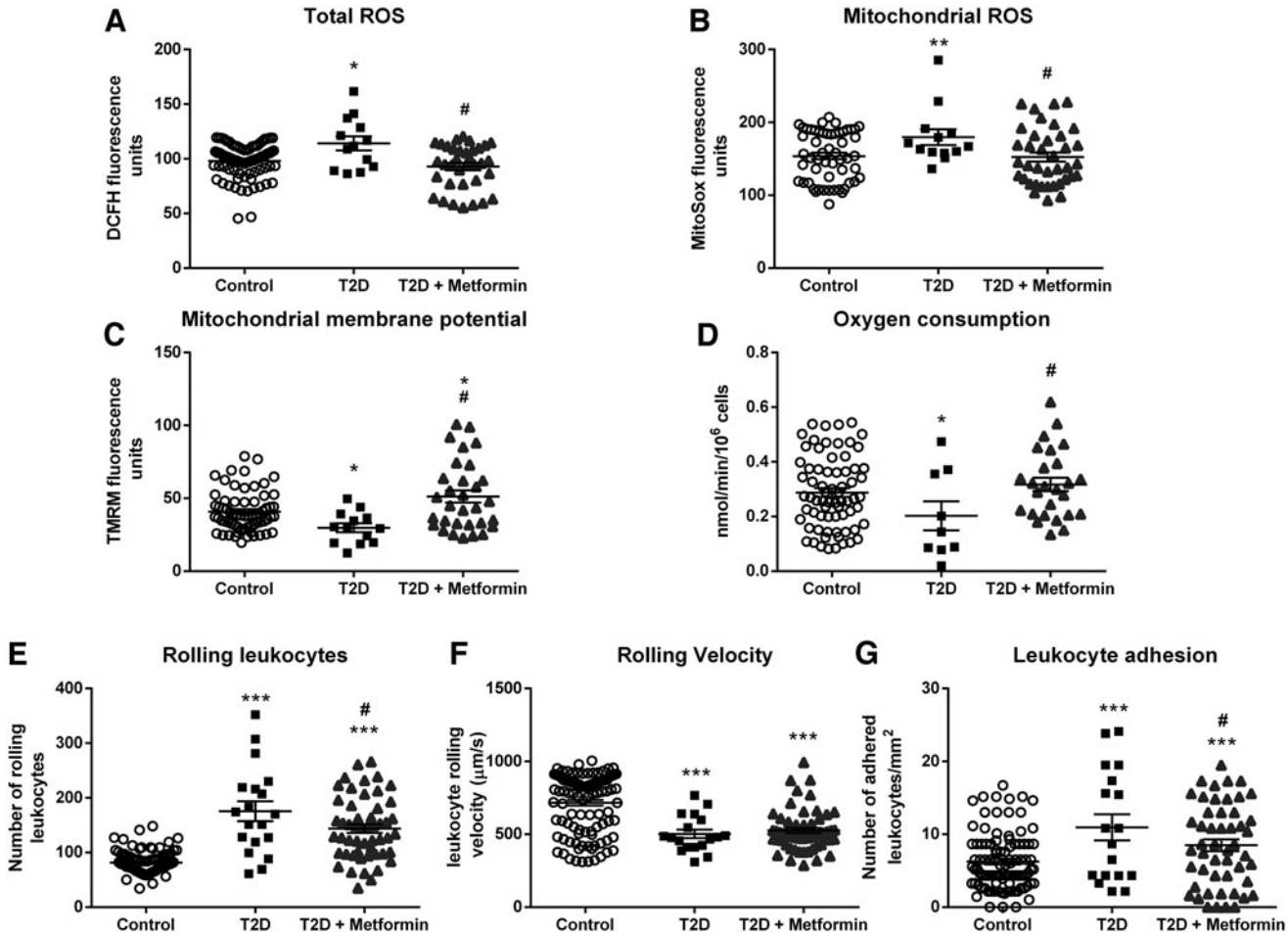

FIG. 1. Mitochondrial ROS production and function parameters and leukocyte/endothelial interaction analysis. (A) Total ROS concentration, measured as relative DCFH fluorescence by static cytometry. **(B)** Mitochondrial ROS concentrations, measured as relative MitoSOX fluorescence by static cytometry. **(C)** Mitochondrial membrane potential, measured as relative TMRM fluorescence by static cytometry. **(D)** O_2 consumption rate of leukocytes, measured by means of a Clark-type oxygen electrode. **(E–G)** Show the three parameters measured in the parallel plate flow chamber experiments. $^{*}p<0.05$, $^{**}p<0.01$, and $^{***}p<0.001$ *versus* control; $^{\#}p<0.05$ *versus* T2D. DCFH, 2′7′-dichlorofluorescein; ROS, reactive oxygen species; T2D, type 2 diabetes; TMRM, tetramethylrhodamine.

($p<0.001$). Metformin treatment reduced leukocyte rolling ($p<0.05$) and adhesion ($p<0.05$), highlighting the anti-inflammatory effect exerted by metformin.

Mitochondrial dynamics

Figure 2 displays how T2D alters mitochondrial dynamics and how metformin treatment modulates it.

The analysis of mRNA expression of fusion genes was diminished in T2D leukocytes (Fig. 2A–E) ($p<0.05$ for *mfn1*, $p<0.001$ for *mfn2*, and $p<0.05$ for *opa1*), and metformin treatment enhanced their expression ($p<0.05$ for *mfn1* and $p<0.01$ for *mfn2*), with the exception of *OPA1* ($p<0.05$ *vs*. control subjects). Furthermore, T2D leukocytes displayed lower levels of fission gene expression than controls ($p<0.01$ for *fis1* and $p<0.001$ for *drp1*). *fis1* expression levels were not modified by metformin treatment ($p<0.05$ *vs*. control subjects), while *drp1* levels returned to normal values ($p<0.001$ *vs*. T2D samples).

Regarding protein expression, mitochondrial fusion (Fig. 2F–J), orchestrated by MFN1, MFN2, and OPA1, was diminished in leukocytes from T2D patients ($p<0.01$, $p<0.05$, and $p<0.01$, respectively). Metformin treatment increased the levels of these proteins significantly ($p<0.05$ in all cases). Furthermore, fission protein FIS1 and DRP1 levels were elevated in T2D leukocytes ($p<0.01$ in both cases), and metformin treatment reversed this increase ($p<0.05$ in both cases), highlighting the beneficial effect of this drug.

Metformin is the gold standard in the management of T2D, thanks mainly to its hypoglycemiant effect (3, 8, 9). Indeed, previous research has shown the remarkable benefits of metformin uptake on some analytical parameters (8). Our T2D patient cohort displayed alterations in classic clinical parameters used to identify the diabetic state; namely, higher weight, BMI, waist circumference, glucose, HbA_{1c}%, SBP, DBP, homeostatic model assessment of insulin resistance (HOMA-IR), and insulin with respect to controls. Metformin treatment reduced glucose and HbA_{1c}%, which is in accordance with the study by van Stee *et al.*

In the case of lipid parameters, T2D patients displayed increased VLDL and triglyceride levels, but reduced cholesterol, HDL, and LDL levels. Research has shown that this

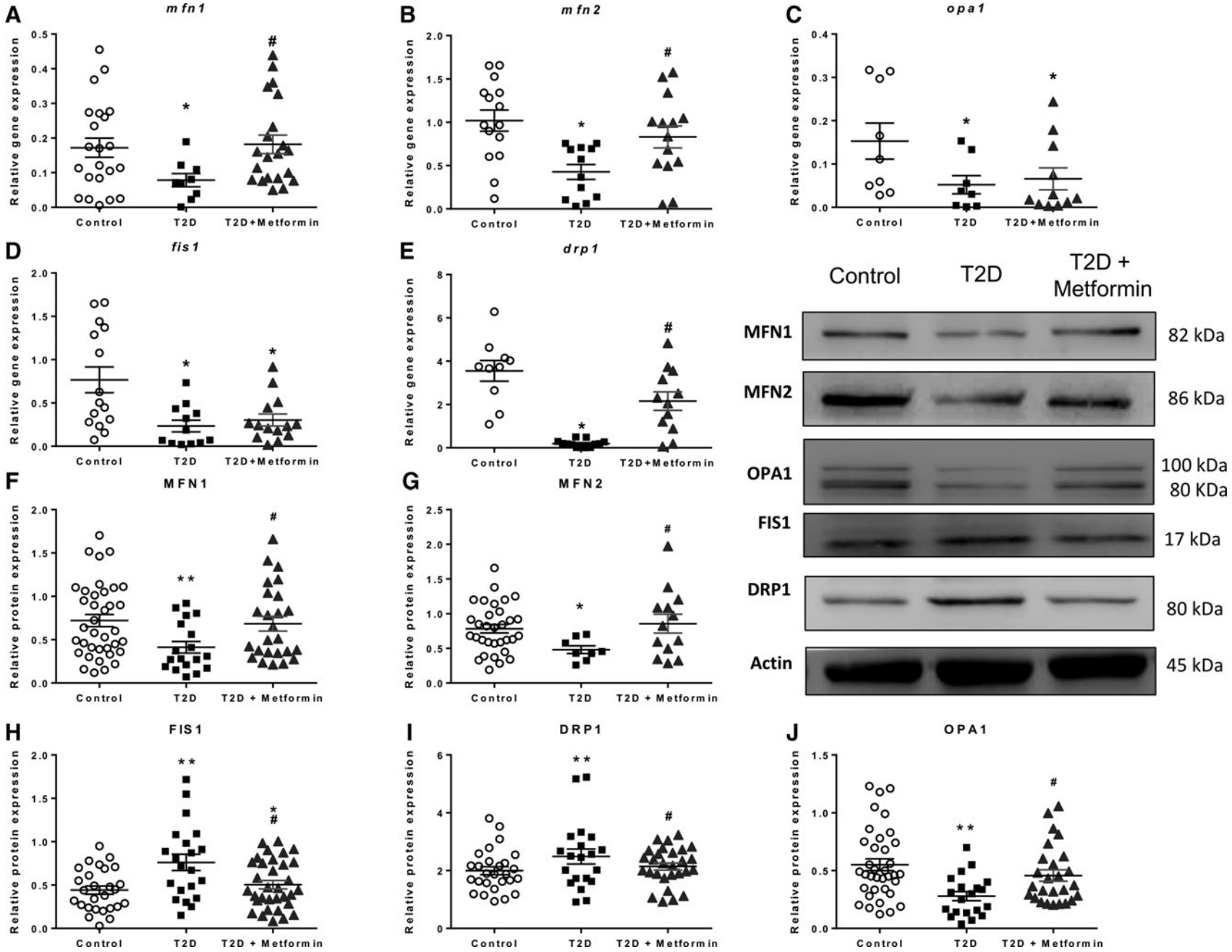

FIG. 2. Fusion and fission gene and protein expression in leukocytes from T2D patients treated (or not) with metformin and from controls. Gene expression in leukocytes from healthy subjects and T2D patients with or without treatment was measured with qRT-PCR. The fusion genes *mfn1* **(A)**, *mfn2* **(B)**, *opa1* **(C)**, *fis1* **(D)**, and *drp1* **(E)** were determined. Protein expression of the corresponding proteins was also measured (fusion proteins MFN1 **(F)**, MFN2 **(G)**, and OPA1 **(J)** and the fission proteins FIS1 **(H)** and DRP1 **(I)**). Representative images of each protein are displayed. In all graphs, *n* (control) = 12, *n* (T2D) = 9, and *n* (T2D + metformin) = 10. $^{*}p < 0.05$ and $^{**}p < 0.01$ *versus* control; $^{\#}p < 0.05$ *versus* T2D. DRP1, dynamin-related protein 1; FIS1, fission protein 1; MFN1, mitofusin 1; MFN2, mitofusin 2; OPA1, optic atrophy 1; qRT-PCR, quantitative real time polymerase chain reaction.

is a result of the hypolipemiant treatment of diabetic dyslipidemia, regardless of whether or not there is metformin treatment (8).

In addition to the biochemical alterations described, we have observed altered mitochondrial function. First, leukocytes from T2D patients expressed increased levels of total and mitochondrial ROS. Although ROS can act as cellular signals, an excess is a signal of cellular stress and can lead to the activation of inflammatory pathways (2). Second, oxygen consumption and mitochondrial potential were altered, suggesting that mitochondrial function was compromised. The loss of membrane potential can be attributed to a leaking mitochondrial membrane, which reduces the electron transport complex's efficiency, thus altering oxygen consumption by leukocytes (4, 7). Such alterations are a sign of mitochondrial dysfunction in T2D leukocytes (1, 7). However, whether it is a cause or a consequence of the pathology of diabetes is still unknown, and future research should address this topic.

In a T2D scenario, the triggers of these mitochondrial alterations are chronic hyperglycemia and hyperlipidemia (2, 7). Therefore, we hypothesized that if metformin can alleviate hyperglycemia, it can also be beneficial for mitochondrial dysfunction. Several previous studies have demonstrated that metformin is beneficial for mitochondrial function and can alleviate the alterations that characterize a diabetic organism. The present study supports this, showing that metformin restores total and mitochondrial reactive oxygen species, mitochondrial membrane potential, and O_2 consumption to control levels.

Mitochondrial dysfunction is closely related to inflammation, as a cause or a consequence (2, 4). Excessive ROS production activates key pathways in inflammation, and reduces the antioxidant capacity of the cell. In immune and endothelial cells, this leads to their overactivation and a nonphysiological activity, both of which contribute to the activation of the endothelial/leukocyte interaction pathway and a subatherosclerotic scenario.

It has previously been reported that altered mitochondrial dynamics increases the endothelial dysfunction in venous endothelial cells from T2D patients and a T2D model of human aortic ring culture (6). Moreover, inhibition of fission has been shown to reduce endothelial impairment, suggesting that mitochondrial dysfunction plays a causative role in T2D. Bearing this in mind, we analyzed the functional repercussions of mitochondrial dysfunction on leukocyte biology in our samples. Our procedure involved us examining leukocyte/endothelial interactions, which were enhanced in T2D patients.

The metformin-treated group displayed less rolling and adhering cells, but velocity remained similar to that in the untreated group. These results suggest that metformin has the capacity to reduce generalized low-grade inflammation. The literature backs our results, confirming that metformin has an anti-inflammatory effect at many different levels (7). The precise mechanism through which the drug acts is yet to be deciphered, although several candidates have been proposed.

Mitochondrial dysfunction involves the deregulation of mitochondrial dynamics. Several *in vitro* and *in vivo* studies have highlighted hampered mitochondrial dynamics in T2D (2, 4, 9). Altogether, T2D seems to promote a profission phenotype and the inhibition of fusion, resulting in the deregulation of mitochondrial dynamics. Conversely, our data show that metformin treatment induces an increase in MFN1, MFN2, and OPA1, and a decrease in FIS1 and DRP1 at the protein level. An increase in mRNA was detected in *mfn1* and *mfn2*, but we did not observe a recovery of *opa-1* mRNA levels in metformin-treated patients, which warrants further research. The inner mitochondrial membrane location of OPA-1 could explain this varying mRNA expression (7).

In the context of these remaining questions, a previous study determined that metformin reduces fission phenotype in diabetic $APOE^{-/-}$ mice and prevents atherosclerotic lesions (9). Based on the present results, we can affirm that metformin restores mitochondrial dynamics in T2D, although we have not identified the exact underlying mechanism. Research to date implicates adenine monophosphate-activated protein kinase (AMPK), which can be effectively activated by metformin (3, 6); whether or not this is the elusive mechanism in question is an object for future research.

Conclusion

In the present study, an improvement in mitochondrial function and dynamics was observed in T2D patients on metformin. Moreover, leukocyte/endothelial cell interactions in the treated subjects were significantly reduced, thus indicating a decrease in inflammation and T2D-related cardiovascular events. Our findings reinforce the idea that metformin plays an important role in modulating the inflammation that occurs in T2D patients. At the same time, it highlights the beneficial effects of this drug, by which it prevents mitochondrial dysfunction and deregulation of mitochondrial dynamics and, in turn, their clinical implications.

Notes

Materials and methods

Subjects. One hundred thirty-five healthy subjects and 120 T2D patients were recruited from the Endocrinology and Nutrition Outpatient's Service of University Hospital Doctor Peset, in Valencia (Spain). Of the 120 T2D patients, 81 had been under 1700 mg/day metformin treatment for at least 1 year. All subjects provided written informed consent to participate in the study. The hospital's Ethics Committee for Clinical Investigation approved the study (ID: 98/19), which was in line with the Helsinki Declaration. T2D was diagnosed following the American Diabetes Association's (ADA) criteria. Exclusion criteria were BMI >35, history of cardiovascular disease, and the presence of autoimmune, infectious, hematological, or malignant disease.

Sample collection and laboratory tests. Subjects attended the Endocrinology Service (Hospital Dr Peset) after 12-h fasting and not having taken any anti-inflammatory drug in the previous 24 h. Peripheral blood was extracted from the brachial vein after measuring blood pressure, weight, height, and waist circumference. Anthropometric parameters were measured as follows: weight and height were measured on a graded scale; SBP and DBP were evaluated with an automatic sphygmomanometer; and waist circumference was evaluated with a measuring tape. BMI was calculated as weight (kg)/(height $(m)^2$.

Insulin was measured with an immunoassay using an Architect Insulin Reagent Kit. Glucose was measured in serum by an automated enzymatic method with a Beckman Synchron LX20 Pro analyzer (Beckman Coulter, Brea, CA). Glycated hemoglobin (HbA_{1c}) was analyzed with an automated Glycohemoglobin analyzer (Arkray, Inc., Kyoto,

Japan). HOMA-IR index was calculated as follows: (Fasting Insulin [μUI/mL] × Fasting Glucose [mg/dL])/405. Cholesterol, HDL, and triglyceride levels were analyzed by means of an enzymatic assay (Beckman Coulter). Friedewald's formula was used to calculate LDL.

Leukocyte isolation. Leukocytes were isolated by means of the Ficoll gradient method. The blood was laid over 7 mL of Ficoll (Hystopaque-1119 Ref. 11191 and Hystopaque-1077 Ref. 10771; both from Sigma-Aldrich, St. Louis, MO) and centrifuged for 25 min at room temperature. Leukocytes were subsequently collected and lysed with erythrocyte lysis buffer (Red Blood Cell Lysis Solution, Ref. 130-096-941; Miltenyi Biotec, Germany) for 5 min. Cells were then washed with Hank's balanced saline solution (HBSS) and stored for future experiments.

Static cytometry assay. Three hundred thousand leukocytes/well were seeded in duplicate in 24-well plates for each sample. An internal control (Hep3b cells) was also seeded at the same density in each plate. After 20 min, when cells were attached to the bottom of the plate, 250 μL tetramethylrhodamine (1 μM) MitoSOX (1 μM), 2′7′dichlorofluorescein (DCFH; 1 μM), and nuclear staining HOECHST 33342 (1 μM), all purchased in Thermo Fisher Scientific, were added to each well and incubated for 20 min at 37°C under gentle shaking. The wells were then washed twice with warm HBSS.

Static cytometry visualization was performed using ScanR software coupled to a IX81 Olympus microscope (both from Olympus Corporation, Shinjuku, Tokyo, Japan). Each experiment was performed in duplicate, with 16 images obtained per well in each experiment and calculating the mean fluorescence intensity. The resulting mean was normalized according to the cell number and internal control.

Oxygen consumption assay. Once leukocytes had been isolated, an aliquot of 5×10^6 cells/mL was placed in a gas-tight chamber. A Clark-Type O_2 electrode (Rank Brothers, Bottisham, United Kingdom) was used to measure O_2 consumption. Sodium cyanide (1 mM), an inhibitor of the electron transport chain, was used to confirm that O_2 consumption was mainly mitochondrial (95%–99%). Duo.18 software (WPI, Stevenage, United Kingdom) was used to visualize and collect the data. The maximal O_2 consumption rate with endogenous substrates was calculated using GraphPad software (GraphPad software, Inc., San Diego, CA). A trypan blue exclusion test was performed after each experiment to determine cell viability, and revealed no significant cell death.

Leukocyte/endothelial interaction assay. An aliquot of 1.2×10^6 leukocytes resuspended in RPMI medium was used for this experiment. Previously, human umbilical cord endothelial cells (HUVECs) isolated from fresh umbilical cords were seeded and grown until a 95% confluent monolayer formed. On the day of the experiment, the leukocyte suspension was perfused over the surface of HUVECs at 0.3 mL/min using a parallel plate flow system, all of which was observed through an inverted microscope. While interacting, cells were recorded with a microscope-coupled camera for 5 min, and, during the last minute, different fields were observed to count the number of adhered leukocytes. The following data were obtained from the videos: number of leukocytes that crossed a 200 μM surface in 1 min (rolling); the time these leukocytes took to cover this distance (rolling velocity); and the number of leukocytes stably adhering to the HUVEC monolayer (adhesion).

Gene and protein expression analysis. To measure gene expression, a GeneAll Ribospin Total RNA extraction kit (GeneAll Biotechnology, Hilden, Germany) was used to isolate RNA from leukocyte samples, following the manufacturers' protocol. We measured gene expression by means of a quantitative real time polymerase chain reaction method (qRT-PCR) using a FastStart universal SYBR Green Master (Sigma Aldrich, St. Louis, MO) and a 7500 Fast RT-PCR system (Life Technologies, Carlsbad, CA). RNA was quantified in a NanoDrop 200c spectrophotometer (Life Technologies, Thermo Fisher Scientific), and purity was confirmed with the 260 nm/280 nm absorbance ratio (A260/280). Next, cDNA was determined with a RevertAid first-strand cDNA synthesis kit (Life Technologies, Thermo Fisher Scientific).

Quantification was performed by means of the comparative $2-\Delta\Delta Ct$ method, and a sample was used as an internal control and *gapdh* expression as an endogenous control in all experiments. Data were analyzed with Expression Suite software (Life Technologies, Thermo Fisher Scientific). Table 2 shows the primers used in the study.

Regarding protein analysis, previously isolated leukocytes were lysed with RIPA buffer, homogenized, and sonicated in an ultrasound bath for 30 s, three times. Samples were then left for 15 min on ice and centrifuged for 15 min at 13,000 rpm at 4°C. The supernatant was collected and quantified following the bicinchoninic acid protein quantification assay (Pierce). Twenty-five micrograms of protein was loaded onto 4%–20% gradient sodium dodecyl sulfate/polyacrylamide gels (Novex Wedge Well 4-20 Tris Glycine Gel, Ref. XP04205B0X; Invitrogen-Life Technology, Carlsbad, CA) and separated at 150 V for 90 min at room temperature. Transference to nitrocellulose membranes (BioRad, CA) was carried out by the wet transference method, running for 60 min at constant amperage (400 mA).

Membranes were then blocked with 5% bovine serum albumin or 5% skimmed milk (depending on the protein of interest) for 1 h at room temperature. Specific antibodies against MFN1, MFN2, OPA1, DRP1, and FIS1 were diluted in blocking buffer. Specific antibody dilutions were incubated with the membranes

Table 2. Forward and Reverse Sequences of the Specific Primers Used in This Study

Target	*Forward*	*Reverse*
Mfn1	CCTCCTCTCCGCCTTTAACT	TATGCTAAGTCTCCGCTCCAAC
Mfn2	CAGCTACACTGGCTCCAACT	TTTCTTGTTCATGGCGGCAA
Opa1	ACCGTTAGCCCTGAGACCATA	GGTAAGTCAACAAGCACCATCC
Fis1	AGAAATTTCAGTCTGAGAAGGCA	CCTCCTTGCTCCCTTTGGG
Drp1	GCTGATGCTTGTGGGCTAATG	TGCCAAAGCACTTGGAACTTT

overnight at 4°C under gentle shaking: rabbit polyclonal anti-MFN1 (Ref. ABC41), rabbit polyclonal anti-MFN2 (Ref. ABC42), mouse monoclonal anti-OPA-1 (Ref. MABN737), rabbit polyclonal anti-FIS-1 (Ref. ABC67), all purchased from Merck-Millipore (Burlington, MA), and mouse monoclonal anti DRP-1 (Ref. GR3248679-1; Abcam, Cambridge, United Kingdom). The following day, specific secondary antibodies (goat anti-rabbit antibody [Ref. PI-1000] from Vector Laboratories, Burlingame, CA, and goat anti-mouse antibody [Ref. 31420] from Thermo Fisher Scientific, Waltham, MA) were incubated for 60 min at room temperature.

Images of the resulting proteins were obtained using Super-Signal West Pico Plus (Ref. 34580) or Femto (Ref. 34095) chemiluminescent substrate (Thermo-Fisher Scientific) and the Fusion FX5 (Vilber Lourmat, Marne-La Vallée, France) imaging system. Densitometric quantification of the images was performed with Bio1D software (Vilber Lourmat). Each membrane was checked several times by cutting different fragments following the guide of the molecular size marker and also with homemade glycine stripping buffer to maximize the results for each sample. Whole-membrane fragments used for the images in Figure 2 are included in Supplementary Figure S1.

Statistical analysis. Normality was confirmed with the Kolmogorov/Smirnov test or the Shapiro/Wilk test depending on the size of the sample. Values are expressed as mean ± SD for normally distributed data, and the median ± (25th–75th percentiles) is presented for non-normally distributed data. One-way analysis of variance with a Tukey *post-hoc* test was used to compare the three groups.

When two groups were compared, a *t*-test was used for normally distributed data, while a Mann/Whitney *U* test was used for non-normal distribution. The influence of sex and BMI was corrected with a covariance analysis (univariate general linear model). Significance was confirmed in all comparisons when $p < 0.05$, with a confidence interval of 95%. SPSS 17.0 (SPSS Statistics, Inc., Chicago, IL) was used in all the tests, and GraphPad (GraphPad, La Jolla, CA) was used to plot the data with bar graphs, representing the media and the standard error of the mean.

Authors' Contributions

Conceptualization: V.M.V. and M.R.; Methodology: A.M.M., Z.A.-J., and F.C.; Resources: A.J., C.M., V.M.V., and M.R.; Data curation: A.M.M., F.C., and V.M.V.; Writing—original draft: A.M.M. and F.C.; Writing—review and editing: V.M.V. and M.R.; Visualization: A.M.M. and Z.A.-J.; Supervision: C.M., V.M.V., and R.M.; Project administration: V.M.V. and M.R.; Funding acquisition: V.M.V. and M.R.

Acknowledgments

The authors thank Brian Normanly (University of Valencia/CIBERehd) for his editorial assistance and Rosa Falcon for her technical assistance.

Funding Information

This study was financed by grants PI19/00838, PI19/0437, and CIBERehd CB06/04/0071 by Carlos III Health Institute and by the European Regional Development Fund (ERDF ''A way to build Europe''); UGP-15-220 by FISABIO; PROMETEO/2019/027 by Ministry of Health of the Valencian Regional Government; and by an unrestricted grant from Menarini. A.M.M. and Z.A.-J. are recipients of PFIS contracts from Carlos III Health Institute (FI17/00126 and FI17/00144, respectively). F.C. is a recipient of a Santiago Grisolía contract from the Valencian Regional Government (GRISOLIAP/2019/091). V.M.V. is a recipient of CES/10/030 contract and M.R. is a recipient of CPII16/00037 contract, both from the Ministry of Health of the Valencian Regional Government and Carlos III Health Institute.

Supplementary Material

Supplementary Figure S1

References

1. Adeshara KA, Bangar NS, Doshi PR, Diwan A, and Tupe RS. Action of metformin therapy against advanced glycation, oxidative stress and inflammation in type 2 diabetes patients: 3 months follow-up study. *Diabetes Metab Syndr* 14: 1449–1458, 2020.
2. Apostolova N, Iannantuoni F, Gruevska A, Muntane J, Rocha M, and Victor VM. Mechanisms of action of metformin in type 2 diabetes: effects on mitochondria and leukocyte-endothelium interactions. *Redox Biol* 34: 101517, 2020.
3. Foretz M, Guigas B, and Viollet B. Understanding the glucoregulatory mechanisms of metformin in type 2 diabetes mellitus. *Nat Rev Endocrinol* 15: 569–589, 2019.
4. Geto Z, Molla MD, Challa F, Belay Y, and Getahun T. Mitochondrial dynamic dysfunction as a main triggering factor for inflammation associated chronic non-communicable diseases. *J Inflamm Res* 13: 97–107, 2020.
5. Pernas L and Scorrano L. Mito-morphosis: mitochondrial fusion, fission, and cristae remodeling as key mediators of cellular function. *Annu Rev Physiol* 78: 505–531, 2016.
6. Shenouda SM, Widlansky ME, Chen K, Xu G, Holbrook M, Tabit CE, Hamburg NM, Frame AA, Caiano TL, Kluge MA, Duess M-A, Levit A, Kim B, Hartman M-L, Joseph L, Shirihai OS, and Vita JA. Altered mitochondrial dynamics contributes to endothelial dysfunction in diabetes mellitus. *Circulation* 124: 444–453, 2011.
7. Sivitz WI and Yorek MA. Mitochondrial dysfunction in diabetes: from Molecular mechanisms to functional significance and therapeutic opportunities. *Antioxid Redox Signal* 12: 537–577, 2010.
8. van Stee MF, de Graaf AA, and Groen AK. Actions of metformin and statins on lipid and glucose metabolism and possible benefit of combination therapy. *Cardiovasc Diabetol* 17: 94, 2018.
9. Wang Q, Zhang M, Torres G, Wu S, Ouyang C, Xie Z, and Zou M-H. Metformin suppresses diabetes-accelerated atherosclerosis via the inhibition of Drp1-mediated mitochondrial fission. *Diabetes* 66: 193–205, 2017.

Address correspondence to:
Dr. Victor M. Victor
Service of Endocrinology and Nutrition
University Hospital Doctor Peset
Foundation for the Promotion of Health and Biomedical Research in the Valencian Region (FISABIO)
Calle Juan de Garay 21
Valencia 46017
Spain

E-mail: victor.victor@uv.es

Dr. Milagros Rocha
Service of Endocrinology and Nutrition
University Hospital Doctor Peset
Foundation for the Promotion of Health and Biomedical Research in the Valencian Region (FISABIO)
Calle Juan de Garay 21
Valencia 46017
Spain

E-mail: milagros.rocha@uv.es

Date of first submission to ARS Central, February 5, 2021; date of acceptance, February 5, 2021.

Abbreviations Used

ADA = American Diabetes Association
AMPK = adenine monophosphate-activated protein kinase
ATP = adenine triphosphate
BMI = body mass index
CT = cholesterol
DBP = diastolic blood pressure
DCFH = 2′7′-dichlorofluorescein
DRP1 = dynamin-related protein 1
ETC = electronic transport complexes
FIS1 = fission protein 1
GTPase = guanylyl triphosphatase
HbA_{1c} = glycated haemoglobin
HBSS = Hank's balanced saline solution
HDL = high-density lipoproteins
HOECHST = 2′-(4-ethoxyphenyl)-5-(4-methyl-1-piperazinyl)-2,5′-bi-1H-benzimidazole
HOMA = homeostatic model assessment
HOMA-IR = homeostatic model assessment of insulin resistance
HUVECs = human umbilical cord endothelial cells
LDL = low-density lipoproteins
MFN1 = mitofusin 1
MFN2 = mitofusin 2
OPA1 = optic atrophy 1
qRT-PCR = quantitative real time polymerase chain reaction method
ROS = reactive oxygen species
SBP = systolic blood pressure
T2D = type 2 diabetes
TMRM = tetramethylrhodamine
VLDL = very low-density lipoproteins

Journal of
Clinical Medicine

MDPI

Article

The Mitochondrial Antioxidant SS-31 Modulates Oxidative Stress, Endoplasmic Reticulum Stress, and Autophagy in Type 2 Diabetes

Irene Escribano-López [1,†], Aranzazu M de Marañon [1,†], Francesca Iannantuoni [1], Sandra López-Domènech [1], Zaida Abad-Jiménez [1], Pedro Díaz [1], Eva Solá [1], Nadezda Apostolova [2], Milagros Rocha [1,2,*] and Víctor M Víctor [1,2,3,*]

1 Service of Endocrinology, University Hospital Doctor Peset, Foundation for the Promotion of Health and Biomedical Research in the Valencian Region (FISABIO), 46017 Valencia, Spain
2 CIBERehd—Department of Pharmacology, University of Valencia, 46010 Valencia, Spain
3 Department of Physiology, University of Valencia, 46010 Valencia, Spain
* Correspondence: milagros.rocha@uv.es (M.R.); victor.victor@uv.es (V.M.V.); Tel.: +34-961-622-757 (M.R. & V.M.V.)
† These authors contributed equally to this work.

Received: 18 July 2019; Accepted: 26 August 2019; Published: 28 August 2019

Abstract: Mitochondrial dysfunction has been shown to play a central role in the pathophysiology of type 2 diabetes (T2D), and mitochondria-targeted agents such as SS-31 are emerging as a promising strategy for its treatment. We aimed to study the effects of SS-31 on leukocytes from T2D patients by evaluating oxidative stress, endoplasmic reticulum (ER) stress and autophagy. Sixty-one T2D patients and 53 controls were included. Anthropometric and analytical measurements were performed. We also assessed reactive oxygen species (ROS) production, calcium content, the expression of ER stress markers GRP78, CHOP, P-eIF2α, and autophagy-related proteins Beclin1, LC3 II/I, and p62 in leukocytes from T2D and control subjects treated or not with SS-31. Furthermore, we have evaluated the action of SS-31 on leukocyte-endothelium interactions. T2D patients exhibited elevated ROS concentration, calcium levels and presence of ER markers (*GRP78* and *CHOP* gene expression, and GRP78 and P-eIF2α protein expression), all of which were reduced by SS-31 treatment. SS-31 also led to a drop in *BECN1* gene expression, and Beclin1 and LC3 II/I protein expression in T2D patients. In contrast, the T2D group displayed reduced p62 protein levels that were restored by SS-31. SS-20 (with non-antioxidant activity) did not change any analyzed parameter. In addition, SS-31 decreased rolling flux and leukocyte adhesion, and increased rolling velocity in T2D patients. Our findings suggest that SS-31 exerts potentially beneficial effects on leukocytes of T2D patients modulating oxidative stress and autophagy, and ameliorating ER stress.

Keywords: Mitochondria; oxidative stress; type 2 diabetes; endoplasmic reticulum stress; autophagy; SS-31

1. Introduction

Type 2 diabetes (T2D) represents a serious global problem with a worryingly high rate worldwide, constituting one of the main public health challenges of the 21st century. T2D is a metabolic disruption characterized by insulin resistance (IR) and β cell failure. In those affected, the persistent exposure to a hyperglycemic environment promotes excessive generation of reactive oxygen species (ROS) and it leads to the imbalance of antioxidant defenses [1], inducing oxidative stress, which contributes to IR and the activation of pro-inflammatory signaling pathways [2], both thought to play key roles in the complications associated with T2D.

Oxidative stress and endoplasmic reticulum (ER) stress are closely linked. Indeed, an altered redox balance has a major impact on ER folding capacity. Under pathological conditions such as T2D, ER homeostasis is disturbed due to an accumulation of misfolded proteins [3,4], in response to which the unfolded protein response (UPR) is activated in order to (i) upregulate the expression of chaperones and aid the folding of ER proteins (ii) and degradation of proteins, and (iii) to prevent protein synthesis [5,6]. It is known that antioxidant production is one of the restorative functions of the UPR, which coordinates the activation of the trans-membrane ER resident protein (PERK) signaling pathway, thus allowing the cell to adapt to oxidative and ER stress [7,8]. The ER stress response also includes mechanisms of autophagy induction, and it has been demonstrated that low-grade autophagy reduces ER stress by destruction of the ubiquitinated unfolded/misfolded dysfunctional proteins and damaged organelles that result from said stress [9]. The onset of autophagy involves the formation of an autophagosome, a process in which several autophagy-related genes coordinate to engulf the defective material in a double membrane. This process is initiated when the complex formed by Beclin1/Vps34/VPs15/UVRAG—known as PI3K complex III—nucleates the formation of the autophagosome. In parallel, the cytosolic protein microtubule-associated to 1B-light chain 3 (LC3 I) is conjugated to a phosphatidylethanolamine to form LC3 II. In this form, LC3 II migrates to the growing autophagosome and helps to build the double membrane. The ubiquitinated protein and defective organelles are detected by sequestosome 1 (SQSTM1)—also known as the p62 protein—which associates itself to membrane-bound LC3 II. The autophagosome then fuses with a lysosome, which pours its hydrolytic enzymes into the inner space of the autophagosome, thereby degrading its content [10,11]. This is usually a rescue mechanism in situations of stress. However, when ER stress is prolonged, the autophagy activated as a result can lead to severe cell damage and, eventually, to apoptosis [12,13]. Incipient insult has serious consequences for the balance of pro- and anti-survival signals. Therefore, the mechanisms of oxidative stress, ER stress and autophagy are closely related to each other and are considered key targets for understanding the development of T2D. In the present work, we have studied these processes by analyzing general markers for their activation.

Mitochondria are essential to the control of cellular homeostasis, cell death and apoptosis. Furthermore, overproduction of ROS occurs mainly in mitochondria, through the electron transport chain [14,15], thus attributing these organelles a key role in the development and control of metabolic diseases such as T2D. For the aforementioned reasons, the identification of novel mitoprotective therapies may lead to the prevention and successful treatment of the complications associated with this disease.

One of the molecules that might be beneficial in mitochondria-based diseases is the mitochondria-targeted antioxidant SS-31 (D-Arg-2′6′-dimethylTyr-Lys-Phe-NH_2), a member of the Szeto–Schiller (SS) peptide family, aromatic-cationic tetrapeptides targeted to cardiolipin on the inner mitochondrial membrane via hydrophobic and electrostatic interactions. There, they increase ATP production, thus restoring cellular function and preserving vital ATP-dependent processes [16–18]. Their antioxidant action is due to two actions, the dimethyltyrosine residue, scavenging H_2O_2 and ONOO- and inhibiting lipid peroxidation. In addition, preclinical studies support their potential use in neurodegenerative disorders and ischaemia-reperfusion injury [19]. Our group has already demonstrated that SS-31 increases SIRT1 levels in leukocytes and ameliorates inflammation, oxidative stress and leukocyte-endothelium interactions in T2D [20].

In the present study, we set out to explore the effects of SS-31 on leukocytes of T2D patients by evaluating different key pathways including oxidative stress, ER stress and autophagy. We have used peripheral blood leukocytes as surrogate model for the general/systemic oxidative stress and its consequences present in T2D. Actually, T2D has been widely related with leukocyte dysfunction [21–25]. Peripheral blood leukocytes are the primary sensors of the alterations in the presence of different soluble molecules in the bloodstream [26–30]. More precisely, we have employed polymorphonuclear cells (PMNs) which present higher vulnerability to oxidative damage in T2D compared to mononuclear cells [21]. Numerous studies suggest that the continuous exposure of leukocytes to high circulating

levels of glucose, lipids, insulin, and proinflammatory cytokines (known as the T2D environment) alters the cell metabolism and affect the cell ability to manage stress situations. These alterations have a direct impact on the leukocytes' function and main pathways such as oxidative stress regulation, ER stress, autophagy, and mitochondrial homeostasis [31–35]. Previous research stated that different molecules, drugs or antioxidants can relieve the stress response [36–39]. Taken into account these facts, we consider that PMNs are a readily available, representative and valid model to evaluate the influence of ROS on the different pathways related to T2D [21].

2. Experimental Section

2.1. Human Subjects

A total of 114 subjects were included in the study population, specifically 61 T2D patients and 53 healthy controls recruited from the Service of Endocrinology and Nutrition of University Hospital Doctor Peset (Valencia, Spain) and adjusted for age and sex. All subjects gave their written informed consent to participate in the study and the protocols followed were approved by our hospital's Ethics Committee for Clinical Investigation (ID: 97/16), in line with the ethical principles of the Helsinki declaration. All T2D patients in this study have suffered from T2D for at least 5 years, which ensures that they display a chronic phenotype.

The American Diabetes Association's criteria were used for T2D diagnosis, and exclusion criteria were history of cardiovascular disease (CVD), presence of morbid obesity or autoimmune, hematological, malignant, infectious, organic, or inflammatory disease, and insulin treatment.

2.2. Sample Collection

Venous blood samples were taken from the antecubital vein and collected in Vacutainer® tubes in fasting conditions, between 8 AM and 10 AM. Anthropometric parameters—weight (kg), height (m), body mass index (BMI; kg/m^2), systolic and diastolic blood pressure (SBP/DBP; mmHg), and waist circumference (cm)—were assessed.

2.3. Laboratory Tests

Fresh blood samples were centrifuged for 10 min at 1500 g at a temperature of 4 °C in order to separate serum from the blood. Serum levels of fasting glucose, total cholesterol and triglycerides were determined by enzymatic method, high-density lipoprotein cholesterol (HDL-c) was recorded employing a Beckman LX-20 autoanalyzer (Beckman Coulter, La Brea, CA, USA) using a direct method, and low-density lipoprotein cholesterol (LDL-c) content was quantified with Friedewald's formula. Insulin levels were obtained by an immunochemiluminescence assay, and HOMA-IR index (fasting insulin (μU/mL) × fasting glucose (mg/dL)/405) was calculated to estimate IR. The percentage of glycated hemoglobin (HbA1c) was determined with an automatic glycohemoglobin analyzer (Arkray, Inc., Kyoto, Japan) and an immunonephelometric assay was used to measure high-sensitive C-reactive protein (hs-CRP) levels.

2.4. Leukocyte Isolation

Human polymorphonuclear leukocytes (PMNs) were isolated from heparinized blood samples incubated for 45 min with 1:2 volumes of dextran solution (3% in NaCl 0.9%; Sigma Aldrich, MO, USA). The supernatant was centrifuged over Fycoll-Hypaque (GE Healthcare, Uppsala, Sweden) at 650 g for 25 min and the pellet lysed to remove the remaining erythrocytes. It was then incubated with lysis buffer (5 min at room temperature) and centrifuged at 240 g. Pellets containing leukocytes were then washed twice and resuspended in Hank's balanced salt solution (HBSS; Sigma Aldrich, MO, USA). A Scepter 2.0 device (Millipore Iberica, Madrid, Spain) was employed for the cell count. The cellular suspension was split into two samples, which were treated under the same conditions with

concentrations that did not affect the cells' viability; one was incubated with SS-31 (100 nM, 30 min), and the other with SS-20 (100 nm, 30 min, without antioxidant activity).

2.5. PMN-Endothelium Interaction Assay

PMNs were isolated as previously described by our group [20]. In this assay, we employed a 1.2 mL aliquot of PMNs obtained from the peripheral blood of control and T2D subjects with a density of 10^6 cells/mL in complete RPMI. Prior to this, primary cultures of human umbilical cord endothelial cells (HUVEC) were established. HUVEC were isolated as previously reported [20]. On the day of the experiment, the PMN aliquot was passed through the endothelial monolayer at a speed of 0.3 mL/min during a 5-min period, which was recorded. Next, the number of rolling PMNs, as well as their velocity and adhesion to the endothelial monolayer were recorded. The number of rolling PMNs was measured as those rolling for 1 min (recorded on video). Velocity was assessed by determining the time in which 15 rolling PMNs covered a distance of 100 micrometers. Adhesion was analyzed by counting the number of PMNs adhering to the endothelium for at least 30 s in 5 fields.

2.6. Quantitative Fluorescence Microscopy

Fluorescence probes 2′,7′-dichlorodihydrofluorescein diacetate (DCFH-DA; 5×10^{-6} mol/L), MitoSOX (5×10^{-6} mol/L) and (acetyloxy)methyl ester (Fluo-4 AM; 1×10^{-6} mol/L) were used to assess total ROS, mitochondrial ROS and calcium levels, respectively. DCFH-DA is routinely used in intact cells, being taken up and deacetylated by endogenous hydrolases to a form (DCFH) that is then oxidized by peroxides to fluorescent 2′,7′-Dichlorofluorescein (DCF). MitoSOX, a mitochondria-targeted dihydroethidium (by addition of a triphenylphosphonium group) is a probe widely used to detect superoxide. To perform these assays, isolated leukocytes were placed in 48-well plates and incubated for 30 min at 37 °C with the appropriate fluorochrome, diluted in phosphate-buffered saline (PBS; Sigma Aldrich, MO, USA). Fluorescence intensity was then recorded with a fluorescence microscope (IX81; Olympus Corporation, Shinjuku-ku, Tokyo, Japan) coupled to the static cytometry software "ScanR" (Olympus). Fluorescence units of these measurements were normalized with respect to the control group, in which the mean fluorescence units were considered 100%, and the data were relativized to that fluorescence value. Experiments were performed in duplicate and 16 images per well were obtained and analyzed obtaining a mean fluorescence value. The mean value of these two replicates of each sample was used for data representation and statistical analysis. Nuclei were detected with Hoechst 33342. All fluorochromes were supplied by Thermo Fisher Scientific, Waltham, MA, USA.

2.7. Flow Cytometry

ROS generation in human leukocytes was analyzed using whole blood by flow cytometry using DCFH-DA (5×10^{-6} mol/L) as marker dye. The distribution of different leukocyte subsets was analyzed in peripheral blood using a single staining (CD45), no-lyse no-wash method. CD45 positive cells (marked with the fluorescent probe APC Mouse Anti-Human CD45, BD Biosciences, San Jose, CA, USA) and the morphological characteristics of the cells (FSC and SSC parameters) were used for determining the PMNs cellular subset as shown in previous work [40,41]. Briefly, 200 µL of heparinized blood were incubated with 4 µL of CD45 monoclonal antibody for 20 min at room temperature in darkness, in the presence and absence of several treatments. For this assay, 500 µL of stained blood diluted 20-fold in PBS was incubated for 30 min at 37 °C with the fluorochrome DCFH-DA. Samples were acquired for 10,000 individual cells by BD Accuri™ C6 Plus Flow Cytometer (BD Biosciences, San Jose, CA, USA) and ROS production was quantified by median fluorescence intensities.

2.8. Western Blotting (WB)

Leukocyte pellets were homogenized and incubated on ice in cell lysis buffer for 15 min (10 mM HEPES pH 7.5, 10 mM NaCl, 2 mM $MgCl_2$, 1 mM EDTA, 1 mM EGTA, 0.5% Nonidet P-40, 1 mM DTT, 'Complete Mini' and 'Pefabloc' protease inhibitor cocktail from Roche Diagnostics and phosphatase inhibitor mixture: 10 mM NaF and 0.1 mM Na_3VO_4); tubes were vortexed to disrupt the cell membranes and centrifuged at 4 °C for 10 min. The supernatants were stored at −70 °C till further use as cytoplasmic extracts. The pelleted nuclei were resuspended in the nuclear extraction buffer (25 mM HEPES pH 7.5, 500 mM NaCl, 9 % glycerol (v/v), 5 mM $MgCl_2$, 0.5 % Nonidet P-40, 1 mM DTT) supplemented with protease inhibitors ('Complete Mini' protease inhibitor cocktail, and 'Pefabloc', both from Roche Diagnostics) and 10 mM NaF as a phosphatase inhibitor, and were incubated on ice for 10 min under sonication. Nuclear extracts were collected by centrifugation for 10 min at 4 °C, and were either immediately used or stored at −70 °C. Protein concentration was determined with a BCA protein assay kit (Thermo Fisher Scientific, Waltham, MA, USA). Next, 25 µg proteins per sample were loaded onto SDS-polyacrilamide gels. Gel electrophoresis was performed at 120 V, 90 min, followed by transfer to nitrocellulose membranes (Bio-Rad, Hercules, CA, USA) at 400 mA, for 1 h. After blocking at RT for 1 h in 5% non-fat milk in TBST buffer containing 25 mM Tris, 150 mM sodium chloride and 0.1% Tween20, at pH 7.5, membranes were incubated overnight at 4 °C with anti-glucose-regulated protein 78 kDa (GRP78) rabbit polyclonal antibody (Abcam, Cambridge, UK), anti-phosphorylated eukaryotic translation initiation factor 2, subunit 1 alpha (eIF2α-pS52) rabbit polyclonal antibody (Life Technologies, Carlsbad, CA USA), anti-Beclin1 (BECN1) rabbit polyclonal antibody (Abcam, Cambridge, UK), anti-light chain 3 (LC3) rabbit polyclonal antibody (Millipore Iberica, Madrid, Spain), anti-sequestosome 1 (SQSTM1/p62) mouse monoclonal antibody (Abnova, Taipei, Taiwan) or anti-Actin rabbit polyclonal antibody (Sigma Aldrich, St Louis, MO, USA), followed by horseradish peroxidase (HRP) goat anti-rabbit (Millipore Iberica, Madrid, Spain) or HRP goat anti-mouse (Thermo Fisher Scientific, Waltham, MA, USA) secondary antibodies as appropriate, for 1 h at RT. Protein expression was assessed with ECL plus reagent (GE Healthcare, Amersham Place, Litte Chalfont, UK) or Supersignal West Femto (Thermo Fisher Scientific, Waltham, MA, USA). A Fusion FX5 acquisition system (Vilbert Lourmat, Marne La Vallée, France) was employed for chemiluminescence signal detection, which was analyzed by densitometry using Bio1D software (Vilbert Lourmat, Marne La Vallée, France). For quantification of the expression level of the studied protein, an internal control was included in each blot and the expression was normalized to that of actin in the same sample.

2.9. Quantitative RT-PCR (qRT-PCR)

Total RNA was isolated from leukocytes with the GeneAll® Ribospin™ kit following the manufacturer's instructions (GeneAll Biotechnology, Hilden, Germany). RNA concentrations were measured using Nanodrop 2000c (Thermo Fisher Scientific, Waltham, MA, USA), and 1 µg of the extracted RNA was employed in the following steps. To detect the expression of genes involved in autophagy and ER stress, the RevertAid First Strand c-DNA Synthesis kit (Thermo Fisher Scientific) and KAPA SYBR FAST universal master mix (Applied Biosystems-Thermo Fisher Scientific, Walthman, MA, USA) were used. RT-qPCR analysis was performed with a 7500 Fast real-time PCR system (Life Technologies, Carlsbad, CA, USA) (Table 1). Fold changes were calculated by the $2^{-\Delta\Delta Ct}$ method through Expression Suite software (Life Technologies) and relative gene expression of *GRP78, DDIT3/CHOP* (CCAAT/enhancer-binding protein (C/EBP) homologous protein), *BECN1* and *SQSTM/p62* was calculated using *GAPDH* as a housekeeping control.

Table 1. Protocol details and primer sequences.

qRT-PCR Protocol				
Temperature	95 °C	95 °C	60 °C	Melting
Time	10 min	10 s	30 s	Curve
No. of Cycles	1	40		
Primers				
Target	**Direction**	**Sequence (5′–3′)**		
BECN1	Forward	CCCCAGAACAGTATAACGGCA		
	Reverse	AGACTGTGTTGCTGCTCCAT		
GRP78	Forward	AAGAACCAGCTCACCTCCAACCC		
	Reverse	TTCAACCACCTTGAACGGCAA		
DDIT3/CHOP	Forward	AGAACCAGGAAACGGAAACAGA		
	Reverse	TCTCCTTCATGCGCTGCTTT		
GAPDH	Forward	CGCATCTTCTTTTGCGTCG		
	Reverse	TTGAGGTCAATGAAGGGGTCA		
SQSTM/P62	Forward	GATTCGCCGCTTCAGCTTCTG		
	Reverse	CTGGAAAAGGCAACCAAGTCC		

2.10. Statistical Analysis

All data were analyzed with SPSS 17.0 software (SPSS Statistics Inc., Chicago, IL, USA). Values are expressed as mean and standard deviation (SD) for parametric data; while the median (25th–75th percentiles) is presented for non-parametric data. Bar graphs show mean and standard error of the mean (SEM) in the figures.

In the case of the variables with normally distributed data, groups were compared with a Student's *t*-test, while a Mann–Whitney *U* test was employed for non-normally distributed ones, and the chi-square test for proportion of frequencies. To examine the main effects of the treatment, the study groups were compared with one-way analysis of variance (ANOVA) followed by a Newman–Keuls post hoc test. In addition, the prominent influence of BMI was reduced by means of an analysis of covariance with a univariate general linear model. Differences were considered to be significant when $p < 0.05$, applying a confidence interval of 95% in every comparison. Graphs were plotted with GraphPad Prism 4.0 (GraphPad, La Jolla, CA, USA).

3. Results

3.1. Clinical and Endocrine Parameters

Our study was carried out in a population of 53 healthy volunteers (mean age 51.7 ± 9.3) and 61 T2D patients (mean age 55.1 ± 10.2), both of which groups had a similar gender distribution. The results of the anthropometric and analytical evaluations are shown in Table 2. As expected, an altered carbohydrate metabolism was observed in T2D patients in comparison with the control group, with glucose, HOMA-IR and HbA1c being significantly higher ($p < 0.001$). Moreover, the T2D group showed higher values for upper waist circumference ($p < 0.01$), SBP, weight, BMI, insulin and hs-CRP levels ($p < 0.001$) than control subjects. Regarding lipid profile, a higher triglyceride concentration ($p < 0.01$) and lower HDL-c ($p < 0.001$) were characteristics of the T2D patients. However, due to lipid-lowering medication received, total cholesterol and LDL-c levels were lower in the diabetic group than in healthy controls ($p < 0.001$) (56.9% were taking statins, 10.3% fibrates, and 3.4% ezetimibe). Given that BMI was significantly different in T2D patients, data were adjusted for this variable, but statistical differences remained similar.

Table 2. Anthropometric and analytical parameters.

	Control	Type 2 Diabetes	*p*-Value	BMI-Adjusted *p*-Value
N	53	61	-	-
Male (%)	47.2	52.5	ns	ns
Age (years)	51.7 ± 9.3	55.1 ± 10.2	ns	ns
Weight (Kg)	72.9 ± 18.8	85.6 ± 15.5	$p < 0.001$	$p < 0.001$
BMI (kg/m^2)	25.8 ± 5.4	31.4 ± 5.6	$p < 0.001$	-
Waist circumference (cm)	85.8 ± 13.2	104.0 ± 11.9	$p < 0.001$	$p < 0.01$
SBP (mmHg)	23.3 ± 19.7	145.8 ± 14.8	$p < 0.001$	$p < 0.001$
DBP (mmHg)	73.6 ± 10.9	74.2 ± 25.6	ns	ns
Glucose (mg/dL)	95.6 ± 13.6	154.0 ± 49.8	$p < 0.001$	$p < 0.001$
Insulin (μUI/mL)	7.56 ± 3.55	16.27 ± 9.09	$p < 0.001$	$p < 0.01$
HOMA-IR	1.71 ± 0.95	6.23 ± 4.64	$p < 0.001$	$p < 0.001$
HbA1c (%)	5.32 ± 0.36	7.42 ± 1.57	$p < 0.001$	$p < 0.001$
Total cholesterol (mg/dL)	198.8 ± 35.5	168.0 ± 37.7	$p < 0.001$	$p < 0.001$
HDL-c (mg/dL)	57.3 ± 19.9	43.1 ± 9.2	$p < 0.001$	$p < 0.001$
LDL-c (mg/dL)	122.1 ± 28.9	93.7 ± 30.6	$p < 0.001$	$p < 0.001$
Triglycerides (mg/dL)	93.0 (26.5–150.5)	133.0 (94.0–170.0)	$p < 0.01$	$p < 0.01$
hs-CRP (mg/L)	1.17 (0.46–2.40)	2.92 (1.88–6.39)	$p < 0.001$	$p < 0.001$

Data are shown as mean ± SD and were compared by a Student's *t* test for parametric variables, while they are shown as median and were compared by a Mann–Whitney *U* test (25th and 75th percentiles) for non-parametric variables. A univariate general linear model was used to adjust changes for BMI. A Chi-Square test was used to compare proportions among groups. ns: not significant.

3.2. Leukocyte Function

For assessing the influence of T2D and SS-31 treatment on one of the main functions of PMN, which is interaction with the endothelial monolayer, we performed a parallel plate flux chamber assay. As stated in methods, PMN were perfused through a monolayer of confluent endothelial cells for assessing those interactions. As shown in Figure S1, T2D enhanced the flux of leukocytes (Figure S1A), reduced its velocity (Figure S1B) which allowed them to adhere more to the endothelial monolayer (Figure S1C). When treated with SS-31, those interactions were significantly reduced. This result shows that leukocyte function is positively affected by SS-31 in T2D PMN. SS-20 did not alter those parameters in any of the analyzed samples.

3.3. Oxidative Stress: ROS Production

Total (DCFH-DA fluorescence) and mitochondrial (MitoSOX fluorescence) ROS were considerably increased in leukocytes of T2D patients in comparison with control subjects (Figure 1A,B; $p < 0.001$), and these effects were reversed by SS-31 (Figure 1A,B; $p < 0.001$, $p < 0.01$ respectively) in leukocytes of T2D patients, while no differences were observed in controls. The SS-20 compound did not alter these oxidative stress parameters. The specificity of the observed response was corroborated by cytometry analysis of the effect of a positive control, rotenone, a well-known inhibitor of Complex I of the electron transport chain whose action induces mitochondrial superoxide production [42]. Incubation with whole blood from control subjects with rotenone (50 μM, 20 min) led to a major increase in total cellular ROS (detected by DCFH-DA) and this effect was reversed with the treatment of both SS-31 and catalase (Figure 1D; $p < 0.05$). Thus, our data show that SS-31 exerts an antioxidant action by reducing total and mitochondrial ROS production.

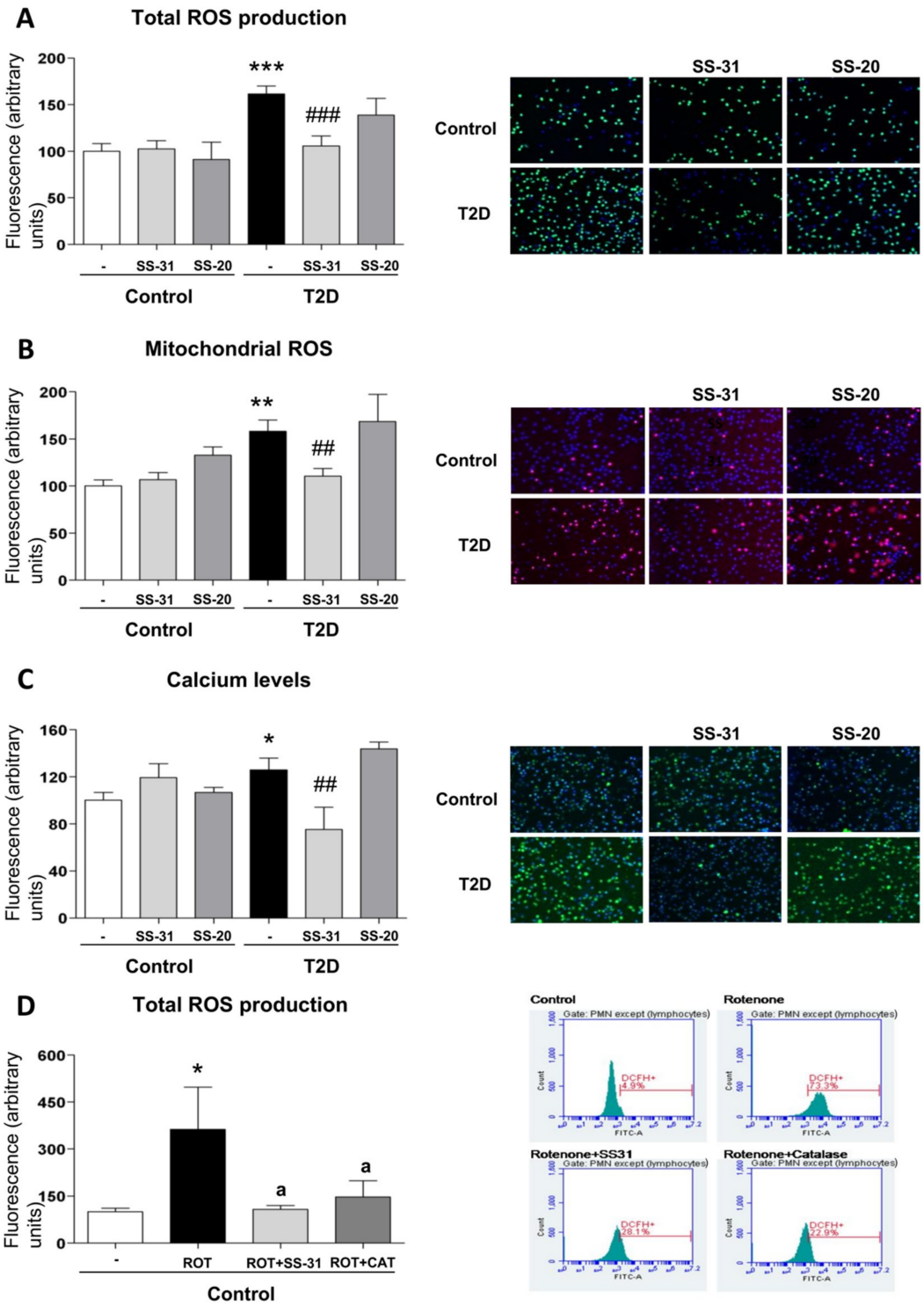

Figure 1. Effects of Szeto–Schiller (SS)-31 (30 min, 100 nM) on total and mitochondrial ROS production, and calcium levels in leukocytes from type 2 diabetes (T2D) patients and healthy subjects. (**A**) reactive oxygen species (ROS) production, measured as deacetylated by endogenous hydrolases to a form (DCFH)-DA fluorescence. (**B**) Mitochondrial ROS production, assessed as MitoSOX fluorescence. (**C**) Calcium levels, determined as Fluo-4 fluorescence. Representative fluorescence microscopy images are also shown. (**D**) Analysis of total ROS levels, measured as DCFH-DA fluorescence in leukocytes from healthy subjects upon a positive control treatment (rotenone, ROT) in the presence or absence of SS-31 or catalase (CAT) and representative cytograms of the 4 groups stained with APC-CD45 and DCFH-DA. 10,000 cells were analyzed in each experiment. $n = 6$. * $p < 0.05$, ** $p < 0.01$ and *** $p < 0.001$ with regard to control group; $^{\#\#}$ $p < 0.01$ $^{\#\#\#}$ $p < 0.001$ vs. non-treated T2D group; ^{a} $p < 0.05$ vs. rotenone treatment.

3.4. Calcium Levels

In the T2D study population, intracellular calcium content—measured as Fluo4-AM fluorescence—was higher than in the control group (Figure 1C; $p < 0.05$), while under treatment with SS-31, calcium levels in T2D patients reached similar values to those in healthy subjects (Figure 1C; $p < 0.01$). The marked decrease of calcium content in the SS-31-treated T2D group in comparison with healthy volunteers may indicate an attenuation of ER stress in these patients given the fact that ER stress is often related to an increase in cytosolic calcium content SS-20 treatment did not modify calcium content in any condition.

3.5. Regulation of UPR Signalling

ER stress markers were determined in order to analyze UPR activation in leukocytes from T2D patients and control subjects. A higher peak in *GRP78* expression was observed in the T2D vs. control group (Figure 2A; $p < 0.05$); similarly, *DDIT3/CHOP* expression was augmented in T2D patients (Figure 2B; $p < 0.05$). Interestingly, SS-31 treatment reduced mRNA levels of both genes in leukocytes from T2D patients (Figure 2A,B; $p < 0.05$). Furthermore, the treatment with the mitochondria-targeted antioxidant SS-31 had no effect about protein levels of GRP78 and P-eIF2α on leukocytes of control subjects (Figure 2C,D) while a reduction in these ER stress parameters was observed in leukocytes from T2D patients with T2D (Figure 2C,D; $p < 0.05$). None of these markers were altered by treatment with SS-20.

These findings suggest that SS-31 can attenuate ER stress in the leukocytes of T2D patients.

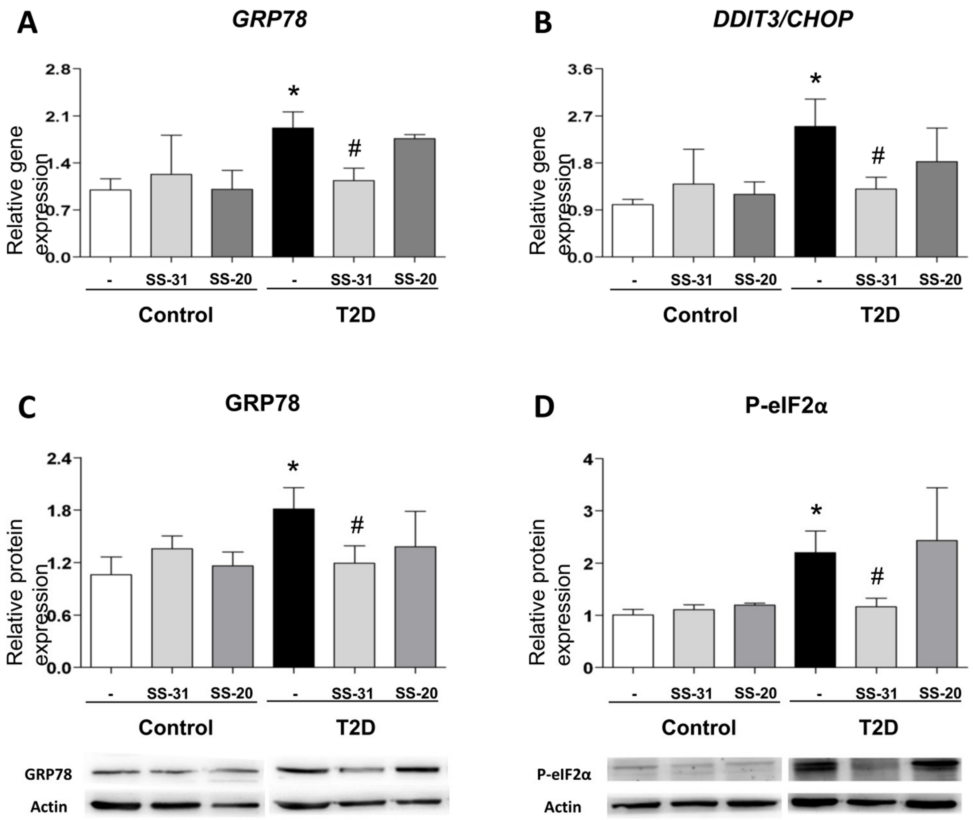

Figure 2. Evaluation of endoplasmic reticulum (ER) stress parameters in leukocytes from T2D patients and controls in the absence and presence of SS-31 (30 min, 100 nM) (**A**) *GRP78* expression. (**B**) *DDIT3/CHOP* expression. (**C**) GRP78 protein levels and representative western blotting (WB) images. (**D**) P-eIF2α protein levels and representative WB images. * $p < 0.05$ with regard to control group # $p < 0.05$ vs. non-treated T2D group.

3.6. Autophagy Assessment

BECN1 gene expression were enhanced in leukocytes from T2D patients with respect to those of healthy controls (Figure 3A; $p < 0.05$), a trend that was reversed by treatment with SS-31 (Figure 3A; $p < 0.05$). In leukocytes from T2D patients treated with SS-31, this trend was also accompanied by a significant reduction of protein expression of distinct markers of autophagy such as Beclin1 and the ratio of LC3 II/I (Figure 3B,C; $p < 0.05$). p62 protein level was significantly lower in leukocytes from diabetic patients compared to controls, however its mRNA levels were more abundant in T2M patients which is indicative of enhanced autophagy. Treatment of leukocytes from T2D patients with SS-31 reversed the protein level of p62 (Figure 3D; $p < 0.05$), while no changes were seen in the gene expression of *SQSTM1/p62* suggesting that SS-31 can modify autophagy at protein level. On the other hand, no significant differences were observed in control group or with SS-20 treatment.

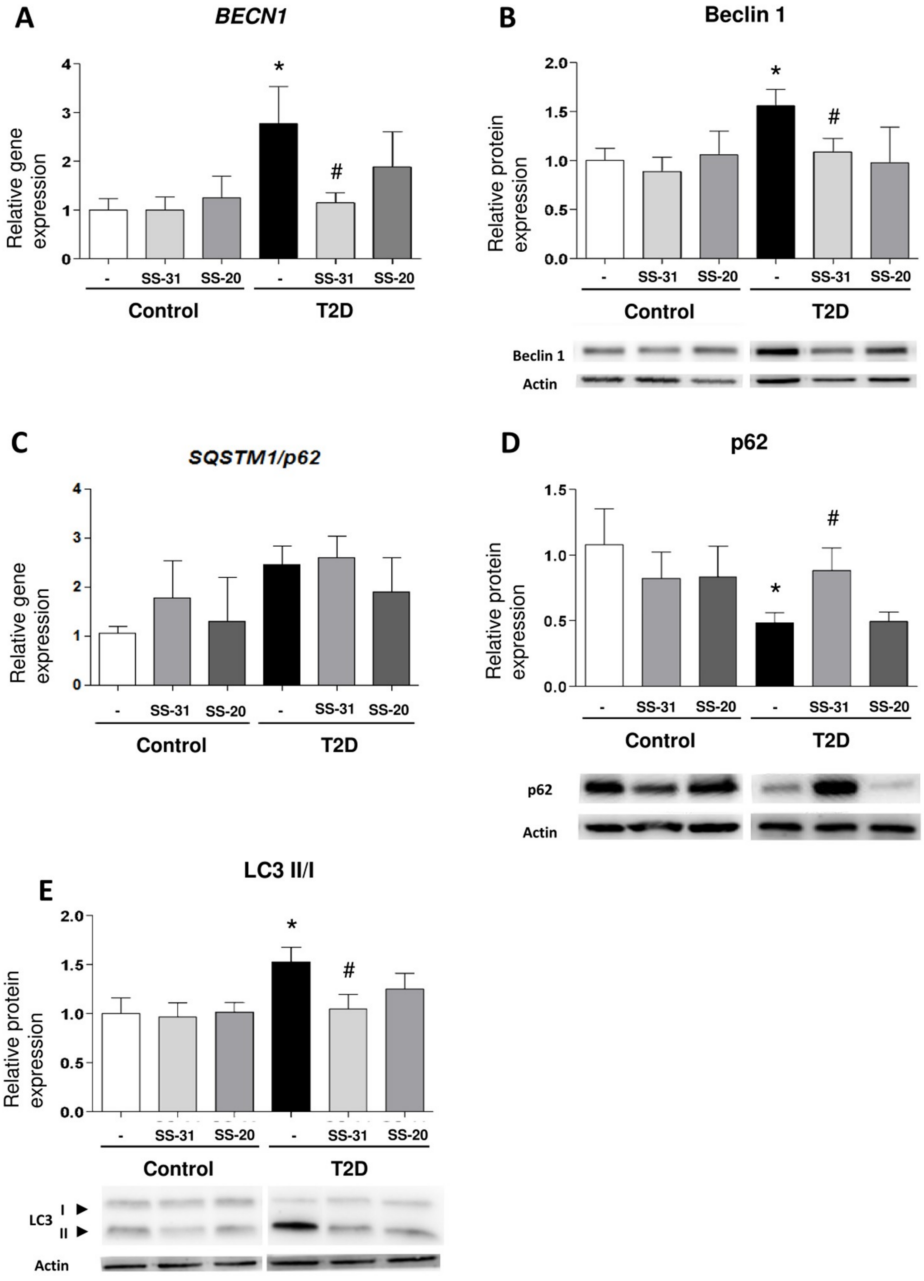

Figure 3. Study of autophagy-related parameters in leukocytes from control subjects and T2D patients

in the presence and absence of SS-31 (30 min, 100 nM). (**A**) *BECN1* expression. (**B**) Beclin 1 protein expression and representative WB images. (**C**) *SQSTM1/p62* expression (**D**) p62 protein expression and representative WB images (**E**) LC3 II/I ratio of protein expression and representative WB images. * $p < 0.05$ with regard to control group, # $p < 0.05$ vs. non-treated T2D group.

These results provide some evidence that the mitochondria-targeted antioxidant SS-31 reduces parameters of autophagy in leukocytes from T2D patients.

3.7. Analysis of Pharmacologically Induced ER Stress and Autophagy

Given that leukocytes from T2D display markers of ER stress and activated autophagy, and the observation that both effects can be alleviated with SS-31 treatment, we set to explore the connection between these processes. For this, we evaluated the capacity of SS-31 to interfere with pharmacologically induced ER stress (thapsigargin) and autophagy (rapamycin). Treatment with thapsigargin (1 μM, 20 min) produced a significant increase in the protein content of P-eIF2α and a slight increase in GRP78, however these effects were not impaired if cells were co-treated with SS-31 (Figure 4A,B). The sesquiterpene alkaloid thapsigargin, a highly selective inhibitor of sarcoplasmic/endoplasmic reticulum Ca^{2+} ATPase (SERCA) prevents Ca^{2+} transport into the ER lumen, which leads to its subsequent increase in the cytosol, and promotes accumulation of unfolded proteins and perturbation of intracellular Ca^{2+} homeostasis [42]. On the contrary, SS-31 was able to prevent the increase in GRP78 protein content when it was induced by the mitochondrial inhibitor rotenone (Figure 4A), a finding that reinforces the ability of SS-31 to act as an antioxidant. Regarding autophagy, as expected, leukocytes from healthy subjects exposed to the pharmacological inducer rapamycin (0.5 μM, 30 min) displayed enhanced autophagy as evidenced by the incremented Beclin1 and LC3 II levels (Figure 4C,D), and the diminished p62 protein content (Figure 4E). Rapamycin inhibits the mTOR complex, a central negative regulator of autophagy in the mammalian cell, thus triggering a strong autophagic response [42,43]. Importantly, SS-31 treatment had no effect on these alterations (Figure 4C–E), a finding that once more underscores the specificity of SS-31 action in the complex metabolic disturbances in leukocytes of T2D patients. We also evaluated autophagy induction in the cells exposed to rotenone and observed no increase in Beclin1 and LC3 II levels. The protein levels of p62 were diminished; however, given the lack of changes in the LC3 II/I ratio the effect may be evidence of an autophagy-independent regulation.

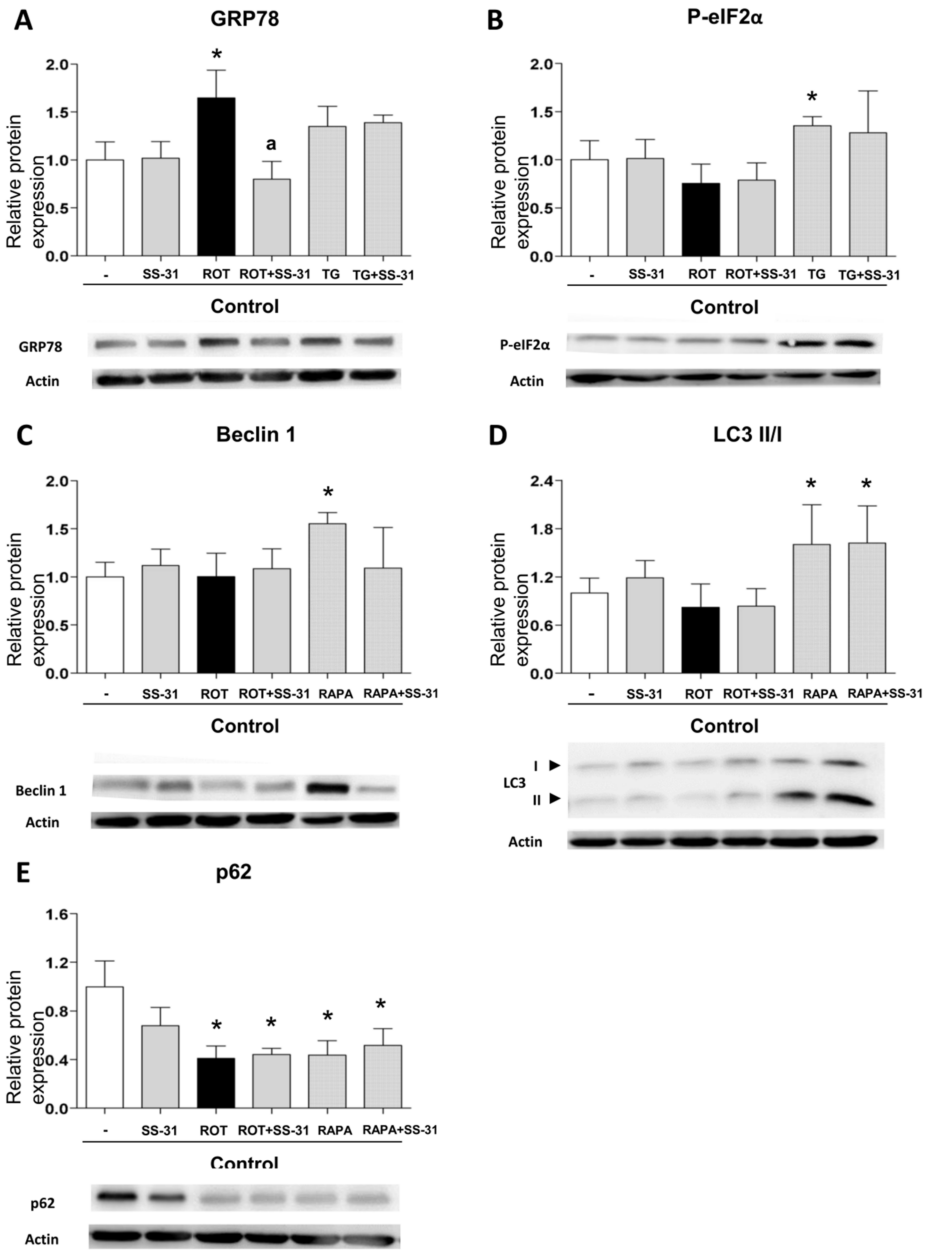

Figure 4. Study of the expression of protein markers of ER stress and autophagy, induced pharmacologically in leukocytes from healthy controls, in the presence and absence of SS-31 (30 min, 100 nM). (**A**) GRP78, (**B**) P-eIF2α, (**C**) Beclin1, (**D**) LC3 II/I ratio, and (**E**) p62. Representative WB images are also shown. * $p < 0.05$ with regard to control group; [a] $p < 0.05$ vs. rotenone-treated group. $n = 6$. ROT, rotenone (50 μM, 20 min); TG, thapsigargin (1 μM, 20 min); RAPA, rapamycin (0.5 μM, 30 min).

4. Discussion

Based on renewed concepts of T2D pathogenesis, the targets of a potential therapy for this chronic progressive disease include, not only glucose homeostasis correction, but also modulation of cellular stress and mitochondrial function in highly metabolic tissues, with the aim of attenuating insulin resistance and low-grade inflammation and ameliorating β cell function and mass, thus preventing the development of macro- and microvascular complications.

In this sense, the mitochondrial antioxidant SS-31 has been described to exert protective effects in several disease models. Indeed, SS-31 has previously been reported to attenuate renal injury in diabetic nephropathy through an antioxidant effect [44]. Furthermore, Zhu et al. have demonstrated

that SS-31 attenuates the severity of lung damage by modulating mitochondrial dysfunction in a mouse model of spinal cord injury [45]. However, the exact pathophysiological mechanism involved in the protective effects of SS-31 on leukocytes in T2D is not fully understood. For this reason, the present study was designed to evaluate whether SS-31 can modulate oxidative stress, ER stress and autophagy in leukocytes of T2D patients, three important pathways involved in the development of T2D.

The pathophysiology of T2D is associated with an impairment of β cell function and, consequently, IR, a hallmark of this disease [46]. Nevertheless, whether cell failure is a primary cause of T2D or secondary to associated long-term metabolic abnormalities is yet to be confirmed, though increased oxidative stress, ER stress and autophagy are thought to be involved [47]. In fact, previous studies have suggested that alterations in $\Delta\Psi_m$ disturb mitochondrial dynamics, eventually promoting a failure in glucose-stimulated insulin secretion [48]. Moreover, our group has previously demonstrated oxidative stress and mitochondrial dysfunction in leukocytes from T2D patients [49]. In this sense, SS-peptides can scavenge ROS, and these molecules have been shown to exert beneficial effects against mitochondrial dysfunction [19,50]. SS-31 protects mitochondria against oxidative damage by accumulating in the inner mitochondrial membrane, a location close to the site of ROS production. In fact, after crossing the mitochondrial outer membrane, SS-31 associates with cardiolipin, an anionic phospholipid expressed exclusively in the inner mitochondrial membrane. Furthermore, SS-31 seems to protect cristae architecture by alleviating mitochondrial oxidative stress and preventing cytochrome c peroxidase activity [17,19].

In the present study, we have found that the leukocytes of T2D patients have functional alterations compared to those of control individuals, as shown in Figure S1. SS-31 is able to rescue the parameters of leucocyte–endothelial interactions which confirms that SS-31 can modulate leukocyte function. The fact that the effects can be ameliorated with SS-31 but not with SS-20 shows that the alterations of the leukocyte function in T2D leukocytes can be due to the high levels of total and mitochondrial ROS levels compared to controls. Fluorescent probes are widely used for ROS detection in biological systems; DCFH–DA has been suggested as a relatively specific probe for H_2O_2, while dihydroethidium seems to be more suitable for superoxide. However, abundant evidence over the past years has shown that all fluorescent probes for ROS detection suffer a lack of selectivity given that they react with various types of ROS, and therefore in living cells or tissues they are generally used for detecting total oxidative activity. In order to reaffirm our findings, we have employed two fluorescent probes and verified the specificity of the detection by studying a positive control of mitochondrial ROS generation, rotenone.

One of the leading hypotheses regarding the onset of IR is that enhanced ROS production triggers ER stress, which leads to activation of the UPR. In relation to this, ER stress is considered a target mechanism under IR conditions. An association between IR and mitochondrial abnormalities, such as lower numbers of mitochondria, reduction in mitochondrial oxidative enzyme activity or mitochondrial dysfunction, have been reported in human studies [51,52]. Furthermore, it has been described that ER stress is related to apoptosis in leukocytes from T2D patients [53]. In addition, a study by Sage et al. demonstrated that levels of ER stress markers such as GRP78, sXBP1 and CHOP correlated positively with glucose levels in leukocytes from patients with metabolic syndrome [54]. In line with such data, we have shown in previous studies that leukocytes from T2D patients exhibit increased ER stress markers which display enhanced GRP78, P-eIF2α and ATF6 protein levels [35]. Interestingly, the present study shows that SS-31 treatment in leukocytes from T2D patients reduces GRP78 and P-eIF2α protein levels, and *GRP78* and *CHOP* mRNA levels, suggesting that this molecule could promote the restoration of cell homeostasis to battle ER stress. The reduction of intracellular calcium levels under treatment with SS-31 described in the present study could also be indicative of lower ER stress compared to untreated T2D leukocytes, but these data need to be considered with caution given that with our methodology we cannot determine the subcellular source of increased calcium. This idea is further enforced by the fact that SS-31 did not alleviate ER stress triggered by other types of stimuli such as thapsigargin, an ER stressor with a direct effect on ER calcium homeostasis.

ER stress can also induce autophagy, and in this sense Gonzalez et al. have described that cleavage and lipidation of microtubule-associated protein LC3 I into LC3 II is mediated by the phosphorylation of PERK/eIF2α [55]. Importantly, we have previously demonstrated in leukocytes from T2D patients that UPR activation occurs in parallel with autophagy [35]. The present study describes an increase in Beclin1 and LC3-II levels in T2D patients compared to controls which is indicative of increased generation of autophagosomes. As this occurs concomitantly with a decrease in p62 protein levels, we believe that it may suggest an increase in the autophagic clearance. Nevertheless, the results presented are not sufficient as to state that autophagy is not only induced but also active/functional in T2D patients.

The expression levels of autophagy-related parameters are significantly decreased in leukocytes of T2D patients under SS-31 therapy. In contrast, p62 protein expression, which is involved in aggresome formation and is itself degraded through autophagy, was increased in leukocytes from T2D patients by addition of SS-31. Of note, this was not due to changes in the gene expression of SQSTM1/p62 suggesting rather a SS-31 effect on autophagy. Our results support the existence of cross-talk between oxidative stress and autophagy in T2D [56], as SS-31 treatment of leukocytes of T2D patients reduces mitochondrial ROS production, which seems to prevent the increase induced by autophagic biomarkers. The specificity of this effect was shown by the fact SS-31 lacked the capacity to prevent the autophagic process induced by the pharmacological inducer of autophagy, rapamycin. As shown in many reports, rapamycin does not increase intracellular ROS levels (or can even diminish them) which is in keeping with our conclusion of SS-31 interfering with the autophagy observed in leukocytes from T2D patients through its capacity to scavenge mitochondrial ROS.

A link between ER stress, ROS production and autophagy could also be established considering the implication of cardiolipin in mitochondrial function including calcium buffering and mitophagy [57–60]. Given that in this work intracellular calcium levels in leukocytes from diabetics are enhanced concomitantly with increased presence of total and mitochondrial ROS, we could speculate that cardiolipin might be altered. With this and considering that SS-31 is a ROS scavenger that binds cardiolipin, we can speculate that cardiolipin may be involved in the effects exerted by SS-31. It could act as a regulator of mitophagy, explaining the reducing effect on autophagy seen in our work and could also affect calcium handling by mitochondria. It is widely known that calcium levels influence leukocyte function [61,62] and this occurs through NLRP3 signaling and the regulation of calmodulins and GTPases which participate in crucial processes in leukocytes such as innate defense and transmigration. Both aspects could reinforce SS-31 as a mitoprotective molecule that prevents leukocyte dysfunction. The effect of SS-31 on cardiolipin in this model and its relation to mitophagy seems a promising idea that needs to be explored in future studies.

It is important to mention that a possible limitation of this study are the potential interactions, synergisms, or detriments that may arise when studying or implementing novel drugs like SS-31 in a background affected by other medications such as statins. In this sense, previous research has stated that statins can have both detrimental [63–66] and beneficial effects [67–77], often unrelated to their lipid-lowering effect and rather associated with their pleiotropic actions. The variation of the effect is explained by the type of statin, the dose, the combination with other treatments and the experimental model. However, to our knowledge, there are no reports about the interference of statins with SS-31 when applied in combination, in patients or in animal studies.

5. Conclusions

In summary, our findings reveal a potential protective effect of novel SS-31 therapy in diseases with increased oxidative and an ER stress state such as T2D. It is important to highlight that mitochondrial accumulation of SS-peptides does not depend on alterations of $\Delta\Psi_m$, which represents a major advantage to respect to other antioxidants [78–80]. The discovery of novel potential therapeutic strategies based on mitochondrial biology is key to future treatments, but further research is essential. The SS-31 peptide in particular represents a possible approach, through targeted delivery of antioxidants

to mitochondria. In fact, in the present study we have demonstrated that SS-31 reduces ROS and could modulate ER stress and autophagy, key molecular pathways in cellular homeostasis, suggesting that this compound may exert beneficial effects that can be channeled for the treatment of T2D. Further investigations including clinical trials are required to elucidate these and other important mechanisms underlying the actions of SS-31 in treatment of T2D.

Supplementary Materials: The following are available online at http://www.mdpi.com/2077-0383/8/9/1322/s1, Figure S1: Leukocyte-enfothelium interaction evaluation under SS-31 and SS-20 treatment.

Author Contributions: Conceptualization, V.M.V. and M.R.; Methodology, I.E.-L., A.M.d.M., Z.A.-J., P.D.-P. and F.I.; Validation, V.M.V. and M.R.; Formal Analysis, I.E.-L., M.R. and V.M.V.; Investigation, I.E.-L., A.M.d.M. and F.I.; Resources, V.M.V., M.R. and E.S.; Data Curation, I.E.-L. and V.M.V.; Writing—Original Draft Preparation, I.E.-L., N.A. and V.M.V.; Writing—Review and Editing, V.M.V., M.R., N.A., E.S., A.M.d.M., Z.A.-J., I.E.-L., F.I., P.D.-P. and S.L.-D.; Visualization, I.E.-L., S.L.-D. and V.M.V.; Supervision, V.M.V. and M.R.; Project Administration, V.M.V. and M.R.; Funding Acquisition, V.M.V. and M.R.

Funding: This research was funded by grants PI16/1083, PI16/0301, and CIBERehd CB06/04/0071 by Carlos III Health Institute, PROMETEOII 2014/035 from the Regional Ministry Education of Valencian Community and by the European Regional Development Fund (ERDF "A way to build Europe"); UGP15-193 and UGP-15-220 by FISABIO and by an unrestricted grant from Menarini S.A. I.E.-L. is recipient of a predoctoral contract from FISABIO (UGP-15-144). A.M.d.M., S.L.-D., Z.A.-J. are recipients of PFIS contracts from Carlos III Health Institute (FI17/00126, FI14/00350, FI17/00144). F.I. is recipient of a contract from Generalitat Valenciana GRISOLIAP/2016/015. M.R. and V.M.V. are recipients of contracts from the Ministry of Health of the Valencian Regional Government and Carlos III Health Institute (CPII16/00037 and CES10/030, respectively).

Acknowledgments: The authors give special thanks to Brian Normanly (University of Valencia-CIBERehd) for his editorial assistance, and Rosa Falcon and Carmen Ramirez (FISABIO) for their technical assistance.

Conflicts of Interest: The authors declare no conflict of interest. The funding bodies had no role in the design of the study; in the collection, analyses or interpretation of data; in the writing of the manuscript, or in the decision to publish the results.

References

1. Giacco, F.; Brownlee, M. Oxidative stress and diabetic complications. *Circ. Res.* **2010**, *107*, 1058–1070. [CrossRef] [PubMed]
2. Akash, M.S.; Rehman, K.; Chen, S. Role of inflammatory mechanisms in pathogenesis of type 2 diabetes mellitus. *J. Cell. Biochem.* **2013**, *114*, 525–531. [CrossRef] [PubMed]
3. Higa, A.; Chevet, E. Redox signaling loops in the unfolded protein response. *Cell. Signal.* **2012**, *24*, 1548–1555. [CrossRef] [PubMed]
4. Klausner, R.D.; Sitia, R. Protein degradation in the endoplasmic reticulum. *Cell* **1990**, *62*, 611–614. [CrossRef]
5. Shamu, C.E.; Cox, J.S.; Walter, P. The unfolded-protein-response pathway in yeast. *Trends Cell Biol.* **1994**, *4*, 56–60. [CrossRef]
6. Hotamisligil, G.S. Inflammation and endoplasmic reticulum stress in obesity and diabetes. *Int. J. Obes.* **2008**, *32*, 52. [CrossRef] [PubMed]
7. Ron, D.; Walter, P. Signal integration in the endoplasmic reticulum unfolded protein response. *Nat. Rev. Mol. Cell Biol.* **2007**, *8*, 519–529. [CrossRef] [PubMed]
8. Wang, S.; Kaufman, R.J. The impact of the unfolded protein response on human disease. *J. Cell. Biol.* **2012**, *197*, 857–867. [CrossRef] [PubMed]
9. Meusser, B.; Hirsch, C.; Jarosch, E.; Sommer, T. ERAD: The long road to destruction. *Nat. Cell Biol.* **2005**, *7*, 766–772. [CrossRef] [PubMed]
10. Tanida, I. Autophagosome formation and molecular mechanism of autophagy. *Antioxid. Redox. Signal.* **2011**, *14*, 2201–2214. [CrossRef]
11. Yin, J.J.; Li, Y.B.; Wang, Y.; Liu, G.D.; Wang, J.; Zhu, X.O.; Pan, S.H. The role of autophagy in endoplasmic reticulum stress-induced pancreatic beta cell death. *Autophagy* **2012**, *8*, 158–164. [CrossRef] [PubMed]
12. Su, J.; Zhou, L.; Kong, X.; Yang, X.; Xiang, X.; Zhang, Y.; Li, X.; Sun, L. Endoplasmic reticulum is at the crossroads of autophagy, inflammation, and apoptosis signaling pathways and participates in the pathogenesis of diabetes mellitus. *J. Diabetes Res.* **2013**, *2013*, 193461. [CrossRef] [PubMed]

13. Demirtas, L.; Guclu, A.; Erdur, F.M.; Akbas, E.M.; Ozcicek, A.; Onk, D.; Turkmen, K. Apoptosis, autophagy & endoplasmic reticulum stress in diabetes mellitus. *Indian J. Med. Res.* **2016**, *144*, 515–524. [CrossRef] [PubMed]
14. Cadenas, E.; Davies, K.J. Mitochondrial free radical generation, oxidative stress, and aging. *Free Radic. Biol. Med.* **2000**, *29*, 222–230. [CrossRef]
15. Murphy, M.P. How mitochondria produce reactive oxygen species. *Biochem. J.* **2009**, *417*, 1–13. [CrossRef]
16. Szeto, H.H. First-in-class cardiolipin-protective compound as a therapeutic agent to restore mitochondrial bioenergetics. *Br. J. Pharmacol.* **2014**, *171*, 2029–2050. [CrossRef]
17. Birk, A.V.; Liu, S.; Soong, Y.; Mills, W.; Singh, P.; Warren, J.D.; Seshan, S.V.; Pardee, J.D.; Szeto, H.H. The mitochondrial-targeted compound SS-31 re-energizes ischemic mitochondria by interacting with cardiolipin. *J. Am. Soc. Nephrol.* **2013**, *24*, 1250–1261. [CrossRef]
18. Szeto, H.H.; Liu, S.; Soong, Y.; Wu, D.; Darrah, S.F.; Cheng, F.Y.; Zhao, Z.; Ganger, M.; Tow, C.Y.; Seshan, S.V. Mitochondria-targeted peptide accelerates ATP recovery and reduces ischemic kidney injury. *J. Am. Soc. Nephrol.* **2011**, *22*, 1041–1052. [CrossRef]
19. Zhao, K.; Zhao, G.M.; Wu, D.; Soong, Y.; Birk, A.V.; Schiller, P.W.; Szeto, H.H. Cell-permeable peptide antioxidants targeted to inner mitochondrial membrane inhibit mitochondrial swelling, oxidative cell death, and reperfusion injury. *J. Biol. Chem.* **2004**, *279*, 34682–34690. [CrossRef]
20. Escribano-López, I.; Díaz-Morales, N.; Iannantuoni, F.; López-Domènech, S.; de Marañón, A.M.; Abad-Jiménez, Z.; Bañuls, C.; Rovira-Llopis, S.; Herance, J.R.; Rocha, M.; et al. The mitochondrial antioxidant SS-31 increases Sirt-1 levels and ameliorates inflammation, oxidative stress and leukocyte-endothelium interactions in type 2 diabetes. *Sci. Rep.* **2018**, *8*, 15862. [CrossRef]
21. Pitozzi, V.; Giovanelli, L.; Bardini, G.; Rotella, C.M.; Dolara, P. Oxidative DNA damage in peripheral blood cells in type 2 diabetes mellitus; higher vulnerability of polymorphonuclear leukocytes. *Mutat. Res.* **2003**, *529*, 129–133. [CrossRef]
22. Bir, S.C.; Kevil, C.G. Diabetic neutrophil mitochondrial dysfunction: an inflammatory situation? *Free Radic. Biol. Med.* **2011**, *50*, 1213–1214. [CrossRef] [PubMed]
23. Zozulinska, D.; Wierusz-Wysocka, B. Type 2 diabetes mellitus as inflammatory disease. *Diabetes Res. Clin. Pract.* **2006**, *74*, S12–S16. [CrossRef]
24. Shurtz-Swirski, R.; Sela, S.; Herskovits, A.T.; Shasha, S.M.; Shapiro, G.; Nasser, L.; Kristal, B. Involvement of Peripheral Polymorphonuclear Leukocytes in Oxidative Stress and Inflammation in Type 2 Diabetic Patients. *Diabetes Care* **2001**, *24*, 104–110. [CrossRef] [PubMed]
25. Pettersson, U.S.; Christoffersson, G.; Massena, S.; Ahl, D.; Jansson, L.; Henriksnäs, J.; Phillipson, M. Increased Recruitment but Impaired Function of Leukocytes during Inflammation in Mouse Models of Type 1 and Type 2 Diabetes. *PLoS ONE* **2011**, *6*, e22480. [CrossRef] [PubMed]
26. Guan, Y.; Zhou, L.; Zhang, Y.; Tian, H.; Li, A.; Han, X. Effects of PP2A/Nrf2 on experimental diabetes mellitus-related cardiomyopathy by regulation of autophagy and apoptosis through ROS dependent pathway. *Cell. Signal.* **2019**, *62*, 109339. [CrossRef] [PubMed]
27. Tampakakis, E.; Tabit, C.E.; Holbrook, M.; Linder, E.A.; Berk, B.D.; Frame, A.A.; Bretón-Romero, R.; Fetterman, J.L.; Gokce, N.; Vita, J.A.; et al. Intravenous lipid infusion induces endoplasmic reticulum stress in endothelial cells and blood mononuclear cells of healthy adults. *J. Am. Heart Assoc.* **2016**, *5*, e002574. [CrossRef]
28. RostamiRad, A.; Ebrahimi, S.S.S.; Sadeghi, A.; Taghikhani, M.; Meshkani, R. Palmitate-induced impairment of autophagy turnover leads to increased apoptosis and inflammation in peripheral blood mononuclear cells. *Immunobiology* **2018**, *223*, 269–278. [CrossRef]
29. Mozzini, C.; Garbin, U.; Stranieri, C.; Pasini, A.; Solani, E.; Tinelli, I.A.; Cominacini, L.; Fratta-Pasini, A.M. Endoplasmic reticulum stress and Nrf2 repression in circulating cells of type 2 diabetic patients without the recommended glycemic goals. *Free Radic. Res.* **2015**, *49*, 244–252. [CrossRef]
30. Rovira-Llopis, S.; Bañuls, C.; Apostolova, N.; Morillas, C.; Hernandez-Mijares, A.; Rocha, M.; Victor, V.M. Is glycemic control modulating endoplasmic reticulum stress in leukocytes of type2 diabetic patients? *Antioxid. Redox. Signal.* **2014**, *21*, 1759–1765. [CrossRef]
31. Szpigel, A.; Hainault, I.; Carlier, A.; Venteclef, N.; Batto, A.F.; Hajduch, E.; Bernard, C.; Ktorza, A.; Gautier, J.F.; Ferré, P.; et al. Lipid environment induces ER stress, TXNIP expression and inflammation in immune cells of individuals with type 2 diabetes. *Diabetologia* **2018**, *61*, 399–412. [CrossRef] [PubMed]

32. Sindhu, S.; Akhter, N.; Kochumon, S.; Thomas, R.; Wilson, A.; Shenouda, S.; Tuomilehto, J.; Ahmad, R. Increased expression of the innate immune receptor TLR10 in obesity and type-2 diabetes: Association with ROS-mediated oxidative stress. *Cell. Physiol. Biochem.* **2018**, *45*, 572–590. [CrossRef] [PubMed]
33. Bañuls, C.; Rovira-Llopis, S.; Lopez-Domenech, S.; Diaz-Morales, N.; Blas-Garcia, A.; Veses, S.; Morillas, C.; Victor, V.M.; Rocha, M.; Hernandez-Mijares, A. Oxidative and endoplasmic reticulum stress is impaired in leukocytes from metabolically unhealthy vs healthy obese individuals. *Int. J. Obes.* **2017**, *41*, 1556–1563.
34. Restaino, R.M.; Deo, S.H.; Parrish, A.R.; Fadel, P.J.; Padilla, J. Increased monocyte-derived reactive oxygen species in type 2 diabetes: Role of endoplasmic reticulum stress. *Exp. Physiol.* **2017**, *102*, 139–153. [CrossRef] [PubMed]
35. Rovira-Llopis, S.; Díaz-Morales, N.; Bañuls, C.; Blas-García, A.; Polo, M.; López-Domenech, S.; Jover, A.; Rocha, M.; Hernández-Mijares, A.; Víctor, V.M. Is Autophagy Altered in the Leukocytes of Type 2 Diabetic Patients? *Antioxid. Redox. Signal.* **2015**, *23*, 1050–1056. [CrossRef]
36. Riek, A.; Oh, J.; Sprague, J.; Timpson, A.; de las Fuentes, L.; Bernal-Mizrachi, L.; Schechtman, K.; Bernal-Mizrachi, C. Vitamin D Suppression of Endoplasmic Reticulum Stress Promotes an Antiatherogenic Monocyte/Macrophage Phenotype in Type 2 Diabetic Patients. *J. Biol. Chem.* **2012**, *287*, 38482–38484. [CrossRef] [PubMed]
37. Lenin, R.; Maria, M.S.; Agrawal, M.; Balasubramanyam, J.; Mohan, V.; Balasubramanyam, M. Amelioration of glucolipotoxicity-induced endoplasmic reticulum stress by a "chemical chaperone" in human THP-1 monocytes. *Exp. Diabetes Res.* **2012**, 356487. [CrossRef]
38. Mehrzadi, S.; Yousefi, B.; Hosseinzadeh, A.; Reiter, R.J.; Safa, M.; Ghaznavi, H.; Naseripour, M. Diabetic retinopathy pathogenesis and the ameliorating effects of melatonin; involvement of autophagy, inflammation and oxidative stress. *Life Sci.* **2018**, *193*, 20–33. [CrossRef]
39. Diaz-Morales, N.; Iannantuoni, F.; Escribano-Lopez, I.; Bañuls, C.; Rovira-Llopis, S.; Sola, E.; Rocha, M.; Hernandez-Mijares, A.; Victor, V.M. Does Metformin Modulate Endoplasmic Reticulum Stress and Autophagy in Type 2 Diabetic Peripheral Blood Mononuclear Cells? *Antioxid. Redox. Signal.* **2018**, *28*, 1562–1569. [CrossRef]
40. Streitz, M.; Miloud, T.; Kapinsky, M.; Reed, M.R.; Magari, R.; Geissler, E.K.; Hutchinson, J.A.; Vogt, K.; Schickeisler, S.; Kverneland, A.H.; et al. Standarization of whole blood immune phenotype monitoring for clinical trials: Panels and methods for the ONE study. *Transplant. Res.* **2013**, *2*, 17. [CrossRef]
41. Fujimoto, H.; Sakata, T.; Hamaguchi, Y.; Shiga, S.; Tohyama, K.; Ichiyama, S.; Wang, F.S.; Houwen, B. Flow cytometric method for enumeration and classification of reactive immature granulocyte populations. *Cytommetry* **2000**, *42*, 371–378. [CrossRef]
42. Fato, R.; Bergamini, C.; Bortolus, M.; Maniero, A.L.; Leoni, S.; Ohnishi, T.; Lenaz, G. Differential effects of mitochondrial Complex I inhibitors on production of reactive oxygen species. *Biochim. Biophys. Acta* **2009**, *1787*, 384–392. [CrossRef]
43. Lytton, J.; Westlin, M.; Hanley, M.R. Thapsigargin inhibits the sarcoplasmic or endoplasmic reticulum Ca-ATPase family of calcium pumps. *J. Biol. Chem.* **1991**, *266*, 17067–17071.
44. Hou, Y.; Li, S.; Wu, M.; Wei, J.; Ren, Y.; Du, C.; Wu, H.; Han, C.; Duan, H.; Shi, Y. Mitochondria-targeted peptide SS-31 attenuates renal injury via an antioxidant effect in diabetic nephropathy. *Am. J. Physiol. Renal Physiol.* **2016**, *310*, 547. [CrossRef]
45. Zhu, L.L.; Li, M.Q.; He, F.; Zhou, S.B.; Jiang, W. Mitochondria Targeted Peptide Attenuates Mitochondrial Dysfunction, Controls Inflammation and Protects Against Spinal Cord Injury-Induced Lung Injury. *Cell. Physiol. Biochem.* **2017**, *44*, 388–400. [CrossRef] [PubMed]
46. Leahy, J.L. Pathogenesis of type 2 diabetes mellitus. *Arch. Med. Res.* **2005**, *36*, 197–209.
47. Mizukami, H.; Takahashi, K.; Inaba, W.; Tsuboi, K.; Osonoi, S.; Yoshida, T.; Yagihashi, S. Involvement of oxidative stress-induced DNA damage, endoplasmic reticulum stress, and autophagy deficits in the decline of beta-cell mass in Japanese type 2 diabetic patients. *Diabetes Care* **2014**, *37*, 1966–1974. [CrossRef] [PubMed]
48. Lo, M.C.; Chen, M.H.; Lee, W.S.; Lu, C.I.; Chang, C.R.; Kao, S.H.; Lee, H.M. Nepsilon-(carboxymethyl) lysine-induced mitochondrial fission and mitophagy cause decreased insulin secretion from beta-cells. *Am. J. Physiol. Endocrinol. Metab.* **2015**, *309*, 829. [CrossRef] [PubMed]

49. Hernandez-Mijares, A.; Rocha, M.; Rovira-Llopis, S.; Bañuls, C.; Bellod, L.; de Pablo, C.; Alvarez, A.; Roldan-Torres, I.; Sola-Izquierdo, E.; Victor, V.M. Human leukocyte/endothelial cell interactions and mitochondrial dysfunction in type 2 diabetic patients and their association with silent myocardial ischemia. *Diabetes Care* **2013**, *36*, 1695–1702. [CrossRef] [PubMed]
50. Whiteman, M.; Spencer, J.P.; Szeto, H.H.; Armstrong, J.S. Do mitochondriotropic antioxidants prevent chlorinative stress-induced mitochondrial and cellular injury? *Antioxid. Redox. Signal.* **2008**, *10*, 641–650. [CrossRef] [PubMed]
51. Petersen, K.F.; Dufour, S.; Befroy, D.; Garcia, R.; Shulman, G.I. Impaired mitochondrial activity in the insulin-resistant offspring of patients with type 2 diabetes. *N. Engl. J. Med.* **2004**, *350*, 664–671. [CrossRef] [PubMed]
52. Kelley, D.E.; He, J.; Menshikova, E.V.; Ritov, V.B. Dysfunction of mitochondria in human skeletal muscle in type 2 diabetes. *Diabetes* **2002**, *51*, 2944–2950. [CrossRef] [PubMed]
53. Komura, T.; Sakai, Y.; Honda, M.; Takamura, T.; Matsushima, K.; Kaneko, S. CD14+ monocytes are vulnerable and functionally impaired under endoplasmic reticulum stress in patients with type 2 diabetes. *Diabetes* **2010**, *59*, 634–643. [CrossRef] [PubMed]
54. Sage, A.T.; Holtby-Ottenhof, S.; Shi, Y.; Damjanovic, S.; Sharma, A.M.; Werstuck, G.H. Metabolic syndrome and acute hyperglycemia are associated with endoplasmic reticulum stress in human mononuclear cells. *Obesity* **2012**, *20*, 748–755. [CrossRef] [PubMed]
55. Gonzalez, C.D.; Lee, M.S.; Marchetti, P.; Pietropaolo, M.; Towns, R.; Vaccaro, M.I.; Watada, H.; Wiley, J.W. The emerging role of autophagy in the pathophysiology of diabetes mellitus. *Autophagy* **2011**, *7*, 2–11. [CrossRef] [PubMed]
56. Liu, H.; Yin, J.J.; Cao, M.M.; Liu, G.D.; Su, Y.; Li, Y.B. Endoplasmic reticulum stress induced by lipopolysaccharide is involved in the association between inflammation and autophagy in INS1 cells. *Mol. Med. Rep.* **2017**, *16*, 5787–5792. [CrossRef] [PubMed]
57. Dudek, J. Role of Cardiolipin in Mitochodnrial signaling pathways. *Front. Cell Dev. Biol.* **2017**, *5*, 90. [CrossRef] [PubMed]
58. Hwang, M.S.; Schwall, C.T.; Pazarentzos, E.; Datler, C.; Alder, N.N.; Grimm, S. Mitochondrial calcium ibnflux targets cardiolipin to disintegrate respiratory chain complex II for cell death induction. *Cell Death Differ.* **2014**, *21*, 1733–1745. [CrossRef] [PubMed]
59. Paradies, G.; Petrosillo, G.; Paradies, V.; Ruggiero, F.M. Role of cardiolipin peroxidation and calcium in mitochondrial dysfunction and disease. *Cell Calcium* **2009**, *45*, 643–650. [CrossRef] [PubMed]
60. Petrosillo, G.; Ruggiero, F.M.; Pistolese, M.; Paradies, G. Calcium-induced Reactive Oxigen Species production promotes Cytocrome C release from rat liver mitochodnria via Mitochondrial Permeability Transition (MPT)-dependent and MPT-independent mechanisms. *J. Biol. Chem.* **2004**, *279*, 53103–53108. [CrossRef] [PubMed]
61. Martinvalet, D. The role of the mitochondria and the rendoplasmic reticulum contact sites in the development of the immune responses. *Cell Death Dis.* **2018**, *9*, 336. [CrossRef] [PubMed]
62. Prahrtana, J.D.; Sullivan, D.P.; Muller, W.A. Exploring the role of calmodulin and calcium signaling in leukocyte transmigration. *FASEB J.* **2018**, *32*, 280.
63. Pal, S.; Ghosh, M.; Ghosh, S.; Bhattacharyya, S.; Sil, P.C. Atorvastatin induced hepatic oxidative stress and apoptotic damage via MAPKs, mitochondria, calpain and caspase 12 dependent pathways. *Food Chem. Toxicol.* **2015**, *83*, 36–47. [CrossRef] [PubMed]
64. Godoy, J.C.; Niesman, I.R.; Busija, A.R.; Kassan, A.; Schilling, J.M.; Schwarz, A.; Alvarez, E.A.; Dalton, N.D.; Drummond, J.C.; Roth, D.M.; et al. Atorvastatin, but not pravastatin, inhibits cardiac Akt/mTOR signaling and disturbs mitochondrial ultrastructure in cardiac myocytes. *FASEB J.* **2019**, *33*, 1209–1225. [CrossRef] [PubMed]
65. Ghavami, S.; Sharma, P.; Yeganeh, B.; Ojo, O.O.; Jha, A.; Mutawe, M.M.; Kashani, H.H.; Los, M.J.; Klonisch, T.; Unruh, H.; et al. Airway mesenchymal cell death by mevalonate cascade inhibition: Integration of autophagy, unfolded protein response and apoptosis focusing on Bcl2 family proteins. *Biochim. Biophys. Acta* **2014**, *1843*, 1259–1271. [CrossRef] [PubMed]
66. Schirris, T.J.; Renkema, G.H.; Ritschel, T.; Voermans, N.C.; Bilos, A.; van Engelen, B.G.; Brandt, U.; Koopman, W.J.; Beyrath, J.D.; Rodenburg, R.J.; et al. Statin-Induced Myopathy Is Associated with Mitochondrial Complex III Inhibition. *Cell Metab.* **2015**, *22*, 399–407. [CrossRef]

67. Costa, S.; Reina-Couto, M.; Albino-Teixeira, A.; Sousa, T. Statins and oxidative stress in chronic heart failure. *Rev. Port. Cardiol.* **2016**, *35*, 41–57. [CrossRef] [PubMed]
68. Escudero, P.; Martinez de Marañón, A.; Collado, A.; Gonzalez-Navarro, H.; Hermenegildo, C.; Peiró, C.; Piqueras, L.; Sanz, M.J. Combined sub-optimal doses of rosuvastatin and bexarotene impair angiotensin II-induced arterial mononuclear cell adhesion through inhibition of Nox5 signaling pathways and increased RXR/PPARα and RXR/PPARγ interactions. *Antiox. Redox. Sign.* **2015**, *22*, 901–920. [CrossRef]
69. Whitehead, N.P. Enhanced autophagy as a potential mechanism for the improved physiological function by simvastatin in muscular dystrophy. *Autophagy* **2016**, *12*, 705–706. [CrossRef]
70. Chen, Y.H.; Chen, Y.C.; Liu, C.S.; Hsieh, M.C. The Different Effects of Atorvastatin and Pravastatin on Cell Death and PARP Activity in Pancreatic NIT-1 Cells. *J. Diabetes Res.* **2016**, 1828071. [CrossRef]
71. Zhang, T.; Lu, D.; Yang, W.; Shi, C.; Zang, J.; Shen, L.; Mai, H.; Xu, A. HMG-CoA Reductase Inhibitors Relieve Endoplasmic Reticulum Stress by Autophagy Inhibition in Rats With Permanent Brain Ischemia. *Front. Neurosci.* **2018**, *12*, 405. [CrossRef] [PubMed]
72. Xu, J.Z.; Chai, Y.L.; Zhang, Y.L. Effect of rosuvastatin on high glucose-induced endoplasmic reticulum stress in human umbilical vein endothelial cells. *Genet. Mol. Res.* **2016**, *15*. [CrossRef] [PubMed]
73. Li, Y.; Lu, G.; Sun, D.; Zuo, H.; Wang, D.W.; Yan, J. Inhibition of endoplasmic reticulum stress signaling pathway: A new mechanism of statins to suppress the development of abdominal aortic aneurysm. *PloS ONE* **2017**, *12*, e0174821. [CrossRef] [PubMed]
74. Kojanian, H.; Szafran-Swietlik, A.; Onstead-Haas, L.M.; Haas, M.J.; Mooradian, A.D. Statins prevent dextrose-induced endoplasmic reticulum stress and oxidative stress in endothelial and HepG2 cells. *Am. J. Ther.* **2016**, *23*, e1456–e1463. [CrossRef] [PubMed]
75. Wu, Z.H.; Chen, Y.Q.; Zhao, S.P. Simvastatin inhibits ox-LDL-induced inflammatory adipokines secretion via amelioration of ER stress in 3T3-L1 adipocyte. *Biochem. Biophys. Res. Commun.* **2013**, *432*, 365–369. [CrossRef] [PubMed]
76. Li, L.; Wang, Y.; Xu, Y.; Chen, L.; Fang, Q.; Yan, X. Atorvastatin inhibits CD68 expression in aortic root through a GRP78-involved pathway. *Cardiovasc. Drugs Ther.* **2014**, *28*, 523–532. [CrossRef] [PubMed]
77. Alaarg, A.; Zheng, K.H.; van der Valk, F.M.; da Silva, A.E.; Versloot, M.; van Ufford, L.C.; Schulte, D.M.; Storm, G.; Metselaar, J.M.; Stroes, E.S.; et al. Multiple pathway assessment to predict anti-atherogenic efficacy of drugs targeting macrophages in atherosclerotic plaques. *Vascul. Pharmacol.* **2016**, *82*, 51–59. [CrossRef] [PubMed]
78. Szeto, H.H.; Schiller, P.W. Novel therapies targeting inner mitochondrial membrane—From discovery to clinical development. *Pharm. Res.* **2011**, *28*, 2669–2679. [CrossRef] [PubMed]
79. Szeto, H.H. Cell-permeable, mitochondrial-targeted, peptide antioxidants. *AAPS J.* **2006**, *8*, 277. [CrossRef]
80. Kelso, G.F.; Porteous, C.M.; Coulter, C.V.; Hughes, G.; Porteous, W.K.; Ledgerwood, E.C.; Smith, R.A.; Murphy, M.P. Selective targeting of a redox-active ubiquinone to mitochondria within cells: Antioxidant and antiapoptotic properties. *J. Biol. Chem.* **2001**, *276*, 4588–4596. [CrossRef]

8.3. Annex III: Additional scientific production during the PhD training

8.3.1. Original articles

1. Rovira-Llopis S, Bañuls C, **de Marañon AM**, Diaz-Morales N, Jover A, Garzon S, Rocha M, Victor VM, Hernandez-Mijares A. Low testosterone levels are related to oxidative stress, mitochondrial dysfunction and altered subclinical atherosclerotic markers in type 2 diabetic male patients. Free Radic Biol Med. 2017 Jul;108:155-162.
   DOI: 10.1016/j.freeradbiomed.2017.03.029.
   Impact Factor: **6.02**
   Category: Endocrinology and metabolism (**Q1**)

2. Bañuls C, Rovira-Llopis S, **Martinez de Marañon A**, Veses S, Jover A, Gomez M, Rocha M, Hernandez-Mijares A, Victor VM. Metabolic syndrome enhances endoplasmic reticulum, oxidative stress and leukocyte-endothelium interactions in PCOS. Metabolism. 2017 Jun;71:153-162.
   DOI: 10.1016/j.metabol.2017.02.012.
   Impact Factor: **6.159**
   Category: Endocrinology and metabolism (**Q1**)

3. López-Domènech S, Bañuls C, **de Marañón AM**, Abab-Jiménez Z, Morillas C, Gómez-Abril SÁ, Rovira-Llopis S, Víctor VM, Hernández-Mijares A, Rocha M. Pinitol alleviates systemic inflammatory cytokines in human obesity by a mechanism involving unfolded protein response and sirtuin 1. Clin Nutr. 2018 Dec;37(6 Pt A):2036-2044.
   DOI: 10.1016/j.clnu.2017.09.015.
   Impact Factor: **6.402**
   Category: Nutrition and dietetics (**D1**)

4. López-Domènech S, Abad-Jiménez Z, Iannantuoni F, **de Marañón AM**, Rovira-Llopis S, Morillas C, Bañuls C, Víctor VM, Rocha M. Moderate weight loss attenuates chronic endoplasmic reticulum stress and mitochondrial dysfunction in human obesity. Mol Metab. 2019 Jan;19:24-33.
   DOI: 10.1016/j.molmet.2018.10.005.
   Impact Factor: **6.448**
   Category: Endocrinology and metabolism (**D1**)

5. Escribano-López I, **de Marañon AM**, Iannantuoni F, López-Domènech S, Abad-Jiménez Z, Díaz P, Solá E, Apostolova N, Rocha M, Víctor VM. The Mitochondrial Antioxidant SS-31 Modulates Oxidative Stress, Endoplasmic Reticulum Stress, and Autophagy in Type 2 Diabetes. J Clin Med. 2019 Aug 28;8(9):1322.
   DOI: 10.3390/jcm8091322
   Impact Factor: **3.303**
   Category: Medicine, general and internal (**Q1**)

6. Bañuls C, **de Marañón AM**, Castro-Vega I, López-Doménech S, Escribano-López I, Salom C, Veses S, Hernández-Mijares A. Role of Endoplasmic Reticulum and Oxidative Stress Parameters in the Pathophysiology of Disease-Related Malnutrition in Leukocytes of an Outpatient Population. Nutrients. 2019 Aug 8;11(8):1838.
   DOI: 10.3390/nu11081838.
   Impact Factor: **4.546**
   Category: Nutrition and dietetics (**Q1**)

7. Iannantuoni F, M **de Marañon A**, Diaz-Morales N, Falcon R, Bañuls C, Abad-Jimenez Z, Victor VM, Hernandez-Mijares A, Rovira-Llopis S. The SGLT2 Inhibitor Empagliflozin Ameliorates the Inflammatory Profile in Type 2 Diabetic Patients and Promotes an Antioxidant Response in Leukocytes. J Clin Med. 2019 Nov 1;8(11):1814.
   DOI: 10.3390/jcm8111814.
   Impact Factor: **3.303**
   Category: Medicine, general and internal (**Q1**)

8. Bañuls C, **de Marañon AM**, Veses S, Castro-Vega I, López-Domènech S, Salom-Vendrell C, Orden S, Álvarez Á, Rocha M, Víctor VM, Hernández-Mijares A. Malnutrition impairs mitochondrial function and leukocyte activation. Nutr J. 2019 Dec 26;18(1):89.
   DOI: 10.1186/s12937-019-0514-7.
   Impact Factor: **3.359**
   Category: Nutrition and dietetics (**Q2**)

9. Iannantuoni F, **M de Marañon A**, Abad-Jiménez Z, Canet F, Díaz-Pozo P, López-Domènech S, Morillas C, Rocha M, Víctor VM. Mitochondrial Alterations and Enhanced Human Leukocyte/Endothelial Cell Interactions in Type 1 Diabetes. J Clin Med. 2020 Jul 8;9(7):2155.
   DOI: 10.3390/jcm9072155.
   Impact Factor: **4.241**
   Category: Medicine, general and internal (**Q1**)

10. Abad-Jiménez Z, López-Domènech S, Gómez-Abril SÁ, Periañez-Gómez D, **de Marañón AM**, Bañuls C, Morillas C, Víctor VM, Rocha M. Effect of Roux-en-Y Bariatric Bypass Surgery on Subclinical Atherosclerosis and Oxidative Stress Markers in Leukocytes of Obese Patients: A One-Year Follow-Up Study. Antioxidants (Basel). 2020 Aug 11;9(8):734.
    DOI: 10.3390/antiox9080734.
    Impact Factor: **6.312**
    Category: Food science & technology (**D1**)

11. Iannantuoni F, Salazar JD, **Martinez de Marañon A**, Bañuls C, López-Domènech S, Rocha M, Hurtado-Murillo F, Morillas C, Gómez-Balaguer M, Víctor VM. Testosterone administration increases leukocyte-endothelium interactions and inflammation in transgender men. Fertil Steril. 2021 Feb;115(2):483-489.
    DOI: 10.1016/j.fertnstert.2020.08.002
    Impact Factor: **7.329**
    Category: Obstetrics and gynecology (**D1**)

12. Canet F, Iannantuoni F, **Marañon AM**, Díaz-Pozo P, López-Domènech S, Vezza T, Navarro B, Solá E, Falcón R, Bañuls C, Morillas C, Rocha M, Víctor VM. Does Empagliflozin Modulate Leukocyte-Endothelium Interactions, Oxidative Stress, and Inflammation in Type 2 Diabetes? Antioxidants (Basel). 2021 Jul 30;10(8):1228.
DOI: 10.3390/antiox10081228..
Impact Factor: **6.312**
Category: Food science & technology (**D1**)

8.3.2. Reviews

1. Burgos-Morón E, Abad-Jiménez Z, **Marañón AM**, Iannantuoni F, Escribano-López I, López-Domènech S, Salom C, Jover A, Mora V, Roldan I, Solá E, Rocha M, Víctor VM. Relationship Between Oxidative Stress, ER Stress, and Inflammation in Type 2 Diabetes: The Battle Continues. J Clin Med. 2019 Sep 4;8(9):1385.
DOI: 10.3390/jcm8091385.
Impact Factor: **3.303**
Category: Medicine, General and Internal (**Q1**)

2. Vezza T, Canet F, **de Marañón AM**, Bañuls C, Rocha M, Víctor VM. Phytosterols: Nutritional Health Players in the Management of Obesity and Its Related Disorders. Antioxidants (Basel). 2020 Dec 12;9(12):1266.
DOI: 10.3390/antiox9121266.
Impact Factor: **5.014**
Category: Food science & technology (**Q1**)

8.3.3. Communications

1. **Martínez de Marañón A.**; Bañuls C.; Veses S.; Castro I.; López I.; Abad Z.; Escribano I.; Iannantuoni F.; Rocha M.; Victor V.M.; Hernandez A.Inflammation parameters and leukocyte-endothelium interactions are enhanced in an outpatient undernourished population. II National Congress of young researchers in Biomedicine. València, Spain,23-24/11/2017. **Poster**.

2. **Martínez de Marañón A.**; Rovira-Llopis S.; Díaz-Morales N.; Escribano-López I.; Abad Z.; Iannantuoni F.;Rocha M.; Víctor V.M. Relationship between autophagy and leukocyte-endothelium interactions in type 2 diabetic patients. SEFAGIA 2018,Madrid,Spain, 14-16/11/2018, **Oral communication**.

3. **de Marañón A.M.**; Canet F.; Iannantuoni F.; Abad-Jiménez Z.; Díaz P.; Rocha M.; Víctor V.M. The iSGLT2 inhibitor empaglifozin promotes antioxidant response in leukocytes and ameliorates the inflammatory profile of type 2 diabetic patients. XXXI Congreso Nacional de la Sociedad Española de Diabetes. XXXI Congreso Nacional de la Sociedad Española de Diabetes, Virtual. 21-23/6/2020. **Oral communication**.

4. **de Marañón A.M.**; Díaz Pozo P.; Iannantuoni F.; Canet F.; Abad Jiménez Z.;López Domènech S.; Falcón R.; Bañuls C.; Jover A.; Morillas C.; Rocha M.; Víctor V.M. SS31 antioxidant reduces leukocyte-endothelium interactions, ROS production and leukocytary inflammation in T2D patients. 88th European Atherosclerosis Society Congress 2020 (Virtual), 4-7/10/2020. **Poster**.

5. **De Marañón A.M.**; Díaz-Pozo P.; Iannantuoni F.; Canet F.; Abad-Jiménez Z.; López-Domènech S.; Falcón R.; Bañuls C.; Jover A.; Morillas C.; Rocha M.; Víctor V.M. SS-31 antioxidant reduces leukocyte-endothelium interactions, ROS production and leukocytary inflammation in T2D patients. European Atherosclerosis Society Congress 2020, Virtual, 4-7/10/2020. **Poster**

6. **Martínez de Marañón Peris A.**; Díaz Pozo P.; Iannantuoni F.; Canet F.; Vezza T.; Abad Jiménez Z.; López Domènech S.; Falcón R.; Zaragoza B.; Bañuls C.; Morillas C.; Rocha M.; Víctor V.M.Good glycaemic control reduces intima-media thickness, inflammation markers and ROS production in type 2 diabetes. 27th Annual Conference of the Society for Redox Biology & Medicine, Virtual, 18-20/11/2020. **Poster**.

7. **de Marañón A.M.**; Díaz Pozo P.; Canet F.; Vezza T.; Abad Jiménez Z.; López Domènech S.; García C.; Falcón R.; Bañuls C.; Rocha M.; Víctor V.M. Metformin reduces mitochondrial ROS levels and improves mitochondrial mass,membrane potential and respiratory complexes in leukocytes of type 2 diabetic subjects 20th Biennial Meeting of the Society for Free Radical Research International, Virtual, 15-18/03/2021. **Oral Communication. Young Investigator Award**

8. **de Marañón A.M.**; Díaz Pozo P.; Canet F.; Vezza T.; Abad Jiménez Z.; García C.; López Domènech S.; Falcón R.; Bañuls C.; Rocha M.; Víctor V.M.Testosterone administration to trasgender men increase inflammation and leukocyte-endothelium interactions. 43º Congreso de la Sociedad Española de Bioquímica y Biología Molecular,Virtual, 19-22/07/2021. **Poster.**